ISSN 1948-5204 (online)

World Journal of

Gastrointestinal Oncology

World J Gastrointest Oncol 2023 October 15; 15(10): 1675-1834

Published by Baishideng Publishing Group Inc

World Journal of Gastrointestinal Oncology

Contents

Monthly Volume 15 Number 10 October 15, 2023

REVIEW

MINIREVIEWS

ORIGINAL ARTICLE

Basic Study

Retrospective Cohort Study

Retrospective Study

World Journal of Gastrointestinal Oncology

Monthly Volume 15 Number 10 October 15, 2023

Contents

CASE REPORT

ABOUT COVER

Editorial Board of *World Journal of Gastrointestinal Oncology*, Claudio Casella, PhD, Assistant Professor, Surgeon, Scientific Sector MED/18 ("General Surgery"), University of Brescia-School of Medicine, Brescia I-25123, Italy. claudio.casella@unibs.it

AIMS AND SCOPE

The primary aim of *World Journal of Gastrointestinal Oncology* (*WJGO*, *World J Gastrointest Oncol*) is to provide scholars and readers from various fields of gastrointestinal oncology with a platform to publish high-quality basic and clinical research articles and communicate their research findings online.

WJGO mainly publishes articles reporting research results and findings obtained in the field of gastrointestinal oncology and covering a wide range of topics including liver cell adenoma, gastric neoplasms, appendiceal neoplasms, biliary tract neoplasms, hepatocellular carcinoma, pancreatic carcinoma, cecal neoplasms, colonic neoplasms, colorectal neoplasms, duodenal neoplasms, esophageal neoplasms, gallbladder neoplasms, *etc*.

INDEXING/ABSTRACTING

The *WJGO* is now abstracted and indexed in PubMed, PubMed Central, Science Citation Index Expanded (SCIE, also known as SciSearch®), Journal Citation Reports/Science Edition, Scopus, Reference Citation Analysis, China National Knowledge Infrastructure, China Science and Technology Journal Database, and Superstar Journals Database. The 2023 edition of Journal Citation Reports® cites the 2022 impact factor (IF) for *WJGO* as 3.0; IF without journal self cites: 2.9; 5-year IF: 3.0; Journal Citation Indicator: 0.49; Ranking: 157 among 241 journals in oncology; Quartile category: Q3; Ranking: 58 among 93 journals in gastroenterology and hepatology; and Quartile category: Q3. The *WJGO*'s CiteScore for 2022 is 4.1 and Scopus CiteScore rank 2022: Gastroenterology is 71/149; Oncology is 197/366.

RESPONSIBLE EDITORS FOR THIS ISSUE

Production Editor: *Xiang-Di Zhang*; **Production Department Director:** *Xiang Li*; **Editorial Office Director:** *Jia-Ru Fan*.

NAME OF JOURNAL
World Journal of Gastrointestinal Oncology

ISSN
ISSN 1948-5204 (online)

LAUNCH DATE
February 15, 2009

FREQUENCY
Monthly

EDITORS-IN-CHIEF
Monjur Ahmed, Florin Burada

EDITORIAL BOARD MEMBERS
https://www.wjgnet.com/1948-5204/editorialboard.htm

PUBLICATION DATE
October 15, 2023

INSTRUCTIONS TO AUTHORS
https://www.wjgnet.com/bpg/gerinfo/204

GUIDELINES FOR ETHICS DOCUMENTS
https://www.wjgnet.com/bpg/GerInfo/287

GUIDELINES FOR NON-NATIVE SPEAKERS OF ENGLISH
https://www.wjgnet.com/bpg/gerinfo/240

PUBLICATION ETHICS
https://www.wjgnet.com/bpg/GerInfo/288

PUBLICATION MISCONDUCT
https://www.wjgnet.com/bpg/gerinfo/208

ARTICLE PROCESSING CHARGE
https://www.wjgnet.com/bpg/gerinfo/242

STEPS FOR SUBMITTING MANUSCRIPTS
https://www.wjgnet.com/bpg/GerInfo/239

ONLINE SUBMISSION
https://www.f6publishing.com

World Journal of Gastrointestinal Oncology

Submit a Manuscript: https://www.f6publishing.com

World J Gastrointest Oncol 2023 October 15; 15(10): 1675-1690

DOI: 10.4251/wjgo.v15.i10.1675

ISSN 1948-5204 (online)

REVIEW

Minimally invasive surgery for gastro-oesophageal junction adenocarcinoma: Current evidence and future perspectives

Rodica Bîrlă, Petre Hoara, Florin Achim, Valeriu Dinca, Diana Ciuc, Silviu Constantinoiu, Adrian Constantin

Specialty type: Oncology

Provenance and peer review: Unsolicited article; Externally peer reviewed.

Peer-review model: Single blind

Peer-review report's scientific quality classification
Grade A (Excellent): A
Grade B (Very good): 0
Grade C (Good): C
Grade D (Fair): 0
Grade E (Poor): 0

P-Reviewer: Kumar M, India; Shiryajev YN, Russia;

Received: July 5, 2023
Peer-review started: July 5, 2023
First decision: August 15, 2023
Revised: September 4, 2023
Accepted: September 22, 2023
Article in press: September 22, 2023
Published online: October 15, 2023

Rodica Bîrlă, Florin Achim, Silviu Constantinoiu, Adrian Constantin, Department of General Surgery, Carol Davila University, Bucharest 011172, Romania

Petre Hoara, Department of General Surgery, Carol Davila University of Medicine and Pharmacy, Bucharest 020021, Romania

Valeriu Dinca, Diana Ciuc, Faculty of Medicine, "Titu Maiorescu" University, Bucharest 031593, Romania

Corresponding author: Petre Hoara, MD, PhD, Assistant Lecturer, Department of General Surgery, Carol Davila University of Medicine and Pharmacy, No. 37 Dionisie Lupu str, District 2, Bucharest 020021, Romania. petre.hoara@umfcd.ro

Abstract

Minimally invasive surgery is increasingly indicated in the management of malignant disease. Although oesophagectomy is a difficult operation, with a long learning curve, there is actually a shift towards the laparoscopic/thoracoscopic/robotic approach, due to the advantages of visualization, surgeon comfort (robotic surgery) and the possibility of the whole team to see the operation as well as and the operating surgeon. Although currently there are still many controversial topics, about the surgical treatment of patients with gastro-oesophageal junction (GOJ) adenocarcinoma, such as the type of open or minimally invasive surgical approach, the type of oesophago-gastric resection, the type of lymph node dissection and others, the minimally invasive approach has proven to be a way to reduce postoperative complications of resection, especially by decreasing pulmonary complications. The implementation of new technologies allowed the widening of the range of indications for this type of surgical approach. The short-term and long-term results, as well as the benefits for the patient - reduced surgical trauma, quick and easy recovery - offer this type of surgical treatment the premises for future development. This article reviews the updates and perspectives on the minimally invasive approach for GOJ adenocarcinoma.

Key Words: Gastro-oesophageal adenocarcinoma; Minimally invasive oesophagectomy; Laparoscopic gastrectomy; Abdomino-mediastinal lymph node dissection; Indocyanine green fluorescence imaging

Core Tip: Minimally invasive surgery is increasingly indicated in the management of malignant disease. Although oesophagectomy is a difficult operation, with a long learning curve, there is actually a shift towards the laparoscopic/thoracoscopic/robotic approach, due to the advantages offered to the patient and surgeon. The short- term and long-term results, as well as the benefits for the patient – reduced surgical aggressiveness, quick and easy recovery, offer this type of surgical treatment the premises for future development. This article reviews the updates and perspectives on the minimally invasive approach for gastro-oesophageal junction adenocarcinoma.

Citation: Bîrlă R, Hoara P, Achim F, Dinca V, Ciuc D, Constantinoiu S, Constantin A. Minimally invasive surgery for gastro-oesophageal junction adenocarcinoma: Current evidence and future perspectives. *World J Gastrointest Oncol* 2023; 15(10): 1675-1690
URL: https://www.wjgnet.com/1948-5204/full/v15/i10/1675.htm
DOI: https://dx.doi.org/10.4251/wjgo.v15.i10.1675

INTRODUCTION

In the last decades, the incidence of adenocarcinomas developed in the vicinity of the gastro-oesophageal junction (GOJ) is increasing[1]. Even from the year 1987, some authors recommend an individualized surgical strategy, guided by tumor stage and topographic location of the tumor center or tumor mass, based on the experience with surgical resection of more than 1000 patients with GOJ adenocarcinoma. This required detailed preoperative staging and classification of tumors, arising in the vicinity of the GOJ, into type I - defined when the tumor center was located 1-5 cm above the esophagogastric junction (EGJ), type II when located from 1 cm above to 2 cm below the EGJ, or type III when located 2-5 cm below the EGJ. type II is also known as "real" carcinoma of the cardia[2].

In patients with type I tumors, transthoracic or transhiatal (TH) oesophagectomy is performed and in patients with type II or type III, an extended total gastrectomy (TG) is more appropriate. In patients with early tumors, staged as uT1 on preoperative endosonography, a limited resection of the proximal stomach, cardia and distal oesophagus, with interposition of a pedicled isoperistaltic jejunal segment, allows a complete tumor removal with adequate lymphadenectomy[3].

Multimodal treatment protocols, with neoadjuvant chemotherapy or combined radiochemotherapy, followed by surgical resection, appear to markedly improve the prognosis, in patients with locally advanced tumors, who respond to preoperative treatment.

Minimally invasive surgery (MIS) is the gold standard in many areas of surgery. The first minimally invasive oesophagectomy was described by Cuschieri[4] in 1993, and one year later, Kitano *et al*[5] reported the first minimally invasive gastrectomy.

Since 1993, techniques for gastric cancer have evolved from laparoscopic-assisted surgery to total laparoscopic surgery, and oesophagectomy techniques have also evolved from hybrid approaches to a completely minimally invasive manner [6,7].

A 2017 study evaluates worldwide trends in surgical techniques, for oesophageal cancer surgery, comparing it to the 2007 survey[8], among the surgical members of the International Society for Diseases of the Esophagus, the World Organization for Specialized Studies in Diseases of the Esophagus, the International Gastric Cancer Association. Participants completed a web-based questionnaire about surgical strategies for esophageal and GOJ cancer. In 2017, minimally invasive transthoracic approach oesophagectomy was preferred by 43% surgeons, compared to 14% in 2007. In a subgroup analysis of oesophageal surgeons, the number of high-volume surgeons increased from 45% to 54%, over the last seven years. The preferred curative surgical treatment of oesophageal cancer was minimally invasive transthoracic oesophagectomy with two-field lymph node dissection (86%) and gastric tube reconstruction (95%).

Actual, most centers propose a laparoscopic abdominal approach, with gastric mobilization and pull-up through the diaphragmatic hiatus. The thoracic phase includes either an open procedure (hybrid technique)[8] or a thoracoscopic approach.

MIS for GOJ adenocarcinoma is associated with a significant operator-dependent learning curve. Data from the literature show a conversion rate of up to 12.5% from minimally invasive esophagectomy to open surgery, in low volume centers[9].

A recent study recognized that 35-40 MIS are required to acquire proficiency[10]. And another cohort study, analyzing the phases and outcomes of the learning curve, required to master minimally invasive, total adventitial resection of the cardia, suggests that there is a long learning curve[11]. A faster course of the learning curve could be facilitated by: gaining experience in open esophageal surgery and in MIS of the digestive tube, using specific high-performance equipment and carrying out training courses, in centers with great experience in this type of surgery.

This article reviews the updates on the MIS for GOJ adenocarcinoma, in terms of indications, types of MIS and resection, lymph node dissection, anastomosis type, short term and long term outcomes, life quality, and the perspectives, in order to provide reference for clinical treatment and research.

METHODS

The article is based on the analysis of data considered relevant for the chosen topic from the studies identified in PubMed Central (PMC) and MEDLINE Complete (EBSCO) since 2013, but also on the experience in minimally invasive surgeryin the General and Esophageal Surgery Clinic of the Sfanta Maria Clinical Hospital, Bucharest, Romania. Trials were sought and used, as well as data from updates of studies, original articles or reviews, regarding minimally invasive surgeryfor GOJ adenocarcinoma. For a sensitive search strategy, the terms used in search engines were: "Oesophagogastric junction adenocarcinoma" and "oesophagogastric junction adenocarcinoma and minimally invasive surgery". The article focused on data that have been updated about the types of indications and types of MIS, oesophago-gastric resection, short-term and long-term results, quality of life, and future perspectives. Only these studies and papers were considered eligible, thus being taken into account in the elaboration of this article. Two authors (Bîrlă R and Constantin A) selected the articles considered relevant, preferring peer-reviewed articles from highly ranked journals, written in English. The decision to select an item was made by agreement of the two. A number of 195 articles were identified for the period 2013–2023, which included the keywords used in the database search, 11 reviews and systematic reviews, 8 meta-analyzes, 5 randomized controlled trials, 10 propensity score-matched studies, 14 comparative studies and 42 observational studies. The reference list from each selected article was screened for additional relevant information. We excluded unpublished data from abstracts, contained in volumes from various congresses or conferences, as we excluded papers that were not in English (Tables 1 and 2).

INDICATIONS AND TYPES OF MIS FOR GOJ ADENOCARCINOMA

Laparo-thoracoscopic surgery

The indications of MIS in GOJ adenocarcinoma have evolved, initially starting from early cases, currently reaching the choice of the minimally invasive or open approach, for each case, considering the patient's preference, biological status, and the surgeon's experience and choice.

Endoscopic resection can be a good therapy for early GOJ adenocarcinoma[12]. When it cannot be applied or fails, the patient is proposed for a minimally invasive surgical resection procedure. In the literature, there are several comparative studies of the results of endoscopic resections and those of MIS. Chen *et al*[13], performed a propensity study to evaluate the survival of patients treated by the two types of approaches and found that no significant difference was observed in the 5-year cumulative incidence of cancer-specific death between the cohorts and that the type of treatment was not a prognostic factor [hazard ratio (HR) = 1.51, 95% confidence interval (95%CI): 0.81-2.81, P = 0.20) in multivariate Cox analysis. Similar results were reported by other authors: Overall survival (OS) rates at 5 years were not statistically significantly different (93.9% *vs* 97.3%)[14], in another study (93.3 *vs* 92.9%; P = 0.282)[15], concluding that endoscopic submucosal dissection (ESD) may be an effective alternative to surgery, for the treatment of early GOJ cancer.

In most cases, with advanced tumors, there is agreement that MIS competes with the open approach. The neoadjuvant treatment can increase the chances of success of MIS, especially in patients with partial or complete clinical response. MIS proves its safety, after neoadjuvant therapy and appears equivalent with the open approach, regarding the perioperative oncologic outcomes[16].

Robotic surgery

Robotic surgery has already found its place in minimally invasive methods. The advantages are multiple, from the improved 3-dimensional(3D) visualization, and the 7 degrees of movement of the working tools, to the comfort of the operating surgeon, accompanied by the reduction of the physiologic tremor of the hands. Robotic surgery has the greatest advantage in narrow spaces and for operations with a single field of interest.

Robot-assisted minimally invasive oesophageal surgery is the newest acquisition, in experienced centers being used with results equivalent to laparoscopic and thoracoscopic surgery[17]. However, the learning curve is long for this operation; therefore many cases are needed to obtain the maximum benefits of the method. A recent study found that to perform a minimally invasive oesophagectomy, with intrathoracic anastomosis, in optimal conditions, 119 cases would be needed, which makes this technique not at all easy to implement[18]. Regarding robotically assisted McKeown oesophagectomy, the number of cases required in the learning curve, to be able to operate in optimal conditions, is 70 [19]. The difference is given by the difficulty of performing intrathoracic anastomosis, which is shown to have a lower risk of fistula compared to cervical anastomosis, but with a more serious and disastrous outcome than that associated with the cervical one.

Studies between robot-assisted oesophagectomy and the classic procedure have shown clear benefits in favour of the minimally invasive approach, with a decrease in the number of days of hospitalization, blood loss, and a more complete lymphadenectomy[20]. However, when compared with laparoscopic/thoracoscopic surgery, regarding the number of resected nodes, the amount of blood loss, pulmonary complications or fistulas, and robotic esophagectomy proved to be similar, less in terms of operative time, which was longer in the last case[21].

Other studies have shown the benefits of robotic surgery *vs* laparoscopic surgery, in terms of lymphadenectomy, at the level of the laryngeal nerve group, with more lymph nodes harvested and fewer recurrent nerve paralyses[22,23].

Currently, robot-assisted Ivor Lewis oesophagectomy can be considered an alternative to laparoscopic/thoracoscopic surgery, with the mention that it is reserved for centers with a large number of cases, which already have experience in minimally invasive oesophageal surgery. Although most centers present robot-assisted oesophagectomy, with one stage of the operation performed laparoscopically, or through a thoracotomy, there are centers where the Ivor Lewis operation

Table 1 The search strategy summary

Items	Specification
Databases and other sources searched	PubMed Central (PMC), MEDLINE Complete (EBSCO)
Search terms used (including MeSH and free text search terms and filters)	Search strategy (see Table 2)
Timeframe	2013–2023
Inclusion and exclusion criteria (study type, language restrictions *etc.*)	Inclusion criteria: Meta-analyzes; trials studies; clinical trials & updates of clinical trials; reviews; original articles; only studies/papers/journals written in English Exclusion criteria: Unpublished data from abstracts contained in volumes from various congresses or conferences; papers that were not in English
Selection process (who conducted the selection, whether it was conducted independently, how consensus was obtained, *etc.*)	RB performed the search in the databases according to the presented criteria. If a study appears relevant by at least one reviewer - Bîrlă R and Constantin A - the full-text article has been retrieved and checked. The selection of full-text articles was made by two reviewers independently Constantin A and Bîrlă R. Assessing content validity required subjective judgment from the reviewers. The citation number was an important selection criterion. Differences were discussed and if consensus could not be reached between the two reviewers, we requested the consultation and recommendation of a third reviewer (Hoara P). The reference list from each selected article was screened for additional relevant information

Table 2 Systematic literature search for oesophagogastric junction adenocarcinoma and minimally invasive surgery

Search terms	Number of articles
1 Search: Oesophagogastric junction adenocarcinoma	2939
2 Search: (Oesophagogastric junction adenocarcinoma) AND (minimally invasive surgery)	429
3 Search: (Oesophagogastric junction adenocarcinoma) AND (minimally invasive surgery) Filters: English, from 2010-2023	230
4 Search: (Oesophagogastric junction adenocarcinoma) AND (minimally invasive surgery) Filters: English, from 2013-2023	195
Final number after review for inclusion and exclusion criteria and addition of articles from review of references[1]	126

[1]Exclusion criteria: No abstract available; non minimally invasive surgery; gastro-oesophageal junction adenocarcinoma not a major focus of article; not published in English; case reports without on minimally invasive surgery.

is performed exclusively with the robot, with very good results, on over 200 cases[24].

There are ongoing studies that try to demonstrate the superiority of robotic oesophagectomy over conventional MIS [25].

OESOPHAGO-GASTRIC RESECTION

For type I and II GOJ adenocarcinomas, there are different minimally invasive techniques, based on transthoracic or TH approaches, as in open surgery. Usually, the minimally invasive Ivor Lewis technique is the primary choice, although intrathoracic anastomosis is sometimes difficult. The operation starts with a laparoscopy, proximal gastrectomy and abdominal lymphadenectomy. Although pyloroplasty was indicated in open surgery, as a mandatory procedure, to improve gastric tube evacuation after vagotomy, in MIS, current studies do not show differences in terms of postoperative gastric evacuation, regardless of whether the pyloroplasty was performed[26].

The second phase right thoracoscopy, includes mobilization of the oesophagus and mediastinal lymph node dissection between the area from the carina to the azygos vein and down to the diaphragm. The oesophagus is divided at least 5 cm proximal to the cranial pole of the tumor, and the specimen is extracted; the gastric tube is pulled up into the thorax through the hiatus, to create an intrathoracic anastomosis. Methods of anastomosis include end-to-side anastomosis, manual or mechanical with a circular stapler[27], or side-to-side anastomosis with a linear stapler[28].

The minimally invasive McKeown procedure begins with a right thoracoscopy, with oesophageal and mediastinal lymph node dissection, which are similar to the previously described Ivor Lewis technique. Subsequently, the patient's position is changed to supine and then a laparoscopic small curvature resection and lymph node dissection are performed. The creation of the gastric tube is also similar to that described in the Ivor Lewis technique. After laparoscopy, a left cervical incision is made and the oesophagus is divided, the specimen is extracted in the abdomen and then outside and the gastric tube is pulled up through the mediastinum, in the cervical region where an end-to-side manually sutured anastomosis, with the proximal oesophagus, is performed[29].

The minimally invasive TH procedure consists of a laparoscopy and a left cervical incision, followed by a longitudinal gastrectomy with lymph nodes dissection and laparoscopic TH dissection of the distal oesophagus. The gastric tube is created extracorporeally and then pulled up in the cervical area, where the anastomosis is done[30].

Also, Ebihara *et al*[31] report considerable advantages, such as securing the proximal margin, intrathoracic oesophago-jejunostomy, and increased exposure in the operative field of the lower mediastinal area for GOJ Siewert type II, through minimally invasive abdominal and left thoracic approach.

For type III cancers, a laparoscopic TG is indicated. A TG with DII lymph node dissection is performed, the duodenum is closed using a linear stapler and a Roux-en-Y limb of the jejunum, is fashioned for the anastomosis with the oesophagus. The diaphragm is opened and the distal oesophagus is mobilized. Only the distal peri oesophageal lymph nodes are resected, and the oesophageal resection is limited. The jejunum is transected at 25 cm distal to the Treitz ligament, distal limb of the jejunum is lifted to prepare the oesophago-jejunostomy. Due to the limited size of the hiatus, the use of OrVil® (Medtronic, Inc., Minneapolis, MN, United States) facilitates the performance of the end-to-side oesophagus-jejunal anastomosis[32]. Finally, a side-to-side jejuno-jejunostomy is performed at 45-50 cm below the oesophago-jejunostomy.

Complete mesenteric resection - new concepts

A new concept, about the type of oesophagogastric resection, extrapolated from the complete resection of the mesorectum, is also configured in resections for GOJ tumors. Zhu *et al*[33], propose a study to evaluate the efficacy and safety of TH laparoscopic surgery of complete mesenteric resection (CME) in comparison with those of the traditional laparoscopic TH approach in the treatment of Siewert II/III GOJ adenocarcinoma, following the short term results. They found that intraoperative blood loss and hospitalization were significantly reduced ($P< 0.05$) in the CME-TH group (patients with CME through TH laparoscopic surgery) compared with those in the TH group (patients without CME through TH laparoscopic surgery), while significantly more lymph nodes were harvested ($P< 0.05$) in the CME-TH than in the TH group, with no significant differences in complications ($P> 0.05$) between two groups. It was concluded that the meso of the stomach and the lower oesophagus can be completely resected, together with the tumor, lymph nodes, adipose tissue and blood vessels blood as an "intact package" GOJ adenocarcinoma, leading to better short-term results.

In the same direction, Lorenzi *et al*[34] propose a minimally invasive technique of circumferential hiatal dissection for the distal oesophagus and GOJ adenocarcinoma in the context of hybrid Ivor Lewis oesophagogastrectomy (laparoscopic/thoracotomy) or minimally invasive procedure. The hiatus dissection included the surrounding peri-oesophageal tissues in a cylindrical fashion, maximizing the distance from the oesophageal wall. Bilateral crural muscle fibers and pleura, anterior pericardial fat, and posterior pre-aortic tissue were excised en bloc. The pathological findings were particularly focused on the involvement of the circumferential resection margin. The results obtained (R0 resection in 92.5%, and negative circumferential resection margin in 91% of patients with pT3 tumors) support the authors' conclusions that the adoption of this technique could reduce the incidence of involvement of the circumferential resection margin and improve the pathological results.

Proximal resection margin –additional procedures

Due to the propensity for intramural invasion of the proximal oesophagus, a clear proximal resection margin is crucial to minimize the rate of anastomotic recurrence, its length being a prognostic factor for survival in multivariate analyses[35]. A length of more than 2 cm of the proximal margin, in resected specimens has been recommended[36] but was difficult to assess because the surgeon cannot estimate the location of the tumor by tactile sense. In most studies, the method of determining the proximal section line of the oesophagus is not described.

Sugita *et al*[37] routinely used intraoperative endoscopy to visualize the tumor location and establish the proximal resection level. In addition, intraoperative pathological examination of frozen sections was performed in all cases or suspected cases[37,38]. Indeed, the combination of intraoperative endoscopy and frozen section analysis may be the perfect way to confirm negative resection margins, but these methods are not always available in all institutions. Therefore, it is essential to carefully assess preoperatively, the extent of oesophageal invasion by preoperative upper endoscopy, upper gastrointestinal barium swallow, and enhanced computed tomography.

Lymph node dissection - current controversies

The extent of lymphadenectomy for GOJ adenocarcinoma has been continuously the subject of discussion. The extent of lymphadenectomy associated with oesophagectomy should be adequate because the number of lymph nodes removed is an independent predictor of survival. To maximize the survival benefit, according to one report, a minimum of 23 regional lymph nodes should be removed[39].

Current German guidelines[40] specify that the standard of care should be a two-field lymph node dissection, both abdominal and mediastinal. In oesophageal cancer, standard two-field lymph node dissection involves :In the chest-posterior mediastinal lymph node dissection from the diaphragm up to the subcarinal nodes and aortopulmonary window; and in the abdomen - D2 Lymphadenectomy: Lymph nodes along the celiac trunk, common hepatic and splenic

arteries, along the lesser gastric curvature, in the lesser omentum. The extended dissection involves the lymph nodes included in the standard two-field lymphadenectomy (2FND)and the right paratracheal nodes along the right recurrent nerve and the brachiocephalic trunk.

Therefore, for oesophageal adenocarcinoma, the advantage of adding a third field during lymph node dissection is less clear; the survival benefit of three-field lymphadenectomy (3FND) applies only to patients with upper- and middle-third oesophageal cancer[41].

Giacopuzzi *et al*[42], in the study published in 2017, pointed out that in Siewert I tumors, the involvement of the middle and upper mediastinal nodes was 5%; for this reason, 3FND should be considered an overtreatment for patients with Siewert I tumors.

In a multicenter prospective study, Kurokawa *et al*[43] evaluated the distribution of lymph node metastases from GOJ tumors and the optimal extent of lymph node dissection in the abdominal and mediastinal fields. If the oesophageal invasion has exceeded 2.0 cm, excision of the lower mediastinal area, which includes the lower thoracic para oesophageal nodes (station 110) is strongly recommended; if oesophageal invasion exceeds 3.0 cm, excision of the upper and middle mediastinal lymph nodes (stations 106recR and 108) is poorly recommended; if the oesophageal involvement exceeds 4.0 cm, excision of the 44 upper mediastinal lymph nodes group (station 106recR) is strongly recommended.

The investigation of lymph node metastasis patterns, proposed by Li *et al*[44], led to the following results: The percentage of patients with positive celiac and lower mediastinal lymph nodes reached 58.3% (42/72) and 8.3%, respectively (6/72). The disease-free survival (DFS) and disease-specific survival of these 72 patients was 94% and 93.4% at 1 year after surgery and 59.8% and 62% at 3 years after surgery, respectively, suggesting the need for inferior mediastinal and celiac D2 Lymph node dissection, to improve oncologic outcome.

The rates of lymph node metastases, for both Siewert type II and type III tumors, were relatively low, but not neglectable, at lower mediastinal nodal stations, particularly station 110[45]. In addition, metastatic involvement in middle and upper mediastinal lymph nodes was significantly higher, when the length of oesophageal invasion was >3 cm [46]. Of note, mediastinal lymph node metastases can be an independent survival factor and are associated with distant metastases and poor survival outcomes[47].

Therefore, special attention should be paid to these nodal stations to anticipate better survival and dissection of stations 110 and 111 have been recommended in Japanese guidelines for tumors invading the oesophagus.

To easily and safely perform lymph node dissection around the lower oesophagus, at a higher level in the lower mediastinal space, it is crucial to ensure a sufficient view, with adequate space for manoeuvres. Even in the open technique, the complex topographical anatomy of the GOJ leads to a narrow and deep surgical field, as well as a rather limited surgical view, which often makes the surgeon unable to see and access the dissection area properly, if the assistant fails to help with a correct exposure. All of these can lead to the failure of a complete lymphadenectomy. In contrast, the laparoscopy can provide both the surgeon and the assistant with a better, magnified surgical view. In addition, fine vascular sealing devices allow for more meticulous dissection under a bloodless field. Sugita *et al*[37], Huang *et al*[48] and Junttila *et al*[49]reported that the number of harvested lymph nodes was significantly higher in the laparoscopic group, for Siewert type II tumors.

Sakaguchi *et al*[50] and Pang *et al*[51], reported a method of dissection of the lower mediastinal lymph nodes en bloc, through a laparoscopic TH approach, by sectioning the tendinous center of the diaphragm, with the excision of the perioesophageal tissue, harvesting an average of five lymph nodes, and observing the correlation of the length of tumor invasion of the oesophagus with the number of metastatic nodes.

To minimize perioperative complications, in the absence of metastatic nodal involvement proximal to the carina and for patients with Siewert type II adenocarcinoma, TH oesophagectomy should therefore be considered a valid surgical approach, transthoracic oesophagectomy should be considered a valid surgical tool in patients with distal oesophageal cancer or Siewert type I cancer, associated with limited metastatic lymph nodal involvement[41].

Antireflux anastomosis

A recent study proposes a semi-embedded valve anastomosis, associated with proximal gastrectomy, to improve postoperative reflux disease, as well as nutritional status, associated with TG[52].

Significant reductions in gastroesophageal reflux (60.7% *vs* 4.2%, $P < 0.001$], postoperative reflux oesophagitis, and improvement of the overall health status were reported by a study[53], comparing the use of an esophago-gastric anastomosis by lateral overlap with fundoplication, by Yamashita (SOFY), with antireflux function, associated with laparoscopic proximal gastrectomy and respectively Roux-en-Y esophago-jejunostomy for laparoscopic TG, in patients with Siewert II/III tumors.

Another study reported acceptable results, for the prevention of reflux oesophagitis, with a side-to-side oesophago-gastric anastomosis, using a linear stapler – the new technique of oesophagogastric tube reconstruction with lateral overlap, which can be performed either after laparoscopic proximal gastrectomy, or after minimally invasive Ivor Lewis oesophagectomy[54].

Lateral anastomosis has been considered a promising approach for creating an intrathoracic oesophago-gastrostomy in minimally invasive oesophagectomy. Manual suturing of the hole left at the level of the anastomosis is a technical challenge in thoracoscopic Ivor Lewis oesophagectomy. Wang *et al*[55] presented initial experience using autostatic suture (barbed suture), with promising short-term results.

Additional intraoperative procedures – indocyanine green fluorescence imaging

Parallel to the improvement of minimally invasive techniques, the development of intraoperative real-time imaging evaluation has brought an additional benefit, regarding the safety of the operative technique, with a direct impact on intraoperative morbidity and the improvement of postoperative results.

Tissue details that cannot be visualized under normal conditions can be highlighted by fluorescence techniques, following the administration of indocyanine green (ICG). The technique shows encouraging results, regarding the evaluation of lymphadenectomy, optimization of the dissection and viability of anastomotic partners[56].

Fistula risk improvement

A specific complication is the anastomotic fistula, which is responsible for decreasing the survival rate and increasing the risk of local recurrence[57]. An important risk factor is inadequate blood perfusion at the level of the anastomosis[58]. Usually, this aspect is evaluated subjectively, through the macroscopic inspection of the tissues, the bleeding at the level of the anastomotic organ's margins and the palpation of the pulse of the vascular pedicles. In the context of a minimally invasive technique, with the use of stapling devices, these manoeuvres are technically very limited. In this sense, different fluorescence imaging methods have been introduced, and among them, ICG angiography (ICG-FA), seems to bring the most benefits. Due to its fluorescent properties, it allows visualization of tissue perfusion in real-time. After endovenous administration, the dye quickly binds to plasma proteins, remaining in the vascular space. With the help of a near-infrared (NIR) light source, the surgeon can observe in detail the diffusion of the dye, at the tissue level. However, the evaluation by ICG-FA is still subjective. By visual assessment, a consensus regarding the quantification of tissue perfusion is not established[59], but an objective parameter can be determined, which is the perfusion speed of the dye in cm/S.

Some authors observed that, even though, fluorescence angiography using ICG, in the evaluation of the vascularization of the gastric stump shows specificity of over 94%, with a negative predictive value of almost 80%, the sensitivity is still below 22%, with a positive predictive value of almost 64%, which suggests that this method does not detect the risk of fistula, instead the measurement of the perfusion speed of the dye in the gastric tube can help to assess this risk[60,61]. Shimada *et al*[62], evaluating the usefulness of ICG-FA for reconstruction after esophagectomy, state that the technique is useful in evaluating the vascularization of the graft and helps to choose the correct site for the anastomosis. However, the rate of fistulas did not change. It can be speculated that the microvascularization highlighted by fluorescence, is not necessarily sufficient for a viable anastomosis. A recent meta-analysis confirms this result[63]. On the other hand, Campbell *et al*[64] reported a decrease in the fistula rate from 20% to 0%, after the introduction of ICG-FA. Koyanagi *et al* [65], confirm the improvement of results after the use of ICG.

Modulation of lymph node dissection and thoracic duct

Logically, the fluorescence evaluation was also taken into account for the intraoperative evaluation of the lymphatic network (node mapping). Several studies have presented encouraging data in this direction by injecting peritumoral ICG, aiming at a better highlight of the lymphatic network and an improvement in specific morbidity of lymphadenectomy[66-68]. Although strongly supported by theoretical foundations, the data provided by the literature in this direction are insufficient and inconclusive.

Although small, the risk of damage to the thoracic duct remains a reality, especially in obese patients[69]. The injection of ICG at the level of the mesentery or bilateral groin, offers the possibility of optimal highlighting of the thoracic duct, allowing its identification during dissection or its ligation in the event of a suspected injury[70].

Limit of oesophageal resection

Last but not least, the use of ICG fluorescence seems to be useful in establishing the resection limit, especially proximal, but also distal, in oncological surgery of the GOJ. The Gastroesophageal Junction Carcinoma Working Group in Japan established that for junctional tumors that invade the oesophagus less than 4 cm, the TH approach can be used[43].

However, the challenge arises from the exact establishment of the topography and the tumor boundary intraoperatively. In MIS, such as laparoscopic and robotic, locating the tumor during surgery is difficult, due to the lack of tactile sensation. Currently, ICG fluorescence imaging can be used for the exact localization of the GOJ tumor[71,72]. In this direction, Sagawa *et al*[73] use the Firefly mode of the da Vinci Xi system, through the capability of NIR visualization and simultaneous intraoperative upper gastrointestinal endoscopy, that precisely indicates the positioning and limits of the tumor injected with ICG.

In conclusion, the need to quantify the data provided by ICG-FA, to issue clear protocols, becomes imperative, and the data from the literature, due to their lack of homogeneity, does not yet provide a close perspective of such an objective. However, the potential of these techniques is obvious.

SHORT-TERM AND LONG-TERM RESULTS

Short-term outcomes

The development of minimally invasive techniques for resection of GOJ adenocarcinoma has the potential advantage of minimizing morbidity. The first randomized controlled trial was conducted in the Netherlands, enrolling 200 patients with the minimally invasive McKeown and Ivor Lewis approach. This clinical trial aimed to identify differences in morbidity, severity of complications and quality of life[74].

A 2017 multicenter study, evaluating short-term results after a minimally invasive Ivor Lewis approach, showed that the rate of anastomotic fistulas is still high (15.2%), possibly due to the technical diversity of anastomotic techniques and a high percentage of patients treated with neoadjuvant chemoradiotherapy (90, 2%); an aggressive approach of the complications (thoracotomy for decortications in 13 patients with empyema) have led to low mortality (2.1%), concluding that further improvements and standardization in anastomotic technique are needed to achieve a safe intrathoracic

anastomosis[75].

Other studies claim that, once the experience is gained in the minimally invasive approach, the results are excellent. In their review of over 1000 MISs, Luketich *et al*[76]reported an overall mortality of 1.7%, vocal cord paresis in 4% of the patients, and an anastomotic fistula rate of 5%. The average number of lymph nodes removed was 20, and 98% of patients obtained a negative histological margin. The average duration of hospitalization was 8 d, with 2 d in the intensive care unit. These numbers speak about what can be achieved, in the context of a dedicated program, with substantial experience and expertise in perfecting a new surgical approach.

There are a few randomized controlled trials, which have compared minimally invasive esophagectomy with open transthoracic esophagectomy. In the TIME trial, conventional thoraco-laparoscopic oesophagectomy was compared with the open approach[76], with a lower incidence of pulmonary infections reported in patients with MIS. In the MIRO trial, hybrid oesophagectomy was compared with transthoracic open oesophagectomy, with the hybrid approach being associated with a lower incidence of major complications[77]. In the MIOMIE trial[78], the hybrid approach was compared with the open approach, with equal results being reported, in terms of morbidity and mortality.

Additional studies found no significant difference in oesophagectomy-related morbidity (anastomotic fistula, anastomotic stricture rate, gastric tube ischemia, chylothorax, vocal cord paralysis) and reduced use of narcotics, due to less postoperative pain. The pain score in the laparoscopic group decreased faster, making it evident that the small wounds generated less stress and pain, which justified the faster recovery[76,79-82]. Similar results have been reported in meta-analysis[83,84], systematic review[85,86], propensity analysis[87], or clinical trials[88-92] comparing MIE with open and hybrid resections.

Zhang *et al*[93] presented in a study the comparative results of open *vs* laparoscopically assisted TH approach and observed that the rate of pleural perforation, requiring the prolonged use of mechanical ventilation, for more than 12 h, was lower in the laparoscopic group, but this lesion, in laparoscopic surgery, may affect the recovery of lung function, possibly due to tension pneumothorax.

Dantoc *et al*[94]studied the oncological outcomes of patients who underwent minimally invasive oesophagectomy. He analyzed 1586 patients (in 17 studies) in which the minimally invasive approach was compared with the open approach: The number of lymph nodes removed was significantly higher in the minimally invasive approach (median of 16 nodes compared to 10 nodes harvested in open oesophagectomies, $P = 0.03$). Similar results were reported after hand-assisted laparoscopic surgery[95], or in other studies that used the minimally invasive approach[48,96].

Other authors conclude that for patients with Siewert type II adenocarcinoma, modified Ivor Lewis surgery, thoraco-laparoscopic oesophago-gastrectomy, 2FND, and intrathoracic anastomosis, is safe and feasible[97].

The use of MIS, in patients with neoadjuvant treatment, did not lead to different short-term results, compared to those of patients with primary surgery. Compared to the group with open surgery, it was found that MIS patients had shorter median intensive care unit time ($P = 0.002$) and hospital lengths of stay ($p< 0.0001$), but the incidence of postoperative complications (open: 54.8% *vs* MIS: 41.1%,$P = 0.155$), mortality at 30 d(open: 2.7% *vs* MIS: 0%,$P = 0.506$) and anastomotic leak rates (open: 1.4% *vs* MIS: 0%, $P = 1.00$) were similar. However, the respiratory complications were significantly reduced after MIS (8.9%) compared with open (29.7%; $P = 0.004$)[98].

Long-term results

Data on long-term survival are limited but encouraging. Several studies compared long-term surgical and oncological outcomes after laparoscopic and open gastrectomy, for GOJ adenocarcinoma, reporting similar 5-year OS and DFS survival rates (44.6% *vs* 42.1%, $P = 0.403$; 40.1% *vs* 37.6%, $P = 0.321$, respectively)[99]. Similar results were reported in another study, after minimally invasive or open esophagectomy, for 5-year OS (12.5%in MIS *vs* 16%in open approach) and DFS (67% in MIS *vs* 16%–57% in open approach, $P = 0.33$)[96]. Other studies found longer but not significantly different 5-year OS and DFS rates between patients in the laparoscopic group *vs* open group, in patients with Stage III disease (HR= 0.42, (95%CI: 0.05-3.47) *vs* HR= 0.47, (95%CI: 0.10-2.12))[100], or a median survival for the laparoscopic approach of 56 mo and 47 mo, respectively, with 5-year OS of 40% and 29.1%, respectively[83].

Another study identified a significantly different five-year survival in oesophagectomy patients (64%-MIS *vs* 35%-open approach, $P< 0.001$), and multivariate analysis demonstrated that patients with an open approach had significantly poorer survival, compared with the minimally invasive procedure, independent of age, rate of excised lymph nodes, radiochemotherapy and pathologic stage (HR=2.00, $P = 0.019$)[101].

Two studies used propensity score matching analysis to adjust for selection bias, leading to more reliable comparisons between laparoscopic and open approaches[83,101]. In the stratified analysis, a better survival was observed in the laparoscopic group for Siewert type II, which may be due to a more thorough lymph node dissection around the lower oesophagus, and a significantly longer median DFS and better OS than the open approach, for types Siewert II/III[83].

The rate and pattern of recurrence did not differ between the two groups, during the follow-up phase[102,103]. Another study reports that, in terms of recurrence, the most common site was the peritoneum[38].

In a comparative study of neoadjuvant *vs* adjuvant therapy, with a median follow-up period of 37.5 mo, a pathological complete responserate of 26% was reported in the neoadjuvant chemoradiotherapy group and a greater rate of R0 resection than in the adjuvant group (95 % *vs* 76%; $P = 0.002$) The multivariable analysis of OS showed lower hazards of death independently associated with neoadjuvant *vs* adjuvant therapy (HR= 0.57; 95%CI: 0.36-0.91; $P = 0.0200$)[104].

Another study showed that preoperative radiochemotherapy determined improvement in R0 resection rate, compared to surgery and preoperative chemotherapy, but there is no significant difference in OS. Both neoadjuvant strategies remain clinically meaningful options for patients with resectable gastroesophageal junction tumors[105,106].

Some authors think that surgical treatment could also be used in tumors with small-volume metastatic disease. A clinical trial evaluated the feasibility and effectiveness of using induction chemotherapy with fluorouracil, leucovorin, oxaliplatin and docetaxelfollowed by surgical resection, with curative intent, for patients with oligometastatic GOJ cancer.

Rigorous criteria were used to include cases, in the group of patients with surgical treatment after 4 chemotherapy sessions. The results showed better survival for patients with surgical resection (gastrectomy and metastasectomy), the OS is 31.3 mo, compared to 9-11 mo for non-operated patients[107].

In patients with neoadjuvant treatment, the long-term results are similar regardless of the approach, OS rates at 5 years (open: 61% *vs* MIS: 50%, $P = 0.933$); MIS was not a significant predictor of OS (HR=1.07; 95%CI: 0.61-1.87; $P = 0.810$)[98].

QUALITY OF LIFE

The surgery of GOJ cancer, due to its amplitude, has a major impact on the quality of life. The specific element, around which the quality of life revolves, is postoperative reflux, with all its consequences. Oesophago-gastrostomy is the traditional and most widespread reconstruction method after proximal gastrectomy with distal oesophagectomy, the accepted technique in the oncological approach to GOJ tumors[103]. The main deficiency of the technique could be the high incidence of reflux oesophagitis, which varies between 9.1% and 35.3%[108,109].

The increased incidence is due to surgical resection, which alters the anatomy of the digestive tube, leading to disruption of anti-reflux mechanisms. In addition, the absence of the gastrointestinal pacemaker and the section of the vagus nerve leads to the impairment of gastric motility, with a direct impact on gastric emptying[110]. Studies have documented that reflux can wake patients from sleep, while sleep disturbances can worsen reflux symptoms, creating a true vicious circle[111]. Long-term sleep disturbances can impair cognitive function and severely impact the quality of life [112].

The long-term postoperative impact is mainly due to the mediastinal adhesion syndrome, with pulmonary involvement, but also in connection with reflux symptoms. Thus, dyspnea, even two years after surgery, seems to be due to pulmonary adhesions, secondary to the thoracic phase of the Ivor Lewis technique. On the other hand, it is known that gastric acidity, even after vagal denervation, normalizes over time. More than three years after surgery, the 24-hour gastric pH metry in most patients is similar to that of healthy subjects[113]. This phenomenon is associated with an increasing incidence of reflux oesophagitis, metaplasia and the need for effective anti-reflux treatment. Some reports indicate that the choice between gastrectomy, oesophagectomy or oeso-gastrectomy, does not have a significant influence on the quality of life, for patients with GOJ adenocarcinoma, six months after surgery[114]. Other studies document higher quality of life parameters, after minimally invasive oesophagectomy than after minimally invasive gastrectomy. Moreover, after thoracoscopic oesophagectomy, it seems to be close to that of the general population[115]. In addition, a meta-analysis of nine studies showed that patients, who underwent minimally invasive transthoracic oesophagectomy, had superior parameters than patients who underwent open transthoracic oesophagectomy, regarding general condition, fatigue, pain, and quality of life[116]. It should be mentioned that these differences were no longer present 6 mo and 1 year after the operation. In this meta-analysis, however, no difference was made between hybrid oesophagectomy or minimally invasive total oesophagectomy, nor between Ivor Lewis, McKeown or Orringer oesophagectomy. In a recent Swedish national study, quality of life was not statistically different at 1 year and 2 years after minimally invasive total esophagectomy, hybrid esophagectomy, and open esophagectomy[117]. Because the robotic technique is relatively new, there are no studies on long-term results using this technique. A recent study reports significant benefit in terms of quality of life 4 mo postoperatively after the robotically assisted Ivor Lewis technique compared with open esophagectomy[118]. Sarkaria *et al*[119] compared early postoperative quality of life after robotic oesophagectomy and open transthoracic oesophagectomy and reported significantly superior outcomes for the robotic technique. However, they included both the Ivor Lewis and McKeown techniques and reported results only for a four-month follow-up, during which 20% of patients were lost.

The search for technical artifices, to restore the continuity of the digestive tract, after proximal gastrectomy with distal oesophagectomy, and improve postoperative reflux is thus a justifiable objective. In the Japanese Gastric Cancer Treatment Guidelines, in addition to the traditional oesophagus-gastro anastomosis, double tract reconstruction is specified as a possible technical alternative[120].

For double tract reconstruction, the jejunum is transected 25 cm distal to the Treitz ligament, distal limb of the jejunum is lifted to prepare the oesophago-jejunostomy. An end-to-side oesophago-jejunostomy is performed with a circular stapler, and the jejunal stump is closed with a linear stapler. Next, a side-to-side gastro-jejunostomy is performed 15 cm below the oesophago-jejunostomy. Finally, a side-to-side jejuno-jejunostomy is performed 15-20 cm below the gastro-jejunostomy[121].

Some studies have reported that this procedure could reduce the incidence of reflux oesophagitis after proximal gastrectomy[122]. A comparative study documents an incidence of reflux oesophagitis of 30.8% in the group with oesophago-gastrostomy and 8.0% for double tract reconstruction. Patients in the group with double tract reconstruction complained less often of dysphagia, pain, reflux, loss of appetite, anxiety, dry mouth and unpleasant taste than those with oesophago-gastrostomy[121]. However, the technique requires additional studies to confirm the advantages.

Another technique that aims to improve postoperative reported reflux is super MIS, through ESD and endoscopic submucosal tunnel dissection which, for the early stages, are equally effective from a curative point of view, with the advantage of avoiding major anatomical changes, secondary to classic surgery[123]. The quality of life is greatly improved, especially regarding reflux and sleep quality. It is believed that this is the result of the less aggressive surgical approach, in that the endoscope does not damage the integrity of the gastrointestinal tract, with relatively few changes in digestive physiology. Moreover, the proportion of patients with postoperative acid reflux, in the group treated by super MIS, is lower than that reported in the healthy group[124]. This may be due to scar contraction after endoscopic manoeuvres, with increased lower oesophageal sphincter pressure[125]. This technique requires confirmation through

additional studies and is indicated in the early stages of the disease.

FUTURE PERSPECTIVES

In recent years, with the improvement of technology, MIS technology has developed rapidly. MIS has wide prospects for use in GOJ adenocarcinoma and its application is the current trend.

Today, MIS uses high-definition 3D imaging systems and 2-dimensional imaging systems with 4K ultra-high-definition cameras. Shortly, this high-definition technology will be available in every dedicated operating room and will help surgeons perform these complex surgical procedures safely.

Although robot-assisted minimally invasive oesophagectomy is indeed attractive to many surgeons, its high cost still limits the use of this technology. As more companies develop robot-assisted surgical systems, in competition with the da Vinci systems, further technical development of less expensive robotic surgical systems is expected shortly.

The role of sentinel node biopsy in the surgical treatment of GOJ adenocarcinoma is still debated. The application of the sentinel node concept could limit the extension of the node dissection, avoiding all associated complications. Undoubtedly, this surgical strategy should be applied only to patients with cT1N0. Shortly, sentinel node mapping and nodal navigation surgery could be considered a promising and interesting tool for early-stage oesophageal cancer, identifying patients who could be treated with individualized, less invasive surgery. However, such complex surgery will be concentrated in high-volume centers and performed by dedicated surgeons, to minimize postoperative complications and improve oncological outcomes.

CONCLUSION

Surgery is still the most important method in the comprehensive treatment of GOJ adenocarcinoma. There is a strong worldwide trend towards MIS, endoscopic methods being used for superficial cancers and robotic and laparo-thoracoscopic methods for early tumors, or locally advanced tumors after neoadjuvant therapy.

The preferred MIS of GOJ tumors is oesophagectomy for Siewert type I tumors and gastrectomy for Siewert type III tumors. Most surgeons favor an extended gastrectomy for Siewert type II tumors. Although pyloroplasty was usually performed in open surgery, in the current MIS, most surgeons have given up on it. The clearly improved visualization and the possibility of fine dissection in narrow spaces, offered by MIS gives the possibility of a much more rigorous lymph node dissection compared with open surgery. Many methods can be adopted for anastomosis, such as manual, circular stapler, linear stapler, and even robot-assisted anastomosis, with comparable results in terms of fistula rate. The use of ICG-FA as an adjunct method for lymph node dissection, or for intraoperative visualization of the vascularization of the gastric tube, is proven to bring important improvement in the performance of the method.

Minimally invasive oesophagectomy may improve short-term results with fewer complications, compared to traditional open oesophagectomy. Most authors note, along with the indisputable benefits of the patient with a minimally invasive approach (quick recovery, reduced need for analgesics, decreased length of hospitalization, *etc.*), the decrease in the incidence of pulmonary complications, and with regard to the rate of anastomotic fistulas, its decrease is especially noticeable when intraoperative ICG-FA was used. In the long term, in advanced cases, the results are similar regardless of the type of approach; some studies, however, note better long-term results in patients with a minimally invasive approach. Also, the quality of life is better after the minimally invasive approach, and with regard to the appearance of reflux symptoms, a lower incidence is noted after the use of double tract reconstruction.

However, there is still no consensus on the ideal type of MIS for GOJ adenocarcinoma. Large randomized controlled trials are still needed to test which minimally invasive technique is best for this tumor.

FOOTNOTES

Author contributions: Birla R and Constantin A designed the article framework; Birla R, Constantin A and Hoara P drafted the manuscript; Achim F, Dinca VG, Ciuc D, and Constantinoiu S critically revised the essential intellectual content of the manuscript; all authors have read and approved the final manuscript.

Conflict-of-interest statement: There is no conflict of interest.

Country/Territory of origin: Romania

ORCID number: Rodica Bîrlă 0000-0002-8799-4524; Petre Hoara 0000-0002-9250-0613; Florin Achim 0000-0003-0095-494X; Valeriu Dinca 0000-0002-1924-4748; Silviu Constantinoiu 0000-0002-3058-5981; Adrian Constantin 0000-0002-9962-2154.

S-Editor: Lin C
L-Editor: A
P-Editor: Zhao S

REFERENCES

1 **Sung H**, Ferlay J, Siegel RL, Laversanne M, Soerjomataram I, Jemal A, Bray F. Global Cancer Statistics 2020: GLOBOCAN Estimates of Incidence and Mortality Worldwide for 36 Cancers in 185 Countries. *CA Cancer J Clin* 2021; **71**: 209-249 [PMID: 33538338 DOI: 10.3322/caac.21660]
2 **Siewert JR**, Hölscher AH, Becker K, Gössner W. [Cardia cancer: attempt at a therapeutically relevant classification]. *Chirurg* 1987; **58**: 25-32 [PMID: 3829805]
3 **Stein HJ**, Feith M, Siewert JR. Individualized surgical strategies for cancer of the esophagogastric junction. *Ann Chir Gynaecol* 2000; **89**: 191-198 [PMID: 11079787]
4 **Cuschieri A**. Endoscopic subtotal oesophagectomy for cancer using the right thoracoscopic approach. *Surg Oncol* 1993; **2** Suppl 1: 3-11 [PMID: 8252219 DOI: 10.1016/0960-7404(93)90052-z]
5 **Kitano S**, Iso Y, Moriyama M, Sugimachi K. Laparoscopy-assisted Billroth I gastrectomy. *Surg Laparosc Endosc* 1994; **4**: 146-148 [PMID: 8180768]
6 **Spector R**, Zheng Y, Yeap BY, Wee JO, Lebenthal A, Swanson SJ, Marchosky DE, Enzinger PC, Mamon HJ, Lerut A, Odze R, Srivastava A, Agoston AT, Tippayawang M, Bueno R; Brigham Esophageal Study Team. The 3-Hole Minimally Invasive Esophagectomy: A Safe Procedure Following Neoadjuvant Chemotherapy and Radiation. *Semin Thorac Cardiovasc Surg* 2015; **27**: 205-215 [PMID: 26686448 DOI: 10.1053/j.semtcvs.2015.06.003]
7 **Kim T**, Hochwald SN, Sarosi GA, Caban AM, Rossidis G, Ben-David K. Review of minimally invasive esophagectomy and current controversies. *Gastroenterol Res Pract* 2012; **2012**: 683213 [PMID: 22919374 DOI: 10.1155/2012/683213]
8 **Haverkamp L**, Seesing MF, Ruurda JP, Boone J, V Hillegersberg R. Worldwide trends in surgical techniques in the treatment of esophageal and gastroesophageal junction cancer. *Dis Esophagus* 2017; **30**: 1-7 [PMID: 27001442 DOI: 10.1111/dote.12480]
9 **Santin BJ**, Price P. Laparoscopic transhiatal esophagectomy at a low-volume center. *JSLS* 2011; **15**: 41-46 [PMID: 21902941 DOI: 10.4293/108680811X13022985131138]
10 **Tapias LF**, Morse CR. Minimally invasive Ivor Lewis esophagectomy: description of a learning curve. *J Am Coll Surg* 2014; **218**: 1130-1140 [PMID: 24698488 DOI: 10.1016/j.jamcollsurg.2014.02.014]
11 **Di Maggio F**, Lee AR, Deere H, Vrakopoulou GZ, Botha AJ. Minimally invasive total adventitial resection of the cardia for tumours of the oesophagogastric junction. *Langenbecks Arch Surg* 2021; **406**: 2273-2285 [PMID: 33904977 DOI: 10.1007/s00423-021-02174-0]
12 **Zhang S**, Orita H, Fukunaga T. Current surgical treatment of esophagogastric junction adenocarcinoma. *World J Gastrointest Oncol* 2019; **11**: 567-578 [PMID: 31435459 DOI: 10.4251/wjgo.v11.i8.567]
13 **Chen H**, Yu X, Yang R, Li S, Zhang G, Si X, Zhou X. The Long-Term Outcomes of Surgery Versus Endoscopic Treatment in Patients With Siewert Type II T1M0N0 Adenocarcinoma of the Esophagogastric Junction. *Cancer Control* 2022; **29**: 10732748221143389 [PMID: 36523149 DOI: 10.1177/10732748221143389]
14 **Gong EJ**, Kim DH, Ahn JY, Jung KW, Lee JH, Choi KD, Song HJ, Lee GH, Jung HY, Kim HS, Lee IS, Kim BS, Yoo MW, Oh ST, Yook JH. Comparison of long-term outcomes of endoscopic submucosal dissection and surgery for esophagogastric junction adenocarcinoma. *Gastric Cancer* 2017; **20**: 84-91 [PMID: 27995482 DOI: 10.1007/s10120-016-0679-0]
15 **Kim HJ**, Chung H, Shin SK, Kim HI, Park JC, Lee SK, Hyung WJ, Lee YC, Noh SH. Comparison of long-term clinical outcomes between endoscopic and surgical resection for early-stage adenocarcinoma of the esophagogastric junction. *Surg Endosc* 2018; **32**: 3540-3547 [PMID: 29417228 DOI: 10.1007/s00464-018-6076-5]
16 **Kurtom S**, Kaplan BJ. Esophagus and Gastrointestinal Junction Tumors. *Surg Clin North Am* 2020; **100**: 507-521 [PMID: 32402297 DOI: 10.1016/j.suc.2020.02.003]
17 **Ackerman JM**, Luketich JD, Sarkaria IS. Robotic Ivor Lewis esophagectomy. *Mini-invasive Surg* 2021; **5**: 14 [DOI: 10.20517/2574-1225.2021.02]
18 **van Workum F**, Stenstra MHBC, Berkelmans GHK, Slaman AE, van Berge Henegouwen MI, Gisbertz SS, van den Wildenberg FJH, Polat F, Irino T, Nilsson M, Nieuwenhuijzen GAP, Luyer MD, Adang EM, Hannink G, Rovers MM, Rosman C. Learning Curve and Associated Morbidity of Minimally Invasive Esophagectomy: A Retrospective Multicenter Study. *Ann Surg* 2019; **269**: 88-94 [PMID: 28857809 DOI: 10.1097/SLA.0000000000002469]
19 **van der Sluis PC**, Ruurda JP, van der Horst S, Goense L, van Hillegersberg R. Learning Curve for Robot-Assisted Minimally Invasive Thoracoscopic Esophagectomy: Results From 312 Cases. *Ann Thorac Surg* 2018; **106**: 264-271 [PMID: 29454718 DOI: 10.1016/j.athoracsur.2018.01.038]
20 **van der Sluis PC**, van der Horst S, May AM, Schippers C, Brosens LAA, Joore HCA, Kroese CC, Haj Mohammad N, Mook S, Vleggaar FP, Borel Rinkes IHM, Ruurda JP, van Hillegersberg R. Robot-assisted Minimally Invasive Thoracolaparoscopic Esophagectomy Versus Open Transthoracic Esophagectomy for Resectable Esophageal Cancer: A Randomized Controlled Trial. *Ann Surg* 2019; **269**: 621-630 [PMID: 30308612 DOI: 10.1097/SLA.0000000000003031]
21 **Zhang Y**, Han Y, Gan Q, Xiang J, Jin R, Chen K, Che J, Hang J, Li H. Early Outcomes of Robot-Assisted Versus Thoracoscopic-Assisted Ivor Lewis Esophagectomy for Esophageal Cancer: A Propensity Score-Matched Study. *Ann Surg Oncol* 2019; **26**: 1284-1291 [PMID: 30843161 DOI: 10.1245/s10434-019-07273-3]
22 **Park S**, Hwang Y, Lee HJ, Park IK, Kim YT, Kang CH. Comparison of robot-assisted esophagectomy and thoracoscopic esophagectomy in esophageal squamous cell carcinoma. *J Thorac Dis* 2016; **8**: 2853-2861 [PMID: 27867561 DOI: 10.21037/jtd.2016.10.39]
23 **Jin D**, Yao L, Yu J, Liu R, Guo T, Yang K, Gou Y. Robotic-assisted minimally invasive esophagectomy versus the conventional minimally invasive one: A meta-analysis and systematic review. *Int J Med Robot* 2019; **15**: e1988 [PMID: 30737881 DOI: 10.1002/rcs.1988]
24 **Kang CH**. Totally Robotic Esophagectomy. *J Chest Surg* 2021; **54**: 302-309 [PMID: 34353971 DOI: 10.5090/jcs.21.069]
25 **Tagkalos E**, van der Sluis PC, Berlth F, Poplawski A, Hadzijusufovic E, Lang H, van Berge Henegouwen MI, Gisbertz SS, Müller-Stich BP,

Ruurda JP, Schiesser M, Schneider PM, van Hillegersberg R, Grimminger PP. Robot-assisted minimally invasive thoraco-laparoscopic esophagectomy versus minimally invasive esophagectomy for resectable esophageal adenocarcinoma, a randomized controlled trial (ROBOT-2 trial). *BMC Cancer* 2021; **21**: 1060 [PMID: 34565343 DOI: 10.1186/s12885-021-08780-x]

26 **De Pasqual CA**, Weindelmayer J, Gobbi L, Alberti L, Veltri A, Giacopuzzi S, de Manzoni G. Effect of Pyloroplasty on Gastric Conduit Emptying and Patients' Quality of Life After Ivor Lewis Esophagectomy. *J Laparoendosc Adv Surg Tech A* 2021; **31**: 692-697 [PMID: 32898448 DOI: 10.1089/lap.2020.0595]

27 **Wiesel O**, Whang B, Cohen D, Fisichella PM. Minimally Invasive Esophagectomy for Adenocarcinomas of the Gastroesophageal Junction and Distal Esophagus: Notes on Technique. *J Laparoendosc Adv Surg Tech A* 2017; **27**: 162-169 [PMID: 27858584 DOI: 10.1089/lap.2016.0430]

28 **Irino T**, Tsai JA, Ericson J, Nilsson M, Lundell L, Rouvelas I. Thoracoscopic side-to-side esophagogastrostomy by use of linear stapler-a simplified technique facilitating a minimally invasive Ivor-Lewis operation. *Langenbecks Arch Surg* 2016; **401**: 315-322 [PMID: 26960591 DOI: 10.1007/s00423-016-1396-1]

29 **Luketich JD**, Alvelo-Rivera M, Buenaventura PO, Christie NA, McCaughan JS, Litle VR, Schauer PR, Close JM, Fernando HC. Minimally invasive esophagectomy: outcomes in 222 patients. *Ann Surg* 2003; **238**: 486-94; discussion 494 [PMID: 14530720 DOI: 10.1097/01.sla.0000089858.40725.68]

30 **Parry K**, Haverkamp L, Bruijnen RC, Siersema PD, Ruurda JP, van Hillegersberg R. Surgical treatment of adenocarcinomas of the gastro-esophageal junction. *Ann Surg Oncol* 2015; **22**: 597-603 [PMID: 25190126 DOI: 10.1245/s10434-014-4047-1]

31 **Ebihara Y**, Kurashima Y, Murakami S, Shichinohe T, Hirano S. Minimally invasive abdominal and left thoracic approach for Siewert type II adenocarcinoma of the oesophagogastric junction: Novel technique for simultaneous combined use of laparoscopy and thoracoscopy. *J Minim Access Surg* 2020; **16**: 285-288 [PMID: 30178772 DOI: 10.4103/jmas.JMAS_228_17]

32 **Ai B**, Zhang Z, Liao Y. Laparoscopic and thoracoscopic esophagectomy with intrathoracic anastomosis for middle or lower esophageal carcinoma. *J Thorac Dis* 2014; **6**: 1354-1357 [PMID: 25276383 DOI: 10.3978/j.issn.2072-1439.2014.07.38]

33 **Zhu TY**, Deng XM, Wang GJ, Gao BL, Li RX, Wang JT. Comparison of short-term surgical outcomes between complete mesenteric resection and traditional transhiatal laparoscopic surgery for Siewert type II/III esophagogastric junction adenocarcinoma. *Langenbecks Arch Surg* 2022; **407**: 3811-3818 [PMID: 36214868 DOI: 10.1007/s00423-022-02676-5]

34 **Lorenzi B**, Davakis S, Syllaios A, Kordzadeh A, Kadri M, Ram M, Fareed K, Barter C, Charalabopoulos A. Minimally Invasive Circumferential Hiatal Dissection for the Treatment of Adenocarcinoma of the Distal Esophagus and Esophago-gastric Junction: Technical Considerations Combined With Histopathological Outcomes. *Anticancer Res* 2019; **39**: 3219-3225 [PMID: 31177171 DOI: 10.21873/anticanres.13462]

35 **Mine S**, Sano T, Hiki N, Yamada K, Kosuga T, Nunobe S, Yamaguchi T. Proximal margin length with transhiatal gastrectomy for Siewert type II and III adenocarcinomas of the oesophagogastric junction. *Br J Surg* 2013; **100**: 1050-1054 [PMID: 23754647 DOI: 10.1002/bjs.9170]

36 **Niclauss N**, Jung MK, Chevallay M, Mönig SP. Minimal length of proximal resection margin in adenocarcinoma of the esophagogastric junction: a systematic review of the literature. *Updates Surg* 2019; **71**: 401-409 [PMID: 31243725 DOI: 10.1007/s13304-019-00665-w]

37 **Sugita S**, Kinoshita T, Kaito A, Watanabe M, Sunagawa H. Short-term outcomes after laparoscopic versus open transhiatal resection of Siewert type II adenocarcinoma of the esophagogastric junction. *Surg Endosc* 2018; **32**: 383-390 [PMID: 28656339 DOI: 10.1007/s00464-017-5687-6]

38 **Lee Y**, Min SH, Park KB, Park YS, Ahn SH, Park DJ, Kim HH. Long-term Outcomes of Laparoscopic Versus Open Transhiatal Approach for the Treatment of Esophagogastric Junction Cancer. *J Gastric Cancer* 2019; **19**: 62-71 [PMID: 30944759 DOI: 10.5230/jgc.2019.19.e1]

39 **Chevallay M**, Bollschweiler E, Chandramohan SM, Schmidt T, Koch O, Demanzoni G, Mönig S, Allum W. Cancer of the gastroesophageal junction: a diagnosis, classification, and management review. *Ann N Y Acad Sci* 2018; **1434**: 132-138 [PMID: 30138540 DOI: 10.1111/nyas.13954]

40 **Hölscher AH**, Stahl M, Messmann H, Stuschke M, Meyer HJ, Porschen R. [New S3 guideline for esophageal cancer : Important surgical aspects]. *Chirurg* 2016; **87**: 865-872 [PMID: 27406251 DOI: 10.1007/s00104-016-0214-1]

41 **Vagliasindi A**, Franco FD, Degiuli M, Papis D, Migliore M. Extension of lymph node dissection in the surgical treatment of esophageal and gastroesophageal junction cancer: seven questions and answers. *Future Oncol* 2023; **19**: 327-339 [PMID: 36942741 DOI: 10.2217/fon-2021-0545]

42 **Giacopuzzi S**, Bencivenga M, Weindelmayer J, Verlato G, de Manzoni G. Western strategy for EGJ carcinoma. *Gastric Cancer* 2017; **20**: 60-68 [PMID: 28039533 DOI: 10.1007/s10120-016-0685-2]

43 **Kurokawa Y**, Takeuchi H, Doki Y, Mine S, Terashima M, Yasuda T, Yoshida K, Daiko H, Sakuramoto S, Yoshikawa T, Kunisaki C, Seto Y, Tamura S, Shimokawa T, Sano T, Kitagawa Y. Mapping of Lymph Node Metastasis From Esophagogastric Junction Tumors: A Prospective Nationwide Multicenter Study. *Ann Surg* 2021; **274**: 120-127 [PMID: 31404008 DOI: 10.1097/SLA.0000000000003499]

44 **Li KK**, Bao T, Wang YJ, Liu XH, Guo W. The Postoperative outcomes of thoracoscopic-laparoscopic Ivor-Lewis surgery plus D2 celiac lymphadenectomy for patients with adenocarcinoma of the esophagogastric junction. *Surg Endosc* 2020; **34**: 4957-4966 [PMID: 31823049 DOI: 10.1007/s00464-019-07288-7]

45 **Chen XD**, He FQ, Chen M, Zhao FZ. Incidence of lymph node metastasis at each station in Siewert types II/III adenocarcinoma of the esophagogastric junction: A systematic review and meta-analysis. *Surg Oncol* 2020; **35**: 62-70 [PMID: 32835903 DOI: 10.1016/j.suronc.2020.08.001]

46 **Kurokawa Y**, Hiki N, Yoshikawa T, Kishi K, Ito Y, Ohi M, Wada N, Takiguchi S, Mine S, Hasegawa S, Matsuda T, Takeuchi H. Mediastinal lymph node metastasis and recurrence in adenocarcinoma of the esophagogastric junction. *Surgery* 2015; **157**: 551-555 [PMID: 25532434 DOI: 10.1016/j.surg.2014.08.099]

47 **Nakamura M**, Iwahashi M, Nakamori M, Naka T, Ojima T, Iida T, Katsuda M, Tsuji T, Hayata K, Mastumura S, Yamaue H. Lower mediastinal lymph node metastasis is an independent survival factor of Siewert type II and III adenocarcinomas in the gastroesophageal junction. *Am Surg* 2012; **78**: 567-573 [PMID: 22546130]

48 **Huang CM**, Lv CB, Lin JX, Chen QY, Zheng CH, Li P, Xie JW, Wang JB, Lu J, Cao LL, Lin M, Tu RH. Laparoscopic-assisted versus open total gastrectomy for Siewert type II and III esophagogastric junction carcinoma: a propensity score-matched case-control study. *Surg Endosc* 2017; **31**: 3495-3503 [PMID: 27981384 DOI: 10.1007/s00464-016-5375-y]

49 **Junttila A**, Helminen O, Kairaluoma V, Mattila A, Sihvo E, Mrena J. Implementation of Multimodality Therapy and Minimally Invasive Surgery: Short- and Long-term Outcomes of Gastric Cancer Surgery in Medium-Volume Center. *J Gastrointest Surg* 2022; **26**: 2061-2069 [PMID: 36002787 DOI: 10.1007/s11605-022-05437-3]

50 **Sakaguchi M**, Hosogi H, Kanaya S. Laparoscopic en bloc lower mediastinal lymph node dissection *via* transhiatal approach for

adenocarcinoma of esophagogastric junction. *Surg Oncol* 2021; **36**: 34-35 [PMID: 33285434 DOI: 10.1016/j.suronc.2020.11.010]

51 **Pang W**, Liu G, Zhang Y, Huang Y, Yuan X, Zhao Z, Zhang C. Total laparoscopic transabdominal-transdiaphragmatic approach for treating Siewert II tumors: a prospective analysis of a case series. *World J Surg Oncol* 2021; **19**: 26 [PMID: 33485350 DOI: 10.1186/s12957-021-02136-2]

52 **Wu Y**, Zhang S, Wang L, Hu X, Zhang Z. Comparative analysis of laparoscopic proximal gastrectomy plus semi-embedded valve anastomosis with laparoscopic total gastrectomy for adenocarcinoma of the esophagogastric junction: a single-center retrospective cohort study. *World J Surg Oncol* 2021; **19**: 50 [PMID: 33588854 DOI: 10.1186/s12957-021-02163-z]

53 **Zhang H**, Zheng Z, Liu X, Xin C, Huang Y, Li Y, Yin J, Zhang J. Safety and efficacy of laparoscopic proximal gastrectomy with SOFY versus laparoscopic total gastrectomy with Roux-en-Y for treating cT1-2 Siewert II/III adenocarcinoma of the esophagogastric junction: a single-center prospective cohort study. *Langenbecks Arch Surg* 2023; **408**: 69 [PMID: 36715889 DOI: 10.1007/s00423-023-02779-7]

54 **Hosogi H**, Sakaguchi M, Yagi D, Onishi R, Hashimoto Y, Sakai Y, Kanaya S. Side-overlap esophagogastric tube (SO-EG) reconstruction after minimally invasive Ivor Lewis esophagectomy or laparoscopic proximal gastrectomy for cancer of the esophagogastric junction. *Langenbecks Arch Surg* 2022; **407**: 861-869 [PMID: 34775522 DOI: 10.1007/s00423-021-02377-5]

55 **Wang F**, Zhang H, Zheng Y, Wang Z, Geng Y, Wang Y. Intrathoracic side-to-side esophagogastrostomy with a linear stapler and barbed suture in robot-assisted Ivor Lewis esophagectomy. *J Surg Oncol* 2019; **120**: 1142-1147 [PMID: 31535396 DOI: 10.1002/jso.25698]

56 **Knospe L**, Gockel I, Jansen-Winkeln B, Thieme R, Niebisch S, Moulla Y, Stelzner S, Lyros O, Diana M, Marescaux J, Chalopin C, Köhler H, Pfahl A, Maktabi M, Park JH, Yang HK. New Intraoperative Imaging Tools and Image-Guided Surgery in Gastric Cancer Surgery. *Diagnostics (Basel)* 2022; **12** [PMID: 35204597 DOI: 10.3390/diagnostics12020507]

57 **Markar S**, Gronnier C, Duhamel A, Mabrut JY, Bail JP, Carrere N, Lefevre JH, Brigand C, Vaillant JC, Adham M, Msika S, Demartines N, Nakadi IE, Meunier B, Collet D, Mariette C; FREGAT (French Eso-Gastric Tumors) working group, FRENCH (Fédération de Recherche EN CHirurgie), and AFC (Association Française de Chirurgie). The Impact of Severe Anastomotic Leak on Long-term Survival and Cancer Recurrence After Surgical Resection for Esophageal Malignancy. *Ann Surg* 2015; **262**: 972-980 [PMID: 26469952 DOI: 10.1097/SLA.0000000000001011]

58 **Ohi M**, Toiyama Y, Mohri Y, Saigusa S, Ichikawa T, Shimura T, Yasuda H, Okita Y, Yoshiyama S, Kobayashi M, Araki T, Inoue Y, Kusunoki M. Prevalence of anastomotic leak and the impact of indocyanine green fluorescein imaging for evaluating blood flow in the gastric conduit following esophageal cancer surgery. *Esophagus* 2017; **14**: 351-359 [PMID: 28983231 DOI: 10.1007/s10388-017-0585-5]

59 **Jansen SM**, de Bruin DM, van Berge Henegouwen MI, Strackee SD, Veelo DP, van Leeuwen TG, Gisbertz SS. Optical techniques for perfusion monitoring of the gastric tube after esophagectomy: a review of technologies and thresholds. *Dis Esophagus* 2018; **31** [PMID: 29701760 DOI: 10.1093/dote/dox161]

60 **Zehetner J**, DeMeester SR, Alicuben ET, Oh DS, Lipham JC, Hagen JA, DeMeester TR. Intraoperative Assessment of Perfusion of the Gastric Graft and Correlation With Anastomotic Leaks After Esophagectomy. *Ann Surg* 2015; **262**: 74-78 [PMID: 25029436 DOI: 10.1097/SLA.0000000000000811]

61 **Talavera-Urquijo E**, Parise P, Palucci M, Olivari G, Turi S, Cossu A, Barbieri L, Elmore U, Rosati R. Perfusion speed of indocyanine green in the stomach before tubulization is an objective and useful parameter to evaluate gastric microcirculation during Ivor-Lewis esophagectomy. *Surg Endosc* 2020; **34**: 5649-5659 [PMID: 32856151 DOI: 10.1007/s00464-020-07924-7]

62 **Shimada Y**, Okumura T, Nagata T, Sawada S, Matsui K, Hori R, Yoshioka I, Yoshida T, Osada R, Tsukada K. Usefulness of blood supply visualization by indocyanine green fluorescence for reconstruction during esophagectomy. *Esophagus* 2011; **8**: 259-266 [PMID: 22557942 DOI: 10.1007/s10388-011-0291-7]

63 **Casas MA**, Angeramo CA, Bras Harriott C, Dreifuss NH, Schlottmann F. Indocyanine green (ICG) fluorescence imaging for prevention of anastomotic leak in totally minimally invasive Ivor Lewis esophagectomy: a systematic review and meta-analysis. *Dis Esophagus* 2022; **35** [PMID: 34378016 DOI: 10.1093/dote/doab056]

64 **Campbell C**, Reames MK, Robinson M, Symanowski J, Salo JC. Conduit Vascular Evaluation is Associated with Reduction in Anastomotic Leak After Esophagectomy. *J Gastrointest Surg* 2015; **19**: 806-812 [PMID: 25791907 DOI: 10.1007/s11605-015-2794-3]

65 **Koyanagi K**, Ozawa S, Oguma J, Kazuno A, Yamazaki Y, Ninomiya Y, Ochiai H, Tachimori Y. Blood flow speed of the gastric conduit assessed by indocyanine green fluorescence: New predictive evaluation of anastomotic leakage after esophagectomy. *Medicine (Baltimore)* 2016; **95**: e4386 [PMID: 27472732 DOI: 10.1097/MD.0000000000004386]

66 **Schlottmann F**, Barbetta A, Mungo B, Lidor AO, Molena D. Identification of the Lymphatic Drainage Pattern of Esophageal Cancer with Near-Infrared Fluorescent Imaging. *J Laparoendosc Adv Surg Tech A* 2017; **27**: 268-271 [PMID: 27992300 DOI: 10.1089/lap.2016.0523]

67 **Hachey KJ**, Gilmore DM, Armstrong KW, Harris SE, Hornick JL, Colson YL, Wee JO. Safety and feasibility of near-infrared image-guided lymphatic mapping of regional lymph nodes in esophageal cancer. *J Thorac Cardiovasc Surg* 2016; **152**: 546-554 [PMID: 27179838 DOI: 10.1016/j.jtcvs.2016.04.025]

68 **Kubota K**, Yoshida M, Kuroda J, Okada A, Ohta K, Kitajima M. Application of the HyperEye Medical System for esophageal cancer surgery: a preliminary report. *Surg Today* 2013; **43**: 215-220 [PMID: 22782594 DOI: 10.1007/s00595-012-0251-4]

69 **Yuasa Y**, Seike J, Yoshida T, Takechi H, Yamai H, Yamamoto Y, Furukita Y, Goto M, Minato T, Nishino T, Inoue S, Fujiwara S, Tangoku A. Sentinel lymph node biopsy using intraoperative indocyanine green fluorescence imaging navigated with preoperative CT lymphography for superficial esophageal cancer. *Ann Surg Oncol* 2012; **19**: 486-493 [PMID: 21792510 DOI: 10.1245/s10434-011-1922-x]

70 **Rao DV**, Chava SP, Sahni P, Chattopadhyay TK. Thoracic duct injury during esophagectomy: 20 years experience at a tertiary care center in a developing country. *Dis Esophagus* 2004; **17**: 141-145 [PMID: 15230727 DOI: 10.1111/j.1442-2050.2004.00391.x]

71 **Turner SR**, Molena DR. The Role of Intraoperative Fluorescence Imaging During Esophagectomy. *Thorac Surg Clin* 2018; **28**: 567-571 [PMID: 30268302 DOI: 10.1016/j.thorsurg.2018.07.009]

72 **Omori T**, Hara H, Shinno N, Yamamoto M, Kanemura T, Takeoka T, Akita H, Wada H, Yasui M, Matsuda C, Nishimura J, Ohue M, Sakon M, Miyata H. Safety and efficacy of preoperative indocyanine green fluorescence marking in laparoscopic gastrectomy for proximal gastric and esophagogastric junction adenocarcinoma (ICG MAP study). *Langenbecks Arch Surg* 2022; **407**: 3387-3396 [PMID: 36227384 DOI: 10.1007/s00423-022-02680-9]

73 **Sagawa H**, Saito M, Ito S, Hayakawa S, Ueno S, Okubo T, Tanaka T, Ogawa R, Takahashi H, Matsuo Y, Mitsui A, Kimura M, Takiguchi S. Near infrared ray-guided surgery using Firefly technology of the daVinci Xi system and intraoperative upper gastrointestinal endoscopy for subtotal gastrectomy and surgery for cancer of the gastroesophageal junction. *BMC Surg* 2022; **22**: 174 [PMID: 35549907 DOI: 10.1186/s12893-022-01633-9]

74 **van Workum F**, Bouwense SA, Luyer MD, Nieuwenhuijzen GA, van der Peet DL, Daams F, Kouwenhoven EA, van Det MJ, van den

Wildenberg FJ, Polat F, Gisbertz SS, Henegouwen MI, Heisterkamp J, Langenhoff BS, Martijnse IS, Grutters JP, Klarenbeek BR, Rovers MM, Rosman C. Intrathoracic versus Cervical ANastomosis after minimally invasive esophagectomy for esophageal cancer: study protocol of the ICAN randomized controlled trial. *Trials* 2016; **17**: 505 [PMID: 27756419 DOI: 10.1186/s13063-016-1636-2]

75 **Straatman J**, van der Wielen N, Nieuwenhuijzen GA, Rosman C, Roig J, Scheepers JJ, Cuesta MA, Luyer MD, van Berge Henegouwen MI, van Workum F, Gisbertz SS, van der Peet DL. Techniques and short-term outcomes for total minimally invasive Ivor Lewis esophageal resection in distal esophageal and gastroesophageal junction cancers: pooled data from six European centers. *Surg Endosc* 2017; **31**: 119-126 [PMID: 27129563 DOI: 10.1007/s00464-016-4938-2]

76 **Luketich JD**, Pennathur A, Awais O, Levy RM, Keeley S, Shende M, Christie NA, Weksler B, Landreneau RJ, Abbas G, Schuchert MJ, Nason KS. Outcomes after minimally invasive esophagectomy: review of over 1000 patients. *Ann Surg* 2012; **256**: 95-103 [PMID: 22668811 DOI: 10.1097/SLA.0b013e3182590603]

77 **Biere SS**, van Berge Henegouwen MI, Maas KW, Bonavina L, Rosman C, Garcia JR, Gisbertz SS, Klinkenbijl JH, Hollmann MW, de Lange ES, Bonjer HJ, van der Peet DL, Cuesta MA. Minimally invasive versus open oesophagectomy for patients with oesophageal cancer: a multicentre, open-label, randomised controlled trial. *Lancet* 2012; **379**: 1887-1892 [PMID: 22552194 DOI: 10.1016/S0140-6736(12)60516-9]

78 **Mariette C**, Markar SR, Dabakuyo-Yonli TS, Meunier B, Pezet D, Collet D, D'Journo XB, Brigand C, Perniceni T, Carrère N, Mabrut JY, Msika S, Peschaud F, Prudhomme M, Bonnetain F, Piessen G; Fédération de Recherche en Chirurgie (FRENCH) and French Eso-Gastric Tumors (FREGAT) Working Group. Hybrid Minimally Invasive Esophagectomy for Esophageal Cancer. *N Engl J Med* 2019; **380**: 152-162 [PMID: 30625052 DOI: 10.1056/NEJMoa1805101]

79 **Paireder M**, Asari R, Kristo I, Rieder E, Zacherl J, Kabon B, Fleischmann E, Schoppmann SF. Morbidity in open versus minimally invasive hybrid esophagectomy (MIOMIE): Long-term results of a randomized controlled clinical study. *Eur Surg* 2018; **50**: 249-255 [PMID: 30546384 DOI: 10.1007/s10353-018-0552-y]

80 **Ben-David K**, Sarosi GA, Cendan JC, Howard D, Rossidis G, Hochwald SN. Decreasing morbidity and mortality in 100 consecutive minimally invasive esophagectomies. *Surg Endosc* 2012; **26**: 162-167 [PMID: 21792712 DOI: 10.1007/s00464-011-1846-3]

81 **Verhage RJ**, Hazebroek EJ, Boone J, Van Hillegersberg R. Minimally invasive surgery compared to open procedures in esophagectomy for cancer: a systematic review of the literature. *Minerva Chir* 2009; **64**: 135-146 [PMID: 19365314]

82 **Bencini L**, Moraldi L, Bartolini I, Coratti A. Esophageal surgery in minimally invasive era. *World J Gastrointest Surg* 2016; **8**: 52-64 [PMID: 26843913 DOI: 10.4240/wjgs.v8.i1.52]

83 **Zhao Y**, Zhang J, Yang D, Tang Z, Wang Q. Feasibility of laparoscopic total gastrectomy for advanced Siewert type II and type III esophagogastric junction carcinoma: A propensity score-matched case-control study. *Asian J Surg* 2019; **42**: 805-813 [PMID: 30685144 DOI: 10.1016/j.asjsur.2018.12.014]

84 **Nagpal K**, Ahmed K, Vats A, Yakoub D, James D, Ashrafian H, Darzi A, Moorthy K, Athanasiou T. Is minimally invasive surgery beneficial in the management of esophageal cancer? A meta-analysis. *Surg Endosc* 2010; **24**: 1621-1629 [PMID: 20108155 DOI: 10.1007/s00464-009-0822-7]

85 **Liao C**, Feng Q, Xie S, Chen J, Shi Y. Laparoscopic versus open gastrectomy for Siewert type II/III adenocarcinoma of the esophagogastric junction: a meta-analysis. *Surg Endosc* 2021; **35**: 860-871 [PMID: 32076857 DOI: 10.1007/s00464-020-07458-y]

86 **Zhou C**, Zhang L, Wang H, Ma X, Shi B, Chen W, He J, Wang K, Liu P, Ren Y. Superiority of Minimally Invasive Oesophagectomy in Reducing In-Hospital Mortality of Patients with Resectable Oesophageal Cancer: A Meta-Analysis. *PLoS One* 2015; **10**: e0132889 [PMID: 26196135 DOI: 10.1371/journal.pone.0132889]

87 **van Workum F**, Berkelmans GH, Klarenbeek BR, Nieuwenhuijzen GAP, Luyer MDP, Rosman C. McKeown or Ivor Lewis totally minimally invasive esophagectomy for cancer of the esophagus and gastroesophageal junction: systematic review and meta-analysis. *J Thorac Dis* 2017; **9**: S826-S833 [PMID: 28815080 DOI: 10.21037/jtd.2017.03.173]

88 **Lin X**, Wan J, Li Z, Yan M, Liu J, Shi Y, Qian F, Zhao Y. Surgical and survival outcomes after laparoscopic and open gastrectomy for serosa-invasive Siewert type II/III esophagogastric junction carcinoma: a propensity score matching analysis. *Surg Endosc* 2022; **36**: 5055-5066 [PMID: 34761283 DOI: 10.1007/s00464-021-08867-3]

89 **Briez N**, Piessen G, Bonnetain F, Brigand C, Carrere N, Collet D, Doddoli C, Flamein R, Mabrut JY, Meunier B, Msika S, Perniceni T, Peschaud F, Prudhomme M, Triboulet JP, Mariette C. Open versus laparoscopically-assisted oesophagectomy for cancer: a multicentre randomised controlled phase III trial - the MIRO trial. *BMC Cancer* 2011; **11**: 310 [PMID: 21781337 DOI: 10.1186/1471-2407-11-310]

90 **Kanamori J**, Watanabe M, Kozuki R, Toihata T, Otake R, Takahashi K, Okamura A, Imamura Y, Mine S. Successful transition from open to minimally invasive approach in Ivor Lewis esophagectomy: a single-center experience in Japan. *Langenbecks Arch Surg* 2021; **406**: 1407-1414 [PMID: 33721088 DOI: 10.1007/s00423-021-02150-8]

91 **Wang J**, Wang JC, Song B, Dai XD, Zhang XY. Comparative study of laparoscopic-assisted and open total gastrectomy for Siewert Types II and III adenocarcinoma of the esophagogastric junction. *J Cell Physiol* 2019; **234**: 11235-11239 [PMID: 30478913 DOI: 10.1002/jcp.27777]

92 **Shi Y**, Li L, Xiao H, Guo S, Wang G, Tao K, Dong J, Zong L. Feasibility of laparoscopic gastrectomy for patients with Siewert-type II/III adenocarcinoma of the esophagogastric junction: A propensity score matching analysis. *PLoS One* 2018; **13**: e0203125 [PMID: 30256806 DOI: 10.1371/journal.pone.0203125]

93 **Zhang YC**, Wu QB, Yang XY, Yang TH, Wang ZQ, Zhou ZG. Laparoscopic-Assisted Transhiatal Esophagogastrectomy Without Thoracic or Cervical Access: A Series of One Hundred Three Consecutive Cases. *J Laparoendosc Adv Surg Tech A* 2018; **28**: 845-852 [PMID: 29641370 DOI: 10.1089/lap.2017.0692]

94 **Dantoc MM**, Cox MR, Eslick GD. Does minimally invasive esophagectomy (MIE) provide for comparable oncologic outcomes to open techniques? A systematic review. *J Gastrointest Surg* 2012; **16**: 486-494 [PMID: 22183862 DOI: 10.1007/s11605-011-1792-3]

95 **Zhang P**, Zhang X, Xue H. Long-term results of hand-assisted laparoscopic gastrectomy for advanced Siewert type II and type III esophagogastric junction adenocarcinoma. *Int J Surg* 2018; **53**: 201-205 [PMID: 29572113 DOI: 10.1016/j.ijsu.2018.03.004]

96 **Andreou A**, Knitter S, Chopra S, Denecke C, Schmelzle M, Struecker B, Heilmann AC, Spenke J, Hofmann T, Thuss-Patience PC, Bahra M, Pratschke J, Biebl M. Laparoscopic Resection for Adenocarcinoma of the Stomach or Gastroesophageal Junction Improves Postoperative Outcomes: a Propensity Score Matching Analysis. *J Gastrointest Surg* 2019; **23**: 730-738 [PMID: 30284200 DOI: 10.1007/s11605-018-3982-8]

97 **Yin Q**, Wang W, Liu H, Yang G, Zhou S, Liu L. Clinical application and observation of modified Ivor-Lewis surgery in Siewert type II adenocarcinoma of the Esophagogastric junction. *J Cardiothorac Surg* 2019; **14**: 207 [PMID: 31775820 DOI: 10.1186/s13019-019-1023-7]

98 **Tapias LF**, Mathisen DJ, Wright CD, Wain JC, Gaissert HA, Muniappan A, Lanuti M, Donahue DM, Morse CR. Outcomes With Open and Minimally Invasive Ivor Lewis Esophagectomy After Neoadjuvant Therapy. *Ann Thorac Surg* 2016; **101**: 1097-1103 [PMID: 26652140 DOI:

10.1016/j.athoracsur.2015.09.062]
99 **Li Z**, Liu Y, Hao Y, Bai B, Yu D, Zhao Q. Surgical and long-term oncologic outcomes of laparoscopic and open gastrectomy for serosa-positive (pT4a) gastric cancer: A propensity score-matched analysis. *Surg Oncol* 2019; **28**: 167-173 [PMID: 30851895 DOI: 10.1016/j.suronc.2019.01.003]
100 **Sugita S**, Kinoshita T, Kuwata T, Tokunaga M, Kaito A, Watanabe M, Tonouchi A, Sato R, Nagino M. Long-term oncological outcomes of laparoscopic versus open transhiatal resection for patients with Siewert type II adenocarcinoma of the esophagogastric junction. *Surg Endosc* 2021; **35**: 340-348 [PMID: 32025923 DOI: 10.1007/s00464-020-07406-w]
101 **Eyck BM**, Klevebro F, van der Wilk BJ, Johar A, Wijnhoven BPL, van Lanschot JJB, Lagergren P, Markar SR, Lagarde SM; LASER study group. Lasting symptoms and long-term health-related quality of life after totally minimally invasive, hybrid and open Ivor Lewis esophagectomy. *Eur J Surg Oncol* 2022; **48**: 582-588 [PMID: 34763951 DOI: 10.1016/j.ejso.2021.10.023]
102 **Palazzo F**, Rosato EL, Chaudhary A, Evans NR 3rd, Sendecki JA, Keith S, Chojnacki KA, Yeo CJ, Berger AC. Minimally invasive esophagectomy provides significant survival advantage compared with open or hybrid esophagectomy for patients with cancers of the esophagus and gastroesophageal junction. *J Am Coll Surg* 2015; **220**: 672-679 [PMID: 25667145 DOI: 10.1016/j.jamcollsurg.2014.12.023]
103 **Kumagai K**, Shimizu K, Yokoyama N, Aida S, Arima S, Aikou T; Japanese Society for the Study of Postoperative Morbidity after Gastrectomy. Questionnaire survey regarding the current status and controversial issues concerning reconstruction after gastrectomy in Japan. *Surg Today* 2012; **42**: 411-418 [PMID: 22391980 DOI: 10.1007/s00595-012-0159-z]
104 **Kim DW**, Lee G, Hong TS, Li G, Horick NK, Roeland E, Keane FK, Eyler C, Drapek LC, Ryan DP, Allen JN, Berger D, Parikh AR, Mullen JT, Klempner SJ, Clark JW, Wo JY. Neoadjuvant versus Postoperative Chemoradiotherapy is Associated with Improved Survival for Patients with Resectable Gastric and Gastroesophageal Cancer. *Ann Surg Oncol* 2022; **29**: 242-252 [PMID: 34480285 DOI: 10.1245/s10434-021-10666-y]
105 **Nishikawa G**, Banik P, Thawani R, Kardosh A, Wood SG, Nabavizadeh N, Chen EY. Comparison of neoadjuvant regimens for resectable gastroesophageal junction cancer: a systematic review of randomized clinical trials across three decades. *J Gastrointest Oncol* 2022; **13**: 1454-1466 [PMID: 35837173 DOI: 10.21037/jgo-22-29]
106 **Ronellenfitsch U**, Schwarzbach M, Hofheinz R, Kienle P, Kieser M, Slanger TE, Jensen K; GE Adenocarcinoma Meta-analysis Group. Perioperative chemo(radio)therapy versus primary surgery for resectable adenocarcinoma of the stomach, gastroesophageal junction, and lower esophagus. *Cochrane Database Syst Rev* 2013; CD008107 [PMID: 23728671 DOI: 10.1002/14651858.CD008107.pub2]
107 **Al-Batran SE**, Homann N, Pauligk C, Illerhaus G, Martens UM, Stoehlmacher J, Schmalenberg H, Luley KB, Prasnikar N, Egger M, Probst S, Messmann H, Moehler M, Fischbach W, Hartmann JT, Mayer F, Höffkes HG, Koenigsmann M, Arnold D, Kraus TW, Grimm K, Berkhoff S, Post S, Jäger E, Bechstein W, Ronellenfitsch U, Mönig S, Hofheinz RD. Effect of Neoadjuvant Chemotherapy Followed by Surgical Resection on Survival in Patients With Limited Metastatic Gastric or Gastroesophageal Junction Cancer: The AIO-FLOT3 Trial. *JAMA Oncol* 2017; **3**: 1237-1244 [PMID: 28448662 DOI: 10.1001/jamaoncol.2017.0515]
108 **Ichikawa D**, Ueshima Y, Shirono K, Kan K, Shioaki Y, Lee CJ, Hamashima T, Deguchi E, Ikeda E, Mutoh F, Oka T, Kurioka H. Esophagogastrostomy reconstruction after limited proximal gastrectomy. *Hepatogastroenterology* 2001; **48**: 1797-1801 [PMID: 11813627]
109 **Nakamura M**, Nakamori M, Ojima T, Katsuda M, Iida T, Hayata K, Matsumura S, Kato T, Kitadani J, Iwahashi M, Yamaue H. Reconstruction after proximal gastrectomy for early gastric cancer in the upper third of the stomach: an analysis of our 13-year experience. *Surgery* 2014; **156**: 57-63 [PMID: 24799083 DOI: 10.1016/j.surg.2014.02.015]
110 **Shen C**, Yang H, Zhang B, Chen H, Chen Z, Chen J. Changes of quality of life after gastric tube reconstruction in adenocarcinoma of the esophagogastric junction. *Pak J Med Sci* 2013; **29**: 1193-1198 [PMID: 24353718 DOI: 10.12669/pjms.295.3879]
111 **Hallit S**, Hajj A, Sacre H, Al Karaki G, Malaeb D, Kheir N, Salameh P, Hallit R. Impact of Sleep Disorders and Other Factors on the Quality of Life in General Population: A Cross-Sectional Study. *J Nerv Ment Dis* 2019; **207**: 333-339 [PMID: 30907768 DOI: 10.1097/NMD.0000000000000968]
112 **Meng M**, Chai N, Liu S, Feng X, Linghu E. Health-related quality of life after super minimally invasive surgery and proximal gastrectomy for early-stage adenocarcinoma of the esophagogastric junction: a propensity score-matched study. *Chin Med J (Engl)* 2022; **135**: 3022-3023 [PMID: 36127801 DOI: 10.1097/CM9.0000000000002410]
113 **Gutschow C**, Collard JM, Romagnoli R, Salizzoni M, Hölscher A. Denervated stomach as an esophageal substitute recovers intraluminal acidity with time. *Ann Surg* 2001; **233**: 509-514 [PMID: 11303132 DOI: 10.1097/00000658-200104000-00005]
114 **Fuchs H**, Hölscher AH, Leers J, Bludau M, Brinkmann S, Schröder W, Alakus H, Mönig S, Gutschow CA. Long-term quality of life after surgery for adenocarcinoma of the esophagogastric junction: extended gastrectomy or transthoracic esophagectomy? *Gastric Cancer* 2016; **19**: 312-317 [PMID: 25627475 DOI: 10.1007/s10120-015-0466-3]
115 **Schmitz SM**, Alizai PH, Eickhoff RM, Schooren L, Kroh A, Roeth AA, Neumann UP, Klink CD. Minimally Invasive Thoracoabdominal Esophagectomy Is Superior to Minimally Invasive Gastrectomy in Terms of Health-Related Quality of Life. *J Laparoendosc Adv Surg Tech A* 2021; **31**: 306-313 [PMID: 32960143 DOI: 10.1089/lap.2020.0509]
116 **Kauppila JH**, Xie S, Johar A, Markar SR, Lagergren P. Meta-analysis of health-related quality of life after minimally invasive versus open oesophagectomy for oesophageal cancer. *Br J Surg* 2017; **104**: 1131-1140 [PMID: 28632926 DOI: 10.1002/bjs.10577]
117 **Klevebro F**, Kauppila JH, Markar S, Johar A, Lagergren P. Health-related quality of life following total minimally invasive, hybrid minimally invasive or open oesophagectomy: a population-based cohort study. *Br J Surg* 2021; **108**: 702-708 [PMID: 34157084 DOI: 10.1002/bjs.11998]
118 **Mehdorn AS**, Möller T, Franke F, Richter F, Kersebaum JN, Becker T, Egberts JH. Long-Term, Health-Related Quality of Life after Open and Robot-Assisted Ivor-Lewis Procedures-A Propensity Score-Matched Study. *J Clin Med* 2020; **9** [PMID: 33142987 DOI: 10.3390/jcm9113513]
119 **Sarkaria IS**, Rizk NP, Goldman DA, Sima C, Tan KS, Bains MS, Adusumilli PS, Molena D, Bott M, Atkinson T, Jones DR, Rusch VW. Early Quality of Life Outcomes After Robotic-Assisted Minimally Invasive and Open Esophagectomy. *Ann Thorac Surg* 2019; **108**: 920-928 [PMID: 31026433 DOI: 10.1016/j.athoracsur.2018.11.075]
120 **Japanese Gastric Cancer Association**. Japanese gastric cancer treatment guidelines 2018 (5th edition). *Gastric Cancer* 2021; **24**: 1-21 [PMID: 32060757 DOI: 10.1007/s10120-020-01042-y]
121 **Ji X**, Jin C, Ji K, Zhang J, Wu X, Jia Z, Bu Z, Ji J. Double Tract Reconstruction Reduces Reflux Esophagitis and Improves Quality of Life after Radical Proximal Gastrectomy for Patients with Upper Gastric or Esophagogastric Adenocarcinoma. *Cancer Res Treat* 2021; **53**: 784-794 [PMID: 33421979 DOI: 10.4143/crt.2020.1064]
122 **Wang S**, Lin S, Wang H, Yang J, Yu P, Zhao Q, Li M. Reconstruction methods after radical proximal gastrectomy: A systematic review. *Medicine (Baltimore)* 2018; **97**: e0121 [PMID: 29538208 DOI: 10.1097/MD.0000000000010121]
123 **Bray F**, Ferlay J, Soerjomataram I, Siegel RL, Torre LA, Jemal A. Global cancer statistics 2018: GLOBOCAN estimates of incidence and

mortality worldwide for 36 cancers in 185 countries. *CA Cancer J Clin* 2018; **68**: 394-424 [PMID: 30207593 DOI: 10.3322/caac.21492]

124 **Wang A**, Li Z, Wang Q, Bai Y, Ji X, Fu T, Ji K, Xue Y, Han T, Wu X, Zhang J, Yang Y, Xu G, Bu Z, Ji J. Diagnostic value of negative enrichment and immune fluorescence in situ hybridization for intraperitoneal free cancer cells of gastric cancer. *Chin J Cancer Res* 2019; **31**: 945-954 [PMID: 31949396 DOI: 10.21147/j.issn.1000-9604.2019.06.10]

125 **Sun W**, Deng J, Zhang N, Liu H, Liu J, Gu P, Du Y, Wu Z, He W, Wang P, Liang H. Prognostic impact of D2-plus lymphadenectomy and optimal extent of lymphadenectomy in advanced gastric antral carcinoma: Propensity score matching analysis. *Chin J Cancer Res* 2020; **32**: 51-61 [PMID: 32194305 DOI: 10.21147/j.issn.1000-9604.2020.01.07]

World Journal of Gastrointestinal Oncology

Submit a Manuscript: https://www.f6publishing.com

World J Gastrointest Oncol 2023 October 15; 15(10): 1691-1705

DOI: 10.4251/wjgo.v15.i10.1691

ISSN 1948-5204 (online)

REVIEW

Systemic treatment for advanced pancreatic cancer

Wattana Leowattana, Pathomthep Leowattana, Tawithep Leowattana

Specialty type: Gastroenterology and hepatology

Provenance and peer review: Invited article; Externally peer reviewed.

Peer-review model: Single blind

Peer-review report's scientific quality classification

Grade A (Excellent): 0
Grade B (Very good): 0
Grade C (Good): C, C
Grade D (Fair): 0
Grade E (Poor): 0

P-Reviewer: Wang GX, China; Zhang C, China

Received: July 11, 2023
Peer-review started: July 11, 2023
First decision: August 15, 2023
Revised: August 24, 2023
Accepted: September 22, 2023
Article in press: September 22, 2023
Published online: October 15, 2023

Wattana Leowattana, Pathomthep Leowattana, Department of Clinical Tropical Medicine, Mahidol University, Rachatawee 10400, Bangkok, Thailand

Tawithep Leowattana, Department of Medicine, Srinakharinwirot University, Wattana 10110, Bangkok, Thailand

Corresponding author: Wattana Leowattana, BMed, MD, MSc, PhD, Full Professor, Department of Clinical Tropical Medicine, Mahidol University, 420/6 Rajavithi Road, Rachatawee 10400, Bangkok, Thailand. wattana.leo@mahidol.ac.th

Abstract

Pancreatic cancer is a deadly disease with an extremely poor 5-year survival rate due to treatment resistance and late-stage detection. Despite numerous years of research and pharmaceutical development, these figures have not changed. Treatment options for advanced pancreatic cancer are still limited. This illness is typically detected at a late stage, making curative surgical resection impossible. Chemotherapy is the most commonly utilized technique for treating advanced pancreatic cancer but has poor efficacy. Targeted therapy and immunotherapy have made significant progress in many other cancer types and have been proven to have extremely promising possibilities; these therapies also hold promise for pancreatic cancer. There is an urgent need for research into targeted treatment, immunotherapy, and cancer vaccines. In this review, we emphasize the foundational findings that have fueled the therapeutic strategy for advanced pancreatic cancer. We also address current advancements in targeted therapy, immunotherapy, and cancer vaccines, all of which continue to improve the clinical outcome of advanced pancreatic cancer. We believe that clinical translation of these novel treatments will improve the low survival rate of this deadly disease.

Key Words: Systemic treatment; Advanced pancreatic cancer; Personalized medicine; Biomarkers; Chemotherapy; Targeted therapy; Immunotherapy

Core Tip: Understanding the pathophysiology of pancreatic cancer and using personalized treatments might improve patients' overall survival. We think that targeted treatment, immunotherapy, and cancer vaccines can improve the prognosis of patients with advanced pancreatic cancer. As a result, additional study is required to identify the best combination of current drugs to help in early treatment and result in a better clinical outcome.

Citation: Leowattana W, Leowattana P, Leowattana T. Systemic treatment for advanced pancreatic cancer. *World J Gastrointest Oncol* 2023; 15(10): 1691-1705
URL: https://www.wjgnet.com/1948-5204/full/v15/i10/1691.htm
DOI: https://dx.doi.org/10.4251/wjgo.v15.i10.1691

INTRODUCTION

It is expected that pancreatic cancer will continue to be the leading cause of cancer-related mortality despite a sharp rise in occurrence over the previous several decades. Many of the observed trends are explained by changes in the identified modifiable risk variables as well as changes in the age structure of the global population, particularly in emerging nations. The chance of developing pancreatic cancer is significantly influenced by genetic factors and modifiable exposures, either acting alone or in concert. In order to limit exposures and identify people most at risk of developing this commonly deadly cancer, preventive initiatives, especially primary prevention techniques, will benefit from an understanding of the underlying risk factors and how they interact. Pancreatic cancer detection rates and the precursor lesions that precede it are increasing. This strategy will assist in lowering the rising prevalence of this deadly disease[1-3]. An overview of the knowledge of known risk factors for pancreatic cancer is given in this review, including inherited genetic risk, lifestyle risk, and risk unique to the disease. In addition, we intend to summarize the most recent guidelines for the systemic treatment of pancreatic cancer. We present the data supporting the recommendations that are currently available, with an emphasis on first-line and second-line situations, based on a thorough evaluation of biomedical and clinical trial databases. Finally, we seek the present state of the art and research paths that can enhance targeted treatment and immunotherapy choices for this high-risk patient population.

EPIDEMIOLOGY AND RISK FACTORS

The frequency of pancreatic cancer diagnoses annually has doubled during the previous two decades. Compared to 196000 cases in 1990, there were 441000 cases of pancreatic cancer in the world in 2017. Given that the risk of developing pancreatic cancer rises with age and that it is uncommon to develop the disease before the age of 40, improved diagnosis techniques and the changing age structure of the global population account for the majority of the rise in pancreatic cancer incidence, especially in high-income countries. Incidence rates in low-income nations have remained low due to limited access to contemporary imaging and a lack of pathology expertise, and there is a dearth of high-quality data on mortality in these regions[4,5]. Obesity, type 2 diabetes, and smoking cigarettes are all modifiable risk factors for the development of pancreatic cancer. A significant National Institutes of Health cohort study found that individuals with a body mass index (BMI) outside the normal range had a higher risk of acquiring this malignancy than those with a BMI within the range, with hazard ratios ranging from 1.15 to 1.53. Pancreatic intraepithelial neoplasia, which is a precursor to pancreatic cancer, has been linked to fatty infiltration of the pancreas. There is a long-standing association between diabetes and the development of pancreatic cancer, with a relative risk (RR) of 2.1, even though cancer of the pancreas is also a risk factor for diabetes development[6-9]. One percent of those with newly diagnosed diabetes over the age of 50 experience diabetes as a result of concurrent pancreatic cancer. Similar to this, those who have had their diabetes diagnosis for less than one year have a greater RR of developing pancreatic cancer of 5.4-fold than those who have had it for a long time, who only have a 1.5-fold higher risk. These findings imply that newly diagnosed diabetes may be a significant risk factor and a sign of pancreatic cancer. Pancreatic cancer is thought to be around twice as common among smokers as in non-smokers, according to estimates; however, unlike other smoking-related malignancies, pancreatic cancer does not yet have a well-defined genetic signature[10,11].

On average, genetic risk factors are thought to be responsible for 5%-10% of all pancreatic malignancies. There are several family cancer syndromes that have been linked to a higher chance of getting pancreatic cancer. A mutation in the tumor suppressor STK11 causes Peutz-Jeghers syndrome, which raises the risk of pancreatic cancer by 35%. The chance of acquiring this kind of cancer is further enhanced by the hereditary breast-ovarian cancer syndrome, which is typically linked to mutations in BRCA1 or BRCA2. Despite the fact that people with a BRCA1 mutation have a relatively low chance of developing the disease—a RR of 2.8 compared with 1.3 in the general population—mutations of BRCA2 are a more common genetic risk factor (RR = 3.5) for pancreatic cancer development[12,13]. An elevated risk of pancreatic cancer of 17% has been attributed to inherited mutations in the *CDKN2A* gene. An elevated risk of acquiring this kind of cancer is also linked to germline abnormalities in genes necessary for DNA damage response and DNA repair. Patients with Lynch syndrome are more likely than the general population to acquire pancreatic cancer by the time that they are 70 years old, and their tumors show microsatellite instability, making them particularly susceptible to immune checkpoint inhibitor treatment. Patients with hereditary pancreatitis syndromes, which are linked to mutations in *SPINK1*

and *PRSS1*, have a 40% lifetime chance of getting pancreatic cancer as a result of chronic pancreatitis[14,15].

CLINICAL PRESENTATION

Only a small percentage of patients with pancreatic cancer initially have the illness that can be surgically removed, which is consistent with the fact that pancreatic cancer often causes minimal symptoms prior to progression to the advanced stage. Tragically, individuals who do experience symptoms frequently have vague complaints, such as nausea, bloating, stomach fullness, or changes in stool consistency, which are frequently appropriately ascribed to other benign causes and delay diagnosis and treatment. At the time of diagnosis, stomach discomfort, abnormal liver function tests, jaundice, newly diagnosed diabetes, nausea, vomiting, dyspepsia, weight loss, and back pain are the clinical symptoms that occur most often[16,17]. Approximately 60%-70% of pancreatic tumors are discovered near the head or neck of the organ, and they are more likely to result in biliary blockage and a patient with an identifiable jaundice-free appearance. The range of jaundice's positive predictive value for detecting pancreatic cancer is 4%-13%. Pancreatic body tumors frequently infiltrate nearby vascular systems, such as the portal vein, hepatic, and superior mesenteric veins, and are therefore more likely to manifest with back discomfort. Because they have fewer anatomical neighbors, pancreatic tail tumors frequently have room to develop unchecked and are typically advanced when discovered (Figure 1)[18,19].

ADVANCED PANCREATIC CANCER

TNM staging and clinical categorization, the two separate staging methods, both have prognostic consequences that are helpful for therapeutic suggestions. Patients with borderline resectable and locally advanced pancreatic cancer are grouped together in stage III of the TNM staging system. Most patients with stage I and stage II cancer will fall into the resectable category, although there are a few people with pancreatic cancer that is borderline resectable who may be categorized as stage II, especially when the superior mesenteric or portal vein is involved. As a result, clinical categorization is more beneficial when choosing a course of treatment. Pancreatic cancer is considered advanced when it is unresectable or cannot be removed surgically. The cancer has spread to neighboring lymph nodes or blood vessels, as well as to organs outside the pancreas. Typically, this is stage III or IV. The majority of pancreatic cancer patients are diagnosed with advanced disease. Patients who are detected at an earlier stage of the disease may acquire advanced cancer if it spreads[20].

ADVANCED PANCREATIC CANCER TREATMENTS

Chemotherapy

More than 33% of pancreatic cancer patients have locally progressive disease at the time of diagnosis, frequently as a result of severe vascular involvement that makes surgical resection impossible. The majority of these individuals have incurable illnesses, while a small percentage who have had a great response to treatment could qualify for surgical excision. This patient group is usually given systemic chemotherapy utilizing protocols that have been authorized for use in the context of metastatic disease. Due to a phase 3 trial that demonstrated gemcitabine's therapeutic advantage over fluorouracil, it has been the standard of care for metastatic pancreatic cancer for many years. However, the median survival time was only 5.6 mo, and the response rate (RR) was only 5%[21]. Since then, several trials have been conducted with gemcitabine serving as the main component of doublet or triplet regimens to enhance patients' overall outcomes. The majority of the trials' results were unsatisfactory, with the exception of one that used erlotinib and gemcitabine together. Gemcitabine with erlotinib resulted in a median survival of 6.2 mo in this randomized phase 3 study, as opposed to 5.9 mo in the gemcitabine-only group. Although the difference in 2-wk survival was statistically significant, the increased toxic effects may prevent it from being clinically important[22]. In 2011, Conroy *et al*[23] conducted a randomized control trial to compare the efficacy and safety of "Folinic acid, fluorouracil, irinotecan, and oxaliplatin" (FOLFIRINOX) with gemcitabine in the first-line treatment of 342 advanced pancreatic cancer patients. The trial lasted 6 mo. In the FOLFIRINOX group, the median overall survival (OS) was 11.1 mo, whereas in the gemcitabine group, it was 6.8 mo. The median progression-free survival (PFS) for the FOLFIRINOX group was 6.4 mo as opposed to 3.3 mo for the gemcitabine group. In comparison to the gemcitabine group, which had a 9.4% objective RR (ORR), the FOLFIRINOX group's ORR was 31.6%. More adverse events were recorded in the FOLFIRINOX group, and 5.4% of the patients in this group experienced febrile neutropenia. In contrast to gemcitabine-treated patients, 31% of FOLFIRINOX-treated patients had a significant deterioration in quality of life at 6 mo. They determined that, as compared to gemcitabine, FOLFIRINOX had a survival benefit but increased toxicity. FOLFIRINOX is a therapy option for people with metastatic pancreatic cancer who have a good performance status. Von Hoff *et al*[24] conducted a phase 3 study in 861 patients with metastatic pancreatic cancer to compare the effectiveness and safety of a combination regimen (nab-paclitaxel-gemcitabine) with gemcitabine alone in 2013. They found that the median OS was 8.5 mo in the nab-paclitaxel-gemcitabine combination group and 6.7 mo in the gemcitabine alone group. The nab-paclitaxel-gemcitabine group had a survival rate of 35% at one year compared to 22% in the gemcitabine alone group and 9% compared to 4% at two years. In comparison to the gemcitabine alone group, which had a median PFS of 3.7 mo, the nab-paclitaxel-gemcitabine group's PFS was 5.5 mo. They observed that gemcitabine combined with nab-paclitaxel importantly improved RR, OS, and PFS in patients with

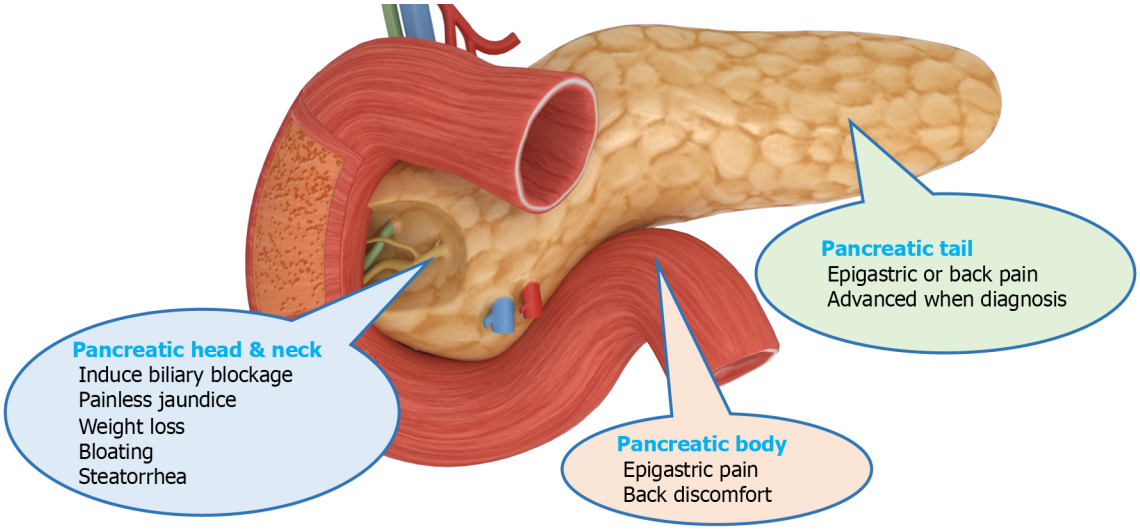

DOI: 10.4251/wjgo.v15.i10.1691

Figure 1 The location of a tumor within the pancreas affects a patient's presentation.

advanced pancreatic cancer but elevated rates of peripheral neuropathy and myelosuppression. Systemic chemotherapy such as FOLFIRINOX or gemcitabine plus nab-paclitaxel continues to be the principal treatment option for patients who have distant metastases at the time of their diagnosis, with the goals of relieving cancer-related symptoms and extending life. Even though first-line gemcitabine plus nab-paclitaxel and FOLFIRINOX have never been directly compared in a randomized controlled trial, real-world retrospective studies reveal that younger and physically fit participants are more likely to be treated with FOLFIRINOX, which results in a better OS in comparison with gemcitabine combined with nab-paclitaxel. Patients whose performance status or comorbidities prevent combination treatment still have the option of gemcitabine monotherapy[25,26]. If a patient's condition allows for chemotherapy and they have advanced on the first-line treatment with FOLFIRINOX, gemcitabine-based chemotherapy is a suitable second-line therapy[27-29].

Targeted therapy

Conventional therapies are treatments that target multiple biological processes; they are unable to distinguish between oncogenic and normal cells, resulting in unfavorable side effects. As a result, tailored therapies using small molecule inhibitors (SMIs) and monoclonal antibodies (mAbs) are required. These drugs work by targeting tumor cell surface receptors, growth factors, or other proteins that are important in disease development and progression. Targeted treatment refers to medications that suppress tumor cell proliferation by interacting with essential molecules in the cells required for cancer development rather than just interfering with rapidly proliferating cells, as typical chemotherapy does. Many researchers are interested in targeted cancer therapy since it is likely to replace systemic chemotherapy in the future[30,31]. Targeted treatment blocks particular pathways useful in cancer initiation and proliferation, resulting in the inhibition of enzymes as well as growth factor receptors required for the evolution of oncogenic cells. Cancer treatment may be substantially better in the future with tailored therapy, and hair loss, the most common adverse effect of systemic chemotherapy, may be decreased.

SMIs: Small molecules are organic chemicals with a low molecular weight that are designed to penetrate the cell membrane, bind particular targets within the cell, and interfere with signaling cascades. The discovery of SMIs was a major breakthrough in cellular biology research. These compounds enable the investigation of numerous biological pathways in order to enhance patient outcomes. Protein kinases linked to cancer initiation and development are key targets in cancer treatment since many SMIs target these kinases. Different proteins and signaling or receptor pathways connected to cancer cells might cause changes in signal transduction cascades. So far, several SMIs with robust and efficient action have been reported, including proteasome inhibitors, VEGF-inhibiting compounds, immune system-regulating drugs, and histone deacetylase (HDAC) inhibitors[32]. Bortezomib, carfilzomib, and ixazomib are examples of proteasome inhibitors. These inhibitors kill pancreatic cancer cells by inducing apoptosis *via* endoplasmic reticulum stress; proapoptotic proteins and their anti-apoptotic target genes are upregulated, whereas numerous anti-apoptotic proteins, as well as signal transducers and transcription activators, are suppressed[33,34]. There was only one randomized study to assess the RR of tumor for bortezomib (PS-341) alone *vs* RR and the survival rate at 6 mo for the combination of bortezomib and gemcitabine in 85 patients with advanced pancreatic cancer. The findings demonstrated that neither bortezomib alone nor in combination with gemcitabine led to an improvement in OS or RR beyond what was anticipated for gemcitabine alone[35]. VEGF-blocking drugs, such as sorafenib and sunitinib, are tyrosine kinase inhibitors used to treat pancreatic cancer. They have two effects: Inhibiting rapidly accelerated fibrosarcoma kinase, which controls cell division and proliferation, as well as the platelet-derived growth factor receptor beta and VEGFR-2 signaling pathways, which block angiogenesis[36] (Figure 2). In a few randomized studies, sorafenib was used to treat advanced pancreatic cancer; however, neither sorafenib alone nor sorafenib in conjunction with gemcitabine showed signs of efficacy that would lead to hope for metastatic pancreatic cancer[37-39]. Sunitinib malate capsules were given

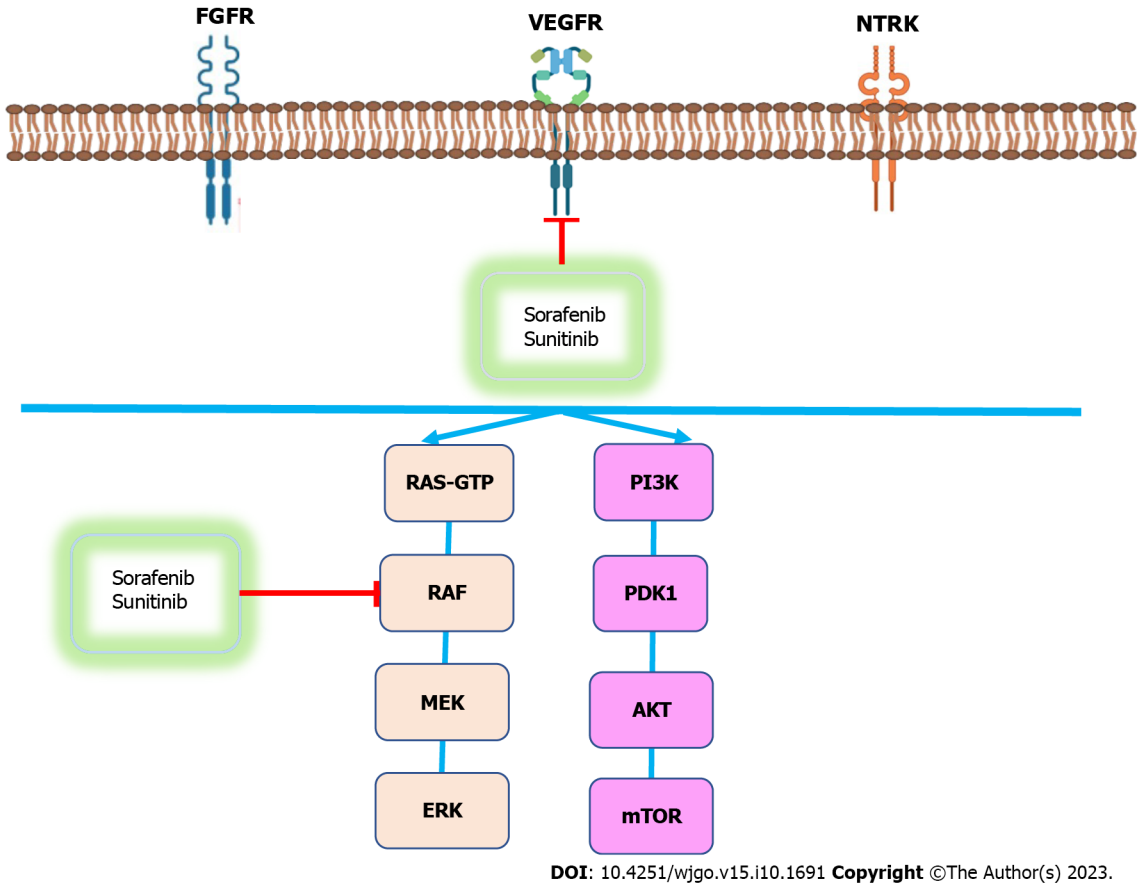

DOI: 10.4251/wjgo.v15.i10.1691

Figure 2 Targeted therapies used in systemic treatment of advanced pancreatic cancers. AKT: Protein kinase B; VEGFR: Vascular epidermal growth factor receptor; ERK: Extracellular signal-related kinase; FGFR: Fibroblast growth factor receptor; GTP: Guanosine triphosphate; MEK: Mitogen-activated protein kinase; mTOR: Mammalian target of rapamycin; NTRK: Neurotrophic tyrosine receptor kinase; PI3K: Phosphoinositide-3-kinase; PKD1: Polycystic kidney disease 1; RAF: Raf proto-oncogene; RAS: RAS proto-oncogene.

Food Drug Administration approval on May 20, 2011, to treat patients with locally progressed or metastatic pancreatic neuroendocrine tumors that are unresectable. One hundred and seventy-one participants were randomly assigned to receive sunitinib (37.5 mg) or a placebo once daily in a phase 3 randomized study. The primary effective outcome was PFS time. OS time, ORR, patient-reported outcomes, and safety were considered secondary goals. For the sunitinib and placebo groups, the median PFS was 10.2 mo and 5.4 mo, respectively. In the sunitinib and placebo groups, the ORRs were 9.3% and 0%, respectively. The OS data lacked maturity[40]. Belinostat, vorinostat, and romidepsin are examples of HDAC inhibitors. They cause cell growth inhibition and apoptosis[41,42]. There has not yet been a randomized control study to assess HDAC inhibitors in advanced pancreatic cancer. SMIs have several advantages over chemotherapeutic drugs and RNA interference agents, including the ability to perform a wide range of *in vivo* assays using different temporal and titration designs, which result in higher penetration in isolation and are useful for testing the combined effects with existing antitumor drugs.

Immunotherapy

The basis for immunotherapy is the distinct antigens that cancer cells release, which T lymphocytes recognize and eliminate. Cancer vaccines enhance the antigen presentation of cancer cells; immune checkpoint inhibitors disrupt the suppressive mechanisms of the immune system that impair effective immunosurveillance of T-cells; and tumor-specific T cells are modified to become more active after being adopted and transplanted. Immunotherapy has been shown in clinical studies to be a possible treatment for numerous solid tumors[43-45]. However, the pancreatic cancer microenvironment, also known as the stroma, contains a variety of noncancer cell components. It has been discovered that stroma, which may account for up to 50% of the overall mass of the tumor in cases with pancreatic cancer, suppresses both naturally occurring and artificially produced antitumor immunity. Immunotherapy for pancreatic cancer is, therefore, extremely challenging. However, there have been several attempts to employ immunotherapy either by itself or in conjunction with other cancer treatment modalities[46].

Immune checkpoint inhibitors: Immune cells include proteins called checkpoints that regulate the immune response. The immune response starts when the checkpoints are activated or deactivated. This process stops immune cells from attacking the body's normal cells, but cancer cells might exploit this defense and evade the immune system. Checkpoint inhibitors interfere with this pathway, causing the immune system to attack tumor cells. These techniques are now being

researched for use in pancreatic cancer. The T-cell immunity inhibitors programmed death-1 (PD-1) and cytotoxic T-lymphocyte-associated antigen-4 (CTLA-4) are the two immunological checkpoints that have attracted the greatest interest. Exocytosis moves CTLA-4 from the naive T cells' intracellular space to their cell surface when they get activated, where it competes with the B7 protein to prevent T cells from becoming activated[47,48]. Numerous immune cells, including T cells, B cells, NK cells, and dendritic cells (DC), express the cell surface receptor PD-1. One of PD-1's ligands, PD-L1, was discovered to be expressed in a variety of cells, including several types of tumor cells. Inhibiting T-cell survival and proliferation, the binding of PD-1 to PD-L1 also allows tumor cells to evade immune surveillance. Upregulation of PD-L1 in pancreatic cancer is associated with tumor growth and a worse prognosis[49].

Anti-CTLA-4 antibodies: Ipilimumab is a anti-CTLA-4 mAb that has been humanized. In a phase 2 study with advanced pancreatic cancer, ipilimumab yielded no response by itself, as measured by the response evaluation criteria in solid tumors (RECIST). In a phase 1 study with previously treated pancreatic cancer patients, ipilimumab was combined with GVAX [granulocyte-macrophage colony-stimulating factor (GM-CSF) gene-transfected tumor cell vaccine]. The efficacy of this combination treatment was demonstrated in this trial as ipilimumab plus GVAX raised median OS (5.7 *vs* 3.6 mo) and 1-year OS rate (27% *vs* 7%)[50] (Table 1). T cell receptor repertoires in peripheral blood from individuals taking ipilimumab with or without GVAX were evaluated using data from the same phase 1 trial. The results demonstrated that participants who had ipilimumab showed more repertoire alterations, particularly when paired with GVAX, which was linked to a much longer life span[51]. Gemcitabine and ipilimumab are a safe and practical treatment option for advanced pancreatic cancer, according to the findings of phase 1 clinical research that examined the long-lasting responses and OS benefit of this combination. Ipilimumab in combination with gemcitabine did not appear to be any more successful than gemcitabine alone in treating advanced pancreatic cancer, despite the fact that one patient in this research had a somewhat persistent response lasting over 20 mo[52] (Figure 3).

A different mAb targeting CTLA-4 is tremelimumab. Tremelimumab plus gemcitabine was well tolerated in a phase 1 investigation with advanced pancreatic cancer, and two participants showed partial responses; nonetheless, this study did not show any RECIST improvement[53]. Tremelimumab did not appear to be beneficial in a separate phase 2 trial in pancreatic cancer patients who had tumor progression after receiving prior conventional first-line 5-FU or gemcitabine-containing treatment[54].

Anti-PD-1 and anti-PD-L1 antibodies: Nivolumab, a monoclonal IG4 anti-PD-1 antibody from human, inhibits the interaction of PD-1 with either PD-L1 or PD-L2. Fifteen pancreatic cancer patients were treated with nivolumab and mogamulizumab, an anti-CC chemokine receptor 4 antibody, in a phase 1 study for patients with advanced or metastatic solid tumors, and only two unconfirmed responses were found[55]. In a multicenter, prospective clinical study, Klein *et al* [56] treated seven advanced cancer patients with pancreatic neuroendocrine neoplasms (NEN) with nivolumab 3 mg/kg and ipilimumab 1 mg/kg every 3 wk for four doses, then nivolumab 3 mg/kg every 2 wk for up to 96 wk, or until severe toxicity or disease progression occurred. They discovered that 43% of pancreatic NEN patients had an objective response. They proposed that combining nivolumab and ipilimumab immunotherapy revealed considerable therapeutic activity in subgroups of patients with advanced, high-grade pancreatic NEN. For 91 advanced pancreatic cancer patients who had not improved after 16 wk platinum-based treatment in 2022, Reiss *et al*[57] conducted a randomized, open-label, phase 1b/2 trial of niraparib with nivolumab or ipilimumab treatment. Using permuted block randomization, the patients were assigned (1:1) to receive four doses of oral niraparib 200 mg daily along with either intravenous nivolumab 240 mg or 480 mg every 2 wk or ipilimumab 3 mg/kg intravenously every 4 wk. They reported that the 6-mo PFS for niraparib plus nivolumab was 20.6% and 59.6% for niraparib plus ipilimumab. They concluded that the main goal was achieved in the niraparib plus ipilimumab maintenance group, while the PFS was reduced in the niraparib plus nivolumab group.

Another monoclonal IG4 antibody from human against PD-1 is pembrolizumab. In a phase 1b study of 11 advanced pancreatic cancer patients, pembrolizumab combined with nab-paclitaxel and gemcitabine produced six cases of stable disease and two cases of partial response. This combination's efficacy was marginally higher than that of gemcitabine combined with nab-paclitaxel in previous studies[58,59]. In comprehensive clinical research involving a variety of cancer types, it was shown that biomarkers related to the clinical success of pembrolizumab included the PD-L1 expression level, T-cell-inflamed gene expression profile, and tumor mutation burden. Patients with pancreatic cancer who received pembrolizumab had an ORR of 0% and an average PFS of 1.7 mo[60]. Another phase 2 clinical trial of pembrolizumab in patients with advanced pancreatic cancer and other solid tumors that are sensitive to the mismatch repair pathway loss-of-function mutations found that the objective radiographic response was 53% and the complete response was 21%[61]. The clinical response was not seen in a phase 1 study that tested the p53-expressing modified vaccinia Ankara virus (p53MVA) alone, but a phase 1 study that combined pembrolizumab with p53MVA showed that three out of 11 patients demonstrated clinical response and the disease was stable for 30, 32, and 49 wk[62,63]. Pembrolizumab was coupled with nab-paclitaxel or gemcitabine in a phase 1/2 clinical study. The OS and PFS were 15.0 and 9.1 mo, respectively, and the disease control rate in the 11 evaluable chemotherapy-naive pancreatic cancer patients was 100%[59]. In a phase 1, multicenter trial, the monoclonal IG4 antibody from human, BMS-936559, against PD-L1 was investigated for the treatment of several advanced cancers. Patients with renal-cell carcinoma, non-small-cell lung cancer, and melanoma all experienced long-term tumor reduction and stable illness as a result of BMS-936559; however, none of the 14 patients with pancreatic cancer who participated in this trial experienced a response[64]. Furthermore, Mehnert *et al*[65] found that pembrolizumab had anticancer efficacy in a subgroup of pancreatic cancer patients with NETs and was well tolerated. Moreover, to examine the CXCR4 antagonist BL-8040 (motixafortide)'s safety, efficacy, and immunobiological effects when combined with pembrolizumab and chemotherapy, Bockorny *et al*[66] conducted a phase 2a, open-label, two-cohort study in 37 chemotherapy-resistant, metastatic pancreatic cancer patients. They stated that further randomized trials should validate their findings before combining CXCR4 and PD-1 inhibition to treat pancreatic cancer

Table 1 Summary of completed clinical trials investigating immunotherapy in advanced pancreatic cancer patients

Ref.	Drug(s)	No. of patients	ORR (%)	Mean OS (mo)	Mean PFS (mo)	Results
Le *et al*[50], 2013	Ipilimumab *vs* ipilimumab plus GVAX	15/15	-	3.6/5.7 1-yr OS (%) 7/27	-	Ipilimumab combined with GVAX was efficacious in advanced pancreatic cancer treatment
Kamath *et al* [52], 2020	Ipilimumab plus gemcitabine	21	14	6.9	2.78	Gemcitabine plus Ipilimumab is a safe and tolerable regimen for advanced pancreatic cancer with a similar response rate to gemcitabine alone
Aglietta *et al* [53], 2014	Tremelimumab plus gemcitabine	34	-	7.4	-	Tremelimumab with gemcitabine had a favorable safety and tolerability profile, indicating that it should be studied further in patients with advanced pancreatic cancer
Renouf *et al* [54], 2022	Gemcitabine, nab-paclitaxel, durvalumab, and tremelimumab *vs* gemcitabine and nab-paclitaxel	119/61	30.3/23.3	9.8/8.8	5.5/5.4	The results did not demonstrate a benefit from adding durvalumab and tremelimumab to gemcitabine and nab-paclitaxel as a first line therapy in advanced pancreatic cancer patients
Reiss *et al* [57], 2022	Niraparib and nivolumab *vs* niraparib and ipilimumab	91 (46/45)	7.1/15.4	13.2/17.3	1.9/8.1	The advantage of niraparib with ipilimumab maintenance treatment extended to patients who did not have known DDR mutations, indicating that the impact is not dependent on DDR deficit
Bockorny *et al*[67], 2021	Motixafortide, pembrolizumab and FOLFIRINOX	43	13.2	6.6	3.8	In a group with poor prognoses and aggressive diseases, motixafortide and pembrolizumab in conjunction with FOLFIRINOX demonstrated effectiveness. The therapy was well tolerated
O'Reilly *et al*[69], 2019	Durvalumab *vs* durvalumab and tremelimumab	64 (32/32)	0/3.1	3.6/3.1	1.5/1.5	The medication was well tolerated, and both durvalumab monotherapy and durvalumab combined with tremelimumab were effective in treating advanced pancreatic cancer patients with a poor prognosis

DDR: DNA damage repair; FOLFIRINOX: Folinic acid, fluorouracil, irinotecan, and oxaliplatin; GVAX: Granulocyte-macrophage colony-stimulating factor gene-transfected tumor cell vaccine; ORR: Objective response rate; OS: Overall survival; PFS: Progression-free survival.

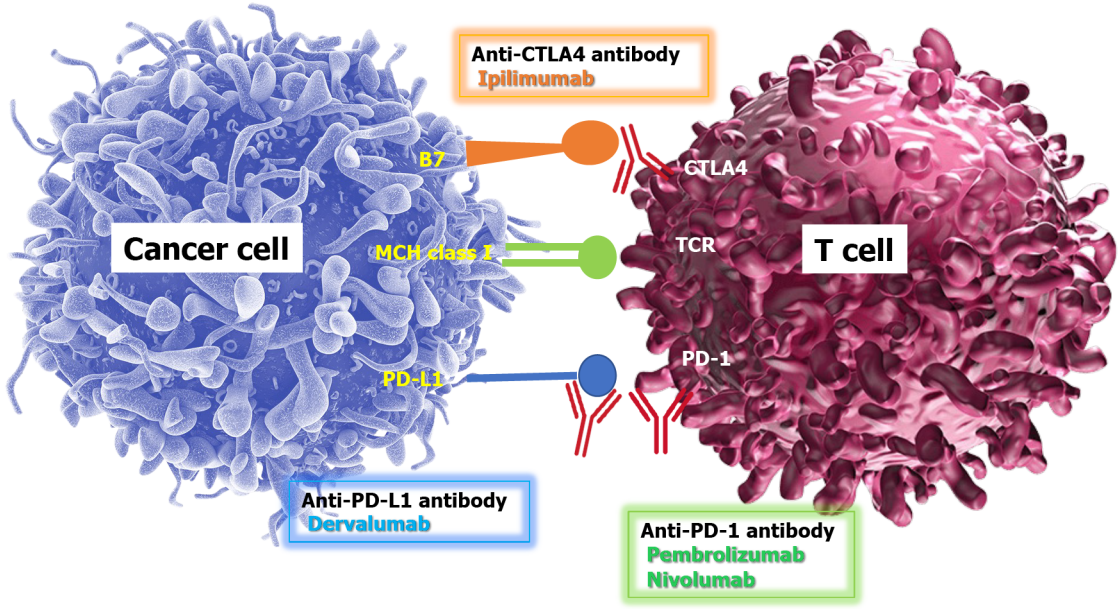

DOI: 10.4251/wjgo.v15.i10.1691

Figure 3 Treatment with immune check point inhibitors for advanced pancreatic cancer. CTLA4: Cytotoxic T-lymphocyte-associated protein 4; MHC: Major histocompatibility complex; PD-1: Programmed cell death protein 1; PD-L1: Programmed death-ligand 1; TCR: T cell receptor.

[67].

Another choice is durvalumab, a monoclonal IgG1 antibody from human that targets PD-L1 and infiltrating T cells in solid tumors. In patients with relapsed or refractory solid tumors, durvalumab was studied in a phase 1b/2 study alongside ibrutinib (a Bruton's tyrosine kinase inhibitor). This study's pancreatic cancer RR was 2% overall, with a median OS of 4.2 mo and median PFS of 1.7 mo. Despite having a good tolerability profile, this regimen had very limited antitumor activity against pancreatic cancer[68]. Another randomized phase 2 study using durvalumab was conducted in individuals with metastatic pancreatic cancer, either alone or in combination with tremelimumab. However, the ORR for individuals receiving tremelimumab plus durvalumab was just 3.1%, and patients treated with durvalumab alone had no response[69]. During a phase 1 study to establish the dose, atezolizumab, an engineered mAb against PD-L1, was found to be well tolerated in a Japanese group[70]. In a phase 1 study for advanced malignancies, atezolizumab was also evaluated in conjunction with navoximod, a small-molecule inhibitor of indoleamine 2,3-dioxygenase 1. There was no evidence to support the addition of navoximod to atezolizumab, but the safety and tolerability of this combination therapy were established, and anticancer efficacy was noted in a variety of tumor types, including pancreatic cancer[71].

Chimeric antigen receptor T-cell therapy

Using modified T-cell receptors or chimeric antigen receptors (CARs), in an effort to target tumor-associated antigens (TAAs), adoptive T-cell immunotherapy, a possible strategy for cancer immunotherapy, alters autologous cells that infiltrate tumors. The optimal target antigen is overexpressed on tumor cells but is seldom or never expressed on normal cells when employed in CAR-T cell therapy. Mesothelin, a cell-surface antigen that is raised in pancreatic cancer but is relatively weakly expressed in the peritoneum, pericardium, and pleura, is the perfect antigen for CAR-T cell treatment [72,73]. A mesothelin-targeted CAR-T-cell therapy has also been demonstrated to be efficient against tumor cells in preclinical conditions, according to several studies. Treatment with modified CAR-T cells targeting mesothelin resulted in strong anticancer action for tumor xenografts and the cell lines of pancreatic cancer[74-76]. In phase 1 research with metastatic pancreatic cancer that had become resistant to chemotherapy, autologous mesothelin-specific CAR-T cells (CARTmeso cells) were found to have potential anticancer benefits and be safe[77]. The cancer stem cell markers CD24 and HER2 are thought to contribute to the emergence of pancreatic cancer[78]. In addition, a phase 1 trial evaluated the safety, viability, and effectiveness of CAR-T cells combined with nab-paclitaxel and cyclophosphamide against HER2 in advanced pancreatic and biliary tract cancers. Five of 11 subjects had stable illness, with a median PFS of 4.8 mo, while one patient had a partial response lasting 4.5 mo. The study established the viability, safety, and the possibility of therapeutic efficacy of HER2-targeting CAR-T treatment[79]. In 60%-80% of pancreatic cancers, prostate stem cell antigen is expressed, but not in healthy tissues. CAR-T cells that target the prostate stem cell antigen have been shown to be beneficial for pancreatic malignancy in two different investigations[80,81]. When used as an antigen in CAR-T therapy, the Tn glycoform of MUC1 demonstrated target-specific cytotoxicity and reduced the development of xenografts made of pancreatic cancer cells[82]. *Ex vivo*-expanded cytokine-induced killer (CIK) cells were used in a phase 2 trial to assess the efficacy and safety of adoptive immunotherapy for advanced pancreatic cancer that is gemcitabine-refractory. The results showed promising improvements in patient quality of life (QoL)[83]. To evaluate the security and efficiency of autologous anti-EGFR CAR T-EGFR cells, Liu *et al*[84] carried out a phase 1 clinical study in patients with advanced pancreatic cancer. Immunohistochemically-detected EGFR expression levels on tumor cells must be over 50%. Six months after being chosen, 16 patients had one to three rounds of CAR T-EGFR cell injection after conditioning with 15 to 35 mg/kg cyclophosphamide and 100 to 200 mg/m^2 nab-paclitaxel. Grade > 3 adverse effects that might be reversed were fever, tiredness, mucosal or cutaneous toxicities, nausea, vomiting, pulmonary interstitial exudation, and pleural effusion. Eight of the 14 patients who were evaluable had stable disease for 2-4 mo, and four of them saw a partial response. The median OS was 4.9 mo for 14 evaluable patients who were treated with CAR T-EGFR cells for the first cycle, and the median PFS was 3 mo. Lower EGFR expression was seen on tumor cells in patients who experienced stable disease and a reduction in liver metastatic lesions. Additionally, the clinical response was enhanced by central memory T cell enrichment in the injected cells. They claimed that patients with advanced pancreatic cancer can get a safe and effective therapy using CAR T-EGFR cells.

Cancer vaccines

Compared to preventive cancer vaccines, therapeutic cancer vaccines have drawn more attention. Vaccines made from a patient's tumor antigens or cells are known as autologous vaccines, whereas allogeneic vaccines are made from biological material from a different individual. Pancreatic cancer has been the subject of research into many therapeutic cancer vaccines, including whole-cell tumor, DNA, idiotype, DC viral vector, and antigen vaccines[85,86].

Whole-cell vaccines: In a preclinical investigation, increased GM-CSF expression was shown to enhance long-term anticancer efficacy in vaccine-based therapy. As a result, GVAX, the first allogenic pancreatic cancer whole-cell-based vaccine, was created using two cell lines from pancreatic cancer patients and had been engineered for the expression of GM-CSF followed by radiation to block cell division in the future. In a phase I clinical investigation, GVAX was initially evaluated in people who had their pancreatic cancer surgically removed. The results of this trial showed that GVAX was risk-free, had few side effects, and looked to prolong at least 25 mo for the disease-free time in 4 of the 14 patients who took part in the study[87]. Furthermore, in these three participants, delayed-type hypersensitivity reactions were exacerbated by GVAX. GVAX was investigated in conjunction with cyclophosphamide in patients with advanced pancreatic cancer in a phase 2 study because of the encouraging outcomes. Pancreatic cancer has an elevated level of mesothelin, a tumor differentiation antigen. In this study, mesothelin-specific T-cell responses were seen in the patients who received GVAX treatment and were shown to be improving. GVAX alone or in combination with cyclophosphamide demonstrated no harm. However, as compared to cyclophosphamide alone, the inclusion of GVAX did not appear to

improve median survival[88]. In a phase 2 trial including surgically resected pancreatic cancer patients, GVAX was used as a neo-adjuvant therapy combined with chemoradiation (5-FU-based). Immunotherapy resulted in the discovery that mesothelin-specific CD8+ T cells were associated with the disease-free survival rate, and when chemoradiation and GVAX were used together, the OS looked to be better than that in previously reported studies for pancreatic cancer that had been surgically removed. In previously treated pancreatic cancer patients, GVAX was also tried in conjunction with ipilimumab. Ipilimumab with the inclusion of GVAX produced a significant longer median OS and 1-year OS of 5.7 *vs* 3.6 mo and 27% *vs* 7%, respectively[89]. Additionally, in patients with an OS of more than 4.3 mo, the peak number of T-cell repertoire and mesothelin-specific T cells was increased. Further research into how immunotherapy affects pancreatic cancer TME revealed that GVAX treatment upregulated immunosuppressive regulatory mechanisms. This indicates that individuals with pancreatic cancer who have received a vaccination may be better candidates for immune checkpoint and other immunomodulatory therapies, such as PD-1/PD-L1 inhibitors, than vaccine-naive patients[90]. The efficiency of the *Listeria monocytogenes* expressing mesothelin (CRS-207) and GVAX booster vaccines combined with cyclophosphamide minimum dose was evaluated in advanced pancreatic cancer patients who had previously received treatment. According to this study, CRS-207 and Cy/GVAX heterologous booster had a superior OS than using only Cy/GVAX (6.1 *vs* 3.9 mo) [91]. However, a recent phase 2b, multicenter trial of CRS-207 and GVAX found no survival advantages for the combination of Cy/GVAX and CRS-207 over single-agent chemotherapy in patients with metastatic pancreatic cancer who had previously received treatment[92]. In a phase 1 clinical trial, CRS-207 produced immunological activation, mesothelin-specific T-cell responses, and listeriolysin O, and and the participant survival rate was 37% within 15 mo. It was also demonstrated to be safe[93]. Two pancreatic cancer cell lines were altered to generate murine 1,3-galactosyl-transferase to create algenpantucel-L, a second allogenic, irradiated, whole-cell-based tumor vaccine. Adoptive transfer of lymphocytes from mice that received melanoma tumor cell lines as a vaccine in a preclinical animal model expressing β-1,3-galactosyltransferase reduced mouse lung metastases[94]. These findings sparked a phase 2, multicenter study of algenpantucel-L in patients with resected pancreatic cancer receiving gemcitabine- or 5-fluorouracil-based chemoradio-therapy. In contrast to recent trials, which found 45% and 65%, respectively, for the median 1-year PFS and OS, the addition of algenpantucel-L to traditional adjuvant therapy may have improved survival in this trial[95]. In a recent multicenter, phase 3, open-label, randomized trial, algenpantucel-L immunotherapy in combination with standard of care (SOC) chemoradiation and chemotherapy therapy was compared to SOC chemoradiation and chemotherapy therapy alone in 303 Locally advanced or borderline resectable pancreatic cancer patients[96]. They found that the experimental group's median OS was 14.3 mo, whereas the SOC group's median OS was 14.9 mo. The median PFS for the SOC group was 13.4 mo as opposed to 12.4 mo for the experimental group. The researchers found that patients who received SOC chemoradiation and neoadjuvant chemotherapy and had locally advanced unresectable or borderline resectable pancreatic cancer had not a longer OS benefit after algenpantucel-L immunotherapy.

Peptide vaccines: About 90% of pancreatic cancers have KRAS mutations, and the mutant KRAS peptide is presented to CD4+ and CD8+ T lymphocytes as a foreign antigen. In a recent study, two out of five pancreatic cancer patients who received treatment with a synthetic KRAS mutant peptide showed a brief KRAS-specific T-cell response[97-99]. In a subsequent phase 1/2 pancreatic cancer research trial, 58% (25/43) of patients developed peptide-specific immunity after receiving a KRAS peptide vaccine and GM-CSF adjuvant therapy, which also helped advanced pancreatic patients live longer (146 *vs* 61 d)[100]. Patients with an immunological response to a KRAS peptide vaccination had a 20% 10-year survival rate compared to 0% in a group of pancreatic cancer patients who had not received the vaccine, and this difference persisted more than ten years after the start of long-term follow-up for these patients[101]. In a recent therapeutic study, individuals with resected pancreatic cancer and detected KRAS mutations received GM-CSF treatment plus a KRAS peptide vaccination. Nine patients (or 25%) had an evaluable immune response, of which three had a delayed-type hypersensitivity reaction and one had a specific immune response to their KRAS mutation[102]. Pancreatic cancers have overexpression of mucin 1 (MUC1), a type I transmembrane protein that is highly immunogenic. Various MUC1 vaccine formulations have been tested in phase 1 trials; however, it appears that MUC1-specific T-cell responses are exclusively induced by the vaccination of DC with the MUC1 peptide[103-105]. Gastrin has been linked to both endocrine and autocrine growth pathways and is overexpressed in pancreatic cancer. An antibody response was found in 67% (20/31) of patients in a phase 2 study employing the anti-gastrin immunogen G17DT in advanced pancreatic cancer, and antibody responders lived much longer than non-responders[106]. Patients who had an anti-G17DT response (73.8%) had a significantly higher median survival than non-responders (151 *vs* 82 d) in a different randomized multicenter trial using G17DT[107]. A vaccine that targets telomerase, called GV1001, was made using the human TERT peptide. Patients with nonresectable pancreatic cancer received treatment with GV1001 and GM-CSF in a phase 1/2 study, and the treatment's safety, tolerability, and immunogenicity were assessed. Immune responses that were seen in 24 of 38 individuals and were connected to longer lifespans served as proof of the safety of GV1001[108]. In a phase 3 study, GV1001 was also evaluated in individuals taking gemcitabine or capecitabine for locally advanced or metastatic pancreatic cancer. However, compared to pancreatic cancer patients receiving chemotherapy alone, the incorporation of GV1001 had no positive impact on OS[109]. The identical outcomes were seen in a different clinical experiment as well [110].

DC vaccines: Because the most important antigen-presenting cells are DCs which excite innocent T cells, a DC vaccine is made by loading TAAs *ex vivo* and then reinfusing them into patients. An autologous DC vaccination containing a MUC1 peptide was tested in resected pancreatic and biliary cancers in an innovative phase 1/2 trial. The DC vaccination was well tolerated and had no obvious side effects. Four of the twelve patients were still alive and had no recurrence throughout a follow-up period of more than four years[105]. In patients with resistant pancreatic cancer, a DC vaccination was also examined in conjunction with gemcitabine and/or S-1 treatment. Two of the 49 patients that were included

experienced complete remission, while five others did so partially, and ten had stable disease[111]. Compared to those who received a DC vaccination and chemotherapy alone, patients who also received lymphokine-activated killer cells had a higher rate of survival. This study established the safety and possible efficacy of combining a DC vaccine with chemotherapy in patients with advanced pancreatic cancer who had not responded to standard treatment. In a phase 1 study, poly-ICLC, a Toll-like receptor-3 agonist, was combined with DC-based immunotherapy. The peripheral blood of HLA-A2+ patients was utilized to generate autologous DCs, which were then combined with three definite A2-restricted peptides and was returned to advanced pancreatic cancer patients. On the days of their vaccinations, subjects concurrently got poly(IC:LC) intramuscularly. The median OS for all 12 subjects was 7.7 mo, and of the eight subjects who received imaging on day 56, four had stable disease and four had progression of the disease[112]. An investigation of the clinical outcomes and safety of immunotherapy using DC-CIK in combination with chemotherapy S-1 in pancreatic cancer was the goal of a phase 1/2 trial. In comparison to DC-CIK alone (85 and 128 d), chemotherapy alone (92 and 141 d), or supportive care alone (43 and 52 d), the combination of DC-CIK infusions and S-1 caused importantly longer median PFS and OS (136 and 212 d), proving that it was safe, changed the peripheral blood immune repertoire, and produced a good PFS and OS[113]. In a phase 1 study of patients with pancreatic cancer that was surgically resected, the Wilms' tumor 1 (WT1) peptide was loaded in a DC (WT1-DC) vaccine and evaluated with chemotherapy. There was no discernible toxicity when WT1-DC was combined with S-1 or S-1 with gemcitabine, and seven out of the eight patients had WT1-specific cytotoxic T-lymphocytes[114].

CONCLUSION

Our understanding of the biology of pancreatic cancer has significantly advanced over the past few decades, but tragically, this has not led to a meaningful increase in the therapeutic management of the majority of patients. The aggressiveness of pancreatic cancer and the lateness of its discovery make it very challenging to cure. The majority of patients have advanced stages, which makes therapy difficult. Although advanced pancreatic cancer can be treated with chemotherapy, radiation therapy, and surgery to increase survival and manage symptoms, there is no definite treatment for the disease. The inability of chemotherapy to distinguish between cancer and healthy cells when it targets a range of biological pathways leads to severe side effects. In order to target growth factors, other proteins involved in the development of the illness, and cancer cell surface receptors, therapies based on SMIs and mAbs are necessary. If the condition is discovered quickly and a focused treatment is employed, patients with pancreatic cancer may have a better chance of living. The majority of the targeted treatments investigated for the treatment of pancreatic malignancies have been shown to be unsuccessful, despite the fact that many of them have been developed. There is a need for innovative treatment approaches for pancreatic cancer, such as cancer vaccines, in addition to the conventional targeted medicines and immunotherapies that have been investigated for years. As an alternative, strategies that combine already-existing technology or therapy modalities might also be very helpful, but this would need further investigation and testing.

FOOTNOTES

Author contributions: Leowattana W wrote the paper; Leowattana T and Leowattana P collected the data.

Conflict-of-interest statement: The authors declare no conflicts of interest related to this article.

Country/Territory of origin: Thailand

ORCID number: Wattana Leowattana 0000-0003-4257-2480; Tawithep Leowattana 0000-0003-2316-3585.

S-Editor: Yan JP
L-Editor: Wang TQ
P-Editor: Yan JP

REFERENCES

1 **GBD 2017 Pancreatic Cancer Collaborators**. The global, regional, and national burden of pancreatic cancer and its attributable risk factors in 195 countries and territories, 1990-2017: a systematic analysis for the Global Burden of Disease Study 2017. *Lancet Gastroenterol Hepatol* 2019; **4**: 934-947 [PMID: 31648972 DOI: 10.1016/S2468-1253(19)30347-4]

2 **Cipora E**, Partyka O, Pajewska M, Czerw A, Sygit K, Sygit M, Kaczmarski M, Mękal D, Krzych-Fałta E, Jurczak A, Karakiewicz-Krawczyk K, Wieder-Huszla S, Banaś T, Bandurska E, Ciećko W, Deptała A. Treatment Costs and Social Burden of Pancreatic Cancer. *Cancers (Basel)*

2023; **15** [PMID: 36980796 DOI: 10.3390/cancers15061911]

3 **Klein AP**. Pancreatic cancer epidemiology: understanding the role of lifestyle and inherited risk factors. *Nat Rev Gastroenterol Hepatol* 2021; **18**: 493-502 [PMID: 34002083 DOI: 10.1038/s41575-021-00457-x]

4 **Rawla P**, Sunkara T, Gaduputi V. Epidemiology of Pancreatic Cancer: Global Trends, Etiology and Risk Factors. *World J Oncol* 2019; **10**: 10-27 [PMID: 30834048 DOI: 10.14740/wjon1166]

5 **Ferlay J**, Colombet M, Soerjomataram I, Mathers C, Parkin DM, Piñeros M, Znaor A, Bray F. Estimating the global cancer incidence and mortality in 2018: GLOBOCAN sources and methods. *Int J Cancer* 2019; **144**: 1941-1953 [PMID: 30350310 DOI: 10.1002/ijc.31937]

6 **Stolzenberg-Solomon RZ**, Schairer C, Moore S, Hollenbeck A, Silverman DT. Lifetime adiposity and risk of pancreatic cancer in the NIH-AARP Diet and Health Study cohort. *Am J Clin Nutr* 2013; **98**: 1057-1065 [PMID: 23985810 DOI: 10.3945/ajcn.113.058123]

7 **Rebours V**, Gaujoux S, d'Assignies G, Sauvanet A, Ruszniewski P, Lévy P, Paradis V, Bedossa P, Couvelard A. Obesity and Fatty Pancreatic Infiltration Are Risk Factors for Pancreatic Precancerous Lesions (PanIN). *Clin Cancer Res* 2015; **21**: 3522-3528 [PMID: 25700304 DOI: 10.1158/1078-0432.CCR-14-2385]

8 **Blackford A**, Parmigiani G, Kensler TW, Wolfgang C, Jones S, Zhang X, Parsons DW, Lin JC, Leary RJ, Eshleman JR, Goggins M, Jaffee EM, Iacobuzio-Donahue CA, Maitra A, Klein A, Cameron JL, Olino K, Schulick R, Winter J, Vogelstein B, Velculescu VE, Kinzler KW, Hruban RH. Genetic mutations associated with cigarette smoking in pancreatic cancer. *Cancer Res* 2009; **69**: 3681-3688 [PMID: 19351817 DOI: 10.1158/0008-5472.CAN-09-0015]

9 **Naudin S**, Viallon V, Hashim D, Freisling H, Jenab M, Weiderpass E, Perrier F, McKenzie F, Bueno-de-Mesquita HB, Olsen A, Tjønneland A, Dahm CC, Overvad K, Mancini FR, Rebours V, Boutron-Ruault MC, Katzke V, Kaaks R, Bergmann M, Boeing H, Peppa E, Karakatsani A, Trichopoulou A, Pala V, Masala G, Panico S, Tumino R, Sacerdote C, May AM, van Gils CH, Rylander C, Borch KB, Chirlaque López MD, Sánchez MJ, Ardanaz E, Quirós JR, Amiano Exezarreta P, Sund M, Drake I, Regnér S, Travis RC, Wareham N, Aune D, Riboli E, Gunter MJ, Duell EJ, Brennan P, Ferrari P. Healthy lifestyle and the risk of pancreatic cancer in the EPIC study. *Eur J Epidemiol* 2020; **35**: 975-986 [PMID: 31564045 DOI: 10.1007/s10654-019-00559-6]

10 **Pereira SP**, Oldfield L, Ney A, Hart PA, Keane MG, Pandol SJ, Li D, Greenhalf W, Jeon CY, Koay EJ, Almario CV, Halloran C, Lennon AM, Costello E. Early detection of pancreatic cancer. *Lancet Gastroenterol Hepatol* 2020; **5**: 698-710 [PMID: 32135127 DOI: 10.1016/S2468-1253(19)30416-9]

11 **Weissman S**, Takakura K, Eibl G, Pandol SJ, Saruta M. The Diverse Involvement of Cigarette Smoking in Pancreatic Cancer Development and Prognosis. *Pancreas* 2020; **49**: 612-620 [PMID: 32433397 DOI: 10.1097/MPA.0000000000001550]

12 **Biller LH**, Wolpin BM, Goggins M. Inherited Pancreatic Cancer Syndromes and High-Risk Screening. *Surg Oncol Clin N Am* 2021; **30**: 773-786 [PMID: 34511196 DOI: 10.1016/j.soc.2021.06.002]

13 **Vietri MT**, D'Elia G, Caliendo G, Albanese L, Signoriello G, Napoli C, Molinari AM. Pancreatic Cancer with Mutation in BRCA1/2, MLH1, and APC Genes: Phenotype Correlation and Detection of a Novel Germline BRCA2 Mutation. *Genes (Basel)* 2022; **13** [PMID: 35205366 DOI: 10.3390/genes13020321]

14 **Kastrinos F**, Mukherjee B, Tayob N, Wang F, Sparr J, Raymond VM, Bandipalliam P, Stoffel EM, Gruber SB, Syngal S. Risk of pancreatic cancer in families with Lynch syndrome. *JAMA* 2009; **302**: 1790-1795 [PMID: 19861671 DOI: 10.1001/jama.2009.1529]

15 **Saba H**, Goggins M. Familial Pancreatic Cancer. *Gastroenterol Clin North Am* 2022; **51**: 561-575 [PMID: 36153110 DOI: 10.1016/j.gtc.2022.06.006]

16 **Walter FM**, Mills K, Mendonça SC, Abel GA, Basu B, Carroll N, Ballard S, Lancaster J, Hamilton W, Rubin GP, Emery JD. Symptoms and patient factors associated with diagnostic intervals for pancreatic cancer (SYMPTOM pancreatic study): a prospective cohort study. *Lancet Gastroenterol Hepatol* 2016; **1**: 298-306 [PMID: 28404200 DOI: 10.1016/S2468-1253(16)30079-6]

17 **Macdonald S**, Macleod U, Campbell NC, Weller D, Mitchell E. Systematic review of factors influencing patient and practitioner delay in diagnosis of upper gastrointestinal cancer. *Br J Cancer* 2006; **94**: 1272-1280 [PMID: 16622459 DOI: 10.1038/sj.bjc.6603089]

18 **Schmidt-Hansen M**, Berendse S, Hamilton W. Symptoms of Pancreatic Cancer in Primary Care: A Systematic Review. *Pancreas* 2016; **45**: 814-818 [PMID: 26495795 DOI: 10.1097/MPA.0000000000000527]

19 **Chang VT**, Sandifer C, Zhong F. GI Symptoms in Pancreatic Cancer. *Clin Colorectal Cancer* 2023; **22**: 24-33 [PMID: 36623952 DOI: 10.1016/j.clcc.2022.12.002]

20 **Gobbi PG**, Bergonzi M, Comelli M, Villano L, Pozzoli D, Vanoli A, Dionigi P. The prognostic role of time to diagnosis and presenting symptoms in patients with pancreatic cancer. *Cancer Epidemiol* 2013; **37**: 186-190 [PMID: 23369450 DOI: 10.1016/j.canep.2012.12.002]

21 **Burris HA 3rd**, Moore MJ, Andersen J, Green MR, Rothenberg ML, Modiano MR, Cripps MC, Portenoy RK, Storniolo AM, Tarassoff P, Nelson R, Dorr FA, Stephens CD, Von Hoff DD. Improvements in survival and clinical benefit with gemcitabine as first-line therapy for patients with advanced pancreas cancer: a randomized trial. *J Clin Oncol* 1997; **15**: 2403-2413 [PMID: 9196156 DOI: 10.1200/JCO.1997.15.6.2403]

22 **Moore MJ**, Goldstein D, Hamm J, Figer A, Hecht JR, Gallinger S, Au HJ, Murawa P, Walde D, Wolff RA, Campos D, Lim R, Ding K, Clark G, Voskoglou-Nomikos T, Ptasynski M, Parulekar W; National Cancer Institute of Canada Clinical Trials Group. Erlotinib plus gemcitabine compared with gemcitabine alone in patients with advanced pancreatic cancer: a phase III trial of the National Cancer Institute of Canada Clinical Trials Group. *J Clin Oncol* 2007; **25**: 1960-1966 [PMID: 17452677 DOI: 10.1200/JCO.2006.07.9525]

23 **Conroy T**, Desseigne F, Ychou M, Bouché O, Guimbaud R, Bécouarn Y, Adenis A, Raoul JL, Gourgou-Bourgade S, de la Fouchardière C, Bennouna J, Bachet JB, Khemissa-Akouz F, Péré-Vergé D, Delbaldo C, Assenat E, Chauffert B, Michel P, Montoto-Grillot C, Ducreux M; Groupe Tumeurs Digestives of Unicancer; PRODIGE Intergroup. FOLFIRINOX *vs* gemcitabine for metastatic pancreatic cancer. *N Engl J Med* 2011; **364**: 1817-1825 [PMID: 21561347 DOI: 10.1056/NEJMoa1011923]

24 **Von Hoff DD**, Ervin T, Arena FP, Chiorean EG, Infante J, Moore M, Seay T, Tjulandin SA, Ma WW, Saleh MN, Harris M, Reni M, Dowden S, Laheru D, Bahary N, Ramanathan RK, Tabernero J, Hidalgo M, Goldstein D, Van Cutsem E, Wei X, Iglesias J, Renschler MF. Increased survival in pancreatic cancer with nab-paclitaxel plus gemcitabine. *N Engl J Med* 2013; **369**: 1691-1703 [PMID: 24131140 DOI: 10.1056/NEJMoa1304369]

25 **Chan KKW**, Guo H, Cheng S, Beca JM, Redmond-Misner R, Isaranuwatchai W, Qiao L, Earle C, Berry SR, Biagi JJ, Welch S, Meyers BM, Mittmann N, Coburn N, Arias J, Schwartz D, Dai WF, Gavura S, McLeod R, Kennedy ED. Real-world outcomes of FOLFIRINOX *vs* gemcitabine and nab-paclitaxel in advanced pancreatic cancer: A population-based propensity score-weighted analysis. *Cancer Med* 2020; **9**: 160-169 [PMID: 31724340 DOI: 10.1002/cam4.2705]

26 **Wang Y**, Camateros P, Cheung WY. A Real-World Comparison of FOLFIRINOX, Gemcitabine Plus nab-Paclitaxel, and Gemcitabine in Advanced Pancreatic Cancers. *J Gastrointest Cancer* 2019; **50**: 62-68 [PMID: 29143916 DOI: 10.1007/s12029-017-0028-5]

27 **Sohal DPS**, Kennedy EB, Khorana A, Copur MS, Crane CH, Garrido-Laguna I, Krishnamurthi S, Moravek C, O'Reilly EM, Philip PA, Ramanathan RK, Ruggiero JT, Shah MA, Urba S, Uronis HE, Lau MW, Laheru D. Metastatic Pancreatic Cancer: ASCO Clinical Practice Guideline Update. *J Clin Oncol* 2018; **36**: 2545-2556 [PMID: 29791286 DOI: 10.1200/JCO.2018.78.9636]

28 **Paluri RK**, Kasi A, Young C, Posey JA. Second-line treatment for metastatic pancreatic cancer. *Clin Adv Hematol Oncol* 2020; **18**: 106-115 [PMID: 32558804]

29 **Petrelli F**, Parisi A, Tomasello G, Mini E, Arru M, Russo A, Garrone O, Khakoo S, Ardito R, Ghidini M. Comparison of different second line treatments for metastatic pancreatic cancer: a systematic review and network meta-analysis. *BMC Gastroenterol* 2023; **23**: 212 [PMID: 37337148 DOI: 10.1186/s12876-023-02853-w]

30 **Zhong L**, Li Y, Xiong L, Wang W, Wu M, Yuan T, Yang W, Tian C, Miao Z, Wang T, Yang S. Small molecules in targeted cancer therapy: advances, challenges, and future perspectives. *Signal Transduct Target Ther* 2021; **6**: 201 [PMID: 34054126 DOI: 10.1038/s41392-021-00572-w]

31 **Roskoski R Jr**. Properties of FDA-approved small molecule protein kinase inhibitors: A 2023 update. *Pharmacol Res* 2023; **187**: 106552 [PMID: 36403719 DOI: 10.1016/j.phrs.2022.106552]

32 **Ayala-Aguilera CC**, Valero T, Lorente-Macías Á, Baillache DJ, Croke S, Unciti-Broceta A. Small Molecule Kinase Inhibitor Drugs (1995-2021): Medical Indication, Pharmacology, and Synthesis. *J Med Chem* 2022; **65**: 1047-1131 [PMID: 34624192 DOI: 10.1021/acs.jmedchem.1c00963]

33 **Murugan NJ**, Voutsadakis IA. Proteasome regulators in pancreatic cancer. *World J Gastrointest Oncol* 2022; **14**: 38-54 [PMID: 35116102 DOI: 10.4251/wjgo.v14.i1.38]

34 **Arpalahti L**, Haglund C, Holmberg CI. Proteostasis Dysregulation in Pancreatic Cancer. *Adv Exp Med Biol* 2020; **1233**: 101-115 [PMID: 32274754 DOI: 10.1007/978-3-030-38266-7_4]

35 **Alberts SR**, Foster NR, Morton RF, Kugler J, Schaefer P, Wiesenfeld M, Fitch TR, Steen P, Kim GP, Gill S. PS-341 and gemcitabine in patients with metastatic pancreatic adenocarcinoma: a North Central Cancer Treatment Group (NCCTG) randomized phase II study. *Ann Oncol* 2005; **16**: 1654-1661 [PMID: 16085692 DOI: 10.1093/annonc/mdi324]

36 **Kim A**, Ha J, Kim J, Cho Y, Ahn J, Cheon C, Kim SH, Ko SG, Kim B. Natural Products for Pancreatic Cancer Treatment: From Traditional Medicine to Modern Drug Discovery. *Nutrients* 2021; **13** [PMID: 34836055 DOI: 10.3390/nu13113801]

37 **El-Khoueiry AB**, Ramanathan RK, Yang DY, Zhang W, Shibata S, Wright JJ, Gandara D, Lenz HJ. A randomized phase II of gemcitabine and sorafenib *vs* sorafenib alone in patients with metastatic pancreatic cancer. *Invest New Drugs* 2012; **30**: 1175-1183 [PMID: 21424698 DOI: 10.1007/s10637-011-9658-9]

38 **Gonçalves A**, Gilabert M, François E, Dahan L, Perrier H, Lamy R, Re D, Largillier R, Gasmi M, Tchiknavorian X, Esterni B, Genre D, Moureau-Zabotto L, Giovannini M, Seitz JF, Delpero JR, Turrini O, Viens P, Raoul JL. BAYPAN study: a double-blind phase III randomized trial comparing gemcitabine plus sorafenib and gemcitabine plus placebo in patients with advanced pancreatic cancer. *Ann Oncol* 2012; **23**: 2799-2805 [PMID: 22771827 DOI: 10.1093/annonc/mds135]

39 **Sinn M**, Liersch T, Riess H, Gellert K, Stübs P, Waldschmidt D, Lammert F, Maschmeyer G, Bechstein W, Bitzer M, Denzlinger C, Hofheinz R, Lindig U, Ghadimi M, Hinke A, Striefler JK, Pelzer U, Bischoff S, Bahra M, Oettle H. CONKO-006: A randomised double-blinded phase IIb-study of additive therapy with gemcitabine + sorafenib/placebo in patients with R1 resection of pancreatic cancer - Final results. *Eur J Cancer* 2020; **138**: 172-181 [PMID: 32890813 DOI: 10.1016/j.ejca.2020.06.032]

40 **Blumenthal GM**, Cortazar P, Zhang JJ, Tang S, Sridhara R, Murgo A, Justice R, Pazdur R. FDA approval summary: sunitinib for the treatment of progressive well-differentiated locally advanced or metastatic pancreatic neuroendocrine tumors. *Oncologist* 2012; **17**: 1108-1113 [PMID: 22836448 DOI: 10.1634/theoncologist.2012-0044]

41 **Damaskos C**, Garmpis N, Karatzas T, Nikolidakis L, Kostakis ID, Garmpi A, Karamaroudis S, Boutsikos G, Damaskou Z, Kostakis A, Kouraklis G. Histone Deacetylase (HDAC) Inhibitors: Current Evidence for Therapeutic Activities in Pancreatic Cancer. *Anticancer Res* 2015; **35**: 3129-3135 [PMID: 26026072]

42 **Li Y**, Seto E. HDACs and HDAC Inhibitors in Cancer Development and Therapy. *Cold Spring Harb Perspect Med* 2016; **6** [PMID: 27599530 DOI: 10.1101/cshperspect.a026831]

43 **Yousefi H**, Yuan J, Keshavarz-Fathi M, Murphy JF, Rezaei N. Immunotherapy of cancers comes of age. *Expert Rev Clin Immunol* 2017; **13**: 1001-1015 [PMID: 28795649 DOI: 10.1080/1744666X.2017.1366315]

44 **Menon S**, Shin S, Dy G. Advances in Cancer Immunotherapy in Solid Tumors. *Cancers (Basel)* 2016; **8** [PMID: 27886124 DOI: 10.3390/cancers8120106]

45 **Mukherji R**, Debnath D, Hartley ML, Noel MS. The Role of Immunotherapy in Pancreatic Cancer. *Curr Oncol* 2022; **29**: 6864-6892 [PMID: 36290818 DOI: 10.3390/curroncol29100541]

46 **Balachandran VP**, Beatty GL, Dougan SK. Broadening the Impact of Immunotherapy to Pancreatic Cancer: Challenges and Opportunities. *Gastroenterology* 2019; **156**: 2056-2072 [PMID: 30660727 DOI: 10.1053/j.gastro.2018.12.038]

47 **Li B**, Chan HL, Chen P. Immune Checkpoint Inhibitors: Basics and Challenges. *Curr Med Chem* 2019; **26**: 3009-3025 [PMID: 28782469 DOI: 10.2174/0929867324666170804143706]

48 **Tison A**, Garaud S, Chiche L, Cornec D, Kostine M. Immune-checkpoint inhibitor use in patients with cancer and pre-existing autoimmune diseases. *Nat Rev Rheumatol* 2022; **18**: 641-656 [PMID: 36198831 DOI: 10.1038/s41584-022-00841-0]

49 **Tang Q**, Chen Y, Li X, Long S, Shi Y, Yu Y, Wu W, Han L, Wang S. The role of PD-1/PD-L1 and application of immune-checkpoint inhibitors in human cancers. *Front Immunol* 2022; **13**: 964442 [PMID: 36177034 DOI: 10.3389/fimmu.2022.964442]

50 **Le DT**, Lutz E, Uram JN, Sugar EA, Onners B, Solt S, Zheng L, Diaz LA Jr, Donehower RC, Jaffee EM, Laheru DA. Evaluation of ipilimumab in combination with allogeneic pancreatic tumor cells transfected with a GM-CSF gene in previously treated pancreatic cancer. *J Immunother* 2013; **36**: 382-389 [PMID: 23924790 DOI: 10.1097/CJI.0b013e31829fb7a2]

51 **Hopkins AC**, Yarchoan M, Durham JN, Yusko EC, Rytlewski JA, Robins HS, Laheru DA, Le DT, Lutz ER, Jaffee EM. T cell receptor repertoire features associated with survival in immunotherapy-treated pancreatic ductal adenocarcinoma. *JCI Insight* 2018; **3** [PMID: 29997287 DOI: 10.1172/jci.insight.122092]

52 **Kamath SD**, Kalyan A, Kircher S, Nimeiri H, Fought AJ, Benson A 3rd, Mulcahy M. Ipilimumab and Gemcitabine for Advanced Pancreatic Cancer: A Phase Ib Study. *Oncologist* 2020; **25**: e808-e815 [PMID: 31740568 DOI: 10.1634/theoncologist.2019-0473]

53 **Aglietta M**, Barone C, Sawyer MB, Moore MJ, Miller WH Jr, Bagalà C, Colombi F, Cagnazzo C, Gioeni L, Wang E, Huang B, Fly KD, Leone F. A phase I dose escalation trial of tremelimumab (CP-675,206) in combination with gemcitabine in chemotherapy-naive patients with metastatic pancreatic cancer. *Ann Oncol* 2014; **25**: 1750-1755 [PMID: 24907635 DOI: 10.1093/annonc/mdu205]

54 **Renouf DJ**, Loree JM, Knox JJ, Topham JT, Kavan P, Jonker D, Welch S, Couture F, Lemay F, Tehfe M, Harb M, Aucoin N, Ko YJ, Tang PA, Ramjeesingh R, Meyers BM, Kim CA, Du P, Jia S, Schaeffer DF, Gill S, Tu D, O'Callaghan CJ. The CCTG PA.7 phase II trial of gemcitabine and nab-paclitaxel with or without durvalumab and tremelimumab as initial therapy in metastatic pancreatic ductal adenocarcinoma. *Nat Commun* 2022; **13**: 5020 [PMID: 36028483 DOI: 10.1038/s41467-022-32591-8]

55 **Doi T**, Muro K, Ishii H, Kato T, Tsushima T, Takenoyama M, Oizumi S, Gemmoto K, Suna H, Enokitani K, Kawakami T, Nishikawa H, Yamamoto N. A Phase I Study of the Anti-CC Chemokine Receptor 4 Antibody, Mogamulizumab, in Combination with Nivolumab in Patients with Advanced or Metastatic Solid Tumors. *Clin Cancer Res* 2019; **25**: 6614-6622 [PMID: 31455681 DOI: 10.1158/1078-0432.CCR-19-1090]

56 **Klein O**, Kee D, Markman B, Michael M, Underhill C, Carlino MS, Jackett L, Lum C, Scott C, Nagrial A, Behren A, So JY, Palmer J, Cebon J. Immunotherapy of Ipilimumab and Nivolumab in Patients with Advanced Neuroendocrine Tumors: A Subgroup Analysis of the CA209-538 Clinical Trial for Rare Cancers. *Clin Cancer Res* 2020; **26**: 4454-4459 [PMID: 32532787 DOI: 10.1158/1078-0432.CCR-20-0621]

57 **Reiss KA**, Mick R, Teitelbaum U, O'Hara M, Schneider C, Massa R, Karasic T, Tondon R, Onyiah C, Gosselin MK, Donze A, Domchek SM, Vonderheide RH. Niraparib plus nivolumab or niraparib plus ipilimumab in patients with platinum-sensitive advanced pancreatic cancer: a randomised, phase 1b/2 trial. *Lancet Oncol* 2022; **23**: 1009-1020 [PMID: 35810751 DOI: 10.1016/S1470-2045(22)00369-2]

58 **Weiss GJ**, Waypa J, Blaydorn L, Coats J, McGahey K, Sangal A, Niu J, Lynch CA, Farley JH, Khemka V. A phase Ib study of pembrolizumab plus chemotherapy in patients with advanced cancer (PembroPlus). *Br J Cancer* 2017; **117**: 33-40 [PMID: 28588322 DOI: 10.1038/bjc.2017.145]

59 **Weiss GJ**, Blaydorn L, Beck J, Bornemann-Kolatzki K, Urnovitz H, Schütz E, Khemka V. Phase Ib/II study of gemcitabine, nab-paclitaxel, and pembrolizumab in metastatic pancreatic adenocarcinoma. *Invest New Drugs* 2018; **36**: 96-102 [PMID: 29119276 DOI: 10.1007/s10637-017-0525-1]

60 **Ott PA**, Bang YJ, Piha-Paul SA, Razak ARA, Bennouna J, Soria JC, Rugo HS, Cohen RB, O'Neil BH, Mehnert JM, Lopez J, Doi T, van Brummelen EMJ, Cristescu R, Yang P, Emancipator K, Stein K, Ayers M, Joe AK, Lunceford JK. T-Cell-Inflamed Gene-Expression Profile, Programmed Death Ligand 1 Expression, and Tumor Mutational Burden Predict Efficacy in Patients Treated With Pembrolizumab Across 20 Cancers: KEYNOTE-028. *J Clin Oncol* 2019; **37**: 318-327 [PMID: 30557521 DOI: 10.1200/JCO.2018.78.2276]

61 **Le DT**, Durham JN, Smith KN, Wang H, Bartlett BR, Aulakh LK, Lu S, Kemberling H, Wilt C, Luber BS, Wong F, Azad NS, Rucki AA, Laheru D, Donehower R, Zaheer A, Fisher GA, Crocenzi TS, Lee JJ, Greten TF, Duffy AG, Ciombor KK, Eyring AD, Lam BH, Joe A, Kang SP, Holdhoff M, Danilova L, Cope L, Meyer C, Zhou S, Goldberg RM, Armstrong DK, Bever KM, Fader AN, Taube J, Housseau F, Spetzler D, Xiao N, Pardoll DM, Papadopoulos N, Kinzler KW, Eshleman JR, Vogelstein B, Anders RA, Diaz LA Jr. Mismatch repair deficiency predicts response of solid tumors to PD-1 blockade. *Science* 2017; **357**: 409-413 [PMID: 28596308 DOI: 10.1126/science.aan6733]

62 **Hardwick NR**, Carroll M, Kaltcheva T, Qian D, Lim D, Leong L, Chu P, Kim J, Chao J, Fakih M, Yen Y, Espenschied J, Ellenhorn JD, Diamond DJ, Chung V. p53MVA therapy in patients with refractory gastrointestinal malignancies elevates p53-specific CD8+ T-cell responses. *Clin Cancer Res* 2014; **20**: 4459-4470 [PMID: 24987057 DOI: 10.1158/1078-0432.CCR-13-3361]

63 **Chung V**, Kos FJ, Hardwick N, Yuan Y, Chao J, Li D, Waisman J, Li M, Zurcher K, Frankel P, Diamond DJ. Evaluation of safety and efficacy of p53MVA vaccine combined with pembrolizumab in patients with advanced solid cancers. *Clin Transl Oncol* 2019; **21**: 363-372 [PMID: 30094792 DOI: 10.1007/s12094-018-1932-2]

64 **Brahmer JR**, Tykodi SS, Chow LQ, Hwu WJ, Topalian SL, Hwu P, Drake CG, Camacho LH, Kauh J, Odunsi K, Pitot HC, Hamid O, Bhatia S, Martins R, Eaton K, Chen S, Salay TM, Alaparthy S, Grosso JF, Korman AJ, Parker SM, Agrawal S, Goldberg SM, Pardoll DM, Gupta A, Wigginton JM. Safety and activity of anti-PD-L1 antibody in patients with advanced cancer. *N Engl J Med* 2012; **366**: 2455-2465 [PMID: 22658128 DOI: 10.1056/NEJMoa1200694]

65 **Mehnert JM**, Bergsland E, O'Neil BH, Santoro A, Schellens JHM, Cohen RB, Doi T, Ott PA, Pishvaian MJ, Puzanov I, Aung KL, Hsu C, Le Tourneau C, Hollebecque A, Élez E, Tamura K, Gould M, Yang P, Stein K, Piha-Paul SA. Pembrolizumab for the treatment of programmed death-ligand 1-positive advanced carcinoid or pancreatic neuroendocrine tumors: Results from the KEYNOTE-028 study. *Cancer* 2020; **126**: 3021-3030 [PMID: 32320048 DOI: 10.1002/cncr.32883]

66 **Bockorny B**, Semenisty V, Macarulla T, Borazanci E, Wolpin BM, Stemmer SM, Golan T, Geva R, Borad MJ, Pedersen KS, Park JO, Ramirez RA, Abad DG, Feliu J, Muñoz A, Ponz-Sarvise M, Peled A, Lustig TM, Bohana-Kashtan O, Shaw SM, Sorani E, Chaney M, Kadosh S, Vainstein Haras A, Von Hoff DD, Hidalgo M. BL-8040, a CXCR4 antagonist, in combination with pembrolizumab and chemotherapy for pancreatic cancer: the COMBAT trial. *Nat Med* 2020; **26**: 878-885 [PMID: 32451495 DOI: 10.1038/s41591-020-0880-x]

67 **Bockorny B**, Macarulla T, Semenisty V, Borazanci E, Feliu J, Ponz-Sarvise M, Abad DG, Oberstein P, Alistar A, Muñoz A, Geva R, Guillén-Ponce C, Fernandez MS, Peled A, Chaney M, Gliko-Kabir I, Shemesh-Darvish L, Ickowicz D, Sorani E, Kadosh S, Vainstein-Haras A, Hidalgo M. Motixafortide and Pembrolizumab Combined to Nanoliposomal Irinotecan, Fluorouracil, and Folinic Acid in Metastatic Pancreatic Cancer: The COMBAT/KEYNOTE-202 Trial. *Clin Cancer Res* 2021; **27**: 5020-5027 [PMID: 34253578 DOI: 10.1158/1078-0432.CCR-21-0929]

68 **Hong D**, Rasco D, Veeder M, Luke JJ, Chandler J, Balmanoukian A, George TJ, Munster P, Berlin JD, Gutierrez M, Mita A, Wakelee H, Samakoglu S, Guan S, Dimery I, Graef T, Borazanci E. A Phase 1b/2 Study of the Bruton Tyrosine Kinase Inhibitor Ibrutinib and the PD-L1 Inhibitor Durvalumab in Patients with Pretreated Solid Tumors. *Oncology* 2019; **97**: 102-111 [PMID: 31230047 DOI: 10.1159/000500571]

69 **O'Reilly EM**, Oh DY, Dhani N, Renouf DJ, Lee MA, Sun W, Fisher G, Hezel A, Chang SC, Vlahovic G, Takahashi O, Yang Y, Fitts D, Philip PA. Durvalumab With or Without Tremelimumab for Patients With Metastatic Pancreatic Ductal Adenocarcinoma: A Phase 2 Randomized Clinical Trial. *JAMA Oncol* 2019; **5**: 1431-1438 [PMID: 31318392 DOI: 10.1001/jamaoncol.2019.1588]

70 **Mizugaki H**, Yamamoto N, Murakami H, Kenmotsu H, Fujiwara Y, Ishida Y, Kawakami T, Takahashi T. Phase I dose-finding study of monotherapy with atezolizumab, an engineered immunoglobulin monoclonal antibody targeting PD-L1, in Japanese patients with advanced solid tumors. *Invest New Drugs* 2016; **34**: 596-603 [PMID: 27363843 DOI: 10.1007/s10637-016-0371-6]

71 **Jung KH**, LoRusso P, Burris H, Gordon M, Bang YJ, Hellmann MD, Cervantes A, Ochoa de Olza M, Marabelle A, Hodi FS, Ahn MJ, Emens LA, Barlesi F, Hamid O, Calvo E, McDermott D, Soliman H, Rhee I, Lin R, Pourmohamad T, Suchomel J, Tsuhako A, Morrissey K, Mahrus S, Morley R, Pirzkall A, Davis SL. Phase I Study of the Indoleamine 2,3-Dioxygenase 1 (IDO1) Inhibitor Navoximod (GDC-0919) Administered with PD-L1 Inhibitor (Atezolizumab) in Advanced Solid Tumors. *Clin Cancer Res* 2019; **25**: 3220-3228 [PMID: 30770348 DOI: 10.1158/1078-0432.CCR-18-2740]

72 **DeSelm CJ**, Tano ZE, Varghese AM, Adusumilli PS. CAR T-cell therapy for pancreatic cancer. *J Surg Oncol* 2017; **116**: 63-74 [PMID: 28346697 DOI: 10.1002/jso.24627]

73 **Akce M**, Zaidi MY, Waller EK, El-Rayes BF, Lesinski GB. The Potential of CAR T Cell Therapy in Pancreatic Cancer. *Front Immunol* 2018; **9**: 2166 [PMID: 30319627 DOI: 10.3389/fimmu.2018.02166]

74 **Sahlolbei M**, Dehghani M, Kheiri Yeghane Azar B, Vafaei S, Roviello G, D'Angelo A, Madjd Z, Kiani J. Evaluation of targetable biomarkers for chimeric antigen receptor T-cell (CAR-T) in the treatment of pancreatic cancer: a systematic review and meta-analysis of preclinical studies. *Int Rev Immunol* 2020; **39**: 223-232 [PMID: 32546036 DOI: 10.1080/08830185.2020.1776274]

75 **O'Hara M**, Stashwick C, Haas AR, Tanyi JL. Mesothelin as a target for chimeric antigen receptor-modified T cells as anticancer therapy. *Immunotherapy* 2016; **8**: 449-460 [PMID: 26973126 DOI: 10.2217/imt.16.4]

76 **Wang J**, Liu X, Ji J, Luo J, Zhao Y, Zhou X, Zheng J, Guo M, Liu Y. Orthotopic and Heterotopic Murine Models of Pancreatic Cancer Exhibit Different Immunological Microenvironments and Different Responses to Immunotherapy. *Front Immunol* 2022; **13**: 863346 [PMID: 35874730 DOI: 10.3389/fimmu.2022.863346]

77 **Beatty GL**, O'Hara MH, Lacey SF, Torigian DA, Nazimuddin F, Chen F, Kulikovskaya IM, Soulen MC, McGarvey M, Nelson AM, Gladney WL, Levine BL, Melenhorst JJ, Plesa G, June CH. Activity of Mesothelin-Specific Chimeric Antigen Receptor T Cells Against Pancreatic Carcinoma Metastases in a Phase 1 Trial. *Gastroenterology* 2018; **155**: 29-32 [PMID: 29567081 DOI: 10.1053/j.gastro.2018.03.029]

78 **Li Z**, Shao C, Liu X, Lu X, Jia X, Zheng X, Wang S, Zhu L, Li K, Pang Y, Xie F, Lu Y, Wang Y. Oncogenic ERBB2 aberrations and KRAS mutations cooperate to promote pancreatic ductal adenocarcinoma progression. *Carcinogenesis* 2020; **41**: 44-55 [PMID: 31046123 DOI: 10.1093/carcin/bgz086]

79 **Feng K**, Liu Y, Guo Y, Qiu J, Wu Z, Dai H, Yang Q, Wang Y, Han W. Phase I study of chimeric antigen receptor modified T cells in treating HER2-positive advanced biliary tract cancers and pancreatic cancers. *Protein Cell* 2018; **9**: 838-847 [PMID: 28710747 DOI: 10.1007/s13238-017-0440-4]

80 **Katari UL**, Keirnan JM, Worth AC, Hodges SE, Leen AM, Fisher WE, Vera JF. Engineered T cells for pancreatic cancer treatment. *HPB (Oxford)* 2011; **13**: 643-650 [PMID: 21843265 DOI: 10.1111/j.1477-2574.2011.00344.x]

81 **Abate-Daga D**, Lagisetty KH, Tran E, Zheng Z, Gattinoni L, Yu Z, Burns WR, Miermont AM, Teper Y, Rudloff U, Restifo NP, Feldman SA, Rosenberg SA, Morgan RA. A novel chimeric antigen receptor against prostate stem cell antigen mediates tumor destruction in a humanized mouse model of pancreatic cancer. *Hum Gene Ther* 2014; **25**: 1003-1012 [PMID: 24694017 DOI: 10.1089/hum.2013.209]

82 **Posey AD Jr**, Schwab RD, Boesteanu AC, Steentoft C, Mandel U, Engels B, Stone JD, Madsen TD, Schreiber K, Haines KM, Cogdill AP, Chen TJ, Song D, Scholler J, Kranz DM, Feldman MD, Young R, Keith B, Schreiber H, Clausen H, Johnson LA, June CH. Engineered CAR T Cells Targeting the Cancer-Associated Tn-Glycoform of the Membrane Mucin MUC1 Control Adenocarcinoma. *Immunity* 2016; **44**: 1444-1454 [PMID: 27332733 DOI: 10.1016/j.immuni.2016.05.014]

83 **Chung MJ**, Park JY, Bang S, Park SW, Song SY. Phase II clinical trial of ex vivo-expanded cytokine-induced killer cells therapy in advanced pancreatic cancer. *Cancer Immunol Immunother* 2014; **63**: 939-946 [PMID: 24916038 DOI: 10.1007/s00262-014-1566-3]

84 **Liu Y**, Guo Y, Wu Z, Feng K, Tong C, Wang Y, Dai H, Shi F, Yang Q, Han W. Anti-EGFR chimeric antigen receptor-modified T cells in metastatic pancreatic carcinoma: A phase I clinical trial. *Cytotherapy* 2020; **22**: 573-580 [PMID: 32527643 DOI: 10.1016/j.jcyt.2020.04.088]

85 **Saxena M**, van der Burg SH, Melief CJM, Bhardwaj N. Therapeutic cancer vaccines. *Nat Rev Cancer* 2021; **21**: 360-378 [PMID: 33907315 DOI: 10.1038/s41568-021-00346-0]

86 **Jou J**, Harrington KJ, Zocca MB, Ehrnrooth E, Cohen EEW. The Changing Landscape of Therapeutic Cancer Vaccines-Novel Platforms and Neoantigen Identification. *Clin Cancer Res* 2021; **27**: 689-703 [PMID: 33122346 DOI: 10.1158/1078-0432.CCR-20-0245]

87 **Jaffee EM**, Hruban RH, Biedrzycki B, Laheru D, Schepers K, Sauter PR, Goemann M, Coleman J, Grochow L, Donehower RC, Lillemoe KD, O'Reilly S, Abrams RA, Pardoll DM, Cameron JL, Yeo CJ. Novel allogeneic granulocyte-macrophage colony-stimulating factor-secreting tumor vaccine for pancreatic cancer: a phase I trial of safety and immune activation. *J Clin Oncol* 2001; **19**: 145-156 [PMID: 11134207 DOI: 10.1200/JCO.2001.19.1.145]

88 **Laheru D**, Lutz E, Burke J, Biedrzycki B, Solt S, Onners B, Tartakovsky I, Nemunaitis J, Le D, Sugar E, Hege K, Jaffee E. Allogeneic granulocyte macrophage colony-stimulating factor-secreting tumor immunotherapy alone or in sequence with cyclophosphamide for metastatic pancreatic cancer: a pilot study of safety, feasibility, and immune activation. *Clin Cancer Res* 2008; **14**: 1455-1463 [PMID: 18316569 DOI: 10.1158/1078-0432.CCR-07-0371]

89 **Lutz E**, Yeo CJ, Lillemoe KD, Biedrzycki B, Kobrin B, Herman J, Sugar E, Piantadosi S, Cameron JL, Solt S, Onners B, Tartakovsky I, Choi M, Sharma R, Illei PB, Hruban RH, Abrams RA, Le D, Jaffee E, Laheru D. A lethally irradiated allogeneic granulocyte-macrophage colony stimulating factor-secreting tumor vaccine for pancreatic adenocarcinoma. A Phase II trial of safety, efficacy, and immune activation. *Ann Surg* 2011; **253**: 328-335 [PMID: 21217520 DOI: 10.1097/SLA.0b013e3181fd271c]

90 **Lutz ER**, Wu AA, Bigelow E, Sharma R, Mo G, Soares K, Solt S, Dorman A, Wamwea A, Yager A, Laheru D, Wolfgang CL, Wang J, Hruban RH, Anders RA, Jaffee EM, Zheng L. Immunotherapy converts nonimmunogenic pancreatic tumors into immunogenic foci of immune regulation. *Cancer Immunol Res* 2014; **2**: 616-631 [PMID: 24942756 DOI: 10.1158/2326-6066.CIR-14-0027]

91 **Le DT**, Wang-Gillam A, Picozzi V, Greten TF, Crocenzi T, Springett G, Morse M, Zeh H, Cohen D, Fine RL, Onners B, Uram JN, Laheru DA, Lutz ER, Solt S, Murphy AL, Skoble J, Lemmens E, Grous J, Dubensky T Jr, Brockstedt DG, Jaffee EM. Safety and survival with GVAX pancreas prime and Listeria Monocytogenes-expressing mesothelin (CRS-207) boost vaccines for metastatic pancreatic cancer. *J Clin Oncol* 2015; **33**: 1325-1333 [PMID: 25584002 DOI: 10.1200/JCO.2014.57.4244]

92 **Le DT**, Picozzi VJ, Ko AH, Wainberg ZA, Kindler H, Wang-Gillam A, Oberstein P, Morse MA, Zeh HJ 3rd, Weekes C, Reid T, Borazanci E, Crocenzi T, LoConte NK, Musher B, Laheru D, Murphy A, Whiting C, Nair N, Enstrom A, Ferber S, Brockstedt DG, Jaffee EM. Results from a Phase IIb, Randomized, Multicenter Study of GVAX Pancreas and CRS-207 Compared with Chemotherapy in Adults with Previously Treated Metastatic Pancreatic Adenocarcinoma (ECLIPSE Study). *Clin Cancer Res* 2019; **25**: 5493-5502 [PMID: 31126960 DOI: 10.1158/1078-0432.CCR-18-2992]

93 **Le DT**, Brockstedt DG, Nir-Paz R, Hampl J, Mathur S, Nemunaitis J, Sterman DH, Hassan R, Lutz E, Moyer B, Giedlin M, Louis JL, Sugar EA, Pons A, Cox AL, Levine J, Murphy AL, Illei P, Dubensky TW Jr, Eiden JE, Jaffee EM, Laheru DA. A live-attenuated Listeria vaccine (ANZ-100) and a live-attenuated Listeria vaccine expressing mesothelin (CRS-207) for advanced cancers: phase I studies of safety and immune induction. *Clin Cancer Res* 2012; **18**: 858-868 [PMID: 22147941 DOI: 10.1158/1078-0432.CCR-11-2121]

94 **Rossi GR**, Mautino MR, Unfer RC, Seregina TM, Vahanian N, Link CJ. Effective treatment of preexisting melanoma with whole cell vaccines expressing alpha(1,3)-galactosyl epitopes. *Cancer Res* 2005; **65**: 10555-10561 [PMID: 16288048 DOI: 10.1158/0008-5472.CAN-05-0627]

95 **Hardacre JM**, Mulcahy M, Small W, Talamonti M, Obel J, Krishnamurthi S, Rocha-Lima CS, Safran H, Lenz HJ, Chiorean EG. Addition of algenpantucel-L immunotherapy to standard adjuvant therapy for pancreatic cancer: a phase 2 study. *J Gastrointest Surg* 2013; **17**: 94-100; discussion p. 100 [PMID: 23229886 DOI: 10.1007/s11605-012-2064-6]

96 **Hewitt DB**, Nissen N, Hatoum H, Musher B, Seng J, Coveler AL, Al-Rajabi R, Yeo CJ, Leiby B, Banks J, Balducci L, Vaccaro G, LoConte N, George TJ, Brenner W, Elquza E, Vahanian N, Rossi G, Kennedy E, Link C, Lavu H. A Phase 3 Randomized Clinical Trial of Chemotherapy

With or Without Algenpantucel-L (HyperAcute-Pancreas) Immunotherapy in Subjects With Borderline Resectable or Locally Advanced Unresectable Pancreatic Cancer. *Ann Surg* 2022; **275**: 45-53 [PMID: 33630475 DOI: 10.1097/SLA.0000000000004669]

97 **Gjertsen MK**, Bakka A, Breivik J, Saeterdal I, Gedde-Dahl T 3rd, Stokke KT, Sølheim BG, Egge TS, Søreide O, Thorsby E, Gaudernack G. Ex vivo ras peptide vaccination in patients with advanced pancreatic cancer: results of a phase I/II study. *Int J Cancer* 1996; **65**: 450-453 [PMID: 8621226 DOI: 10.1002/(SICI)1097-0215(19960208)65:4<450::AID-IJC10>3.0.CO;2-E]

98 **Gjertsen MK**, Bjorheim J, Saeterdal I, Myklebust J, Gaudernack G. Cytotoxic CD4+ and CD8+ T lymphocytes, generated by mutant p21-ras (12Val) peptide vaccination of a patient, recognize 12Val-dependent nested epitopes present within the vaccine peptide and kill autologous tumour cells carrying this mutation. *Int J Cancer* 1997; **72**: 784-790 [PMID: 9311595 DOI: 10.1002/(sici)1097-0215(19970904)72:5<784::aid-ijc14>3.0.co;2-9]

99 **Gjertsen MK**, Bakka A, Breivik J, Saeterdal I, Solheim BG, Søreide O, Thorsby E, Gaudernack G. Vaccination with mutant ras peptides and induction of T-cell responsiveness in pancreatic carcinoma patients carrying the corresponding RAS mutation. *Lancet* 1995; **346**: 1399-1400 [PMID: 7475823 DOI: 10.1016/s0140-6736(95)92408-6]

100 **Gjertsen MK**, Buanes T, Rosseland AR, Bakka A, Gladhaug I, Søreide O, Eriksen JA, Møller M, Baksaas I, Lothe RA, Saeterdal I, Gaudernack G. Intradermal ras peptide vaccination with granulocyte-macrophage colony-stimulating factor as adjuvant: Clinical and immunological responses in patients with pancreatic adenocarcinoma. *Int J Cancer* 2001; **92**: 441-450 [PMID: 11291084 DOI: 10.1002/ijc.1205]

101 **Wedén S**, Klemp M, Gladhaug IP, Møller M, Eriksen JA, Gaudernack G, Buanes T. Long-term follow-up of patients with resected pancreatic cancer following vaccination against mutant K-ras. *Int J Cancer* 2011; **128**: 1120-1128 [PMID: 20473937 DOI: 10.1002/ijc.25449]

102 **Abou-Alfa GK**, Chapman PB, Feilchenfeldt J, Brennan MF, Capanu M, Gansukh B, Jacobs G, Levin A, Neville D, Kelsen DP, O'Reilly EM. Targeting mutated K-ras in pancreatic adenocarcinoma using an adjuvant vaccine. *Am J Clin Oncol* 2011; **34**: 321-325 [PMID: 20686403 DOI: 10.1097/COC.0b013e3181e84b1f]

103 **Ramanathan RK**, Lee KM, McKolanis J, Hitbold E, Schraut W, Moser AJ, Warnick E, Whiteside T, Osborne J, Kim H, Day R, Troetschel M, Finn OJ. Phase I study of a MUC1 vaccine composed of different doses of MUC1 peptide with SB-AS2 adjuvant in resected and locally advanced pancreatic cancer. *Cancer Immunol Immunother* 2005; **54**: 254-264 [PMID: 15372205 DOI: 10.1007/s00262-004-0581-1]

104 **Kaufman HL**, Kim-Schulze S, Manson K, DeRaffele G, Mitcham J, Seo KS, Kim DW, Marshall J. Poxvirus-based vaccine therapy for patients with advanced pancreatic cancer. *J Transl Med* 2007; **5**: 60 [PMID: 18039393 DOI: 10.1186/1479-5876-5-60]

105 **Lepisto AJ**, Moser AJ, Zeh H, Lee K, Bartlett D, McKolanis JR, Geller BA, Schmotzer A, Potter DP, Whiteside T, Finn OJ, Ramanathan RK. A phase I/II study of a MUC1 peptide pulsed autologous dendritic cell vaccine as adjuvant therapy in patients with resected pancreatic and biliary tumors. *Cancer Ther* 2008; **6**: 955-964 [PMID: 19129927]

106 **Brett BT**, Smith SC, Bouvier CV, Michaeli D, Hochhauser D, Davidson BR, Kurzawinski TR, Watkinson AF, Van Someren N, Pounder RE, Caplin ME. Phase II study of anti-gastrin-17 antibodies, raised to G17DT, in advanced pancreatic cancer. *J Clin Oncol* 2002; **20**: 4225-4231 [PMID: 12377966 DOI: 10.1200/JCO.2002.11.151]

107 **Gilliam AD**, Broome P, Topuzov EG, Garin AM, Pulay I, Humphreys J, Whitehead A, Takhar A, Rowlands BJ, Beckingham IJ. An international multicenter randomized controlled trial of G17DT in patients with pancreatic cancer. *Pancreas* 2012; **41**: 374-379 [PMID: 22228104 DOI: 10.1097/MPA.0b013e31822ade7e]

108 **Bernhardt SL**, Gjertsen MK, Trachsel S, Møller M, Eriksen JA, Meo M, Buanes T, Gaudernack G. Telomerase peptide vaccination of patients with non-resectable pancreatic cancer: A dose escalating phase I/II study. *Br J Cancer* 2006; **95**: 1474-1482 [PMID: 17060934 DOI: 10.1038/sj.bjc.6603437]

109 **Middleton G**, Silcocks P, Cox T, Valle J, Wadsley J, Propper D, Coxon F, Ross P, Madhusudan S, Roques T, Cunningham D, Falk S, Wadd N, Harrison M, Corrie P, Iveson T, Robinson A, McAdam K, Eatock M, Evans J, Archer C, Hickish T, Garcia-Alonso A, Nicolson M, Steward W, Anthoney A, Greenhalf W, Shaw V, Costello E, Naisbitt D, Rawcliffe C, Nanson G, Neoptolemos J. Gemcitabine and capecitabine with or without telomerase peptide vaccine GV1001 in patients with locally advanced or metastatic pancreatic cancer (TeloVac): an open-label, randomised, phase 3 trial. *Lancet Oncol* 2014; **15**: 829-840 [PMID: 24954781 DOI: 10.1016/S1470-2045(14)70236-0]

110 **Staff C**, Mozaffari F, Frödin JE, Mellstedt H, Liljefors M. Telomerase (GV1001) vaccination together with gemcitabine in advanced pancreatic cancer patients. *Int J Oncol* 2014; **45**: 1293-1303 [PMID: 24919654 DOI: 10.3892/ijo.2014.2496]

111 **Kimura Y**, Tsukada J, Tomoda T, Takahashi H, Imai K, Shimamura K, Sunamura M, Yonemitsu Y, Shimodaira S, Koido S, Homma S, Okamoto M. Clinical and immunologic evaluation of dendritic cell-based immunotherapy in combination with gemcitabine and/or S-1 in patients with advanced pancreatic carcinoma. *Pancreas* 2012; **41**: 195-205 [PMID: 21792083 DOI: 10.1097/MPA.0b013e31822398c6]

112 **Mehrotra S**, Britten CD, Chin S, Garrett-Mayer E, Cloud CA, Li M, Scurti G, Salem ML, Nelson MH, Thomas MB, Paulos CM, Salazar AM, Nishimura MI, Rubinstein MP, Li Z, Cole DJ. Vaccination with poly(IC:LC) and peptide-pulsed autologous dendritic cells in patients with pancreatic cancer. *J Hematol Oncol* 2017; **10**: 82 [PMID: 28388966 DOI: 10.1186/s13045-017-0459-2]

113 **Jiang N**, Qiao G, Wang X, Morse MA, Gwin WR, Zhou L, Song Y, Zhao Y, Chen F, Zhou X, Huang L, Hobeika A, Yi X, Xia X, Guan Y, Song J, Ren J, Lyerly HK. Dendritic Cell/Cytokine-Induced Killer Cell Immunotherapy Combined with S-1 in Patients with Advanced Pancreatic Cancer: A Prospective Study. *Clin Cancer Res* 2017; **23**: 5066-5073 [PMID: 28611200 DOI: 10.1158/1078-0432.CCR-17-0492]

114 **Yanagisawa R**, Koizumi T, Koya T, Sano K, Koido S, Nagai K, Kobayashi M, Okamoto M, Sugiyama H, Shimodaira S. WT1-pulsed Dendritic Cell Vaccine Combined with Chemotherapy for Resected Pancreatic Cancer in a Phase I Study. *Anticancer Res* 2018; **38**: 2217-2225 [PMID: 29599342 DOI: 10.21873/anticanres.12464]

World Journal of Gastrointestinal Oncology

Submit a Manuscript: https://www.f6publishing.com

World J Gastrointest Oncol 2023 October 15; 15(10): 1706-1716

DOI: 10.4251/wjgo.v15.i10.1706

ISSN 1948-5204 (online)

MINIREVIEWS

Role of inositol polyphosphate-4-phosphatase type II in oncogenesis of digestive system tumors

Le Han, Shuo Chen, Shi-Yu Du

Specialty type: Oncology

Provenance and peer review: Unsolicited article; Externally peer reviewed.

Peer-review model: Single blind

Peer-review report's scientific quality classification

Grade A (Excellent): 0
Grade B (Very good): 0
Grade C (Good): C, C
Grade D (Fair): 0
Grade E (Poor): 0

P-Reviewer: Boon CS, United Kingdom; Tanabe S, Japan

Received: June 13, 2023
Peer-review started: June 13, 2023
First decision: July 31, 2023
Revised: August 22, 2023
Accepted: September 19, 2023
Article in press: September 19, 2023
Published online: October 15, 2023

Le Han, Peking University China-Japan Friendship School of Clinical Medicine, Peking University, Beijing 100029, China

Shuo Chen, Shi-Yu Du, Department of Gastroenterology, China-Japan Friendship Hospital, Beijing 100029, China

Corresponding author: Shuo Chen, MD, Doctor, Department of Gastroenterology, China-Japan Friendship Hospital, No. 2 East Yinghua Street, Chaoyang District, Beijing 100029, China. 2111210566@bjmu.edu.cn

Abstract

Inositol polyphosphate-4-phosphatase type II (INPP4B) is a newly discovered PI(3,4,5)P3 phosphatase. Many studies have revealed that INPP4B is upregulated or downregulated in tumors of the digestive system, and the abnormal expression of INPP4B may be attributed to the occurrence, development, and prognosis of tumors of the digestive system. This paper reviews studies on the correlations between INPP4B and digestive system tumors and the roles of INPP4B in the development of different tumors to provide a theoretical basis for further research on its molecular mechanism and clinical application. "INPP4B" and "tumor" were searched as key words in PubMed and in the CNKI series full text database retrieval system from January 2000 to August 2023. A total of 153 English-language studies and 30 Chinese-language studies were retrieved. The following enrollment criteria were applied: (1) Studies contained information on the biological structure and functions of INPP4B; (2) studies covered the influence of abnormal expression of INPP4B in digestive system tumors; and (3) studies covered the role of INPP4B in the diagnosis, treatment, and prognosis of digestive system tumors. After excluding the literature irrelevant to this study, 61 papers were finally included in the analysis. INPP4B expression is low in gastric cancer, colon cancer, pancreatic cancer, and liver cancer but it has high expression in esophageal cancer, colon cancer, pancreatic cancer, and gallbladder cancer. INPP4B is involved in the occurrence and development of digestive system tumors through the regulation of gene expression and signal transduction. The abnormal expression of INPP4B plays an important role in the development of digestive system tumors. Studies on INPP4B provide new molecular insights for the diagnosis, treatment, and prognosis evaluation of digestive system tumors.

Key Words: Inositol polyphosphate-4-phosphatase type II; Tumors of the digestive system; Protein kinase B; Serum and glucocorticoid-regulated kinase 3

Core Tip: Inositol polyphosphate-4-phosphatase type II (INPP4B) is a newly discovered PI(3,4,5)P3 phosphatase. This paper reviews studies on the correlations between INPP4B and digestive system tumors and the roles of INPP4B in the development of different tumors to provide a theoretical basis for further research on its molecular mechanism and clinical application. The abnormal expression of INPP4B plays an important role in the development of digestive system tumors. Studies on INPP4B provide new molecular insights for the diagnosis, treatment, and prognosis evaluation of digestive system tumors.

Citation: Han L, Chen S, Du SY. Role of inositol polyphosphate-4-phosphatase type II in oncogenesis of digestive system tumors. *World J Gastrointest Oncol* 2023; 15(10): 1706-1716
URL: https://www.wjgnet.com/1948-5204/full/v15/i10/1706.htm
DOI: https://dx.doi.org/10.4251/wjgo.v15.i10.1706

INTRODUCTION

Tumors of the digestive system, including esophageal cancer, stomach cancer, colorectal cancer, liver cancer, pancreatic cancer, and gallbladder cancer, have high morbidity and mortality rates in China and abroad. According to the 2020 global cancer statistics released by *CA: A Cancer Journal for Clinicians*[1,2], the top five cancers in the world were breast, lung, colorectal, prostate, and stomach cancers, and the top five cancers in China were lung, colorectal, stomach, breast, and liver cancers. Lung, colorectal, liver, stomach and breast cancers rank as the top five in terms of mortality worldwide, and lung, liver, stomach, esophageal, and colorectal cancers rank as the top five in terms of mortality in China. Thus, the diagnosis and treatment of digestive tumors at home and abroad are still important issues since these cancers seriously endanger the lives and health of people worldwide. The pathogenesis of digestive tumors is complex, and the risk factors are numerous. There are few early screening and diagnosis techniques for these tumors; in addition, the treatment response of patients with late-stage disease is poor, and the metastasis rate is high. In recent years, studies have found that inositol polyphosphate-4-phosphatase type II (INPP4B) is underexpressed or overexpressed in a variety of digestive system tumors and that it can regulate the gene expression and transcription of tumor cells, thus playing an important role in tumor inhibition or promotion.

To provide a theoretical basis and new ideas for the study of digestive system tumors, the correlation between INPP4B and digestive system tumors and the corresponding molecular mechanisms related to the occurrence and development of digestive system cancers are reviewed in this paper (Table 1).

Structure of INPP4B

INPP4B is a newly discovered PI(3,4,5)P3 phosphatase independent of Mg^{2+}. Its gene is located at 4q31.21 of chromosome 8[3,4]. The molecular weight is approximately 110 kDa. INPP4B is highly expressed in human skeletal muscle, breast, heart, brain, liver, pancreas, and prostate tissues[5]. The INPP4B structure consists of three parts: An N-terminal C2 Lipid binding domain, NHR2, and a C-terminal phosphatase domain. Among them, the C2 Lipid binding domain and the C-terminal phosphatase domain can bind to PI(3,4,5)P3. The C-terminal phosphatase domain contains the conserved sequence of amino acids 842-849 (CKSAKDRT), including the catalytic active site C(X)5R, which leads to the phosphorylation of lipids and proteins. INPP4B can dephosphorylate the D4 phosphate group of PI(3,4)P2 and degrade it to PI(3)P, thereby inhibiting protein kinase B (AKT) activation[4-8].

Effects of INPP4B in digestive system tumors

At present, there are different experimental conclusions on the relationship between INPP4B and tumors. In a variety of malignancies, such as breast cancer of the reproductive system[9], hepatocellular carcinoma (HCC) of the digestive system[10], prostate cancer of the urinary system[11], and leukemia of the blood system[12], INPP4B has a high frequency of decreased expression, and this phenotype is often closely related to a poor prognosis in patients. The decrease in INPP4B is particularly pronounced in some highly metastatic tumors, such as highly metastatic colorectal cancer[13]. This suggests that INPP4B may play an anticancer role in tumor tissues. However, in estrogen-receptor-positive breast cancer [14], *BCR/ABL1* fusion gene-positive acute myeloid leukemia[15], pancreatic ductal adenocarcinomas[16], and other types of tumors, INPP4B overexpression can promote the development of tumors. This indicates that INPP4B may play a role in promoting tumor progression. As a result, INPP4B may have dual and complex effects on tumors.

In tumors of the digestive system, INPP4B mainly functions through the phosphoinositide 3-kinase/protein kinase B (PI3K/AKT) and PI3K/serum and glucocorticoid-regulated kinase 3 (PI3K/SGK3) pathways.

INPP4B and PI3K/AKT: The PI3K/AKT signaling pathway is closely related to cell proliferation and apoptosis. Extracellular stimulation can activate PI3K, and the downstream factor of PI3K (AKT) can be phosphorylated and activated by the combination of the PH domain with PI(3,4,5)P3 or PI(3,4)P2, thus triggering the proliferation and apoptosis of regulated cells. INPP4B can be generated by activating PI3K to produce PI(3,4)P2. PI(3,4)P2 is further

Table 1 Role of inositol polyphosphate-4-phosphatase type II in tumors of the digestive system

Cancer	Role	Molecular pathway	Ref.
Gastric cancer	Carcinostasis	AKT, p-AKT, SGK3, SGK3	[29-34,39]
	Dual function	AKT, p-AKT, SGK3, SGK3, HIF-1A	[40,41]
Colon cancer	Carcinostasis	MiR-1290, p27, cyclin D1	[42-44]
	Carcinogenesis	Ets-1, PTEN, PI3K/AKT, PI3K/SGK3	[18,19,45-48]
	Dual function	Sox2, Nanog	[13]
Pancreatic cancer	Carcinostasis	Methylation inhibitors, PI3K/AKT, Ecad	[16,49,50]
	Carcinogenesis	PI3K/AKT	[51]
Liver cancer	Carcinostasis	MiR-765, AKT, p-AKT, Cyclin D1, p-FOXO3a, p21	[10,53-56]
Esophageal cancer	Carcinogenesis	AKT, pAKT	[20]
Gallbladder cancer	Dual function	AKT, p-AKT, SGK3, p-SGK3	[41,57]

AKT: Protein kinase B; p-AKT: Phosphorylated AKT; SGK3: Serum and glucocorticoid-regulated kinase 3; p-SGK3: Phosphorylated SGK3; HIF-1A: Hypoxia inducible factor-1A; Ets-1: E26 transformation-specific 1; PTEN: Phosphate and tensin homolog deleted on chromosome 1; PI3K: Phosphoinositide 3-kinase; SOX2: Recombinant sex determining region Y box protein 2; Ecad: E-cadherin; p-FOXO3a: Phosphorylated Forkhead box O3.

hydrolyzed to PI(3)P, which blocks the PI3K/AKT signal, thus affecting downstream signaling. Therefore, INPP4B has a significantly negative regulatory effect on the PI3K/AKT signaling pathway, thus inhibiting the proliferation of tumor cells. Therefore, INPP4B has become a potential tumor suppressor of the PI(3,4,5)P3 phosphatase family (Figure 1A)[3-7, 17]. However, other studies have come to a different conclusion: The overexpression of INPP4B can promote cancer by promoting the expression of AKT[18-20]. This process may be related to the expression of phosphate and tensin homolog deleted on chromosome 1/PI3K/AKT (PTEN/PI3K/AKT). PTEN is an analog of INPP4B. PTEN also regulates PI3K/AKT to promote cell proliferation[21,22]. Some researchers believe that overexpression of INPP4B inhibits the expression of PTEN and activates the PI3K/AKT pathway, which plays a role in promoting cancer (Figure 1B)[18-20]. Therefore, through the PI3K/AKT pathway, INPP4B may play both anticancer and procancer roles.

INPP4B and PI3K/SGK3: Aside from AKT, SGK is another serine/threonine protein kinase family. There are three isoforms of the SGK family: SGK1, SGK2, and SGK3. These three isoforms are highly homologous with AKT and share a common substrate specificity. The SKG3 protein has an approximately 55% sequence similarity with AKT. The hydrolytic product of INPP4B, PI(3)P, can bind to and activate SKG3[23,24]. Activation of the PIK3/SGK3 signaling pathway may enhance the growth, proliferation, and migration of tumor cells[23-25]. The overexpression of INPP4B in tumor cells may promote the occurrence and development of tumors and resist the process of apoptosis of tumor cells by activating the PIK3/SGK3 signaling pathway (Figure 2)[18,26]. INPP4B is highly expressed in PIK3CA-mutant breast cancer. Breast cancer with oncogenic PIK3CA mutations activates SGK3 signaling while inhibiting AKT, thus mediating the proliferation of estrogen-receptor-positive breast cancer cells[9,26]. Overexpression of INPP4B through the activation of SGK3 to play a role in promoting cancer has also been found in melanoma[27,28]. Therefore, INPP4B plays a role in promoting cancer in tumor cells through the PIK3/SGK3 pathway.

The above studies confirm that INPP4B is closely related to the occurrence and development of cancers through the PIK3/AKT and PIK3/SGK3 signaling pathways. INPP4B may play a role in inhibiting or promoting cancer in different tumor cells, which may be related to its effect on different signaling pathways.

INPP4B AND GASTRIC CANCER

Gastric cancer is one of the most common malignant tumors of the digestive system. Early diagnosis relies on invasive examination, such as gastroscopy. Gastric cancer is highly malignant, invasive, and metastatic. At present, the study of INPP4B in gastric cancer is still in the preliminary stage.

INPP4B is downregulated in gastric cancer *vs* normal tissues. Hu *et al*[29] used quantitative real-time polymerase chain reaction (qRT-PCR) and immunohistochemistry (IHC) to detect the expression of INPP4B mRNA and protein in the cancer tissues and adjacent tissues of 50 patients with gastric cancer, respectively. The results of qRT-PCR revealed that the mRNA expression of *INPP4B* in gastric cancer tissues was significantly lower than that in paracancerous tissues ($P < 0.01$). The results of IHC revealed the positive rate of INPP4B protein expression in gastric cancer tissues was significantly lower than that in paracancerous tissues (28.0% *vs* 82.0%, $P < 0.01$). Moreover, INPP4B mRNA and protein expression are considered to be related to the differentiation degree, lymph node metastasis, and tumor-node-metastasis (TNM) stage of gastric cancer ($P < 0.01$). Fan[30] used qRT-PCR and IHC to determine the expression of INPP4B in gastric cancer tissues,

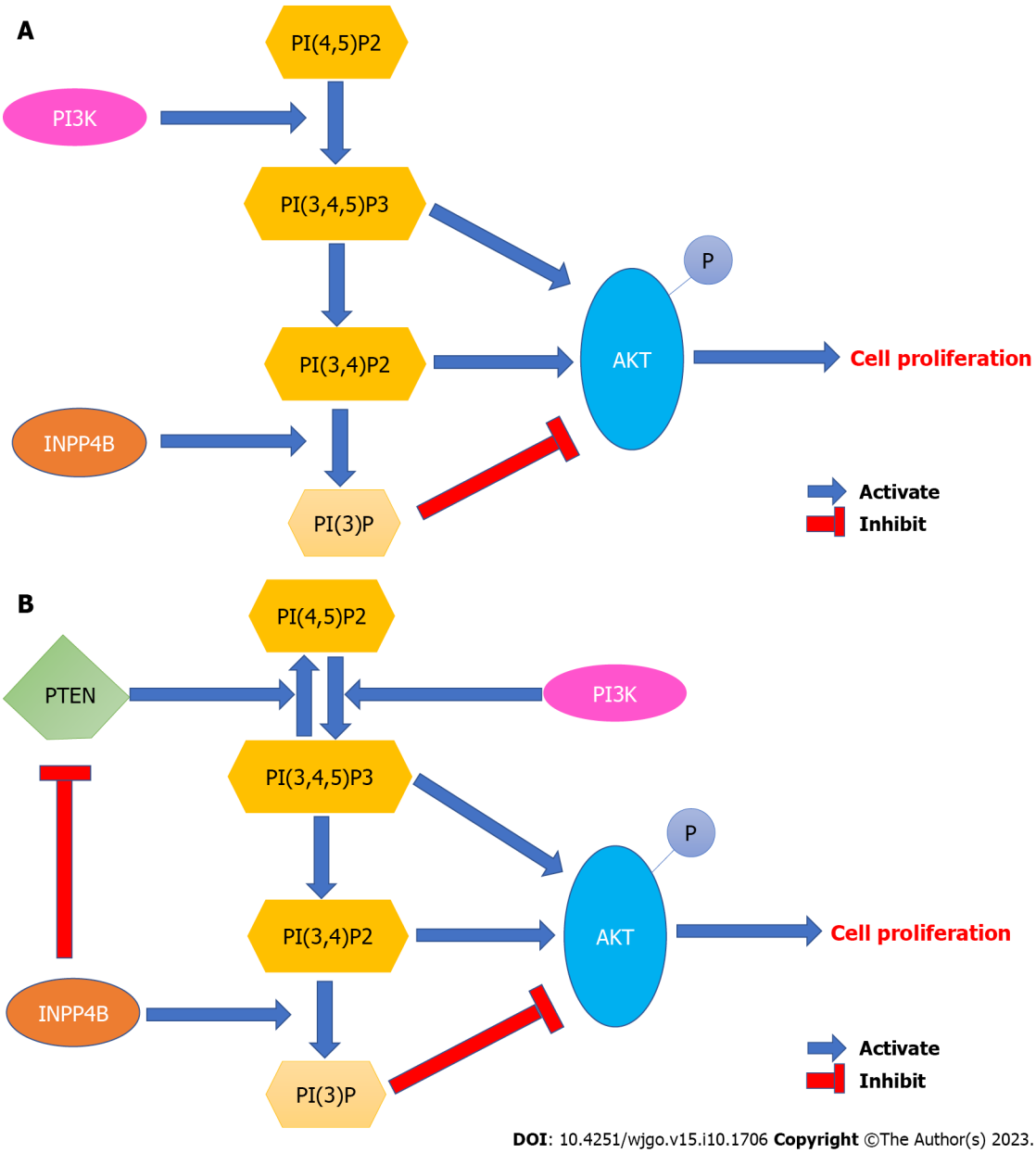

DOI: 10.4251/wjgo.v15.i10.1706

Figure 1 Molecular mechanism of inositol polyphosphate-4-phosphatase type II in cancer proliferation through the phosphoinositide 3-kinase/protein kinase B pathway. A: Phosphoinositide 3-kinase can activate cell membrane receptors, which increases the content of PI(3,4,5)P3 and PI(3,4)P2. PI(3,4,5)P3 and PI(3,4)P2 further bind and activate the downstream factor protein kinase B (AKT). Activation of AKT promotes cell proliferation and ultimately tumor development. Inositol polyphosphate-4-phosphatase type II promotes the conversion of PI(3,4)P2 to PI(3)P, thereby reducing the content of PI(3,4,5)P3 and PI(3,4)P2, which inhibits the AKT pathway; B: Phosphate and tensin homolog deleted on chromosome 10 can reduce the content of PI(3,4,5)P3 and PI(3,4)P2 by dephosphorylating PI(3,4,5)P3 into PI(4,5)P2, thereby inhibiting the AKT pathway. INPP4B was found to inhibit PTEN, which resulted in increased intracellular PI(3,4,5)P3 and PI(3,4)P2. PI(3,4,5)P3 and PI(3,4)P2 activate the AKT pathway, leading to the proliferation of tumor cells. INPP4B: Inositol polyphosphate-4-phosphatase type II; PI3K: Phosphoinositide 3-kinase; AKT: Protein kinase B; PTEN: Phosphate and tensin homolog deleted on chromosome 10.

normal tissues, and tumor-adjacent tissues and the expression of AKT and phosphorylated AKT (p-AKT) in 36 patients. The expression of INPP4B in cancer tissues was significantly lower than that in normal tissues and paracancerous tissues. Moreover, the expression of AKT and p-AKT in cancer tissues was significantly higher than that in normal tissues and paracancerous tissues ($P < 0.001$). INPP4B was negatively correlated with AKT and p-AKT ($P < 0.001$). Therefore, INPP4B plays a role as a tumor suppressor in gastric cancer. Decreased INPP4B expression activates the phosphorylation of AKT, which leads to the occurrence and development of gastric cancer.

Yang *et al*[31] used qRT-PCR and ELISA to determine the mRNA and protein expression levels of INPP4B in peripheral blood samples from 50 patients with gastric cancer and 30 healthy volunteers, respectively. The mRNA and protein expression levels of INPP4B in the peripheral blood of gastric cancer patients were significantly lower than those in the blood of healthy volunteers ($P < 0.05$). Moreover, the mRNA and protein expression levels of INPP4B in the peripheral blood of gastric cancer patients were correlated with TNM stage, lymph node metastasis, and infiltration depth ($P < 0.05$), and the sensitivity and specificity values were 78.0% and 84.0%, respectively. Li *et al*[32] also found that the positive rate of INPP4B protein expression in gastric adenocarcinoma tissues (21.43%) was lower than that in tumor-adjacent tissues

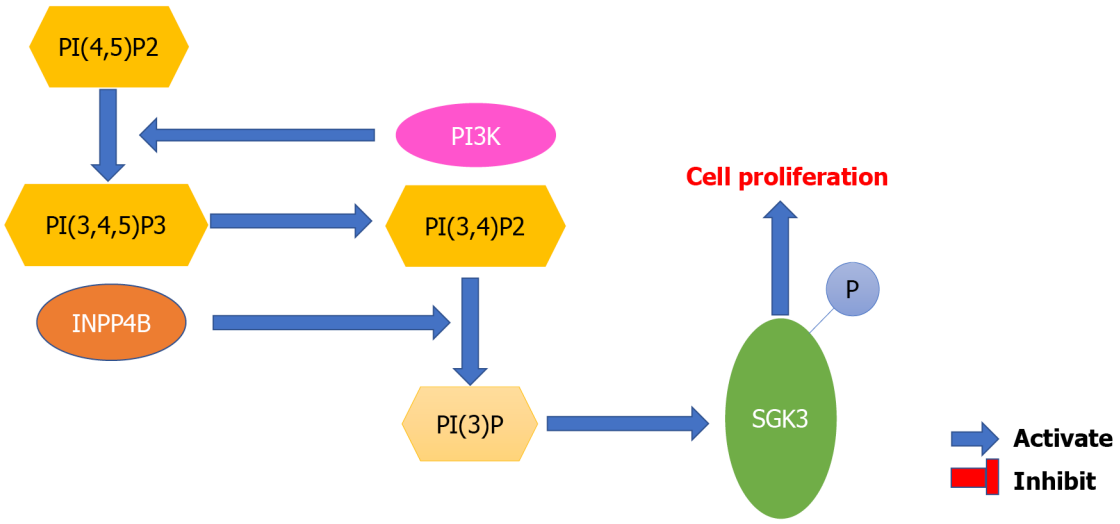

DOI: 10.4251/wjgo.v15.i10.1706

Figure 2 Molecular mechanism of inositol polyphosphate-4-phosphatase type II in cancer proliferation through the phosphoinositide 3-kinase/serum and glucocorticoid-regulated kinase 3 pathway. PI(3)P, produced by inositol polyphosphate-4-phosphatase type II, can bind to and activate serum and glucocorticoid-regulated kinase 3, which promotes the occurrence and development of tumors and resists the process of apoptosis of tumor cells. INPP4B: Inositol polyphosphate-4-phosphatase type II; PI3K: Phosphoinositide 3-kinase; SGK3: Serum and glucocorticoid-regulated kinase 3.

(83.57%), and the difference was statistically significant ($P < 0.01$). The expression levels of INPP4B protein in gastric adenocarcinoma tissues were negatively associated with lymph node metastasis, differentiation degree, and TNM stage ($P < 0.01$). The survival time of the INPP4B high-expression group was significantly longer than that of the low-expression group. A total of 79 patients with advanced gastric cancer and 40 healthy people were selected for analysis of the expression of *INPP4B* mRNA in peripheral blood in the research of Liu Z *et al*[33]. They found that the relative expression of *INPP4B* mRNA in the study group was lower ($P < 0.05$); among patients with low mRNA expression of *INPP4B*, the proportion of patients with stage IV gastric cancer was higher than that of patients with stage IIIB ($P < 0.05$). Compared to that in the treatment-sensitive group, the expression of *INPP4B* mRNA in the treatment-resistant group was lower, and the expression of *PI3K* and *AKT* mRNA was higher ($P < 0.05$). The median survival time of the high-expression group was also longer than that of the low-expression group ($P = 0.006$). Therefore, the expression of INPP4B mRNA and protein in gastric cancer tissues and peripheral blood may become an effective molecular index to indicate progression, facilitate early diagnosis, and predict prognosis in gastric cancer patients.

Recently, IHC and *in situ* hybridization studies of EBER expression were used to assess the cancer tissues and paracancerous tissues of 301 patients with gastric cancer; these studies showed that the expression of INPP4B protein was decreased in most gastric cancer tissues infected with Epstein-Barr virus (EBV) compared to those not infected ($P < 0.05$)[34]. According to the gastric cancer typing in the 2014 American Cancer Genome Atlas Research Network[35], EBV-positive gastric cancer is often considered to have a poor prognosis, and this type of gastric cancer is characterized by more extensive DNA hypermethylation, PIK3CA mutation, PD-L1/2 overexpression, and *CDKN2A* gene silencing. In this type of gastric cancer, INPP4B protein is hypermethylated by EBV, which further explains the pathogenesis and poor prognosis of EBV nucleic acid-positive gastric cancer. Yuen *et al*[36] used RT-PCR, methylation-specific PCR, and other experimental techniques to find that in EBV-infected nasopharyngeal carcinoma tissues, the downregulation of INPP4B protein was closely related to the hypermethylation of the *INPP4B* promoter region. The latent membrane protein 1 of EBV changes the methylation state of the host genome by inducing the methyltransferase activity of the host cell, which may indicate the mechanism[37,38]. Moreover, Ma *et al*[39] discovered that before treatment of EBV-positive and EBV-negative gastric cancer cell lines with methylation inhibitors, the methylation level of CpG islands in the promoter region of the *INPP4B* gene was decreased, and the transcription and expression levels of the *INPP4B* gene were increased. CpG island methylation in the promoter region is one of the important mechanisms of *INPP4B* gene inactivation, and methylation inhibitor treatment can promote the transcription and expression of the *INPP4B* gene in EBV-positive and EBV-negative gastric cancer cell lines[39]. Therefore, the downregulated expression of *INPP4B*, an anticancer gene in gastric cancer[34] and nasopharyngeal carcinoma[36], is related to EBV infection-mediated hypermethylation of the *INPP4B* promoter region. These preliminary studies provide new research directions regarding the mechanism by which EBV infection causes nasopharyngeal carcinoma and gastric cancer.

However, a study showed that *INPP4B* may play dual roles as an oncogene and tumor suppressor gene in different tissue grades and clinical stages[40].

Using gastric cancer cells, Wu *et al*[40] found that knockdown of INPP4B in BGC-823 cells could increase the apoptosis rate, decrease cell migration capability, and suppress proliferation and colony formation, while overexpression of INPP4B in AGS cells had opposite effects, suggesting that *INPP4B* is an oncogene in gastric cancer cells. Using *in vitro* analyses of gastric cancer cells, Wu *et al*[40] discovered that downregulation of INPP4B in BGC-823 cells resulted in an elevation of the apoptosis rate, a reduction in cell migration capability, and inhibition of proliferation and colony formation. Conversely, upregulation of INPP4B in AGS cells exhibited contrasting effects, indicating its oncogenic role in gastric

cancer cells. Mechanistically, INPP4B overexpression increased the level of phosphorylated SGK3 (p-SGK3) in AGS cells, while INPP4B knockdown increased the p-AKT level in BGC-823 cells. Wu[41] also found that INPP4B was positively correlated with cytoplasmic hypoxia inducible factor-1A (HIF-1A) ($P = 0.003$), which might affect the microvessel density and the occurrence of tumors. Hence, the roles of INPP4B in the prognosis of gastric cancer patients may be paradoxical.

In summary, *INPP4B* is thought to act as an oncogene by regulating AKT in gastric cancer. INPP4B plays a negative regulatory role in the occurrence, development, invasion, and metastasis of gastric cancer. Downregulation of INPP4B expression has been associated with EBV infection. The detection of INPP4B mRNA and protein expression in peripheral blood or cancer tissues has appreciated guiding significance for the determination of cancer subtypes and prognosis. The identification of INPP4B as a potential therapeutic target suggests its promising role in the management of gastric cancer.

INPP4B AND CONLON CANCER

Colon cancer is a common malignancy of the digestive system. The early diagnosis of colon cancer depends on colonoscopy and other invasive examinations, and the prognosis is usually poor. The in-depth study of INPP4B and colon cancer may provide a new direction for early diagnosis, treatment, and prognosis judgment in this malignancy.

Role of INPP4B in inhibiting colon cancer

Sung *et al*[42] determined the expression of INPP4B in the colorectal cancer cell lines HCT-116, SW620, DLD-1, and WiDr by RT-PCR, Western blot, and IHC. INPP4B expression levels were significantly reduced in colorectal cancer cell lines ($P < 0.001$). Choi *et al*[43] studied the expression of INPP4B in colorectal cancer tissues in the public genome database and discovered that the expression level of INPP4B was significantly reduced in colorectal cancer. Studies by Ma *et al*[44] have shown that the downregulation of INPP4B can lead to a decrease in p27 expression and an increase in cyclin D1 expression in colorectal cancer cells, thus promoting the occurrence and development of the tumors. This supports that *INPP4B* acts as an anticancer gene in colon cancer. One of the upstream regulatory signals of INPP4B is miR-1290 ($P < 0.05$). MiR-1290 may inhibit the expression of INPP4B by binding to the 3'-untranslated region of *INPP4B* and thus promote the proliferation of colorectal cancer ($P < 0.05$)[44]. Therefore, the above research indicates that *INPP4B* also plays a role as a tumor suppressor gene in colon cancer.

Role of INPP4B in promoting colon cancer

However, some studies have shown that high expression of INPP4B in colon cancer may have a carcinogenic effect. Guo *et al*[18] used IHC to detect INPP4B expression in 124 pairs of colon cancer and tumor-adjacent tissues. INPP4B was upregulated in more than half of the cancer tissues ($P < 0.01$). This may be due to an increase in the transcription of *INPP4B* in colon cancer cells mediated by E26 transformation-specific 1 (Ets-1). The overexpression of INPP4B promoted the development and progression of colon cancer by promoting the expression of AKT and SGK3. The study also found that the activation of AKT and SGK3 was blocked by silencing INPP4B ($P < 0.05$), thereby inhibiting the proliferation of colon cancer cells and delaying the growth of xenograft tumors of colon cancer. Ruan *et al*[19] found that INPP4B promoted colorectal cancer by activating the mTORC1 signaling pathway and cap-dependent cAMP-activated protein ($P < 0.05$). This process was also found to be associated with increased AKT and SGK3 expression ($P < 0.05$). High INPP4B expression in colon cancer is often accompanied by high SGK3 expression, which explains why INPP4B appears to promote cancer in some colon cancers[18,45]. Therefore, the PI3K/SGK3 pathway may be the pathway *via* which INPP4B plays a role in promoting colon cancer.

Previous results also indicate that INPP4B overexpression in colon cancer activates AKT[18,19]. A similar phenomenon in which INPP4B overexpression leads to increased AKT expression has also been found in esophageal cancer[20]. Therefore, the carcinogenic effect of INPP4B in colon cancer and other digestive system tumors may also be related to the activation of the PI3K/AKT pathway. Some studies suggest that this process may be related to the interaction between INPP4B and PTEN[18,46,47]. Guo *et al*[18] found that the increase in INPP4B expression was accompanied by the downregulation of PTEN in colon cancer cells, while the upregulation of PTEN was observed in INPP4B knockout cells. Therefore, overexpression of INPP4B leads to activation of PI3K/AKT in colon cancer cells, which may be related to downregulation of PTEN ($P < 0.05$).

Croft *et al*[42] reported a new small transcript variant of *INPP4B* (*INPP4B-S*). *INPP4B-S* differs from full-length *INPP4B* (*INPP4B-FL*) in that a new small exon is inserted between its 15th and 16th exons, and exons 20-24 are deleted. *INPP4B-S* was found to promote the proliferation of colon and breast cancer cells ($P < 0.01$). This suggests that INPP4B may have different isoforms. Different isoforms of INPP4B may have different procancer or anticancer effects and thus may affect the differences in the degree of malignancy and prognosis of tumors. In addition, Chen[48] found that the expression levels of IRF-2 and INPP4B in colorectal cancer tissues were positively correlated and that INPP4B may be involved in the development of microsatellite instability in colorectal cancer. This suggests that there may be other mechanisms for the carcinogenic effects of INPP4B.

These results suggest that INPP4B may be a carcinogenic driver of colon cancer. Therefore, INPP4B could potentially serve as a novel therapeutic target for colon cancer treatment.

Dual function of INPP4B in colon cancer

Recently, Yang *et al*[13] confirmed the dual role of INPP4B in colorectal cancer in animal experiments. This effect may be attributed to the regulation of Sox2 and Nanog expression by the PTEN/PI3K/AKT signaling pathway. The team used qRT-PCR to find that the expression of INPP4B was decreased in primary colorectal cancer ($P < 0.05$), accompanied by the

overexpression of Recombinant Sex Determining Region Y Box Protein 2 (Sox2) and Nanog ($P < 0.05$). In metastatic colorectal cancer, the expression of INPP4B was increased ($P < 0.05$), while antagonism between Sox2 and Nanog and INPP4B was observed ($P < 0.05$). It is suggested that the expression of INPP4B is closely related to the origin of colon cancer.

In summary, the dual role of INPP4B in colon cancer has been demonstrated. This dual function may be related to the PI3K/AKT and PI3K/SGK3 pathways or to the existence of different subtypes of INPP4B. The specific mechanism needs further research and discussion.

INPP4B AND PANCREATIC CANCER

Pancreatic cancer is a kind of digestive system malignancy with high mortality. Pancreatic cancer is characterized by its difficult early diagnosis, high drug resistance rate, and poor prognosis. At present, the study of INPP4B in pancreatic cancer is in the preliminary stage.

Role of INPP4B in inhibiting pancreatic cancer

At present, there are few studies on the role of INPP4B in pancreatic cancer. The INPP4B level in pancreatic cancer cells (ASPC-1, BXPC-3, SW1990, and PANC-1) was significantly reduced compared to that in normal controls, as detected by using Western blot and qRT-PCR ($P < 0.05$). Overexpression of INPP4B inhibited the activation of AKT signaling and partially reversed epithelial-mesenchymal transition (EMT) in pancreatic cancer cells ($P < 0.05$) to reduce invasion[49]. Therefore, *INPP4B* is a tumor suppressor gene in pancreatic cancer. In addition, the expression of INPP4B and E-cadherin (Ecad) in pancreatic cancer tissues was found to be consistent to a certain extent by using gene overexpression and interference techniques ($P < 0.05$). This process is related not only to the inhibition of AKT expression (the activation of AKT can reduce the expression level of Ecad) but also to the direct effect of INPP4B on Ecad[16,49]. A study of 39 primary pancreatic ductal cell adenocarcinoma specimens surgically removed found that INPP4B was involved in the endocytosis and circulation of Ecad[16]. A reduction in the level of INPP4B resulted in the loss of Ecad. The loss of Ecad is often the first step of epithelial-mesenchymal transformation in tumorigenesis[50]. Therefore, the decrease in INPP4B expression initiated the development of pancreatic cancer. In addition, although the methylation inhibitor failed to reverse the methylation state of the *INPP4B* gene promoter region in cancer cells, it upregulated the expression of INPP4B and Ecad ($P < 0.05$)[16]. Therefore, the identification of methylation inhibitors that can be effectively employed in clinical settings may represent a novel avenue of research on the treatment of pancreatic cancer characterized by low INPP4B and Ecad expression. Furthermore, an in-depth exploration into the underlying mechanism is warranted.

Role of INPP4B in promoting pancreatic cancer

However, recent studies have collected INPP4B expression data in pancreatic cancer tissues and normal tissues in Gene Expression Profiling Interactive Analysis. Statistical analysis revealed that the expression level of INPP4B in pancreatic cancer tissues was significantly increased ($P < 0.05$). INPP4B downregulation inhibited the proliferation of pancreatic cancer cells, promoted cell apoptosis, and reduced the phosphorylation level of AKT ($P < 0.05$). *INPP4B* has been identified as a significant oncogene in pancreatic cancer. INPP4B can be considered a potential diagnostic marker and independent prognostic marker and may even be a new therapeutic target for pancreatic cancer[51].

Above all, the role of INPP4B in pancreatic cancer is controversial. The controversial point is also related to the regulatory effect of INPP4B on AKT. Similar to colon cancer studies, other studies have found that decreased PTEN expression in pancreatic cancer leads to increased phosphorylation of AKT, which promotes the proliferation of pancreatic cancer cells[52]. Therefore, the specific mechanism by which PTEN is involved in the regulatory effect of INPP4B on AKT may be the focus of future studies in pancreatic cancer.

INPP4B AND LIVER CANCER

Liver cancer is the second most common cause of cancer-related death in China, and HCC accounts for approximately 90% of primary liver cancer cases. HCC is often caused by viral hepatitis, alcoholism, nonalcoholic fatty liver disease, and aflatoxin exposure. HCC is difficult to diagnose early and is highly invasive, with a poor overall prognosis and low survival rate. At present, the specific role of INPP4B in liver cancer has not been fully studied.

Zhang *et al*[53] used IHC to detect the expression of INPP4B and PTEN in 74 Liver cancer tissues, 74 paracancerous tissues, and 30 normal liver tissues. The expression levels of INPP4B and PTEN in liver cancer tissues were significantly decreased ($P < 0.05$), and their expression levels were positively correlated ($P = 0.000$). INPP4B and PTEN are closely related to the occurrence, development, invasion, and metastasis of liver cancer, and they have obvious antitumor effects and synergistic effects in liver cancer. However, the specific mechanism is not completely clear[53,54].

Xie *et al*[10] assessed eight HCC cell lines (Hep3B, Huh7, HepG2, HCCC-9810, BEL-7402, QGY-7703, MHCC97L, and MHCC97H) and eight surgically excised specimens and found that miR-765 was highly expressed in HCC. MiR-765 promoted the proliferation and development of HCC. The results of the dual-luciferase reporter and Western blot assays showed that the high expression of miR-765 inhibited the expression of INPP4B ($P < 0.05$). Therefore, INPP4B is a target of miR-765. By inhibiting the expression of INPP4B, miR-765 Leads to upregulation of p-AKT and cyclin D1 and downregulation of phosphorylated forkhead box O3 (p-FOXO3a) and p21 in HCC, thus promoting the development of

HCC[55]. In the latest research, Tang *et al*[56] used qRT-PCR and Western blot to determine INPP4B elevation in both metastatic and nonmetastatic HCC samples of 86 human HCC patients ($P < 0.001$). The positive rate of INPP4B expression in metastatic HCC tissues was higher than that in primary HCC tissues. INPP4B was negatively correlated with AKT and p-AKT in HCC cells ($P < 0.05$). This suggests that INPP4B plays an antitumor role in HCC by inhibiting the PI3K/AKT pathway and that INPP4B inhibits the metastasis and invasion of HCC by inhibiting the EMT process of HCC.

Therefore, it is currently believed that INPP4B plays an anticancer role in HCC mainly by inhibiting the PI3K/AKT pathway. The signaling pathway mechanism of INPP4B in HCC is the next research focus. MiR-765 and INPP4B may be new targets for the diagnosis and treatment of HCC.

INPP4B AND ESOPHAGEAL CANCER

There is only one study on INPP4B in esophageal cancer. High expression of INPP4B mRNA and protein in esophageal squamous carcinoma ($P < 0.05$) was found by qRT-PCR and IHC, respectively. INPP4B was positively correlated with the expression of AKT and pAKT in esophageal cancer ($P = 0.000$). This suggests that high expression of INPP4B may play a role in promoting esophageal cancer[20]. Since the role of NPP4B in esophageal cancer has been poorly studied, this conclusion needs to be further confirmed with more research.

INPP4B AND GALLBLADDER CANCER

There are only two studies on INPP4B in gallbladder cancer (GBC) from Wu *et al*[57]. Wu *et al*[57] found that INPP4B was upregulated in human GBC tissues compared with normal gallbladder tissues, but INPP4B was highly expressed in highly-moderately differentiated GBC and was not associated with the overall survival of GBC patients ($P = 0.071$). In GBC-SD cells, overexpression of INPP4B increased the expression levels of p-SGK3 and p-Akt, and interference with INPP4B decreased the expression levels of p-SGK3 and p-Akt. In SGC996 cells, overexpression of INPP4B enhanced the expression level of p-SGK3. These results suggest that INPP4B plays an oncogenic role in GC cells and GBC cells and may affect their biological functions through different signaling pathways in different GBCs. In GBC cells, INPP4B knockdown inhibited proliferation, colony formation, migration, and invasion, while INPP4B overexpression had opposite effects *in vitro*. These findings suggest that INPP4B may play a dual role in GBC.

CONCLUSION

In summary, INPP4B plays different roles in a variety of digestive system tumors. INPP4B plays an obvious anticancer role in a variety of digestive system cancers, such as gastric cancer, colon cancer, pancreatic cancer, and liver cancer. However, INPP4B is also believed to have promoting roles in colon, pancreatic, and esophageal cancers. The roles of INPP4B in digestive system tumors mainly include the following: (1) EBV and microRNAs can regulate the expression of INPP4B; (2) INPP4B can regulate PI3K/AKT to exert an anticancer effect and can also promote the procancer effect of PI3K/AKT by affecting PTEN; (3) INPP4B can regulate PI3K/SGK3 to promote cancer; and (4) INPP4B can affect the EMT process of some tumor cells.

At present, the understanding of the role of INPP4B in digestive system tumors is still superficial. There are still few studies on its mechanism of action, clinical development, and application in different digestive system tumors. Based on the contradiction and duality shown in current INPP4B research, further research and discussion may be needed regarding the upstream and downstream pathways of INPP4B and the mechanism of action of various subtypes of INPP4B. Future studies should aim to determine its role in promoting or inhibiting cancer in different types of digestive tumors and further consider whether it is possible for it to be clinically detected and applied for treatment by assessing, blocking, or promoting the expression of INPP4B. INPP4B has been found to be associated with drug resistance and radiation resistance in malignant tumors such as ovarian, laryngeal, and lung cancers[58-61]. At present, there is a lack of relevant research on this aspect in digestive tumors. In addition, the correlation of INPP4B expression with the features of other digestive system tumors, such as gastrointestinal pancreatic neuroendocrine tumors and tumors in the bile duct, duodenum, and ileum, remains unknown. With the development of this area of research, broad prospects may emerge for the use of INPP4B in the early diagnosis, monitoring, prognosis assessment, and treatment of digestive system malignancies.

ACKNOWLEDGEMENTS

We would like to give our heartfelt thanks to all the people who have helped us with this paper. Our sincere appreciation goes first to China-Japan Friendship Hospital.

FOOTNOTES

Author contributions: Han L contributed significantly to conceptualization, data analysis, and manuscript preparation; Du SY and Chen S helped perform data analysis with constructive discussions; all authors read and approved the final version of the manuscript.

Supported by the China-Japan Friendship Hospital Foundation, No. 2019-1-QN-2.

Conflict-of-interest statement: The authors declare that they have no competing interests to disclose.

Country/Territory of origin: China

ORCID number: Le Han 0000-0002-7591-0805; Shuo Chen 0000-0002-2808-2787.

S-Editor: Yan JP
L-Editor: Wang TQ
P-Editor: Yan JP

REFERENCES

1 **Sung H**, Ferlay J, Siegel RL, Laversanne M, Soerjomataram I, Jemal A, Bray F. Global Cancer Statistics 2020: GLOBOCAN Estimates of Incidence and Mortality Worldwide for 36 Cancers in 185 Countries. *CA Cancer J Clin* 2021; **71**: 209-249 [PMID: 33538338 DOI: 10.3322/caac.21660]

2 **Lai SQ**. Cancer's Current Situation and Predicament, Prospect and Way Out: Analysis of Cancer's Development Tendency and Control Measures of 2017. *Yixue Yu Zhexue* 2018; **40**: 20-23

3 **Kofuji S**, Kimura H, Nakanishi H, Nanjo H, Takasuga S, Liu H, Eguchi S, Nakamura R, Itoh R, Ueno N, Asanuma K, Huang M, Koizumi A, Habuchi T, Yamazaki M, Suzuki A, Sasaki J, Sasaki T. INPP4B Is a PtdIns(3,4,5)P3 Phosphatase That Can Act as a Tumor Suppressor. *Cancer Discov* 2015; **5**: 730-739 [PMID: 25883023 DOI: 10.1158/2159-8290.CD-14-1329]

4 **Ferron M**, Vacher J. Characterization of the murine Inpp4b gene and identification of a novel isoform. *Gene* 2006; **376**: 152-161 [PMID: 16631325 DOI: 10.1016/j.gene.2006.02.022]

5 **Gewinner C**, Wang ZC, Richardson A, Teruya-Feldstein J, Etemadmoghadam D, Bowtell D, Barretina J, Lin WM, Rameh L, Salmena L, Pandolfi PP, Cantley LC. Evidence that inositol polyphosphate 4-phosphatase type II is a tumor suppressor that inhibits PI3K signaling. *Cancer Cell* 2009; **16**: 115-125 [PMID: 19647222 DOI: 10.1016/j.ccr.2009.06.006]

6 **Agoulnik IU**, Hodgson MC, Bowden WA, Ittmann MM. INPP4B: the new kid on the PI3K block. *Oncotarget* 2011; **2**: 321-328 [PMID: 21487159 DOI: 10.18632/oncotarget.260]

7 **Woolley JF**, Dzneladze I, Salmena L. Phosphoinositide signaling in cancer: INPP4B Akt(s) out. *Trends Mol Med* 2015; **21**: 530-532 [PMID: 26150301 DOI: 10.1016/j.molmed.2015.06.006]

8 **Lopez SM**, Hodgson MC, Packianathan C, Bingol-Ozakpinar O, Uras F, Rosen BP, Agoulnik IU. Determinants of the tumor suppressor INPP4B protein and lipid phosphatase activities. *Biochem Biophys Res Commun* 2013; **440**: 277-282 [PMID: 24070612 DOI: 10.1016/j.bbrc.2013.09.077]

9 **Bertucci MC**, Mitchell CA. Phosphoinositide 3-kinase and INPP4B in human breast cancer. *Ann N Y Acad Sci* 2013; **1280**: 1-5 [PMID: 23551093 DOI: 10.1111/nyas.12036]

10 **Xie BH**, He X, Hua RX, Zhang B, Tan GS, Xiong SQ, Liu LS, Chen W, Yang JY, Wang XN, Li HP. Mir-765 promotes cell proliferation by downregulating INPP4B expression in human hepatocellular carcinoma. *Cancer Biomark* 2016; **16**: 405-413 [PMID: 27062697 DOI: 10.3233/CBM-160579]

11 **Hodgson MC**, Shao LJ, Frolov A, Li R, Peterson LE, Ayala G, Ittmann MM, Weigel NL, Agoulnik IU. Decreased expression and androgen regulation of the tumor suppressor gene INPP4B in prostate cancer. *Cancer Res* 2011; **71**: 572-582 [PMID: 21224358 DOI: 10.1158/0008-5472.CAN-10-2314]

12 **Rijal S**, Fleming S, Cummings N, Rynkiewicz NK, Ooms LM, Nguyen NY, Teh TC, Avery S, McManus JF, Papenfuss AT, McLean C, Guthridge MA, Mitchell CA, Wei AH. Inositol polyphosphate 4-phosphatase II (INPP4B) is associated with chemoresistance and poor outcome in AML. *Blood* 2015; **125**: 2815-2824 [PMID: 25736313 DOI: 10.1182/blood-2014-09-603555]

13 **Yang L**, Ding C, Tang W, Yang T, Liu M, Wu H, Wen K, Yao X, Feng J, Luo J. INPP4B exerts a dual function in the stemness of colorectal cancer stem-like cells through regulating Sox2 and Nanog expression. *Carcinogenesis* 2020; **41**: 78-90 [PMID: 31179504 DOI: 10.1093/carcin/bgz110]

14 **Wang Y**, Zhou D, Phung S, Masri S, Smith D, Chen S. SGK3 is an estrogen-inducible kinase promoting estrogen-mediated survival of breast cancer cells. *Mol Endocrinol* 2011; **25**: 72-82 [PMID: 21084382 DOI: 10.1210/me.2010-0294]

15 **Dzneladze I**, He R, Woolley JF, Son MH, Sharobim MH, Greenberg SA, Gabra M, Langlois C, Rashid A, Hakem A, Ibrahimova N, Arruda A, Löwenberg B, Valk PJ, Minden MD, Salmena L. INPP4B overexpression is associated with poor clinical outcome and therapy resistance in acute myeloid leukemia. *Leukemia* 2015; **29**: 1485-1495 [PMID: 25736236 DOI: 10.1038/leu.2015.51]

16 **Zhang B**, Wang W, Li C, Liu R. Inositol polyphosphate-4-phosphatase type II plays critical roles in the modulation of cadherin-mediated adhesion dynamics of pancreatic ductal adenocarcinomas. *Cell Adh Migr* 2018; **12**: 548-563 [PMID: 29952716 DOI: 10.1080/19336918.2018.1491496]

17 **Ma K**, Cheung SM, Marshall AJ, Duronio V. PI(3,4,5)P3 and PI(3,4)P2 Levels correlate with PKB/akt phosphorylation at Thr308 and Ser473,

respectively; PI(3,4)P2 Levels determine PKB activity. *Cell Signal* 2008; **20**: 684-694 [PMID: 18249092 DOI: 10.1016/j.cellsig.2007.12.004]
18 **Guo ST**, Chi MN, Yang RH, Guo XY, Zan LK, Wang CY, Xi YF, Jin L, Croft A, Tseng HY, Yan XG, Farrelly M, Wang FH, Lai F, Wang JF, Li YP, Ackland S, Scott R, Agoulnik IU, Hondermarck H, Thorne RF, Liu T, Zhang XD, Jiang CC. INPP4B is an oncogenic regulator in human colon cancer. *Oncogene* 2016; **35**: 3049-3061 [PMID: 26411369 DOI: 10.1038/onc.2015.361]
19 **Ruan XH**, Liu XM, Yang ZX, Zhang SP, Li QZ, Lin CS. INPP4B promotes colorectal cancer cell proliferation by activating mTORC1 signaling and cap-dependent translation. *Onco Targets Ther* 2019; **12**: 3109-3117 [PMID: 31114251 DOI: 10.2147/OTT.S186365]
20 **Zhang L**. Clinical significance and correlation to prognosis of expression of INPP4B, Akt and pAkt in esophageal squamous carcinoma. MS Thesis, Shanxi Medical University. 2017
21 **Carracedo A**, Alimonti A, Pandolfi PP. PTEN level in tumor suppression: how much is too little? *Cancer Res* 2011; **71**: 629-633 [PMID: 21266353 DOI: 10.1158/0008-5472.CAN-10-2488]
22 **Vo TT**, Fruman DA. INPP4B Is a Tumor Suppressor in the Context of PTEN Deficiency. *Cancer Discov* 2015; **5**: 697-700 [PMID: 26152921 DOI: 10.1158/2159-8290.CD-15-0609]
23 **Moniz LS**, Vanhaesebroeck B. AKT-ing out: SGK kinases come to the fore. *Biochem J* 2013; **452**: e11-e13 [PMID: 23725458 DOI: 10.1042/BJ20130617]
24 **Bruhn MA**, Pearson RB, Hannan RD, Sheppard KE. Second AKT: the rise of SGK in cancer signalling. *Growth Factors* 2010; **28**: 394-408 [PMID: 20919962 DOI: 10.3109/08977194.2010.518616]
25 **Xu J**, Liu D, Gill G, Songyang Z. Regulation of cytokine-independent survival kinase (CISK) by the Phox homology domain and phosphoinositides. *J Cell Biol* 2001; **154**: 699-705 [PMID: 11514587 DOI: 10.1083/jcb.200105089]
26 **Gasser JA**, Inuzuka H, Lau AW, Wei W, Beroukhim R, Toker A. SGK3 mediates INPP4B-dependent PI3K signaling in breast cancer. *Mol Cell* 2014; **56**: 595-607 [PMID: 25458846 DOI: 10.1016/j.molcel.2014.09.023]
27 **Tsao H**, Goel V, Wu H, Yang G, Haluska FG. Genetic interaction between NRAS and BRAF mutations and PTEN/MMAC1 inactivation in melanoma. *J Invest Dermatol* 2004; **122**: 337-341 [PMID: 15009714 DOI: 10.1046/j.0022-202X.2004.22243.x]
28 **Chi MN**, Guo ST, Wilmott JS, Guo XY, Yan XG, Wang CY, Liu XY, Jin L, Tseng HY, Liu T, Croft A, Hondermarck H, Scolyer RA, Jiang CC, Zhang XD. INPP4B is upregulated and functions as an oncogenic driver through SGK3 in a subset of melanomas. *Oncotarget* 2015; **6**: 39891-39907 [PMID: 26573229 DOI: 10.18632/oncotarget.5359]
29 **Hu QL**, Wang HB, Yang M. Significance of expression of INPP4B in gastric cancer. *Shijie Huaren Xiaohua Zazhi* 2016; **24**: 2478-2484
30 **Fan CJ**. Expression of INPP4B in gastric cancer. MS Thesis, Shanxi Medical University. 2016
31 **Yang M**, Wang HB, Hu QL. Significance of the expression of INPP4B mRNA and protein in peripheral blood of gastric cancer patient. *Xiandai Zhongliu Yixue* 2016; **24**: 3443-3446
32 **Li Z**, Yu JS, Jia YH, Li Y, Xu Y, Ding B. Expression and clinicopathologic significance of INPP4B protein in gastric adenocarcinoma. *Xiandai Yiyao Weisheng* 2020; **36**: 1614-1617
33 **Liu Z**, Gong XL, Yu DZ, Zhao YY, Xu AF, Song Y. Relationship between the expression of INPP4B in peripheral blood and clinicopathological features, chemosensitivity and PI3K/AKT pathway in patients with gastric cancer. *Zhongguo Shiyan Zhenduanxue* 2023; **l27**: 516-521
34 **Ma YW**, Tan JC, Zhang Y, Dai WH, Lin RJ, Luo Y, Xu Y. Reduced Expression of INPP4B in Epstein-Barr Virus-Associated Gastric Carcinoma. *Zhongguo Yike Daxue Xuebao* 2019; **48**: 587-590, 600
35 **Cancer Genome Atlas Research Network**. Comprehensive molecular characterization of gastric adenocarcinoma. *Nature* 2014; **513**: 202-209 [PMID: 25079317 DOI: 10.1038/nature13480]
36 **Yuen JW**, Chung GT, Lun SW, Cheung CC, To KF, Lo KW. Epigenetic inactivation of inositol polyphosphate 4-phosphatase B (INPP4B), a regulator of PI3K/AKT signaling pathway in EBV-associated nasopharyngeal carcinoma. *PLoS One* 2014; **9**: e105163 [PMID: 25126743 DOI: 10.1371/journal.pone.0105163]
37 **Niller HH**, Banati F, Salamon D, Minarovits J. Epigenetic Alterations in Epstein-Barr Virus-Associated Diseases. *Adv Exp Med Biol* 2016; **879**: 39-69 [PMID: 26659263 DOI: 10.1007/978-3-319-24738-0_3]
38 **Shinozaki-Ushiku A**, Kunita A, Fukayama M. Update on Epstein-Barr virus and gastric cancer (review). *Int J Oncol* 2015; **46**: 1421-1434 [PMID: 25633561 DOI: 10.3892/ijo.2015.2856]
39 **Ma YW**. A research about the expression and mechanism of INPP4B in EBV-associated gastric cancer. MS Thesis, China Medical University. 2019
40 **Wu Y**, Wang X, Lu Y, Wang H, Wang M, You Y, Su X, Sun D, Sun Y, Li Y. INPP4B exerts a dual role in gastric cancer progression and prognosis. *J Cancer* 2021; **12**: 7201-7213 [PMID: 34729121 DOI: 10.7150/jca.58397]
41 **Wu Y**. Clinical significance and mechanism of INPP4B in gastric cancer and gallbladder cancer. MS Thesis, Anhui Medical University. 2022
42 **Sung JY**, Na K, Kim HS. Down-regulation of Inositol Polyphosphate 4-Phosphatase Type II Expression in Colorectal Carcinoma. *Anticancer Res* 2017; **37**: 5525-5531 [PMID: 28982866 DOI: 10.21873/anticanres.11984]
43 **Choi EJ**, Kim MS, Yoo NJ, Lee SH. Inactivating Frameshift Mutation of INPP4B Encoding a PI3K Pathway Phosphatase in Gastric and Colorectal Cancers. *Pathol Oncol Res* 2016; **22**: 653-654 [PMID: 27068714 DOI: 10.1007/s12253-016-0062-9]
44 **Ma Q**, Wang Y, Zhang H, Wang F. miR-1290 Contributes to Colorectal Cancer Cell Proliferation by Targeting INPP4B. *Oncol Res* 2018; **26**: 1167-1174 [PMID: 28915933 DOI: 10.3727/096504017X15051741798389]
45 **Song TN**. The expression and clinical significance of INPP4B, SGK3 and Ki-67 in colon cancer. MS Thesis, Chengde Medical University. 2018
46 **Rodgers SJ**, Ferguson DT, Mitchell CA, Ooms LM. Regulation of PI3K effector signalling in cancer by the phosphoinositide phosphatases. *Biosci Rep* 2017; **37** [PMID: 28082369 DOI: 10.1042/BSR20160432]
47 **Croft A**, Guo ST, Sherwin S, Farrelly M, Yan XG, Zhang XD, Jiang CC. Functional identification of a novel transcript variant of INPP4B in human colon and breast cancer cells. *Biochem Biophys Res Commun* 2017; **485**: 47-53 [PMID: 28189677 DOI: 10.1016/j.bbrc.2017.02.012]
48 **Chen DG**. Expression and Clincopathological Significance of IRF-2 and INPP4B in Colorectal Adenocarcinoma Tissues. MS Thesis, Gansu Medical University. 2022
49 **Zhang B**. Inositol polyphosphate-4-phosphatase type II plays critical roles in the modulation of cadherin-mediated adhesion dynamics of pancreatic ductal adenocarcinomas. MS Thesis, Chinese People's Liberation Army General Hospital. 2018
50 **Krantz SB**, Shields MA, Dangi-Garimella S, Munshi HG, Bentrem DJ. Contribution of epithelial-to-mesenchymal transition and cancer stem cells to pancreatic cancer progression. *J Surg Res* 2012; **173**: 105-112 [PMID: 22099597 DOI: 10.1016/j.jss.2011.09.020]

51 **Zhai S**, Liu Y, Lu X, Qian H, Tang X, Cheng X, Wang Y, Shi Y, Deng X. INPP4B As A Prognostic And Diagnostic Marker Regulates Cell Growth Of Pancreatic Cancer Via Activating AKT. *Onco Targets Ther* 2019; **12**: 8287-8299 [PMID: 31632078 DOI: 10.2147/OTT.S223221]

52 **Asano T**, Yao Y, Zhu J, Li D, Abbruzzese JL, Reddy SA. The PI 3-kinase/Akt signaling pathway is activated due to aberrant Pten expression and targets transcription factors NF-kappaB and c-Myc in pancreatic cancer cells. *Oncogene* 2004; **23**: 8571-8580 [PMID: 15467756 DOI: 10.1038/sj.onc.1207902]

53 **Zhang YY**. Significance of expression of INPP4B and PTEN in hepatocellular carcinoma. MS Thesis, Zhengzhou University. 2014

54 **Zhang YY**, Li JS, He DZ, Jiang D. Significance of expression of INPP4B and PTEN in hepatocellular carcinoma. *Shijie Huaren Xiaohua Zazhi* 2014; **22**: 695-699

55 **Xie X**, Wang XX, Xie BH, He X, Xie YK, Zeng QS. Mir-765 regulates hepatocellular carcinoma cell proliferation through targeting INPP4B. *Zhongguo Zhongliu Shengwu Zhiliao Zazhi* 2017; **24**: 43-47

56 **Tang W**, Yang L, Yang T, Liu M, Zhou Y, Lin J, Wang K, Ding C. INPP4B inhibits cell proliferation, invasion and chemoresistance in human hepatocellular carcinoma. *Onco Targets Ther* 2019; **12**: 3491-3507 [PMID: 31123408 DOI: 10.2147/OTT.S196832]

57 **Wu Y**, Meng D, Xu X, Bao J, You Y, Sun Y, Li Y, Sun D. Expression and functional characterization of INPP4B in gallbladder cancer patients and gallbladder cancer cells. *BMC Cancer* 2021; **21**: 433 [PMID: 33879096 DOI: 10.1186/s12885-021-08143-6]

58 **Ip LR**, Poulogiannis G, Viciano FC, Sasaki J, Kofuji S, Spanswick VJ, Hochhauser D, Hartley JA, Sasaki T, Gewinner CA. Loss of INPP4B causes a DNA repair defect through loss of BRCA1, ATM and ATR and can be targeted with PARP inhibitor treatment. *Oncotarget* 2015; **6**: 10548-10562 [PMID: 25868852 DOI: 10.18632/oncotarget.3307]

59 **Min JW**, Kim KI, Kim HA, Kim EK, Noh WC, Jeon HB, Cho DH, Oh JS, Park IC, Hwang SG, Kim JS. INPP4B-mediated tumor resistance is associated with modulation of glucose metabolism *via* hexokinase 2 regulation in laryngeal cancer cells. *Biochem Biophys Res Commun* 2013; **440**: 137-142 [PMID: 24051093 DOI: 10.1016/j.bbrc.2013.09.041]

60 **Kim JS**, Yun HS, Um HD, Park JK, Lee KH, Kang CM, Lee SJ, Hwang SG. Identification of inositol polyphosphate 4-phosphatase type II as a novel tumor resistance biomarker in human laryngeal cancer HEp-2 cells. *Cancer Biol Ther* 2012; **13**: 1307-1318 [PMID: 22895072 DOI: 10.4161/cbt.21788]

61 **Stjernström A**, Karlsson C, Fernandez OJ, Söderkvist P, Karlsson MG, Thunell LK. Alterations of INPP4B, PIK3CA and pAkt of the PI3K pathway are associated with squamous cell carcinoma of the lung. *Cancer Med* 2014; **3**: 337-348 [PMID: 24500884 DOI: 10.1002/cam4.191]

World Journal of Gastrointestinal Oncology

Submit a Manuscript: https://www.f6publishing.com

World J Gastrointest Oncol 2023 October 15; 15(10): 1717-1738

DOI: 10.4251/wjgo.v15.i10.1717

ISSN 1948-5204 (online)

ORIGINAL ARTICLE

Basic Study

Identification of tumor antigens and immune subtypes of hepatocellular carcinoma for mRNA vaccine development

Tai-Liang Lu, Cheng-Long Li, Yong-Qiang Gong, Fu-Tao Hou, Chao-Wu Chen

Specialty type: Oncology

Provenance and peer review: Unsolicited article; Externally peer reviewed.

Peer-review model: Single blind

Peer-review report's scientific quality classification

Grade A (Excellent): A, A
Grade B (Very good): 0
Grade C (Good): 0
Grade D (Fair): 0
Grade E (Poor): 0

P-Reviewer: Jiraviriyakul A, Thailand; Sahin TT, Turkey

Received: June 13, 2023
Peer-review started: June 13, 2023
First decision: July 25, 2023
Revised: August 10, 2023
Accepted: September 18, 2023
Article in press: September 18, 2023
Published online: October 15, 2023

Tai-Liang Lu, Cheng-Long Li, Yong-Qiang Gong, Fu-Tao Hou, Chao-Wu Chen, Department of General Surgery, Hunan Provincial People's Hospital, The First Affiliated Hospital of Hunan Normal University, Changsha 410005, Hunan Province, China

Corresponding author: Chao-Wu Chen, MD, Chief Physician, Department of General Surgery, Hunan Provincial People's Hospital, The First Affiliated Hospital of Hunan Normal University, No. 61 Jiefang Xi Road, Furong District, Changsha 410005, Hunan Province, China. dr.chencw@hunnu.edu.cn

Abstract

BACKGROUND

mRNA vaccines have been investigated in multiple tumors, but limited studies have been conducted on their use for hepatocellular carcinoma (HCC).

AIM

To identify candidate mRNA vaccine antigens for HCC and suitable subpopulations for mRNA vaccination.

METHODS

Gene expression profiles and clinical information of HCC datasets were obtained from International Cancer Genome Consortium and The Cancer Genome Atlas. Genes with somatic mutations and copy number variations were identified by cBioPortal analysis. The differentially expressed genes with significant prognostic value were identified by Gene Expression Profiling Interactive Analysis 2 website analysis. The Tumor Immune Estimation Resource database was used to assess the correlation between candidate antigens and the abundance of antigen-presenting cells (APCs). Tumor-associated antigens were overexpressed in tumors and associated with prognosis, genomic alterations, and APC infiltration. A consensus cluster analysis was performed with the Consensus Cluster Plus package to identify the immune subtypes. The weighted gene coexpression network analysis (WGCNA) was used to determine the candidate biomarker molecules for appropriate populations for mRNA vaccines.

RESULTS

AURKA, CCNB1, CDC25C, CDK1, TRIP13, PES1, MCM3, PPM1G, NEK2, KIF2C, PTTG1, KPNA2, and *PRC1* were identified as candidate HCC antigens for mRNA vaccine development. Four immune subtypes (IS1-IS4) and five immune gene modules of HCC were identified that were consistent in both patient cohorts. The

immune subtypes showed distinct cellular and clinical characteristics. The IS1 and IS3 immune subtypes were immunologically "cold". The IS2 and IS4 immune subtypes were immunologically "hot", and the immune checkpoint genes and immunogenic cell death genes were upregulated in these subtypes. IS1-related modules were identified with the WGCNA algorithm. Ultimately, five hub genes (*RBP4, KNG1, METTL7A, F12,* and *ABAT*) were identified, and they might be potential biomarkers for mRNA vaccines.

CONCLUSION

AURKA, CCNB1, CDC25C, CDK1, TRIP13, PES1, MCM3, PPM1G, NEK2, KIF2C, PTTG1, KPNA2, and *PRC1* have been identified as candidate HCC antigens for mRNA vaccine development. The IS1 and IS3 immune subtypes are suitable populations for mRNA vaccination. *RBP4, KNG1, METTL7A, F12,* and *ABAT* are potential biomarkers for mRNA vaccines.

Key Words: mRNA vaccine; Hepatocellular carcinoma; Immunotype; Antigens; Immune subtypes

Core Tip: In this study, bioinformatics methods were used to explore novel hepatocellular carcinoma (HCC)-specific antigens for mRNA vaccine development and construct an immune subtype of HCC to select the appropriate vaccination population. Tumor-specific antigens were defined as highly expressed, genetically altered, and prognostic genes associated with antigen-presenting cell infiltration. *AURKA, CCNB1, CDC25C, CDK1, TRIP13, PES1, MCM3, PPM1G, NEK2, KIF2C, PTTG1, KPNA2,* and *PRC1* were recognized candidate HCC antigens for mRNA vaccine development. The IS1 and IS3 immune subtypes of HCC were suitable populations for mRNA vaccination. *RBP4, KNG1, METTL7A, F12*, and *ABAT* were potential biomarkers for mRNA vaccines.

Citation: Lu TL, Li CL, Gong YQ, Hou FT, Chen CW. Identification of tumor antigens and immune subtypes of hepatocellular carcinoma for mRNA vaccine development. *World J Gastrointest Oncol* 2023; 15(10): 1717-1738
URL: https://www.wjgnet.com/1948-5204/full/v15/i10/1717.htm
DOI: https://dx.doi.org/10.4251/wjgo.v15.i10.1717

INTRODUCTION

Primary liver cancer is one of the leading causes of malignant tumor death in China. According to the latest cancer report published in Advances in Cancer Science[1], there were 389000 new cases of liver cancer in China, ranking fourth among malignant tumors. With an annual death rate of 336400, liver cancer is the second leading cause of cancer deaths; thus, it leads to a heavy disease burden[1]. Early diagnosis and treatment of liver cancer are critical. The five-year survival rate of patients with early-stage liver cancer is more than 50%, and the treatment cost is low[2]. However, the five-year survival rate of patients with advanced liver cancer is only 0%-20%, and the treatment is expensive[2]. In the past decade, the surgical technique for liver cancer has developed considerably, and its treatment effect has improved, making it more accurate and safer. Efficient minimally invasive endoscopic and ablation procedures and perioperative management can significantly reduce the surgical trauma of patients, but the surgical resection rate is only 20%-30%[3]. Hepatocellular carcinoma (HCC) is not sensitive to conventional chemotherapy and radiotherapy[4]. However, drug therapy, represented by targeted therapy and immunotherapy, has progressed dramatically[5]. Immunotherapy may be an essential therapeutic tool to improve the clinical outcomes of HCC.

With the impact of coronavirus disease 2019 (COVID-19), mRNA technology has entered a new fast track of development, and mRNA vaccines, as a future shield against COVID-19, have also attracted attention[6]. Moreover, mRNA vaccines have attracted much attention in cancer treatment[7-11]. Immunotherapy, which suppresses tumor development by altering or enhancing the immune system, is the mainstream tumor immune treatment and serves a new direction for tumor treatment. mRNA vaccines have become an important platform for cancer immunotherapy. At present, mRNA vaccine research has made progress in prostate cancer[12], non-small cell lung cancer[13], and melanoma [8]. mRNA cancer vaccines are a promising alternative to traditional vaccine approaches due to their high efficiency, safe administration, rapid development potential, and low-cost production[14]. DNA vaccines, dendritic cell vaccines, and peptide vaccines[15-17] are currently available for patients with HCC. In a clinical trial of the tumor vaccine phosphatidylglycan in patients with advanced HCC, patients with high cytotoxic T-cell expression had a median progression-free survival (mPFS) of 12.2 mo *in vivo*; the mPFS of patients with low cytotoxic T-cell expression was 8.5 mo [18]. mRNA cannot integrate into the genome and thus does not cause insertion mutations. The therapeutic HCC vaccine HePAVAC-101 was first tested in phase I/II clinical trials[19]. The results provided preliminary evidence for the safety and immunogenicity of the vaccine. Although tumor antigens have the characteristics of diversity and heterogeneity, with tremendous individual differences, mRNA sequences can be designed and modified to encode any pathological antigen. Thus, mRNA vaccines are ideally suited for targeting tumor-specific antigens[20,21]. Therefore, it is feasible and urgently necessary to develop and apply mRNA vaccines to improve the prognosis of HCC patients. It is also vital to

identify HCC patient subpopulations who are suitable for vaccination.

The antigens encoded by mRNA vaccines can be classified as tumor-associated antigens (TAAs) and tumor-specific antigens (TSAs)[22]. The core mechanism of mRNA cancer vaccines is to encode specific antigens based on the characteristics of cancer, which are successfully recognized by immune cells to activate the immune response[23]. TSAs, also known as "tumor neoantigens", are derived from gene mutations in cancer cells, so they are theoretically not constrained by immune tolerance[23]. The differences in mutation profiles of different tumors provide the possibility of tailoring highly individualized cancer vaccines.

This study aimed to explore novel HCC-associated antigens for mRNA vaccine development and construct an immune subtype of HCC to select the appropriate vaccination population. TSAs were overexpressed in tumors and associated with prognosis, genomic alterations, and antigen-presenting cell (APC) infiltration. By integrating multiomics data, 13 potential tumor antigens were identified for HCC mRNA vaccine development. The high expression of these antigens was associated with a poor prognosis and positively correlated with APC infiltration. Based on the clustering of immune-related genes *via* consensus clustering analysis, we defined four robust immune subtypes of HCC and identified an immune subtype population with "cold" tumors suitable for vaccination, which was validated in an independent cohort. Furthermore, five functional modules and five potential biomarkers for mRNA vaccines were identified by weighted gene coexpression network analysis (WGCNA). This study will provide new insights into developing HCC mRNA vaccines and screening suitable patients for vaccination.

MATERIALS AND METHODS

Data collection and processing

The RNA-seq and clinicopathological data of 371 HCC patients (Supplementary Table 1) were downloaded from The Cancer Genome Atlas (TCGA, https://www.cancer.gov/tcga). The normalized gene expression and clinical follow-up data of 235 HCC patients (Supplementary Table 1) were downloaded from the International Cancer Genome Consortium (ICGC, https://www.icgc-argo.org). The immune subtype data of the TCGA HCC samples were obtained from Supplementary material in a previously published study[24]. A total of 2108 immune-related genes (Supplementary Table 2) were obtained from previously published research[25]. First, samples with incomplete clinicopathological and follow-up data were removed. Then, genes that were not expressed in all samples were removed. In the TCGA cohort, we excluded 377 genes and 6 samples and finally obtained the expression matrix of 20153 genes in 365 samples. In the ICGC cohort, no genes or samples were excluded, and an expression matrix of 22911 genes in 235 samples was obtained. The gene expression was converted into log2 (TPM + 1). Finally, 2012 immune-related genes expressed in both the TCGA and ICGC datasets were included for the subsequent analysis.

Gene differential expression and mutation analysis

Gene Expression Profiling Interactive Analysis (GEPIA) 2 (http://gepia2.cancer-pku.cn) is a free public website for gene differential expression analysis and prognostic analysis of TCGA using a standard processing pipeline. The differentially expressed genes were identified using ANOVA by $|Log2FC| > 1$ and q value < 0.01. A chromosome distribution map of differentially expressed genes in HCC was downloaded from this website. The cBioCancer Genomics Portal (cBioPortal, http://www.cbioportal.org) was used for gene mutation analysis of HCC patients from TCGA. The overexpressed genes were regarded as potential tumor antigens filtered by analyzing amplification of copy number variation categories and mutation counts in individual samples. P values < 0.05 were considered statistically significant.

Survival analysis and Tumor Immune Estimation Resource analysis

The R package "survival" was used to analyze the correlation between candidate tumor antigen genes and overall survival (OS) and recurrence-free survival (RFS) of HCC patients. The HCC patients from TCGA were divided into two groups according to the median cutoff. A P value < 0.05 was considered statistically significant. Tumor Immune Estimation Resource (https://cistrome.shinyapps.io/timer/) was used to analyze the correlation between the candidate tumor antigen genes and APCs (B cells, macrophages, and dendritic cells). The P value cutoff was set as 0.05.

Identification and validation of immune subtypes

The 33 significant immune-related survival genes were identified *via* univariate Cox hazard analysis in TCGA datasets with a P value less than 0.05. Then, the R package "ConsensusClusterPlus"[26] was used to determine the immune subtypes of HCC in the TCGA datasets (training sets) and ICGC datasets (validation sets). The distance parameter was set to "Pearson", and the reps and pItem parameters were set to 1000 and 0.8, respectively. The maxk was set to 10, and the optimal k was defined by evaluating the consensus matrix and the consensus cumulative distribution function.

Estimation of clinicopathological characteristics and prognosis of immune subtypes

The clinical characteristics of patients with different immune subtypes, such as age, sex, grade, p stage, T stage, N stage, and M stage, were explored. The log-rank test was used to estimate the prognostic value of different immune subtypes. The tumor mutational burden (TMB) of each patient was obtained from the cBioPortal database. The differences in TMB, mutation count, and fraction genome altered between immune subtypes were tested by the Kruskal-Wallis test. A P value less than 0.05 was considered statistically significant.

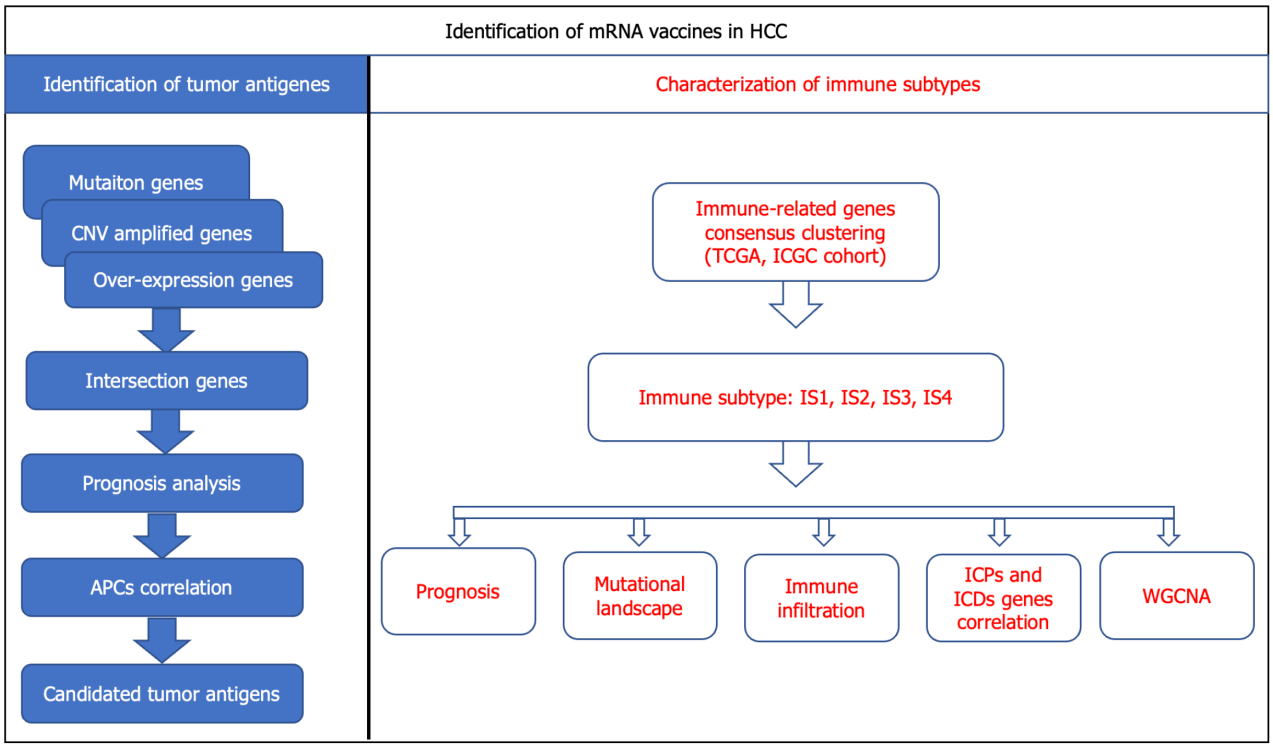

DOI: 10.4251/wjgo.v15.i10.1717

Figure 1 Workflow of this study. APCs: Antigen-presenting cells; CNV: Copy number variation; HCC: Hepatocellular carcinoma; ICGC: International Cancer Genome Consortium; ICPs: Immune checkpoints; ICDs: Immune cell death modulators; TCGA: The Cancer Genome Atlas; WGVNA: Weighted gene coexpression network analysis.

Immune microenvironment and molecular characteristics of different immune subtypes

ssGSEA[27] was used to calculate the immune enrichment scores of 28 immune cells for TCGA and ICGC HCC samples. The 28 immune signatures were obtained from a previously published study[28]. The R package "estimate" was used to calculate the immune score, stromal score, and estimate score of each sample. Immune cell death modulator (ICD)- and immune checkpoint (ICP)-related genes (Supplementary Tables 3 and 4) were obtained from previous studies[29]. The *t* test was used to determine the differences between the scores and the molecular characteristics of immune subtypes.

WGCNA

WGCNA[30] was used to find modules associated with immune subtypes and identify the hub genes of these modules. These hub genes may be potential mRNA vaccine biomarkers. The TCGA dataset was used for WGCNA, and eight gene modules were identified. Univariate Cox regression analysis was performed to assess the prognostic value of different gene modules. The GO and KEGG enrichment analysis of interesting module genes was performed *via* the R package "clusterProfiler"[31].

RESULTS

Screening of candidate tumor antigen genes in HCC

The workflow of this study is shown in Figure 1. A total of 1482 overexpressed genes in HCC were identified by the GEPIA database (Figure 2A, Supplementary Table 5), and these genes were considered potential tumor antigens. Then, a total of 13678 mutant genes and 11519 amplified genes were identified in individual samples by the cBioPortal website (Figure 2B and C). Tenascin N, tumor protein p53, catenin beta 1, cub and sushi multiple domains 3, pkdh1-like 1, and transcriptional repressor GATA binding 1 were found to be the top frequently mutated genes in terms of both altered genome fraction and mutation counts (Figure 2D and E). In addition, thyroglobulin, TBC1 domain family member 31, CUB and sushi multiple domains 1, and fer-1-like family member 6 were among the top 10 genes with altered genome fractions (Figure 2D). High mutation counts were also observed in t-SNARE domain containing 1, thyrotropin releasing hormone receptor, annexin A13, and ryanodine receptor 2 (Figure 2E). Altogether, 472 genes were identified as candidate tumor antigen genes.

Identification of tumor antigens associated with HCC prognosis and antigen presentation

The prognostic value of the candidate tumor antigen genes was estimated to identify the candidate genes for developing mRNA vaccines. Thirteen genes were closely related to OS and RFS in HCC (Figure 3A). High expression levels of

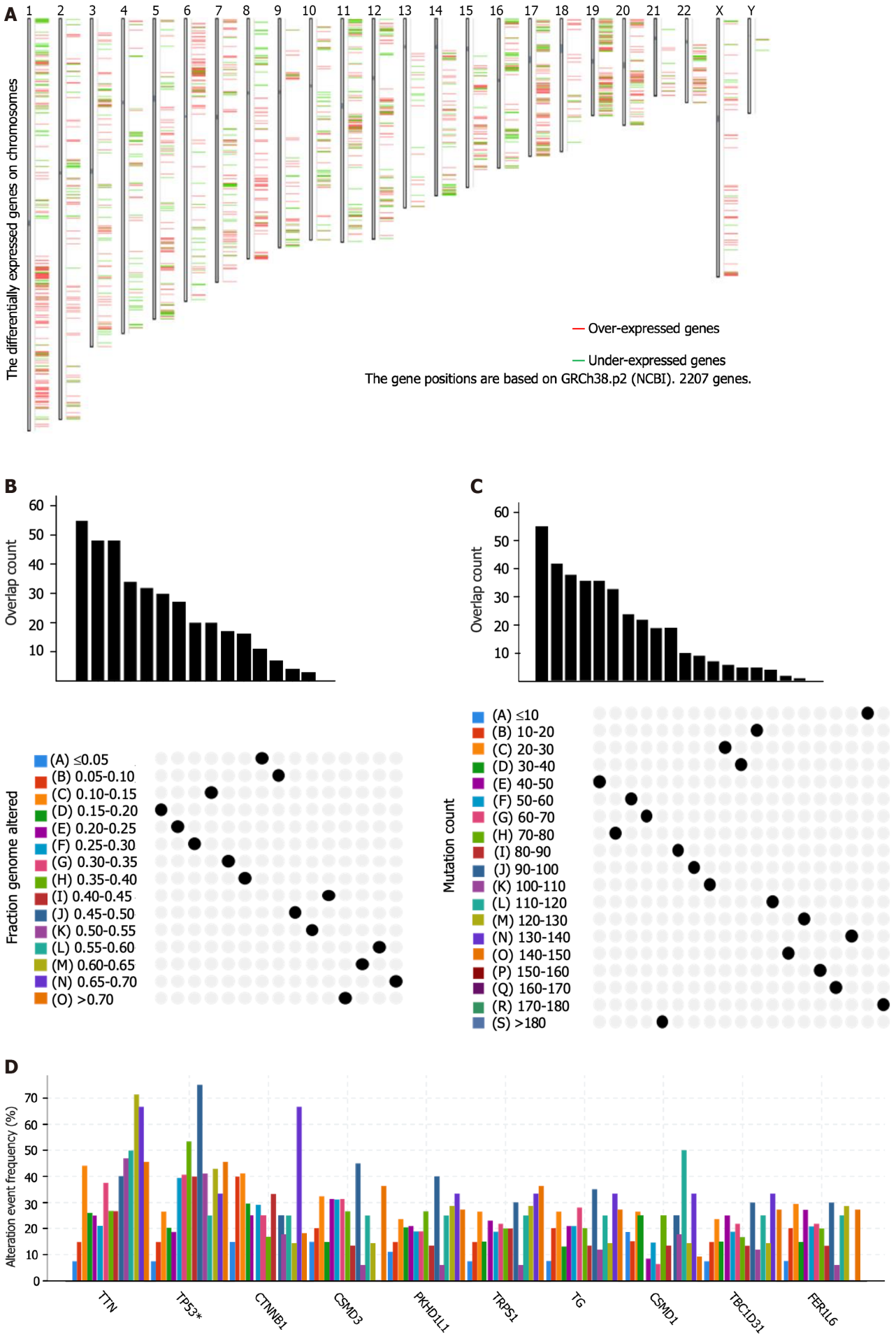
A
1 2 3 4 5 6 7 8 9 10 11 12 13 14 15 16 17 18 19 20 21 22 X Y
The differentially expressed genes on chromosomes
Over-expressed genes
Under-expressed genes
The gene positions are based on GRCh38.p2 (NCBI). 2207 genes.
B
Overlap count
Fraction genome altered
(A) ≤0.05
(B) 0.05-0.10
(C) 0.10-0.15
(D) 0.15-0.20
(E) 0.20-0.25
(F) 0.25-0.30
(G) 0.30-0.35
(H) 0.35-0.40
(I) 0.40-0.45
(J) 0.45-0.50
(K) 0.50-0.55
(L) 0.55-0.60
(M) 0.60-0.65
(N) 0.65-0.70
(O) >0.70
C
Overlap count
Mutation count
(A) ≤10
(B) 10-20
(C) 20-30
(D) 30-40
(E) 40-50
(F) 50-60
(G) 60-70
(H) 70-80
(I) 80-90
(J) 90-100
(K) 100-110
(L) 110-120
(M) 120-130
(N) 130-140
(O) 140-150
(P) 150-160
(Q) 160-170
(R) 170-180
(S) >180
D
Alteration event frequency (%)
TTN
TP53*
CTNNB1
CSMD3
PKHD1L1
TRPS1
TG
CSMD1
TBC1D31
FER1L6

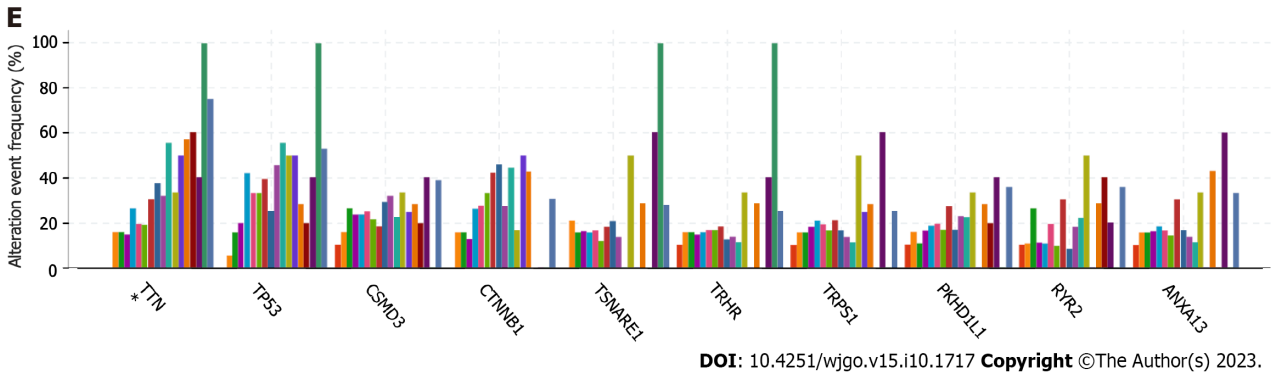

DOI: 10.4251/wjgo.v15.i10.1717

Figure 2 Screening of candidate tumor antigen genes in hepatocellular carcinoma. A: Chromosome distribution of differentially expressed genes; B: Overlapping samples in altered genome fraction groups; C: Overlapping samples in mutation count groups; D: Genes with the highest frequency in altered genome fraction groups; E: Genes with the highest frequency in mutation count groups.

AURKA, CCNB1, CDC25C, CDK1, TRIP13, PES1, MCM3, PPM1G, NEK2, KIF2C, PTTG1, KPNA2, and *PRC1* were found to be associated with a poor OS and RFS (Figure 3B-N, Supplementary Figure 1). mRNA vaccines should be recognized by APCs, which include B cells, dendritic cells, and macrophages. Therefore, we further evaluated the correlation between tumor antigens and these APCs. The results showed that all the 13 genes positively correlated with the abundance of macrophages, dendritic cells, and B cells (Supplementary Figure 2). These results implied that these 13 genes were promising candidates for developing mRNA vaccines against HCC.

Identification of immune subtypes of HCC

Immunotyping could help screen suitable patients for immunotherapy and vaccination. The TCGA datasets were chosen as the training set. Thirty-three out of 2012 immune-related genes were identified as associated with the prognosis of HCC patients *via* univariate Cox regression analysis and were selected for subsequent cluster analysis. The results showed that 365 samples in the TCGA datasets could be clustered into four groups (Figure 4A-C). The survival analysis showed that the OS significantly differed among the four subtypes (IS1, IS2, IS3, and IS4) (Figure 4D). IS4 and IS1 were associated with a better prognosis, whereas IS2 had the poorest survival probability. Next, we used the ICGC datasets as the validation set to verify the clustering stability. Consistent with the results obtained with the TCGA cohort (Figure 4E-G), the immune subtype was prognostically relevant in the ICGC cohort as well (Figure 4H). The clinicopathological characteristics of the immune subtypes were analyzed. As shown in the heatmap (Figure 5A and B), the candidate mRNA vaccine genes were highly expressed in the immune subtypes with a worse prognosis in both the TCGA and ICGA cohorts. In addition, the distribution of immune subtypes in different pathological stages of patients was similar in both the TCGA and ICGC cohorts (Figure 5C and D). Altogether, these data showed that HCC samples could be classified into four distinct immune subtypes, which could be used to predict the prognosis of HCC patients.

Correlation between immune subtypes and tumor mutational landscape

Studies have shown that a high TMB is correlated with tumor immunotherapy and mRNA vaccine therapy. Therefore, we next analyzed the correlation between immune subtypes and genomic heterogeneity in HCC. There were no significant differences in the mutational landscape among the four immune subtypes (Figure 6A), and consistently, there were no differences in TMB or the number of mutations (Figure 6B and C). However, the frequency of altered genome fractions was higher in IS2 and IS3 than in IS1 and IS4 (Figure 6D). These results suggest that TMB may not predict the immune response to mRNA vaccines.

Immune microenvironment characteristics of immune subtypes

The immune microenvironment of HCC affects the immunotherapy response rate, including the mRNA vaccine effect. First, we calculated the immune and stromal scores for the immune subtypes of the TCGA and ICGC cohorts using the R package "estimate". The results showed that in the TCGA cohort, the IS2 and IS4 subtypes had higher immune scores (Figure 7A-C). Similarly, in the ICGC cohort, immune scores were higher in the IS2 and IS4 subtypes (Figure 7D-F). Second, we evaluated the infiltrating abundance of 28 immune cells in both TCGA and ICGC cohort samples using the ssGSEA algorithm with the 28 previously reported immune cell signatures. In the TCGA cohort, the abundance of immune cell infiltration was consistently higher in the IS2 and IS4 subtypes than in the IS1 and IS3 subtypes (Figure 7G). Consistent results were also observed in the ICGC cohort. The abundance of immune cell infiltration was higher in the IS2 and IS4 subtypes in ICGC than in the IS1 and IS3 subtypes (Figure 7H). Therefore, the IS2 and IS4 subtypes belong to the immunological "hot" phenotypes, while the IS1 and IS3 subtypes belong to the immunological "cold" phenotypes. These results suggested that our immunotyping could reflect the immune status of HCC patients. Now that antigen stimulation by mRNA vaccines can remodel the tumor immune microenvironment, subtypes with lower immune infiltration, referred to as "cold" tumors, may be suitable for mRNA vaccines.

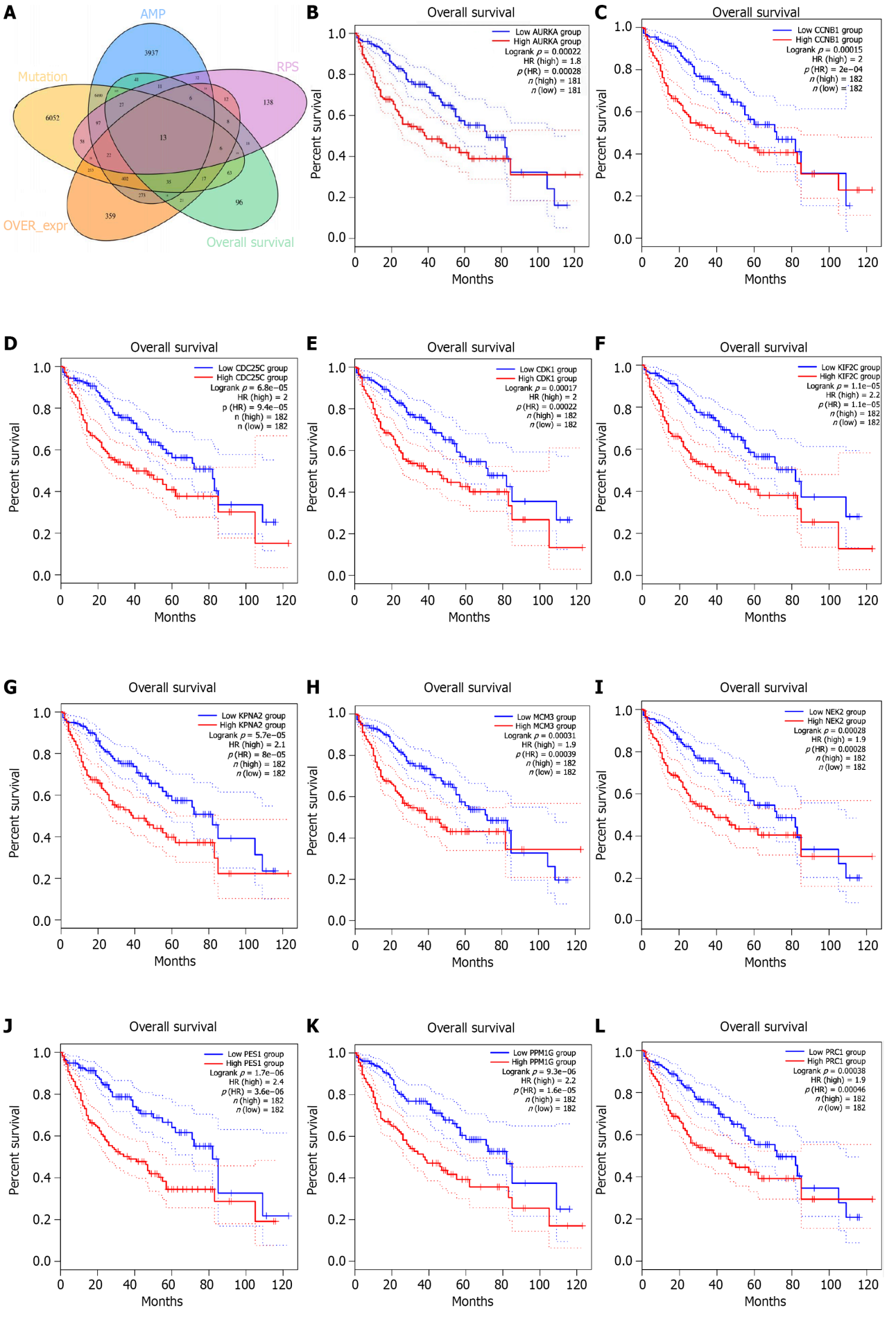
A
AMP
Mutation
RPS
OVER_expr
Overall survival
3937
6052
138
13
359
96
B
Overall survival
Low AURKA group
High AURKA group
Logrank p = 0.00022
HR (high) = 1.8
p (HR) = 0.00028
n (high) = 181
n (low) = 181
Percent survival
Months
C
Overall survival
Low CCNB1 group
High CCNB1 group
Logrank p = 0.00015
HR (high) = 2
p (HR) = 2e−04
n (high) = 182
n (low) = 182
D
Overall survival
Low CDC25C group
High CDC25C group
Logrank p = 6.8e−05
HR (high) = 2
p (HR) = 9.4e−05
n (high) = 182
n (low) = 182
E
Overall survival
Low CDK1 group
High CDK1 group
Logrank p = 0.00017
HR (high) = 2
p (HR) = 0.00022
n (high) = 182
n (low) = 182
F
Overall survival
Low KIF2C group
High KIF2C group
Logrank p = 1.1e−05
HR (high) = 2.2
p (HR) = 1.1e−05
n (high) = 182
n (low) = 182
G
Overall survival
Low KPNA2 group
High KPNA2 group
Logrank p = 5.7e−05
HR (high) = 2.1
p (HR) = 8e−05
n (high) = 182
n (low) = 182
H
Overall survival
Low MCM3 group
High MCM3 group
Logrank p = 0.00031
HR (high) = 1.9
p (HR) = 0.00039
n (high) = 182
n (low) = 182
I
Overall survival
Low NEK2 group
High NEK2 group
Logrank p = 0.00028
HR (high) = 1.9
p (HR) = 0.00028
n (high) = 182
n (low) = 182
J
Overall survival
Low PES1 group
High PES1 group
Logrank p = 1.7e−06
HR (high) = 2.4
p (HR) = 3.6e−06
n (high) = 182
n (low) = 182
K
Overall survival
Low PPM1G group
High PPM1G group
Logrank p = 9.3e−06
HR (high) = 2.2
p (HR) = 1.6e−05
n (high) = 182
n (low) = 182
L
Overall survival
Low PRC1 group
High PRC1 group
Logrank p = 0.00038
HR (high) = 1.9
p (HR) = 0.00046
n (high) = 182
n (low) = 182

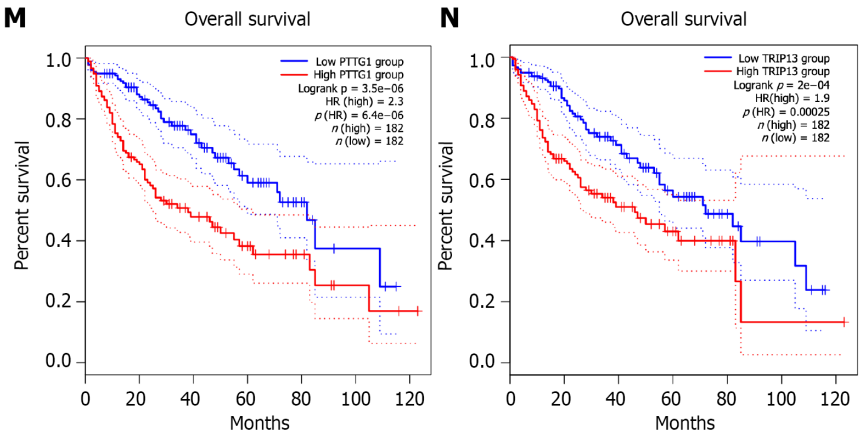

DOI: 10.4251/wjgo.v15.i10.1717

Figure 3 Identification of tumor antigens associated with hepatocellular carcinoma prognosis. A: Venn diagram of mutated genes, amplified genes, highly expressed genes, and prognostic genes; B-N: Kaplan-Meier curves showing that high expression of *AURKA* (B), *CCNB1* (C), *CDC25C* (D), *CDK1* (E), *KIF2C* (F), *KPNA2* (G), *MCM3* (H), *NEK2* (I), *PES1* (J), *PPM1G* (K), *PRC1* (L), *PTTG1* (M), and *TRIP13* (N) indicates a worse overall survival in hepatocellular carcinoma patients. AMP: Amplification; HR: Hazard ratio; RFS: Recurrence-free survival.

Association between immune subtypes and ICP/ICD-related genes

Antitumor immunity is closely related to regulating ICPs and ICDs. Hence, we further analyzed the correlation between immunophenotypes and the expression levels of ICPs and ICD regulators. Sixty ICP regulatory genes and 34 ICD regulatory genes were included in the TCGA and ICGC cohorts for differential expression analysis between immune subtypes. Figure 8A and B shows that the expression of most ICP genes was different among the immune subtypes. Moreover, in the TCGA cohort, most ICP genes were highly expressed in IS2 and IS4. Similarly, in the ICGC cohort, most ICP genes were also highly expressed in IS2 and IS4. In addition, the differential expression trend of ICD genes in the TCGA and ICGC cohorts was similar to that of ICP genes (Figure 8C and D). Therefore, immunotyping correlated with the expression levels of ICPs and ICD modulators, indicating that they might be used as potential therapeutic biomarkers for mRNA vaccines.

Identification of immune gene co-expression modules

We identified the coexpression modules of immune-related genes by clustering the samples using the WGCNA algorithm (Supplementary Figure 3A). The soft threshold was set at 3 for a scale-free network (Supplementary Figure 3B). After selecting the soft threshold, the adjacency matrix and topological overlap matrix were constructed based on the gene matrix using the adjacency function and TOMsimilarity function. Each gene module contained at least 30 genes, and five coexpressed gene modules were obtained (the gray module was not counted) (Supplementary Figure 3C and D). We further analyzed the relationship between each module and the prognosis of gastric cancer patients by univariate Cox regression analysis. The yellow and green modules were significantly associated with the prognosis of HCC ($P < 0.01$) (Supplementary Figure 3E). Next, we analyzed the distribution of the two immune subtypes in eigengenes of five modules and found that only four modules were significantly different (Figure 9A). The IS1 subtype showed the highest eigengenes in yellow and the lowest eigengenes in the green module. In contrast, IS2 showed the highest eigengenes in the green module and the lowest eigengenes in the yellow module (Figure 9A). Moreover, we analyzed the relationship between the modules and the clinical traits of HCC samples. We found that the yellow and green modules were the most significantly associated with the IS1 and IS2 subtypes (Figure 9B). We extracted genes from the yellow module and performed GO and KEGG enrichment analyses. The results showed that these genes were involved in multiple immune-related functions and cell adhesion functions, such as T-cell activation, leukocyte proliferation, lymphocyte proliferation, the JAK-STAT signaling pathway, antigen processing and presentation, Th17 cell differentiation, and the regulation of leukocyte cell-cell adhesion (Figure 9C and D). However, the hub genes extracted from the green module were mainly associated with the cell cycle. Therefore, we further analyzed the prognosis-relevant genes of the yellow module. The results showed that higher expression scores were associated with a better prognosis in the TCGA cohorts (Figure 9E and F). The six previously reported pancancer immune subtypes showed that the C4 subtype was lymphocyte depleted. We compared the immune subtypes with the former immune cluster and found that IS1 was associated with C4 (Figure 9G). Accordingly, patients in the IS1 subtype with high expression of genes clustered into the yellow module might be candidates for mRNA vaccines. Five hub genes (*RBP4, KNG1, METTL7A, F12,* and *ABAT*) with a more than 80% correlation with the yellow module were identified, and these genes might be potential biomarkers for mRNA vaccines.

DISCUSSION

HCC is a malignant tumor with a high mortality rate due to its unique blood supply, nerve distribution, and functional characteristics. Traditional surgery and medical treatment are not ideal for treating advanced HCC. Immunotherapy can

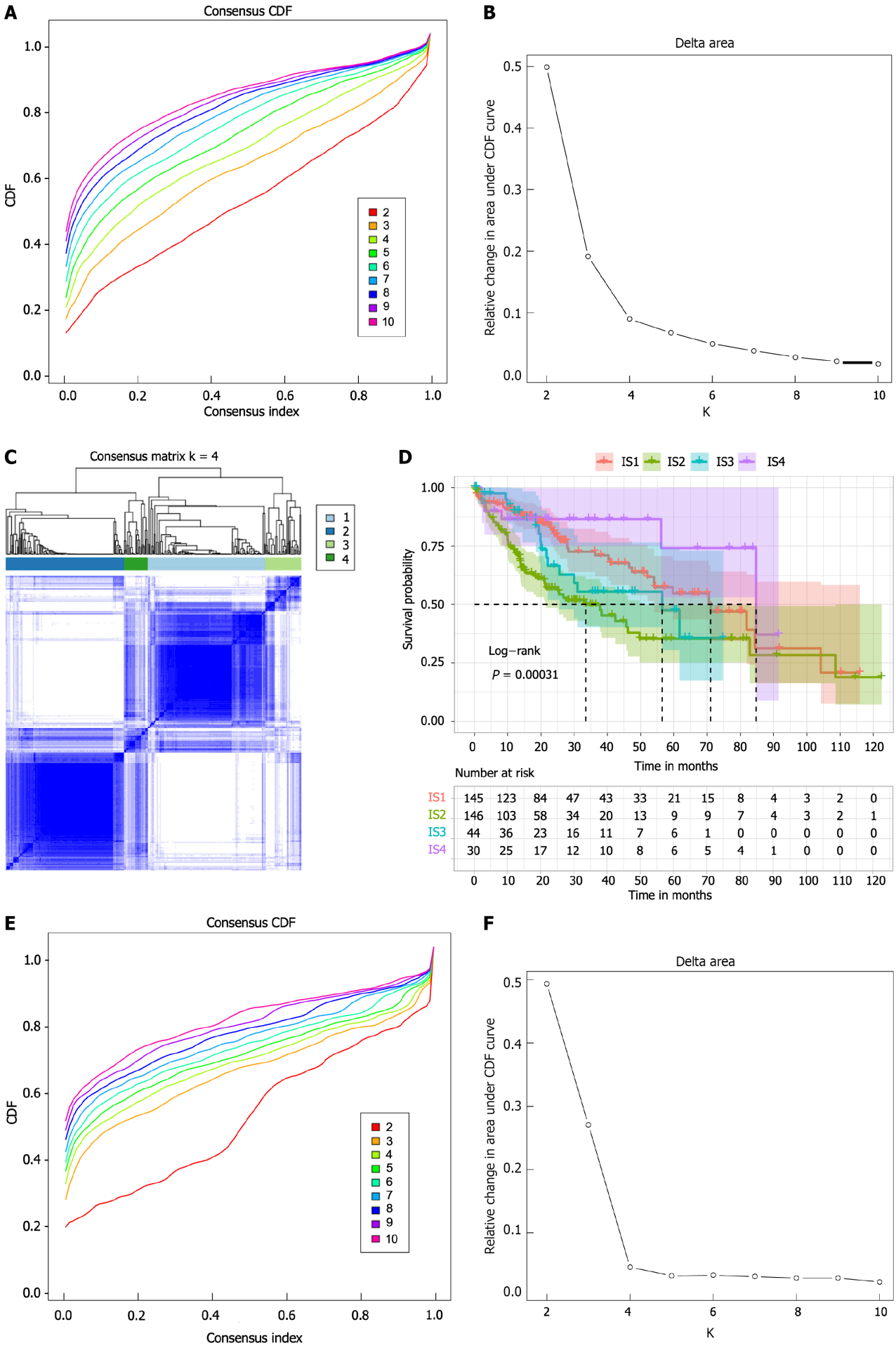
A
Consensus CDF
CDF
Consensus index
2
3
4
5
6
7
8
9
10
B
Delta area
Relative change in area under CDF curve
K
C
Consensus matrix k = 4
1
2
3
4
D
IS1
IS2
IS3
IS4
Survival probability
Log−rank
P = 0.00031
Time in months
Number at risk
IS1 145 123 84 47 43 33 21 15 8 4 3 2 0
IS2 146 103 58 34 20 13 9 9 7 4 3 2 1
IS3 44 36 23 16 11 7 6 1 0 0 0 0 0
IS4 30 25 17 12 10 8 6 5 4 1 0 0 0
E
Consensus CDF
CDF
Consensus index
F
Delta area
Relative change in area under CDF curve
K

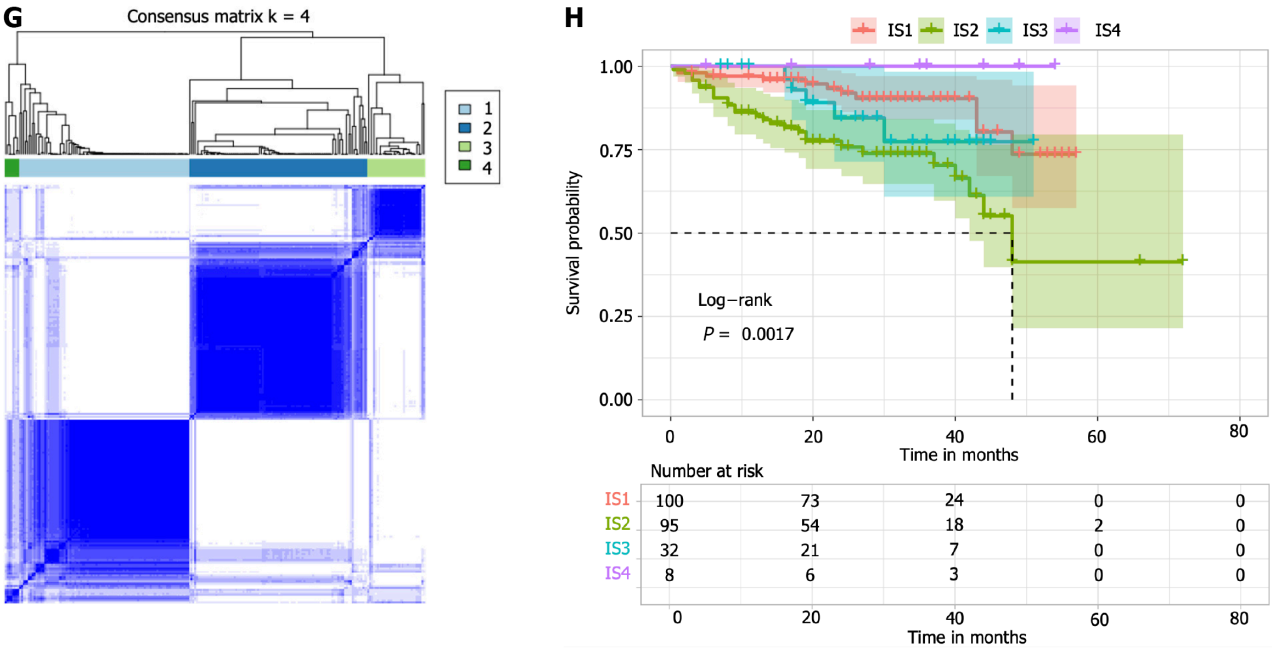

DOI: 10.4251/wjgo.v15.i10.1717 **Copyright** ©The Author(s) 2023.

Figure 4 Identification of immune subtypes of hepatocellular carcinoma. A: Cumulative distribution function curve of immune-related genes in the The Cancer Genome Atlas (TCGA) cohort; B: Delta area of immune-related genes in the TCGA cohort; C: Sample clustering heatmap in the TCGA cohort; D: Kaplan-Meier curves showing the overall survival of the hepatocellular carcinoma immune subtypes in the TCGA cohort; E: Cumulative distribution function curve of immune-related genes in the International Cancer Genome Consortium (ICGC) cohort; F: Delta area of immune-related genes in the ICGC cohort; G: Sample clustering heatmap in the ICGC cohort; H: Kaplan-Meier curves showing the overall survival of the hepatocellular carcinoma immune subtypes in the ICGC cohort. CDF: Cumulative Distribution Function.

be combined with surgery and medical treatment in the future because of its high specificity and minor side effects to achieve the ideal treatment goal of advanced HCC. mRNA tumor vaccines target TSAs and are innovative immunotherapies[21]. The mRNA cannot be integrated into the genome and can be degraded by cellular RNases. mRNA has a short and controllable half-life *in vivo* and has good safety[32,33]. However, only DNA vaccines, dendritic cell vaccines, and peptide vaccines are currently available for liver cancer. Studies on mRNA vaccines for HCC are limited.

In this study, we integrated the mutational and mRNA sequencing data of the TCGA-LICH cohort and identified a series of targeted antigens, of which *AURKA, CCNB1, CDC25C, CDK1, TRIP13, PES1, MCM3, PPM1G, NEK2, KIF2C, PTTG1, KPNA2,* and *PRC1* are promising candidates for mRNA vaccines. The overexpression of these genes was not only associated with a poor OS and RFS but also positively correlated with the abundance of macrophages, dendritic cells, and infiltrating B cells. Therefore, these antigens play a crucial role in the development of HCC and can be recognized by APCs and presented to B cells to promote lymphocyte infiltration in the tumor microenvironment and induce an immune attack. Previous studies have shown that *AURKA* is upregulated in HCC tissues and is associated with distant metastasis [34]. It can regulate the epithelial-mesenchymal transition and cancer stemness through the PI3K/AKT pathway[35]. High expression of *CCNB1* is closely related to the poor prognosis of HCC patients[36,37]. *CDK1* encodes a Ser/Thr protein kinase essential for cellular G1/S and G2/M phase transitions. *CDK1* may play an important oncogenic role in HCC progression[38]. *CDC25C* is a novel TAA that is overexpressed in several cancers, including lung cancer[39], stomach cancer[40], bladder cancer[41], prostate cancer[42], esophageal squamous cell carcinoma[43], breast cancer[44], acute myeloid leukemia[45], and colon cancer[46]. *TRIP13* is highly expressed in multiple tumors and is associated with a poor prognosis[47]. The abnormal expression of *TRIP13* can lead to chromosomal instability and aneuploidy, which may promote tumorigenesis[47]. *PES1*, also known as Pescadillo or *NOP7*, encodes a protein involved in DNA replication and ribosome biogenesis[48]. Studies have found that *PES1* is involved in the regulation of cell proliferation, and its abnormal expression can lead to tumorigenic transformation and tumor progression[48]. A series of studies have shown that *PES1* is highly expressed in various tumors and is associated with a poor prognosis. Thus, it may play a role in promoting tumor development[49-51]. This implies that *PES1* may serve as a molecular target for cancer therapy. Previous studies have shown that *MCM3* is highly expressed in medulloblastoma[52], melanoma[53], and prostate cancer[54] and is associated with nonanchored cell growth, cell migration, and invasion ability. High *MCM3* expression was associated with high AFP levels and a poor OS and RFS[55]. *PPM1G* is highly expressed in HCC and is associated with a poor prognosis[56]. PPM1G can promote the progression of HCC by phosphorylating and regulating the alternative splicing protein SRSF3[56]. *NEK2* encodes a serine/threonine kinase that is highly expressed in multiple tumors and promotes tumorigenesis through abnormal cell cycle regulation. NEK2 can affect the expression of PD-L1, thereby mediating tumor immune escape[57]. *KIF2C* encodes an important cell cycle regulator that is highly expressed in multiple tumors and is associated with a poor prognosis. Its abnormal expression can promote tumor progression[58]. *PTTG1* is a proto-oncogene involved in proliferation, metabolism, cell cycle progression, DNA damage/repair, and apoptosis[59]. Previous studies have shown that *PTTG1* is overexpressed in HCC cell lines and HCC tissues[60]. *KPNA2* encodes a member of the

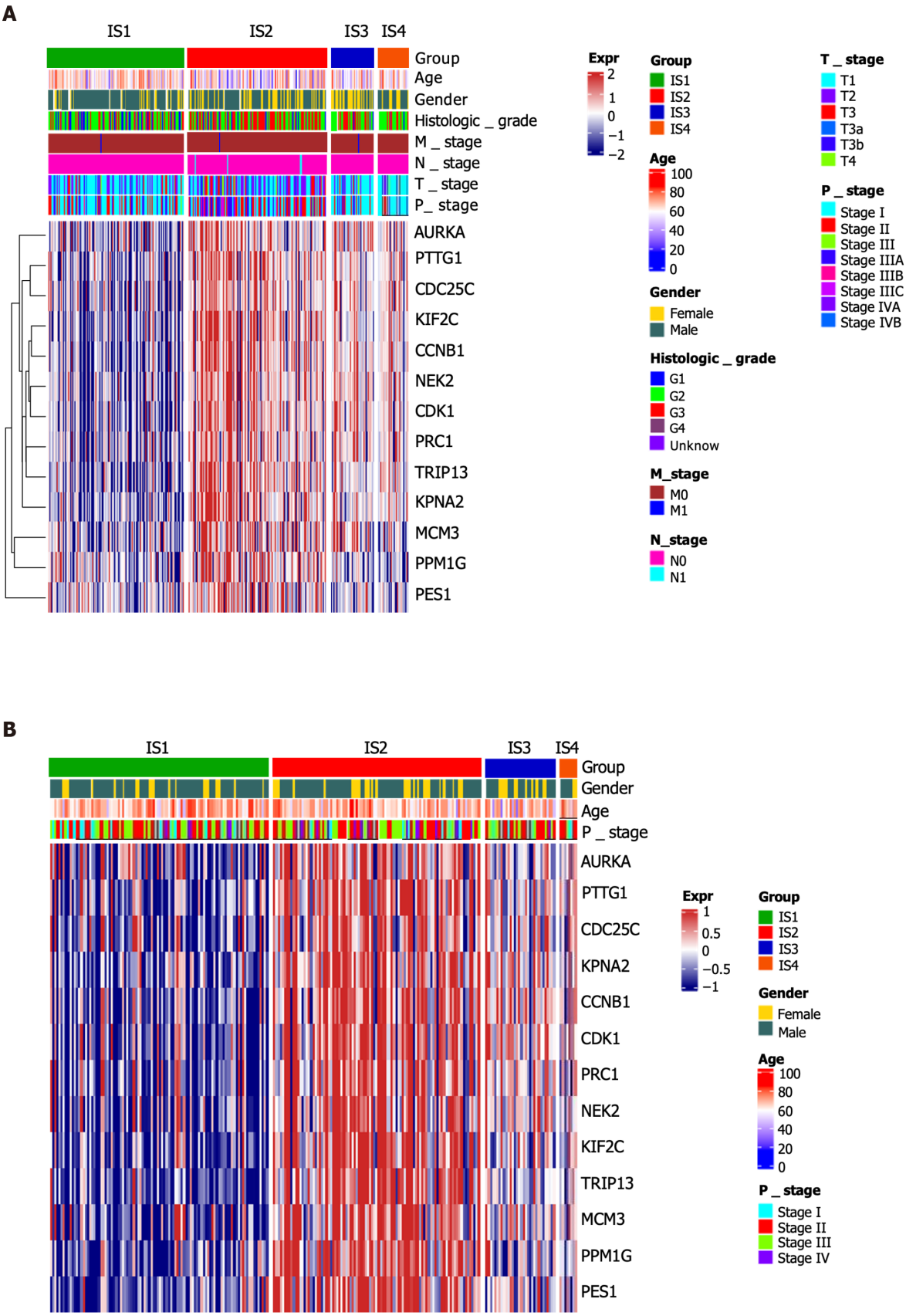
A
IS1
IS2
IS3
IS4
Group
Age
Gender
Histologic _ grade
M _ stage
N _ stage
T _ stage
P_ stage
AURKA
PTTG1
CDC25C
KIF2C
CCNB1
NEK2
CDK1
PRC1
TRIP13
KPNA2
MCM3
PPM1G
PES1
Expr
2
1
0
−1
−2
Group
IS1
IS2
IS3
IS4
Age
100
80
60
40
20
0
Gender
Female
Male
Histologic _ grade
G1
G2
G3
G4
Unknow
M_stage
M0
M1
N_stage
N0
N1
T _ stage
T1
T2
T3
T3a
T3b
T4
P _ stage
Stage I
Stage II
Stage III
Stage IIIA
Stage IIIB
Stage IIIC
Stage IVA
Stage IVB
B
IS1
IS2
IS3
IS4
Group
Gender
Age
P _ stage
AURKA
PTTG1
CDC25C
KPNA2
CCNB1
CDK1
PRC1
NEK2
KIF2C
TRIP13
MCM3
PPM1G
PES1
Expr
1
0.5
0
−0.5
−1
Group
IS1
IS2
IS3
IS4
Gender
Female
Male
Age
100
80
60
40
20
0
P _ stage
Stage I
Stage II
Stage III
Stage IV

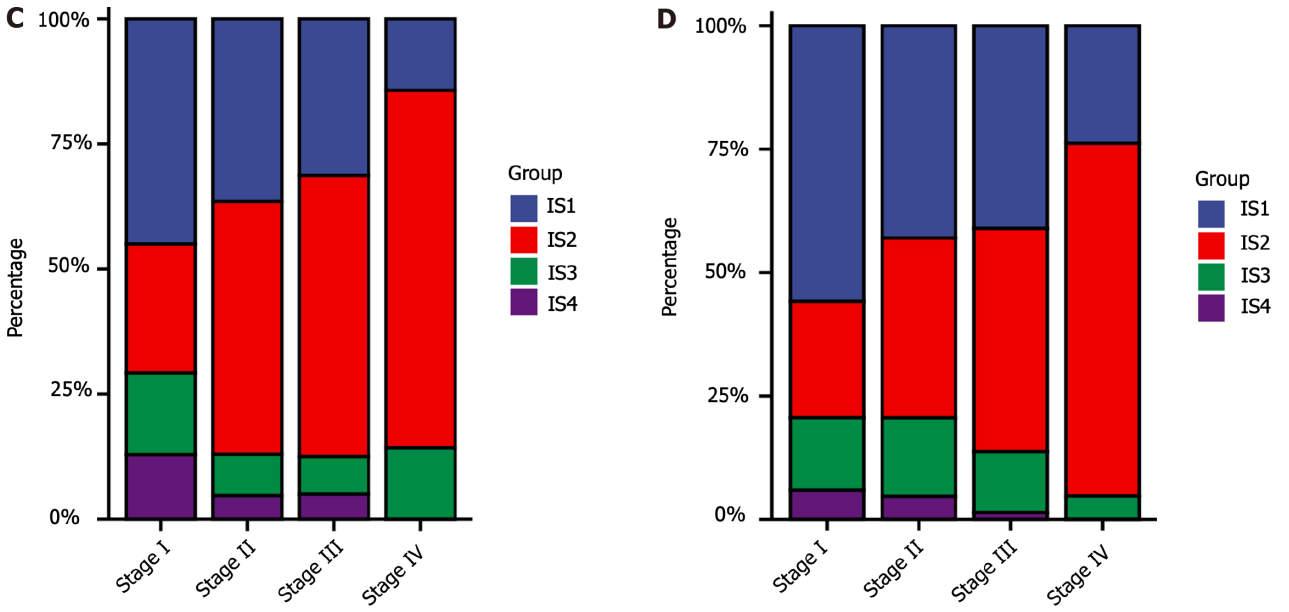

DOI: 10.4251/wjgo.v15.i10.1717

Figure 5 Clinicopathological characteristics of immune subtypes of hepatocellular carcinoma. A and B: Complex heatmap of clinicopathological characteristics of immune subtypes of hepatocellular carcinoma (HCC) patients in the The Cancer Genome Atlas (TCGA) (A) and International Cancer Genome Consortium (ICGC) (B) cohorts; C and D: Distribution of immune subtypes across HCC pStage in the TCGA (C) and ICGC (D) cohorts.

nuclear transporter family also known as importin α1. Recent studies have shown that *KPNA2* is highly expressed in various cancers and is a poor prognostic marker[61]. *PRC1* is associated with tumor proliferation, metastasis, and tumorigenesis. It is highly expressed in multiple tumors and is regulated by nuclear β-catenin and WNT expression[62]. Additionally, some studies have reported that PRC1 controls chromatin structure mainly through posttranslational histone modifications. Taken together, reports from previous studies of these genes support their potential for the development of mRNA vaccines.

Individual differences in the tumor microenvironment affect the efficacy of immunotherapy and vaccine response for liver cancer. To screen the appropriate population for mRNA vaccines, we used consensus cluster analysis to classify HCC patients into four immune subtypes based on the expression of immune-related genes. The ICGC cohort was also used to verify the robustness of the immune subtypes. There were significant survival differences among patients with different immune subtypes. Subtypes with better prognoses had lower expression levels of candidate mRNA vaccine antigens. This is consistent with the results of our analysis mentioned earlier. In the TCGA cohort, IS1 and IS4 had better prognoses and contained more stage I HCC patients. IS2 had the worst prognosis and contained more stage IV HCC patients. The same results were observed in the ICGC cohort. This indicates that immunophenotyping can predict the prognosis of HCC patients and is more accurate than traditional staging. Interestingly, there were no significant differences in the mutation landscape, TMB, or mutation counts among the four immune subtypes. This may be related to the fact that the threshold for high TMB should differ in different cancers[63]. TMB may not predict the immune response to mRNA vaccines in HCC. Published literature has reported that the tumor immune microenvironment varies among different individuals, including the "cold" and "hot" types of microenvironment[24]. Patients with a "cold" tumor immune microenvironment respond poorly to immunotherapy. In the TCGA cohort, the immune scores and the abundance of immune cell infiltration were higher in IS2 and IS4 subtypes than in IS1 and IS3 subtypes. Hence, IS2 and IS4 are immunologically "hot" phenotypes, while IS1 and IS3 are immunologically "cold" phenotypes. Consistent results were also observed in the ICGC cohort. ICD is vital in transforming tumors from "cold" to "hot". However, high expression of ICP-related genes represents an immunosuppressive tumor microenvironment, which may suppress the immune response to mRNA vaccines. Therefore, we further evaluated the differential expression of ICPs and ICDs among the four immune subtypes. The results showed that ICPs were highly expressed in the IS2 and IS4 subtypes. Similarly, high ICD expression was observed in the IS2 and IS4 subtypes in both the TCGA cohort and ICGC cohort. To verify the robustness of immunotyping, we compared the immune subtypes with the former immune cluster. We found that IS1 in the TCGA cohort was associated with the C4 subtype, which was lymphocyte depleted. This further shows that IS1 is suitable for mRNA vaccines. We also found that IS4 in the TCGA cohort was associated with C3, which was associated with superior prognoses. These results were consistent with a better survival probability of IS4. In conclusion, IS1 in the TCGA cohort and IS2 in the ICGC cohort may be suitable populations for mRNA vaccination.

To further explore the marker molecules for predicting the appropriate population for mRNA vaccines, we used the WGCNA algorithm to identify five coexpression modules of immune-related genes. The yellow module was associated with prognosis and positively associated with IS1. The genes extracted from the yellow module were involved in multiple immune-related functions and cell adhesion functions, such as T-cell activation, leukocyte proliferation, lymphocyte proliferation, the JAK-STAT signaling pathway, antigen processing and presentation, Th17 cell differentiation, and regulation of leukocyte cell-cell adhesion. Ultimately, five hub genes (*RBP4*, *KNG1*, *METTL7A*, *F12*, and *ABAT*) with a

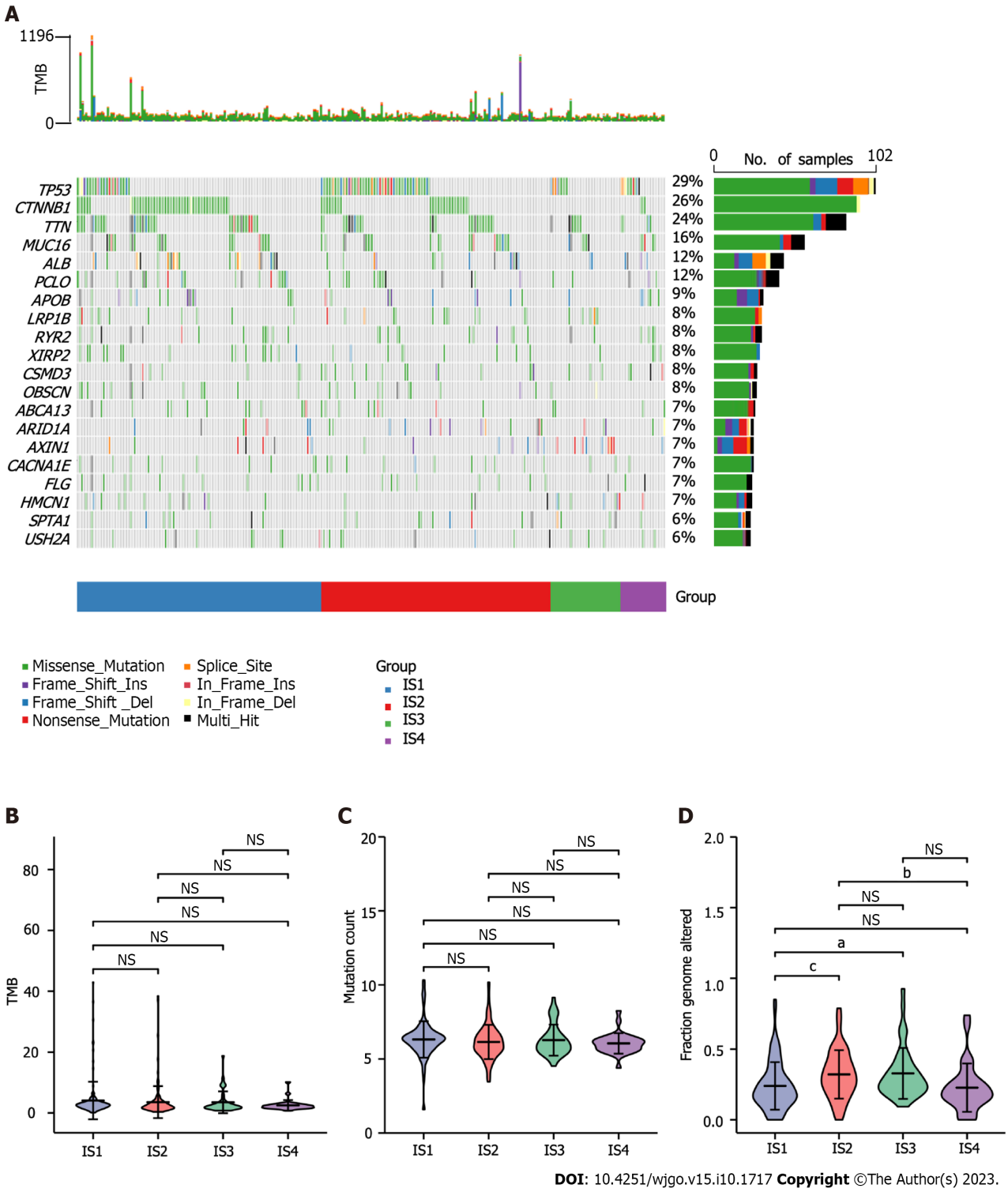

DOI: 10.4251/wjgo.v15.i10.1717 **Copyright** ©The Author(s) 2023.

Figure 6 Mutational landscape of distinct immune subtypes. A: Mutational landscape oncoplot of the top 20 mutated genes in the hepatocellular carcinoma (HCC) immune subtypes; B to D: Tumor mutational burden (B), mutation number (C), and altered genome fractions (D) in HCC IS1-IS4. [a]*P* value < 0.05; [b]*P* value < 0.01; [c]*P* value < 0.001; TMB: Tumor mutational burden; NS: Not significant.

more than 80% correlation with the yellow module were identified, which might be potential biomarkers for mRNA vaccines. *RBP4* encodes a protein that belongs to the lipoprotein family and is the main transport protein of hydrophobic retinol[64]. Previous studies have shown that RBP4 plays a crucial role in maintaining the self-renewing ability of colon cancer and promoting tumorigenesis[65]. Studies have found that RBP4 is overexpressed in ovarian cancer and promotes the proliferation and metastasis of ovarian cancer cells by regulating the RhoA/Rock1 pathway[66]. The protein encoded by *KNG1* is degraded to kinin in malignant gliomas, which further activates TH-1 immunity. Thus, it may become a therapeutic target for malignant gliomas[67]. *KNG1* has been identified as a biomarker for advanced colorectal cancer [68], lung squamous cell carcinoma[69], and multiple myeloma[70]. The role of *METTL7A* in cancers has rarely been investigated. Previous studies have shown that *METTL7A* may be involved in the development of thyroid cancer[71].

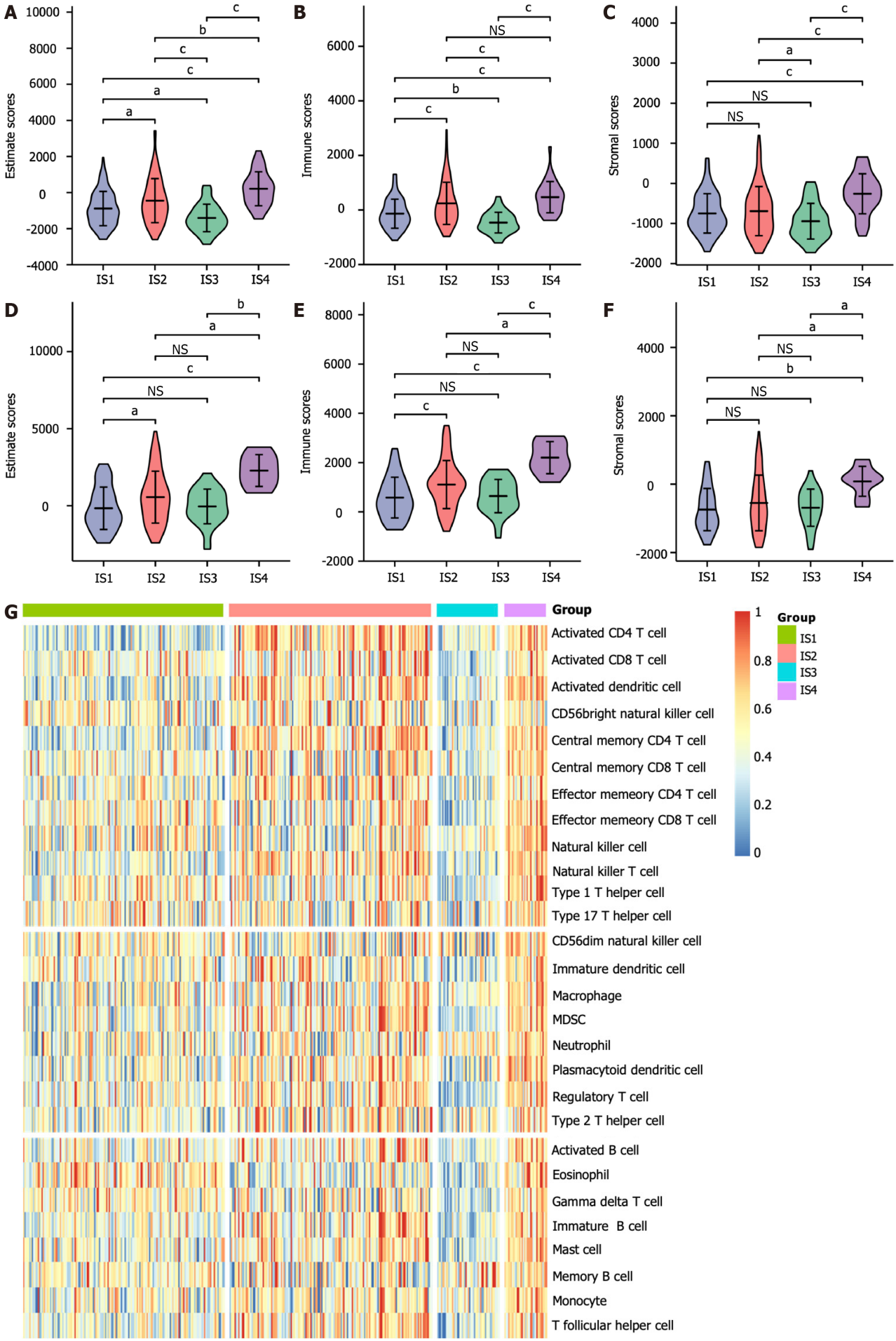
A
Estimate scores
IS1
IS2
IS3
IS4
B
Immune scores
C
Stromal scores
D
Estimate scores
E
Immune scores
F
Stromal scores
G
Group
Activated CD4 T cell
Activated CD8 T cell
Activated dendritic cell
CD56bright natural killer cell
Central memory CD4 T cell
Central memory CD8 T cell
Effector memeory CD4 T cell
Effector memeory CD8 T cell
Natural killer cell
Natural killer T cell
Type 1 T helper cell
Type 17 T helper cell
CD56dim natural killer cell
Immature dendritic cell
Macrophage
MDSC
Neutrophil
Plasmacytoid dendritic cell
Regulatory T cell
Type 2 T helper cell
Activated B cell
Eosinophil
Gamma delta T cell
Immature B cell
Mast cell
Memory B cell
Monocyte
T follicular helper cell

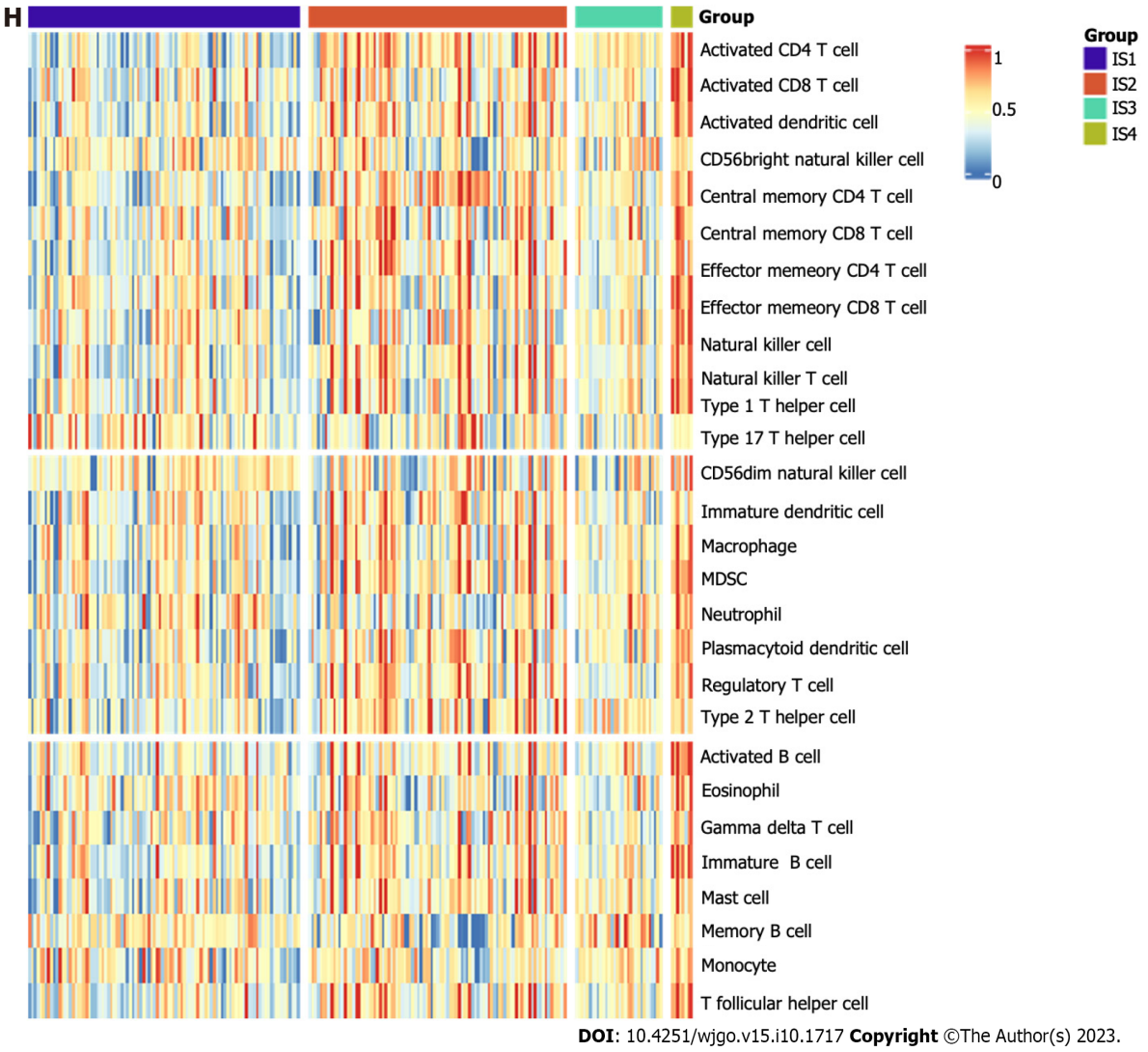

DOI: 10.4251/wjgo.v15.i10.1717

Figure 7 Immune microenvironment characteristics of immune subtypes. A to C: Estimate scores (A), immune scores (B), and stromal scores (C) of hepatocellular carcinoma (HCC) immune subtypes in The Cancer Genome Atlas (TCGA) cohort; D to F: Estimate scores (D), immune scores (E), and stromal scores (F) of HCC immune subtypes in International Cancer Genome Consortium (ICGC) cohort; G and H: Heatmap of enrichment scores of 28 immune cell signatures among HCC immune subtypes in the (G) TCGA and (H) ICGC cohorts. [a]*P* value < 0.05; [b]*P* value < 0.01; [c]*P* value < 0.001; NS: Not significant.

METTL7A can participate in adipocyte-induced myeloma drug resistance by regulating lncRNA m6A methylation[72]. F12, produced by hepatocytes, is underexpressed in colorectal[73], gastric[74], and lung cancers[75] and is involved in antigen processing and presentation and glutathione metabolism. Studies have shown that *ABAT* expression is downregulated in HCC, and low *ABAT* expression is associated with a poor prognosis, which is an independent risk factor for HCC patients[76]. These data suggest that these hub genes may play a key role in HCC tumorigenesis and progression.

CONCLUSION

In conclusion, *AURKA, CCNB1, CDC25C, CDK1, TRIP13, PES1, MCM3, PPM1G, NEK2, KIF2C, PTTG1, KPNA2,* and *PRC1* have been identified as candidate HCC antigens for mRNA vaccine development. The IS1 and IS3 immune subtypes are suitable populations for mRNA vaccination. *RBP4, KNG1, METTL7A, F12,* and *ABAT* are potential biomarkers for mRNA vaccines.

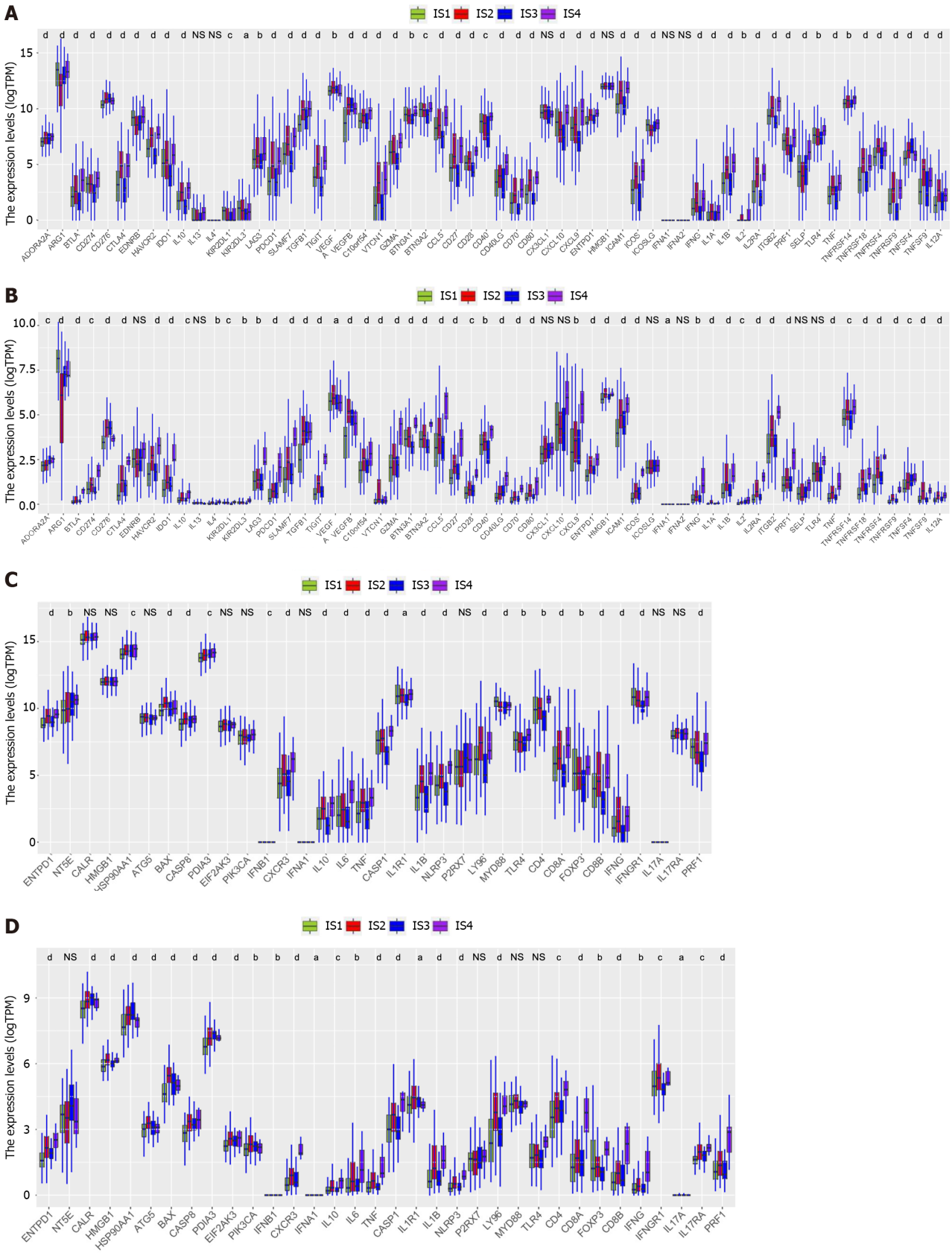

DOI: 10.4251/wjgo.v15.i10.1717

Figure 8 Association between immune subtypes and immune checkpoint/immune cell death modulator-related genes. A and B: Box plot of differential expression of immune checkpoint genes among immune subtypes in the The Cancer Genome Atlas (TCGA) (A) and International Cancer Genome Consortium (ICGC) (B) cohorts; C and D: Box plot of differential expression of immune cell death modulator genes among immune subtypes in the TCGA (C) and ICGC (D) cohorts. [a]*P* value < 0.05; [b]*P* value < 0.01; [c]*P* value < 0.001; [d]*P* value < 0.0001; NS: Not significant.

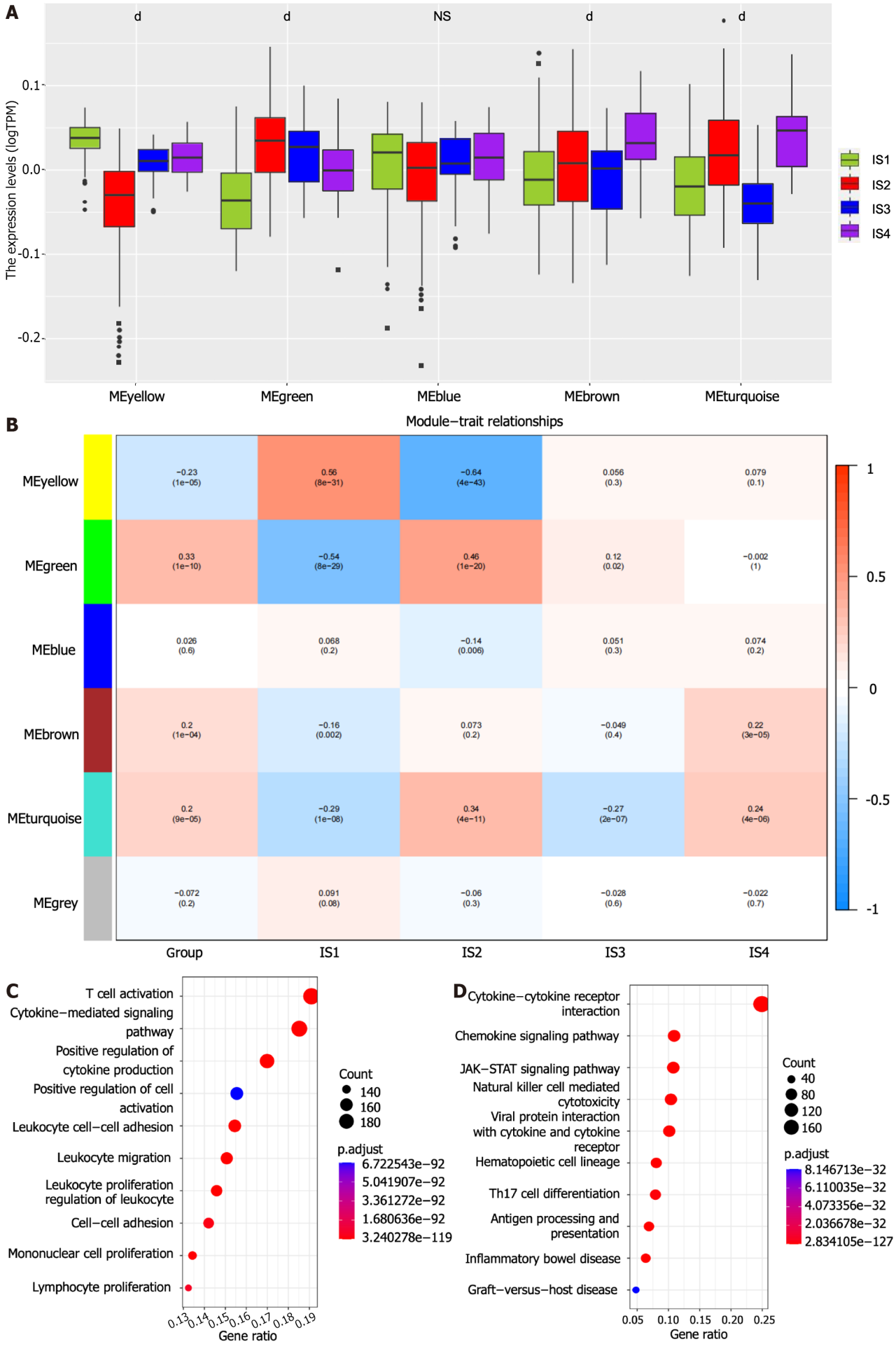
A
d
d
NS
d
d
The expression levels (logTPM)
0.1
0.0
-0.1
-0.2
MEyellow
MEgreen
MEblue
MEbrown
MEturquoise
IS1
IS2
IS3
IS4
B
Module−trait relationships
MEyellow
MEgreen
MEblue
MEbrown
MEturquoise
MEgrey
−0.23 (1e−05)
0.56 (8e−31)
−0.64 (4e−43)
0.056 (0.3)
0.079 (0.1)
0.33 (1e−10)
−0.54 (8e−29)
0.46 (1e−20)
0.12 (0.02)
−0.002 (1)
0.026 (0.6)
0.068 (0.2)
−0.14 (0.006)
0.051 (0.3)
0.074 (0.2)
0.2 (1e−04)
−0.16 (0.002)
0.073 (0.2)
−0.049 (0.4)
0.22 (3e−05)
0.2 (9e−05)
−0.29 (1e−08)
0.34 (4e−11)
−0.27 (2e−07)
0.24 (4e−06)
−0.072 (0.2)
0.091 (0.08)
−0.06 (0.3)
−0.028 (0.6)
−0.022 (0.7)
Group
IS1
IS2
IS3
IS4
1
0.5
0
-0.5
-1
C
T cell activation
Cytokine−mediated signaling pathway
Positive regulation of cytokine production
Positive regulation of cell activation
Leukocyte cell−cell adhesion
Leukocyte migration
Leukocyte proliferation regulation of leukocyte
Cell−cell adhesion
Mononuclear cell proliferation
Lymphocyte proliferation
0.13
0.14
0.15
0.16
0.17
0.18
0.19
Gene ratio
Count
140
160
180
p.adjust
6.722543e−92
5.041907e−92
3.361272e−92
1.680636e−92
3.240278e−119
D
Cytokine−cytokine receptor interaction
Chemokine signaling pathway
JAK−STAT signaling pathway
Natural killer cell mediated cytotoxicity
Viral protein interaction with cytokine and cytokine receptor
Hematopoietic cell lineage
Th17 cell differentiation
Antigen processing and presentation
Inflammatory bowel disease
Graft−versus−host disease
0.05
0.10
0.15
0.20
0.25
Gene ratio
Count
40
80
120
160
p.adjust
8.146713e−32
6.110035e−32
4.073356e−32
2.036678e−32
2.834105e−127

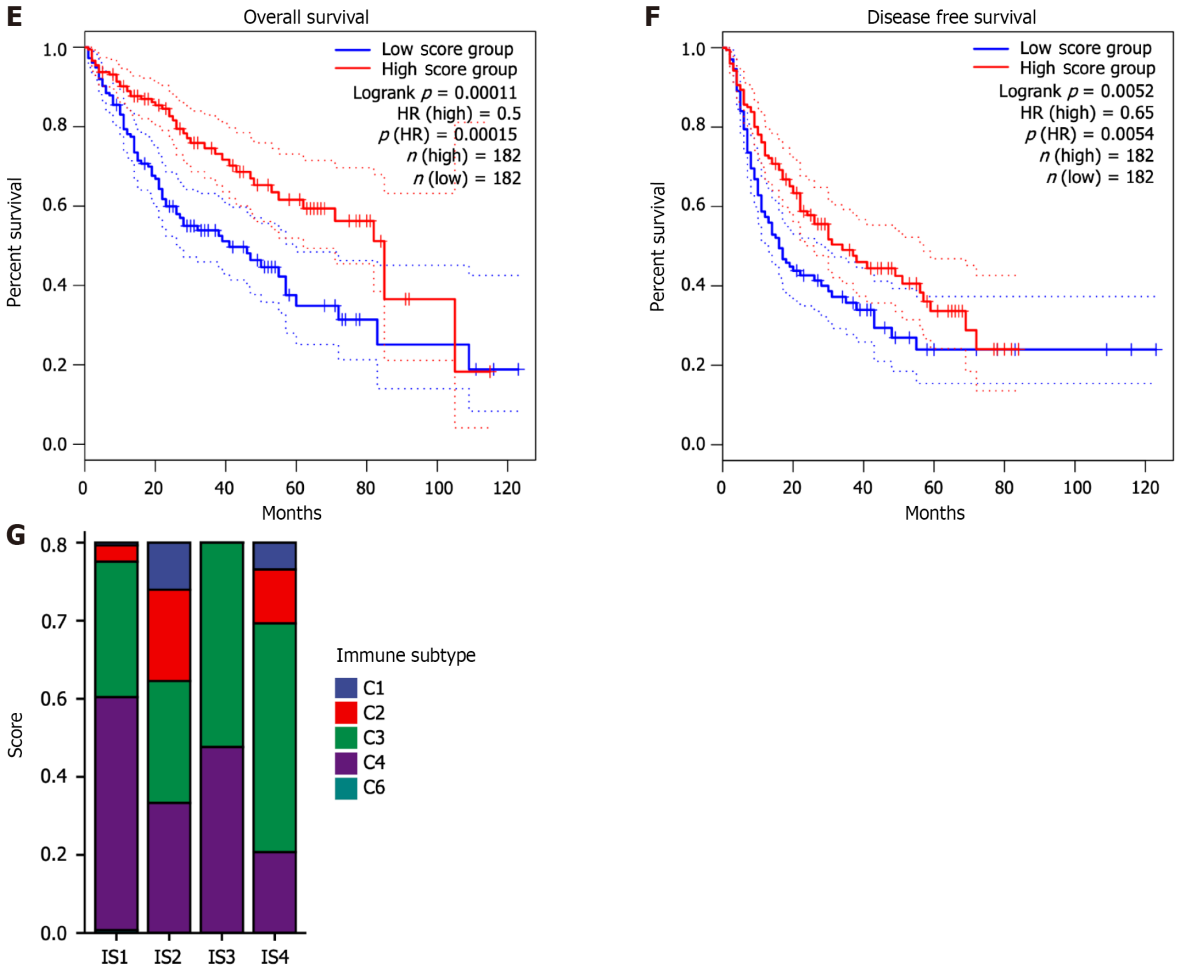

DOI: 10.4251/wjgo.v15.i10.1717

Figure 9 Identification of potential biomarkers for mRNA vaccines. A: Differential distribution of module eigengenes among distinct hepatocellular carcinoma immune subtypes; B: Heatmap of module trait relationships; C: Dot plot showing the top 10 GO terms in the yellow module; D: Dot plot showing the top 10 KEGG terms in the yellow module; E and F: Kaplan-Meier plots showing overall survival (E) and recurrence-free survival (F) of the yellow module prognostic gene expression score; G: Distribution of six previously reported pancancer immune subtypes among IS1-IS4. ^{d}P value < 0.0001; NS: Not significant; HR: Hazard ratio.

ARTICLE HIGHLIGHTS

Research background

Primary liver cancer is one of the leading causes of malignant tumor death in China. Hepatocellular carcinoma (HCC) is not sensitive to conventional chemotherapy and radiotherapy. However, drug therapy, represented by targeted therapy and immunotherapy, has progressed dramatically. mRNA vaccines have become an important platform for cancer immunotherapy. mRNA vaccines have been investigated in multiple tumors, but limited studies have been conducted on their use for HCC.

Research motivation

mRNA vaccines are ideally suited for targeting tumor-specific antigens. It is feasible and urgently necessary to develop and apply mRNA vaccines to improve the prognosis of HCC patients. It is also vital to identify HCC patient subpopulations who are suitable for vaccination.

Research objectives

The present study aimed to identify candidate mRNA vaccine antigens for HCC and suitable subpopulations for mRNA vaccination in order to provide new insights into developing HCC mRNA vaccines and screening suitable patients for vaccination.

Research methods

Gene expression profiles and clinical information of HCC datasets were obtained from International Cancer Genome Consortium and The Cancer Genome Atlas. Genes with somatic mutations and copy number variations were identified by cBioPortal analysis. The differentially expressed genes with significant prognostic value were identified by Gene Expression Profiling Interactive Analysis 2 website analysis. The Tumor Immune Estimation Resource database was used

to assess the correlation between candidate antigens and the abundance of antigen-presenting cells (APCs). Tumor-associated antigens were overexpressed in tumors and associated with prognosis, genomic alterations, and APC infiltration. A consensus cluster analysis was performed with the Consensus Cluster Plus package to identify the immune subtypes. The weighted gene coexpression network analysis (WGCNA) was used to determine the candidate biomarker molecules for appropriate populations for mRNA vaccines.

Research results

AURKA, CCNB1, CDC25C, CDK1, TRIP13, PES1, MCM3, PPM1G, NEK2, KIF2C, PTTG1, KPNA2, and *PRC1* were identified as candidate HCC antigens for mRNA vaccine development. Four immune subtypes (IS1-IS4) and five immune gene modules of HCC were identified that were consistent in both patient cohorts. The immune subtypes showed distinct cellular and clinical characteristics. The IS1 and IS3 immune subtypes were immunologically "cold". The IS2 and IS4 immune subtypes were immunologically "hot", and the immune checkpoint genes and immunogenic cell death genes were upregulated in these subtypes. IS1-related modules were identified with the WGCNA algorithm. Ultimately, five hub genes *(RBP4, KNG1, METTL7A, F12,* and *ABAT*) were identified, and they might be potential biomarkers for mRNA vaccines.

Research conclusions

AURKA, CCNB1, CDC25C, CDK1, TRIP13, PES1, MCM3, PPM1G, NEK2, KIF2C, PTTG1, KPNA2, and *PRC1* have been identified as candidate HCC antigens for mRNA vaccine development. The IS1 and IS3 immune subtypes are suitable populations for mRNA vaccination. *RBP4, KNG1, METTL7A, F12,* and *ABAT* are potential biomarkers for mRNA vaccines.

Research perspectives

Immunotherapy may be an essential therapeutic tool to improve the clinical outcomes of HCC. The immunotherapy of HCC should be studied in more dimensions.

FOOTNOTES

Author contributions: Lu TL conceived the study, performed the literature search and bioinformatics analysis, and prepared the figures; Li CL, Gong YQ, and Hou FT helped with data collection, analysis, and interpretation; Lu TL and Chen CW wrote and revised the manuscript.

Institutional review board statement: This article is a bioinformatics analysis and does not involve experiments on humans or animals. So Institutional Review Board Approval Form or Document is not applicable.

Conflict-of-interest statement: The authors declare no conflict of interest for this article.

Data sharing statement: The datasets ANALYZED for this study can be found in The Cancer Genome Atlas (TCGA, https://www.cancer.gov/tcga) and International Cancer Genome Consortium (ICGC, https://www.icgc-argo.org).

Country/Territory of origin: China

ORCID number: Yong-Qiang Gong 0000-0002-9215-8790; Chao-Wu Chen 0000-0003-0653-4102.

S-Editor: Lin C
L-Editor: Wang TQ
P-Editor: Zhang XD

REFERENCES

1 **Zheng R**, Zhang S, Zeng H, Wang S, Sun K, Chen R, Li L, Wei W, He J. Cancer incidence and mortality in China, 2016. J Nat Cancer Cent 2022; 2: 1-9 [DOI: 10.1016/j.jncc.2022.02.002]

2 **Lin J**, Zhang H, Yu H, Bi X, Zhang W, Yin J, Zhao P, Liang X, Qu C, Wang M, Hu M, Liu K, Wang Y, Zhou Z, Wang J, Tan X, Liu W, Shao Z, Cai J, Tang W, Cao G. Epidemiological Characteristics of Primary Liver Cancer in Mainland China From 2003 to 2020: A Representative Multicenter Study. *Front Oncol* 2022; **12**: 906778 [PMID: 35800051 DOI: 10.3389/fonc.2022.906778]

3 **Zeng H**, Chen W, Zheng R, Zhang S, Ji JS, Zou X, Xia C, Sun K, Yang Z, Li H, Wang N, Han R, Liu S, Mu H, He Y, Xu Y, Fu Z, Zhou Y, Jiang J, Yang Y, Chen J, Wei K, Fan D, Wang J, Fu F, Zhao D, Song G, Jiang C, Zhou X, Gu X, Jin F, Li Q, Li Y, Wu T, Yan C, Dong J, Hua Z, Baade P, Bray F, Jemal A, Yu XQ, He J. Changing cancer survival in China during 2003-15: a pooled analysis of 17 population-based

cancer registries. *Lancet Glob Health* 2018; **6**: e555-e567 [PMID: 29653628 DOI: 10.1016/S2214-109X(18)30127-X]
4 **Chakraborty E**, Sarkar D. Emerging Therapies for Hepatocellular Carcinoma (HCC). *Cancers (Basel)* 2022; **14** [PMID: 35681776 DOI: 10.3390/cancers14112798]
5 **Pinter M**, Jain RK, Duda DG. The Current Landscape of Immune Checkpoint Blockade in Hepatocellular Carcinoma: A Review. *JAMA Oncol* 2021; **7**: 113-123 [PMID: 33090190 DOI: 10.1001/jamaoncol.2020.3381]
6 **Yang L**, Tang L, Zhang M, Liu C. Recent Advances in the Molecular Design and Delivery Technology of mRNA for Vaccination Against Infectious Diseases. *Front Immunol* 2022; **13**: 896958 [PMID: 35928814 DOI: 10.3389/fimmu.2022.896958]
7 **Chen J**, Ye Z, Huang C, Qiu M, Song D, Li Y, Xu Q. Lipid nanoparticle-mediated lymph node-targeting delivery of mRNA cancer vaccine elicits robust CD8(+) T cell response. *Proc Natl Acad Sci U S A* 2022; **119**: e2207841119 [PMID: 35969778 DOI: 10.1073/pnas.2207841119]
8 **Ping H**, Yu W, Gong X, Tong X, Lin C, Chen Z, Cai C, Guo K, Ke H. Analysis of melanoma tumor antigens and immune subtypes for the development of mRNA vaccine. *Invest New Drugs* 2022; **40**: 1173-1184 [PMID: 35962880 DOI: 10.1007/s10637-022-01290-y]
9 **Tang TY**, Huang X, Zhang G, Lu MH, Liang TB. mRNA vaccine development for cholangiocarcinoma: a precise pipeline. *Mil Med Res* 2022; **9**: 40 [PMID: 35821067 DOI: 10.1186/s40779-022-00399-8]
10 **Valentin A**, Bergamaschi C, Rosati M, Angel M, Burns R, Agarwal M, Gergen J, Petsch B, Oostvogels L, Loeliger E, Chew KW, Deeks SG, Mullins JI, Pavlakis GN, Felber BK. Comparative immunogenicity of an mRNA/LNP and a DNA vaccine targeting HIV gag conserved elements in macaques. *Front Immunol* 2022; **13**: 945706 [PMID: 35935984 DOI: 10.3389/fimmu.2022.945706]
11 **You W**, Ouyang J, Cai Z, Chen Y, Wu X. Comprehensive Analyses of Immune Subtypes of Stomach Adenocarcinoma for mRNA Vaccination. *Front Immunol* 2022; **13**: 827506 [PMID: 35874675 DOI: 10.3389/fimmu.2022.827506]
12 **Zheng X**, Xu H, Yi X, Zhang T, Wei Q, Li H, Ai J. Tumor-antigens and immune landscapes identification for prostate adenocarcinoma mRNA vaccine. *Mol Cancer* 2021; **20**: 160 [PMID: 34872584 DOI: 10.1186/s12943-021-01452-1]
13 **Valanparambil RM**, Carlisle J, Linderman SL, Akthar A, Millett RL, Lai L, Chang A, McCook-Veal AA, Switchenko J, Nasti TH, Saini M, Wieland A, Manning KE, Ellis M, Moore KM, Foster SL, Floyd K, Davis-Gardner ME, Edara VV, Patel M, Steur C, Nooka AK, Green F, Johns MA, O'Brein F, Shanmugasundaram U, Zarnitsyna VI, Ahmed H, Nyhoff LE, Mantus G, Garett M, Edupuganti S, Behra M, Antia R, Wrammert J, Suthar MS, Dhodapkar MV, Ramalingam S, Ahmed R. Antibody Response to COVID-19 mRNA Vaccine in Patients With Lung Cancer After Primary Immunization and Booster: Reactivity to the SARS-CoV-2 WT Virus and Omicron Variant. *J Clin Oncol* 2022; **40**: 3808-3816 [PMID: 35759727 DOI: 10.1200/JCO.21.02986]
14 **McNamara MA**, Nair SK, Holl EK. RNA-Based Vaccines in Cancer Immunotherapy. *J Immunol Res* 2015; **2015**: 794528 [PMID: 26665011 DOI: 10.1155/2015/794528]
15 **Mizukoshi E**, Nakagawa H, Tamai T, Kitahara M, Fushimi K, Nio K, Terashima T, Iida N, Arai K, Yamashita T, Sakai Y, Honda M, Kaneko S. Peptide vaccine-treated, long-term surviving cancer patients harbor self-renewing tumor-specific CD8(+) T cells. *Nat Commun* 2022; **13**: 3123 [PMID: 35660746 DOI: 10.1038/s41467-022-30861-z]
16 **Cai Z**, Su X, Qiu L, Li Z, Li X, Dong X, Wei F, Zhou Y, Luo L, Chen G, Chen H, Wang Y, Zeng Y, Liu X. Personalized neoantigen vaccine prevents postoperative recurrence in hepatocellular carcinoma patients with vascular invasion. *Mol Cancer* 2021; **20**: 164 [PMID: 34903219 DOI: 10.1186/s12943-021-01467-8]
17 **Sun K**, Wang L, Zhang Y. Dendritic cell as therapeutic vaccines against tumors and its role in therapy for hepatocellular carcinoma. *Cell Mol Immunol* 2006; **3**: 197-203 [PMID: 16893500]
18 **Nobuoka D**, Yoshikawa T, Sawada Y, Fujiwara T, Nakatsura T. Peptide vaccines for hepatocellular carcinoma. *Hum Vaccin Immunother* 2013; **9**: 210-212 [PMID: 23442593 DOI: 10.4161/hv.22473]
19 **Löffler MW**, Gori S, Izzo F, Mayer-Mokler A, Ascierto PA, Königsrainer A, Ma YT, Sangro B, Francque S, Vonghia L, Inno A, Avallone A, Ludwig J, Alcoba DD, Flohr C, Aslan K, Mendrzyk R, Schuster H, Borrelli M, Valmori D, Chaumette T, Heidenreich R, Gouttefangeas C, Forlani G, Tagliamonte M, Fusco C, Penta R, Iñarrairaegui M, Gnad-Vogt U, Reinhardt C, Weinschenk T, Accolla RS, Singh-Jasuja H, Rammensee HG, Buonaguro L. Phase I/II Multicenter Trial of a Novel Therapeutic Cancer Vaccine, HepaVac-101, for Hepatocellular Carcinoma. *Clin Cancer Res* 2022; **28**: 2555-2566 [PMID: 35421231 DOI: 10.1158/1078-0432.CCR-21-4424]
20 **Luo W**, Yang G, Luo W, Cao Z, Liu Y, Qiu J, Chen G, You L, Zhao F, Zheng L, Zhang T. Novel therapeutic strategies and perspectives for metastatic pancreatic cancer: vaccine therapy is more than just a theory. *Cancer Cell Int* 2020; **20**: 66 [PMID: 32158356 DOI: 10.1186/s12935-020-1147-9]
21 **Pardi N**, Hogan MJ, Porter FW, Weissman D. mRNA vaccines - a new era in vaccinology. *Nat Rev Drug Discov* 2018; **17**: 261-279 [PMID: 29326426 DOI: 10.1038/nrd.2017.243]
22 **Lin MJ**, Svensson-Arvelund J, Lubitz GS, Marabelle A, Melero I, Brown BD, Brody JD. Cancer vaccines: the next immunotherapy frontier. *Nat Cancer* 2022; **3**: 911-926 [PMID: 35999309 DOI: 10.1038/s43018-022-00418-6]
23 **Saxena M**, van der Burg SH, Melief CJM, Bhardwaj N. Therapeutic cancer vaccines. *Nat Rev Cancer* 2021; **21**: 360-378 [PMID: 33907315 DOI: 10.1038/s41568-021-00346-0]
24 **Wellenstein MD**, de Visser KE. Cancer-Cell-Intrinsic Mechanisms Shaping the Tumor Immune Landscape. *Immunity* 2018; **48**: 399-416 [PMID: 29562192 DOI: 10.1016/j.immuni.2018.03.004]
25 **Wang G**, Gao Y, Chen Y, Wang K, Zhang S, Li G. Identification of Novel Tumor Antigens and the Immune Landscapes of Bladder Cancer Patients for mRNA Vaccine Development. *Front Oncol* 2022; **12**: 921711 [PMID: 35814377 DOI: 10.3389/fonc.2022.921711]
26 **Wilkerson MD**, Hayes DN. ConsensusClusterPlus: a class discovery tool with confidence assessments and item tracking. *Bioinformatics* 2010; **26**: 1572-1573 [PMID: 20427518 DOI: 10.1093/bioinformatics/btq170]
27 **Hänzelmann S**, Castelo R, Guinney J. GSVA: gene set variation analysis for microarray and RNA-seq data. *BMC Bioinformatics* 2013; **14**: 7 [PMID: 23323831 DOI: 10.1186/1471-2105-14-7]
28 **Charoentong P**, Finotello F, Angelova M, Mayer C, Efremova M, Rieder D, Hackl H, Trajanoski Z. Pan-cancer Immunogenomic Analyses Reveal Genotype-Immunophenotype Relationships and Predictors of Response to Checkpoint Blockade. *Cell Rep* 2017; **18**: 248-262 [PMID: 28052254 DOI: 10.1016/j.celrep.2016.12.019]
29 **Garg AD**, De Ruysscher D, Agostinis P. Immunological metagene signatures derived from immunogenic cancer cell death associate with improved survival of patients with lung, breast or ovarian malignancies: A large-scale meta-analysis. *Oncoimmunology* 2016; **5**: e1069938 [PMID: 27057433 DOI: 10.1080/2162402X.2015.1069938]
30 **Langfelder P**, Horvath S. Fast R Functions for Robust Correlations and Hierarchical Clustering. *J Stat Softw* 2012; **46** [PMID: 23050260 DOI: 10.18637/jss.v046.i11]

31 **Wu T**, Hu E, Xu S, Chen M, Guo P, Dai Z, Feng T, Zhou L, Tang W, Zhan L, Fu X, Liu S, Bo X, Yu G. clusterProfiler 4.0: A universal enrichment tool for interpreting omics data. *Innovation (Camb)* 2021; **2**: 100141 [PMID: 34557778 DOI: 10.1016/j.xinn.2021.100141]

32 **Mockey M**, Bourseau E, Chandrashekhar V, Chaudhuri A, Lafosse S, Le Cam E, Quesniaux VF, Ryffel B, Pichon C, Midoux P. mRNA-based cancer vaccine: prevention of B16 melanoma progression and metastasis by systemic injection of MART1 mRNA histidylated lipopolyplexes. *Cancer Gene Ther* 2007; **14**: 802-814 [PMID: 17589432 DOI: 10.1038/sj.cgt.7701072]

33 **Grunwitz C**, Kranz LM. mRNA Cancer Vaccines-Messages that Prevail. *Curr Top Microbiol Immunol* 2017; **405**: 145-164 [PMID: 28401358 DOI: 10.1007/82_2017_509]

34 **Wu M**, Zhou Y, Fei C, Chen T, Yin X, Zhang L, Ren Z. ID1 overexpression promotes HCC progression by amplifying the AURKA/Myc signaling pathway. *Int J Oncol* 2020; **57**: 845-857 [PMID: 32705157 DOI: 10.3892/ijo.2020.5092]

35 **Chen C**, Song G, Xiang J, Zhang H, Zhao S, Zhan Y. AURKA promotes cancer metastasis by regulating epithelial-mesenchymal transition and cancer stem cell properties in hepatocellular carcinoma. *Biochem Biophys Res Commun* 2017; **486**: 514-520 [PMID: 28322787 DOI: 10.1016/j.bbrc.2017.03.075]

36 **Chai N**, Xie HH, Yin JP, Sa KD, Guo Y, Wang M, Liu J, Zhang XF, Zhang X, Yin H, Nie YZ, Wu KC, Yang AG, Zhang R. FOXM1 promotes proliferation in human hepatocellular carcinoma cells by transcriptional activation of CCNB1. *Biochem Biophys Res Commun* 2018; **500**: 924-929 [PMID: 29705704 DOI: 10.1016/j.bbrc.2018.04.201]

37 **Zhuang L**, Yang Z, Meng Z. Upregulation of BUB1B, CCNB1, CDC7, CDC20, and MCM3 in Tumor Tissues Predicted Worse Overall Survival and Disease-Free Survival in Hepatocellular Carcinoma Patients. *Biomed Res Int* 2018; **2018**: 7897346 [PMID: 30363964 DOI: 10.1155/2018/7897346]

38 **Tavakolian S**, Goudarzi H, Faghihloo E. Cyclin-dependent kinases and CDK inhibitors in virus-associated cancers. *Infect Agent Cancer* 2020; **15**: 27 [PMID: 32377232 DOI: 10.1186/s13027-020-00295-7]

39 **Chen CY**, Hsu YL, Tsai YC, Kuo PL. Kotomolide A arrests cell cycle progression and induces apoptosis through the induction of ATM/p53 and the initiation of mitochondrial system in human non-small cell lung cancer A549 cells. *Food Chem Toxicol* 2008; **46**: 2476-2484 [PMID: 18511169 DOI: 10.1016/j.fct.2008.04.016]

40 **Kim M**, Ju H, Lim B, Kang C. Maspin genetically and functionally associates with gastric cancer by regulating cell cycle progression. *Carcinogenesis* 2012; **33**: 2344-2350 [PMID: 22962304 DOI: 10.1093/carcin/bgs280]

41 **Skowron KB**, Pitroda SP, Namm JP, Balogun O, Beckett MA, Zenner ML, Fayanju O, Huang X, Fernandez C, Zheng W, Qiao G, Chin R, Kron SJ, Khodarev NN, Posner MC, Steinberg GD, Weichselbaum RR. Basal Tumor Cell Isolation and Patient-Derived Xenograft Engraftment Identify High-Risk Clinical Bladder Cancers. *Sci Rep* 2016; **6**: 35854 [PMID: 27775025 DOI: 10.1038/srep35854]

42 **Al Nakouzi N**, Cotteret S, Commo F, Gaudin C, Rajpar S, Dessen P, Vielh P, Fizazi K, Chauchereau A. Targeting CDC25C, PLK1 and CHEK1 to overcome Docetaxel resistance induced by loss of LZTS1 in prostate cancer. *Oncotarget* 2014; **5**: 667-678 [PMID: 24525428 DOI: 10.18632/oncotarget.1574]

43 **Li BZ**, Chen ZL, Shi SS, Feng XL, Tan XG, Zhou F, He J. Overexpression of Cdc25C predicts response to radiotherapy and survival in esophageal squamous cell carcinoma patients treated with radiotherapy followed by surgery. *Chin J Cancer* 2013; **32**: 403-409 [PMID: 23470146 DOI: 10.5732/cjc.012.10233]

44 **Yan M**, Zhang L, Li G, Xiao S, Dai J, Cen X. Long noncoding RNA linc-ITGB1 promotes cell migration and invasion in human breast cancer. *Biotechnol Appl Biochem* 2017; **64**: 5-13 [PMID: 26601916 DOI: 10.1002/bab.1461]

45 **Yoshimi A**, Toya T, Kawazu M, Ueno T, Tsukamoto A, Iizuka H, Nakagawa M, Nannya Y, Arai S, Harada H, Usuki K, Hayashi Y, Ito E, Kirito K, Nakajima H, Ichikawa M, Mano H, Kurokawa M. Recurrent CDC25C mutations drive malignant transformation in FPD/AML. *Nat Commun* 2014; **5**: 4770 [PMID: 25159113 DOI: 10.1038/ncomms5770]

46 **Natarajan G**, Ramalingam S, Ramachandran I, May R, Queimado L, Houchen CW, Anant S. CUGBP2 downregulation by prostaglandin E2 protects colon cancer cells from radiation-induced mitotic catastrophe. *Am J Physiol Gastrointest Liver Physiol* 2008; **294**: G1235-G1244 [PMID: 18325984 DOI: 10.1152/ajpgi.00037.2008]

47 **Lu S**, Qian J, Guo M, Gu C, Yang Y. Insights into a Crucial Role of TRIP13 in Human Cancer. *Comput Struct Biotechnol J* 2019; **17**: 854-861 [PMID: 31321001 DOI: 10.1016/j.csbj.2019.06.005]

48 **Li YZ**, Zhang C, Pei JP, Zhang WC, Zhang CD, Dai DQ. The functional role of Pescadillo ribosomal biogenesis factor 1 in cancer. *J Cancer* 2022; **13**: 268-277 [PMID: 34976188 DOI: 10.7150/jca.58982]

49 **Cheng L**, Li J, Han Y, Lin J, Niu C, Zhou Z, Yuan B, Huang K, Jiang K, Zhang H, Ding L, Xu X, Ye Q. PES1 promotes breast cancer by differentially regulating ERα and ERβ. *J Clin Invest* 2012; **122**: 2857-2870 [PMID: 22820289 DOI: 10.1172/JCI62676]

50 **Jiang Z**, Zhang Y, Chen X, Wang Y, Wu P, Wu C, Chen D. microRNA-1271 impedes the development of prostate cancer by downregulating PES1 and upregulating ERβ. *J Transl Med* 2020; **18**: 209 [PMID: 32448371 DOI: 10.1186/s12967-020-02349-1]

51 **Wang J**, Sun J, Zhang N, Yang R, Li H, Zhang Y, Chen K, Kong D. PES1 enhances proliferation and tumorigenesis in hepatocellular carcinoma *via* the PI3K/AKT pathway. *Life Sci* 2019; **219**: 182-189 [PMID: 30630006 DOI: 10.1016/j.lfs.2018.12.054]

52 **Lau KM**, Chan QK, Pang JC, Li KK, Yeung WW, Chung NY, Lui PC, Tam YS, Li HM, Zhou L, Wang Y, Mao Y, Ng HK. Minichromosome maintenance proteins 2, 3 and 7 in medulloblastoma: overexpression and involvement in regulation of cell migration and invasion. *Oncogene* 2010; **29**: 5475-5489 [PMID: 20661220 DOI: 10.1038/onc.2010.287]

53 **Nodin B**, Fridberg M, Jonsson L, Bergman J, Uhlén M, Jirström K. High MCM3 expression is an independent biomarker of poor prognosis and correlates with reduced RBM3 expression in a prospective cohort of malignant melanoma. *Diagn Pathol* 2012; **7**: 82 [PMID: 22805320 DOI: 10.1186/1746-1596-7-82]

54 **Stewart PA**, Khamis ZI, Zhau HE, Duan P, Li Q, Chung LWK, Sang QA. Upregulation of minichromosome maintenance complex component 3 during epithelial-to-mesenchymal transition in human prostate cancer. *Oncotarget* 2017; **8**: 39209-39217 [PMID: 28424404 DOI: 10.18632/oncotarget.16835]

55 **Zhang L**, Yuan L, Li D, Tian M, Sun S, Wang Q. Identification of potential prognostic biomarkers for hepatocellular carcinoma. *J Gastrointest Oncol* 2022; **13**: 812-821 [PMID: 35557563 DOI: 10.21037/jgo-22-303]

56 **Chen D**, Zhao Z, Chen L, Li Q, Zou J, Liu S. PPM1G promotes the progression of hepatocellular carcinoma *via* phosphorylation regulation of alternative splicing protein SRSF3. *Cell Death Dis* 2021; **12**: 722 [PMID: 34290239 DOI: 10.1038/s41419-021-04013-y]

57 **Huang X**, Zhang G, Tang T, Gao X, Liang T. One shoot, three birds: Targeting NEK2 orchestrates chemoradiotherapy, targeted therapy, and immunotherapy in cancer treatment. *Biochim Biophys Acta Rev Cancer* 2022; **1877**: 188696 [PMID: 35157980 DOI: 10.1016/j.bbcan.2022.188696]

58 **Ritter A**, Kreis NN, Louwen F, Wordeman L, Yuan J. Molecular insight into the regulation and function of MCAK. *Crit Rev Biochem Mol*

Biol 2015; **51**: 228-245 [PMID: 27146484 DOI: 10.1080/10409238.2016.1178705]

59 **Perramón M**, Jiménez W. Pituitary Tumor-Transforming Gene 1/Delta like Non-Canonical Notch Ligand 1 Signaling in Chronic Liver Diseases. *Int J Mol Sci* 2022; **23** [PMID: 35805898 DOI: 10.3390/ijms23136897]

60 **Cho-Rok J**, Yoo J, Jang YJ, Kim S, Chu IS, Yeom YI, Choi JY, Im DS. Adenovirus-mediated transfer of siRNA against PTTG1 inhibits liver cancer cell growth *in vitro* and in vivo. *Hepatology* 2006; **43**: 1042-1052 [PMID: 16628636 DOI: 10.1002/hep.21137]

61 **Han Y**, Wang X. The emerging roles of KPNA2 in cancer. *Life Sci* 2020; **241**: 117140 [PMID: 31812670 DOI: 10.1016/j.lfs.2019.117140]

62 **Melo GA**, Calôba C, Brum G, Passos TO, Martinez GJ, Pereira RM. Epigenetic regulation of T cells by Polycomb group proteins. *J Leukoc Biol* 2022; **111**: 1253-1267 [PMID: 35466423 DOI: 10.1002/JLB.2RI0122-039R]

63 **Heine A**, Juranek S, Brossart P. Clinical and immunological effects of mRNA vaccines in malignant diseases. *Mol Cancer* 2021; **20**: 52 [PMID: 33722265 DOI: 10.1186/s12943-021-01339-1]

64 **Steinhoff JS**, Lass A, Schupp M. Biological Functions of RBP4 and Its Relevance for Human Diseases. *Front Physiol* 2021; **12**: 659977 [PMID: 33790810 DOI: 10.3389/fphys.2021.659977]

65 **Karunanithi S**, Levi L, DeVecchio J, Karagkounis G, Reizes O, Lathia JD, Kalady MF, Noy N. RBP4-STRA6 Pathway Drives Cancer Stem Cell Maintenance and Mediates High-Fat Diet-Induced Colon Carcinogenesis. *Stem Cell Reports* 2017; **9**: 438-450 [PMID: 28689994 DOI: 10.1016/j.stemcr.2017.06.002]

66 **Wang Y**, Wang Y, Zhang Z. Adipokine RBP4 drives ovarian cancer cell migration. *J Ovarian Res* 2018; **11**: 29 [PMID: 29642915 DOI: 10.1186/s13048-018-0397-9]

67 **Monteiro AC**, Scovino A, Raposo S, Gaze VM, Cruz C, Svensjö E, Narciso MS, Colombo AP, Pesquero JB, Feres-Filho E, Nguyen KA, Sroka A, Potempa J, Scharfstein J. Kinin danger signals proteolytically released by gingipain induce Fimbriae-specific IFN-gamma- and IL-17-producing T cells in mice infected intramucosally with Porphyromonas gingivalis. *J Immunol* 2009; **183**: 3700-3711 [PMID: 19687097 DOI: 10.4049/jimmunol.0900895]

68 **Wang J**, Wang X, Lin S, Chen C, Wang C, Ma Q, Jiang B. Identification of kininogen-1 as a serum biomarker for the early detection of advanced colorectal adenoma and colorectal cancer. *PLoS One* 2013; **8**: e70519 [PMID: 23894665 DOI: 10.1371/journal.pone.0070519]

69 **Wang W**, Wang S, Zhang M. Evaluation of kininogen 1, osteopontin and α-1-antitrypsin in plasma, bronchoalveolar lavage fluid and urine for lung squamous cell carcinoma diagnosis. *Oncol Lett* 2020; **19**: 2785-2792 [PMID: 32218831 DOI: 10.3892/ol.2020.11376]

70 **Chanukuppa V**, Taware R, Taunk K, Chatterjee T, Sharma S, Somasundaram V, Rashid F, Malakar D, Santra MK, Rapole S. Proteomic Alterations in Multiple Myeloma: A Comprehensive Study Using Bone Marrow Interstitial Fluid and Serum Samples. *Front Oncol* 2020; **10**: 566804 [PMID: 33585190 DOI: 10.3389/fonc.2020.566804]

71 **Zhou S**, Shen Y, Zheng M, Wang L, Che R, Hu W, Li P. DNA methylation of METTL7A gene body regulates its transcriptional level in thyroid cancer. *Oncotarget* 2017; **8**: 34652-34660 [PMID: 28416772 DOI: 10.18632/oncotarget.16147]

72 **Wang Z**, He J, Bach DH, Huang YH, Li Z, Liu H, Lin P, Yang J. Induction of m(6)A methylation in adipocyte exosomal LncRNAs mediates myeloma drug resistance. *J Exp Clin Cancer Res* 2022; **41**: 4 [PMID: 34980213 DOI: 10.1186/s13046-021-02209-w]

73 **Battistelli S**, Stefanoni M, Lorenzi B, Dell'Avanzato R, Varrone F, Pascucci A, Petrioli R, Vittoria V. Coagulation factor levels in non-metastatic colorectal cancer patients. *Int J Biol Markers* 2008; **23**: 36-41 [PMID: 28207105 DOI: 10.5301/JBM.2008.4255]

74 **Roeise O**, Sivertsen S, Ruud TE, Bouma BN, Stadaas JO, Aasen AO. Studies on components of the contact phase system in patients with advanced gastrointestinal cancer. *Cancer* 1990; **65**: 1355-1359 [PMID: 1689607 DOI: 10.1002/1097-0142(19900315)65:6<1355::aid-cncr2820650618>3.0.co;2-1]

75 **Pan J**, Qian Y, Weiser P, Zhou X, Lu H, Studelska DR, Zhang L. Glycosaminoglycans and activated contact system in cancer patient plasmas. *Prog Mol Biol Transl Sci* 2010; **93**: 473-495 [PMID: 20807657 DOI: 10.1016/S1877-1173(10)93020-2]

76 **Gao X**, Jia X, Xu M, Xiang J, Lei J, Li Y, Lu Y, Zuo S. Regulation of Gamma-Aminobutyric Acid Transaminase Expression and Its Clinical Significance in Hepatocellular Carcinoma. *Front Oncol* 2022; **12**: 879810 [PMID: 35847853 DOI: 10.3389/fonc.2022.879810]

World Journal of Gastrointestinal Oncology

Submit a Manuscript: https://www.f6publishing.com

World J Gastrointest Oncol 2023 October 15; 15(10): 1739-1755

DOI: 10.4251/wjgo.v15.i10.1739

ISSN 1948-5204 (online)

ORIGINAL ARTICLE

Basic Study

Deltonin enhances gastric carcinoma cell apoptosis and chemosensitivity to cisplatin *via* inhibiting PI3K/AKT/mTOR and MAPK signaling

Lin Yang, Ya-Nan Liu, Yi Gu, Qi Guo

Specialty type: Oncology

Provenance and peer review: Unsolicited article; Externally peer reviewed.

Peer-review model: Single blind

Peer-review report's scientific quality classification

Grade A (Excellent): 0
Grade B (Very good): B
Grade C (Good): C
Grade D (Fair): 0
Grade E (Poor): 0

P-Reviewer: Delko T, Switzerland; Thakur U, India

Received: April 6, 2023
Peer-review started: April 6, 2023
First decision: April 19, 2023
Revised: May 23, 2023
Accepted: July 19, 2023
Article in press: July 19, 2023
Published online: October 15, 2023

Lin Yang, Intensive Care Unit, Second Affiliated Hospital of Soochow University, Suzhou 215006, Jiangsu Province, China

Ya-Nan Liu, Department of Obstetrics and Gynecology, Second Affiliated Hospital of Soochow University, Suzhou 215006, Jiangsu Province, China

Yi Gu, Nursing Department of Obstetrics and Gynecology, Second Affiliated Hospital of Soochow University, Suzhou 215006, Jiangsu Province, China

Qi Guo, Department of Radiotherapy, Second Affiliated Hospital of Soochow University, Suzhou 215006, Jiangsu Province, China

Corresponding author: Qi Guo, Doctor, Doctor, Department of Radiotherapy, Second Affiliated Hospital of Soochow University, No. 1055 Sanxiang Road, Suzhou 215006, Jiangsu Province, China. guoqi456258@163.com

Abstract

BACKGROUND

As an active ingredient derived from *Dioscorea zingiberensis* C.H. Wright, deltonin has been reported to show anti-cancer effects in a variety of malignancies.

AIM

To investigate the role and mechanism of action of deltonin in promoting gastric carcinoma (GC) cell apoptosis and chemosensitivity to cisplatin.

METHODS

The GC cell lines AGS, HGC-27, and MKN-45 were treated with deltonin and then subjected to flow cytometry and 3-(4,5-dimethylthiazol-2-yl)-3,5-diphenyltetrazolium bromide assays for cell apoptosis and viability determination. Western blot analysis was conducted to examine alterations in the expression of apoptosis-related proteins (Bax, Bid, Bad, and Fas), DNA repair-associated proteins (Rad51 and MDM2), and phosphatidylinositol 3-kinase/protein kinase B/mammalian target of the rapamycin (PI3K/AKT/mTOR) and p38-mitogen-activated protein kinase (MAPK) axis proteins. Additionally, the influence of deltonin on GC cell chemosensitivity to cisplatin was evaluated both *in vitro* and *in vivo*.

RESULTS
Deltonin treatment weakened viability, enhanced apoptosis, and dampened DNA repair in GC cell lines in a dose-dependent pattern. Furthermore, deltonin mitigated PI3K, AKT, mTOR, and p38-MAPK phosphorylation. HS-173, an inhibitor of PI3K, attenuated GC cell viability and abolished deltonin inhibition of GC cell viability and PI3K/AKT/mTOR and p38-MAPK pathway activation. Deltonin also promoted the chemosensitivity of GC cells to cisplatin *via* repressing GC cell proliferation and growth and accelerating apoptosis.

CONCLUSION
Deltonin can boost the chemosensitivity of GC cells to cisplatin *via* inactivating p38-MAPK and PI3K/AKT/mTOR signaling.

Key Words: Deltonin; Gastric carcinoma; Cisplatin; Apoptosis; Chemotherapy; Axis

Core Tip: Chemoradiotherapy is currently the mainstay of clinical treatment for advanced gastric carcinoma (GC). However, chemoradiotherapy is difficult to achieve the desired results due to the challenges of early diagnosis of GC and the characteristics of distant metastasis and drug resistance. This study attempted to enhance the efficacy of GC clinical treatment from a pharmacological mechanism perspective.

Citation: Yang L, Liu YN, Gu Y, Guo Q. Deltonin enhances gastric carcinoma cell apoptosis and chemosensitivity to cisplatin *via* inhibiting PI3K/AKT/mTOR and MAPK signaling. *World J Gastrointest Oncol* 2023; 15(10): 1739-1755
URL: https://www.wjgnet.com/1948-5204/full/v15/i10/1739.htm
DOI: https://dx.doi.org/10.4251/wjgo.v15.i10.1739

INTRODUCTION

Gastric carcinoma (GC) is a digestive tract malignancy prevalent worldwide, ranking second in cancer-related deaths[1]. Currently, it is still associated with a high incidence and mortality rate in developing countries[2]. There are several risk factors for GC, including diet patterns, smoking and drinking, family/genetic history, and *Helicobacter pylori* infection[3-5]. At present, chemoradiotherapy is the main clinical treatment for advanced GC. However, owing to the challenges in the early diagnosis of GC and the features of distant metastasis and drug resistance in the advanced stage, it is difficult for radiotherapy to achieve the expected results[6]. This experiment attempted to enhance the efficacy of GC clinical treatment from the perspective of drug mechanism.

Deltonin, an active ingredient in traditional Chinese medicine, is derived from *Dioscorea zingiberensis* C.H. Wright, and shows anti-cancer effects on many malignancies like colon cancer and breast cancer[7]. For instance, deltonin activates autophagy through the protein kinase B/mammalian target of the rapamycin (AKT/mTOR) axis and prevents FaDu, a head and neck squamous cell carcinoma cell line, from proliferating through cell cycle arrest and apoptosis induction, thus boosting cell apoptosis[8]. Moreover, through reactive oxygen species (ROS)-mediated mitochondrial disorders and extracellular signal-regulated kinase/AKT axis, deltonin restrains human breast carcinoma cell proliferation and promotes cell apoptosis[9]. Although previous studies have demonstrated that deltonin functions in most cancers, there are few studies on its role in GC cells and the relevant mechanisms.

The phosphatidylinositol 3-kinase (PI3K)/AKT/mTOR signaling pathway is activated in multiple tumors and regulates various processes such as tumor cell growth, apoptosis, migration, invasiveness, autophagy, and survival[10]. Currently, this signaling pathway is deemed to be a crucial therapeutic target for tumors. Some studies have verified that apigenin inhibits the PI3K/AKT/mTOR axis to suppress liver cancer cell proliferation, thus eliciting autophagy in liver cancer cells and facilitating cell apoptosis[11]. Diallyl disulfide inhibits the PI3K/AKT/mTOR signaling pathway to elicit G2/M phase arrest of human osteosarcoma cells, as well as their apoptosis and autophagic death[12]. p38 mitogen-activated protein kinases (p38-MAPK), as a type of serine/threonine MAPK, participate in the signaling cascades of cytokines and stress cell responses and influence the occurrence, metastasis, and drug resistance of tumor cells[13,14]. For instance, diosgenin suppresses ovarian cancer cell activity by modulating the PI3K/AKT/p38-MAPK axis-associated protein profiles[15]. Another example is inotilone, which inhibits lung carcinoma cell migration and invasiveness through the ROS-mediated PI3K/AKT/p38-MAPK axis[16]. Thus, both p38-MAPK and PI3K/AKT/mTOR signals play essential regulatory roles in multiple malignancies. Nevertheless, whether deltonin influences drug resistance and disease progression in GC *via* the two signaling pathways still needs further investigation.

This study aimed at investigating the underlying anti-tumor function of deltonin in GC cells. Our experiments revealed that deltonin boosted cell apoptosis and improved the chemosensitivity of GC cells to cisplatin. Furthermore, deltonin inhibited PI3K/AKT/mTOR and p38-MAPK signaling pathway activation. Thus, our work provides a new therapeutic avenue to explore novel drugs for patients with GC undergoing end-stage chemotherapy.

MATERIALS AND METHODS

Cell culture

The culture medium of GC (AGS, HGC-27, and MKN-45) and human gastric epithelial (GES-1) cell lines, all from the Chinese Academy of Sciences, Shanghai, China, was RPMI1640 medium (Thermo Fisher Scientific, MA, United States) + 1% penicillin/streptomycin (Thermo Fisher Scientific) + 10% fetal bovine serum (FBS; Invitrogen, CA, United States), and the culture condition was 37 °C and 5% CO_2. Cells in logarithmic growth phase were trypsinized using 0.25% trypsin (Thermo Fisher HyClone, United States) and then harvested through centrifugation at 170 *g* for 5 min.

Cell treatment

The three GC cell lines were treated with cisplatin (Cat. No. 15663-27-1, Sigma-Aldrich, United States; 5 μg/mL)[17], deltonin (Cat. No. HYN2283, MedChemExpress; 0, 0.625, 1.25, 2.5, 5, 10, and 20 μM)[9,18], and/or HS-173 (a PI3K inhibitor; Cat. No. HY-15868, MedChemExpress; 1 μM)[19], or 740 Y-P (a PI3K activator; Cat. No. HY-P0175, MedChemExpress; 20 μM)[20]. Thereafter, the cells were harvested in preparation for the following experiments.

3-(4,5-dimethylthiazol-2-yl)-2,5-diphenyltetrazolium bromide assay

The three GC cell lines in logarithmic growth phase were inoculated into 96-well plates (4×10^3 cells/well, 100 μL) and incubated for 24 h under conditions of 100% humidity, 37 °C, and 5% CO_2 in air. They were then treated with cisplatin, deltonin, and/or the PI3K inhibitor HS-173; the control group was treated with phosphate buffered saline (PBS) of the same volume. Each group contained five replicates. Cells were immersed in 50 μL of 3-(4,5-dimethylthiazol-2-yl)-3,5-diphenyltetrazolium bromide (MTT) (5 g/L) (Beyotime Biotechnology, Shanghai, China) after 24-h culture, and the supernatant was aspirated following 4-h incubation at 37 °C. The cells were treated with DMSO at 150 μL per well, and then placed on a plate shaker. Ultimately, a microplate reader was used to examine each well's OD value at 450 nm at 24, 48, and 72 h.

Western blot analysis

After cell treatment mentioned in section 2.2 and cultivation in 6-well plates, the cells were subjected to two PBS washes and 30 min of lysis in 200 μL RIPA (Beyotime Biotechnology, Shanghai, China). Thereafter, the lysates were collected for a 15-min centrifugation at 14000 rpm to obtain total protein. Protein concentrations were measured using Bradford dye (Bio-Rad). Following 2 h of separation on a polyacrylamide gel by electrophoresis at a voltage maintained at 100 V, the protein samples were electroblotted onto polyvinylidene fluoride membranes (Millipore, Bedford, MA, United States). They were then blocked with 5% nonfat-dried milk for 1 h at room temperature (RT), followed by three 10-min Tris-buffered saline with 0.1% Tween® 20 detergent (TBST) rinses and overnight incubation at 4 °C with primary antibodies at 1:1000 dilution that were procured from Abcam (MA, United States): Anti-Bax (ab32503), anti-Bid (ab32060), anti-Bak (ab32371), anti-Fas (ab133619), anti-Rad51 (ab133534), anti-MDM2 (ab16895), anti-PI3K (ab32089), anti-mTOR (ab134903), anti-p-mTOR (ab137133), anti-p-PI3K (ab182651), anti-AKT (ab8805), anti-p-AKT (ab38449), anti-p38-MAPK (ab170099), anti-p-p38-MAPK (ab178867), and anti-β-actin (ab115777). Following TBST washes, the membranes were subjected to 1 h of RT incubation with horseradish peroxidase-labeled anti-rabbit secondary antibody (1:300 dilution). Thereafter, TBST was used to rinse the membranes again thrice (10-min rinses). Eventually, the membranes were imaged and the staining intensity was assessed using BeyoECL Plus (Beyotime Biotechnology, Shanghai, China) and ImageJ, respectively.

Flow cytometry

The human GC cell lines in logarithmic growth phase were harvested and prepared as single-cell suspensions for inoculation in a 25 cm^2 culture flask. Following adherent culture overnight, the original medium was replaced with fresh medium containing 0.3% FBS for the experimental group and a comparable volume of PBS medium for the control group, followed by 24 h of incubation with 5% CO_2 at 37 °C and cell supernatant collection. Thereafter, the cells were subjected to cold PBS flushing for 3 times, trypsinization using EDTA-free trypsin, and harvesting. Then, the cells were treated as instructed in the Annexin V-PI Apoptosis Detection Kit (Yeasen Biotech Co., Ltd.) protocol. Subsequently, flow cytometry was performed within 1 h for analyzing cell apoptosis.

In vivo experiments in nude mice

We acquired 12 female athymic BALB/c nude mice (6 wk old with a weight of 22-24 g) from Shandong University Experimental Animal Center (Jinan, China) and reared them under normal specific pathogen-free conditions (24 °C, 12-h/12-h light/dark regime, and free access to food and water). Then, AGS cells were administered hypodermically at 2×10^6 cells/0.1 mL PBS into mouse right back according to a previous study[21]. Seven days later, the animals were randomly distributed to one of the following groups: Sham (treated with normal saline *via* intraperitoneal injection), cisplatin (once every 3 d at 3 mg/kg, for 3 times)[22,23], deltonin (once every 3 d at 50 mg/kg, for 3 times)[8], and cisplatin (once every 3 d at 1.5 mg/kg, for 3 times) + deltonin (once every 3 d at 25 mg/kg, for 3 times). During the following 28 d after drug treatment, a caliper was used for measuring the tumor volume ($0.5 \times \text{length} \times \text{width}^2$) weekly. Four weeks later, the nude mice were sacrificed using 30 mg/kg phenobarbital sodium, and the tumor was resected and weighed. The animal experiments were approved by the Ethics Review Committee of the Second Affiliated Hospital of Soochow University (approval No. SZSH-2020-042), and were implemented strictly following the Declaration of Helsinki and the Regulations of the People's Republic of China on the Management of Laboratory Animals issued on October 31, 2017.

Immunofluorescence assay

Tumor tissue specimens were treated with 4% paraformaldehyde and then paraffin-embedded. Tumor sections were prepared (4 μm in thickness), dewaxed using gradient alcohol, and rehydrated. Following RT sealing with bovine serum albumin (5%) for half an hour, the sections were incubated with anti-p-PI3K/AKT/mTOR/p38 MAPK antibodies (ab191606, ab131443, ab109268, and ab38238) at RT for 1 h. After washing with PBS, they were incubated with the Cy3-(ab98416) or fluorescein isothiocyanate-labelled goat anti-rabbit secondary antibody (ab6717) for 60 min at RT. All antibodies were procured from Abcam. Following nuclei labeling with 4',6-diamidino-2-phenylindole (Beyotime Technology, Shanghai, China), a confocal immunofluorescence microscope (Leica LSM 800, Wetzlar, Germany) was used to visualize the images.

Statistical analysis

SPSS16.0 from SPSS Inc. (Chicago, IL, United States) was used for performing all statistical analyses, and $P < 0.05$ indicated statistical significance. Between-group differences were analyzed by unpaired, two-sided Student's *t*-tests, and multi-group differences were determined by one-way ANOVA followed by Tukey's post-hoc tests. All data are described as the mean ± SD.

RESULTS

Deltonin prevents GC cell proliferation and accelerates apoptosis

GES-1, AGS, HGC-27, and MKN-45 cells were all treated with 0-20 μM of deltonin for 24 h, after which their viability was examined using MTT assays. GC cell viability was observed to significantly decrease when the dose of deltonin exceeded 2.5 μM, while only 20 μM of deltonin exerted an inhibitory effect on GES-1 viability ($P < 0.05$ *vs* control, Figure 1A). The IC_{50} values were gauged for AGS, HGC-27, and MKN-45 cells following treatment with deltonin at different concentrations; the IC_{50} values were 3.487, 2.343, and 2.78 for AGS, HGC-27, and MKN-45 cells, respectively (Figure 1B). The GC cells were treated with 2.5 μM deltonin and then subjected to the MTT assay to examine cell viability at different time points. Deltonin inhibited GC cell viability in a time-dependent manner ($P < 0.05$ *vs* control, Figure 1C). Flow cytometry analysis revealed that deltonin treatment promoted cell apoptosis ($P < 0.05$ *vs* control, Figure 1D). And as indicated by Western blot analysis, deltonin treatment enhanced the protein levels of pro-apoptotic markers Bax, Bak, Bid, and Fas but reduced those of Rad51 and MDM2, which are associated with DNA repair processes ($P < 0.05$ *vs* control, Figure 1E). Western blot assays also indicated that deltonin (2.5 μM) treatment markedly lowered PI3K/AKT/mTOR and p38-MAPK protein levels in GC cells (including AGS and HGC-27), with the expression gradually decreasing with time (0, 24, 48, and 72 h) ($P < 0.05$ *vs* control, Figure 1F and G). Additionally, these proteins presented decreased expression in GC cells in a deltonin concentration-dependent manner (0, 2.5, 5, and 10 μM) ($P < 0.05$ *vs* control, Figure 1H and I). The above results demonstrated the ability of deltonin to exert an inhibitory effect on GC cell growth and enhance apoptosis while inactivating p38-MAPK and PI3K/AKT/mTOR axes in these cells.

Repressing PI3K/AKT/mTOR and p38-MAPK signaling suppresses deltonin-mediated anti-tumor effects

GC cells treated with deltonin (2.5 μM) and HS-173 (0.8 nM) showed remarkably lower viability compared to the control ($P < 0.05$, Figure 2A and B). Nevertheless, deltonin + HS-173 exerted no additional influence on cell viability compared to the HS-173 alone group ($P > 0.05$, Figure 2A and B). The determination of apoptosis-related protein profiles also determined that deltonin and HS-173 individually increased the expression of Bax, Bak, Bid, and Fas, whereas co-treatment with HS-173 and deltonin barely influenced their expression levels ($P < 0.05$, Figure 2C and D). Western blot analysis also showed that phosphorylated PI3K/AKT/mTOR and p38-MAPK protein levels were substantially reduced with deltonin or HS-173 treatment, whereas the administration of deltonin and HS-173 exerted no inhibitory effect on p38-MAPK and PI3K/AKT/mTOR axes (*vs* HS-173 group alone, $P > 0.05$, Figure 2E and F). Therefore, deltonin may repress GC cell viability by suppressing p38-MAPK and PI3K/AKT/mTOR signaling.

Impact of activating PI3K/AKT/mTOR and p38-MAPK signaling on deltonin-mediated effects

Next, we treated GC cells (AGS and HGC-27) with deltonin (2.5 μM) and the PI3K activator 740 Y-P (20 μM), and found that deltonin notably enhanced cell viability *vs* the control, wherein cell viability was inhibited by the addition of deltonin ($P < 0.05$, Figure 3A and B). Furthermore, Western blot analysis showed reduced expression of apoptosis-related proteins (Bax, Bak, Bid, and Fas) in the 740 Y-P group, while the deltonin + 740 Y-P group showed increased expression of these proteins in comparison to 740 Y-P alone treatment ($P < 0.05$, Figure 3C and D). Western blot analysis also indicated augmented PI3K, AKT, mTOR, and p38-MAPK phosphorylation in AGS and HGC-27 cells in the 740 Y-P group, whereas deltonin co-treatment suppressed such increased phosphorylation ($P < 0.05$ *vs* 740 Y-P group, Figure 3E and F). Together, these results suggest that activating PI3K/AKT/mTOR and p38-MAPK signaling may facilitate cell proliferation and weaken the anti-cancer effects of deltonin.

Deltonin enhances chemosensitivity of GC cells to cisplatin

AGS and HGC-27 cells were treated with 2.5 μM of deltonin or 5 μg/mL of cisplatin or cisplatin (2.5 μg/mL) + deltonin (1.25 μM). Treatment with cisplatin or deltonin considerably attenuated cell viability, whereas cisplatin + deltonin co-treatment reduced cell viability compared to the cisplatin alone group ($P < 0.05$, Figure 4A and B). According to flow cytometry analysis, the apoptosis of cisplatin- or deltonin-treated cells was dramatically increased compared to the

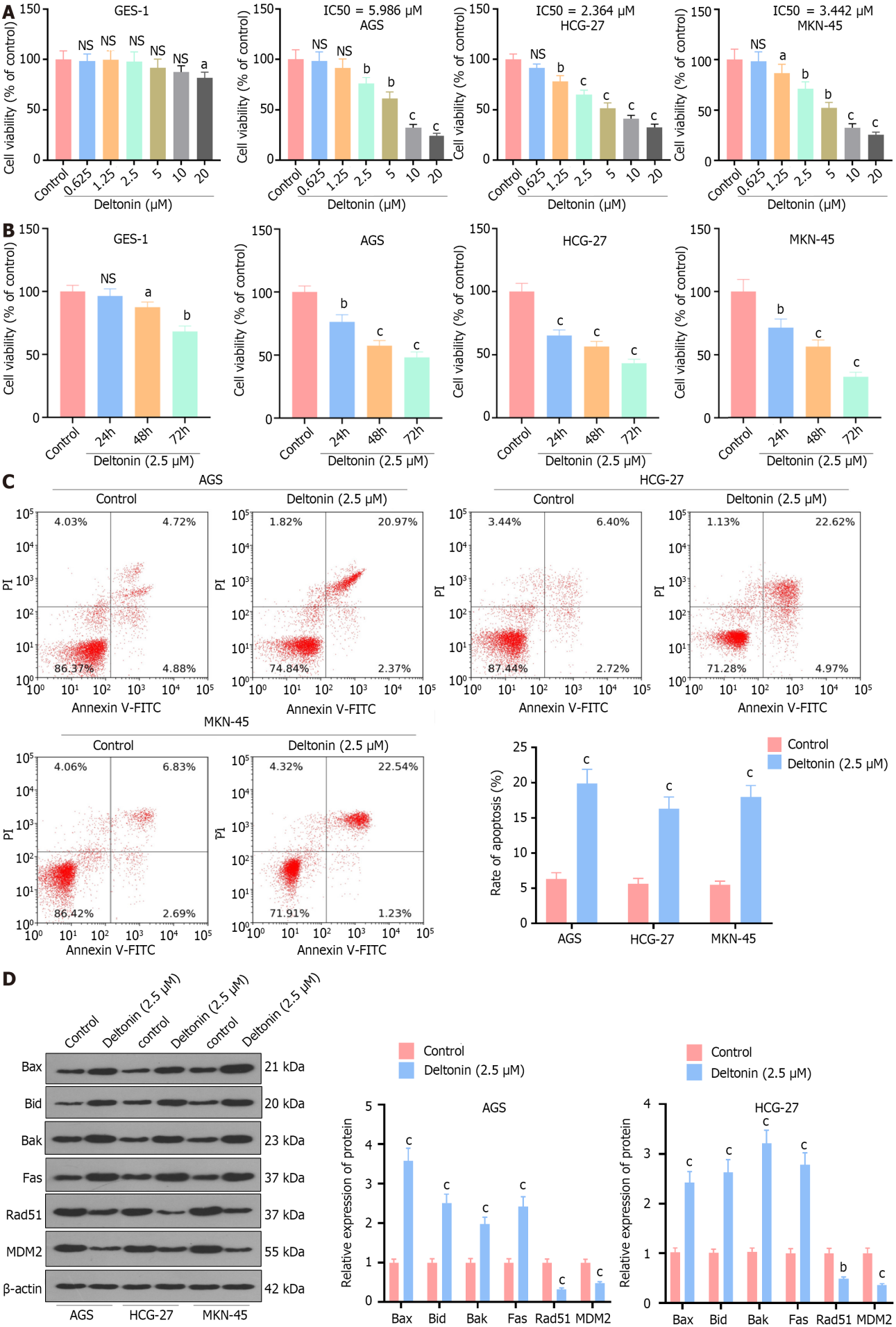
A
GES-1
IC50 = 5.986 μM
AGS
IC50 = 2.364 μM
HCG-27
IC50 = 3.442 μM
MKN-45
Cell viability (% of control)
Control
0.625
1.25
2.5
5
10
20
Deltonin (μM)
B
GES-1
AGS
HCG-27
MKN-45
24h
48h
72h
Deltonin (2.5 μM)
C
AGS
HCG-27
MKN-45
Control
Deltonin (2.5 μM)
PI
Annexin V-FITC
4.03%
4.72%
86.37%
4.88%
1.82%
20.97%
74.84%
2.37%
3.44%
6.40%
87.44%
2.72%
1.13%
22.62%
71.28%
4.97%
4.06%
6.83%
86.42%
2.69%
4.32%
22.54%
71.91%
1.23%
Rate of apoptosis (%)
D
Bax
Bid
Bak
Fas
Rad51
MDM2
β-actin
21 kDa
20 kDa
23 kDa
37 kDa
37 kDa
55 kDa
42 kDa
Relative expression of protein

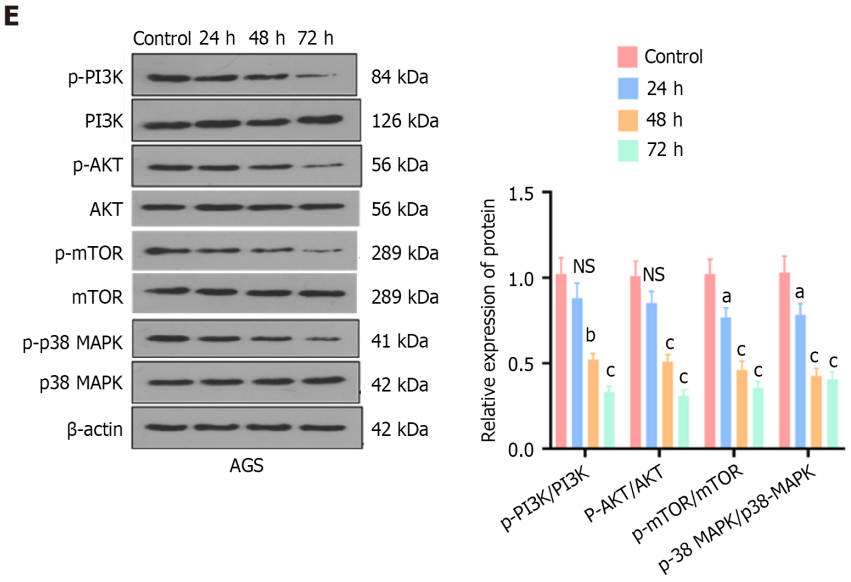
E
Control 24 h 48 h 72 h
p-PI3K
PI3K
p-AKT
AKT
p-mTOR
mTOR
p-p38 MAPK
p38 MAPK
β-actin
84 kDa
126 kDa
56 kDa
56 kDa
289 kDa
289 kDa
41 kDa
42 kDa
42 kDa
AGS
Control
24 h
48 h
72 h
Relative expression of protein
1.5
1.0
0.5
0.0
NS
NS
a
a
b
c
c
c
c
c
c
c
p-PI3K/PI3K
P-AKT/AKT
p-mTOR/mTOR
p-38 MAPK/p38-MAPK

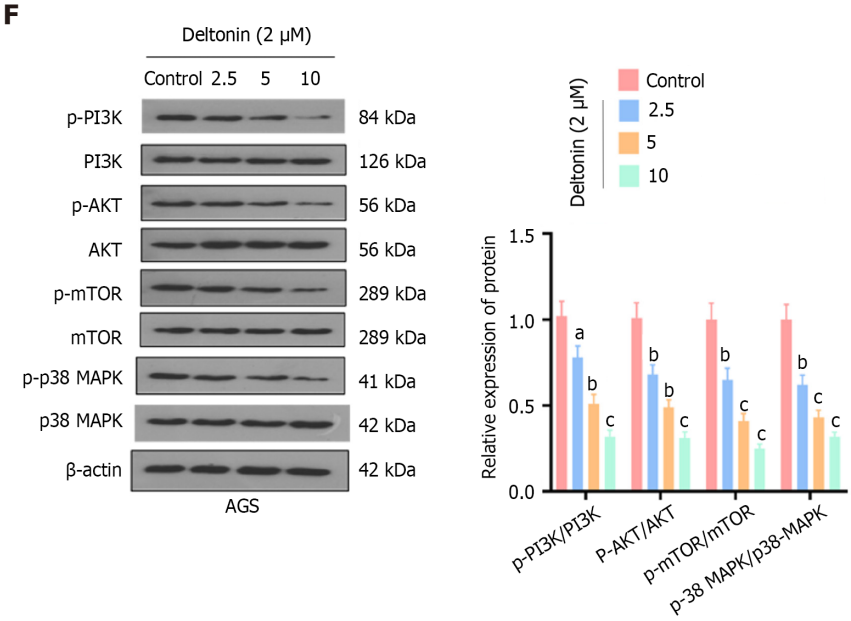
F
Deltonin (2 μM)
Control 2.5 5 10
p-PI3K
PI3K
p-AKT
AKT
p-mTOR
mTOR
p-p38 MAPK
p38 MAPK
β-actin
84 kDa
126 kDa
56 kDa
56 kDa
289 kDa
289 kDa
41 kDa
42 kDa
42 kDa
AGS
Deltonin (2 μM)
Control
2.5
5
10
Relative expression of protein
1.5
1.0
0.5
0.0
a
b
c
b
b
c
c
b
c
c
p-PI3K/PI3K
P-AKT/AKT
p-mTOR/mTOR
p-38 MAPK/p38-MAPK

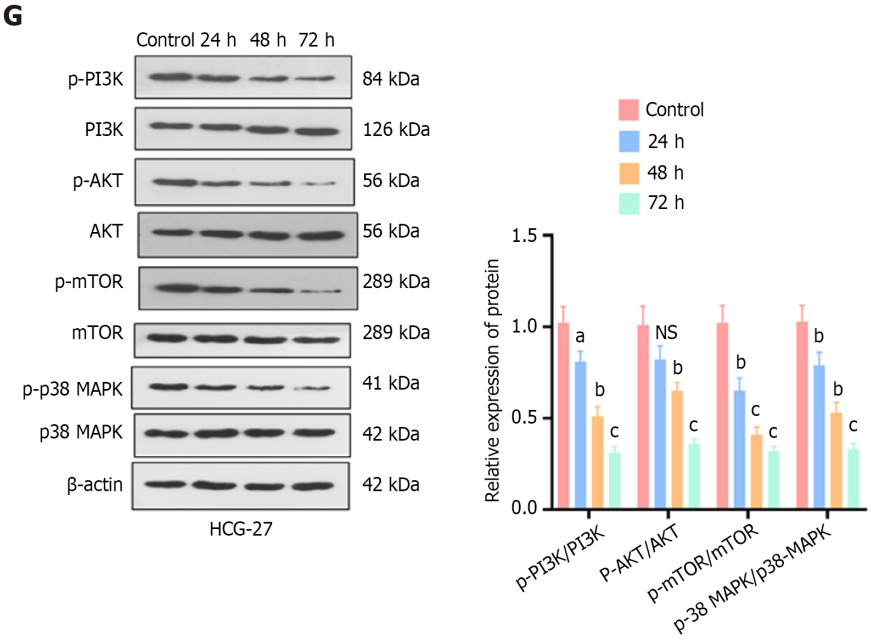
G
Control 24 h 48 h 72 h
p-PI3K
PI3K
p-AKT
AKT
p-mTOR
mTOR
p-p38 MAPK
p38 MAPK
β-actin
84 kDa
126 kDa
56 kDa
56 kDa
289 kDa
289 kDa
41 kDa
42 kDa
42 kDa
HCG-27
Control
24 h
48 h
72 h
Relative expression of protein
1.5
1.0
0.5
0.0
a
b
c
NS
b
c
b
b
c
c
b
b
c
p-PI3K/PI3K
P-AKT/AKT
p-mTOR/mTOR
p-38 MAPK/p38-MAPK

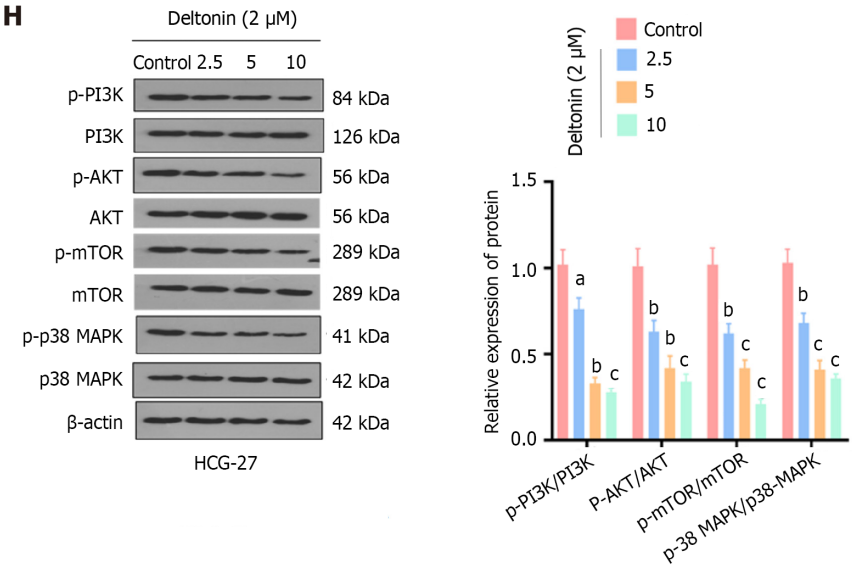

DOI: 10.4251/wjgo.v15.i10.1739 **Copyright** ©The Author(s) 2023.

Figure 1 Deltonin inhibits gastric carcinoma cell proliferation and expedites their apoptosis. A: Gastric carcinoma (GC) cell lines AGS, HGC-27, and MKN-45 were treated with deltonin (0 μM, 0.625 μM, 1.25 μM, 2.5 μM, 5 μM, 10 μM, and 20 μM) for 24 h. 3-(4,5-dimethylthiazol-2-yl)-3,5-diphenyltetrazolium bromide (MTT) assay was used to examine cell viability; B: IC_{50} values of AGS, HGC-27, and MKN-45 cells treated with deltonin of different concentrations; C: Flow cytometry analysis of apoptosis of AGS, HGC-27, and MKN-45 cells treated with 2.5 μM deltonin for 24 h; D: Western blot analysis of expression of apoptosis-concerned proteins (Bax, Bak, Bid, and Fas) and DNA repair-associated proteins (Rad51 and MDM2) in GC cells; E: Western blot analysis of protein expression in AGS cells treated with 2.5 μM of deltonin for 0 h, 24 h, 48 h, and 72 h; F: Western blot analysis of protein expression in AGS cells treated with deltonin (0, 2.5, 5, and 10 μM) for 24 h; G: Western blot analysis of protein expression in HGC-27 cells treated with 2.5 μM of deltonin for 0 h, 24 h, 48 h, and 72 h; H: Western blot analysis of protein expression in HGC-27 cells treated with deltonin (0, 2.5, 5, and 10 μM) for 24 h; NS: $P > 0.05$, $^{a}P < 0.05$, $^{b}P < 0.01$, $^{c}P < 0.001$ *vs* control group. $n = 3$. NS: No significance; PI3K: Phosphatidylinositol 3-kinase; AKT: Protein kinase B; mTOR: Mammalian target of the rapamycin; p38-MAPK: p38-mitogen-activated protein kinase.

control ($P < 0.05$, Figure 4C and D), and it was further enhanced in the cisplatin + deltonin group ($P < 0.05$, Figure 4C and D, *vs* cisplatin group). Western blot analysis also showed elevated Bax and Bid and reduced Rad51 protein expression in cisplatin- or deltonin-treated cells *vs* the control. Moreover, Bax and Bid protein expression in the cisplatin + deltonin group was further increased, while Rad51 expression was considerably reduced in comparison to the expression levels in the cisplatin alone group ($P < 0.05$, Figure 4E and F). Based on the above findings, deltonin may exert a pro-apoptotic effect and promote the chemosensitivity of GC cells to cisplatin.

Deltonin increases chemosensitivity of GC cells to cisplatin in vivo through PI3K/AKT/mTOR and p38-MAPK signaling inhibition

To further verify the function and mechanism of deltonin in chemosensitivity of GC cells to cisplatin, we conducted *in vivo* experiments in nude mice. The tumor-bearing mice were intervened with saline, deltonin (50 mg/kg), cisplatin (3 mg/kg), or deltonin (25 mg/kg) + cisplatin (1.5 mg/kg). Treatment with deltonin or cisplatin both reduced tumor volume and weight compared to the sham group ($P < 0.05$, Figure 5A-C), but failed to reduce mouse body weight ($P > 0.05$, Figure 5D). Interestingly, the joint application of deltonin + cisplatin further mitigated the mouse tumor volume and weight in comparison to cisplatin treatment alone ($P < 0.01$, Figure 5A-C), but barely altered the body weight ($P > 0.05$, Figure 5D). We then carried out immunofluorescence assays to determine PI3K/AKT/mTOR and p38-MAPK phosphorylation levels in the tumor tissues. Both deltonin and cisplatin reduced the levels of phosphorylated p38-MAPK and PI3K/AKT/mTOR, and their combination further reduced the levels compared to the cisplatin alone group (Figure 5E-H). These findings suggest that deltonin enhances chemosensitivity of GC cells to cisplatin by suppressing p38-MAPK and PI3K/AKT/mTOR signaling activation (Figure 6).

DISCUSSION

GC is a prevalent internal gastrointestinal malignancy with a high clinical fatality rate[24]. The current methods are ineffective for early GC diagnosis, owing to which GC is often diagnosed at the end stage when it is accompanied by distant metastasis and chemotherapy resistance. Moreover, surgical treatment and drug chemotherapy display poor efficacy[25]. Cisplatin is a frequently used chemotherapy drug for many malignant tumor diseases and is also extensively adopted in the context of GC[26,27]. Regarding the primary mechanism of cisplatin in cancer treatment, it triggers DNA damage in tumor cells. Unfortunately, cisplatin treatment can easily contribute to the drug resistance of tumor cells and influence the function of chemotherapy[28]. Hence, probing the drug action mechanisms in GC has great clinical implications for its treatment. Here, we discovered that deltonin hinders p38-MAPK and PI3K/AKT/mTOR signaling

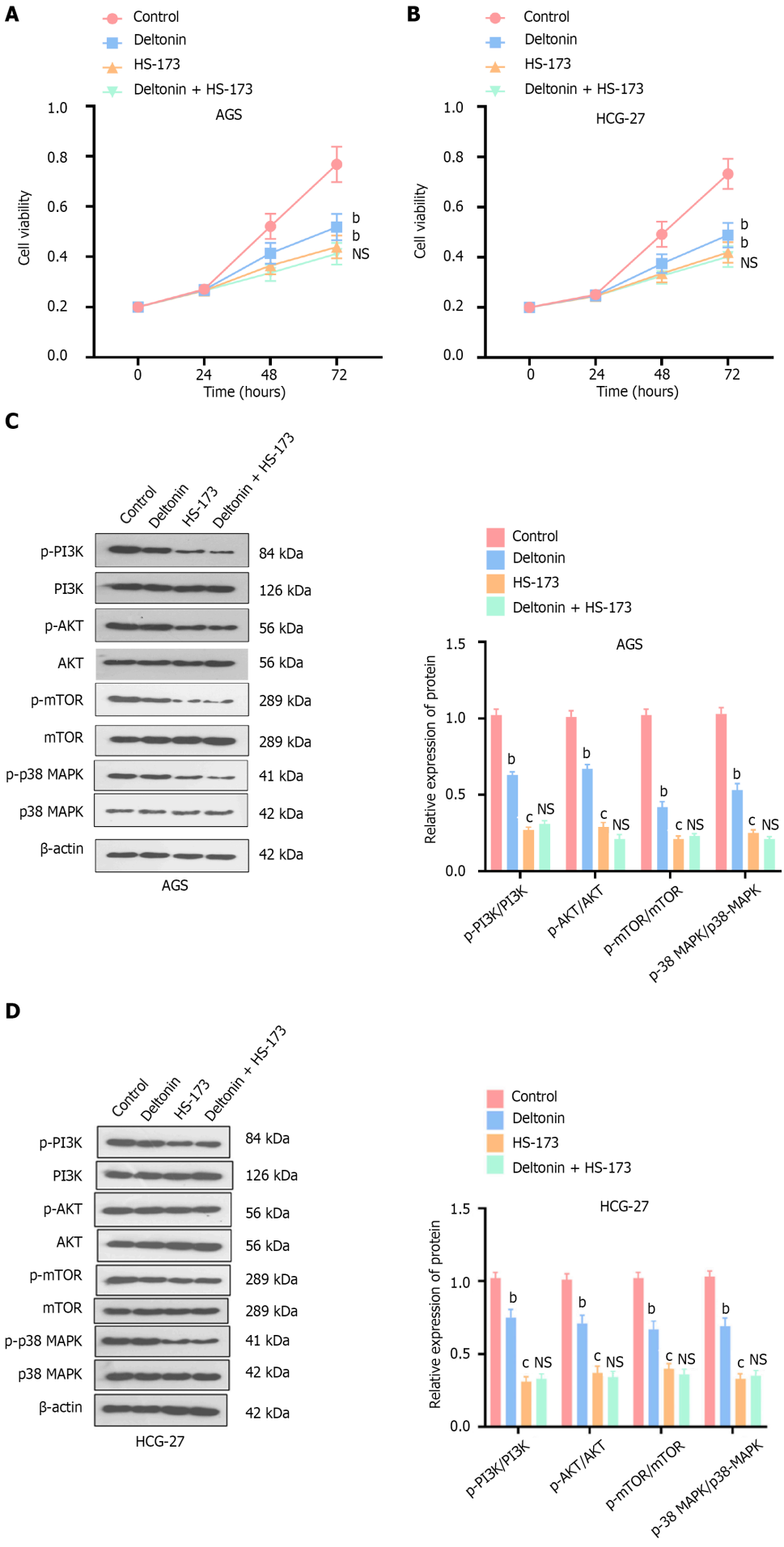
A
Control
Deltonin
HS-173
Deltonin + HS-173
AGS
Cell viability
1.0
0.8
0.6
0.4
0.2
0.0
0
24
48
72
Time (hours)
b
b
NS
B
Control
Deltonin
HS-173
Deltonin + HS-173
HCG-27
Cell viability
Time (hours)
b
b
NS
C
Control
Deltonin
HS-173
Deltonin + HS-173
p-PI3K
PI3K
p-AKT
AKT
p-mTOR
mTOR
p-p38 MAPK
p38 MAPK
β-actin
84 kDa
126 kDa
56 kDa
56 kDa
289 kDa
289 kDa
41 kDa
42 kDa
42 kDa
AGS
Control
Deltonin
HS-173
Deltonin + HS-173
AGS
Relative expression of protein
1.5
1.0
0.5
0.0
b
c
NS
p-PI3K/PI3K
p-AKT/AKT
p-mTOR/mTOR
p-38 MAPK/p38-MAPK
D
Control
Deltonin
HS-173
Deltonin + HS-173
p-PI3K
PI3K
p-AKT
AKT
p-mTOR
mTOR
p-p38 MAPK
p38 MAPK
β-actin
84 kDa
126 kDa
56 kDa
56 kDa
289 kDa
289 kDa
41 kDa
42 kDa
42 kDa
HCG-27
Control
Deltonin
HS-173
Deltonin + HS-173
HCG-27
Relative expression of protein
b
c
NS
p-PI3K/PI3K
p-AKT/AKT
p-mTOR/mTOR
p-38 MAPK/p38-MAPK

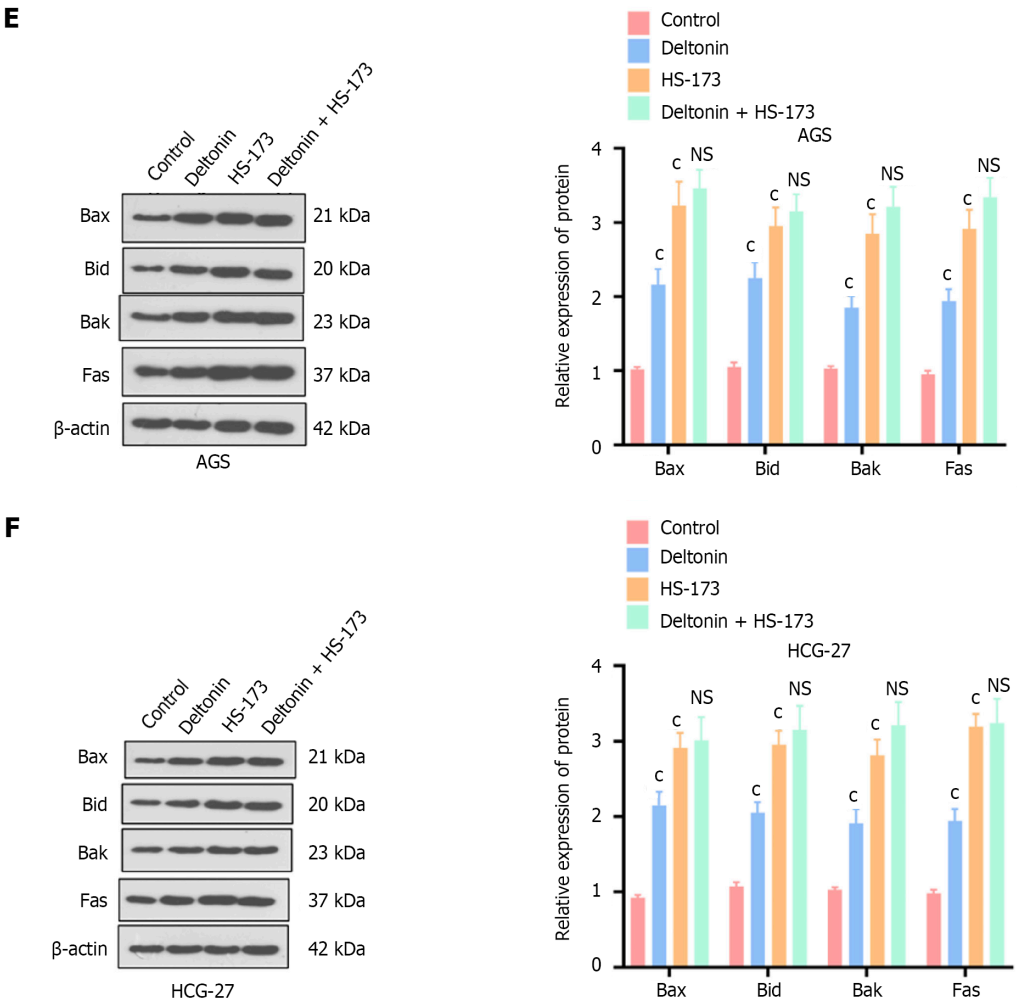

DOI: 10.4251/wjgo.v15.i10.1739 **Copyright** ©The Author(s) 2023.

Figure 2 Deltonin attenuates gastric carcinoma cell viability by dampening the phosphatidylinositol 3-kinase/protein kinase B/mammalian target of the rapamycin mitogen-activated protein kinase pathways. HGC-27 and AGS cells were treated with 2.5 μM of deltonin and/or 0.8 nM of HS-173 for 24 h. A and B: 3-(4,5-dimethylthiazol-2-yl)-3,5-diphenyltetrazolium bromide assay for cell viability examination; C and D: Western blot analysis of the profiles of apoptosis-correlated proteins; E and F: Western blot confirmation of the protein profiles of phosphatidylinositol 3-kinase/protein kinase B/mammalian target of the rapamycin p38-mitogen-activated protein kinase. $^{b}P < 0.01$, $^{c}P < 0.001$ *vs* control group; NS: $P > 0.05$ *vs* HS-173 group, $n = 3$. PI3K: Phosphatidylinositol 3-kinase; AKT: Protein kinase B; mTOR: Mammalian target of the rapamycin; p38-MAPK: p38-mitogen-activated protein kinase.

activation to boost GC cell apoptosis and promote their chemosensitivity to cisplatin.

Deltonin is known as an anti-tumor drug that curbs tumor cell angiogenesis to restrain tumor growth and facilitate apoptosis[29]. Deltonin inhibits AKT and p38-MAPK signaling pathway activation to further inhibit mouse colon cancer cell proliferation and bolster tumor cell apoptosis[18]. Furthermore, the intake of deltonin significantly suppresses colon cancer C26 cell proliferation in tumor-bearing mice, restricts tumor angiogenesis, and elicits cell apoptosis, thus prolonging the life cycle of the mice[30]. All the above studies confirm that deltonin enhances cancer cell apoptosis and represses cancer in a multitude of tumor diseases, which aligns with the observations in this study. Here, we demonstrated that deltonin considerably inhibits proliferation, boosts apoptosis, and dampens DNA repair in GC cells.

Chemotherapy is a prevailing method for GC, effectively extending patients' life. Cisplatin is a typical drug used in GC chemotherapy. Nonetheless, GC resistance is a leading contributor to chemotherapy failure[31,32]. Many studies have evaluated drug resistance in GC, including the most complicated molecular and drug mechanisms[33]. For instance, ten-eleven translocation-2 (TET2), a DNA demethylase, modulates interleukin (IL)-6 levels in the tumor microenvironment *via* histone acetylation, thus influencing cell resistance, and TET2 overexpression notably mitigates cisplatin resistance in GC cells[34]. Curcumin also augments the sensitivity of GC cells to adriamycin and other chemotherapy drugs by down-regulating the nuclear factor-kappaB (NF-κB) axis in human GC SGC-7901 cells and a downstream anti-apoptotic target gene of NF-κB[35]. Most of the prior studies have investigated the tolerance of chemotherapeutic drugs in GC from the aspect of molecular and drug mechanisms. Here, we unveiled that deltonin efficaciously augmented the chemosensitivity of GC cells to cisplatin and thereby boosted the anti-tumor function of cisplatin *via* eliciting apoptosis and DNA damage.

PI3K/AKT/mTOR and p38-MAPK signals were initially considered as factors that could regulate inflammation and immune response and affect inflammatory reactions, cell proliferation, differentiation, apoptosis, and other cellular processes[36,37]. Recent evidence has also demonstrated the pro-oncogenic functions of p38-MAPK and PI3K/AKT/mTOR in several tumors[38,39]. For instance, an *in vitro* experiment on GC cells has revealed that blocking PI3K/AKT/

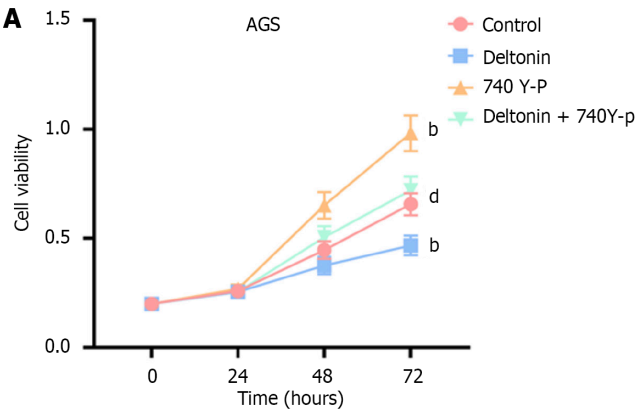
A
AGS
Control
Deltonin
740 Y-P
Deltonin + 740Y-p
Cell viability
Time (hours)
b
d
b

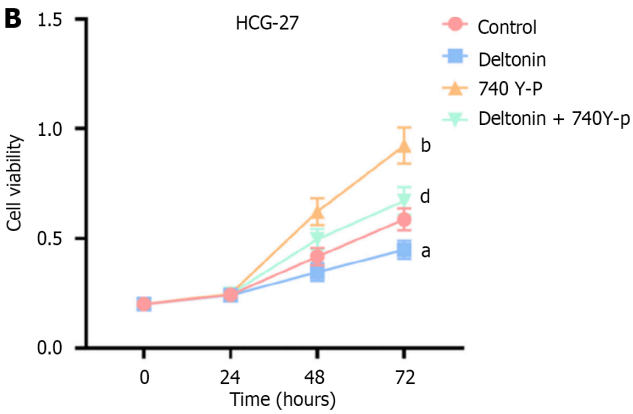
B
HCG-27
Control
Deltonin
740 Y-P
Deltonin + 740Y-p
Cell viability
Time (hours)
b
d
a

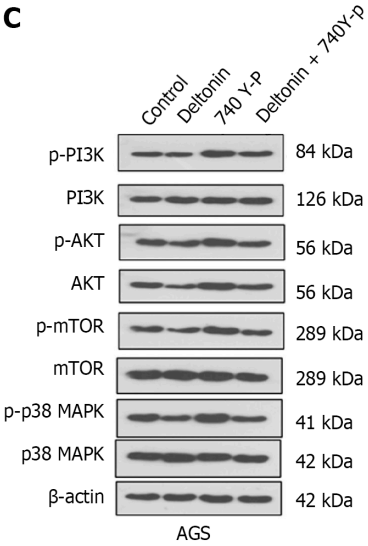
C
Control
Deltonin
740 Y-P
Deltonin + 740Y-p
p-PI3K
PI3K
p-AKT
AKT
p-mTOR
mTOR
p-p38 MAPK
p38 MAPK
β-actin
84 kDa
126 kDa
56 kDa
56 kDa
289 kDa
289 kDa
41 kDa
42 kDa
42 kDa
AGS

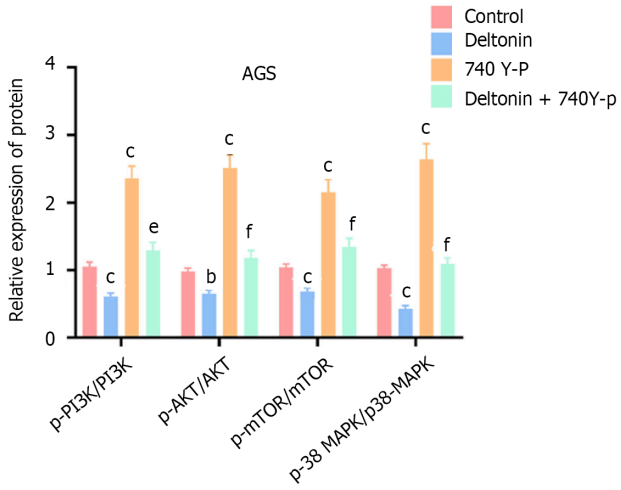
Control
Deltonin
740 Y-P
Deltonin + 740Y-p
AGS
Relative expression of protein
p-PI3K/PI3K
p-AKT/AKT
p-mTOR/mTOR
p-38 MAPK/p38-MAPK

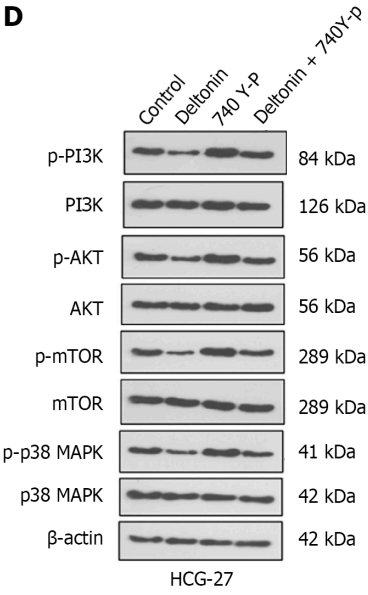
D
Control
Deltonin
740 Y-P
Deltonin + 740Y-p
p-PI3K
PI3K
p-AKT
AKT
p-mTOR
mTOR
p-p38 MAPK
p38 MAPK
β-actin
84 kDa
126 kDa
56 kDa
56 kDa
289 kDa
289 kDa
41 kDa
42 kDa
42 kDa
HCG-27

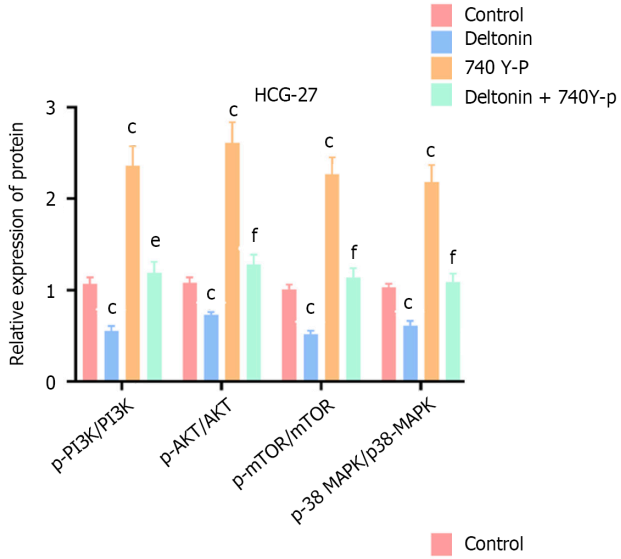
Control
Deltonin
740 Y-P
Deltonin + 740Y-p
HCG-27
Relative expression of protein
p-PI3K/PI3K
p-AKT/AKT
p-mTOR/mTOR
p-38 MAPK/p38-MAPK

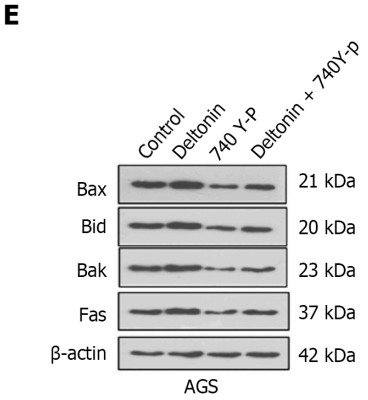
E
Control
Deltonin
740 Y-P
Deltonin + 740Y-p
Bax
Bid
Bak
Fas
β-actin
21 kDa
20 kDa
23 kDa
37 kDa
42 kDa
AGS

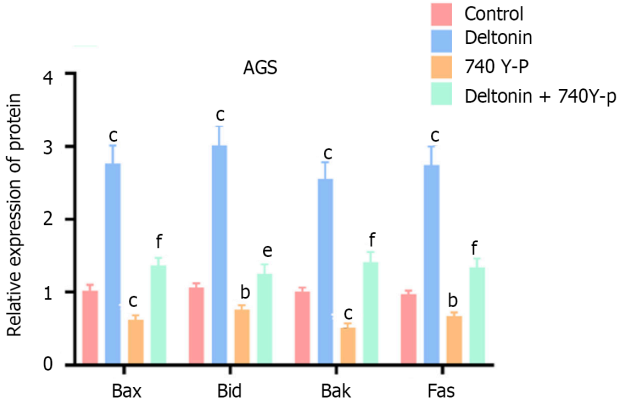
Control
Deltonin
740 Y-P
Deltonin + 740Y-p
AGS
Relative expression of protein
Bax
Bid
Bak
Fas

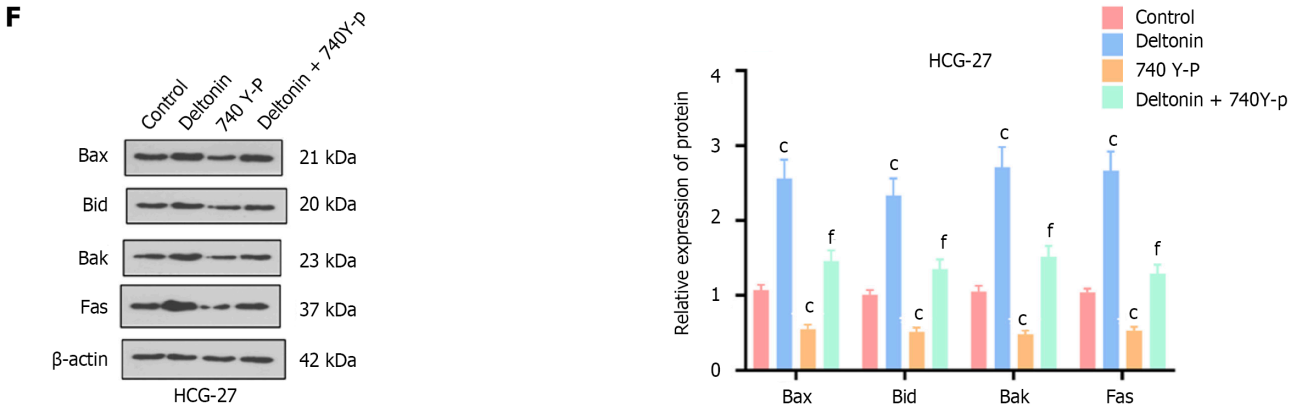

DOI: 10.4251/wjgo.v15.i10.1739 **Copyright** ©The Author(s) 2023.

Figure 3 Influence of phosphatidylinositol 3-kinase/protein kinase B/mammalian target of the rapamycin p38-mitogen-activated protein kinase signaling pathway activation on the effects mediated by deltonin. HGC-27 and AGS cells were treated with 2.5 μM of deltonin and/or 20 μM of phosphatidylinositol 3-kinase activator 740 Y-P for 24 h. A and B: 3-(4,5-dimethylthiazol-2-yl)-3,5-diphenyltetrazolium bromide assay for cell viability; C and D: Western blot verification of the profiles of apoptosis-concerned proteins; E and F: Western blot determination of the protein profiles of phosphatidylinositol 3-kinase/protein kinase B/mammalian target of the rapamycin and p38-mitogen-activated protein kinase. $^{a}P < 0.05$, $^{b}P < 0.01$, $^{c}P < 0.001$ *vs* control group; $^{d}P < 0.05$, $^{e}P < 0.01$, $^{f}P < 0.001$ *vs* 740 Y-P group, $n = 3$. PI3K: Phosphatidylinositol 3-kinase; AKT: Protein kinase B; mTOR: Mammalian target of the rapamycin; p38-MAPK: p38-mitogen-activated protein kinase.

mTOR signaling activation augments the resistance of GC cells to paclitaxel and promotes their apoptosis[40]. Afatinib dampens p38-MAPK and PI3K/AKT/mTOR signaling activation, thereby eliciting GC cell apoptosis and bolstering their resistance to chemotherapy[41]. All these conclusions align with our current study findings. Here, we discovered that deltonin significantly hinders p38-MAPK and PI3K/AKT/mTOR signaling activation, thereby bolstering GC cell apoptosis and attenuating the resistance of GC cells to cisplatin.

CONCLUSION

In summary, through a series of experiments, we uncovered that treating GC cells (AGS, HGC-27, and MKN-45) with deltonin results in reduced proliferation ability and increased apoptosis rate; of these, HGC-27 cells exhibited the best proliferation capability and the lowest apoptosis rate. Therefore, we exploited AGS and HGC-27 cells for further experiments and analyses. Our experiments demonstrated the ability of deltonin to promote GC cell apoptosis and chemosensitivity to cisplatin by lowering PI3K/AKT/mTOR and p38-MAPK-associated protein levels, offering novel insights into the mechanism of drug action. Nevertheless, further investigations are required to understand how deltonin represses these two axes, and *in vivo* experiments should be conducted using both male and female nude mice and other GC cell lines.

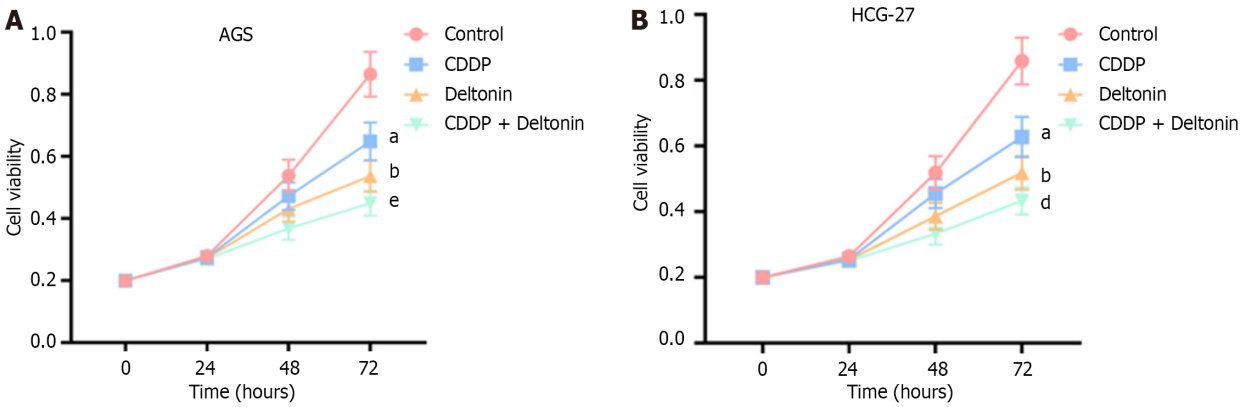

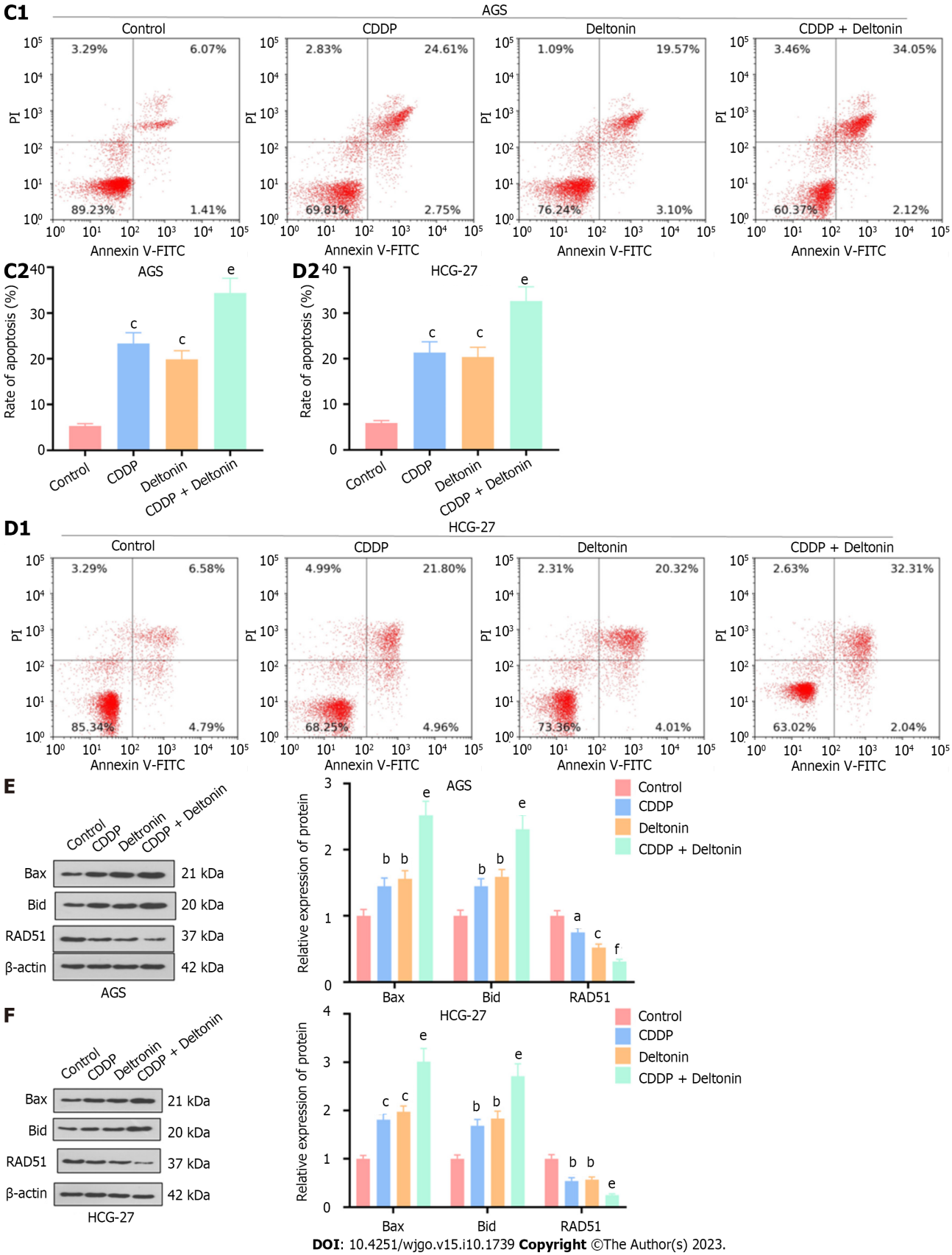

DOI: 10.4251/wjgo.v15.i10.1739 **Copyright** ©The Author(s) 2023.

Figure 4 Deltonin enhances the chemosensitivity of gastric carcinoma cells to cisplatin. AGS and HGC-27 gastric carcinoma cells were treated with 2.5 μM of deltonin or 5 μg/mL of cisplatin or deltonin (1.25 μM) plus cisplatin (2.5 μg/mL) for 24 h. A and B: 3-(4,5-dimethylthiazol-2-yl)-3,5-diphenyltetrazolium bromide assay for examination of cell viability; C and D: Flow cytometry analysis of cell apoptosis; E and F: Western blot analysis of expression of apoptosis-correlated proteins (Bax and Bid) and the DNA repair-associated protein Rad51. $^{a}P < 0.05$, $^{b}P < 0.01$, $^{c}P < 0.001$ *vs* control group; $^{d}P < 0.01$, $^{e}P < 0.01$, $^{f}P < 0.001$ *vs* cisplatin group, $n = 3$. CDDP: Cisplatin.

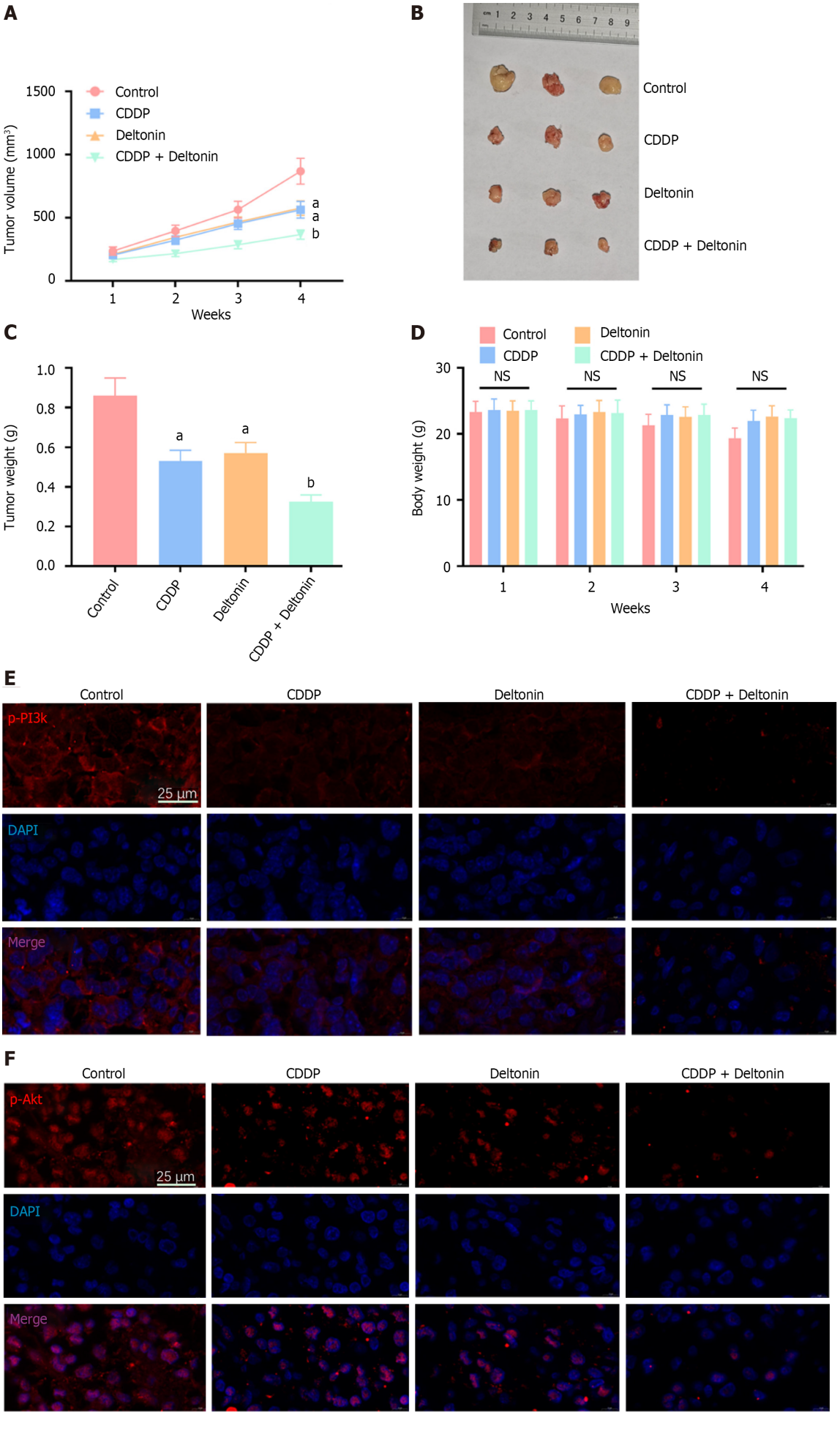
A
Control
CDDP
Deltonin
CDDP + Deltonin
Tumor volume (mm³)
1500
1000
500
0
1
2
3
4
Weeks
a
a
b
B
Control
CDDP
Deltonin
CDDP + Deltonin
C
Tumor weight (g)
1.0
0.8
0.6
0.4
0.2
0.0
a
a
b
Control
CDDP
Deltonin
CDDP + Deltonin
D
Control
CDDP
Deltonin
CDDP + Deltonin
Body weight (g)
30
20
10
0
NS
NS
NS
NS
1
2
3
4
Weeks
E
Control
CDDP
Deltonin
CDDP + Deltonin
p-PI3k
25 μm
DAPI
Merge
F
Control
CDDP
Deltonin
CDDP + Deltonin
p-Akt
25 μm
DAPI
Merge

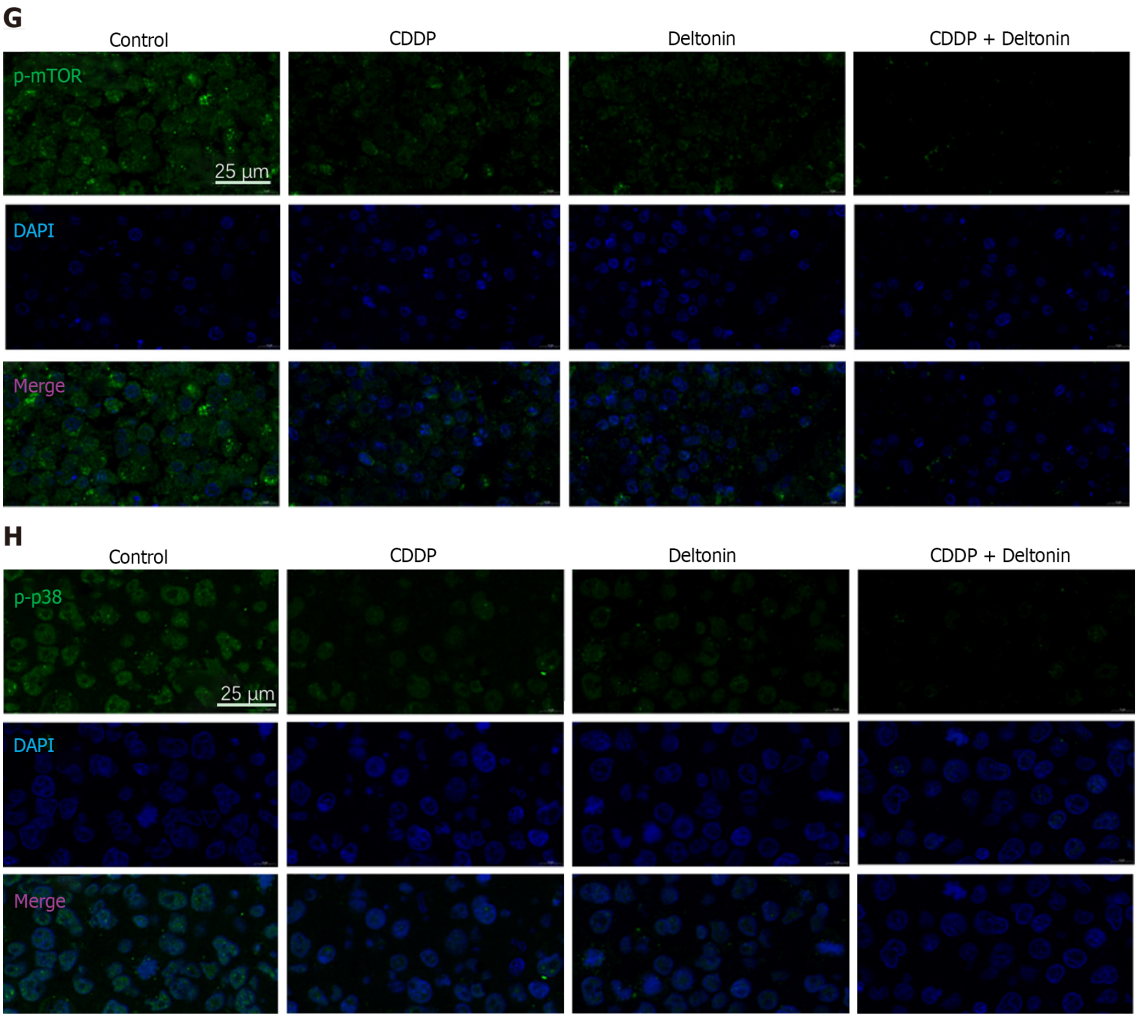

DOI: 10.4251/wjgo.v15.i10.1739 **Copyright** ©The Author(s) 2023.

Figure 5 Deltonin augmentes the chemosensitivity to cisplatin *in vivo* by dampening the phosphatidylinositol 3-kinase/protein kinase B/mammalian target of the rapamycin and mitogen-activated protein kinase signaling pathways. Tumor-bearing mice were treated with saline, deltonin (50 mg/kg), and cisplatin (3 mg/kg) or deltonin (25 mg/kg) + cisplatin (1.5 mg/kg). A: The tumor volume was calculated during the 28 d; B and C: On the 28th d, the mice were sacrificed, the tumor images were taken, and the tumor weight was gauged; D: The body weight of the nude mice in different groups was figured out; E-H: Immunofluorescence measurement of the levels of phosphorylated phosphatidylinositol 3-kinase/protein kinase B/mammalian target of the rapamycin and p38-mitogen-activated protein kinase in the tumor tissues. NS: $P > 0.05$, $^{a}P < 0.01$ *vs* sham group, $^{b}P < 0.01$ *vs* cisplatin group, $n = 3$. NS: No significance; PI3K: Phosphatidylinositol 3-kinase; AKT: Protein kinase B; mTOR: Mammalian target of the rapamycin; DAPI: 4',6-diamidino-2-phenylindole; CDDP: Cisplatin.

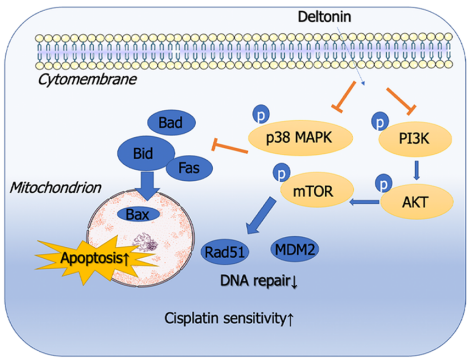

DOI: 10.4251/wjgo.v15.i10.1739 **Copyright** ©The Author(s) 2023.

Figure 6 Mechanism diagram. Deltonin bolsteres the apoptosis of gastric cancer cells and enhances their chemosensitivity to cisplatin *via* the phosphatidylinositol 3-kinase/protein kinase B/mammalian target of the rapamycin and mitogen-activated protein kinase signaling pathways. PI3K: Phosphatidylinositol 3-kinase; AKT: Protein kinase B; mTOR: Mammalian target of the rapamycin; p38-MAPK: p38-mitogen-activated protein kinase.

ARTICLE HIGHLIGHTS

Research background

Despite being the main clinical treatment modality for advanced gastric cancer (GC), chemoradiotherapy is still difficult to achieve the expected effect due to the early diagnosis of GC and the characteristics of distant metastasis and drug resistance. Deltonin, an active ingredient in traditional Chinese medicine, shows anti-cancer effects on many malignancies.

Research motivation

This study attempted to optimize the treatment strategies for advanced GC and enhance the therapeutic effect on patients from a pharmacological mechanism perspective.

Research objectives

Here, we investigated the role and mechanism of action of deltonin in promoting GC cell apoptosis and chemosensitivity to cisplatin.

Research methods

In this study, gastric cancer cell lines (AGS, HGC-27, and MKN-45 cells) were treated with deltonin. Then, apoptosis was observed, and the expression of apoptosis-related proteins (Bax, Bid, Bad, and Fas), DNA repair-related proteins (Rad51 and MDM2), and phosphatidylinositol 3-kinase/protein kinase B/mammalian target of the rapamycin (PI3K/AKT/mTOR-MAPK) proteins was detected by Western blot analysis. In addition to this, the effect of deltonin on the chemosensitivity of GC cells to cisplatin was evaluated by *in vivo* and *in vitro* experiments

Research results

Treating GC cells (AGS, HGC-27, and MKN-45) with deltonin resulted in reduced proliferation ability and increased apoptosis rate; of these, HGC-27 cells exhibited the best proliferation capability and the lowest apoptosis rate. Our experiments demonstrated the ability of deltonin to promote GC cell apoptosis and chemosensitivity to cisplatin by lowering PI3K/AKT/mTOR and p38-MAPK-associated protein levels, offering novel insights into the mechanism of drug action.

Research conclusions

Deltonin enhances the chemosensitivity of GC cells to cisplatin by inhibiting the p38-MAPK and PI3K/AKT/mTOR signaling pathways.

Research perspectives

This study has verified that deltonin is able to regulate GC cell apoptosis as well as chemosensitivity to cisplatin through the PI3K/AKT/mTOR and p38-AMPK signaling pathways by *in vivo* and *in vitro* experiments. Such results provide a new direction for drug therapy of gastric cancer. However, the study of the regulatory role of the pathways in this study was limited and could not fully elucidate its mechanism of action. Therefore, further analysis as well as nude mouse experiments and more cellular experiments are needed to excavate the mechanism.

FOOTNOTES

Author contributions: Yang L and Liu YN contributed equally to this work and are co-first authors. Yang L and Liu YN conceived and designed the experiments; Yang L, Liu YN, Gu Y, and Guo Q performed the experiments; Yang L, Liu YN, Gu Y, and Guo Q contributed to the statistical analysis; Yang L, Liu YN, and Guo Q wrote the paper; and all authors read and approved the final manuscript.

Institutional review board statement: Our study was approved by the Ethics Review Committee of the Second Affiliated Hospital of Soochow University (approval No.: SZSH-2020-042).

Institutional animal care and use committee statement: The animal experiments were approved by the Ethics Review Committee of the Second Affiliated Hospital of Soochow University (approval No. SZSH-2020-042).

Conflict-of-interest statement: All the authors report no relevant conflicts of interest for this article.

Data sharing statement: The data sets used and analyzed during the current study are available from the corresponding author on reasonable request.

ARRIVE guidelines statement: The authors have read the ARRIVE guidelines, and the manuscript was prepared and revised according to the ARRIVE guidelines.

Country/Territory of origin: China

ORCID number: Qi Guo 0000-0002-2996-5987.

S-Editor: Wang JJ
L-Editor: Wang TQ
P-Editor: Zhang XD

REFERENCES

1 **Joshi SS**, Badgwell BD. Current treatment and recent progress in gastric cancer. *CA Cancer J Clin* 2021; **71**: 264-279 [PMID: 33592120 DOI: 10.3322/caac.21657]
2 **Jemal A**, Center MM, DeSantis C, Ward EM. Global patterns of cancer incidence and mortality rates and trends. *Cancer Epidemiol Biomarkers Prev* 2010; **19**: 1893-1907 [PMID: 20647400 DOI: 10.1158/1055-9965.EPI-10-0437]
3 **Freedman ND**, Abnet CC, Leitzmann MF, Mouw T, Subar AF, Hollenbeck AR, Schatzkin A. A prospective study of tobacco, alcohol, and the risk of esophageal and gastric cancer subtypes. *Am J Epidemiol* 2007; **165**: 1424-1433 [PMID: 17420181 DOI: 10.1093/aje/kwm051]
4 **Yaghoobi M**, Bijarchi R, Narod SA. Family history and the risk of gastric cancer. *Br J Cancer* 2010; **102**: 237-242 [PMID: 19888225 DOI: 10.1038/sj.bjc.6605380]
5 **Kamangar F**, Sheikhattari P, Mohebtash M. Helicobacter pylori and its effects on human health and disease. *Arch Iran Med* 2011; **14**: 192-199 [PMID: 21529109]
6 **Song Z**, Wu Y, Yang J, Yang D, Fang X. Progress in the treatment of advanced gastric cancer. *Tumour Biol* 2017; **39**: 1010428317714626 [PMID: 28671042 DOI: 10.1177/1010428317714626]
7 **Zhang Y**, Tian Z, Wan H, Liu W, Kong F, Ma G. Deltonin Ameliorates Cerebral Ischemia/Reperfusion Injury in Correlation with Modulation of Autophagy and Inflammation. *Neuropsychiatr Dis Treat* 2020; **16**: 871-879 [PMID: 32280228 DOI: 10.2147/NDT.S227988]
8 **Xie YL**, Fan M, Jiang RM, Wang ZL, Li Y. Deltonin induced both apoptosis and autophagy in head and neck squamous carcinoma FaDu cell. *Neoplasma* 2015; **62**: 419-431 [PMID: 25866222 DOI: 10.4149/neo_2015_050]
9 **Zhang S**, He Y, Tong Q, Chen Q, Wu X, Huang W. Deltonin induces apoptosis in MDAMB231 human breast cancer cells *via* reactive oxygen speciesmediated mitochondrial dysfunction and ERK/AKT signaling pathways. *Mol Med Rep* 2013; **7**: 1038-1044 [PMID: 23314115 DOI: 10.3892/mmr.2013.1273]
10 **Aoki M**, Fujishita T. Oncogenic Roles of the PI3K/AKT/mTOR Axis. *Curr Top Microbiol Immunol* 2017; **407**: 153-189 [PMID: 28550454 DOI: 10.1007/82_2017_6]
11 **Yang J**, Pi C, Wang G. Inhibition of PI3K/Akt/mTOR pathway by apigenin induces apoptosis and autophagy in hepatocellular carcinoma cells. *Biomed Pharmacother* 2018; **103**: 699-707 [PMID: 29680738 DOI: 10.1016/j.biopha.2018.04.072]
12 **Yue Z**, Guan X, Chao R, Huang C, Li D, Yang P, Liu S, Hasegawa T, Guo J, Li M. Diallyl Disulfide Induces Apoptosis and Autophagy in Human Osteosarcoma MG-63 Cells through the PI3K/Akt/mTOR Pathway. *Molecules* 2019; **24** [PMID: 31340526 DOI: 10.3390/molecules24142665]
13 **Coulthard LR**, White DE, Jones DL, McDermott MF, Burchill SA. p38(MAPK): stress responses from molecular mechanisms to therapeutics. *Trends Mol Med* 2009; **15**: 369-379 [PMID: 19665431 DOI: 10.1016/j.molmed.2009.06.005]
14 **Cuadrado A**, Nebreda AR. Mechanisms and functions of p38 MAPK signalling. *Biochem J* 2010; **429**: 403-417 [PMID: 20626350 DOI: 10.1042/BJ20100323]
15 **Guo X**, Ding X. Dioscin suppresses the viability of ovarian cancer cells by regulating the VEGFR2 and PI3K/AKT/MAPK signaling pathways. *Oncol Lett* 2018; **15**: 9537-9542 [PMID: 29805675 DOI: 10.3892/ol.2018.8454]
16 **Chao W**, Deng JS, Li PY, Kuo YH, Huang GJ. Inotilone from Inonotus linteus suppresses lung cancer metastasis *in vitro* and *in vivo* through ROS-mediated PI3K/AKT/MAPK signaling pathways. *Sci Rep* 2019; **9**: 2344 [PMID: 30787353 DOI: 10.1038/s41598-019-38959-z]
17 **Xue M**, Liu X, Cheng B, Rui X, Wu M, Lv J. Epigallocatechin Gallate Enhances Inhibition Effect of DDP on the Proliferation of Gastric Cancer BGC-823 Cells by Regulating p19Arf-p53-p21Cip1 Signaling Pathway. *Asian Pac J Cancer Prev* 2021; **22**: 1263-1270 [PMID: 33906321 DOI: 10.31557/APJCP.2021.22.4.1263]
18 **Shu D**, Qing Y, Tong Q, He Y, Xing Z, Zhao Y, Li Y, Wei Y, Huang W, Wu X. Deltonin isolated from Dioscorea zingiberensis inhibits cancer cell growth through inducing mitochondrial apoptosis and suppressing Akt and mitogen activated protein kinase signals. *Biol Pharm Bull* 2011; **34**: 1231-1239 [PMID: 21804211 DOI: 10.1248/bpb.34.1231]
19 **Son MK**, Ryu YL, Jung KH, Lee H, Lee HS, Yan HH, Park HJ, Ryu JK, Suh JK, Hong S, Hong SS. HS-173, a novel PI3K inhibitor, attenuates the activation of hepatic stellate cells in liver fibrosis. *Sci Rep* 2013; **3**: 3470 [PMID: 24326778 DOI: 10.1038/srep03470]
20 **Feng X**, Chen L, Guo W, Zhang Y, Lai X, Shao L, Li Y. Graphene oxide induces p62/SQSTM-dependent apoptosis through the impairment of autophagic flux and lysosomal dysfunction in PC12 cells. *Acta Biomater* 2018; **81**: 278-292 [PMID: 30273743 DOI: 10.1016/j.actbio.2018.09.057]
21 **Wang J**, Liu R, Mo H, Xiao X, Xu Q, Zhao W. Deubiquitinase PSMD7 promotes the proliferation, invasion, and cisplatin resistance of gastric cancer cells by stabilizing RAD23B. *Int J Biol Sci* 2021; **17**: 3331-3342 [PMID: 34512150 DOI: 10.7150/ijbs.61128]
22 **Li H**, Xu W, Liu X, Ye J, Li P, Shang F, Yu X. Curcumin Alleviates the Side Effects of Cisplatin on Gastric Emptying of Mice by Inhibiting the Signal Changes of Acetylcholine and Interstitial Cells of Cajal. *J Med Food* 2020; **23**: 920-927 [PMID: 32833554 DOI: 10.1089/jmf.2019.4599]
23 **Ando K**, Takagi K, Tsubone H. Enhanced gastric retention of solid resin beads as a marker for emetic potential of agents in rats. *J Toxicol Sci* 2012; **37**: 549-553 [PMID: 22687994 DOI: 10.2131/jts.37.549]
24 **Digklia A**, Wagner AD. Advanced gastric cancer: Current treatment landscape and future perspectives. *World J Gastroenterol* 2016; **22**: 2403-

2414 [PMID: 26937129 DOI: 10.3748/wjg.v22.i8.2403]
25 **Choi AH**, Kim J, Chao J. Perioperative chemotherapy for resectable gastric cancer: MAGIC and beyond. *World J Gastroenterol* 2015; **21**: 7343-7348 [PMID: 26139980 DOI: 10.3748/wjg.v21.i24.7343]
26 **Hayashi N**, Kataoka H, Yano S, Kikuchi JI, Tanaka M, Nishie H, Kinoshita Y, Hatano M, Nomoto A, Ogawa A, Inoue M, Mizoshita T, Shimura T, Mori Y, Kubota E, Tanida S, Joh T. Anticancer Effects of a New Aminosugar-conjugated Platinum Complex Agent Against Cisplatin-resistant Gastric Cancer. *Anticancer Res* 2016; **36**: 6005-6009 [PMID: 27793927 DOI: 10.21873/anticanres.11189]
27 **Wang D**, Lippard SJ. Cellular processing of platinum anticancer drugs. *Nat Rev Drug Discov* 2005; **4**: 307-320 [PMID: 15789122 DOI: 10.1038/nrd1691]
28 **Galluzzi L**, Senovilla L, Vitale I, Michels J, Martins I, Kepp O, Castedo M, Kroemer G. Molecular mechanisms of cisplatin resistance. *Oncogene* 2012; **31**: 1869-1883 [PMID: 21892204 DOI: 10.1038/onc.2011.384]
29 **Tong Q**, Zhao Q, Qing Y, Hu X, Jiang L, Wu X. Deltonin inhibits angiogenesis by regulating VEGFR2 and subsequent signaling pathways in endothelial cells. *Steroids* 2015; **96**: 30-36 [PMID: 25554580 DOI: 10.1016/j.steroids.2014.12.019]
30 **Tong QY**, Qing Y, Shu D, He Y, Zhao YL, Li Y, Wang ZL, Zhang SY, Xing ZH, Xu C, Wei YQ, Huang W, Wu XH. Deltonin, a steroidal saponin, inhibits colon cancer cell growth *in vitro* and tumor growth *in vivo via* induction of apoptosis and antiangiogenesis. *Cell Physiol Biochem* 2011; **27**: 233-242 [PMID: 21471712 DOI: 10.1159/000327949]
31 **Archie V**, Kauh J, Jones DV Jr, Cruz V, Karpeh MS Jr, Thomas CR Jr. Gastric cancer: standards for the 21st century. *Crit Rev Oncol Hematol* 2006; **57**: 123-131 [PMID: 16412659 DOI: 10.1016/j.critrevonc.2005.09.004]
32 **Zhang XL**, Shi HJ, Wang JP, Tang HS, Cui SZ. MiR-218 inhibits multidrug resistance (MDR) of gastric cancer cells by targeting Hedgehog/smoothened. *Int J Clin Exp Pathol* 2015; **8**: 6397-6406 [PMID: 26261515]
33 **Chen C**, Tang X, Liu Y, Zhu J, Liu J. Induction/reversal of drug resistance in gastric cancer by non-coding RNAs (Review). *Int J Oncol* 2019; **54**: 1511-1524 [PMID: 30896792 DOI: 10.3892/ijo.2019.4751]
34 **Zhou K**, Guo H, Zhang J, Zhao D, Zhou Y, Zheng Z, Xu Y, Li Y, Wang D. Potential role of TET2 in gastric cancer cisplatin resistance. *Pathol Res Pract* 2019; **215**: 152637 [PMID: 31570278 DOI: 10.1016/j.prp.2019.152637]
35 **Yu LL**, Wu JG, Dai N, Yu HG, Si JM. Curcumin reverses chemoresistance of human gastric cancer cells by downregulating the NF-κB transcription factor. *Oncol Rep* 2011; **26**: 1197-1203 [PMID: 21811763 DOI: 10.3892/or.2011.1410]
36 **Ono K**, Han J. The p38 signal transduction pathway: activation and function. *Cell Signal* 2000; **12**: 1-13 [PMID: 10676842 DOI: 10.1016/s0898-6568(99)00071-6]
37 **Polivka J Jr**, Janku F. Molecular targets for cancer therapy in the PI3K/AKT/mTOR pathway. *Pharmacol Ther* 2014; **142**: 164-175 [PMID: 24333502 DOI: 10.1016/j.pharmthera.2013.12.004]
38 **Cai C**, Dang W, Liu S, Huang L, Li Y, Li G, Yan S, Jiang C, Song X, Hu Y, Gu J. Anthrax toxin receptor 1/tumor endothelial marker 8 promotes gastric cancer progression through activation of the PI3K/AKT/mTOR signaling pathway. *Cancer Sci* 2020; **111**: 1132-1145 [PMID: 31977138 DOI: 10.1111/cas.14326]
39 **Du F**, Sun L, Chu Y, Li T, Lei C, Wang X, Jiang M, Min Y, Lu Y, Zhao X, Nie Y, Fan D. DDIT4 promotes gastric cancer proliferation and tumorigenesis through the p53 and MAPK pathways. *Cancer Commun (Lond)* 2018; **38**: 45 [PMID: 29976242 DOI: 10.1186/s40880-018-0315-y]
40 **Chen D**, Lin X, Zhang C, Liu Z, Chen Z, Li Z, Wang J, Li B, Hu Y, Dong B, Shen L, Ji J, Gao J, Zhang X. Dual PI3K/mTOR inhibitor BEZ235 as a promising therapeutic strategy against paclitaxel-resistant gastric cancer *via* targeting PI3K/Akt/mTOR pathway. *Cell Death Dis* 2018; **9**: 123 [PMID: 29374144 DOI: 10.1038/s41419-017-0132-2]
41 **Chen Z**, Liu Z, Zhang M, Huang W, Li Z, Wang S, Zhang C, Dong B, Gao J, Shen L. EPHA2 blockade reverses acquired resistance to afatinib induced by EPHA2-mediated MAPK pathway activation in gastric cancer cells and avatar mice. *Int J Cancer* 2019; **145**: 2440-2449 [PMID: 30957241 DOI: 10.1002/ijc.32313]

World Journal of Gastrointestinal Oncology

Submit a Manuscript: https://www.f6publishing.com

World J Gastrointest Oncol 2023 October 15; 15(10): 1756-1770

DOI: 10.4251/wjgo.v15.i10.1756

ISSN 1948-5204 (online)

ORIGINAL ARTICLE

Basic Study

Pomolic acid and its glucopyranose ester promote apoptosis through autophagy in HT-29 colon cancer cells

Li-Yan Liu, Teng-Hua Yu, Tie-Song Liao, Peng Xu, Ying Wang, Min Shi, Bin Li

Specialty type: Oncology

Provenance and peer review: Unsolicited article; Externally peer reviewed.

Peer-review model: Single blind

Peer-review report's scientific quality classification

Grade A (Excellent): 0
Grade B (Very good): B, B
Grade C (Good): 0
Grade D (Fair): 0
Grade E (Poor): 0

P-Reviewer: Kim K, South Korea; Rau B, Germany

Received: May 21, 2023
Peer-review started: May 21, 2023
First decision: June 1, 2023
Revised: July 5, 2023
Accepted: August 31, 2023
Article in press: August 31, 2023
Published online: October 15, 2023

Li-Yan Liu, Tie-Song Liao, Bin Li, Workstation of Academician, Jiangxi University of Chinese Medicine, Nanchang 330004, Jiangxi Province, China

Li-Yan Liu, Department of Pharmacy, Jiangxi Cancer Hospital and Jiangxi Cancer Center, Nanchang 330029, Jiangxi Province, China

Teng-Hua Yu, Department of Breast Surgery, Jiangxi Cancer Hospital and Jiangxi Cancer Center, Nanchang 330029, Jiangxi Province, China

Peng Xu, Min Shi, Laboratory Animal Science and Technology Center, Jiangxi University of Chinese Medicine, Nanchang 330004, Jiangxi Province, China

Ying Wang, Department of Pharmacy, Shangrao Health School, Shangrao 334000, Jiangxi Province, China

Corresponding author: Bin Li, PhD, Professor, Workstation of Academician, Jiangxi University of Chinese Medicine, No. 1688 Meiling Road, Nanchang 330004, Jiangxi Province, China. emilylly2013@sina.com

Abstract

BACKGROUND

Colon cancer remains a leading cause of death globally. Pomolic acid (PA) can be separated from the ethyl acetate fraction of achyrocline satureioides.

AIM

To determine the effects of PA and its glucopyranose ester, pomolic acid-28-O-β-D-glucopyranosyl ester (PAO), on colon cancer HT-29 cells.

METHODS

3-(4, 5-dimethylthiazol-2-yl)-2, 5-diphenyl tetrazolium bromide assay was used to measure cell viability. Apoptosis was detected *via* hoechst 33342 staining. PI single staining was identified by flow cytometry to determine the cycle and scratch assay was used to observe the migration of HT-29 cells. The levels of mRNA and proteins were evaluated by q polymerase chain reaction and western blotting, respectively.

RESULTS

PA and PAO considerably inhibited the growth of the HT-29 cell line in a time and dose-dependent manner. After the administration of PA and PAO for 24 and

48 h, cell apoptosis was significantly promoted and HT-29 cells were arrested in the G_0/G_1 stage. The Bax/Bcl2 ratio was also increased, which activated cysteinyl aspartate specific proteinase 3, leading to apoptosis; it also increased the expression of light chain 3 II/I and Beclin1, which activated autophagy and caused cell death. This in turn increased the expression of p62 to promote cell apoptosis, inhibiting the levels of signal transducer and activator of transcription 3 (STAT3) and p-STAT3, suppressing the level of Bcl2, and promoting cell.

CONCLUSION
Both PA and PAO provide novel therapeutic strategies for treating colorectal cancer.

Key Words: Colon cancer; Achyrocline satureioides; Pomolic acid; Pomolic acid-28-O-β-D-glucopyranose

Core Tip: Compounds pomolic acid (PA) and pomolic acid-28-O-β-D-glucopyranosyl ester (PAO) exhibited a considerable growth inhibitory effect against HT-29 cell lines in a time-dose-dependent manner. PA and PAO promote apoptosis through autophagy in HT-29 colon tumor cells. Both PA and PAO provide novel therapeutic strategy for colorectal cancers treatment.

Citation: Liu LY, Yu TH, Liao TS, Xu P, Wang Y, Shi M, Li B. Pomolic acid and its glucopyranose ester promote apoptosis through autophagy in HT-29 colon cancer cells. *World J Gastrointest Oncol* 2023; 15(10): 1756-1770
URL: https://www.wjgnet.com/1948-5204/full/v15/i10/1756.htm
DOI: https://dx.doi.org/10.4251/wjgo.v15.i10.1756

INTRODUCTION

Colon cancer remains a leading cause of death globally[1], while colorectal cancer has become the third most common tumor with the highest incidence[2]. Surgical treatment is generally the best choice for early-stage colon cancer patients, but unfortunately many patients are diagnosed at an advanced stage. Surgery-based postoperative adjuvant chemotherapy is currently the most important method for treating colon cancer. However, resistance and toxicity of chemotherapy have severely hampered the implementation of chemotherapy regimens. There is thus a need for new therapeutic options for patients at an advanced stage of the disease, so the search for new drugs and targets has become a key component of efforts to treat colon cancer.

There are abundant active substances in nature, especially in plants of medicine food homology. Achyrocline satureioides is a plant from the achyrocline genus brassica, which is a medicinal herb widely used in Latin America for gastrointestinal diseases, bacterial infections, anti-inflammatory effects, pain relief, and for treating other diseases[3-7]. We previously isolated many compounds from the flowers of *A. satureioides*, including triterpenics, anthraquinones, and flavonoids. Research has shown that pomolic acid (PA) and its glucopyranose ester have effects against breast cancer[8-10], prostate cancer[11], leukemia[12-15], and other malignant tumors. Because of its high safety, these agents have been increasingly used in the treatment of cancer. However, there has been little research on the use of PA and its glucopyranose ester in treating colon cancer, or on the mechanisms behind their effects. We thus investigated the influence of PA and its glucopyranose ester on colon cancer cells. In this study, PA and its glucopyranose ester showed good inhibitory effects on colon cancer cells and have potential as new drugs for future use in a clinical context.

MATERIALS AND METHODS

Materials and chemicals

PA was separated and purified from *A. satureioides* (purity > 98%). Pomolic acid-28-O-β-D-glucopyranosyl ester (PAO) was obtained from Chengdu Alpha Biological Co., Ltd. (cas: 83725-25-0), with purity exceeding 94%. Oxaliplatin was obtained from Hengrui Medicine (China). Annexin-V-fluorescein isothiocyanate and propidium iodide (BD Biosciences, Franklin Lake, NJ, United States), McCoys' 5A (Modified; Gibco, United States), and [fetal bovine serum (FBS); EXCEll, China] were also obtained. Bcl2, anti-sequestosome-1 (p62), anti-light chain 3 (LC3) A/B, Bax, Beclin-1, anti-janus kinase (JAK), anti-p-signal transducer and activator of transcription 3 (STAT3), and anti-STAT3 antibodies were obtained from cell signaling technology (United States). Anti-β-actin was purchased Protech (China). 3-(4, 5-dimethylthiazol-2-yl)-2, 5-diphenyl tetrazolium bromide (MTT) and dimethyl sulfoxide (DMSO) were obtained from Solarbio (China). The HT-29 cell line was purchased from National Collection of Authenticated Cell Cultures. Finally, the laser confocal microscope leica DMI3000B was used (Leica, Germany).

Methods

Preparation of PA: *A. Satureioides* was identified by Professor Peng HS of Anhui University of Chinese Medicine. Nine kilograms of dried *A. satureioides* was pulverized mechanically and extracted five times with the amount of 95% ethanol. It was then heated and refluxed two times for 1 h each, and subsequently heated and refluxed three times with the amount of 50% ethanol two times for 1 h each. Then, the ethanol extracts were combined and concentrated under reduced pressure to give a brown solid material (1.6 kg), which was extracted using ethyl acetate. Next, this ethyl acetate fraction (950 g) was subjected to silica gel column chromatography (petroleum ether: Acetone 100: 0, 50: 1, 20: 1, 5: 1, and 0: 100) to obtain six fractions (Fr. 1-6). Among them, Fr. 2 (110 g) was eluted by silica gel column chromatography (petroleum ether: Acetone 50: 1–1: 50) to obtain 10 fractions. Among these, Fr. 2-10 were subjected to medium-pressure preparative chromatography (methanol: Water 30: 70-100: 0) gradient elution to obtain five fractions. Fr. 2-10-3-5 was then subjected to gel column chromatography (CH_2Cl_2/MeOH gradient elution system), silica gel column chromatography (petroleum ether/acetone gradient elution system), and preparative thin-layer chromatography (petroleum ether/acetone gradient elution system) to afford the compound PA (116.6 mg). The concentrations of PA and PAO in this study were determined based on previous publications[16,17] and our preliminary experiment.

Nuclear magnetic resonance (NMR) assay: DMSO-d6 was used to dissolve the compound PA. An NMR spectrometer (Bruker Corporation, Solna, Sweden) was used to record C-NMR (125 MHz) and H-NMR (500 MHz) spectra. All chemical shifts were reported in δ (ppm) relative to tetramethylsilane.

Cell culture and proliferation assay: Cells were cultured in McCoy's 5A (modified) medium containing 50 U/mL penicillin, 50 mg/mL streptomycin, and 10% FBS under conditions of 5% CO_2 at 37 ℃. The medium was replaced with serum-free medium 24 h before the different treatments.

The MTT method was used to detect cell proliferation. Cells (1×10^4) were seeded in a 96-well plate. After 12 h, the cells were treated with different concentrations of PA (5, 6.25, 7.5, 10, 12.5, 15, and 20 μg/mL equivalent to 10.59, 13.24, 15.89, 21.18, 26.48, 31.77, and 42.36 μM, respectively) or PAO (10, 20, 40, 60, 80, and 100 μM, respectively) medium with 0.1% DMSO. After different durations of incubation (24, 48, and 72 h), MTT reagents were used to incubate cells for 3 h. Then, the OD value was detected with an enzyme-linked immunosorbent assay reader (Thermo Fisher Scientific, United States) at a wavelength of 490 nm. The IC_{50} values and inhibition rate were calculated.

Hoechst 33342 staining: Cells (2×10^3/well) were seeded in a 24-well plate and cell slides were added in per well. After being synchronized, the cells were treated with the medium or PA for 24 and 48 h. The cells were then washed in phosphate buffer saline (PBS) three times, while Hoechst 33342 (10 μg/mL) was added to each well for 30 min. The cell slides were taken out, placed on a glass slide, and observed under a laser scanning confocal microscope.

Acridine orange/ethidium bromide (AO/EB) double staining: Cells (2×10^3/well) were seeded in a 24-well plate and cell slides were added in per well. After being synchronized, the cells were treated with the medium or PA for 24 and 48 h. The cells were washed in PBS three times, while 10 μL of AO/EB solution was added for incubation (5 min). Then, the cell slides were taken out and observed under a confocal microscope.

Cell apoptosis analysis: Cells (4×10^5/well) were seeded in a six-well plate. After the administration of drugs for 24 and 48 h, the cells were collected and washed with PBS three times. Annexin V-FITC and PI were used for staining, and the cells were analyzed with a FACS verse instrument (BD Biosciences, San Jose, CA, United States).

Cell cycle analysis: Cells (4×10^5/well) were seeded in a six-well plate. After the administration of drugs for 24 and 48 h, the cells were collected and washed with PBS three times. The cells were then fixed in ice-cold 70% ethanol overnight. They were then stained with 500 μL of a PI RNase solution for 15 min and analyzed by flow cytometry (FACS verse; BD Biosciences, United States). FlowJo version 10 software (BD Biosciences, United States) was used for cell phase analysis.

Scratch motility assay: Cells (4×10^5/well) were seeded in a six-well plate and cultured under conditions of 37 ℃ and 5% CO_2. A 10 μL sterilized pipette tip was then used to scrape the cell monolayer. The particular drug was added in the form of serum-free medium containing different drug concentrations, while the vehicle group was treated with 0.1% DMSO serum-free medium. The distance of cell movement was measured every 24 h until 48 h. The migration area was measured by ImageJ[18].

Reverse-transcription and real-time polymerase chain reaction (RT-PCR): HT-29 cells were exposed to the drugs for 48 h. TRIzol reagent was used for RNA extraction. Reverse-transcription PCR was performed using an RT-PCR Kit (TransGen Biotech, China). Real-time PCR was performed with TransStart® Top Green qPCR SuperMix (TransGen Biotech, China). The $2^{-\Delta\Delta t}$ method was used for gene expression analysis. The primers used are listed in Supplementary Table 1.

Western blotting: After the administration of drugs for 24 and 48 h, cell lysates were collected. Protein samples (30 μg) were separated by 10% SDS-PAGE and transferred to PVDF membranes. These PVDF membranes were incubated with related primary antibodies overnight. These membranes were then incubated with secondary antibodies for 4 h. An enhanced chemiluminescence kit (Transgen, Beijing, China) was used to detect immunolabeling. Grayscale values were measured using ImageJ.

Statistical analysis: All data are presented here as mean ± SD from at least three independent experiments. In the figures, data representative of the experiments are presented. The statistical significance of differences was assessed by one-way

analysis of variance. $P < 0.05$ was considered to reflect statistical significance.

RESULTS

PA and PAO suppressed HT-29 cell proliferation in vitro

To investigate the effects of PA and PAO on colon cancer cells, the MTT assay was performed. PA treatment at 6.25, 7.5, 10, 12.5, 15, and 20 μg/mL exerted significant inhibitory effects. IC_{50} values for the treatments lasting 24, 48, and 72 h were 9.7, 7.6, and 8.8 μg/mL, respectively (Figure 1A). Meanwhile, PAO treatments at 10, 20, 40, 60, 80, and 100 μM also exerted significant inhibitory effects in a concentration- and time-dependent manner ($P < 0.05$). Here the IC_{50} values for the treatments lasting 24, 48, and 72 h were 50.4 (79.4 μg/mL), 24.3 μM (38.3 μg/mL), and 11.96 μM (18.8 μg/mL), respectively (Figure 1B). Compared with that in the vehicle control group, the cell cycle distribution was changed and the cells were arrested at the G_0/G_1 phase in the groups treated with PA (Figure 1C and D) and PAO (Figure 1E and F) for 24 (Figure 1C and E) and 48 h (Figure 1D and F).

PA and PAO can induce apoptosis of HT-29 cells

After drug administration for 24 or 48 h, the cells were stained with Hoechst 33342. In this approach, live cells with an intact cellular structure could be distinguished from dead cells with an incomplete structure in which the nucleus was stained. The drug-administered group, especially the high-dose group and the positive group, showed more dead cells, as indicated in Figure 2A and B. Morphologically, the live cells were normal, with the nucleus being uniformly fluorescent green, while the early apoptotic cells were condensed into a hanging bead, with a green or yellow-green color or fragmented coloration. The late apoptotic cells were orange in color and the chromatin was concentrated. Meanwhile, the necrotic cells were round or elliptical, in which the nucleus was dyed orange, and the sizes were relatively small. Among PA-treated cells, there were increases in apoptotic cells compared with the rate of 2.67% in control cells to 12.07%, 14.14%, and 15.11% in groups treated with 7.5, 10, and 12.5 μg/mL for 24 h (Figure 2C) and from 4.36% to 7.02%-21.45% in groups treated with 7.5, 10, and 12.5 μg/mL for 48 h (Figure 2D). After PAO treatment, the apoptosis rate in the 80 μM and positive group was markedly higher than in the control group (Figure 2E).

PA and PAO reduced scratch healing

After the administration of drugs, the speed and extent of scratch healing in the drug group were lower than those in the vehicle group. A concentration of 12.5 μg/mL could significantly reduce the scratch healing rate ($P < 0.05$ and $P < 0.001$ at 24 and 48 h, respectively) (Figure 3A). There was no significant difference at 24 h, but the PAO concentrations of 60 and 80 μM significantly reduced the healing rate of scratches at 48 h ($P < 0.05$ and $P < 0.0001$, Figure 3B).

PA and PAO induced apoptosis via the autophagy pathway

To expand these findings, the mechanisms behind the anti-colon cancer effects of PA and PAO were explored further. More protein levels were determined. We found that the levels of Bax/Bcl2, cysteinyl aspartate specific proteinase (Caspase) 3, LC3II/I, Beclin1, and p62 proteins were markedly enhanced in HT-29 cells under PA or PAO treatment and the expression of JAK STAT3 or p-STAT3 was downregulated (Figure 4). Meanwhile, no effect on the expression of Beclin1 was noted in the PA or PAO group (Figure 5A). Notably, the mRNA expression of Caspase3 and LC3II/I was upregulated while p62 was downregulated after treatment with PA or PAO (Figure 5B-D). These results are basically consistent with the results of phenotypic research mentioned above.

DISCUSSION

Colon cancer has the highest morbidity and mortality among gastrointestinal tumors, making it a major threat to health and a particular focus for researchers[19]. Owing to the serious side effects of chemotherapy and the high cost of targeted drugs, patient compliance and overall survival are poor. Combination therapy with fluorouracil, oxaliplatin, and calcium folinate is a common method for treating colon cancer. However, severe side effects including gastrointestinal reactions, bone marrow suppression, liver damage, and individual differences in drug sensitivity limit its application[20]. Natural products with strong biological activity are optional drugs for clinical application. *A. satureioides*, an edible dual-use plant, has been used to cure a variety of diseases in Brazilian folk medicine. In this study, we searched for the active component, in the form of PA, from the plant for its anti-colon cancer effects, high safety, and strong medicinal properties. We also clarified its mechanism of action against colon cancer. PA has the particular advantage of having minimal side effects.

Our study showed that PA can inhibit HT-29 cell proliferation in a time- and dose-dependent manner and promote HT-29 cell apoptosis, as well as changing the distribution of HT-29 cells among the phases of the cell cycle. Specifically, HT-29 cells were arrested at the G_0/G_1 phase and their rate of migration was significantly reduced. The results also showed that, after the administration of PA or PAO, the levels of Bax/Bcl2, Caspase3, LC3II/I, Beclin1, and p62 in HT-29 cells were markedly elevated.

In the process of tumor development, apoptosis is usually downregulated. Therefore, reduced apoptosis is considered to be a sign of cancer[21-24]. Members of the Bcl2 family play key roles in regulating cell apoptosis[25]. Bax and Bak (known as multi-domain pro-apoptotic proteins) can promote apoptosis by forming oligomers on the mitochondrial

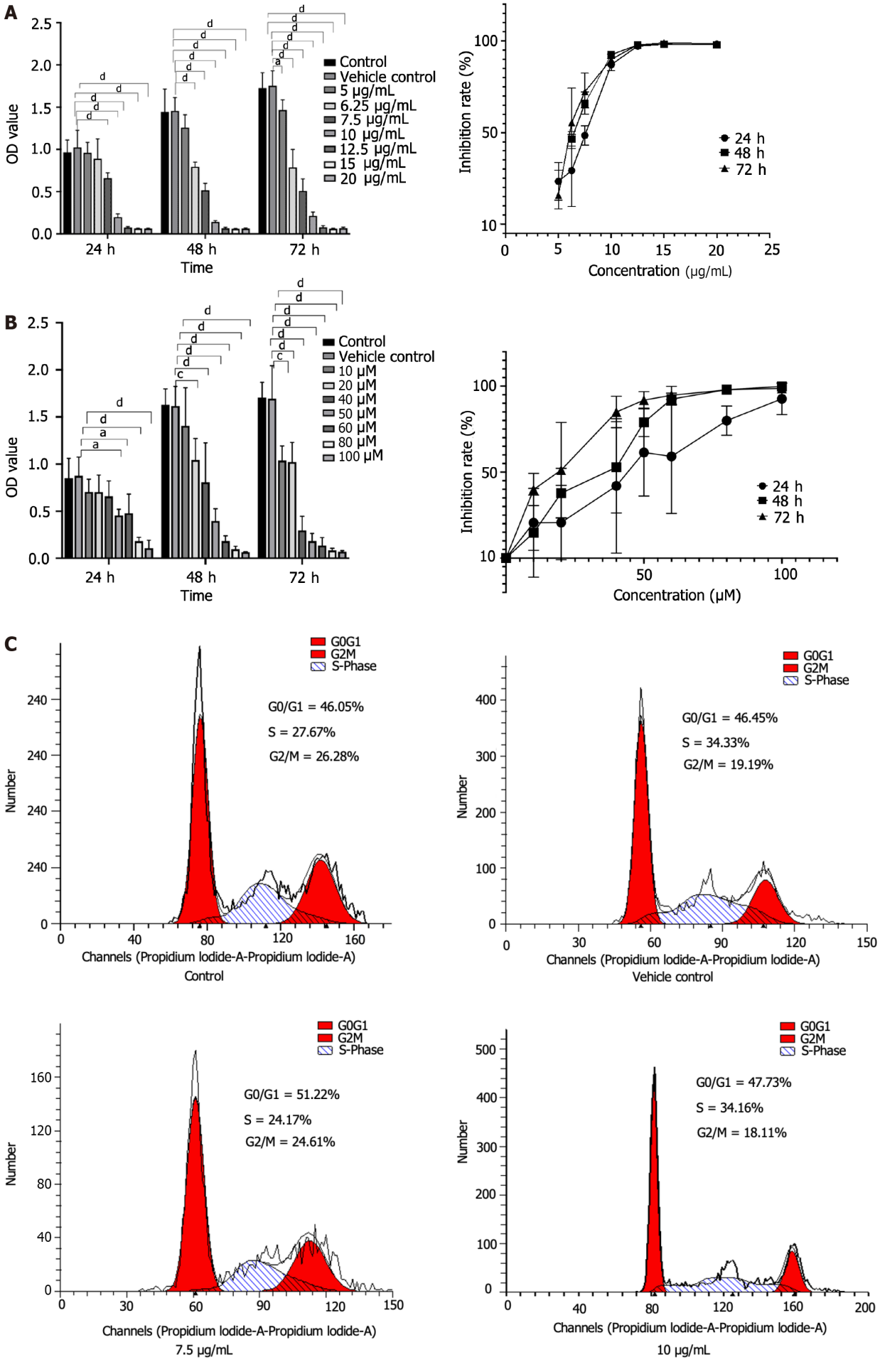
A
OD value
Time
24 h
48 h
72 h
Control
Vehicle control
5 μg/mL
6.25 μg/mL
7.5 μg/mL
10 μg/mL
12.5 μg/mL
15 μg/mL
20 μg/mL
Inhibition rate (%)
Concentration (μg/mL)
B
10 μM
20 μM
40 μM
50 μM
60 μM
80 μM
100 μM
Concentration (μM)
C
G0G1
G2M
S-Phase
G0/G1 = 46.05%
S = 27.67%
G2/M = 26.28%
Number
Channels (Propidium Iodide-A-Propidium Iodide-A)
Control
G0/G1 = 46.45%
S = 34.33%
G2/M = 19.19%
Vehicle control
G0/G1 = 51.22%
S = 24.17%
G2/M = 24.61%
7.5 μg/mL
G0/G1 = 47.73%
S = 34.16%
G2/M = 18.11%
10 μg/mL

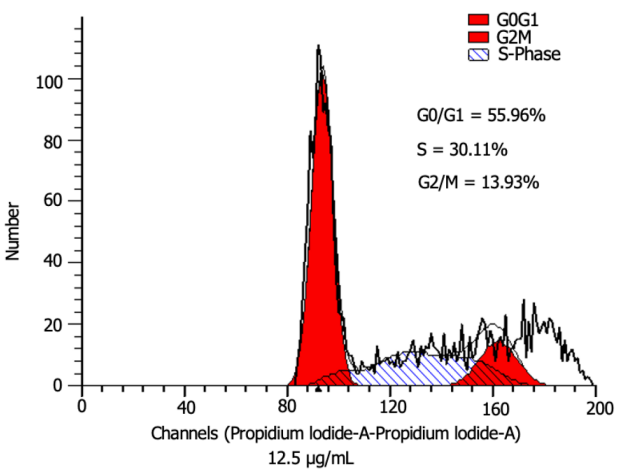
G0G1
G2M
S-Phase
G0/G1 = 55.96%
S = 30.11%
G2/M = 13.93%
Number
Channels (Propidium Iodide-A-Propidium Iodide-A)
12.5 μg/mL

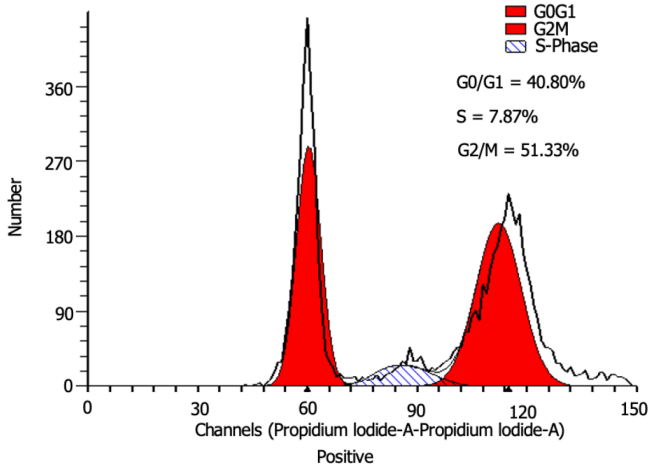
G0G1
G2M
S-Phase
G0/G1 = 40.80%
S = 7.87%
G2/M = 51.33%
Number
Channels (Propidium Iodide-A-Propidium Iodide-A)
Positive

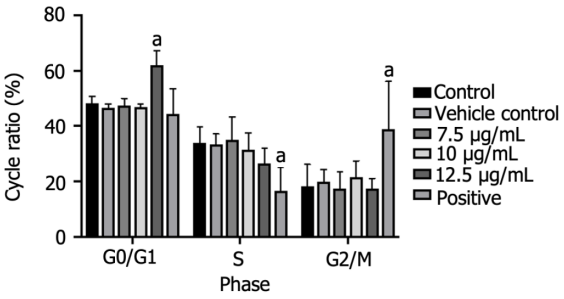
Cycle ratio (%)
G0/G1
S
G2/M
Phase
Control
Vehicle control
7.5 μg/mL
10 μg/mL
12.5 μg/mL
Positive

D

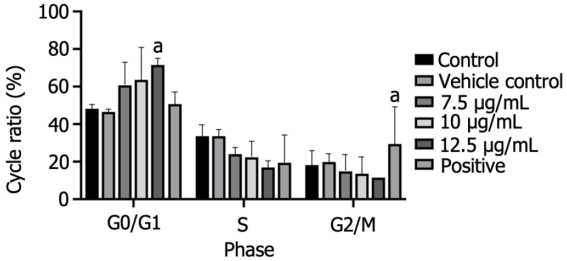
Cycle ratio (%)
G0/G1
S
G2/M
Phase
Control
Vehicle control
7.5 μg/mL
10 μg/mL
12.5 μg/mL
Positive

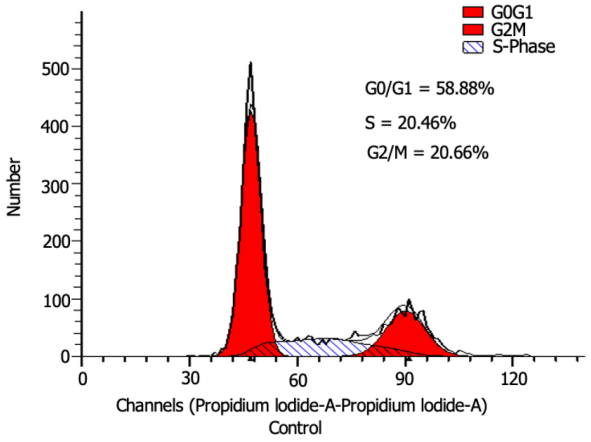
G0G1
G2M
S-Phase
G0/G1 = 58.88%
S = 20.46%
G2/M = 20.66%
Number
Channels (Propidium Iodide-A-Propidium Iodide-A)
Control

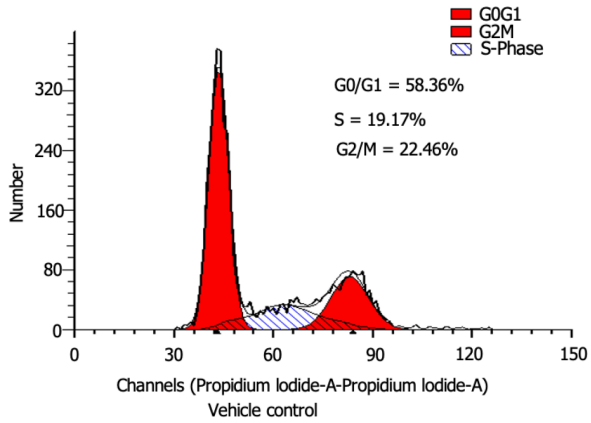
G0G1
G2M
S-Phase
G0/G1 = 58.36%
S = 19.17%
G2/M = 22.46%
Number
Channels (Propidium Iodide-A-Propidium Iodide-A)
Vehicle control

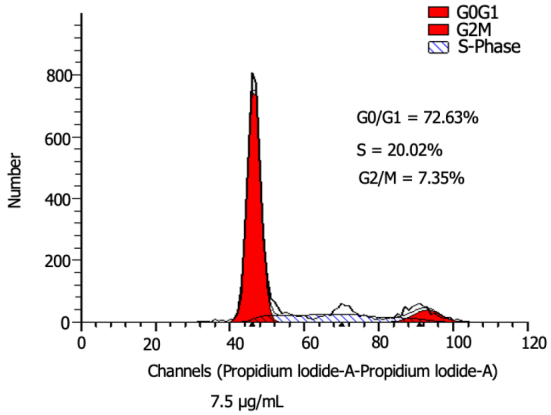
G0G1
G2M
S-Phase
G0/G1 = 72.63%
S = 20.02%
G2/M = 7.35%
Number
Channels (Propidium Iodide-A-Propidium Iodide-A)
7.5 μg/mL

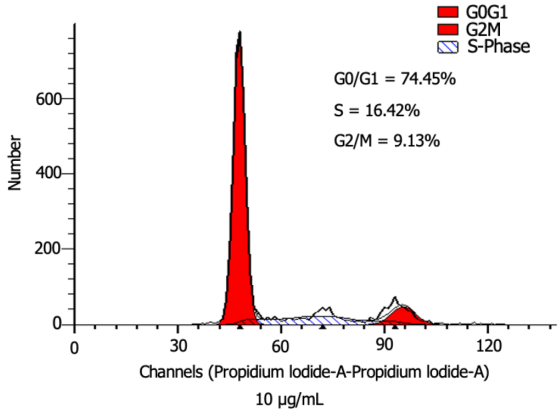
G0G1
G2M
S-Phase
G0/G1 = 74.45%
S = 16.42%
G2/M = 9.13%
Number
Channels (Propidium Iodide-A-Propidium Iodide-A)
10 μg/mL

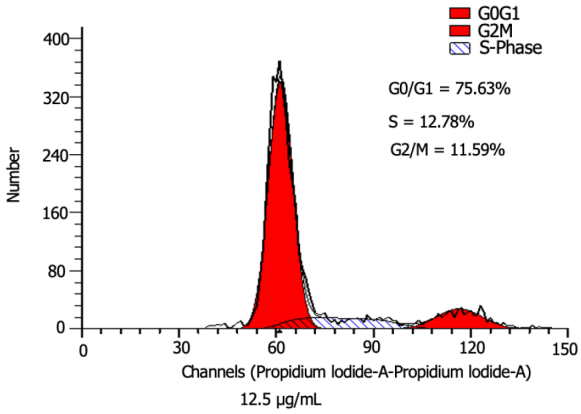
G0G1
G2M
S-Phase
G0/G1 = 75.63%
S = 12.78%
G2/M = 11.59%
Number
Channels (Propidium Iodide-A-Propidium Iodide-A)
12.5 μg/mL

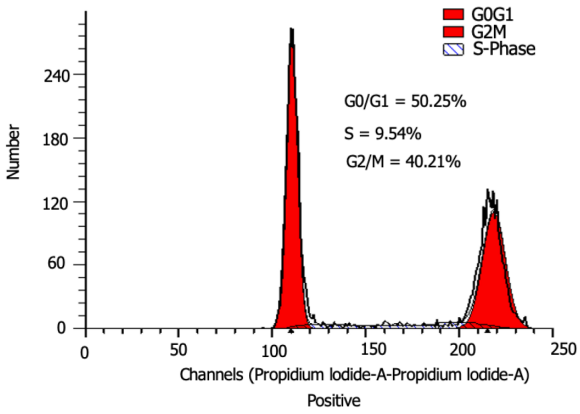
G0G1
G2M
S-Phase
G0/G1 = 50.25%
S = 9.54%
G2/M = 40.21%
Number
Channels (Propidium Iodide-A-Propidium Iodide-A)
Positive

E

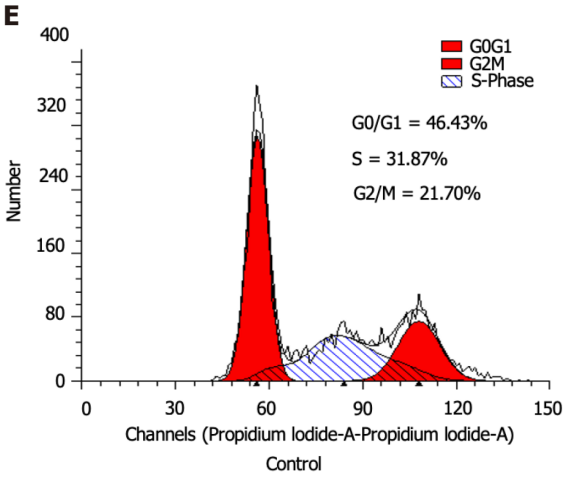
G0G1
G2M
S-Phase
G0/G1 = 46.43%
S = 31.87%
G2/M = 21.70%
Number
Channels (Propidium Iodide-A-Propidium Iodide-A)
Control

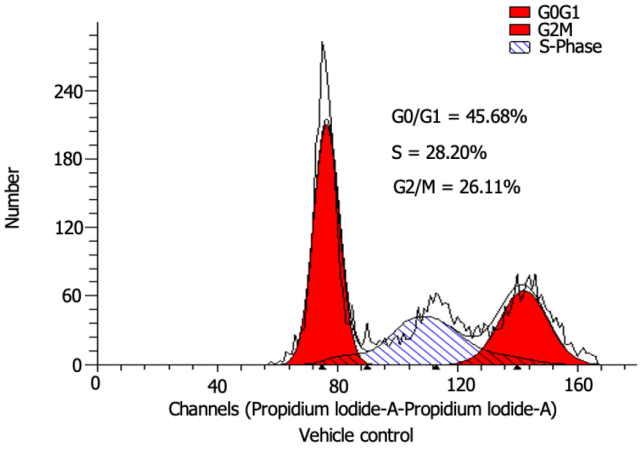
G0G1
G2M
S-Phase
G0/G1 = 45.68%
S = 28.20%
G2/M = 26.11%
Number
Channels (Propidium Iodide-A-Propidium Iodide-A)
Vehicle control

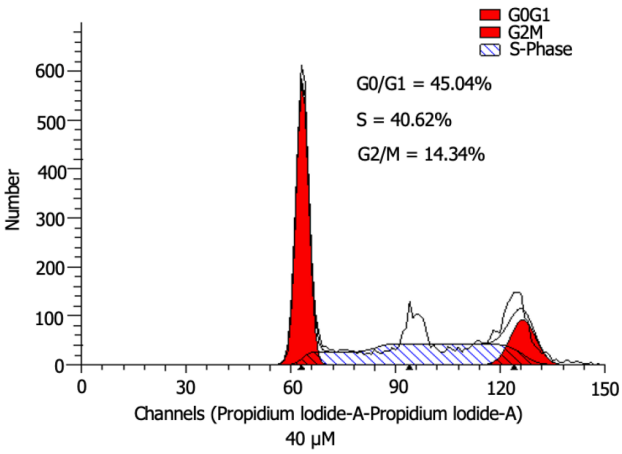
G0G1
G2M
S-Phase
G0/G1 = 45.04%
S = 40.62%
G2/M = 14.34%
Number
Channels (Propidium Iodide-A-Propidium Iodide-A)
40 μM

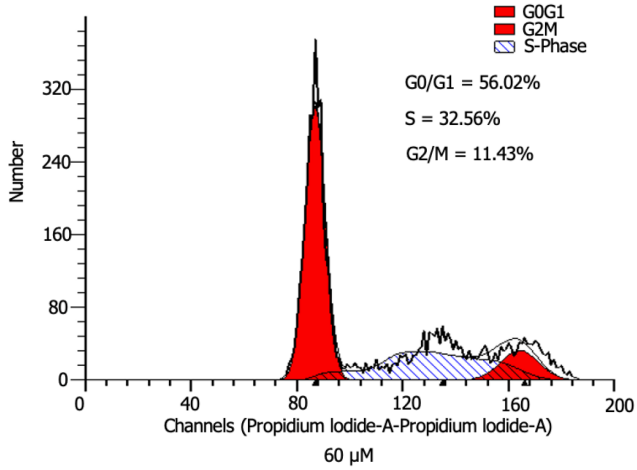
G0G1
G2M
S-Phase
G0/G1 = 56.02%
S = 32.56%
G2/M = 11.43%
Number
Channels (Propidium Iodide-A-Propidium Iodide-A)
60 μM

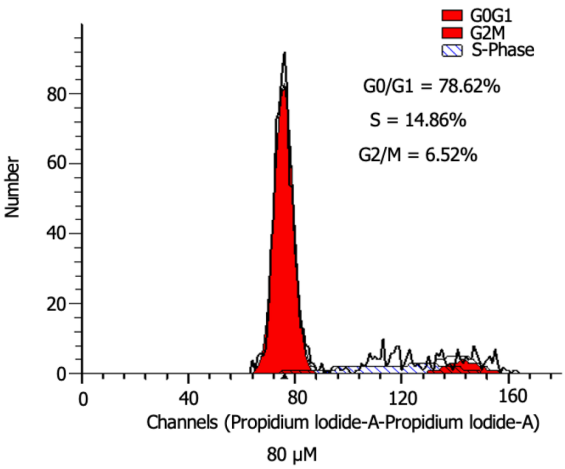
G0G1
G2M
S-Phase
G0/G1 = 78.62%
S = 14.86%
G2/M = 6.52%
Number
Channels (Propidium Iodide-A-Propidium Iodide-A)
80 μM

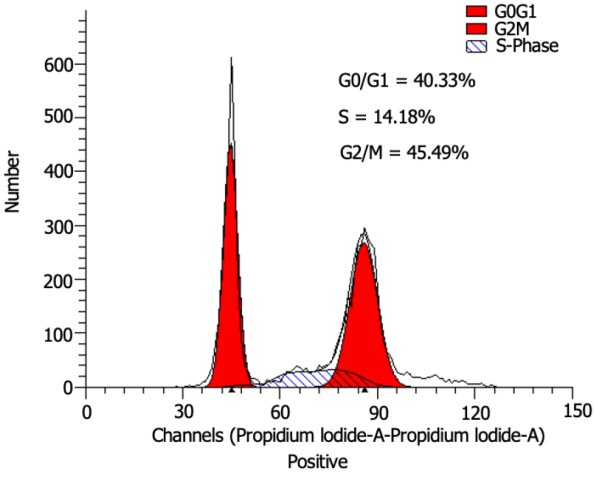
G0G1
G2M
S-Phase
G0/G1 = 40.33%
S = 14.18%
G2/M = 45.49%
Number
Channels (Propidium Iodide-A-Propidium Iodide-A)
Positive

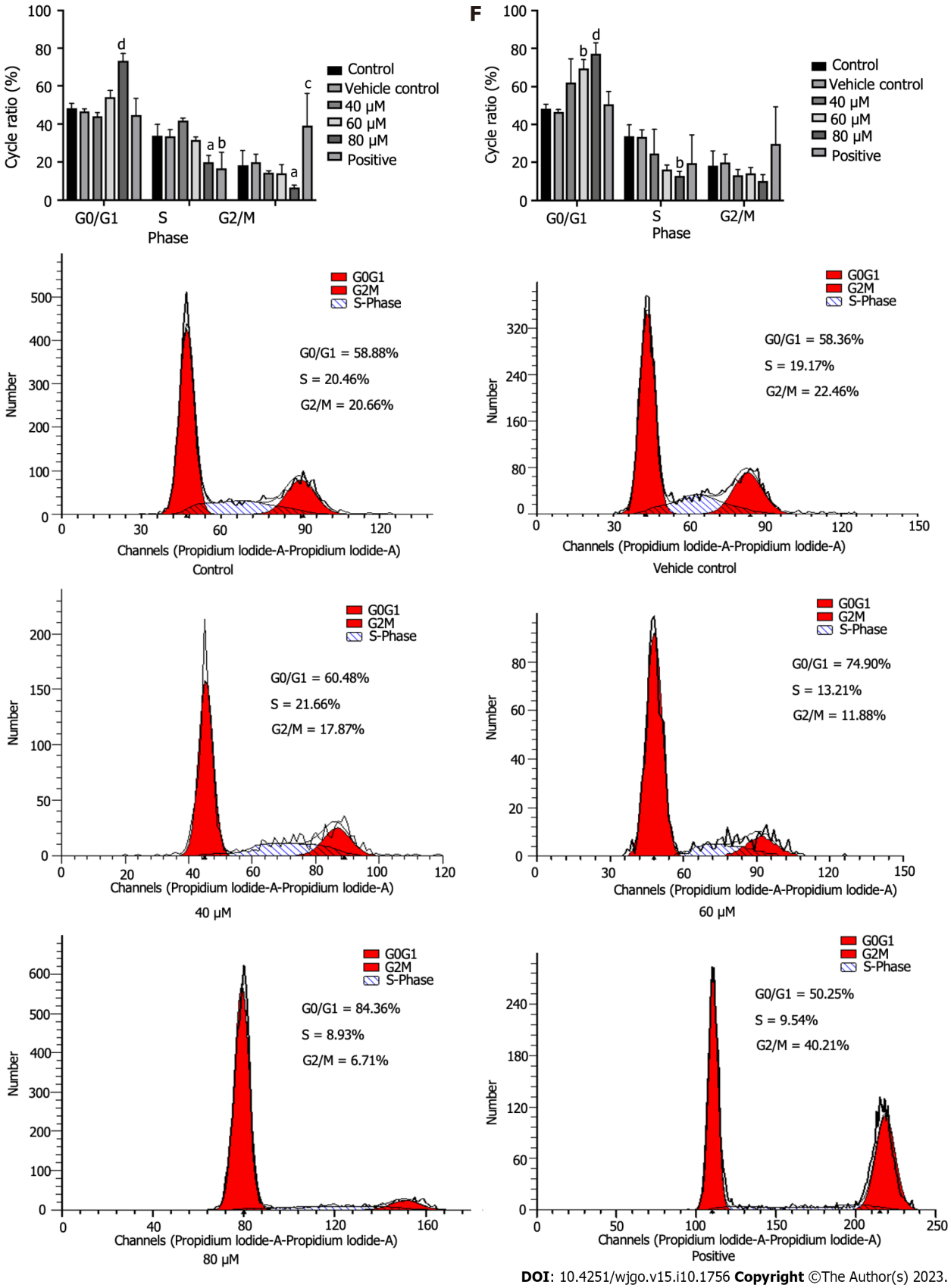

DOI: 10.4251/wjgo.v15.i10.1756

Figure 1 The effects of pomolic acid and pomolic acid-28-O-β-D-glucopyranosyl ester on proliferation of colon cancer cells. A: The proliferation of HT-29 cells after treatment with different concentrations of pomolic acid (PA) for 24, 48, and 72 h; B: The proliferation of HT-29 cells after treatment with different concentrations of pomolic acid-28-O-β-D-glucopyranosyl ester (PAO) for 24, 48, and 72 h; C: The cell cycle distribution of HT-29 cells after treatment with different concentrations of PA for 24 h; D: The cell cycle distribution of HT-29 cells after treatment with different concentrations of PA for 48 h; E: The cell cycle distribution of HT-29 cells after treatment with different concentrations of PAO for 24 h; F: The cell cycle distribution of HT-29 cells after treatment with different concentrations of PAO for 48 h. $^{a}P < 0.05$, $^{b}P < 0.01$, $^{c}P < 0.001$, $^{d}P < 0.0001$.

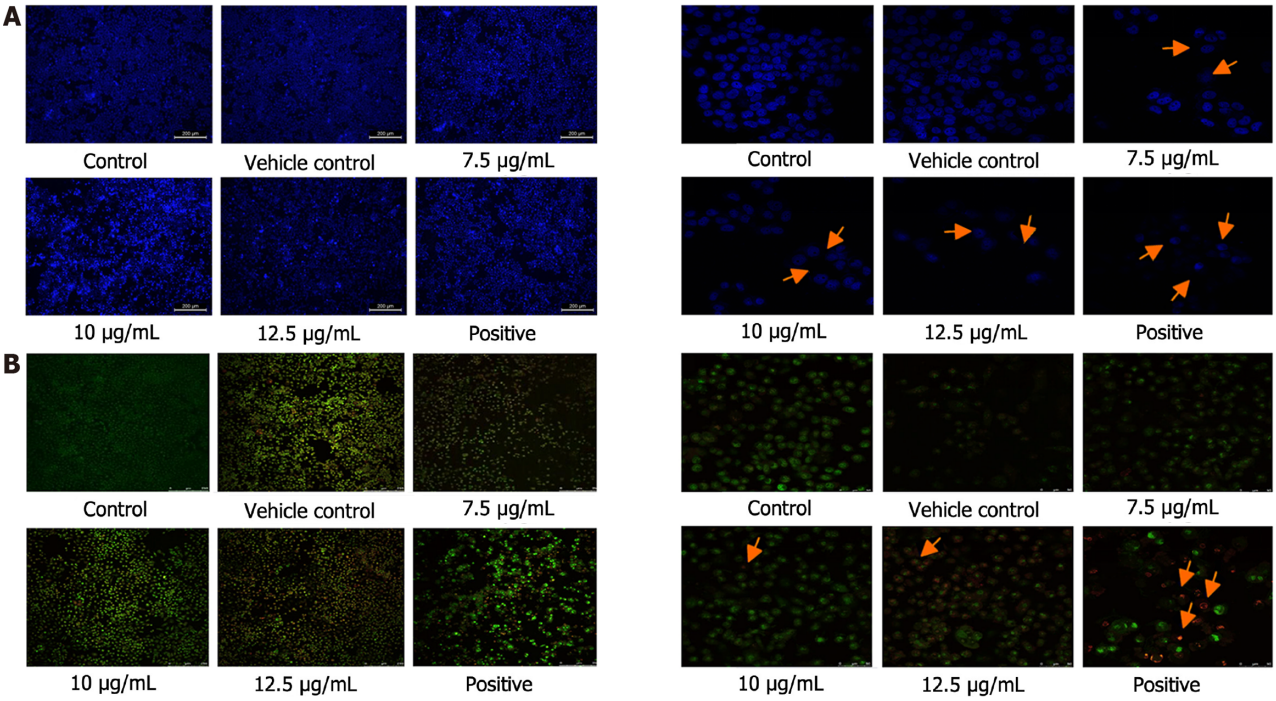
A
Control
Vehicle control
7.5 μg/mL
10 μg/mL
12.5 μg/mL
Positive
B
Control
Vehicle control
7.5 μg/mL
10 μg/mL
12.5 μg/mL
Positive

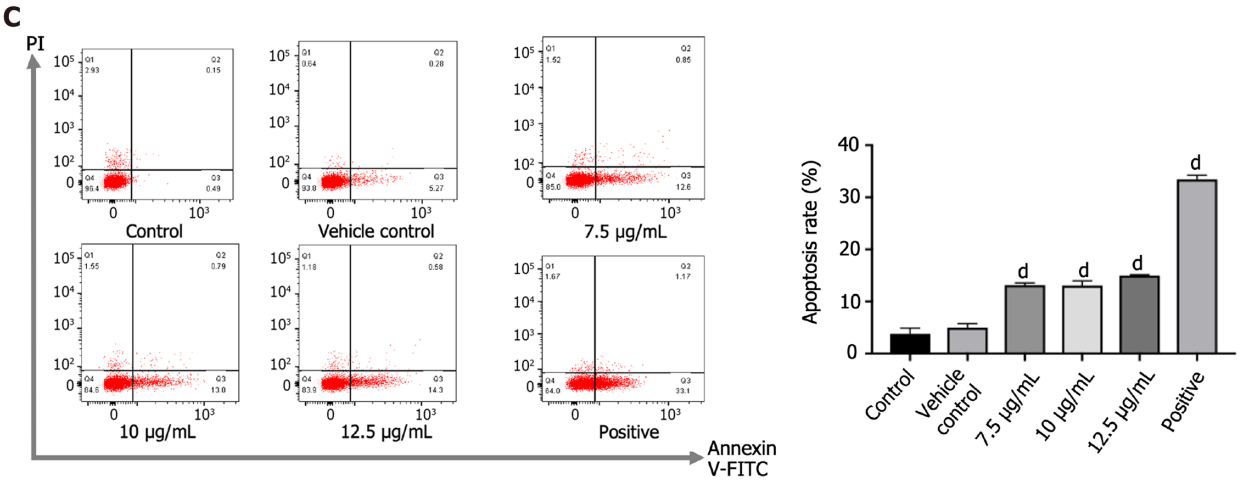
C
PI
Control
Vehicle control
7.5 μg/mL
10 μg/mL
12.5 μg/mL
Positive
Annexin V-FITC
Apoptosis rate (%)
Control
Vehicle control
7.5 μg/mL
10 μg/mL
12.5 μg/mL
Positive

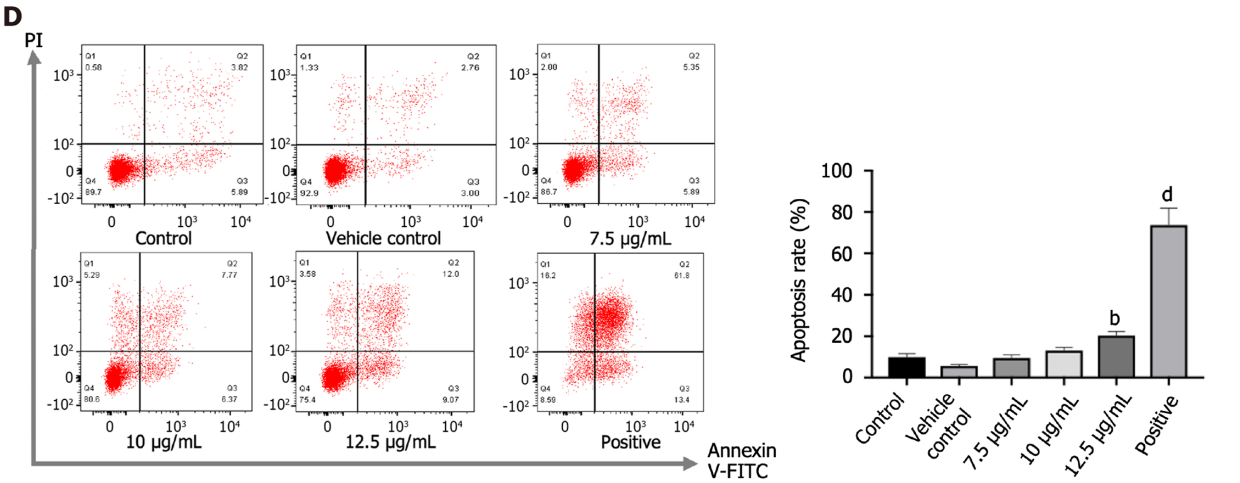
D
PI
Control
Vehicle control
7.5 μg/mL
10 μg/mL
12.5 μg/mL
Positive
Annexin V-FITC
Apoptosis rate (%)
Control
Vehicle control
7.5 μg/mL
10 μg/mL
12.5 μg/mL
Positive

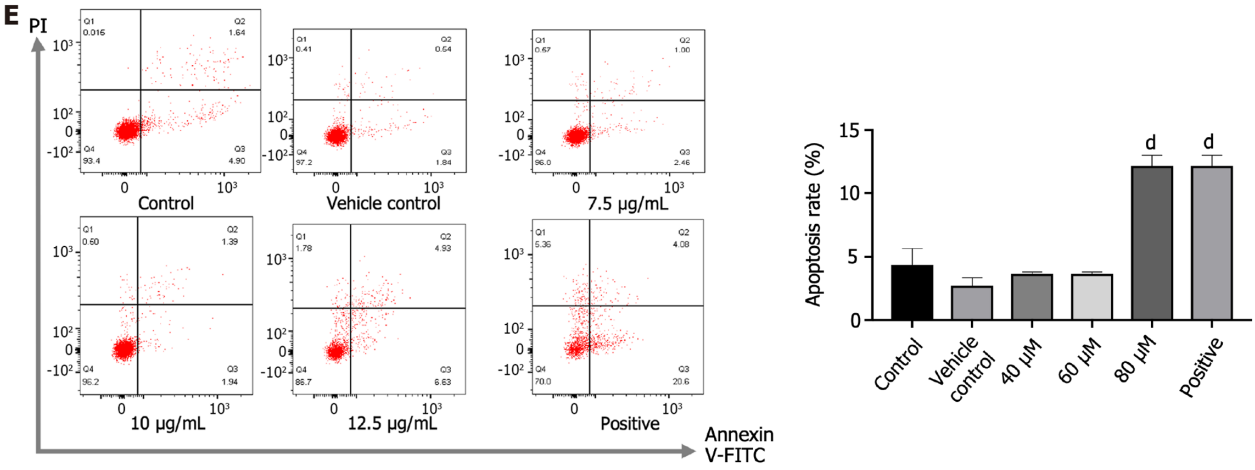

DOI: 10.4251/wjgo.v15.i10.1756 **Copyright** ©The Author(s) 2023.

Figure 2 Apoptosis of HT-29 cells after drug administration. A: HT-29 cells were stained with Hoechst 33342 and observed under an inverted fluorescence microscope (40 ×); B: HT-29 cells were stained with Hoechst 33342 and observed under an inverted fluorescence microscope (400 ×); C: Apoptosis of cells after treated with pomolic acid (PA) for 24 h; D: Apoptosis of cells after treated with PA for 48 h; E: Apoptosis of cells after treated with pomolic acid-28-O-β-D-glucopyranosyl ester for 48 h. $^{b}P < 0.01$, $^{d}P < 0.0001$.

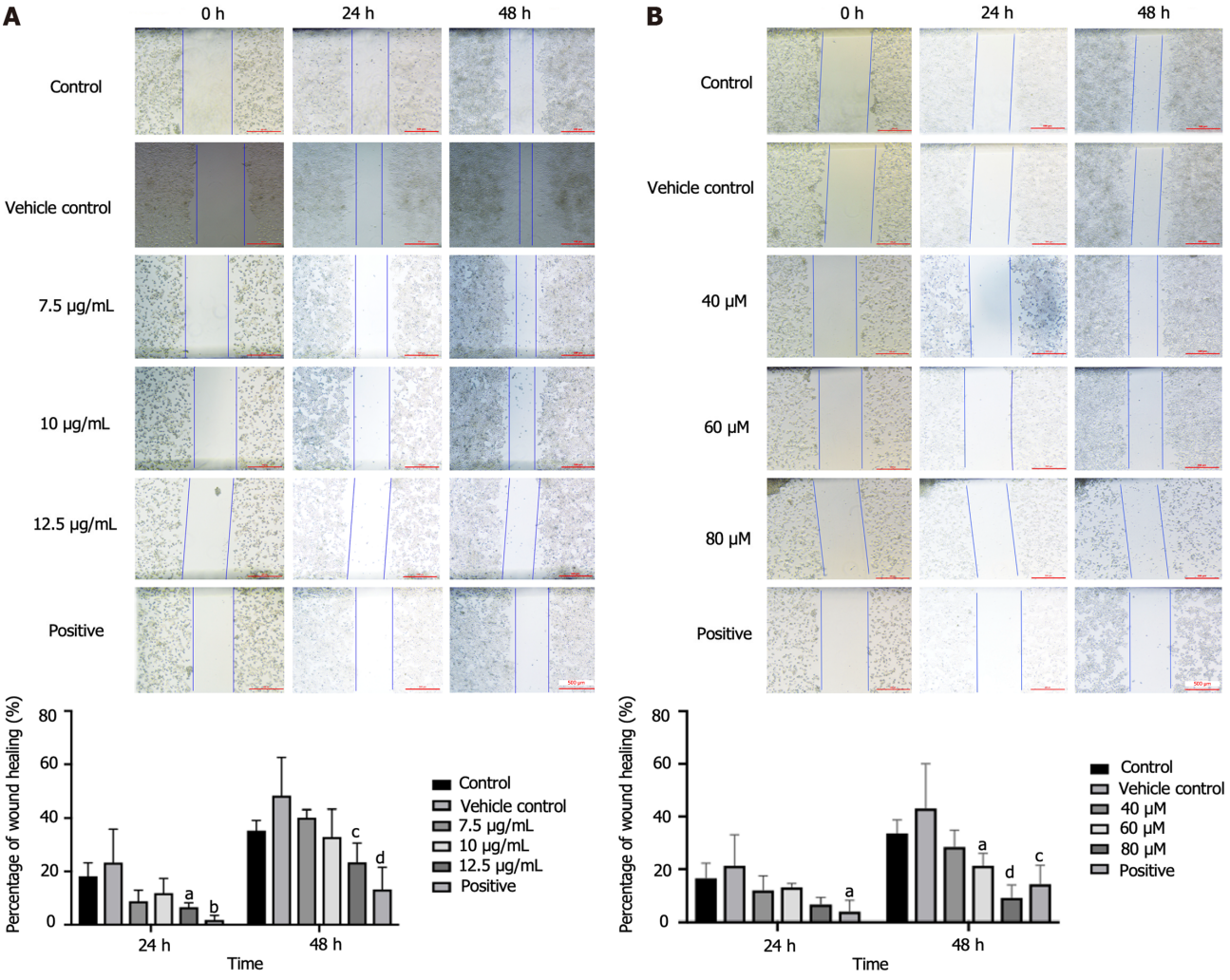

DOI: 10.4251/wjgo.v15.i10.1756 **Copyright** ©The Author(s) 2023.

Figure 3 Effects of pomolic acid and pomolic acid-28-O-β-D-glucopyranosyl ester on scratch assay in HT-29 cells. A: The speed and extent of scratch healing of cells after treated with different concentration of pomolic acid; B: The speed and extent of scratch healing of cells after treated with different concentration of pomolic acid-28-O-β-D-glucopyranosyl ester. $^{a}P < 0.05$, $^{b}P < 0.01$, $^{c}P < 0.001$, $^{d}P < 0.0001$.

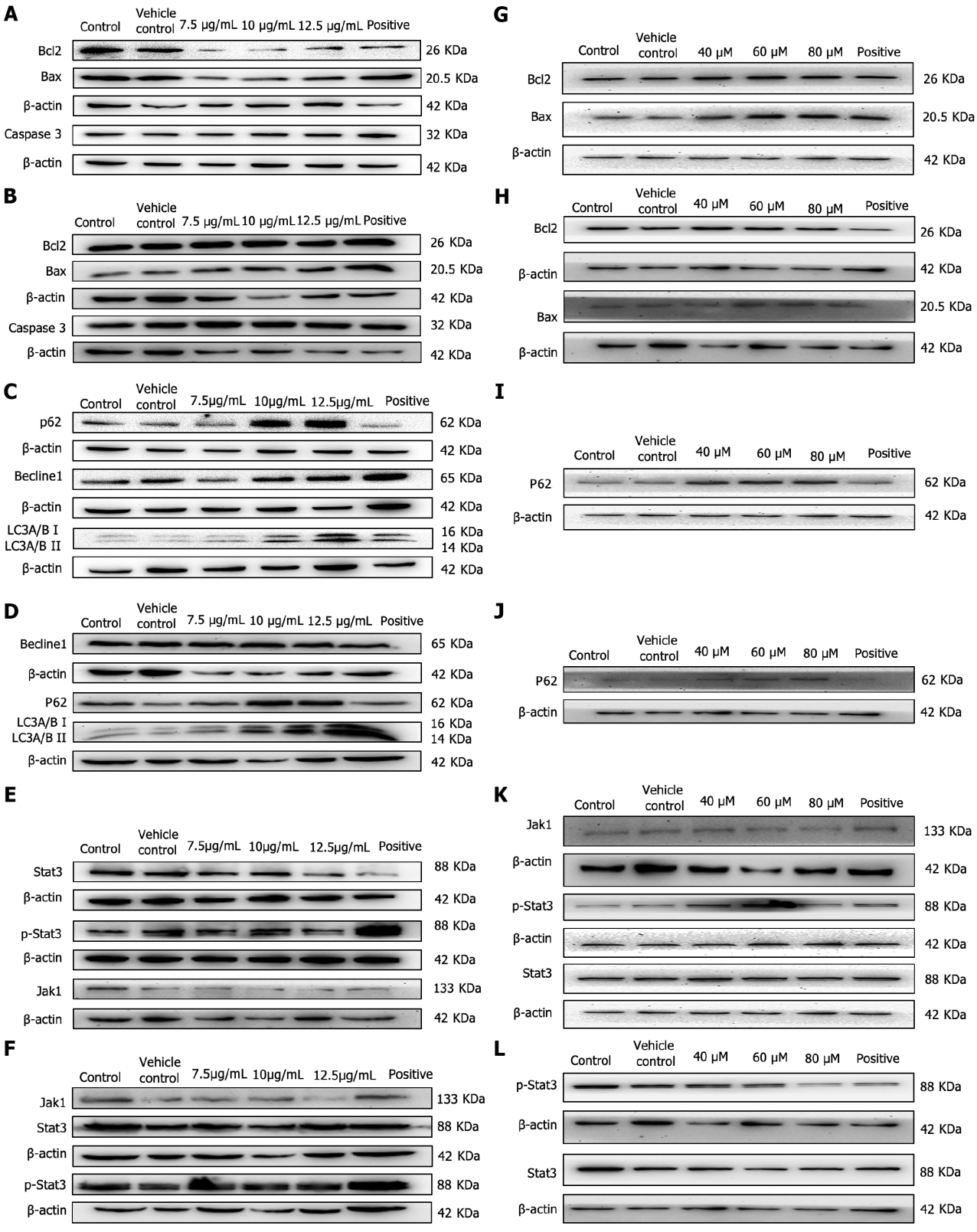

DOI: 10.4251/wjgo.v15.i10.1756

Figure 4 Effects of pomolic acid and pomolic acid-28-O-β-D-glucopyranosyl ester on the relative expression of proteins. A and B: The expression of apoptosis related protein in HT-29 cells treated with pomolic acid (PA) for 24 h and 48 h; C and D: The expression of autophagy related protein in HT-29 cells treated with PA for 24 h and 48 h; E and F: The expression of signal transducer and activator of transcription 3 (STAT3) and janus kinase (JAK) protein in HT-29 cells treated with PA for 24 h and 48 h; G and H: The expression of apoptosis related protein in HT-29 cells treated with pomolic acid-28-O-β-D-glucopyranosyl ester (PAO) for 24 h and 48 h; I and J: The expression of p62 protein in HT-29 cells treated with PAO for 24 h and 48 h; K: The expression of STAT3 and JAK1 protein in HT-29 cells treated with PAO for 24h; L: The expression of STAT3 protein in HT-29 cells treated with PAO for 48 h. Caspase: Cysteinyl aspartate specific proteinase; LC3: Light chain 3; STAT3: Signal transducer and activator of transcription 3; JAK: Janus kinase.

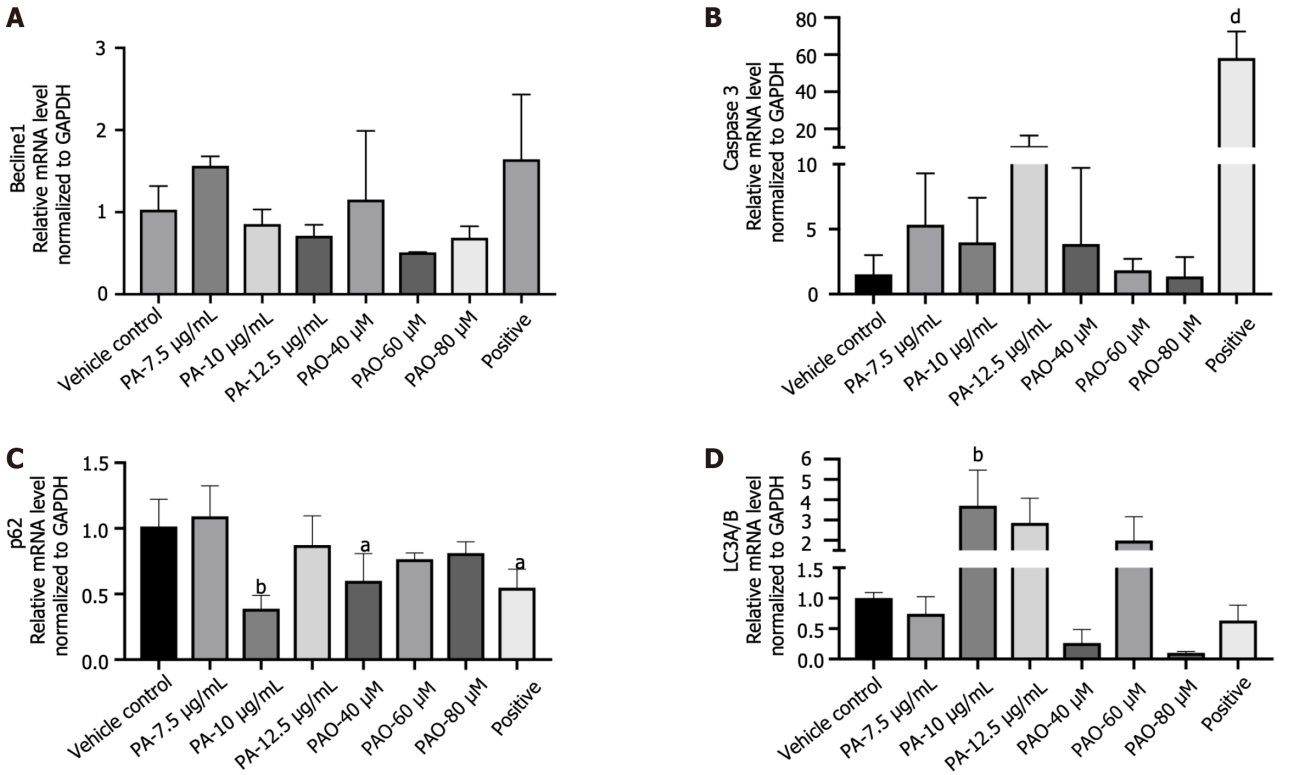

DOI: 10.4251/wjgo.v15.i10.1756

Figure 5 Effects of pomolic acid and pomolic acid-28-O-β-D-glucopyranosyl ester on the mRNA expression of Beclin1, cysteinyl aspartate specific proteinase 3, p62, and light chain 3A/B. A: mRNA expression of Beclin1; B: mRNA expression of cysteinyl aspartate specific proteinase 3; C: mRNA expression of light chain 3A/B; D: mRNA expression of p62. $^{a}P < 0.05$, $^{b}P < 0.01$, $^{d}P < 0.0001$. PA: Pomolic acid; PAO: Pomolic acid-28-O-β-D-glucopyranosyl ester; Caspase 3: Cysteinyl aspartate specific proteinase 3; LC3: Light chain 3.

membrane. There, they directly induce apoptosis after receiving the death signal, resulting in the release of cytochrome c, and apoptotic protease activator-activating factor 1 and Caspase activation[26]. Our research has shown that PA and PAO can significantly reduce the Bcl2/Bax ratio, which is basically consistent with the findings in the above literature.

In cancer, autophagy plays two roles of restricting the occurrence of tumors in the early stage but also promoting tumor development in cancers that have already become established. When autophagy is activated, LC3 is catalyzed and cleaved by the corresponding protease, so that the C-terminal glycine residue of LC3 is exposed to form LC3I, which is then processed by ubiquitination. This in turn upregulates autophagy. Beclin1 is a homolog of mammalian ATG6, which is encoded by the only confirmed mammalian "autophagy gene". It is an executor of autophagy and plays an important role in autophagy. It has been reported that Beclin1 monoallelic deletion can promote cancer development and progression[27]. Beclin1 can form a complex with type III phosphatidylinositol-3 kinase, which can recruit autophagy-related protein LC3 to regulate the maturation and formation of autophagosomes, leading to autophagy. Defects in autophagy can lead to the accumulation of p62, which is an autophagy substrate protein and also a ubiquitin-binding protein. The sustained expression of p62 can change the regulatory expression of NF-κB and promote tumorigenesis[28-30]. The involvement of Bcl2 in the process of autophagy is mainly related to Beclin 1, which binds to and is inhibited by Bcl-2 or the Bcl-2 homolog Bcl-XL under physiological conditions. Our study showed that PA significantly increased the LC3II/I ratio and upregulated Beclin1. Interestingly, our experimental results revealed that PA can increase the level of p62 protein after PA administration for 24 and 48 h, but the positive drugs showed a decrease. This might be linked to the fact that, in addition to acting as a marker of autophagy activation, p62 can also serve as an important bridge for Caspase8-dependent cell activation, promoting the accumulation of Caspase8 and leading to apoptosis[31,32]. Our study showed that, after PA or PAO treatment, the level of Bcl2 decreased while the level of Beclin1 increased, which may have resulted in autophagy activation.

CONCLUSION

PA can promote the apoptosis of colon cancer cells, possibly through upregulating the expression of LC3II/I and Beclin1 and then activating autophagy, while upregulating the expression of p62, Bax/Bcl2, and Caspase3. These results indicate the PA is a potential anticancer agent.

ARTICLE HIGHLIGHTS

Research background

Colon cancer remains as a high death leading cause in the world. Pomolic acid (PA) is separated from the ethyl acetate fraction of achyrocline satureioides.

Research motivation

We want to explore a novel, safe, effective agent for the treatment of colon cancer.

Research objectives

We aimed to examine the effects of PA and its glucopyranose ester, pomolic acid-28-O-β-D-glucopyranosyl ester (PAO) on colon cancer HT-29 cells.

Research methods

3-(4, 5-dimethylthiazol-2-yl)-2, 5-diphenyl tetrazolium bromide assay was used to measure cell viability. Apoptosis was detected *via* Hoechst 33342 Staining. PI single staining by flow cytometry was determine the cycle and scratch assay was used to observe the migration of HT-29 cells. The levels of mRNA and proteins were evaluated with the q-polymerase chain reaction and western blot assay, respectively.

Research results

Compounds PA and PAO exhibited a considerable growth inhibitory effect against HT-29 cell lines in a time-dose-dependent manner. After administration of drugs for 24h and 48h, it showed that PA and PAO could significantly promote the cell apoptosis, and arrested HT-29 cells at G_0/G_1 stage; the ratio of Bax/Bcl2 was increased and activated the cysteinyl aspartate specific proteinase 3 which leading to an apoptosis, and the expression of anti-light chain 3 II/I and Beclin1 activate autophagy and cause cell death, increasing the expression of p62 promotes a cell apoptosis, inhibiting the level of signal transducer and activator of transcription 3 (STAT3) and p-STAT3 can suppress the level of Bcl2 and promote cell.

Research conclusions

Both PA and PAO provide novel therapeutic strategy for colorectal cancers treatment.

Research perspectives

The inhibitions of colon cancer by PA and PAO were validated with HT-29 cells.

ACKNOWLEDGEMENTS

The authors thank Professor Peng HS from Anhui University of Chinese Medicine for identifying achyrocline satureioides.

FOOTNOTES

Author contributions: Liu LY, Liao TS, Wang Y, and Yu TH were responsible for the design, data collection, data management, and statistical analysis; Liu LY, Yu TH, and Shi M contributed to the writing of the manuscript; Xu P and Li B contributed to supervising data collection, improved the manuscript, and were responsible for supervision or mentorship; Liu LY and Li B were responsible for the research idea and interpretation of the results; All authors reviewed and approved the final version of the manuscript.

Supported by Central Level Major Increase and Decrease Expenditures Project, No. 2060302-2101-11, No. 2060302-1701-01; Workstation Project, No. YSGZZ201801; Open Fund for Scientific Research of Jiangxi Cancer Hospital, No. 2021J16; Distinguished Young Scholars Fund of Jiangxi Cancer Hospital, No. 2021DYS04; Jiangxi Provincial Natural Science Foundation, No. 20212BAB216063; National Natural Science Foundation of China, No. 82160565.

Conflict-of-interest statement: The authors declare that they have no competing interests.

Data sharing statement: No additional data are available.

Country/Territory of origin: China

ORCID number: Bin Li 0009-0003-6010-6720.

S-Editor: Qu XL
L-Editor: A
P-Editor: Zhang XD

REFERENCES

1 **Siegel RL**, Miller KD, Jemal A. Cancer statistics, 2020. *CA Cancer J Clin* 2020; **70**: 7-30 [PMID: 31912902 DOI: 10.3322/caac.21590]
2 **Bray F**, Ferlay J, Soerjomataram I, Siegel RL, Torre LA, Jemal A. Global cancer statistics 2018: GLOBOCAN estimates of incidence and mortality worldwide for 36 cancers in 185 countries. *CA Cancer J Clin* 2018; **68**: 394-424 [PMID: 30207593 DOI: 10.3322/caac.21492]
3 **Retta D**, Dellacassa E, Villamil J, Suárez SA, Bandoni AL. Marcela, a promising medicinal and aromatic plant from Latin America: A review. *Industrial Crops & Products* 2012; **38**: 27-38 [DOI: 10.1016/j.indcrop.2012.01.006]
4 **Pereira CG**, Gualtieri IP, Meireles MAA. Effect of Different Extraction Processes on the Recovery of Extracts from Achyrocline satureioides D.C.: An Evaluation of Antioxidant Activity. *Separation Science & Technology* 2008; **43**: 1549-1563 [DOI: 10.1080/01496390801955562]
5 **Puhlmann J**, Knaus U, Tubaro L, Schaefer W, Wagner H. Immunologically active metallic ion-containing polysaccharides of Achyrocline satureioides. *Phytochemistry* 1992; **31**: 2617-2621 [PMID: 1368417 DOI: 10.1016/0031-9422(92)83597-r]
6 **Sabini MC**, Escobar FM, Tonn CE, Zanon SM, Contigiani MS, Sabini LI. Evaluation of antiviral activity of aqueous extracts from Achyrocline satureioides against Western equine encephalitis virus. *Nat Prod Res* 2012; **26**: 405-415 [PMID: 20623427 DOI: 10.1080/14786419.2010.490216]
7 **Baldissera MD**, Oliveira CB, Rech VC, Rezer JF, Sagrillo MR, Alves MP, da Silva AP, Leal DB, Boligon AA, Athayde ML, Da Silva AS, Mendes RE, Monteiro SG. Treatment with essential oil of Achyrocline satureioides in rats infected with Trypanosoma evansi: relationship between protective effect and tissue damage. *Pathol Res Pract* 2014; **210**: 1068-1074 [PMID: 25017420 DOI: 10.1016/j.prp.2014.06.008]
8 **Kim B**, Kim JH, Park B. Pomolic acid inhibits invasion of breast cancer cells through the suppression of CXC chemokine receptor type 4 expression. *J Cell Biochem* 2016; **117**: 1296-1307 [PMID: 27870282 DOI: 10.1002/jcb.25730]
9 **Kim B**, Kim YC, Park B. Pomolic acid inhibits metastasis of HER2 overexpressing breast cancer cells through inactivation of the ERK pathway. *Int J Oncol* 2016; **49**: 744-752 [PMID: 27277173 DOI: 10.3892/ijo.2016.3568]
10 **Park JH**, Yoon J, Park B. Pomolic acid suppresses HIF1α/VEGF-mediated angiogenesis by targeting p38-MAPK and mTOR signaling cascades. *Phytomedicine* 2016; **23**: 1716-1726 [PMID: 27912873 DOI: 10.1016/j.phymed.2016.10.010]
11 **Martins CA**, Rocha GDG, Gattass CR, Takiya CM. Pomolic acid exhibits anticancer potential against a docetaxel-resistant PC3 prostate cell line. *Oncol Rep* 2019; **42**: 328-338 [PMID: 31002376 DOI: 10.3892/or.2019.7132]
12 **Pereira MXG**, Hammes ASO, Vasconcelos FC, Pozzo AR, Pereira TH, Caffarena ER, Gattass CR, Maia RC. Antitumor Effect of Pomolic Acid in Acute Myeloid Leukemia Cells Involves Cell Death, Decreased Cell Growth and Topoisomerases Inhibition. *Anticancer Agents Med Chem* 2018; **18**: 1457-1468 [PMID: 29651965 DOI: 10.2174/1871520618666180412120128]
13 **Kuete V**, Sandjo LP, Seukep JA, Zeino M, Mbaveng AT, Ngadjui B, Efferth T. Cytotoxic compounds from the fruits of Uapaca togoensis towards multifactorial drug-resistant cancer cells. *Planta Med* 2015; **81**: 32-38 [PMID: 25473921 DOI: 10.1055/s-0034-1383362]
14 **Fernandes J**, Weinlich R, Castilho RO, Kaplan MA, Amarante-Mendes GP, Gattass CR. Pomolic acid triggers mitochondria-dependent apoptotic cell death in leukemia cell line. *Cancer Lett* 2005; **219**: 49-55 [PMID: 15694664 DOI: 10.1016/j.canlet.2004.09.001]
15 **Vasconcelos FC**, Gattass CR, Rumjanek VM, Maia RC. Pomolic acid-induced apoptosis in cells from patients with chronic myeloid leukemia exhibiting different drug resistance profile. *Invest New Drugs* 2007; **25**: 525-533 [PMID: 17520174 DOI: 10.1007/s10637-007-9064-5]
16 **Guimarães LPTP**, Rocha GDG, Queiroz RM, Martins CA, Takiya CM, Gattass CR. Pomolic acid induces apoptosis and inhibits multidrug resistance protein MRP1 and migration in glioblastoma cells. *Oncol Rep* 2017; **38**: 2525-2534 [PMID: 28849227 DOI: 10.3892/or.2017.5895]
17 Martins CA, Rocha GDG, Gattass CR, Takiya CM. Pomolic acid exhibits anticancer potential against a docetaxelresistant PC3 prostate cell line. Oncol Rep 2019; 42: 328-338 [PMID: 31002376 DOI: 10.3892/or.2019.7132]
18 **Chung DJ**, Wang CJ, Yeh CW, Tseng TH. Inhibition of the Proliferation and Invasion of C6 Glioma Cells by Tricin *via* the Upregulation of Focal-Adhesion-Kinase-Targeting MicroRNA-7. *J Agric Food Chem* 2018; **66**: 6708-6716 [PMID: 29877083 DOI: 10.1021/acs.jafc.8b00604]
19 **Siegel RL**, Miller KD, Jemal A. Cancer statistics, 2019. *CA Cancer J Clin* 2019; **69**: 7-34 [PMID: 30620402 DOI: 10.3322/caac.21551]
20 **Gosavi R**, Chia C, Michael M, Heriot AG, Warrier SK, Kong JC. Neoadjuvant chemotherapy in locally advanced colon cancer: a systematic review and meta-analysis. *Int J Colorectal Dis* 2021; **36**: 2063-2070 [PMID: 33945007 DOI: 10.1007/s00384-021-03945-3]
21 **Dai H**, Meng WX, Kaufmann SH. BCL2 Family, Mitochondrial Apoptosis, and Beyond. *Cancer Transl Med* 2016; **2** [DOI: 10.4103/2395-3977.177558]
22 **Thandapani P**, Aifantis I. Apoptosis, Up the Ante. *Cancer Cell* 2017; **32**: 402-403 [PMID: 29017053 DOI: 10.1016/j.ccell.2017.09.009]
23 **Pullarkat VA**, Newman EM. BCL2 Inhibition by Venetoclax: Targeting the Achilles' Heel of the Acute Myeloid Leukemia Stem Cell? *Cancer Discov* 2016; **6**: 1082-1083 [PMID: 27698099 DOI: 10.1158/2159-8290.cd-16-0921]
24 **Hata AN**, Engelman JA, Faber AC. The BCL2 Family: Key Mediators of the Apoptotic Response to Targeted Anticancer Therapeutics. *Cancer Discov* 2015; **5**: 475-487 [PMID: 25895919 DOI: 10.1158/2159-8290.CD-15-0011]
25 **Fesik SW**. Promoting apoptosis as a strategy for cancer drug discovery. *Nat Rev Cancer* 2005; **5**: 876-885 [PMID: 16239906 DOI: 10.1038/nrc1736]
26 **Wei MC**, Zong WX, Cheng EH, Lindsten T, Panoutsakopoulou V, Ross AJ, Roth KA, MacGregor GR, Thompson CB, Korsmeyer SJ. Proapoptotic BAX and BAK: a requisite gateway to mitochondrial dysfunction and death. *Science* 2001; **292**: 727-730 [PMID: 11326099 DOI: 10.1126/science.1059108]
27 **Peng Y**, Miao H, Wu S, Yang W, Zhang Y, Xie G, Xie X, Li J, Shi C, Ye L, Sun W, Wang L, Liang H, Ou J. ABHD5 interacts with BECN1 to regulate autophagy and tumorigenesis of colon cancer independent of PNPLA2. *Autophagy* 2016; **12**: 2167-2182 [PMID: 27559856 DOI: 10.1080/15548627.2016.1217380]
28 **Pankiv S**, Clausen TH, Lamark T, Brech A, Bruun JA, Outzen H, Øvervatn A, Bjørkøy G, Johansen T. p62/SQSTM1 binds directly to Atg8/

LC3 to facilitate degradation of ubiquitinated protein aggregates by autophagy. *J Biol Chem* 2007; **282**: 24131-24145 [PMID: 17580304 DOI: 10.1074/jbc.m702824200]

29 **Mathew R**, Karp CM, Beaudoin B, Vuong N, Chen G, Chen HY, Bray K, Reddy A, Bhanot G, Gelinas C, Dipaola RS, Karantza-Wadsworth V, White E. Autophagy suppresses tumorigenesis through elimination of p62. *Cell* 2009; **137**: 1062-1075 [PMID: 19524509 DOI: 10.1016/j.cell.2009.03.048]

30 **Ichimura Y**, Kumanomidou T, Sou YS, Mizushima T, Ezaki J, Ueno T, Kominami E, Yamane T, Tanaka K, Komatsu M. Structural basis for sorting mechanism of p62 in selective autophagy. *J Biol Chem* 2008; **283**: 22847-22857 [PMID: 18524774 DOI: 10.1074/jbc.M802182200]

31 **Zhang YB**, Gong JL, Xing TY, Zheng SP, Ding W. Autophagy protein p62/SQSTM1 is involved in HAMLET-induced cell death by modulating apotosis in U87MG cells. *Cell Death Dis* 2013; **4**: e550 [PMID: 23519119 DOI: 10.1038/cddis.2013.77]

32 **Jin Z**, Li Y, Pitti R, Lawrence D, Pham VC, Lill JR, Ashkenazi A. Cullin3-based polyubiquitination and p62-dependent aggregation of caspase-8 mediate extrinsic apoptosis signaling. *Cell* 2009; **137**: 721-735 [PMID: 19427028 DOI: 10.1016/j.cell.2009.03.015]

World Journal of Gastrointestinal Oncology

Submit a Manuscript: https://www.f6publishing.com

World J Gastrointest Oncol 2023 October 15; 15(10): 1771-1783

DOI: 10.4251/wjgo.v15.i10.1771

ISSN 1948-5204 (online)

ORIGINAL ARTICLE

Retrospective Cohort Study

Modified albumin-bilirubin predicted survival of unresectable hepatocellular carcinoma patients treated with immunotherapy

Huttakan Navadurong, Thaninee Prasoppokakorn, Nanicha Siriwong, Chonlada Phathong, Nattaya Teeyapun, Suebpong Tanasanvimon, Kessarin Thanapirom, Piyawat Komolmit, Pisit Tangkijvanich, Sombat Treeprasertsuk, Roongruedee Chaiteerakij

Specialty type: Oncology

Provenance and peer review: Unsolicited article; Externally peer reviewed.

Peer-review model: Single blind

Peer-review report's scientific quality classification

Grade A (Excellent): 0
Grade B (Very good): 0
Grade C (Good): C, C, C
Grade D (Fair): 0
Grade E (Poor): 0

P-Reviewer: Bi JF, China; Liang HL, Taiwan; Maher H, China

Received: March 12, 2023
Peer-review started: March 12, 2023
First decision: April 19, 2023
Revised: July 1, 2023
Accepted: August 15, 2023
Article in press: August 15, 2023
Published online: October 15, 2023

Huttakan Navadurong, Thaninee Prasoppokakorn, Nanicha Siriwong, Chonlada Phathong, Kessarin Thanapirom, Piyawat Komolmit, Sombat Treeprasertsuk, Roongruedee Chaiteerakij, Department of Medicine, Division of Gastroenterology, Faculty of Medicine, Chulalongkorn University, Bangkok 10330, Thailand

Huttakan Navadurong, Thaninee Prasoppokakorn, Nanicha Siriwong, Chonlada Phathong, Nattaya Teeyapun, Suebpong Tanasanvimon, Kessarin Thanapirom, Piyawat Komolmit, Sombat Treeprasertsuk, Roongruedee Chaiteerakij, The Thai Red Cross Society, Bangkok 10330, Thailand

Nattaya Teeyapun, Suebpong Tanasanvimon, Department of Medicine, Division of Oncology, Faculty of Medicine, Chulalongkorn University, Bangkok 10330, Thailand

Pisit Tangkijvanich, Center of Excellence in Hepatitis and Liver Cancer, Faculty of Medicine, Chulalongkorn University, Bangkok 10330, Thailand

Roongruedee Chaiteerakij, Center of Excellence for Innovation and Endoscopy in Gastrointestinal Oncology, Division of Gastroenterology, Faculty of Medicine, Chulalongkorn University, Bangkok 10330, Thailand

Corresponding author: Roongruedee Chaiteerakij, MD, PhD, Associate Professor, Department of Medicine, Division of Gastroenterology, Faculty of Medicine, Chulalongkorn University, 1873 Rama IV Rd, Khwaeng Pathum Wan, Khet Pathum Wan, Bangkok 10330, Thailand. roon.chaiteerakij@chula.md

Abstract

BACKGROUND

Modified albumin-bilirubin (mALBI) grade has been established as a survival determinant in hepatocellular carcinoma (HCC) patients who receive locoregional and targeted therapies.

AIM

To investigate whether mALBI could predict survival in unresectable HCC (uHCC) patients who were treated with atezolizumab plus bevacizumab (AB).

METHODS

A single-center, retrospective cohort study enrolled uHCC patients who received AB treatment between September 2020 and April 2023 and were followed up until June 2023. An association between mALBI and patient survival was determined using Cox proportional hazards analysis.

RESULTS

Of the 83 patients, 67 patients (80.7%) were male with the mean age of 60.6 years. Among them, 22 patients (26.5%) were classified as Barcelona Clinic Liver Cancer B, and 61 patients (73.5%) were classified as Barcelona Clinic Liver Cancer C. Cirrhosis was present in 76 patients (91.6%), with 58 patients classified as Child-Turcotte-Pugh (CTP) A and 18 as CTP B. The median overall survival (OS) and progression-free survival were 13.0 mo [95% confidence interval (CI): 5.2-20.8] and 9.0 mo (95%CI: 5.0-13.0), respectively. The patients were divided into two groups based on mALBI grades: 42 patients (50.6%) in the mALBI 1 + 2a group; and 41 patients (49.4%) in the mALBI 2b + 3 group. During the median follow-up period of 7.0 mo, the mALBI 1 + 2a group exhibited significantly better survival compared to the mALBI 2b + 3 group, with a median OS that was not reached *vs* 3.0 mo (95%CI: 0.1-6.0, $P < 0.001$). In a subgroup of patients with CTP A, the mALBI 1 + 2a group also showed significantly longer survival compared to the mALBI 2b + 3 group, with a median OS that was not reached *vs* 6.0 mo (95%CI: 3.4-8.6, $P < 0.001$). In the multivariate analysis, both CTP class and mALBI grade were independently associated with survival, with adjusted hazard ratios (95%CI) of 2.63 (1.19-5.78, $P = 0.020$) and 3.90 (1.71-8.90, $P = 0.001$), respectively.

CONCLUSION

mALBI grades can determine survival of uHCC patients receiving AB treatment, particularly those who have mildly impaired liver function. This highlights the importance of assessing mALBI before initiating AB treatment to optimize therapeutic efficacy in clinical practice.

Key Words: Unresectable hepatocellular carcinoma; Atezolizumab plus bevacizumab; Modified albumin-bilirubin grade; Immunotherapy; Liver function

Core Tip: The modified albumin-bilirubin (mALBI) grade has been shown to determine survival in hepatocellular carcinoma patients receiving locoregional and targeted therapies. This study demonstrated that mALBI can also predict survival in unresectable hepatocellular carcinoma patients receiving atezolizumab plus bevacizumab. To improve the therapeutic outcome of atezolizumab plus bevacizumab treatment in clinical practice, mALBI assessment before initiating treatment can help in identifying suitable candidates for immunotherapy.

Citation: Navadurong H, Prasoppokakorn T, Siriwong N, Phathong C, Teeyapun N, Tanasanvimon S, Thanapirom K, Komolmit P, Tangkijvanich P, Treeprasertsuk S, Chaiteerakij R. Modified albumin-bilirubin predicted survival of unresectable hepatocellular carcinoma patients treated with immunotherapy. *World J Gastrointest Oncol* 2023; 15(10): 1771-1783
URL: https://www.wjgnet.com/1948-5204/full/v15/i10/1771.htm
DOI: https://dx.doi.org/10.4251/wjgo.v15.i10.1771

INTRODUCTION

Hepatocellular carcinoma (HCC) represents a growing global health concern due to its increasing incidence and poor prognosis[1]. The survival of HCC patients is primarily influenced by tumor burden, liver functional reserve, and patient performance status[2]. The Child-Turcotte-Pugh (CTP) score has long been utilized to assess liver functional reserve in patients with cirrhosis. The score was initially designed to evaluate the prognosis of patients with cirrhosis undergoing shunt surgery for variceal bleeding[3]. It has several limitations including the subjectivity of certain parameters, such as grade of ascites and encephalopathy, which reduce its accuracy. Additionally, the CTP score is incapable of distinguishing between CTP class C patients with higher serum bilirubin levels and more severe coagulopathy from those with lower bilirubin levels and less severe coagulopathy. Notably, some HCC patients do not have cirrhosis, and therefore the CTP score may not accurately reflect their liver functional reserve.

To address the limitations of the CTP classification, the albumin-bilirubin (ALBI) grade was developed to specifically evaluate the liver functional reserve of HCC patients. The ALBI grade is calculated using albumin and bilirubin levels, making it more objective than the CTP classification. Overall, the ALBI grade has performed similarly to CTP classification in predicting the survival of HCC patients treated with various modalities, including resection, transplantation, radiofrequency ablation, microwave ablation, transarterial chemoembolization (TACE), transarterial radioembolization, external beam radiotherapy (EBRT), and targeted therapy[4,5]. Moreover, the ALBI grade has outperformed the CTP class since it can differentiate between patients with good and poor prognoses within the same CTP class. For instance, when CTP A patients were separated into two groups based on ALBI grade, there was a 10-mo difference in survival between

those with ALBI grade 1 and those with ALBI grade 2[4].

Although ALBI has been proposed as an index for evaluating liver functional reserve and prognosis in HCC patients [2], its performance remains suboptimal. Despite the greater granularity of the ALBI compared to the CTP score, the distribution of HCC patients across the ALBI grades remains uneven, with 52%-65% of patients classified as ALBI grade 2 and very few classified as ALBI grade 3[4]. Accordingly, some ALBI grade 2 patients had survival comparable to ALBI grade 1 patients, while others had survival similar to ALBI grade 3 patients. To overcome the limitation of the original ALBI score, a modified ALBI (mALBI) grading system was recently developed. The mALBI score showed better predictive performance than the original ALBI grade in assessing liver functional reserve and predicting prognosis in HCC patients. The mALBI score divides the ALBI grade 2 into 2a and 2b, resulting in a more balanced distribution of patients across all grades and better performance in stratifying patients into different groups with different outcomes[6]. The mALBI score also demonstrated superior stratification performance than the original ALBI score in patients treated with resection, radiofrequency ablation, microwave ablation, TACE, and targeted therapy[7].

The current first-line treatment for unresectable HCC (uHCC) is atezolizumab plus bevacizumab (AB)[2], which has demonstrated a significant prolongation of overall survival (OS) and progression-free survival (PFS)[8]. However, few studies have explored the relationship between mALBI grade and prognosis in uHCC patients treated with AB[9,10]. Previous research has suggested that patients with mALBI 1 or 2a experienced significantly longer PFS and a higher objective response rate (ORR) than those with mALBI 2b or 3[10]. Nonetheless, the predictive value of mALBI grade for predicting outcomes of HCC patients receiving AB treatment has yet to be fully investigated. In this study, we aimed to investigate the association between mALBI grade and survival in uHCC patients treated with AB as the first-line, second-line, or subsequent line of treatment after locoregional and systemic therapies.

MATERIALS AND METHODS

Patient enrollment

A single-center, retrospective cohort study was conducted at the King Chulalongkorn Memorial Hospital in Bangkok, Thailand. Patients were enrolled between September 2020 and April 2023. The inclusion criteria were patients aged ≥ 18 years who received AB and were diagnosed with HCC by either pathologically or typical radiologically *via* contrast-enhanced magnetic resonance imaging or dynamic computed tomography[11]. The exclusion criteria were patients with other malignancies and mixed hepatocholangiocarcinoma (Figure 1).

Patient baseline characteristics were collected including performance status, tumor burden, underlying chronic liver disease, presence of cirrhosis, liver functional reserve, and alpha fetoprotein level. Patient performance status was evaluated using the Eastern Cooperative Oncology Group Performance Status (ECOG-PS) score[12]. The ECOG-PS scores were defined as follows: 0 (fully active); 1 (restricted in physically strenuous activity but able to perform light work); 2 (unable to perform any work activities > 50% of waking hours); 3 (confined to bed or chair > 50% of waking hours); and 4 (totally confined to bed).

Tumor burden was assessed using the 2022 Barcelona Clinic Liver Cancer (BCLC) staging system[2], which classified HCC into 5 stages as BCLC stage 0 (very early stage) for solitary nodule ≤ 2 cm, BCLC stage A (early stage) for multifocal HCCs up to three nodules with size ≤ 3 cm, BCLC stage B (intermediate stage) for multifocal HCCs exceeding the stage A criteria, BCLC stage C (advanced stage) for the presence of vascular invasion or extrahepatic spread, and BCLC stage D (end stage) for patients with ECOG-PS > 2 and/or impaired liver function who are not transplant candidates. Tumor size was determined by measuring the maximum diameter of the largest intrahepatic lesion.

The liver functional reserve was evaluated using several measures, including the CTP score, ALBI, and mALBI grades. The ALBI and mALBI grades were calculated using the following equation: ($\log_{10}$ bilirubin in μmol/L × 0.66) + [albumin in g/L × (-0.085)]. The cutoff points for ALBI grades 1, 2, and 3 were ≤ -2.60, > -2.60 to ≤ -1.39, and >-1.39, respectively. For mALBI grades, the cutoff points were ≤ -2.60, > -2.60 to ≤ -2.27, and > -2.27 to ≤ -1.39, and > -1.39 for grades 1, 2a, 2b, and 3, respectively[4,7].

All patients received 1200 mg of atezolizumab and 15 mg/kg of bevacizumab intravenously every 3 wk. The administration of AB was discontinued when the disease progressed by radiologic evidence or by the patient's preference. If any adverse events grade 3 or 4 occurred as defined by the Common Terminology Criteria for Adverse Events version 5.0, AB was temporarily withheld and resumed when the adverse event improved to a milder grade.

The response to AB treatment was evaluated every three cycles using dynamic computed tomography or magnetic resonance imaging and classified according to the Modified Response Evaluation Criteria in Solid Tumors. A complete response was defined as the absence of intratumoral arterial enhancement in all lesions, while a partial response was defined as at least a 30% decrease in the sum of diameters of viable lesions. Progressive disease was defined as at least 20% increase in the sum of the diameters of viable lesions, while stable disease was defined as not in the criteria of either partial response or progressive disease[13]. Regardless of AB treatment, all patients received optimal treatment decided by a multidisciplinary team including hepatologists, surgeons, interventionists, and oncologists. All patients were followed for disease progression and OS.

Statistical analysis

Continuous variables with normal distribution were presented as mean and standard deviation, while variables with non-normal distribution were presented as median and interquartile range (IQR). They were compared using independent *t* tests or the Mann–Whitney *U*, as appropriate. Categorical variables were presented as numbers and percentages and compared using Fisher's exact test or χ^2 test, as appropriate. Patients were divided into two groups based

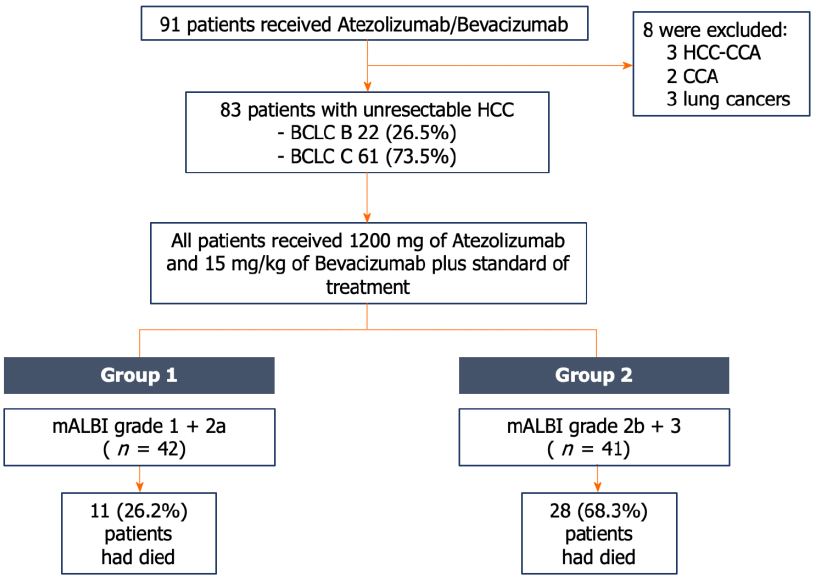

DOI: 10.4251/wjgo.v15.i10.1771 **Copyright** ©The Author(s) 2023.

Figure 1 Flow diagram of patient enrollment. BCLC: Barcelona Clinic Liver Cancer; CCA: Cholangiocarcinoma; HCC: Hepatocellular carcinoma; mALBI: Modified albumin-bilirubin.

on their mALBI grades: group 1 (mALBI grades 1 and 2a) and group 2 (mALBI grades 2b and 3). The patient's survival was calculated from the enrollment date until death or the last follow-up date, which was on June 8, 2023. OS and PFS were estimated using the Kaplan-Meier survival method and compared using the log-rank test. An association between mALBI and patient survival was determined using Cox proportional hazards analysis. Other factors associated with patient survival were also determined using the univariate Cox proportional hazards model. Age, sex, and other factors with a P value of < 0.05 in the univariate model were included in the multivariate model. A P value of < 0.05 was considered statistically significant. Statistical analyses were performed using the SPSS package version 22.0.0 (SPSS Inc., Chicago, IL, United States). The study protocol was approved by the Institutional Review Board of the Faculty of Medicine, Chulalongkorn University (IRB No.892/63), and was in accordance with the Helsinki Declaration of 1983.

RESULTS

Patient characteristics

A total of 91 patients received AB in our hospital. Of those, 83 patients were uHCC and included in the study. Eight patients were excluded due to other cancer diagnoses (three hepatocholangiocarcinomas, two cholangiocarcinomas, and three lung cancers). Among the 83 uHCC patients, 67 patients (80.7%) were male with a mean age of 60.6 ± 12.8 years. Baseline characteristics of the entire cohort are displayed in Table 1. Chronic liver disease was primarily caused by viral hepatitis B/C infection (53 patients, 63.9%), followed by nonalcoholic steatohepatitis (23, 27.7%), alcohol liver disease (7, 8.4%), and autoimmune hepatitis (1, 1.2%). Cirrhosis was present in 76 patients (91.6%), with 58 patients (69.9%) classified as CTP class A and 18 patients (21.7%) classified as CTP class B. The baseline median alpha fetoprotein level in the entire cohort was 339.0 ng/mL (IQR 10.7, 6300.0).

At the time of AB initiation, 22 patients (26.5%) were classified as BCLC stage B with extensive tumor involvement, while 61 patients (73.5%) were classified as BCLC stage C. Among them, 30 patients (36.1%) had portal vein invasion, and 40 patients (48.2%) had extrahepatic metastasis. AB was utilized as first-line therapy in 20 patients (24.1%), with 17 patients (20.5%) receiving AB monotherapy and 3 patients (3.6%) receiving AB in combination with EBRT. Sixty-three patients (75.9%) received AB as a second or subsequent line of treatment. Among them, 62 patients (74.7%) had received prior locoregional treatment (48 TACE, 22 resections, 19 EBRT, 17 ablations, and 9 transarterial radioembolization), and 10 patients (12.0%) had received prior systemic therapies (5 sorafenib, 4 lenvatinib, and 2 had at least two systemic therapy regimens).

Regarding the mALBI classification, there were 23 patients (27.7%), 19 patients (22.9%), 32 patients (38.9%), and 9 patients (10.8%) classified as grade 1, 2a, 2b, and 3, respectively. This distribution resulted in 42 patients (50.6%) being categorized to group 1 (mALBI 1 + 2a), and 41 patients (49.4%) being categorized to group 2 (mALBI 2b + 3).

Regarding liver functional reserve, patients in group 1 with a lower mALBI grade showed a significantly higher percentage of CTP A compared to those in group 2 with a higher mALBI grade [35 patients (83.3%) *vs* 23 patients (56.1%), P < 0.001]. As for tumor burden, patients in group 1 had a higher percentage of BCLC C compared to those in group 2 [36 patients (85.7%) *vs* 25 patients (61.0%), P = 0.010]. When considering patients with BCLC C, there was no significant difference in the number of patients with macrovascular invasion between the two groups [15 patients (35.7%) *vs* 15 patients (36.6%), P = 0.930]. We did find a significantly higher number of patients with extrahepatic metastasis in group 1

Table 1 Baseline characteristics of the unresectable hepatocellular carcinoma patients who received atezolizumab plus bevacizumab therapy, *n* (%)

Variables	Total, *n* = 83	mALBI 1+2a, *n* = 42	mALBI 2b+3, *n* = 41	*P* value
Age in yr, mean ± SD	60.6 ± 12.8	59.8 ± 14.0	61.5 ± 11.5	0.560
Male	67 (80.7)	34 (81.0)	33 (80.5)	0.960
ECOG-PS				0.680
0	78 (94.0)	40 (95.2)	38 (92.7)	
1	5 (6.0)	2 (4.8)	3 (7.3)	
Presence of cirrhosis	76 (91.6)	35 (83.3)	41 (100)	< 0.001
CTP A	58 (69.9)	35 (83.3)	23 (56.1)	
CTP B	18 (21.7)	0 (0)	18 (43.9)	
Etiology of disease				
Viral hepatitis	53 (63.9)	27 (64.3)	26 (63.4)	0.930
NASH	23 (27.7)	11 (26.2)	12 (29.3)	0.750
Alcohol related	7 (8.4)	1 (2.4)	6 (14.6)	0.060
Others	1 (1.2)	1 (2.4)	0 (0)	1.000
BCLC staging				
BCLC B	22 (26.5)	6 (14.3)	16 (39.0)	0.010
BCLC C	61 (73.5)	36 (85.7)	25 (61.0)	
Macrovascular invasion	30 (36.1)	15 (35.7)	15 (36.6)	0.930
Extrahepatic metastasis	40 (48.2)	25 (59.5)	15 (36.6)	0.040
AFP in ng/mL, median (IQR)	339.0 (10.7, 6300.0)	581.5 (11.5, 6869.5)	339.0 (10.5, 9144.5)	0.880
Tumor size in cm, median (IQR)	5.3 (1.7, 12.0)	4.8 (1.7, 11.0)	5.6 (1.7, 14.3)	0.730
Portal vein invasion grade of 2/3/4	8 (26.7)/13 (43.3)/9 (30.0)	4 (26.7)/7 (46.7)/4 (26.7)	4 (26.7)/6 (40.0)/5 (33.3)	1.000
EHM bone/lymph node/lung/peritoneum	11 (27.5)/14 (35.0)/21 (52.5)/9 (22.5)	8 (32.0)/7 (28.0)/13 (52.0)/3 (12.0)	3 (20.0)/7 (46.7)/8 (53.3)/6 (40.0)	0.350
ALBI score, median (IQR)	-2.270 (-2.628 to -1.826)	-2.622 (-2.836 to -2.398)	-1.826 (-2.067 to -1.434)	< 0.001
mALBI grade				< 0.001
1: ≤ -2.60	23 (27.7)	23 (54.8)	0 (0)	
2a: > -2.60 to ≤ -2.27	19 (22.9)	19 (45.2)	0 (0)	
2b: > -2.27 to ≤ -1.39	32 (38.6)	0 (0)	32 (78.0)	
3: > -1.39	9 (10.8)	0 (0)	9 (22.0)	
Prior local therapy for HCC	62 (74.7)	33 (78.6)	29 (70.7)	0.410
Resection	22 (35.5)	17 (51.5)	5 (17.2)	0.005
Ablation	17 (27.4)	9 (27.3)	8 (27.6)	0.980
TACE	48 (77.4)	23 (69.7)	25 (86.2)	0.120
TARE	9 (14.5)	5 (15.2)	4 (13.8)	1.000
EBRT	19 (30.6)	11 (33.3)	8 (27.6)	0.620
Prior systemic therapy for HCC	10 (12.0)	4 (9.5)	6 (14.6)	0.460
Sorafenib	5 (50.0)	1 (25.0)	4 (66.7)	0.530
Lenvatinib	4 (40.0)	2 (50.0)	2 (33.3)	1.000
> 2 lines of systemic therapy	2 (20.0)	1 (25.0)	1 (16.7)	1.000
AB as first-line treatment	20 (24.1)	9 (21.4)	11 (26.8)	0.570

Combination of AB and other local therapy as first-line treatment	3 (3.6)	3 (7.1)	0 (0)	0.240
Resection/TACE/TARE/EBRT	0 (0)/0 (0)/0 (0)/3 (100)	0 (0)/0 (0)/0 (0)/3 (100.0)	0 (0)/0 (0)/0 (0)/0 (0)	0.240
Number of AB cycle, median (IQR)	4.0 (2.0, 9.0)	5.0 (4.0, 11.3)	3.0 (1.0, 4.5)	< 0.001

AB: Atezolizumab plus bevacizumab; AFP: Alpha fetoprotein; ALBI: Albumin-bilirubin; BCLC: Barcelona Clinic Liver Cancer; CTP: Child-Turcotte-Pugh; EBRT: External beam radiotherapy; ECOG-PS: Eastern Cooperative Oncology Group Performance Status; EHM: Extrahepatic metastasis; HCC: Hepatocellular carcinoma; IQR: Interquartile range; mALBI: Modified albumin-bilirubin; NASH: Nonalcoholic steatohepatitis; SD: Standard deviation; TACE: Transarterial chemoembolization; TARE: Transarterial radioembolization.

compared to group 2 [25 patients (59.5%) *vs* 15 patients (36.6%), $P = 0.040$] (Table 1).

Treatment outcomes

During the median follow-up period of 7 mo (range 0.75-30.0 mo), 39 patients (47.0%) had died. The median OS and PFS were 13.0 mo [95% confidence interval (CI): 5.2-20.8] and 9.0 mo (95%CI: 5.0-13.0), respectively (Figure 2A and B). Of those, 61 patients were evaluated for treatment responses. The disease control rate was 62.3% ($n = 38$), with a complete response rate of 6.6% ($n = 4$), a partial response rate of 21.3% ($n = 13$), and a stable disease rate of 34.4% ($n = 21$). The disease progression rate was 37.7% ($n = 23$). However, there were no statistically significant differences in the ORR and disease control rate between the two groups (Table 2).

We further performed subgroup analyses based on CTP, tumor size, and tumor stages. We found that patients with CTP class A had a significantly longer median OS compared to those with CTP class B, with values of 17 mo (95%CI: not estimated) and 2.0 mo (95%CI: 1.1-2.9), respectively ($P < 0.001$) (Table 3).

Regarding tumor characteristics, there was no significant difference in survival among the following groups: tumor size less than or equal 5.0 cm *vs* 5.0 cm or more; BCLC stage C with and without portal vein invasion; and BCLC stage C with and without extrahepatic metastasis. However, the PFS in BCLC stage C with portal vein invasion was significantly longer compared to those without portal vein invasion, with values of 24.0 mo (95%CI: Not estimated) *vs* 6.0 mo (95%CI: 3.2-8.8), respectively ($P = 0.030$) (Table 3).

Number of treatments and treatments following AB failure

The median number of AB cycles administered in the cohort was 4.0 cycles (IQR: 2.0, 9.0). Patients in group 1 received a significantly higher number of AB cycles than those in group 2 [5.0 cycles (4.0, 11.3) *vs* 3.0 cycles (1.0, 4.5), $P < 0.001$] (Table 1).

Of the 83 study patients, 37 patients experienced disease progression after AB treatment. Among them, 32 patients (86.5%) received additional systemic therapies (19 received lenvatinib, 3 received chemotherapy, 1 received sorafenib, and 9 received two or more consecutive systemic therapies). Other treatment options included EBRT (8 patients, 21.6%), TACE (4 patients, 10.8%), and best supportive care (4 patients, 10.8%). In the cohort, 6 patients (16.2%) were treated with a combination of systemic treatment and EBRT, 3 patients (8.1%) received a combination of systemic treatment and TACE, and 1 patient (2.7%) received a combination of systemic treatment, TACE, and EBRT (Table 4).

Among patients who experienced disease progression after AB treatment, those who received subsequent therapeutic interventions had longer survival than those who received the best supportive care. However, the survival difference did not reach statistical significance. The median survival time was not reached *vs* 5.0 mo (95%CI: 1.8-8.2, $P = 0.050$).

Predictors of survival in uHCC patients treated with AB

In the univariate analysis, mALBI grade 2b + 3 showed a significant association with survival, with a hazard ratio (HR) of 5.20 (95%CI: 2.52-10.76, $P < 0.001$). Similarly, CTP class B was also significantly associated with survival, with an HR of 5.38 (95%CI: 2.66-10.89, $P < 0.001$). In the multivariate analysis adjusted for age and sex, both mALBI grade 2b + 3 and CTP class B remained independently associated with worse survival, with adjusted HRs of 3.90 (95%CI: 1.71-8.90, $P = 0.001$) and 2.63 (95%CI: 1.19-5.78, $P = 0.020$), respectively (Table 5).

Patients in group 1 (lower mALBI grade) exhibited a significantly longer survival than those in group 2 (higher mALBI grade), *i.e.* not reached *vs* 3.0 mo (95%CI: 0.1–6.0, $P < 0.001$) (Figure 3A). When considering the classification based on CTP class, the OS of patients with CTP class A was 17 mo (95%CI: Not estimated), while it was only 2 mo (95%CI: 1.1-2.9) for those with CTP class B ($P < 0.001$). Among CTP class A patients, the median survival for those in group 1 remained significantly longer than for those in group 2, *i.e.* not reached *vs* 6.0 mo (95%CI: 3.4–8.6, $P < 0.001$) (Figure 3B).

Furthermore, among patients with CTP class A and a CTP score of 5 ($n = 46$), group 1 patients exhibited a significantly longer survival than group 2 patients [not reached *vs* 6.0 mo (95%CI: 3.4-8.6), $P < 0.001$], suggesting that mALBI grades performed better than CTP score and CTP classification in predicting survival. In contrast, among patients with CTP class A and a CTP score of 6 ($n = 19$), there was no significant difference in survival between group 2 and group 1 [11.0 mo (95%CI: 2.5-19.5) *vs* 3 mo (95%CI: not estimated), $P = 0.830$]. Likewise, the median PFS of group 1 and group 2 showed no significant difference [8.0 mo (95%CI: 3.2-12.8) *vs* 9.0 mo (95%CI: 4.5–13.5), respectively, $P = 0.920$].

Similar findings were observed when considering the classification based on BCLC stages. In the BCLC C subgroup, patients in group 1 had an estimated median survival that was not reached, while those in group 2 had a median survival of 3.0 mo (95%CI: 0.0-7.6, $P < 0.001$). In the BCLC B subgroup, death was not reported in group 1, while those in group 2 had a median survival of 3.0 mo (95%CI: 0.0-6.7, $P = 0.014$) (Figure 4).

Table 2 Efficacy outcomes of atezolizumab plus bevacizumab[1], *n* (%)

Variables	Total, *n* = 61	mALBI 1 + 2a, *n* = 39	mALBI 2b + 3, *n* = 22	*P* value
Complete response	4 (6.6)	3 (7.7)	1 (4.5)	1.000
Partial response	13 (21.3)	11 (28.2)	2 (9.1)	0.110
Stable disease	21 (34.4)	12 (30.8)	9 (40.9)	0.420
Objective response rate	17 (27.9)	14 (35.9)	3 (13.6)	0.060
Disease control rate	38 (62.3)	26 (66.7)	12 (54.5)	0.350
Progressive disease	23 (37.7)	13 (33.3)	10 (45.5)	0.350

[1]The number of patients who had available data on treatment response evaluation were 61/83 patients (73.5%), and 22/83 patients (26.5%) had died prior to treatment response evaluation. mALBI: Modified albumin-bilirubin.

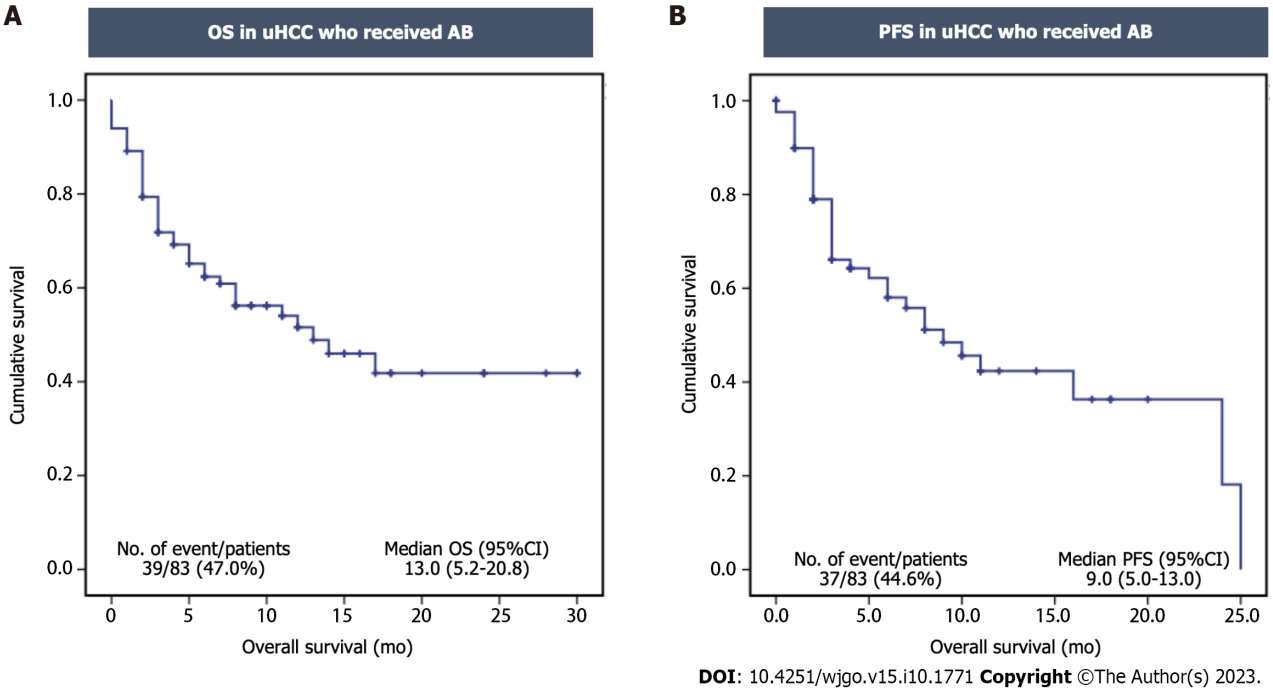

DOI: 10.4251/wjgo.v15.i10.1771

Figure 2 Kaplan–Meier analysis of overall survival and progression free survival of the unresectable hepatocellular carcinoma patients who received atezolizumab plus bevacizumab therapy. A: Overall survival (OS) in unresectable hepatocellular carcinoma (uHCC) patients who received atezolizumab plus bevacizumab (AB); B: Progression-free survival (PFS) in uHCC patients who received AB. CI: Confidence interval.

DISCUSSION

This study presented the efficacy of AB treatment for uHCC and highlighted the significance of liver functional reserve as assessed by mALBI grades in relation to patient survival. The findings of the study suggested that mALBI grades offer a more reliable prognostic ability compared to CTP classification because mALBI grades can distinguish between patients who share the same CTP score or classification but exhibit different outcomes.

The landmark phase III clinical trial for AB treatment in uHCC showed prolonged patient survival of 19.2 mo and PFS of 6.9 mo over a follow-up period of 15.6 mo. However, in real-world cohorts, patients receiving AB treatment had shorter survival, ranging from 10.6-15.0 mo, but similar PFS, ranging from 5.1-6.9 mo[14-16]. Our cohort demonstrated an OS of 13 mo and a PFS of 9 mo. The shorter survival observed in our study compared to the landmark study was likely explained by differences in patient characteristics, particularly the liver functional reserve. The AB combination was tested in a phase III clinical trial for its efficacy in CTP class A patients. In practice, however, AB was given not only to CTP class A patients but also to CTP class B patients. The OS and PFS of patients in our study were relatively similar to a real-world cohort. Focusing on a subgroup of CTP A patients, our study found a survival rate of 17 mo, which was similar to the clinical trial results. These findings underscore the significance of liver functional reserve in determining outcomes for patients receiving AB treatment.

The mALBI grades exhibited a significant correlation with survival in uHCC patients who underwent systemic therapy, where patients with mALBI grades 2a had a survival rate of 11 mo compared to 7 mo for those with mALBI

Table 3 Median overall survival and progression-free survival of unresectable hepatocellular carcinoma patients who received atezolizumab plus bevacizumab therapy stratified by liver function, tumor size, and tumor stage

Variables	No. of events/No. of patients	Median OS (95%CI), mo	*P* value	No. of events/No. of patients	Median OS (95%CI), mo	*P* value
A. Entire cohort, *n* = 83						
CTP class			< 0.001			NE
CTP A	25/65	17 (-)		34/65	9.0 (5.1-12.9)	
CTP B	14/18	2.0 (1.1-2.9)		3/18	NE	
Tumor size in cm			0.790			0.130
≤ 5.0	21/41	12.0 (4.8-19.2)		21/41	7.0 (2.8-11.2)	
> 5.0	18/42	NE		16/42	16.0 (6.5-25.5)	
B. BCLC C group, *n* = 61	27/61	14.0 (-)		28/61	10.0 (0.5-19.5)	
CTP class			< 0.001			0.810
CTP A	18/49	NE		26/49	10.0 (0.3-19.7)	
CTP B	9/12	1.0 (0.1-2.5)		2/12	NE	
Tumor size in cm			0.850			0.060
≤ 5.0	13/26	12.0 (3.4-20.6)		15/26	6.0 (2.5-9.5)	
> 5.0	14/35	NE		13/35	24.0 (9.4-38.6)	
With PV invasion, *n* = 30			0.140			0.030
No	12/31	NE		20/31	6.0 (3.2-8.8)	
Yes	15/30	13.0 (2.0-24.0)		8/30	24.0 (-)	
With EHM metastasis, *n* = 40			0.540			0.170
No	10/21	13.0 (0.1-27.3)		7/21	24 (-)	
Yes	17/40	NE		21/40	6.0 (1.1-10.9)	
C. BCLC B group, *n* = 22	12/22	11.0 (2.7-19.3)		9/22	8.0 (1.3-14.7)	
CTP class			0.020			0.660
CTP A	7/16	11.0 (5.6-16.4)		8/16	8.0 (1.5-14.5)	
CTP B	5/6	2.0 (0.8-3.2)		1/6	5.0 (-)	
Tumor size in cm			0.490			0.140
≤ 5.0	8/15	11.0 (0.1-24.1)		6/15	9.0 (6.9-11.1)	
> 5.0	4/7	7.0 (0.1-17.3)		3/7	5.0 (-)	

CI: Confidence interval; BCLC: Barcelona Clinic Liver Cancer; CTP: Child-Turcotte-Pugh; EHM: Extrahepatic metastasis; NE: Not estimated; OS: Overall survival; PFS: Progression-free survival; PV: Pulmonary vein.

grades 2b who received lenvatinib or ramucirumab[6]. Our study consistently demonstrated that mALBI grades are reliable predictors of OS in patients with uHCC undergoing AB treatment. Patients with mALBI grades 1 or 2a had significantly longer survival compared to those with mALBI grades 2b or 3, with a median survival that was not reached compared to 3.0 mo, respectively. The more precise scoring system of mALBI grade may account for its superior predictive performance, as it breaks down ALBI grade 2 into 2a and 2b using a cutoff value of 30% indocyanine green retention rate at 15 min (ICG-R15). ICG-R15 was initially developed to evaluate liver functional reserve in patients undergoing hepatic resection; those with an ICG-R15 of ≤ 30% were eligible for segmentectomy[17]. The mALBI grades demonstrated superior performance compared to the original ALBI in identifying patients with favorable or unfavorable survival outcomes, especially among those with a CTP score of 5. Our study consistently observed this trend[7].

The observed PFS in our cohort was 9 mo. In a retrospective study involving 71 Japanese uHCC patients who received AB treatment, the PFS was significantly longer in the mALBI 1 + 2a group compared to the mALBI 2b + 3 group (10.5 mo *vs* 3.0 mo, $P < 0.010$)[10]. This suggests that AB therapy was more effective in patients with mALBI 1 + 2a. However, our study found that the mALBI 1 + 2a and 2b + 3 groups had similar PFS durations of 8-9 mo. This could be attributed to the

Table 4 Treatment after progression on atezolizumab plus bevacizumab therapy[1], *n* (%)

Treatment	Total, *n* = 37	mALBI 1 + 2a, *n* = 24	mALBI 2b + 3, *n* = 13	*P* value
Systemic therapy	32 (86.5)	22 (91.7)	10 (76.9)	0.320
TACE	4 (10.8)	4 (16.7)	0 (0)	0.280
EBRT	8 (21.6)	6 (25.0)	2 (15.4)	0.690
Best supportive care	4 (10.8)	1 (4.2)	3 (23.1)	0.120

[1]There were 37/83 (44.6%) patients who had disease progression after atezolizumab plus bevacizumab therapy. EBRT: External beam radiotherapy; mALBI: Modified albumin-bilirubin; TACE: Transarterial chemoembolization.

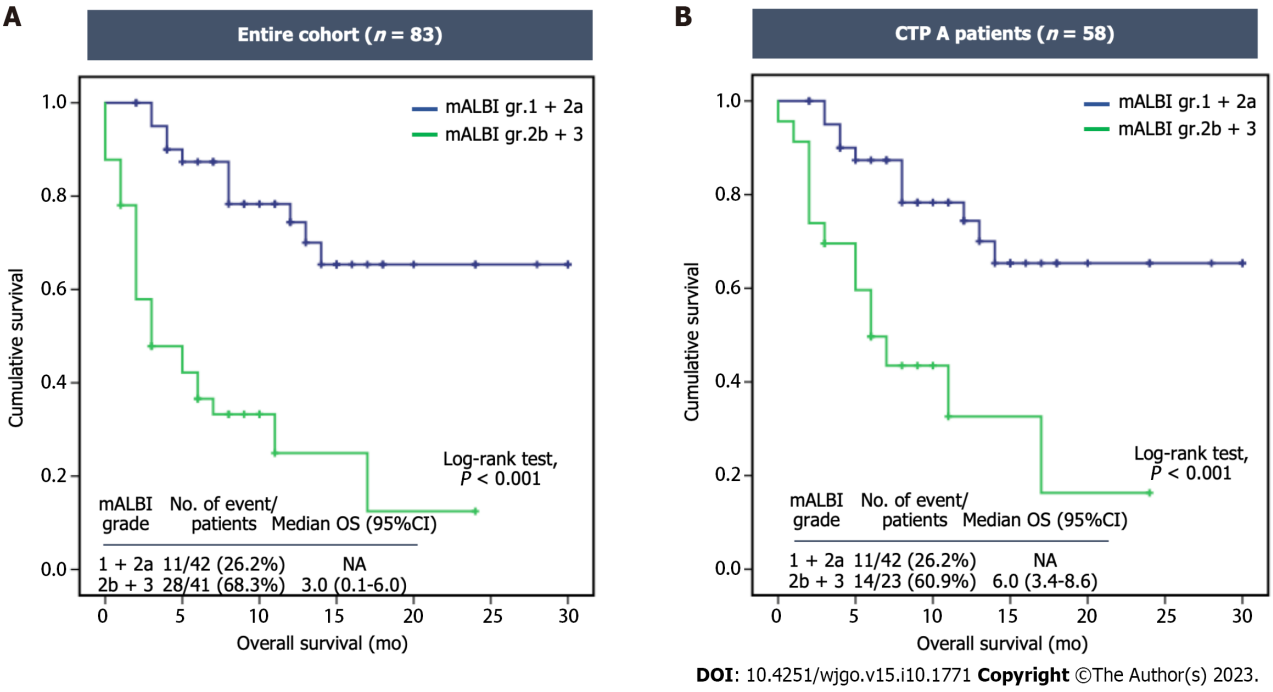

DOI: 10.4251/wjgo.v15.i10.1771

Figure 3 Kaplan-Meier curves for overall survival in patients undergoing atezolizumab plus bevacizumab therapy stratified by modified albumin-bilirubin grade. A: Entire cohort; B: Child-Turcotte-Pugh (CTP) class A. CI: Confidence interval; gr: Group; mALBI: Modified albumin-bilirubin; NA: Not available; OS: Overall survival.

higher proportion of BCLC stage C patients in the mALBI 1 + 2a group compared to the mALBI 2b + 3 group. Advanced stages of HCC are associated with reduced efficacy of AB therapy, as indicated in a previous study involving BCLC stage C patients, which reported a significantly lower ORR compared to BCLC stage B patients (32% *vs* 62%, $P < 0.050$)[10]. In our study, we found that the ORR in the mALBI grade 1 + 2a group was not significantly higher than in the mALBI grade 2b group (35.9% *vs* 13.6%, $P = 0.060$). Similarly, another retrospective study involving 115 uHCC patients treated with AB showed no significant difference in ORR between the mALBI grade 1 + 2a and mALBI grade 2b groups (21.9% *vs* 12.9%, $P = 0.460$), which is consistent with our findings[9].

In patients with uHCC, the treatment outcome is more dependent on liver functional reserve rather than tumor burden. Within our cohort, we observed that patients with a low mALBI grade of 1 + 2a had a longer survival compared to those with a high mALBI grade of 2b + 3, specifically within the BCLC B and C subgroups. Among patients with a low mALBI grade in the BCLC B subgroup, there were no deaths by the end of the study period. Conversely, patients with a high mALBI grade in the BCLC C subgroup experienced poor survival. In our study, patients with BCLC B and C HCCs exhibited comparable survival of 11 mo and 14 mo, respectively. This finding was consistent with a previous study that reported survival of 25.8 mo and 24.6 mo in BCLC stage B and C patients, respectively[18]. These findings support the notion that the effectiveness of AB therapy is primarily influenced by the liver's functional reserve rather than the stage of the tumor.

Among patients with progressive disease, we observed that those who received subsequent treatment, including additional systemic therapies or locoregional therapies, had slightly longer survival compared to those who received the best supportive care, although the difference did not reach statistical significance. We believe it remains worth considering the continuation of treatment with alternative options if feasible, as it has the potential to extend the survival of uHCC patients who face disease progression after AB treatment.

Table 5 Predictors of overall survival in unresectable hepatocellular carcinoma patients who received atezolizumab plus bevacizumab therapy

Variables	Univariate		Multivariate	
	Hazard ratio (95%CI)	*P* value	Adjusted hazard ratio (95%CI)	*P* value
Age	1.00 (0.97-1.02)	0.970	0.99 (0.96-1.02)	0.540
Male sex	1.15 (0.51-2.60)	0.740	0.97 (0.41-2.28)	0.940
ECOG-PS				
0	1.00 (Reference)			
1	2.03 (0.62-6.66)	0.240		
Presence of cirrhosis				
No	1.00 (Reference)			
Yes	2.19 (0.53-9.13)	0.280		
Etiology of disease				
NASH	0.70 (0.32-1.52)	0.360		
Viral hepatitis	1.48 (0.73-2.97)	0.280		
Alcohol	2.09 (0.81-5.39)	0.130		
BCLC stage				
B	1.00 (Reference)			
C	0.66 (0.33-1.31)	0.230		
Extrahepatic metastasis				
No	1.00 (Reference)			
Yes	0.70 (0.37-1.32)	0.270		
Portal invasion				
No	1.00 (Reference)			
Yes	1.29 (0.68-2.47)	0.440		
AFP > 500 ng/mL	1.26 (0.67-2.36)	0.480		
CTP class				
A	1.00 (Reference)			
B	5.38 (2.66-10.89)	< 0.001	2.63 (1.19-5.78)	0.020
mALBI grade				
1 + 2a	1.00 (Reference)			
2b + 3	5.20 (2.52-10.76)	< 0.001	3.90 (1.71-8.90)	0.001
Prior treatment for HCC				
No	1.00 (Reference)			
Yes	0.87 (0.42-1.78)	0.700		
Prior local therapy for HCC				
No	1.00 (Reference)			
Yes	0.79 (0.39-1.58)	0.500		
Prior systemic therapy for HCC				
No	1.00 (Reference)			
Yes	1.80 (0.79-4.11)	0.160		
Combination of AB and local treatment as first-line treatment				
No	1.00 (Reference)			

Yes	0.05 (0.01-27.12)	0.340

AB: Atezolizumab plus bevacizumab; AFP: Alpha fetoprotein; BCLC: Barcelona Clinic Liver Cancer; CI: Confidence interval; CTP: Child-Turcotte-Pugh; ECOG-PS: Eastern Cooperative Oncology Group Performance Status; HCC: Hepatocellular carcinoma; mALBI: Modified albumin-bilirubin; NASH: Nonalcoholic steatohepatitis.

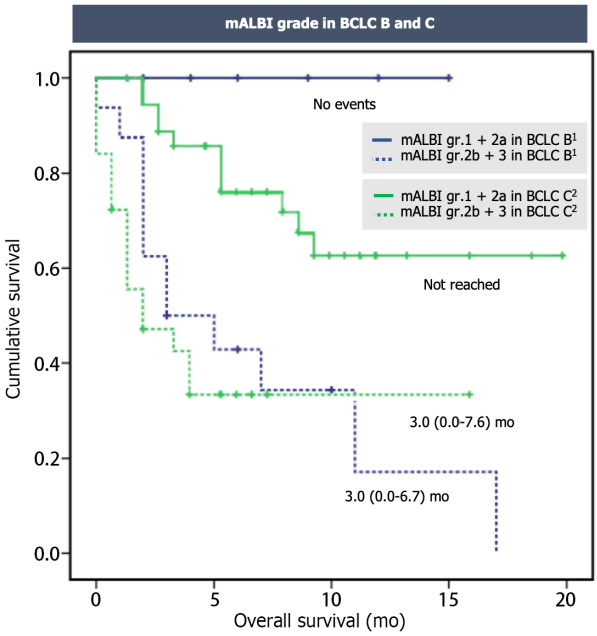

DOI: 10.4251/wjgo.v15.i10.1771

Figure 4 Kaplan-Meier curves for overall survival in patients undergoing atezolizumab plus bevacizumab therapy stratified by modified albumin-bilirubin grade in Barcelona Clinic Liver Cancer B and C. $^{1}P = 0.014$; $^{2}P < 0.001$. BCLC: Barcelona Clinic Liver Cancer; gr: Group; mALBI: Modified albumin-bilirubin.

Our study had several strengths. First, we included diverse uHCC patients who received real-world AB treatment, including those with liver functional reserve in CTP B, which extends beyond the recommended guidelines. This reflects the practical treatment approach in the Asian population, where various treatment options are commonly used, deviating from recommended guidelines. Second, we were able to track post-AB treatment and disease progression, providing real-life survival outcomes. Despite these strengths, our study also had some limitations due to its retrospective nature, relatively short follow-up period, and a small number of patients in the BCLC B subgroup. A large, multicenter prospective cohort study with an extended follow-up duration is necessary to gain a deeper understanding of the efficacy of AB therapy in HCC.

CONCLUSION

In uHCC patients, liver functional reserve plays a significant role as a prognostic factor and is essential for maximizing the effectiveness of AB therapy in clinical practice. Our study demonstrated that mALBI grades are a reliable prognostic factor, particularly for distinguishing patients with CTP A. The assessment of liver functional reserve using mALBI before initiating AB treatment can assist in identifying appropriate candidates for this therapy.

ARTICLE HIGHLIGHTS

Research background

Modified albumin-bilirubin (mALBI) grade has been established as a survival determinant in hepatocellular carcinoma (HCC) patients who receive locoregional and targeted therapies.

Research motivation

The predictive value of mALBI grade for predicting outcomes of HCC patients receiving atezolizumab plus bevacizumab (AB) treatment has yet to be fully investigated.

Research objectives
To assess whether mALBI could predict survival in unresectable HCC patients who were treated with AB.

Research methods
A single-center, retrospective cohort study enrolled unresectable HCC patients who received AB treatment between September 2020 and April 2023 and were followed up until June 2023. An association between mALBI and patient survival was determined using Cox proportional hazards analysis.

Research results
Of the 83 patients, the median overall survival (OS) was 13.0 mo [95% confidence interval (CI): 5.2-20.8]. The median progression-free survival was 9.0 mo (95%CI: 5.0-13.0). The patients were divided into two groups based on mALBI grades: 42 patients (50.6%) in the mALBI 1 + 2a group and 41 patients (49.4%) in the mALBI 2b + 3 group. The mALBI 1 + 2a group exhibited significantly better survival compared to the mALBI 2b + 3 group, with a median OS that was not reached *vs* 3.0 mo (95%CI: 0.1-6.0) ($P < 0.001$). In a subgroup of patients with Child-Turcotte-Pugh (CTP) A, the mALBI 1 + 2a group also showed significantly longer survival compared to the mALBI 2b + 3 group, with a median OS that was not reached *vs* 6.0 mo (95%CI: 3.4-8.6, $P < 0.001$).

Research conclusions
Our study demonstrated that mALBI grades are a more reliable prognostic factor than CTP classification, particularly for distinguishing outcomes of patients within the CTP A class.

Research perspectives
The assessment of liver functional reserve using mALBI before initiating AB treatment can assist in identifying appropriate candidates for this therapy.

ACKNOWLEDGEMENTS

This work was supported by the Division of Gastroenterology, Faculty of Medicine Foundation, Chulalongkorn University.

FOOTNOTES

Author contributions: Navadurong H and Chaiteerakij R designed the study; Navadurong H, Prasoppokakorn T, Siriwong N, and Phathong C contributed to data acquisition; Teeyapun N, Tanasanvimon S, Thanapirom K, Komolmit P, Tangkijvanich T, and Treeprasertsuk S recruited and managed the patients; Navadurong H, Prasoppokakorn T, and Phathong C analyzed and interpreted the data; Navadurong H, and Prasoppokakorn T drafted the manuscript; Prasoppokakorn T and Chaiteerakij R revised the manuscripts critically for important intellectual content; All the authors read and approved the final manuscript.

Institutional review board statement: The study protocol was approved by the Institutional Review Board of the Faculty of Medicine, Chulalongkorn University (No.892/63).

Conflict-of-interest statement: The authors have no conflicts of interest to declare.

Data sharing statement: No additional data are available.

STROBE statement: The authors have read the STROBE Statement—checklist of items, and the manuscript was prepared and revised according to the STROBE Statement—checklist of items.

Country/Territory of origin: Thailand

ORCID number: Thaninee Prasoppokakorn 0000-0002-1012-9874; Chonlada Phathong 0000-0002-8474-9654; Piyawat Komolmit 0000-0002-1357-9547; Sombat Treeprasertsuk 0000-0001-6459-8329; Roongruedee Chaiteerakij 0000-0002-7191-3881.

S-Editor: Lin C
L-Editor: Filipodia
P-Editor: Zhang XD

REFERENCES

1 **Forner A**, Reig M, Bruix J. Hepatocellular carcinoma. *Lancet* 2018; **391**: 1301-1314 [PMID: 29307467 DOI: 10.1016/S0140-6736(18)30010-2]

2 **Reig M**, Forner A, Rimola J, Ferrer-Fàbrega J, Burrel M, Garcia-Criado Á, Kelley RK, Galle PR, Mazzaferro V, Salem R, Sangro B, Singal AG, Vogel A, Fuster J, Ayuso C, Bruix J. BCLC strategy for prognosis prediction and treatment recommendation: The 2022 update. *J Hepatol* 2022; **76**: 681-693 [PMID: 34801630 DOI: 10.1016/j.jhep.2021.11.018]

3 **Child CG**, Turcotte JG. Surgery and portal hypertension. *Major Probl Clin Surg* 1964; **1**: 1-85 [PMID: 4950264]

4 **Johnson PJ**, Berhane S, Kagebayashi C, Satomura S, Teng M, Reeves HL, O'Beirne J, Fox R, Skowronska A, Palmer D, Yeo W, Mo F, Lai P, Iñarrairaegui M, Chan SL, Sangro B, Miksad R, Tada T, Kumada T, Toyoda H. Assessment of liver function in patients with hepatocellular carcinoma: a new evidence-based approach-the ALBI grade. *J Clin Oncol* 2015; **33**: 550-558 [PMID: 25512453 DOI: 10.1200/JCO.2014.57.9151]

5 **Toyoda H**, Johnson PJ. The ALBI score: From liver function in patients with HCC to a general measure of liver function. *JHEP Rep* 2022; **4**: 100557 [PMID: 36124124 DOI: 10.1016/j.jhepr.2022.100557]

6 **Kudo M**. Newly Developed Modified ALBI Grade Shows Better Prognostic and Predictive Value for Hepatocellular Carcinoma. *Liver Cancer* 2022; **11**: 1-8 [PMID: 35222503 DOI: 10.1159/000521374]

7 **Hiraoka A**, Kumada T, Tsuji K, Takaguchi K, Itobayashi E, Kariyama K, Ochi H, Tajiri K, Hirooka M, Shimada N, Ishikawa T, Tachi Y, Tada T, Toyoda H, Nouso K, Joko K, Hiasa Y, Michitaka K, Kudo M. Validation of Modified ALBI Grade for More Detailed Assessment of Hepatic Function in Hepatocellular Carcinoma Patients: A Multicenter Analysis. *Liver Cancer* 2019; **8**: 121-129 [PMID: 31019902 DOI: 10.1159/000488778]

8 **Finn RS**, Qin S, Ikeda M, Galle PR, Ducreux M, Kim TY, Kudo M, Breder V, Merle P, Kaseb AO, Li D, Verret W, Xu DZ, Hernandez S, Liu J, Huang C, Mulla S, Wang Y, Lim HY, Zhu AX, Cheng AL; IMbrave150 Investigators. Atezolizumab plus Bevacizumab in Unresectable Hepatocellular Carcinoma. *N Engl J Med* 2020; **382**: 1894-1905 [PMID: 32402160 DOI: 10.1056/NEJMoa1915745]

9 **Sho T**, Suda G, Yamamoto Y, Furuya K, Baba M, Ogawa K, Kubo A, Tokuchi Y, Fu Q, Yang Z, Kimura M, Kitagataya T, Maehara O, Ohnishi S, Nakamura A, Yamada R, Ohara M, Kawagishi N, Natsuizaka M, Nakai M, Suzuki K, Izumi T, Meguro T, Terashita K, Takagi T, Ito J, Kobayashi T, Miyagishima T, Sakamoto N. Efficacy and Effect on Liver Functional Reserve of Atezolizumab and Bevacizumab for Unresectable Hepatocellular Carcinoma in Patients Who Do Not Meet Eligibility Criteria of IMbrave150. *Cancers (Basel)* 2022; **14** [PMID: 36010930 DOI: 10.3390/cancers14163938]

10 **Tomonari T**, Tani J, Sato Y, Tanaka H, Tanaka T, Taniguchi T, Asahiro M, Okamoto K, Sogabe M, Miyamoto H, Muguruma N, Masaki T, Takayama T. Initial therapeutic results of atezolizumab plus bevacizumab for unresectable advanced hepatocellular carcinoma and the importance of hepatic functional reserve. *Cancer Med* 2023; **12**: 2646-2657 [PMID: 35964253 DOI: 10.1002/cam4.5145]

11 **Tzartzeva K**, Obi J, Rich NE, Parikh ND, Marrero JA, Yopp A, Waljee AK, Singal AG. Surveillance Imaging and Alpha Fetoprotein for Early Detection of Hepatocellular Carcinoma in Patients With Cirrhosis: A Meta-analysis. *Gastroenterology* 2018; **154**: 1706-1718.e1 [PMID: 29425931 DOI: 10.1053/j.gastro.2018.01.064]

12 **Oken MM**, Creech RH, Tormey DC, Horton J, Davis TE, McFadden ET, Carbone PP. Toxicity and response criteria of the Eastern Cooperative Oncology Group. *Am J Clin Oncol* 1982; **5**: 649-655 [PMID: 7165009]

13 **Lencioni R**, Llovet JM. Modified RECIST (mRECIST) assessment for hepatocellular carcinoma. *Semin Liver Dis* 2010; **30**: 52-60 [PMID: 20175033 DOI: 10.1055/s-0030-1247132]

14 **de Castro T**, Jochheim LS, Bathon M, Welland S, Scheiner B, Shmanko K, Roessler D, Ben Khaled N, Jeschke M, Ludwig JM, Marquardt JU, Weinmann A, Pinter M, Lange CM, Vogel A, Saborowski A. Atezolizumab and bevacizumab in patients with advanced hepatocellular carcinoma with impaired liver function and prior systemic therapy: a real-world experience. *Ther Adv Med Oncol* 2022; **14**: 17588359221080298 [PMID: 35251317 DOI: 10.1177/17588359221080298]

15 **Fulgenzi CAM**, Cheon J, D'Alessio A, Nishida N, Ang C, Marron TU, Wu L, Saeed A, Wietharn B, Cammarota A, Pressiani T, Personeni N, Pinter M, Scheiner B, Balcar L, Napolitano A, Huang YH, Phen S, Naqash AR, Vivaldi C, Salani F, Masi G, Bettinger D, Vogel A, Schönlein M, von Felden J, Schulze K, Wege H, Galle PR, Kudo M, Rimassa L, Singal AG, Sharma R, Cortellini A, Gaillard VE, Chon HJ, Pinato DJ. Reproducible safety and efficacy of atezolizumab plus bevacizumab for HCC in clinical practice: Results of the AB-real study. *Eur J Cancer* 2022; **175**: 204-213 [PMID: 36148739 DOI: 10.1016/j.ejca.2022.08.024]

16 **Himmelsbach V**, Pinter M, Scheiner B, Venerito M, Sinner F, Zimpel C, Marquardt JU, Trojan J, Waidmann O, Finkelmeier F. Efficacy and Safety of Atezolizumab and Bevacizumab in the Real-World Treatment of Advanced Hepatocellular Carcinoma: Experience from Four Tertiary Centers. *Cancers (Basel)* 2022; **14** [PMID: 35406493 DOI: 10.3390/cancers14071722]

17 **Miyagawa S**, Makuuchi M, Kawasaki S, Kakazu T. Criteria for safe hepatic resection. *Am J Surg* 1995; **169**: 589-594 [PMID: 7771622 DOI: 10.1016/s0002-9610(99)80227-x]

18 **Kudo M**. A New Era in Systemic Therapy for Hepatocellular Carcinoma: Atezolizumab plus Bevacizumab Combination Therapy. *Liver Cancer* 2020; **9**: 119-137 [PMID: 32399427 DOI: 10.1159/000505189]

World Journal of Gastrointestinal Oncology

Submit a Manuscript: https://www.f6publishing.com

World J Gastrointest Oncol 2023 October 15; 15(10): 1784-1795

DOI: 10.4251/wjgo.v15.i10.1784

ISSN 1948-5204 (online)

ORIGINAL ARTICLE

Retrospective Cohort Study

Association between the Khorana risk score and all-cause mortality in Japanese patients with gastric and colorectal cancer: A retrospective cohort study

Yu-Feng Zhang, Guo-Dong Wang, Min-Guang Huang, Zhao-Qi Qiu, Jia Si, Mao-Yi Xu

Specialty type: Oncology

Provenance and peer review: Unsolicited article; Externally peer reviewed.

Peer-review model: Single blind

Peer-review report's scientific quality classification

Grade A (Excellent): 0
Grade B (Very good): 0
Grade C (Good): C, C, C
Grade D (Fair): 0
Grade E (Poor): 0

P-Reviewer: Lieto E, Italy; Toyoshima O, Japan

Received: June 15, 2023
Peer-review started: June 15, 2023
First decision: August 7, 2023
Revised: August 21, 2023
Accepted: September 18, 2023
Article in press: September 18, 2023
Published online: October 15, 2023

Yu-Feng Zhang, Guo-Dong Wang, Min-Guang Huang, Zhao-Qi Qiu, Department of Oncology Radiotherapy, Zhuji Affiliated Hospital of Wenzhou Medical University, Zhuji 311800, Zhejiang Province, China

Jia Si, Department of Electrocardiography, Zhuji Affiliated Hospital of Wenzhou Medical University, Zhuji 311800, Zhejiang Province, China

Mao-Yi Xu, Department of Oncology, The First Hospital of Jiaxing (Affiliated Hospital of Jiaxing University), Jiaxing 314000, Zhejiang Province, China

Corresponding author: Mao-Yi Xu, MD, Doctor, Department of Oncology, The First Hospital of Jiaxing (Affiliated Hospital of Jiaxing University), No. 1882 South Central Road, Jiaxing 314000, Zhejiang Province, China. maoyixu1991@163.com

Abstract

BACKGROUND

The Khorana risk score (KRS) has poor predictive value for cancer-associated thrombosis in a single tumor type but is associated with early all-cause mortality from cancer. Evidence for the association between KRS and all-cause mortality in Japanese patients with gastric and colorectal cancer is limited.

AIM

To investigate whether KRS was independently related to all-cause mortality in Japanese patients with gastric and colorectal cancer after adjusting for other covariates and to shed light on its temporal validity.

METHODS

Data from Dryad database were used in this study. Patients in the Gastroenterology Department of Sapporo General Hospital, Sapporo, Japan, were enrolled. The starting and ending dates of the enrollment were January 1, 2008 and January 5, 2015, respectively. The cutoff date for follow-up was May 31, 2016. The independent and dependent (target) variables were the baseline measured using the KRS and final all-cause mortality, respectively. The KRS was categorized into three groups: Low-risk group (= 0 score), intermediate-risk group (1-2 score), and high-risk group (≥ 3 score).

RESULTS
Men and patients with Eastern Cooperative Oncology Group Performance Status (ECOG PS) ≥ 2 displayed a higher 2-year risk of death than women and those with ECOG PS 0-1 in the intermediate/high risk group for KRS. The higher the score, the higher the risk of early death; however, the relevance of this independent prediction decreased with longer survival. The overall survival of each patient was recorded *via* real-world follow-up and retrospective observations, and this study yielded the overall relationship between KRS and all-cause mortality.

CONCLUSION
The prechemotherapy baseline of KRS was independently associated with all-cause mortality within 2 years; however, this independent predictive relationship weakened as survival time increased.

Key Words: Gastric cancer; Colorectal cancer; Khorana risk score; All-cause mortality; Cancer-associated thrombosis; Overall survival

Core Tip: The Khorana risk score (KRS) has poor predictive value for cancer-associated thrombosis in a single tumor type but is associated with early all-cause mortality from cancer. In Japanese patients with gastric and colorectal cancer, the prechemotherapy baseline of KRS was independently associated with all-cause mortality within 2 years. The concept of time-sensitive management needs to be established for clinicians and community workers as well. The earlier the stratified intervention for patients with intermediate/high KRS, the more likely long-term survival benefit will be achieved.

Citation: Zhang YF, Wang GD, Huang MG, Qiu ZQ, Si J, Xu MY. Association between the Khorana risk score and all-cause mortality in Japanese patients with gastric and colorectal cancer: A retrospective cohort study. *World J Gastrointest Oncol* 2023; 15(10): 1784-1795
URL: https://www.wjgnet.com/1948-5204/full/v15/i10/1784.htm
DOI: https://dx.doi.org/10.4251/wjgo.v15.i10.1784

INTRODUCTION

In recent years, the incidence of and mortality associated with gastric and colorectal cancers have reached the top five positions in Japan[1]. Of late, the cure rate of tumors has been immensely improved owing to advancements in chemotherapy, targeted therapy, radiotherapy, immunotherapy, surgery and other therapeutic modalities. However, at the same time, several treatment-related complications have emerged. Cancer-associated thrombosis (CAT) is one of the most dangerous complications and is directly related to patient prognosis[2]. CAT includes arterial embolic events, such as stroke and myocardial infarction; venous embolic events, such as deep vein thrombosis; pulmonary embolism; and visceral venous thrombosis. The Khorana risk score (KRS) is a risk scoring tool developed by Khorana *et al*[3] and has been internally and externally validated for stratifying thrombotic risks in patients with cancer. The 2019 revision of the American Society of Clinical Oncology (ASCO) thrombosis guidelines also recommend the use of KRS[4]. Nevertheless, a 2018 systematic review observed that the score exhibited poor predictive power for individual tumor types, and unexpectedly, higher scores were associated with a higher risk of early death[5]. Some prospective studies have demonstrated its ability to predict early death in lung and colorectal cancers[6,7]. However, studies on the relationship between KRS and all-cause mortality are limited. In addition, investigations in Asian populations are especially lacking, and the follow-up observation time for predicting early mortality is not long, which does not exclude the possibility that KRS possesses the ability to predict long-term survival. Therefore, this study aimed to determine whether the KRS is independently associated with all-cause mortality in Japanese patients with gastric and colorectal cancer and to show its temporal validity.

MATERIALS AND METHODS

Study design

Patient's KRS obtained at baseline prior to chemotherapy served as the independent variable, and all-cause mortality (dichotomous variable: death = 1; survival = 0) served as the dependent (target) variable. The overall survival (OS) time of each patient was recorded as of May 31, 2016.

Study population

Data from the Dryad database were used in this study[8]. Patients in the Gastroenterology Department of Sapporo General Hospital, Sapporo, Japan, were enrolled. The starting and ending dates of the enrollment were January 1, 2008

and January 5, 2015, respectively. The cutoff date for follow-up was May 31, 2016. Complete inclusion/exclusion criteria, collection of patient history, and diagnostic methods for CAT have been described in the study by Aonuma *et al*[9]. The flowchart for the selection of the study cohort is depicted in Figure 1. The requirement for informed consent was waived owing to the retrospective nature of the study. The institutional review board of Affiliated Hospital of Jiaxing University approved this study.

Variables

The KRS at baseline before chemotherapy was obtained and recorded for stratification of categorical variables. The KRS is a predictive scoring system to determine the risk of venous thromboembolic events (VTE) in patients receiving chemotherapy and comprises five parameters: primary cancer site, platelet count, hemoglobin and/or erythropoietin use, white blood cell count, and body mass index (BMI). Patients were classified into three risk categories based on the total risk model: low-risk group (score = 0), intermediate-risk group (score = 1-2), and high-risk group (score = ≥ 3).

The following were selected as covariates: (1) Demographic data; (2) variables affecting the KRS or all-cause mortality have been reported in previous studies; and (3) variables based on our clinical experience. The full adjustment model was constructed using the following variables: (1) Continuous variables: age (obtained at baseline); (2) categorical variables: sex, CAT, arterial thromboembolism (ATE), Eastern Cooperative Oncology Group Performance Status (ECOG PS), cancer type [gastric cancer (GC); colorectal cancer (CRC)], pathological type, primary site surgery, adjuvant chemotherapy, single or multiple primary tumor, active cancer (AC), opportunity for diagnosis, central venous catheter (CVC) placement.

AC was defined as unresectable advanced gastric and colorectal tumors that recur during or after the completion of adjuvant chemotherapy and/or other unrelated malignancies. The opportunity for diagnosis was defined as the final clinical diagnosis of a patient based on the presentation of symptoms associated with CAT.

Based on the results of the retrospective and follow-up observations, the outcome variables for all-cause mortality (dichotomous variables) and OS were obtained. The term "all-cause mortality" refers to deaths due to any cause.

Treatment protocol

Patients diagnosed with GC and CRC were treated according to the then-current ASCO or National Comprehensive Cancer Network guidelines, and who developed CAT were administered anticoagulation therapy.

Statistical analysis

Categorical variables were expressed as frequency or percentage. Chi-squared (categorical variables, normal distribution) or Kruskal-Wallis *H* test (skewed distribution) were used to test for differences among different KRS groups (clinical cut point). Step 1: To examine the association between KRS and all-cause mortality, univariate and multivariate Cox proportional hazards models were employed. Four models were constructed: crude model, no covariates were adjusted; model 1: Only adjusted for sociodemographic data; model 2: Model 1 + those considerable covariates ($P < 0.10$ or having significant clinical significance); model 3: All covariates. To ensure the robustness of the experimental results, a sensitivity analysis was simultaneously performed by converting the KRS to categorical variables and calculating the trend in *P*-value. Step 2: Subgroup analyses were performed using the hierarchical Cox proportional hazards model. Continuous variables were initially converted to categorical variables according to the clinical cut point, and subsequently, an interaction test was performed. Tests for effect modification of subgroup indicators were followed by the likelihood ratio test. Step 3: The OS time of each group was recorded, and Kaplan-Meier (KM) survival curves were plotted to compare the median survival time of each group. Step 4: The multivariate Cox proportional hazards model was employed to calculate the risk ratios over a given number of years, and a trend graph was plotted. All analyses were performed using the statistical software packages R 3.3.2 (http://www.R-project.org, The R Foundation) and Free Statistics software version 1.7. A two-tailed test was performed and $P < 0.05$ was considered statistically significant.

RESULTS

Baseline characteristics of selected participants

A total of 500 participants were selected for the final data analysis (Figure 1 for the flow chart). Their median follow-up time was 22.0 mo. The baseline characteristics of these participants are listed in Table 1 based on the clinical grouping of the KRS. Their average age was 68.9 (62.5 ± 75.9) years, and 38.8% were women. There were 194 participants in the KRS low-risk group, 218 in the moderate-risk group, and 88 in the high-risk group. There were group differences among the three KRS groups in terms of cancer type, pathological type, primary site surgery, and CVC placement ($P < 0.001$); however, there were no statistically significant differences in terms of additional covariates (all *P* values > 0.05). Furthermore, it was observed that the number of patients with CVC placement ($n = 55$), primary site surgery ($n = 43$), well and mod pathological type ($n = 28$), and cancer type (CRC, $n = 5$) was lower in the KRS high-risk group than in the other groups. The final diagnosis of CAT was made in 70 (14%) of the 500 patients, of which 11 (2.2%) were diagnosed with ATE.

Univariate analysis

Results of the univariate analysis for mortality within 2 years are presented in Table 2. The univariate Cox proportional hazards model, revealed that sex, CAT, ATE, single or multiple primary tumor, thrombosis treatment, and opportunity

Table 1 Baseline characteristics of the study participants

Variables	Total, *n* = 500	Low-risk group, *n* = 194	Intermediate-risk group, *n* = 218	High-risk group, *n* = 88	*P* value
Age, median (IQR)	68.9 (62.5, 75.9)	69.1 (62.9, 75.2)	68.6 (62.6, 76.2)	69.0 (61.4, 76.8)	0.93
Sex, *n* (%)					0.459
Male	306 (61.2)	117 (60.3)	130 (59.6)	59 (67)	
Female	194 (38.8)	77 (39.7)	88 (40.4)	29 (33)	
CAT, *n* (%)					0.254
Non	430 (86.0)	161 (83)	190 (87.2)	79 (89.8)	
All CAT	70 (14.0)	33 (17)	28 (12.8)	9 (10.2)	
ATE	11 (2.2)	0 (0)	6 (2.8)	5 (5.7)	
ECOG PS, *n* (%)					0.053
0-1	449 (89.8)	181 (93.3)	194 (89)	74 (84.1)	
≥ 2	51 (10.2)	13 (6.7)	24 (11)	14 (15.9)	
Cancer type, *n* (%)					< 0.001
GC	206 (41.2)	0 (0)	123 (56.4)	83 (94.3)	
CRC	294 (58.8)	194 (100)	95 (43.6)	5 (5.7)	
Adjuvant chemotherapy, *n* (%)					0.069
No	306 (61.2)	111 (57.2)	132 (60.6)	63 (71.6)	
Yes	194 (38.8)	83 (42.8)	86 (39.4)	25 (28.4)	
Active cancer (AC), *n* (%)					0.201
Non-AC	141 (28.2)	57 (29.4)	66 (30.3)	18 (20.5)	
AC	359 (71.8)	137 (70.6)	152 (69.7)	70 (79.5)	
Single or multiple primary tumor, *n* (%)					0.95
Single	450 (90.0)	174 (89.7)	196 (89.9)	80 (90.9)	
Multiple	50 (10.0)	20 (10.3)	22 (10.1)	8 (9.1)	
Pathological type, *n* (%)					< 0.001
Well and mod	317 (63.4)	169 (87.1)	120 (55)	28 (31.8)	
Others	169 (33.8)	19 (9.8)	95 (43.6)	55 (62.5)	
Unknown	14 (2.8)	6 (3.1)	3 (1.4)	5 (5.7)	
Primary site surgery, *n* (%)					< 0.001
No	122 (24.4)	19 (9.8)	58 (26.6)	45 (51.1)	
Yes	378 (75.6)	175 (90.2)	160 (73.4)	43 (48.9)	
CVC placement, *n* (%)					< 0.001
No	168 (33.6)	46 (23.7)	89 (40.8)	33 (37.5)	
Yes	332 (66.4)	148 (76.3)	129 (59.2)	55 (62.5)	
Opportunity for Diagnosis, *n* (%)					0.714
Asymptomatic	495 (99.0)	193 (99.5)	215 (98.6)	87 (98.9)	
Symptomatic	5 (1.0)	1 (0.5)	3 (1.4)	1 (1.1)	
Thrombosis treatment, *n* (%)					0.424
No	470 (94.0)	179 (92.3)	207 (95)	84 (95.5)	
Yes	30 (6.0)	15 (7.7)	11 (5)	4 (4.5)	

CAT: Cancer associated thrombosis; ATE: Arterial thromboembolism; ECOG PS: Eastern Cooperative Oncology Group; GC: Gastric cancer; CRC: Colorectal cancer; AC: Active cancer; Well: Well-differentiated adenocarcinoma; Mod: Moderately differentiated adenocarcinoma; CVC: Central venous catheter; IQR: Interquartile range.

Table 2 Univariate analyses of all-cause death within 2 years

Variables	HR (95%CI)	*P* value
Age (≥ 65 yr *vs* < 65 yr)	1.22 (1.02-1.47)	0.034
KRS (intermediate *vs* low)	1.60 (1.21-2.13)	0.001
KRS (high *vs* low)	2.67 (1.91-3.73)	< 0.001
Sex (female *vs* male)	1.02 (0.79-1.30)	0.900
CAT (yes *vs* no)	1.01 (0.71-1.43)	0.965
ATE (yes *vs* no)	1.36 (0.60-3.05)	0.481
ECOG PS (≥ 2 *vs* 0-1)	4.05 (2.93-5.61)	< 0.001
Cancer type (CRC *vs* GC)	0.60 (0.47-0.76)	< 0.001
Pathological type (others *vs* well and mod)	1.53 (1.19-1.96)	< 0.001
Pathological type (unknown *vs* well and mod)	1.45 (0.68-3.09)	0.338
Primary site surgery (yes *vs* no)	0.30 (0.23-0.39)	< 0.001
Adjuvant chemotherapy (yes *vs* no)	0.28 (0.21-0.38)	< 0.001
Active cancer (yes *vs* no)	4.28 (2.94-6.24)	< 0.001
Multiple primary *vs* single primary	0.94 (0.62-1.44)	0.784
CVC placement (yes *vs* no)	1.92 (1.44-2.55)	< 0.001
Thrombosis treatment (yes *vs* no)	0.92 (0.56-1.53)	0.761
Opportunity for diagnosis (symptomatic *vs* asymptomatic)	1.57 (0.50-4.91)	0.436

KRS: Khorana risk score; CAT: Cancer associated thrombosis; ATE: Arterial thromboembolism; ECOG PS: Eastern Cooperative Oncology Group; GC: Gastric cancer; CRC: Colorectal cancer; Well: Well-differentiated adenocarcinoma; Mod: Moderately differentiated adenocarcinoma; CVC: Central venous catheter; HR: Hazard ratios; CI: Confidence intervals.

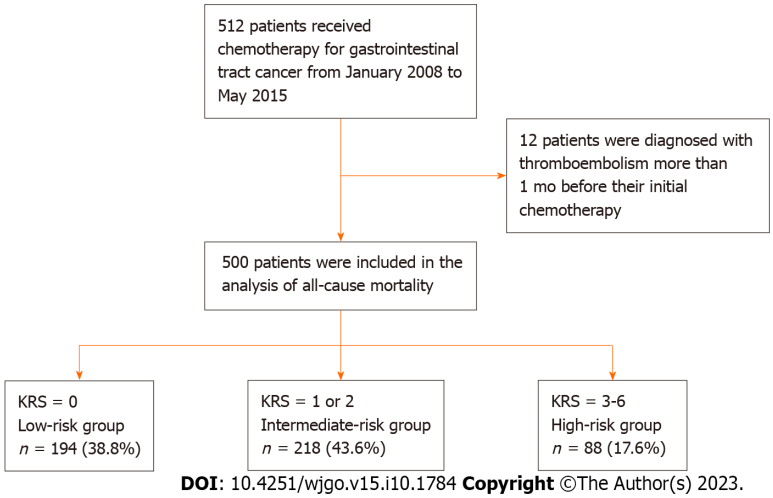

DOI: 10.4251/wjgo.v15.i10.1784

Figure 1 Flowchart depicting the patient selection process. KRS: Khorana risk score.

for diagnosis were not associated with all-cause mortality. Moreover, cancer type, primary site surgery, and adjuvant chemotherapy were negatively associated with all-cause mortality ($P < 0.001$). In contrast, univariate analysis indicated that age ($P = 0.034$), KRS intermediate/high-risk group, ECOG PS, pathological type (others *vs* well and mod), AC and CVC placement were positively correlated with all-cause mortality ($P < 0.001$).

Results of the unadjusted and adjusted Cox proportional hazards model

In this study, four models were constructed to analyze the independent effects of KRS on all-cause mortality within 2 years (univariate and multivariate Cox proportional hazards model). The effect sizes [hazard ratios (HRs) and their 95% confidence intervals (CIs)] are listed in Table 3. In the unadjusted model (crude mode), the model-based effect size can be explained as the difference in each group of KRS associated with risk of death. For example, in the unadjusted model, the effect size for all-cause mortality denotes the strength of the correlation between the KRS and the risk of death (KRS, intermediate *vs* low, HR: 1.6; 95%CI: 1.21-2.13; $P = 0.001$; KRS, high *vs* low, HR: 2.67; 95%CI: 1.91-3.73; $P < 0.001$). In the minimum-adjusted model (model 1), compared with the low-risk group, the medium-risk group demonstrated a 60% increased risk of all-cause death (95%CI: 1.20-2.12; $P = 0.001$), whereas the high-risk group exhibited a 2.64-fold increase (95%CI: 1.89-3.69; $P < 0.001$). Similar results were obtained for model 2 (adjusting for significant covariates) and model 3 (full adjustment), which indicated a 45% increased risk of death in the intermediate risk group compared with the low-risk group (95%CI: 1.02-2.06; $P = 0.041$). On the contrary, the high-risk group showed a two-fold increase (95%CI: 1.26-3.24; $P = 0.004$). For sensitivity analysis, the KRS was converted from a continuous variable to a categorical variable (clinical grouping of KRS). The p value of the trend test for the different models was < 0.05, which suggesting the same trend effect and stable study results (Table 3).

Subgroup analysis

Age, sex, cancer type, primary site surgery, ECOG PS, CVC placement, CAT were used as stratification variables to examine the trend of effect sizes in these variables (Figure 2). No interactions were seen in these variables based on our a priori specification (all P values for interaction < 0.05). In this study, a stronger association was detected in men (KRS, intermediate *vs* low, HR: 1.8; 95%CI: 1.06-3.03; KRS, high *vs* low, HR: 2.17; 95%CI: 1.04-4.51), and ECOG PS ≥ 2 (KRS, intermediate *vs* low, HR: 2.71; 95%CI: 1.04-7.04; KRS, high *vs* low, HR: 3.02; 95%CI: 0.89-10.28). In contrast, a weaker association was perceived in women (ECOG PS 0-1). Patients in the intermediate-risk group aged < 65 years exhibited a lower 2-year relative risk of death (HR: 1.33, 95%CI: 0.66-2.67) than those aged ≥ 65 years and other intermediate/high-risk groups, with a mortality rate of 45.2%. The KRS high-risk group showed a higher mortality rate regardless of cancer type (68.7% in GC and 80% in CRC). In addition, the risk of death was more than two times higher in the high-risk group than in the low-risk group for KRS regardless of surgeries in the primary tumor site (HR: 2.49; 95%CI: 1.31-4.73 in the operated group; HR: 2.13; 95%CI: 0.85-5.32 in the non-operated group). However, the risk of death was not higher with CAT in the KRS high-risk group than in the low-risk group (HR: 0.92, 95%CI: 0.17-4.9).

KM survival curves and risk ratio trend

Figure 3 depicts the KM curves of OS for different risk groups. The median OS for the three groups was 28.0 mo in the low-risk group, 20.0 mo in the intermediate-risk group, and 10.5 mo in the high-risk group ($P < 0.001$). Furthermore, the mortality was higher in the intermediate/high-risk group with KRS in the early/middle period. Nevertheless, all three curves converged as the survival time increased, which suggested that the relationship between KRS and all-cause mortality was unknown at later times. To further test this idea, the OS time was categorized into specific periods, and a separate multivariate Cox proportional hazards model was constructed to plot the trend of risk ratio (Figure 4). The findings indicated that the risk of death within 6 mo was 2.17 times higher in the KRS intermediate-risk group than in the low-risk group (95%CI: 1.01-4.67; $P = 0.047$) and 2.37 times higher in the KRS high-risk group than in the low-risk group (95%CI: 0.89-3.29; $P = 0.083$). At the same time, the risk of death within 2 years was 1.45 times higher in the intermediate-risk group than in the low-risk group (95%CI: 1.02-2.06; $P = 0.041$) and 2.02 times higher in the high-risk group than in the low-risk group (95%CI: 1.26-3.24; $P = 0.004$). Subsequent risk ratios decreased gradually over 3, 5, and 8 years and at $P > 0.05$.

DISCUSSION

The findings from this study indicated that the KRS was independently associated with all-cause mortality within 2 years in Japanese patients with GC and CRC before receiving chemotherapy. Subgroup analysis aided in better understanding the trend of KRS and all-cause mortality in different populations. Men and patients with ECOG PS ≥ 2 displayed a higher 2-year risk of death than women and those with ECOG PS 0-1 in the intermediate/high risk group for KRS. Hence, the higher the score, the higher the risk of early death; however, the relevance of this independent prediction decreased with longer survival. The OS of each patient was recorded *via* real-world follow-up and retrospective observations, and this study yielded the overall relationship between KRS and all-cause mortality, which provides a good guide for future prospective studies.

A multivariate Cox proportional hazards model was constructed based on various factors associated with the prognosis of patients with GC and CRC, including age, CAT, cancer type, ECOG PS, primary site surgery, adjuvant chemotherapy, active cancer and CVC placement. The findings pointed to the presence of an independent predictive relationship between baseline KRS before chemotherapy and death within 2 years in patients with GC and CRC. This result is comparable to a global prospective study by Sohal *et al*[7], which observed that KRS predicted mortality within 6

Table 3 Multivariate analysis of the association between Khorana risk score and all-cause death within 2 years

Variable	Crude mode		Multivariable-adjusted model 1		Multivariable-adjusted model 2		Multivariable-adjusted model 3	
	HR (95%CI)	*P* value	HR (95%CI)	*P* value	HR (95%CI)	*P* value	HR (95%CI)	*P* value
Trend test[1]	1.63 (1.38-1.93)	< 0.001	1.62 (1.37-1.92)	< 0.001	1.39 (1.10-1.76)	0.005	1.42 (1.12-1.8)	0.004
KRS, low-risk group	1 (Ref)		1 (Ref)		1 (Ref)		1 (Ref)	
KRS, intermediate-risk group	1.6 (1.21-2.13)	0.001	1.6 (1.20-2.12)	0.001	1.43 (1.00-2.04)	0.047	1.45 (1.02-2.06)	0.041
KRS, high-risk group	2.67 (1.91-3.73)	< 0.001	2.64 (1.89-3.69)	< 0.001	1.95 (1.22-3.12)	0.005	2.02 (1.26-3.24)	0.004

[1]A test for linear trend was performed for each model.

Multivariable-adjusted model 1: Adjusted for age and sex; Multivariable-adjusted model 2: Adjusted for age, sex, cancer-associated thrombosis (CAT), Eastern Cooperative Oncology Group (ECOG PS), cancer type, primary site surgery, adjuvant chemotherapy, active cancer and central venous catheter (CVC); Multivariable-adjusted model 3: Adjusted for age, sex, CAT, ECOG PS, cancer type, pathological type, primary site surgery, adjuvant chemotherapy, active cancer, single or multiple primary, CVC, thrombosis treatment, opportunity for diagnosis. KRS: Khorana risk score; HR: Hazard ratios; CI: Confidence intervals.

mo in patients with CRC treated using chemotherapy. Moreover, similar findings have been reported for different tumor types in studies by Shibata *et al*[10], Kuderer *et al*[11], Mansfield *et al*[12], and Vathiotis *et al*[13]. Without emphasizing the length of the observations, their conclusions agree with the findings from this study. However, all of their follow-up observations were short or had limited sample sizes, and therefore none of the results indicated the dynamic trends in baseline KRS and mortality in patients with tumors.

Using univariate regression analysis, a study by Salazar Adum *et al*[14] showed that KRS predicted death in various cancer types, but additional Cox multifactorial analysis indicated the lack of an independent correlation between the two (with a maximum observation period of 25 mo). This parallel comparison confirmed our question about the time frame in which KRS predicts death. Another study demonstrated that KRS did not accurately identify patients with lung cancer who were at an elevated risk for VTE but predicted lung cancer mortality. This study noted a predictive relationship between KRS and long-term survival (180 mo) using KM survival curves but failed to perform additional multivariate Cox regression analysis. Merely based on the trend of KM survival curves, the study found that KRS was significantly associated with death within 2 years, and the grouping curves converged as the survival time increased[12]. Another study that analyzed a large population from the NHIS-HEALS database observed that maintaining hemoglobin levels in the normal range was associated with a reduction in all-cause mortality[15]. It is therefore hypothesized that the possible cause of the time effect is the survival benefit offered by early and timely intervention in the intermediate/high risk group of KRS.

Subgroup analysis performed in this study revealed that men and those with ECOG PS ≥ 2 for GC and CRC belonging to the intermediate/high risk group of KRS exhibited a higher risk of mortality. This elevated risk may be due to the higher number of smokers among men, which has been shown to exacerbate the risk of CRC mortality by 9.8% compared with nonsmokers in a large case–control study[16]. It is well known that lower ECOG PS signifies shorter survival for patients with tumor. However, ECOG PS ≥ 2 was also an unfavorable factor for survival in the GC and CRC population in this study (ECOG PS ≥ 2 *vs* 0-1, HR: 4.05; 95%CI: 2.93-5.61, $P < 0.001$), which might exert a dual effect with intermediate/high KRS, implying that this population requires special attention from clinicians for early intervention. Further analysis revealed that primary site surgery did not alleviate the 2-year risk of death in the KRS intermediate/high-risk group (KRS, intermediate *vs* low, HR: 1.57; 95%CI: 1.04-2.37; KRS, high *vs* low, HR: 2.49; 95%CI: 1.31-4.73; *P* for interaction = 0.675). This finding is related to the five parameters comprising the KRS.

A large retrospective study by the Japanese Association of Clinical Cancer Centers reported a higher 5-year survival rate of 72.2% for patients with colon cancer (5054 patients) than the rate of 68.7% for those with GC (15353 patients)[17], which is consistent with our findings (cancer type CRC *vs* GC, HR: 0.60; 95%CI: 0.47-0.76, $P < 0.001$). In addition, the KRS was higher for GC, which suggests that this score predicts death and CAT shares the same pathophysiological features. Several studies have proved that anemia is associated with local recurrence-free survival, recurrence-free survival, and OS not only in GC[18] and CRC[19] but also in other cancers, such as lung, breast, head and neck, and bladder cancer[20-25]. Furthermore, leukocytosis and thrombocytosis, which imply a physiologic inflammatory response, are associated with lower survival in patients with CRC, lung and cervical cancers[19,26-28]. The second World Cancer Research Fund/American Institute for Cancer Research indicated that CRC is strongly associated with obesity[29]. Another meta-analysis that pooled several prospective studies observed that class II/III obesity (BMI ≥ 35 kg/m^2) was linked to significantly increased all-cause mortality from CRC[30].

Interestingly, our study did not identify a correlation between the occurrence of CAT and OS in this population (CAT yes *vs* no, HR: 1.22; 95%CI: 0.95-1.58, $P = 0.119$). This discrepancy could be attributed to limitations in screening equipment and follow-up, which make it impossible to confirm the diagnosis in all patients who developed CAT in the clinic, which resulted in an underestimation of its incidence. This finding is in contrast to the study by Fuentes *et al*[31], which signified that VTE was an independent predictor of mortality in patients with GC (112 cases). However, because their results were not subjected to additional multivariate Cox regression analysis and sensitivity analysis, further

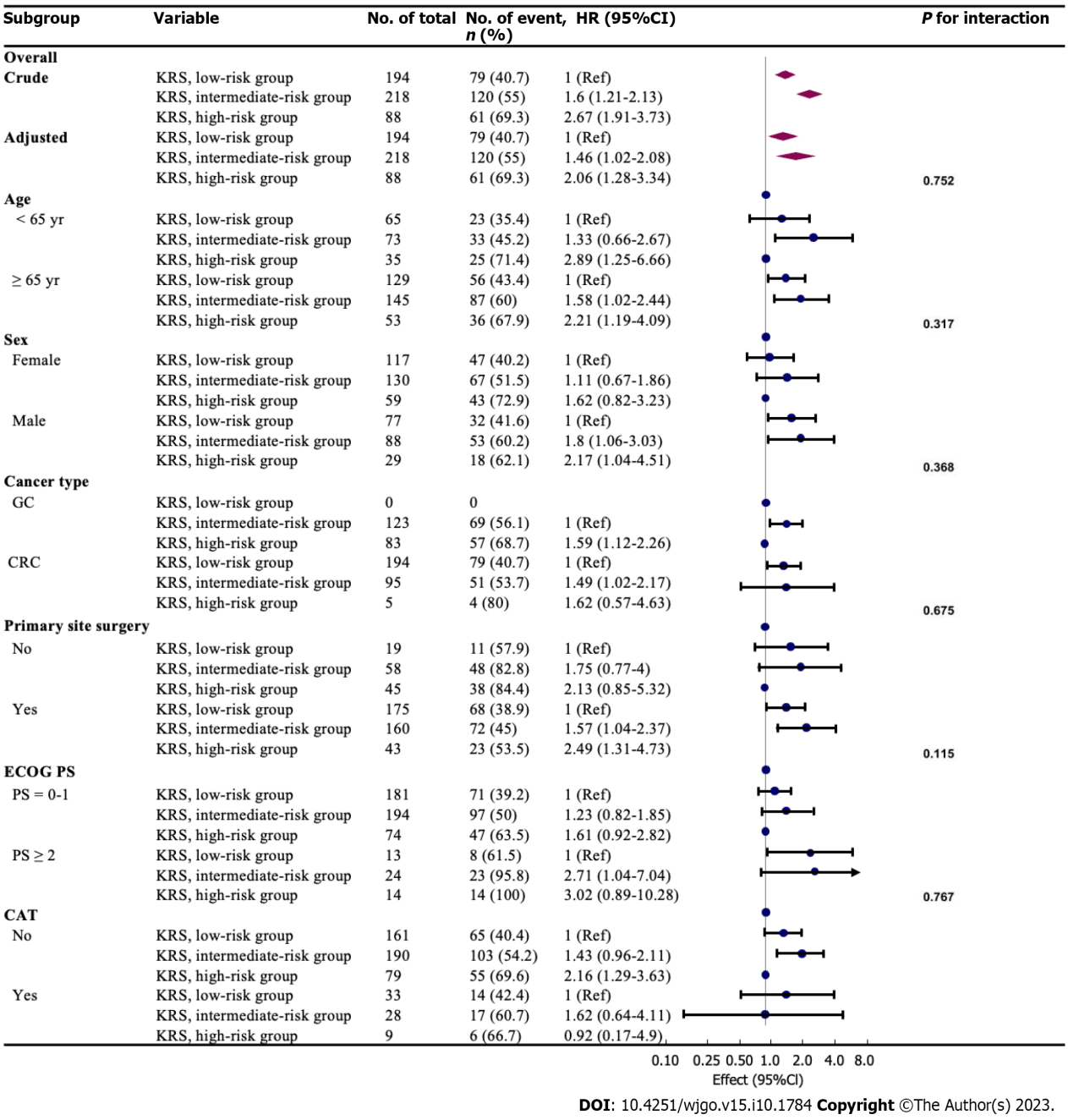

DOI: 10.4251/wjgo.v15.i10.1784

Figure 2 Stratified analyses of the association between Khorana risk score and all-cause death within 2 years in accordance to baseline characteristics. The *P* value for interaction represents the likelihood of interaction between the variable and Khorana risk score. KRS: Khorana risk score; CAT: Cancer-associated thrombosis; ECOG PS: Eastern Cooperative Oncology Group; GC: Gastric cancer; CRC: Colorectal cancer; HR: Hazard ratios; CI: Confidence intervals.

validation is required. In another study, the incidence of CAT in patients with CRC was highest in the first 6 mo after diagnosis and declined rapidly thereafter. CAT reduces survival in patients with local or regional disease[32]. Not coincidentally, in a prospective multi-cancer study involving 2488 patients in the United States, CAT was associated with lower survival rates in different KRS subgroups[33]. Overall, the relationship between CAT and mortality in gastrointestinal tumors needs to be investigated further.

The clinical values of this study are as follows: (1) To the best of our knowledge, the first independent correlation and time sensitivity between KRS and all-cause mortality was observed in Japanese patients with stomach and colorectal cancer.; (2) It may guide the follow-up time issue in relevant prospective studies and improve the economic efficacy; (3) It will be helpful for health care professionals working in the clinic to give stratified management of cancer patients in a specific time period and to establish a time-efficient management concept, *i.e.*, the earlier the intervention for blood picture and BMI, the higher the survival benefit is likely to be; and (4) The results of this study will contribute to additional research on what survival benefits this intervention provides to patients with stomach and colorectal cancer, as well as the development of future all-cause mortality prediction models.

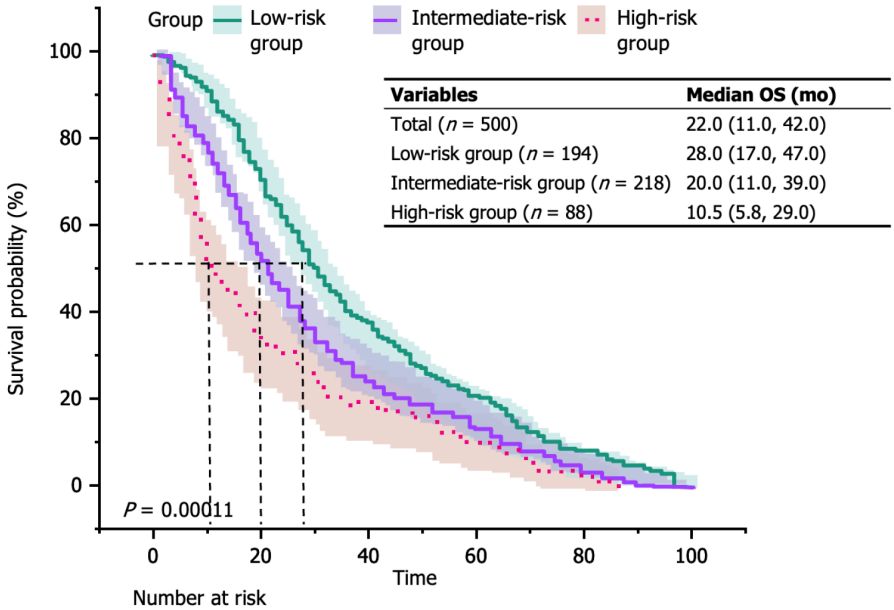

Variables	Median OS (mo)
Total (n = 500)	22.0 (11.0, 42.0)
Low-risk group (n = 194)	28.0 (17.0, 47.0)
Intermediate-risk group (n = 218)	20.0 (11.0, 39.0)
High-risk group (n = 88)	10.5 (5.8, 29.0)

Number at risk						
Low-risk group	194	132	62	32	10	1
Intermediate-risk group	218	114	54	31	10	0
High-risk group	88	29	17	9	2	0

DOI: 10.4251/wjgo.v15.i10.1784

Figure 3 The Kaplan-Meier curves of overall survival in different risk groups. The median overall survival for the three groups was 28.0 mo in the low-risk group, 20.0 mo in the intermediate-risk group, and 10.5 mo in the high-risk group (P < 0.001). OS: Overall survival.

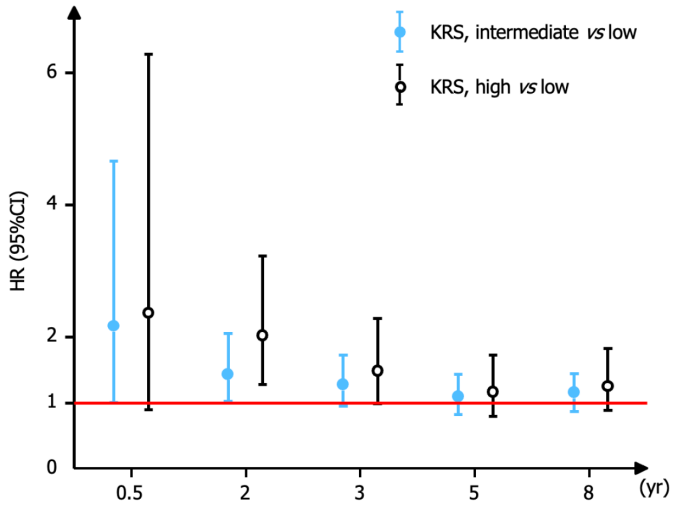

HR (95%CI)	KRS, intermediate *vs* low	2.17 (1.01-4.67)	1.45 (1.02-2.06)	1.28 (0.94-1.74)	1.09 (0.83-1.45)	1.14 (0.88-1.47)
	KRS, high *vs* low	2.37 (0.89-3.29)	2.02 (1.26-3.24)	1.50 (0.98-2.29)	1.16 (0.78-1.73)	1.26 (0.87-1.83)
P value	KRS, intermediate *vs* low	0.047	0.041	0.113	0.534	0.310
	KRS, high *vs* low	0.083	0.004	0.062	0.452	0.215

DOI: 10.4251/wjgo.v15.i10.1784

Figure 4 A multivariable-adjusted Cox proportional hazards models was applied to observe the mortality risk ratio over a given number of years. Multivariable-adjusted Cox proportional hazards models: Adjusted for age, sex, cancer-associated thrombosis, Eastern Cooperative Oncology Group, cancer type, pathological type, primary site surgery, adjuvant chemotherapy, active cancer, single or multiple primary, central venous catheter, thrombosis treatment, opportunity for diagnosis. The graph depicts the risk ratios and their trends across different years. KRS: Khorana risk score; HR: Hazards ratio.

This study has several advantages: (1) The sample size was larger compared with previous similar studies; (2) This study observed and recorded the OS of each patient with GC and CRC in Japan and analyzed it entirely as well as by time period; (3) This study is the first to explain the temporal validity of KRS at the baseline in predicting cancer-related mortality; and (4) The effect modifier factor analysis enhanced the use of data and yielded stable conclusions in different models and subgroups.

However, there are certain limitations in this study: (1) This research was a retrospective observational cohort study with selection bias and bias for unknown confounders, which might have affected the findings; (2) The study population comprised Japanese patients with gastrointestinal tract tumors. Therefore, generalizability and extrapolation of the results are somewhat lacking; (3) Regarding the time effect of KRS in predicting mortality, only the approximate period could be derived and not the exact time; and (4) As patients in whom CAT occurred > 1 mo before the start of chemotherapy were excluded, the results cannot be applied to these individuals.

CONCLUSION

In Japanese patients with GC and CRC, the prechemotherapy baseline of KRS was independently associated with all-cause mortality within 2 years; however, this independent predictive relationship decreased as survival time increased.

ARTICLE HIGHLIGHTS

Research background

The incidence of and mortality associated with gastric and colorectal cancers have reached the top five positions in Japan. Cancer-associated thrombosis is one of the most dangerous complications and is directly related to patient prognosis. The Khorana risk score (KRS) is a risk scoring tool and has been internally and externally validated for stratifying thrombotic risks in patients with cancer.

Research motivation

Studies on the relationship between KRS and all-cause mortality are limited. In addition, investigations in Asian populations are especially lacking, and the follow-up observation time for predicting early mortality is not long, which does not exclude the possibility that KRS possesses the ability to predict long-term survival.

Research objectives

We performed a retrospective analysis to investigate whether KRS was independently related to all-cause mortality in Japanese patients with gastric and colorectal cancer after adjusting for other covariates and to shed light on its temporal validity.

Research methods

This retrospective study was conducted using data from the Dryad database. Patient's KRS obtained at baseline prior to chemotherapy served as the independent variable, and all-cause mortality (dichotomous variable: Death = 1; survival = 0) served as the dependent (target) variable. The KRS was categorized into three groups: low-risk group, intermediate-risk group, and high-risk group. All analyses were performed using the statistical software packages R 3.3.2 and Free Statistics software version 1.7.

Research results

In our study, a total of 500 participants were selected for the final data analysis . Their median follow-up time was 22.0 mo. The average age was 68.9 (62.5 ± 75.9) years, and 38.8% were women. There were 194 participants in the KRS low-risk group, 218 in the moderate-risk group, and 88 in the high-risk group. The risk of death within 6 mo was 2.17 times higher in the KRS intermediate-risk group than in the low-risk group (95%CI: 1.01-4.67; $P = 0.047$) and 2.37 times higher in the KRS high-risk group than in the low-risk group (95%CI: 0.89-3.29; $P = 0.083$). At the same time, the risk of death within 2 years was 1.45 times higher in the intermediate-risk group than in the low-risk group (95%CI: 1.02-2.06; $P = 0.041$) and 2.02 times higher in the high-risk group than in the low-risk group (95%CI: 1.26-3.24; $P = 0.004$). Men and patients with Eastern Cooperative Oncology Group Performance Status (ECOG PS) ≥ 2 displayed a higher 2-year risk of death than women and those with ECOG PS 0-1 in the intermediate/high risk group for KRS.

Research conclusions

The overall survival of each patient was recorded *via* real-world follow-up and retrospective observations, and this study yielded the overall relationship between KRS and all-cause mortality. In Japanese patients with gastric and colorectal cancer, the prechemotherapy baseline of KRS was independently associated with all-cause mortality within 2 years. The higher the score, the higher the risk of early death; however, the relevance of this independent prediction decreased with longer survival.

Research perspectives

A concept of time-sensitive management needs to be established for clinicians and community workers as well, i.e., the earlier the stratified intervention for patients with intermediate/high KRS, the more likely long-term survival benefit will be achieved. Further study with large sample size and more comprehensive prognostic information is desired to verify our findings.

ACKNOWLEDGEMENTS

The authors thank all the staff members of our institution. We are grateful to Dr. Liu L of Department of Vascular and Endovascular Surgery, Chinese PLA General Hospital for his contribution to the statistical support, study design consultations, and comments regarding the manuscript.

FOOTNOTES

Author contributions: Xu MY contributed to the study design and manuscript composition; Zhang YF and Si J helped to perform and check the statistical analysis; Qiu ZQ contributed to data collection and analysis; Wang GD and Huang MG contributed to proofreading and final approval of the article.

Supported by the Key Medical Disciplines Jointly Established by the Zhejiang Province and Jiaxing City: Oncology, No. 2023-SSGJ-001; and Jiaxing Key Laboratory of Tumor Radiotherapy, No. 2021-zlzdsys.

Institutional review board statement: The institutional review board of Affiliated Hospital of Jiaxing University approved this study (Approval No. 2023-LY-244).

Informed consent statement: Patients were not required to give informed consent to the study because the analysis used anonymous clinical data that were obtained after each patient agreed to treatment by written consent.

Conflict-of-interest statement: The authors declare no conflicts of interest.

Data sharing statement: Participants gave informed consent for data sharing.

STROBE statement: The authors have read the STROBE Statement—checklist of items, and the manuscript was prepared and revised according to the STROBE Statement—checklist of items.

Country/Territory of origin: China

ORCID number: Mao-Yi Xu 0000-0001-8532-5370.

S-Editor: Yan JP
L-Editor: A
P-Editor: Zhang XD

REFERENCES

1 **Foundation for Promotion of Cancer Research**. Cancer statistics in Japan-2021. [cited 2022 Nov 27]. Available from: http://ganjoho.jp/reg_stat/statistics/stat/summary.html
2 **Khorana AA**, Francis CW, Culakova E, Kuderer NM, Lyman GH. Thromboembolism is a leading cause of death in cancer patients receiving outpatient chemotherapy. *J Thromb Haemost* 2007; **5**: 632-634 [PMID: 17319909 DOI: 10.1111/j.1538-7836.2007.02374.x]
3 **Khorana AA**, Kuderer NM, Culakova E, Lyman GH, Francis CW. Development and validation of a predictive model for chemotherapy-associated thrombosis. *Blood* 2008; **111**: 4902-4907 [PMID: 18216292 DOI: 10.1182/blood-2007-10-116327]
4 **Key NS**, Khorana AA, Kuderer NM, Bohlke K, Lee AYY, Arcelus JI, Wong SL, Balaban EP, Flowers CR, Francis CW, Gates LE, Kakkar AK, Levine MN, Liebman HA, Tempero MA, Lyman GH, Falanga A. Venous Thromboembolism Prophylaxis and Treatment in Patients With Cancer: ASCO Clinical Practice Guideline Update. *J Clin Oncol* 2020; **38**: 496-520 [PMID: 31381464 DOI: 10.1200/JCO.19.01461]
5 **Khorana AA**, Francis CW. Risk prediction of cancer-associated thrombosis: Appraising the first decade and developing the future. *Thromb Res* 2018; **164** Suppl 1: S70-S76 [PMID: 29395243 DOI: 10.1016/j.thromres.2018.01.036]
6 **Kuderer NM**, Poniewierski MS, Culakova E, Lyman GH, Khorana AA, Pabinger I, Agnelli G, Liebman HA, Vicaut E, Meyer G, Shepherd FA. Predictors of Venous Thromboembolism and Early Mortality in Lung Cancer: Results from a Global Prospective Study (CANTARISK). *Oncologist* 2018; **23**: 247-255 [PMID: 28951500 DOI: 10.1634/theoncologist.2017-0205]
7 **Sohal DPS**, Kuderer NM, Shepherd FA, Pabinger I, Agnelli G, Liebman HA, Meyer G, Kalady MF, McCrae K, Lyman GH, Khorana AA. Clinical Predictors of Early Mortality in Colorectal Cancer Patients Undergoing Chemotherapy: Results From a Global Prospective Cohort Study. *JNCI Cancer Spectr* 2017; **1**: pkx009 [PMID: 31360835 DOI: 10.1093/jncics/pkx009]
8 **Aonuma AO**, Nakamura M, Sakamaki K, Murai T, Matsuda C, Itaya K, Sone T, Yagisawa M, Koike Y, Endo A, Tsukuda Y, Ono Y, Nagasaka A, Nishikawa S, Yamanaka T, Sakamoto N. Data from: Incidence of cancer-associated thromboembolism in Japanese gastric and colorectal cancer patients receiving chemotherapy: a single-institutional retrospective cohort analysis (Sapporo CAT study) [Dataset]. Dryad. 2019. Available from: https://doi.org/10.5061/dryad.84s01sv

9 **Aonuma AO**, Nakamura M, Sakamaki K, Murai T, Matsuda C, Itaya K, Sone T, Yagisawa M, Koike Y, Endo A, Tsukuda Y, Ono Y, Nagasaka A, Nishikawa S, Yamanaka T, Sakamoto N. Incidence of cancer-associated thromboembolism in Japanese gastric and colorectal cancer patients receiving chemotherapy: a single-institutional retrospective cohort analysis (Sapporo CAT study). *BMJ Open* 2019; **9**: e028563 [PMID: 31439602 DOI: 10.1136/bmjopen-2018-028563]

10 **Shibata K**, Tokushige A, Imamura M, Ikeda Y, Ohishi M. Evaluating the Khorana risk score of gastrointestinal cancer patients during initial chemotherapy as a predictor of patient mortality: A retrospective study. *J Cardiol* 2022; **79**: 655-663 [PMID: 34924239 DOI: 10.1016/j.jjcc.2021.11.024]

11 **Kuderer NM**, Culakova E, Lyman GH, Francis C, Falanga A, Khorana AA. A Validated Risk Score for Venous Thromboembolism Is Predictive of Cancer Progression and Mortality. *Oncologist* 2016; **21**: 861-867 [PMID: 27125754 DOI: 10.1634/theoncologist.2015-0361]

12 **Mansfield AS**, Tafur AJ, Wang CE, Kourelis TV, Wysokinska EM, Yang P. Predictors of active cancer thromboembolic outcomes: validation of the Khorana score among patients with lung cancer. *J Thromb Haemost* 2016; **14**: 1773-1778 [PMID: 27273134 DOI: 10.1111/jth.13378]

13 **Vathiotis I**, Dimakakos EP, Boura P, Ntineri A, Charpidou A, Gerotziafas G, Syrigos K. Khorana Score: New Predictor of Early Mortality in Patients With Lung Adenocarcinoma. *Clin Appl Thromb Hemost* 2018; **24**: 1347-1351 [PMID: 29806470 DOI: 10.1177/1076029618777153]

14 **Salazar Adum JP**, Diaz Quintero L, Fuentes HE, Lind BB, Caprini JA, Tafur AJ. Predictors of active cancer thromboembolic outcomes: mortality associated with calf deep vein thrombosis. *Int Angiol* 2017; **36**: 553-557 [PMID: 28541021 DOI: 10.23736/S0392-9590.17.03846-9]

15 **Lee G**, Choi S, Kim K, Yun JM, Son JS, Jeong SM, Kim SM, Park SM. Association of Hemoglobin Concentration and Its Change With Cardiovascular and All-Cause Mortality. *J Am Heart Assoc* 2018; **7** [PMID: 29378732 DOI: 10.1161/JAHA.117.007723]

16 **Hou L**, Jiang J, Liu B, Nasca PC, Wu Y, Zou X, Han W, Chen Y, Zhang B, Xue F, Pang H, Li J. Association between smoking and deaths due to colorectal malignant carcinoma: a national population-based case-control study in China. *Br J Cancer* 2014; **110**: 1351-1358 [PMID: 24481400 DOI: 10.1038/bjc.2014.9]

17 **Okamoto N**, Saruki N, Mikami H, Yamashita K, Maruyama Y, Yano T, Imamura Y, Kaneko S, Tanaka H. 5-year survival rates for primary cancer sites at cancer-treatment-oriented hospitals in Japan. *Asian Pac J Cancer Prev* 2006; **7**: 46-50 [PMID: 16629514]

18 **Shen JG**, Cheong JH, Hyung WJ, Kim J, Choi SH, Noh SH. Pretreatment anemia is associated with poorer survival in patients with stage I and II gastric cancer. *J Surg Oncol* 2005; **91**: 126-130 [PMID: 16028285 DOI: 10.1002/jso.20272]

19 **Qiu MZ**, Yuan ZY, Luo HY, Ruan DY, Wang ZQ, Wang FH, Li YH, Xu RH. Impact of pretreatment hematologic profile on survival of colorectal cancer patients. *Tumour Biol* 2010; **31**: 255-260 [PMID: 20336401 DOI: 10.1007/s13277-010-0024-x]

20 **Yovino S**, Kwok Y, Krasna M, Bangalore M, Suntharalingam M. An association between preoperative anemia and decreased survival in early-stage non-small-cell lung cancer patients treated with surgery alone. *Int J Radiat Oncol Biol Phys* 2005; **62**: 1438-1443 [PMID: 16029805 DOI: 10.1016/j.ijrobp.2004.12.038]

21 **Zhang Y**, Chen Y, Chen D, Jiang Y, Huang W, Ouyang H, Xing W, Zeng M, Xie X, Zeng W. Impact of preoperative anemia on relapse and survival in breast cancer patients. *BMC Cancer* 2014; **14**: 844 [PMID: 25406979 DOI: 10.1186/1471-2407-14-844]

22 **Zhu W**, Xu B. Association of Pretreatment Anemia with Pathological Response and Survival of Breast Cancer Patients Treated with Neoadjuvant Chemotherapy: A Population-Based Study. *PLoS One* 2015; **10**: e0136268 [PMID: 26291454 DOI: 10.1371/journal.pone.0136268]

23 **Dietl B**, Marienhagen J, Schäfer C, Kölbl O. The prognostic value of anaemia at different treatment times in patients with locally advanced head and neck cancer treated with surgery and postoperative radiotherapy. *Clin Oncol (R Coll Radiol)* 2007; **19**: 228-233 [PMID: 17433968 DOI: 10.1016/j.clon.2007.02.009]

24 **Gorphe P**, Bouhir S, Garcia GCTE, Alali A, Even C, Breuskin I, Tao Y, Janot F, Bidault F, Temam S. Anemia and neutrophil-to-lymphocyte ratio in laryngeal cancer treated with induction chemotherapy. *Laryngoscope* 2020; **130**: E144-E150 [PMID: 31006874 DOI: 10.1002/lary.28021]

25 **Chen C**, Hu L, Li X, Hou J. Preoperative Anemia as a Simple Prognostic Factor in Patients with Urinary Bladder Cancer. *Med Sci Monit* 2017; **23**: 3528-3535 [PMID: 28723884 DOI: 10.12659/msm.902855]

26 **Tomita M**, Shimizu T, Hara M, Ayabe T, Onitsuka T. Preoperative leukocytosis, anemia and thrombocytosis are associated with poor survival in non-small cell lung cancer. *Anticancer Res* 2009; **29**: 2687-2690 [PMID: 19596947]

27 **Kang S**, Wu J, Li J, Hou Q, Tang B. Prognostic Significance of Clinicopathological Factors Influencing Overall Survival and Event-Free Survival of Patients with Cervical Cancer: A Systematic Review and Meta-Analysis. *Med Sci Monit* 2022; **28**: e934588 [PMID: 35260545 DOI: 10.12659/MSM.934588]

28 **Holgersson G**, Sandelin M, Hoye E, Bergström S, Henriksson R, Ekman S, Nyman J, Helsing M, Friesland S, Holgersson M, Lundström KL, Janson C, Birath E, Mörth C, Blystad T, Ewers SB, Löden B, Bergqvist M. Swedish lung cancer radiation study group: the prognostic value of anaemia, thrombocytosis and leukocytosis at time of diagnosis in patients with non-small cell lung cancer. *Med Oncol* 2012; **29**: 3176-3182 [PMID: 22565809 DOI: 10.1007/s12032-012-0247-3]

29 **Wiseman M**. The second World Cancer Research Fund/American Institute for Cancer Research expert report. Food, nutrition, physical activity, and the prevention of cancer: a global perspective. *Proc Nutr Soc* 2008; **67**: 253-256 [PMID: 18452640 DOI: 10.1017/S002966510800712X]

30 **Doleman B**, Mills KT, Lim S, Zelhart MD, Gagliardi G. Body mass index and colorectal cancer prognosis: a systematic review and meta-analysis. *Tech Coloproctol* 2016; **20**: 517-535 [PMID: 27343117 DOI: 10.1007/s10151-016-1498-3]

31 **Fuentes HE**, Oramas DM, Paz LH, Wang Y, Andrade XA, Tafur AJ. Venous Thromboembolism Is an Independent Predictor of Mortality Among Patients with Gastric Cancer. *J Gastrointest Cancer* 2018; **49**: 415-421 [PMID: 28634671 DOI: 10.1007/s12029-017-9981-2]

32 **Alcalay A**, Wun T, Khatri V, Chew HK, Harvey D, Zhou H, White RH. Venous thromboembolism in patients with colorectal cancer: incidence and effect on survival. *J Clin Oncol* 2006; **24**: 1112-1118 [PMID: 16505431 DOI: 10.1200/JCO.2005.04.2150]

33 **Khorana AA**, Kuderer NM, McCrae K, Milentijevic D, Germain G, Laliberté F, MacKnight SD, Lefebvre P, Lyman GH, Streiff MB. Cancer associated thrombosis and mortality in patients with cancer stratified by khorana score risk levels. *Cancer Med* 2020; **9**: 8062-8073 [PMID: 32954653 DOI: 10.1002/cam4.3437]

World Journal of Gastrointestinal Oncology

Submit a Manuscript: https://www.f6publishing.com

World J Gastrointest Oncol 2023 October 15; 15(10): 1796-1806

DOI: 10.4251/wjgo.v15.i10.1796

ISSN 1948-5204 (online)

ORIGINAL ARTICLE

Retrospective Study

Real-world clinical effectiveness of sorafenib among patients with unresectable hepatocellular carcinoma at two centers in the United States

Daneng Li, Stephen B Gruber, Shrividya Iyer, Sanjay Gupta, Mohamedtaki Tejani

Specialty type: Oncology

Provenance and peer review: Unsolicited article; Externally peer reviewed.

Peer-review model: Single blind

Peer-review report's scientific quality classification

Grade A (Excellent): 0
Grade B (Very good): B, B
Grade C (Good): C
Grade D (Fair): 0
Grade E (Poor): 0

P-Reviewer: Li YW, China; Shomura M, Japan; Zhang XF, China

Received: May 31, 2023
Peer-review started: May 31, 2023
First decision: June 26, 2023
Revised: July 7, 2023
Accepted: September 1, 2023
Article in press: September 1, 2023
Published online: October 15, 2023

Daneng Li, Department of Medical Oncology and Therapeutics Research, City of Hope Comprehensive Cancer Center, Duarte, CA 91010, United States

Stephen B Gruber, Center for Precision Medicine, City of Hope Comprehensive Cancer Center, Duarte, CA 91010, United States

Shrividya Iyer, Sanjay Gupta, Department of Oncology, Worldwide Real-World Evidence, Eisai Inc., Nutley, NJ 07110, United States

Mohamedtaki Tejani, Department of Oncology and Hematology, Advent Health Cancer Institute, Orlando, FL 32804, United States

Corresponding author: Daneng Li, MD, Associate Professor, Department of Medical Oncology and Therapeutics Research, City of Hope Comprehensive Cancer Center, 1500 E. Duarte Road, Duarte, CA 91010, United States. danli@coh.org

Abstract

BACKGROUND

In the United States, sorafenib monotherapy was approved in 2007 for first-line (1L) treatment of patients with unresectable hepatocellular carcinoma (uHCC). As other therapies have been approved in recent years for hepatocellular carcinoma treatment in later lines, it is essential to assess clinical effectiveness of older therapies in actual clinical practice to inform healthcare practitioners' decisions for better patient care.

AIM

To assess patient characteristics/clinical effectiveness of 1L sorafenib in uHCC patients treated in United States academic and community practice settings.

METHODS

A retrospective observational study was conducted among adult patients (≥ 18 years) in the United States initiating sorafenib monotherapy as 1L systemic therapy for uHCC with Eastern Cooperative Oncology Group status of 0 or 1 between January 2016 and December 2019 at City of Hope and Advent Health. Data were extracted by trained abstractionists from individual patients' electronic health records and captured in electronic case report forms. Institutional Review

Board approvals were obtained prior to study initiation. Data were captured from the time of sorafenib initiation until death or the end of follow-up. All data were de-identified prior to analyses. Clinical outcomes assessed included provider-reported best response, progression-free survival (PFS), and overall survival (OS). PFS and OS were estimated using Kaplan-Meier methods.

RESULTS

Among 134 uHCC patients treated with 1L sorafenib, majority were male (75%), and most were Caucasian (62%) or Asian (19%). Median patient age was 64 years. The most common etiologies of liver disease were hepatitis C (54%), alcohol-related liver disease (16%), and hepatitis B (11%). Most patients were reported to have Barcelona Clinic Liver Cancer stage B (19%) or stage C (70%) disease. Of 134 patients, 110 (82%) were reported to have discontinued treatment or died during follow-up. Primary reasons for sorafenib discontinuation were reported as progression (35%) and toxicity (30%). Best overall response was reported for 124 patients, of which 7.3% reported complete or partial response. Median time to treatment discontinuation was 2.3 mo. Overall, 103 patients (77%) had disease progression or died during sorafenib therapy. Median PFS was estimated to be 2.9 mo. At the end of follow-up, 82 patients (61%) were deceased. Median OS was 8.5 mo.

CONCLUSION

Newer therapeutic options that have reported higher PFS and OS in real-world clinical practice should be considered to enhance patient outcomes.

Key Words: Retrospective observational study; Sorafenib; Hepatocellular carcinoma; Clinical effectiveness

Core Tip: As treatment options evolve for hepatocellular carcinoma (HCC) it is important to assess and understand the clinical outcomes with older treatment options in diverse real-world clinical practice settings to inform clinical decision making and identify the right patient for the right drug. The current study aimed to assess the patient characteristics and clinical effectiveness of sorafenib as first-line therapy in unresectable HCC patients treated in both academic and community practice settings in the United States.

Citation: Li D, Gruber SB, Iyer S, Gupta S, Tejani M. Real-world clinical effectiveness of sorafenib among patients with unresectable hepatocellular carcinoma at two centers in the United States. *World J Gastrointest Oncol* 2023; 15(10): 1796-1806
URL: https://www.wjgnet.com/1948-5204/full/v15/i10/1796.htm
DOI: https://dx.doi.org/10.4251/wjgo.v15.i10.1796

INTRODUCTION

Primary liver cancer is the sixth most commonly diagnosed cancer and the third leading cause of cancer death worldwide in 2020, with approximately 906000 new cases and 830000 deaths[1]. Hepatocellular carcinoma (HCC) is the most common type of liver cancer and accounts for approximately 75% of liver cancer cases in the United States[2]. Systemic treatments may benefit patients with advanced-stage HCC. Sorafenib was the first systemic drug approved by the United States Food and Drug Administration in 2007 and was considered standard of care until 2018[3].

Sorafenib was approved for the treatment of unresectable HCC (uHCC) after two phase III trials [Sorafenib HCC assessment randomized protocol (SHARP) and Asia-Pacific] demonstrated significant improvements in overall survival (OS)[4,5]. However, rapid advances during the last four years have led to the approval of other molecular targeted drugs and several immune checkpoint inhibitors[3] for first- or second/later-line use. In the first-line (1L) setting, lenvatinib was approved in July 2018 for the treatment of advanced uHCC patients[6]. Additional systemic treatment options are currently available and approved for use in sorafenib-treated patients (in second or later lines), including the tyrosine kinase inhibitors regorafenib and cabozantinib, the vascular endothelial growth factor receptor inhibitor ramucirumab, and the programmed cell death protein 1 inhibitor pembrolizumab[7-11].

Though previous retrospective and prospective real-world observational studies have evaluated clinical effectiveness of sorafenib[12-17], with the evolving landscape it is important to reassess clinical outcomes like OS in patients treated with 1L sorafenib, given there are many more options. Understanding OS with sorafenib becomes more critical given sorafenib is now a generic drug in the United States and progression-free survival (PFS)/OS are critical elements in assessing cost-benefit ratios of treatments, especially when comparing to novel branded therapeutic options. In our study we assess clinical outcomes of uHCC patients treated with 1L sorafenib at an academic cancer center and a community cancer practice.

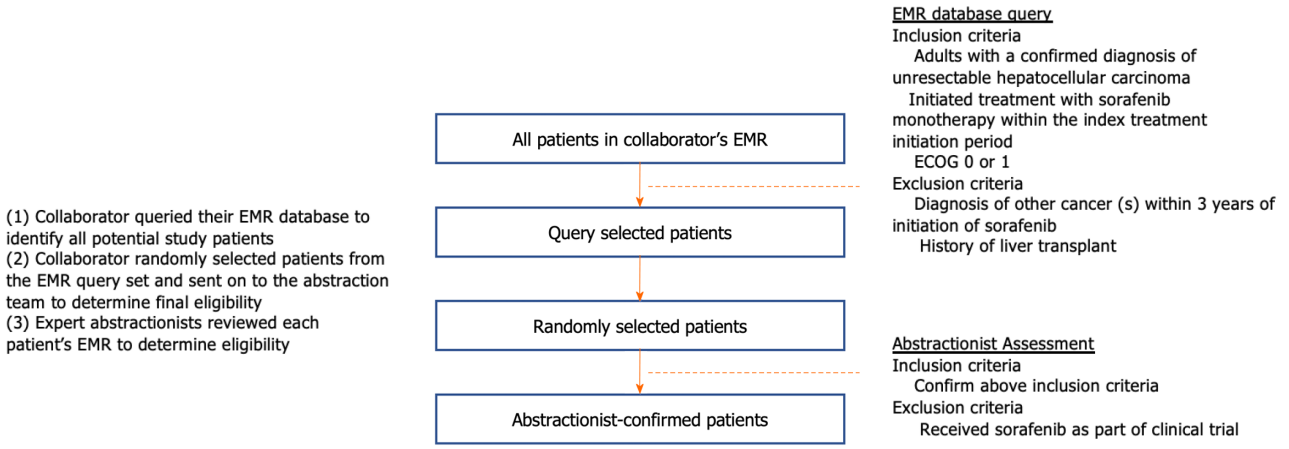

DOI: 10.4251/wjgo.v15.i10.1796

Figure 1 Study overview. Flow diagram detailing patient record selection process. ECOG: Eastern Cooperative Oncology Group; EMR: Electronic medical record.

MATERIALS AND METHODS

Patient Population

A retrospective observational study was conducted among adult patients (≥ 18 years) in the United States who had initiated sorafenib monotherapy as 1L systemic therapy for uHCC with an Eastern Cooperative Oncology Group (ECOG) status of 0 or 1 between January 2016 and December 2019 at an academic cancer center (City of Hope) and a community cancer practice (Advent Health). City of Hope is an academic and National Cancer Institute-designated Comprehensive Cancer Center located in the state of California. Advent Health is a large regional community health system headquartered in Florida serving 5 million patients across 9 states (Colorado, Florida, Georgia, Illinois, Kansas, Kentucky, North Carolina, Texas, and Wisconsin). Patients were excluded if there was evidence of other malignant neoplasms within 3 years prior to initiation of sorafenib, liver transplant recorded at any point in their medical history, or if they had received sorafenib as part of a clinical trial. Each collaborating center had the study protocol reviewed and approved by their respective Institutional Review Board. All data transmitted from the data collaborators in support of the study were de-identified pursuant to Health Insurance Portability and Accountability Act Privacy Rule 164.514 (b) and (c).

Patient medical records were selected randomly in a three-part process as depicted in Figure 1. Each center used a database query to identify a superset of patients that contained all eligible patients (and likely some that were ineligible). Data were collected using a standard electronic case report form (eCRF) at both centers. Structured data were automatically collected from de-identified electronic medical records (EMR). Data explicitly stated in the EMR and not requiring any inference or clinical judgment were entered into the eCRF by expert oncology chart abstractionists trained on the study protocol at each center. Data abstracted by the abstractionists were reviewed by the study oncologist for completeness and quality assurance. Treating oncologists who were specifically trained on the study protocol also captured certain key data that were not expressly stated in the EMR but could be determined through clinical judgment from evidence in the patient EMR (including unstructured physician notes *e.g.*, response, progression).

Treatment

Sorafenib monotherapy initiated as 1L systemic therapy for uHCC between January 2016 and December 2019.

Follow-Up

Data on these patients were captured from the time of sorafenib initiation until their death, lost to contact, or the end of follow-up.

Study Variables and Endpoints

Patient demographics and clinical history were extracted from the EMR. Demographics of interest included age at sorafenib initiation, sex, and race/ethnicity. Clinical history included liver disease etiology (hepatitis B, hepatitis C, alcohol-related, and nonalcoholic fatty liver disease), cirrhosis severity (Child-Pugh score), ECOG performance status, and Barcelona Clinic Liver Cancer (BCLC) stage. Patients' treatment characteristics included receipt of treatments or procedures prior to and after sorafenib. Information about treatment with sorafenib start and end dates was ascertained. The reasons for discontinuation were captured at a category-level only (*e.g.*, toxicity, progression, patient preference, death, not reported).

After baseline tumor assessment, subsequent assessments by the treating oncologist recorded the tumor response as progressive disease (PD), stable disease (SD), partial response (PR), complete response (CR), not evaluable. When these observations were stated explicitly in the patient medical record, they were captured by the abstractionists. When the tumor response was not explicitly stated by the treating oncologist in the EMR the abstractionist recorded that an

Table 1 Patient demographics

Characteristic	Overall (*n* = 134)	Advent Health (*n* = 62)	City of Hope (*n* = 72)
Age at diagnosis (yr)			
Mean	65	64	65
Median (range)	64 (33-90)	63 (44-79)	66 (33-90)
Sex, *n* (%)			
Male	101 (75)	50 (81)	51 (71)
Female	33 (25)	12 (19)	21 (29)
BMI, *n* (%)			
< 18.5	4 (3)	4 (6)	-
18.5-24.9	48 (36)	20 (32)	28 (39)
25-29.9	38 (28)	14 (23)	24 (33)
≥ 30	34 (25)	21 (34)	13 (18)
Not reported	10 (8)	3 (5)	7 (10)
Race, *n* (%)			
Asian	25 (19)	3 (5)	22 (31)
African-American	15 (11)	11 (18)	4 (6)
Native Hawaiian or other Pacific Islander	1 (1)	-	1 (1)
Caucasian	83 (62)	41 (66)	42 (58)
Not reported	10 (7)	7 (11)	3 (4)
Ethnicity, *n* (%)			
Hispanic or Latino	34 (25)	16 (26)	18 (25)
Non-Hispanic or Non-Latino	94 (70)	45 (73)	49 (68)
Not reported	6 (5)	1 (1)	5 (7)

BMI: Body mass index.

assessment was done but tumor response was "not stated". The reviewing oncologist recorded the patients' best overall response (BOR) on sorafenib based on the treating oncologists' explicitly stated assessment or, if that was not available, by applying their clinical judgment based on the evidence in the EMR. The physician-reported criteria used to evaluate best clinical response [*e.g.*, Response Evaluation Criteria in Solid Tumors (RECIST) 1.1, modified (m) RECIST, or physician assessment, if no specific criteria were reported in patient charts] were collected. PFS was defined as time from sorafenib initiation to clinical progression or death during sorafenib treatment, and OS was defined as time from sorafenib initiation to death. For PFS, patients who did not progress during sorafenib treatment were censored at sorafenib treatment stop date; for OS, those who were still alive at the time of data collection were censored at the date of their last available medical record.

Statistical Analysis

Our study did not involve formal hypothesis testing or comparative analyses and was primarily descriptive; therefore, the sample size was based on available resources rather than a formal statistical power calculation. Descriptive statistics were reported for patients' demographic, clinical, and treatment characteristics as well as for physicians' characteristics. Missing data were not extrapolated or estimated and were calculated as percentage of patients of the total that had a particular characteristic as missing or not reported. Clinical outcomes are reported for the overall cohort. Real-world BOR (rwBOR) was calculated as percentage of patients who had a real-world best response reported as partial or complete. Disease control rate (DCR) was calculated as percentage of patients who had a rwBOR of SD, PR, or CR. Time-to-event outcomes (*i.e.*, PFS and OS) were estimated using the Kaplan-Meier method. PFS and OS between subgroups were compared using log-rank tests. A P value of $P < 0.05$ was considered statistically significant. The statistical methods of this study were reviewed by Shrividya Iyer from Eisai.

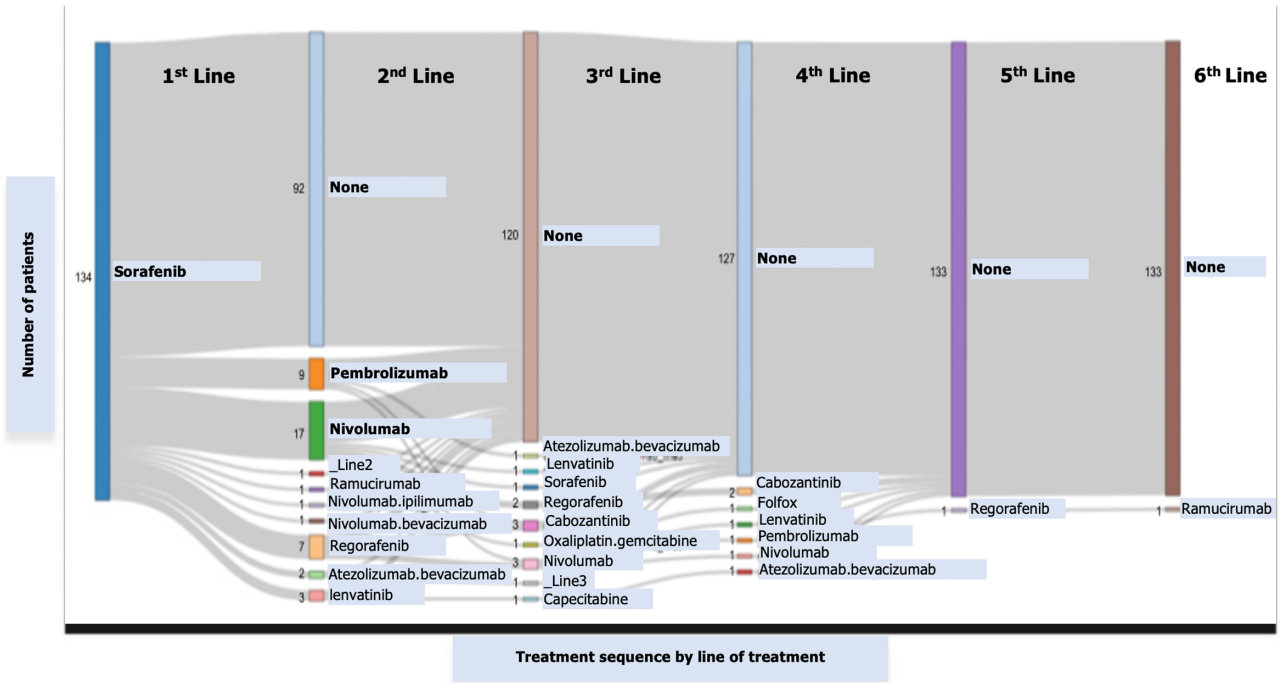

DOI: 10.4251/wjgo.v15.i10.1796

Figure 2 Therapeutic sequences. Sankey plot detailing subsequent treatments received by patients.

RESULTS

Patient Demographics and Clinical Characteristics

Patient demographics and clinical characteristics of the 134 patients who received 1L sorafenib are shown in Table 1 and Table 2, respectively. Patients' median age was 64 years, and most patients were male (75%) and Caucasian (62%) or Asian (19%) (Table 1). Majority of the patients had either Child-Pugh class A cirrhosis (36%) or Child-Pugh class B cirrhosis (40%), with 9% showing more severe liver dysfunction with Child-Pugh class C cirrhosis. More than half (54%) of patients were diagnosed with hepatitis C and 11% with hepatitis B infection, whereas 16% of patients had alcohol-related liver disease and 8% had nonalcoholic fatty liver disease. Majority (70%) of patients were BCLC stage C, whereas 19% were BCLC stage B, and 9% BCLC stage A at initiation of 1L sorafenib (Table 2). Portal vein thrombosis was reported in 13% of patients.

Treatment Characteristics

Of the 134 patients treated with 1L sorafenib, 110 were known to have discontinued treatment or died during the observation period. Median real-world time to treatment discontinuation (rwTTD) was 69 d (2.3 mo) from initiation of 1L sorafenib. Among patients with Child-Pugh class A cirrhosis, median rwTTD was 2.4 mo; among patients with Child-Pugh class B cirrhosis, median rwTTD was 1.9 mo, while patients with Child-Pugh class C cirrhosis had a median rwTTD of 1 mo.

Reason for discontinuation of 1L sorafenib was available for 102 patients. For majority of patients, sorafenib was discontinued due to progression (35%) and toxicity (30%). Death (5%), patient preference (3%), and hospice or palliative care (2%) were other reasons listed as a reason for discontinuation.

Majority of the patients (69%) received only one line of therapy. Of those who went on to receive subsequent lines of therapy, 17 (40%) received second-line nivolumab and 9 (21%) received second-line pembrolizumab. Figure 2 shows the therapeutic sequences observed.

RWBOR and DCR

Of the 134 patients that received 1L sorafenib, 124 patients had response information captured from the EMR. The response findings were based on the treating physicians' assessment. Overall, 9 patients (7.3%) had best response reported as CR or PR on 1L sorafenib; 55 patients reported a best response as CR, PR, or SD with a DCR of 44.4%. BOR for subgroups are presented in Table 3.

Real-World PFS (rwPFS)

Overall, 103 of 134 patients had disease progression or died during sorafenib therapy. Median rwPFS was 88 d (2.9 mo) from initiation of 1L sorafenib (Figure 3A). Median rwPFS was estimated to be 3.1 mo among patients with Child-Pugh class A cirrhosis, 2.6 mo among patients with Child-Pugh class B cirrhosis, and 1.4 mo among patients with Child-Pugh class C cirrhosis. RwPFS was observed to be significantly lower in Child-Pugh C patients compared to Child-Pugh A patients [hazard ratio (HR) = 3.27, 95% confidence interval (CI): 1.57-6.79, $P < 0.05$] and in patients with an ECOG status

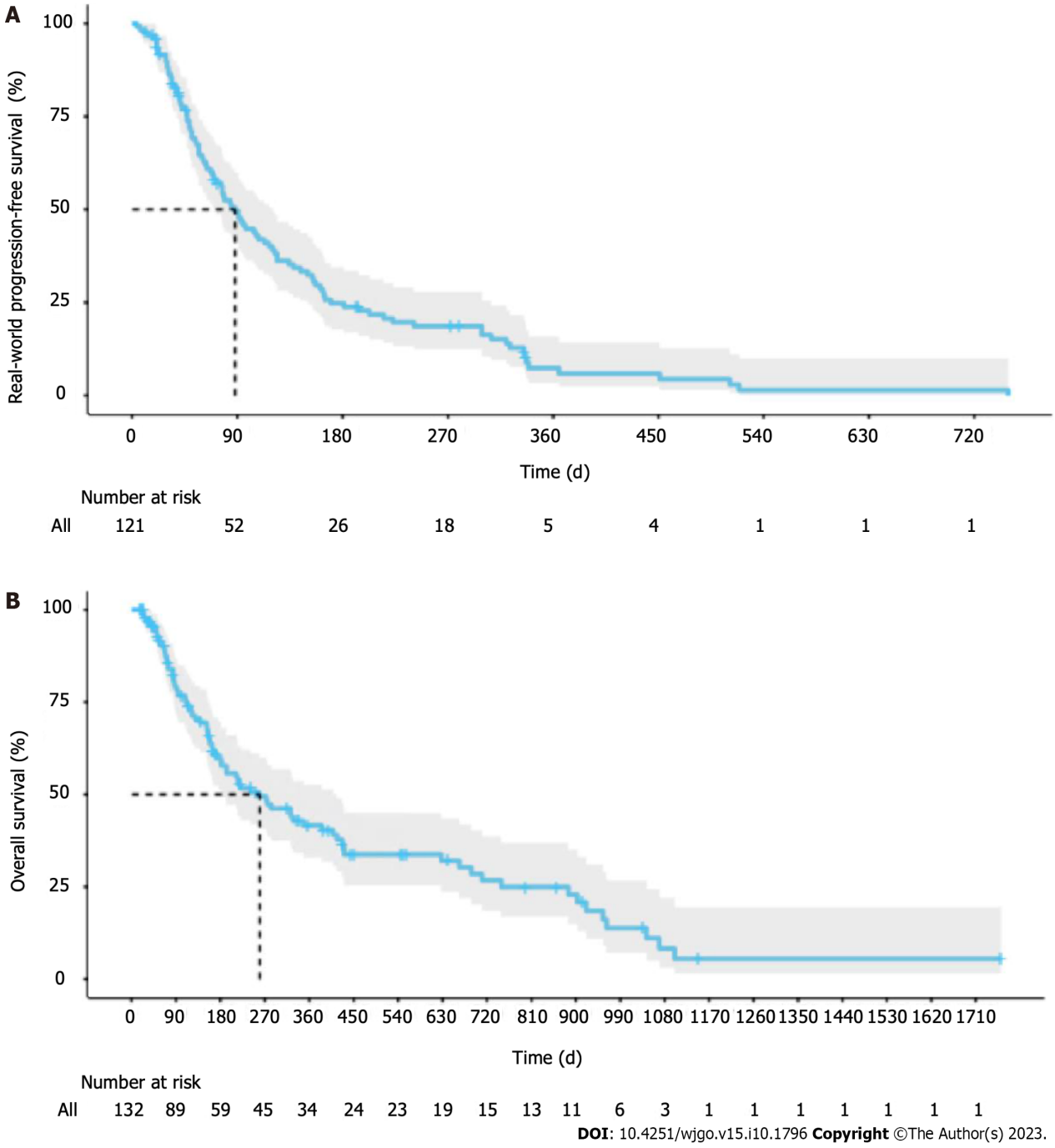

DOI: 10.4251/wjgo.v15.i10.1796

Figure 3 Real-world progression-free survival and overall survival. A: Kaplan-Meier plot of Real-world progression-free survival (rwPFS), median rwPFS (88 d) is shown as a dashed line; B: Kaplan-Meier plot of overall survival (OS), median OS (258 d) is shown as a dashed line.

of 1 compared to patients with an ECOG status of 0 (HR = 1.70, 95% CI: 1.03-2.83, $P < 0.05$) (Table 3).

OS

At the end of the observation period, 82 patients (61%) were deceased. Median OS was 258 d (8.5 mo) from initiation of 1L sorafenib (Figure 3B). Median OS was 10.6 mo among patients with Child-Pugh class A cirrhosis, 6.3 mo among patients with Child-Pugh class B cirrhosis, and 3 mo among patients with Child-Pugh class C cirrhosis. Median OS was significantly lower in Child-Pugh C patients compared to Child-Pugh A patients (HR = 4.49, 95% CI: 1.87-10.8, $P < 0.05$). No statistically significant differences in OS were observed between other subgroups (Table 3).

DISCUSSION

Our retrospective real-world study evaluated clinical outcomes among a demographically and clinically diverse adult uHCC patient population treated at an academic cancer center and a community health care system, thus including

Table 2 Patient clinical characteristics

	Overall (*n* = 134)	Advent Health (*n* = 62)[1]	City of Hope (*n* = 72)
Child-Pugh class, *n* (%)			
A	48 (36)	26 (42)	22 (31)
B	54 (40)	25 (40)	29 (40)
C	12 (9)	7 (11)	5 (7)
Not reported	20 (15)	4 (6)	16 (22)
BCLC stage, *n* (%)			
0	1 (1)	1 (2)	-
A	12 (9)	2 (3)	10 (14)
B	25 (19)	22 (35)	3 (4)
C	94 (70)	36 (58)	58 (81)
D	1 (1)	-	1 (1)
Not reported	1 (1)	1 (2)	0
ECOG, *n* (%)			
0	28 (21)	10 (16)	18 (25)
1	103 (77)	49 (79)	54 (75)
Not reported	3 (2)	3 (5)	0
Etiology, *n* (%)			
Hepatitis B	15 (11)	5 (8)	10 (14)
Hepatitis C	72 (54)	35 (56)	37 (51)
Alcohol-related liver disease	21 (16)	10 (16)	11 (15)
Nonalcoholic fatty liver disease	11 (8)	4 (6)	7 (10)
Not reported/none of the above	15 (11)	8 (13)	7 (10)

[1]Due to rounding, percentages may not add to 100%.
BCLC: Barcelona Clinic Liver Cancer; ECOG: Eastern Cooperative Oncology Group.

uHCC patients treated with 1L sorafenib in diverse health care settings from multiple states in the United States.

The clinical outcomes observed in our study were similar to previously published real-world data studies as well as the sorafenib arm clinical outcomes in major clinical trials. The results of the SHARP study demonstrated the clinical effectiveness of sorafenib in the treatment of uHCC. Compared to the placebo group, the sorafenib treatment group had significantly prolonged median OS (10.7 *vs* 7.9 mo)[4,5]. In the Asia-Pacific study, patients treated with sorafenib had a longer median OS (6.4 *vs* 4.2 mo) and median time to progression (2.8 *vs* 1.4 mo) compared to placebo[5]. Notably, the patient population in our real-world study had Child-Pugh scores ranging from A to C, while the majority (> 95%) of patients in SHARP had Child-Pugh A scores[4].

In line with previous clinical and prospective real-world data studies, median PFS and median OS in patients treated with sorafenib in our study were shorter in Child-Pugh B patients compared with Child-Pugh A patients[13,14]. In a multi-center phase 2 trial, the median PFS (range) for the total patient population was 3.9 (0.1-35.3) mo; median PFS (range) for patients with Child-Pugh A or B cirrhosis was 4.3 (0.1-35.3) mo and 2.1 (0.3-27.3) mo, respectively (log-rank $P < 0.001$). In the multivariate analysis in the same trial, Child-Pugh B patients had a greater risk of disease progression or death compared to Child-Pugh A patients (HR 1.87, 95%CI: 1.41-2.48, $P < 0.001$)[14].

The global investigation of therapeutic decisions in HCC and of its treatment with sorafenib trial was a large prospective, observational cross-regional registry study undertaken to evaluate the real-life use, safety, and effectiveness of sorafenib in HCC patients; it included patients with baseline Child-Pugh B (21%) and C (2%) liver function[13]. Median OS was longer in Child-Pugh A patients (13.6 mo) than in Child-Pugh B patients (5.2 mo) and Child-Pugh C patients (2.6 mo)[13]. In a smaller retrospective real-world study of patients treated with sorafenib in Portugal ($n = 36$), median OS was reported to be 6.8 mo (95%CI: 3-10.6). Median OS differed according to Child-Pugh class [Child-Pugh A: 17.3 mo (95%CI: 5.3-29.4) *vs* Child-Pugh B: 3.2 mo (95%CI: 0.9-5.5); $P = 0.001$][17]. In the same study by Cardoso *et al*[17], two patients (6%) had PR, nine patients (25%) were classified as SD, and seven patients (19%) reported PD. Sixteen patients were also evaluated according to mRECIST criteria; one patient reached CR, four patients (11%) had PR, three patients (8%) had SD, and eight patients (22%) reported PD.

Table 3 Clinical outcomes by subgroup

Cohort/subgroup	Best overall response, % (CR + PR)	N (PFS)	Median PFS (Q1, Q3), months	HR (95%CI)	N (OS)	Median OS (Q1, Q3), months	HR (95%CI)
Overall	7.3	121	2.9 (1.5, 5.6)		134	8.5 (3.6, 24.6)	
Age group (yr)							
< 65[1]	7.7	61	3.5 (1.8, 7.1)		69	8.5 (3.6, 23.4)	
65-75	9.8	42	2.3 (1, 10.3)	1.40 (0.90-2.15)	45	10.6 (4, 29.7)	0.87 (0.53-1.44)
> 75	0	18	3.8 (1.5, 7.9)	0.85 (0.48-1.52)	18	6 (3.1, 31.6)	1.09 (0.58-2.02)
Sex							
Male[1]	7.4	91	2.8 (1.6, 5.4)		92	7.1 (3.6, 21.8)	
Female	6.9	30	3.6 (1.3, 7.9)	0.84 (0.53-1.32)	31	14.2 (3.7, 30.3)	0.68 (0.41-1.15)
Race							
Asian[1]	12.0	25	3 (1.5, 5.4)		25	10.6 (5.4, 23.4)	
African-American	7.7	12	4.5 (1.9, 6.7)	0.90 (0.43-1.89)	15	13.7 (1.8, 36.2)	1.03 (0.47-2.27)
Native Hawaiian or other Pacific Islander	0	1	2.8 (2.8, 2.8)	1.37 (0.18-10.3)	1	2.8 (2.8, 2.8)	6.52 (0.82-51.7)
Caucasian	6.4	77	2.6 (1.5, 6.4)	0.89 (0.54-1.47)	82	9.3 (4, 29.7)	1.05 (0.59-1.84)
Child-Pugh Class							
A[1]	9.1	43	3.1 (1.9, 5.4)		47	10.6 (5.2, 24.6)	
B	10.2	50	2.6 (1.5, 5.6)	1.23 (0.79-1.93)	54	6.3 (2.8, 14.2)	1.36 (0.84-2.19)
C	0	11	1.4 (0.7, 2.5)	3.27 (1.57-6.79)[a]	12	3 (1.7, 4.2)	4.49 (1.87-10.8)[a]
BCLC stage							
0	0	1	1 (1, 1)	NA	1	Not reached	NA
A[1]	9.1	10	10.8 (1, 14.8)		12	23.4 (23.4, -)	
B	21.7	23	2.9 (1.5, 9.8)	1.64 (0.68-3.96)	24	9 (3.1, 22.6)	4.67 (1.08-20.1)
C	3.4	85	3 (1.6, 5.3)	1.79 (0.80-3.98)	93	7.1 (3.6, 24.6)	4.35 (1.06-17.8)
D	0	1	2.1 (2.1, 2.1)	NA	1	5.4 (5.4, 5.4)	NA
ECOG							
0[1]	12.5	25	5.1 (3, 10.5)		27	29.1 (6, 30.3)	
1	6.2	94	2.4 (1.4, 5.2)	1.70 (1.03-2.83)[a]	102	6.3 (3.1, 14.2)	2.02 (1.13-3.60)
Hepatitis B							
No[1]	6.5	106	3 (1.5, 6)		116	7.9 (3.6, 29.7)	
Yes	13.3	14	3 (1.9, 7.3)	0.90 (0.48-1.70)	15	9 (5.4, 21.8)	1.31 (0.70-2.42)
Hepatitis C							
No[1]	5.5	54	2.8 (1.5, 5.4)		60	7.9 (5, 21.8)	
Yes	8.8	66	3 (1.5, 7.1)	0.94 (0.63-1.39)	71	9.3 (3.6, 29.1)	0.85 (0.54-1.32)

Alcohol-related liver disease							
No[1]	7.8	102	3 (1.5, 6.4)		110	9 (3.7, 29.1)	
Yes	4.8	18	2.6 (2.1, 4.1)	1.17 (0.68-2.00)	21	7.1 (3.1, 13.4)	1.46 (0.81-2.61)
Nonalcoholic fatty liver disease							
No[1]	7.1	110	3 (1.6, 5.6)		120	7.9 (3.7, 23.4)	
Yes	10.0	10	2.8 (1.4, 10.6)	0.79 (0.38-1.63)	11	10.6 (3.1, 29.7)	0.71 (0.31-1.64)

[1]Reference. The subgroup within a categorical variable (*e.g.* age) that the other subgroup/s (within the same variable) are compared to for calculation of the Hazard Ratios reported.

[a]$P < 0.05$. BCLC: Barcelona Clinic Liver Cancer; CI: Confidence interval; CR: Complete response; ECOG: Eastern Cooperative Oncology Group; HR: Hazard ratio; NA: Not applicable; OS: Overall survival; PFS: Progression-free survival; PR: Partial response; Q1: Quartile 1; Q3: Quartile 3.

Our real-world study has a few limitations. Clinical data were entered directly into the eCRFs by data abstractionists based on medical records available at the time of data entry; therefore, the data are potentially subject to inadvertent entry, keying errors, or missing data. Review of the eCRFs by treating oncologists was enforced to minimize these errors. Frequency of scans in clinical practice might vary between patients and could be less frequent than commonly mandated in clinical trials. While published response criteria were provided as guidance in eCRFs, clinical responses were based on physician assessment and a criterion (if used) was asked to be reported. No safety data were collected. Our study may have also missed ascertainment of care received outside of the study clinics, and the convenience sample of United States-based centers likely limits the generalizability of our findings to other countries. Despite these limitations, our study provides useful information on the use and outcomes of sorafenib in real-world clinical practice in the United States.

CONCLUSION

To our knowledge, no other retrospective study has evaluated real-world outcomes of sorafenib in the United States combining data from an established academic cancer center and a multi-state community health care system. Real-world median PFS and OS of sorafenib in 1L uHCC were < 3 mo and < 9 mo, respectively. Newer therapeutic options that have reported higher PFS and OS in real-world clinical practice should be considered as 1L treatment choices to enhance uHCC patient outcomes.

ARTICLE HIGHLIGHTS

Research background

Sorafenib has been approved for use in unresectable hepatocellular carcinoma (uHCC) patients for more than a decade. As other therapies have been approved in recent years for uHCC treatment in later lines, it is essential to assess clinical effectiveness of older therapies in actual clinical practice to inform healthcare practitioners' decisions for better patient care.

Research motivation

Limited recent data on real-world clinical effectiveness of sorafenib in diverse clinical practice settings in the United States.

Research objectives

To assess clinical effectiveness of sorafenib as first-line (1L) therapy in uHCC patients treated in both academic and community practice settings in the United States.

Research methods

In a retrospective observational study we assessed clinical outcomes including best response, progression-free survival (PFS), and overall survival (OS) among adult uHCC patients (≥ 18 years) in the United States initiating 1L sorafenib monotherapy at City of Hope (academic) and Advent Health (community practice) between January 2016 and December 2019.

Research results

Median time to treatment discontinuation was 2.3 mo. Overall, 103 patients (77%) had disease progression or died during sorafenib therapy. Median PFS was 2.9 mo and median OS was 8.5 mo.

Research conclusions

Median PFS and OS of sorafenib in 1L uHCC were < 3 mo and < 9 mo, respectively.

Research perspectives

Newer therapeutic options that have reported higher PFS and OS in real-world clinical practice should be considered to enhance patient outcomes.

ACKNOWLEDGEMENTS

We would like to acknowledge Christiana Crook, clinical research assistant at City of Hope, for providing editorial assistance, and Xiaoyu Xia, Ethan Truong, Kimber Slater, Yvette Estrada, Katherine Roth, Sidney Lindsey, and Joseph Bonner from City of Hope Center for Precision Medicine. The authors would like to acknowledge Samir Courdy and Srisairam Achuthan from City of Hope Center for Informatics for the utilization of the POSEIDON platform for data exploration, visualization, analysis, and discovery.

FOOTNOTES

Author contributions: Li D, Gruber SB, and Tejani M contributed to study design, data collection, data interpretation, and manuscript development; Iyer S and Gupta S contributed to study design, data interpretation, and manuscript development; all authors read and approved the final version.

Institutional review board statement: The study was reviewed and approved by the Ethics Committees of Advent Health Orlando and City of Hope.

Informed consent statement: Informed consent was not required for this study as it was a retrospective analysis and data were de-identified prior to analysis. Waivers for informed consent were provided by each site's Institutional Review Board.

Conflict-of-interest statement: Dr.Li reports personal fees and other from AstraZeneca, other from Brooklyn ImmunoTherapeutics, personal fees from Adagene, personal fees from Coherus, personal fees from Delcath, personal fees from Eisai, personal fees from Exelixis, personal fees from Genentech, personal fees from Ipsen Biopharmaceuticals, personal fees from Merck, personal fees from Servier, personal fees from Sumitomo Pharma, and personal fees from TerSera Therapeutics, outside the submitted work.

Data sharing statement: No additional data are available.

Country/Territory of origin: United States

ORCID number: Daneng Li 0000-0001-5330-7522; Stephen B Gruber 0000-0001-8656-7822; Shrividya Iyer 0000-0002-1770-2311; Sanjay Gupta 0009-0003-5857-9772.

S-Editor: Qu XL
L-Editor: A
P-Editor: Zhang XD

REFERENCES

1 **World Health Organization**. Globocan: The IARC Global Cancer Observatory. 2020. [cited 3 February 2022]. Available from: http://globocan.iarc.fr/old/FactSheets/cancers/Liver-new.asp

2 **Petrick JL**, Kelly SP, Altekruse SF, McGlynn KA, Rosenberg PS. Future of Hepatocellular Carcinoma Incidence in the United States Forecast Through 2030. *J Clin Oncol* 2016; **34**: 1787-1794 [PMID: 27044939 DOI: 10.1200/JCO.2015.64.7412]

3 **Zhang H**, Zhang W, Jiang L, Chen Y. Recent advances in systemic therapy for hepatocellular carcinoma. *Biomark Res* 2022; **10**: 3 [PMID: 35000616 DOI: 10.1186/s40364-021-00350-4]

4 **Llovet JM**, Ricci S, Mazzaferro V, Hilgard P, Gane E, Blanc JF, de Oliveira AC, Santoro A, Raoul JL, Forner A, Schwartz M, Porta C, Zeuzem S, Bolondi L, Greten TF, Galle PR, Seitz JF, Borbath I, Häussinger D, Giannaris T, Shan M, Moscovici M, Voliotis D, Bruix J; SHARP Investigators Study Group. Sorafenib in advanced hepatocellular carcinoma. *N Engl J Med* 2008; **359**: 378-390 [PMID: 18650514 DOI: 10.1056/NEJMoa0708857]

5 **Cheng AL**, Kang YK, Chen Z, Tsao CJ, Qin S, Kim JS, Luo R, Feng J, Ye S, Yang TS, Xu J, Sun Y, Liang H, Liu J, Wang J, Tak WY, Pan H, Burock K, Zou J, Voliotis D, Guan Z. Efficacy and safety of sorafenib in patients in the Asia-Pacific region with advanced hepatocellular

carcinoma: a phase III randomised, double-blind, placebo-controlled trial. *Lancet Oncol* 2009; **10**: 25-34 [PMID: 19095497 DOI: 10.1016/S1470-2045(08)70285-7]

6 **Kudo M**, Finn RS, Qin S, Han KH, Ikeda K, Piscaglia F, Baron A, Park JW, Han G, Jassem J, Blanc JF, Vogel A, Komov D, Evans TRJ, Lopez C, Dutcus C, Guo M, Saito K, Kraljevic S, Tamai T, Ren M, Cheng AL. Lenvatinib versus sorafenib in first-line treatment of patients with unresectable hepatocellular carcinoma: a randomised phase 3 non-inferiority trial. *Lancet* 2018; **391**: 1163-1173 [PMID: 29433850 DOI: 10.1016/S0140-6736(18)30207-1]

7 **Foerster F**, Galle PR. Comparison of the current international guidelines on the management of HCC. *JHEP Rep* 2019; **1**: 114-119 [PMID: 32039359 DOI: 10.1016/j.jhepr.2019.04.005]

8 **Bruix J**, Qin S, Merle P, Granito A, Huang YH, Bodoky G, Pracht M, Yokosuka O, Rosmorduc O, Breder V, Gerolami R, Masi G, Ross PJ, Song T, Bronowicki JP, Ollivier-Hourmand I, Kudo M, Cheng AL, Llovet JM, Finn RS, LeBerre MA, Baumhauer A, Meinhardt G, Han G; RESORCE Investigators. Regorafenib for patients with hepatocellular carcinoma who progressed on sorafenib treatment (RESORCE): a randomised, double-blind, placebo-controlled, phase 3 trial. *Lancet* 2017; **389**: 56-66 [PMID: 27932229 DOI: 10.1016/S0140-6736(16)32453-9]

9 **Abou-Alfa GK**, Meyer T, Cheng AL, El-Khoueiry AB, Rimassa L, Ryoo BY, Cicin I, Merle P, Chen Y, Park JW, Blanc JF, Bolondi L, Klümpen HJ, Chan SL, Zagonel V, Pressiani T, Ryu MH, Venook AP, Hessel C, Borgman-Hagey AE, Schwab G, Kelley RK. Cabozantinib in Patients with Advanced and Progressing Hepatocellular Carcinoma. *N Engl J Med* 2018; **379**: 54-63 [PMID: 29972759 DOI: 10.1056/NEJMoa1717002]

10 **Zhu AX**, Kang YK, Yen CJ, Finn RS, Galle PR, Llovet JM, Assenat E, Brandi G, Pracht M, Lim HY, Rau KM, Motomura K, Ohno I, Merle P, Daniele B, Shin DB, Gerken G, Borg C, Hiriart JB, Okusaka T, Morimoto M, Hsu Y, Abada PB, Kudo M; REACH-2 study investigators. Ramucirumab after sorafenib in patients with advanced hepatocellular carcinoma and increased α-fetoprotein concentrations (REACH-2): a randomised, double-blind, placebo-controlled, phase 3 trial. *Lancet Oncol* 2019; **20**: 282-296 [PMID: 30665869 DOI: 10.1016/S1470-2045(18)30937-9]

11 **Finn RS**, Ryoo BY, Merle P, Kudo M, Bouattour M, Lim HY, Breder V, Edeline J, Chao Y, Ogasawara S, Yau T, Garrido M, Chan SL, Knox J, Daniele B, Ebbinghaus SW, Chen E, Siegel AB, Zhu AX, Cheng AL; KEYNOTE-240 investigators. Pembrolizumab As Second-Line Therapy in Patients With Advanced Hepatocellular Carcinoma in KEYNOTE-240: A Randomized, Double-Blind, Phase III Trial. *J Clin Oncol* 2020; **38**: 193-202 [PMID: 31790344 DOI: 10.1200/JCO.19.01307]

12 **Jo M**, Yasui K, Kirishima T, Shima T, Niimi T, Katayama T, Mori T, Funaki J, Sumida Y, Fujii H, Takami S, Kimura H, Mitsumoto Y, Minami M, Yamaguchi K, Yoshinami N, Mizuno M, Sendo R, Tanaka S, Shintani H, Kagawa K, Okanoue T, Itoh Y. Efficacy and safety of sorafenib in very elderly patients aged 80 years and older with advanced hepatocellular carcinoma. *Hepatol Res* 2014; **44**: 1329-1338 [PMID: 24528772 DOI: 10.1111/hepr.12308]

13 **Marrero JA**, Kudo M, Venook AP, Ye SL, Bronowicki JP, Chen XP, Dagher L, Furuse J, Geschwind JH, de Guevara LL, Papandreou C, Takayama T, Sanyal AJ, Yoon SK, Nakajima K, Lehr R, Heldner S, Lencioni R. Observational registry of sorafenib use in clinical practice across Child-Pugh subgroups: The GIDEON study. *J Hepatol* 2016; **65**: 1140-1147 [PMID: 27469901 DOI: 10.1016/j.jhep.2016.07.020]

14 **Pressiani T**, Boni C, Rimassa L, Labianca R, Fagiuoli S, Salvagni S, Ferrari D, Cortesi E, Porta C, Mucciarini C, Latini L, Carnaghi C, Banzi M, Fanello S, De Giorgio M, Lutman FR, Torzilli G, Tommasini MA, Ceriani R, Covini G, Tronconi MC, Giordano L, Locopo N, Naimo S, Santoro A. Sorafenib in patients with Child-Pugh class A and B advanced hepatocellular carcinoma: a prospective feasibility analysis. *Ann Oncol* 2013; **24**: 406-411 [PMID: 23041587 DOI: 10.1093/annonc/mds343]

15 **Wong H**, Tang YF, Yao TJ, Chiu J, Leung R, Chan P, Cheung TT, Chan AC, Pang RW, Poon R, Fan ST, Yau T. The outcomes and safety of single-agent sorafenib in the treatment of elderly patients with advanced hepatocellular carcinoma (HCC). *Oncologist* 2011; **16**: 1721-1728 [PMID: 22135121 DOI: 10.1634/theoncologist.2011-0192]

16 **Morimoto M**, Numata K, Kondo M, Hidaka H, Takada J, Shibuya A, Kobayashi S, Ohkawa S, Okuse C, Morita S, Taguri M, Tanaka K. Higher discontinuation and lower survival rates are likely in elderly Japanese patients with advanced hepatocellular carcinoma receiving sorafenib. *Hepatol Res* 2011; **41**: 296-302 [PMID: 21348907 DOI: 10.1111/j.1872-034X.2011.00778.x]

17 **Cardoso H**, Alves AM, Marques M, Vale AM, Pereira P, Macedo G. Hepatocellular Carcinoma Treatment With Sorafenib: Real-Life Evaluation of Prognostic Factors and a Practical Clue for Patient Management. *GE Port J Gastroenterol* 2016; **23**: 243-248 [PMID: 28868469 DOI: 10.1016/j.jpge.2016.04.006]

World Journal of Gastrointestinal Oncology

Submit a Manuscript: https://www.f6publishing.com

World J Gastrointest Oncol 2023 October 15; 15(10): 1807-1822

DOI: 10.4251/wjgo.v15.i10.1807

ISSN 1948-5204 (online)

CASE REPORT

Synchronous occurrence of gastric cancer and gastrointestinal stromal tumor: A case report and review of the literature

Jie Liu, Bin-Jie Huang, Fei-Fei Ding, Fu-Tian Tang, Yu-Min Li

Specialty type: Gastroenterology and hepatology

Provenance and peer review: Unsolicited article; Externally peer reviewed.

Peer-review model: Single blind

Peer-review report's scientific quality classification

Grade A (Excellent): A
Grade B (Very good): B, B
Grade C (Good): 0
Grade D (Fair): D
Grade E (Poor): 0

P-Reviewer: Baryshnikova NV, Russia; Moshref L, Saudi Arabia; Shah OJ, India; Sumi K, Japan

Received: May 31, 2023
Peer-review started: May 31, 2023
First decision: July 31, 2023
Revised: August 20, 2023
Accepted: September 14, 2023
Article in press: September 14, 2023
Published online: October 15, 2023

Jie Liu, Bin-Jie Huang, Fei-Fei Ding, Fu-Tian Tang, Yu-Min Li, Department of General Surgery, Lanzhou University Second Hospital, Lanzhou 730030, Gansu Province, China

Jie Liu, Bin-Jie Huang, Fei-Fei Ding, Fu-Tian Tang, Yu-Min Li, Key Laboratory of the Digestive System Tumors of Gansu Province, Lanzhou University Second Hospital, Lanzhou 730030, Gansu Province, China

Corresponding author: Yu-Min Li, MD, PhD, Chief Physician, Professor, Surgeon, Surgical Oncologist, Department of General Surgery, Lanzhou University Second Hospital, No. 80 Cuiyingmen, Lanzhou 730030, Gansu Province, China. liym@lzu.edu.cn

Abstract

BACKGROUND

To evaluate the clinicopathological features and prognosis of gastric cancer (GC) occurring synchronously with gastrointestinal stromal tumor (GIST).

CASE SUMMARY

We report 19 patients with concurrent GC and GIST (17 male and 2 female, median age 62 years). GC was most often located in the lower third of the stomach. GIST was diagnosed preoperatively in four patients. GIST was most often located in the gastric body (n = 8, 42%). The most common growth pattern in GIST was extraluminal (n = 12, 63%). The positive expression rates of CD117 and CD34 in GIST were 100% and 95%, respectively. Most patients with GIST (n = 17, 89%) were very low or low risk. There was no recurrence of GIST during follow-up. The 3-year cumulative survival rate was 73.9%, and the 5-year cumulative survival rate was 59.2%. The combined analysis of this study and literature reports (47 reports, 157 patients) found that GC and GIST were usually located in the lower third (42%) and middle third (51%) of the stomach. GC was usually early (stage I: 42%), poorly differentiated (42%) intestinal-type adenocarcinoma (51%). GISTs were primarily small in diameter (median: 1.2 cm) and very low or low risk (89%).

CONCLUSION

Synchronous GC and GIST may not be rare. They have specific clinicopathological characteristics, and may have mutual inhibition in pathogenesis and progression.

Key Words: Gastric cancer; Gastrointestinal stromal tumor; Synchronous occurrence; Diagnosis; Prognosis; Case report

Core Tip: We conclude that there are specific clinicopathological features in gastric cancer (GC) and gastrointestinal stromal tumor (GIST), as is often seen in older men; GC is usually a poorly differentiated enterotype early adenocarcinoma located in the lower third of the stomach. GIST is usually small in diameter, low or very low risk, and located in the body of the stomach. We hypothesized that GC and GIST might be affected by the same unknown carcinogen, leading to the simultaneous proliferation of epithelial and mesenchymal cells. GC and GIST may inhibit each other in the occurrence and development of the disease.

Citation: Liu J, Huang BJ, Ding FF, Tang FT, Li YM. Synchronous occurrence of gastric cancer and gastrointestinal stromal tumor: A case report and review of the literature. *World J Gastrointest Oncol* 2023; 15(10): 1807-1822
URL: https://www.wjgnet.com/1948-5204/full/v15/i10/1807.htm
DOI: https://dx.doi.org/10.4251/wjgo.v15.i10.1807

INTRODUCTION

Gastric cancer (GC) is a common malignant tumor originating from epithelial tissue. Gastrointestinal stromal tumor (GIST) accounts for 1%-2% of gastrointestinal tumors[1,2]. The prevalence of GC varies widely between western and eastern countries. However, there is no significant difference in GIST[3,4]. GIST is most common in the stomach (60%-70%) and small intestine (20%-30%)[5]. Nevertheless, it is rare for GIST and gastric epithelial tumors to co-occur in the stomach. Maiorana *et al*[6] first reported the synchronous occurrence of gastric epithelial and stromal tumors in 2000. Globally, most studies on concurrent GC and GIST are case reports[7-41]. Collision tumor formed by combined GC and GIST is also rare, a particular case of GC and GIST occurring synchronously[2,32,37-44]. At present, the etiology of GC occurring simultaneously with GIST is unclear. Several studies have reported the synchronous occurrence of GC and GIST with specific pathological features[45]. Some researchers believe that it is an accidental phenomenon[6,11]. Other researchers believe that several unknown carcinogens induce simultaneous proliferation and tumorigenesis of epithelial and stromal cells, such as gene mutation, nitrite, and *Helicobacter pylori*[6,7,9-11,18,30,34,37,38,46-49]. In addition, the impact of co-occurrence of GC and GIST on treatment options and prognosis is controversial.

From December 1, 2011 to December 31, 2021, 5408 GC patients were treated at the Lanzhou University Second Hospital, China. We analyzed 19 patients with synchronously occurring GC and GIST in our institution and reviewed previous studies. The Ethics Committee of Lanzhou University Second Hospital approved this retrospective study (2021A-585). This study aimed to provide some auxiliary data for deepening the understanding of concurrent GC and GIST.

CASE PRESENTATION

Chief complaints

The chief complaints at initial admission were upper abdominal pain (n = 8, 42%), epigastric discomfort (n = 6, 32%), abdominal distension (n = 4), black stools (n = 3), acid reflux (n = 2) and progressive dysphagia (n = 2). Among them, two patients with the chief complaint of "acid reflux" had symptoms of heartburn and eructation. Some patients had more than one of these symptoms.

History of present illness

The disease duration ranged from 15 d to 4 years (median, 4 mo). The outpatients were admitted to the hospital for gastric malignant tumors.

History of past illness

Eight patients (42%) had weight loss (range: 1-20 kg) within the last year. Six patients (32%) had prior surgical history, including three cases of cholecystectomy, one of appendectomy, two of fracture surgery and one of cataract surgery. Six patients (32%) had comorbidities, including three with hypertension, two with type 2 diabetes, and one with both.

Personal and family history

None of the patients had a family history of GC or GIST.

Physical examination

Specialist physical examination showed eight cases (42%) with positive signs; all of which were mild tenderness under the xiphoid process. The median body mass index was 22.8 kg/m^2 (range: 13.1-27.9 kg/m^2).

Laboratory examinations

Preoperative laboratory tests showed six (32%) patients with elevated tumor markers. The most frequently observed tumor markers with elevated reference values were CEA and CA72-4, followed by CA125 and CA199 (Table 1). Six patients (32%) with anemia (hemoglobin: No. 1 = 108 g/L; No. 7 = 102 g/L; No. 8 = 124 g/L; No. 10 = 129 g/L; No. 11 = 119 g/L; and No. 17 = 88 g/L). Four patients (21%) had positive occult blood tests.

Imaging examinations

The results of preoperative abdominal contrast-enhanced computed tomography (CT) and esophagogastroduodenoscopy (EGD) suggested that GC was most commonly located in the lower third of the stomach (n = 7, 37%), followed by the middle third (n = 6, 31%), upper third (n = 5, 26%) and multiple distributions in the stomach (n = 1, 5%). The median maximum diameter was 3.5 cm (range, 1.5-10.0 cm). The most common gross appearances were ulcerative type (Figure 1A) (n = 10, 53%) and ulcerative infiltrative type (n = 4). The detailed clinicopathological data of all GC patients are shown in Table 1. Preoperative CT found suspected GIST in three cases (15%) (Figure 1B and C). All 19 patients underwent EGD, and four (21%) were found to be suspicious of GIST (Figure 1D); of whom, three were diagnosed by endoscopic ultrasonography (Figure 1E). The clinicopathological data of GIST are shown in Table 2.

For the histological subtype, 18 cases were adenocarcinoma (Figure 2A) and one was high-grade intraepithelial neoplasia. Seven cases (39%) were classified as moderately to poorly differentiated, five were moderately differentiated, five were poorly differentiated, and one was well differentiated. For the Lauren classification, six patients (32%) were classified as diffuse type, five as intestinal type and three as mixed type. In pTNM staging, there was one stage 0, three stage IA, three stage IB, three stage IIA, three stage IIB, four stage IIIA, and two stage IIIC.

Intraoperative exploration revealed suspicious GIST in 12 cases (63%). The location of GIST was most commonly in the gastric body (n = 8, 42%), followed by gastric fundus (n = 3, 15%), gastric antrum (n = 2), gastric cardia (n = 2), duodenum (n = 2), and jejunum (n = 2). The median maximum diameter of GIST was 1.4 cm (range: 0.2-12.0 cm), and the diameters of two were 9 cm (Figure 1B) and 12 cm (Figure 1C), respectively. Seven cases (50%) of GIST were subserosal, five were muscular, and two were submucosal. For the growth pattern of GIST, 12 (63%) were extraluminal, two were intraluminal, of which one caused pyloric obstruction (Figure 1B), four were intramural, and one was both intraluminal and extraluminal, with compression of the spleen and left kidney (Figure 1C). Eighteen GISTs had a mitotic index < 5/50 HPF. According to the risk category for malignant behavior of GIST, 17 (89%) patients were classified as low or very low risk, and two as high risk. Sixteen GISTs were composed of spindle cells (Figure 2B), and one of spindle and epithelial cells. All GISTs were positive for CD117 (Figure 2C), 18 were positive for CD34 (Figure 2D), 18 for Dog-1 (Figure 2E), and nine for vimentin. S-100 protein was negative in 17 cases, and SMA protein was negative in 15 cases.

MULTIDISCIPLINARY EXPERT CONSULTATION

Xiao Chen, Professor, Chief of Gastroenterology; Ai-Lin Song, Professor, Chief of Gastroenterology; Ying-Xin Kang, Professor, Chief of Gastroenterology.

FINAL DIAGNOSIS

Synchronous occurrence of GC and GIST.

TREATMENT

According to the Japanese Classification of Gastric Cancer, all GC patients underwent D2 Lymphadenectomy and postoperative chemotherapy. Complete resection or local resection with adequate margins was performed for all GIST, and oral imatinib mesylate (IM) was administered postoperatively for medium- or high-risk GIST. All 19 patients received radical gastrectomy combined with complete stromal tumor resection, including four (21%) with laparotomy and 15 cases (79%) with laparoscopy. For GC, total gastrectomy was performed in six cases (31%), distal gastrectomy in 11 (58%) and proximal gastrectomy in two (11%). For postoperative treatment of GIST, two patients were given oral IM because GIST was classified as high risk, but the rest were not treated.

OUTCOME AND FOLLOW-UP

Patients were followed up by outpatient review or telephone; the primary event was death, and the last follow-up date was March 2022. During follow-up, two patients were lost, 12 survived, and five died of GC recurrence or distant metastasis (Table 1). No recurrence of GIST was found in 17 patients who were successfully followed up. The 3-year cumulative survival rate of 19 patients with synchronously occurring GC and GIST was 73.9%, and the 5-year cumulative survival rate was 59.2% (Figure 3A).

Table 1 Clinicopathological features, treatment and outcome of gastric cancer in 19 patients

No.	Age in yr	Sex	BMI	Chief complaint	Disease duration (mo)	Comorbidities in yr	Tumor marker	Primary site	Size (cm)	pTNM	Gross appearance	Differentiation	Lauren type	Outcome
1	66	M	17.9	Epigastric discomfort	12.0	HBP/20	(-)	Pylorus	1.5	T3N0M0/IIA	Ulcerativeinfiltrative	M-P	Mixed	38 m, PFS
2	56	M	24.2	CT found by accident	2.0	No	(-)	Cardia, body, antrum	10.0	T3N1M0/IIB	Diffuse infiltrative	P, SRCC	Diffuse	NA
3	53	M	19.5	Upper abdominal pain	0.5	No	CA72-4↑	Body	4.5	T3N0M0/IIA	Ulcerative infiltrative	P, SRCC	NA	48 m, PFS
4	71	M	21.5	Epigastric discomfort	6.0	No	(-)	Body	2.0	T2N0M0/IB	NA	M-P	Mixed	53 m, PFS
5	45	M	21.8	Bloating, acid reflux	6.0	No	(-)	Pylorus	3.5	T3N2M0/IIIA	Ulcerative	M-P, SRCC	Diffuse	48 m, DOD
6	55	M	25.5	Epigastric discomfort	2.0	No	(-)	Antrum	4.0	T1bN0M0/IA	Ulcerative	M-P, SRCC	Intestinal	6 m, PFS
7	79	F	22.2	Heartburn, abdominal pain, black stools	2.0	HBP/10, DM/10	(-)	Antrum	3.0	TisN0M0/0	NA	HGIEN	NA	27 m, PFS
8	58	M	27.9	Upper abdominal pain	4.0	No	(-)	Antrum	5.0	T4aN0M0/IIB	Ulcerative	P	Diffuse	26 m, PFS
9	71	M	23.8	Epigastric pain, acid reflux	1.0	HBP/10	(-)	Antrum	3.5	T1bN0M0/IA	NA	M	Intestinal	23 m, PFS
10	56	M	23.2	Upper abdominal pain, choking eating, black stools	1.0	No	(-)	Cardia	1.5	T2N0M0/IB	Ulcerative infiltrative	M	Intestinal	NA
11	55	M	23.7	Abdominal distension	9.0	No	CEA↑	Fundus	3.0	T4aN3bM0/IIIC	Ulcerative	M	Intestinal	10 m, DOD
12	59	M	23.1	Abdominal distension, black stools	1.0	DM/6	(-)	Body	5.0	T2N0M0/IB	Ulcerative	P	Diffuse	20 m, PFS
13	62	M	22.9	Upper abdominal pain	12.0	No	CEA↑, CA724↑	Body	2.0	T3N0M0/IIA	Ulcerative	P, SRCC	Diffuse	9 m, PFS
14	49	M	13.1	Epigastric discomfort	12.0	No	(-)	Cardia, fundus	5.0	T4bN0M0/IIIA	Ulcerative	M-P	Mixed	45 m, PFS
15	65	F	23.6	Epigastric discomfort, abdominal distension	12.0	No	(-)	Cardia, body	2.5	T4aN1M0/IIIA	Ulcerative	M	NA	5 m, DOD
16	73	M	21.3	Epigastric discomfort	48.0	No	CA724↑	Body	5.0	T4aN3bM0/IIIC	Ulcerative	M-P	Diffuse	12 m, DOD
17	62	M	22.8	Upper abdominal	6.0	DM/6	CEA↑,	Antrum	3.5	T4aN0M0/IIB	Ulcerative infiltrative	M	Intestinal	70 m, PFS

				pain			CA125↑						
18	62	M	21.2	Progressive dysphagia	3.0	HBP/30	CA199↑	Cardia	4.5	T4aN2M0/IIIA	Ulcerative	M-P	Mixed	12 m, DOD
19	72	M	22.4	Upper abdominal pain	0.5	No	(-)	Body	1.5	T1bN0M0/IA	NA	W	NA	63 m, PFS

M: Male; F: Female; HBP: High blood pressure; DM: Diabetes Mellitus (Type 2); TG: Total gastrectomy; DG: Distal gastrectomy; PG: Proximal gastrectomy; pTNM: Pathological tumor-node-metastasis; SRCC: Signet-ring cell carcinoma; HGIEN: High-grade intraepithelial neoplasia; NA: Not assessed; PFS: Progression-free survival; DOD: Dead of disease; M-P: Moderately to poorly differentiated; M: Moderately differentiated; P: Poorly differentiated; W: Well differentiated.

DISCUSSION

It has been reported that the incidence of GC accompanied by GIST is 0.29%-0.53%[6,30,52]. As the diagnostic criteria for GIST have changed and awareness has increased, data surveys in the United States and the Netherlands showed that the incidence of GIST has increased year by year[4,53]. Kawanowa *et al*[54] found that microscopic GIST was found in 35% of GC patients undergoing resection. In our series, the incidence of synchronous GC and GIST was 0.35% (19/5408). It is possible that the incidence of GC simultaneously occurring with GIST is higher because most GISTs are small (68% ≤ 2 cm, Table 3) and it is easy to miss diagnosis[7-41]. In addition to the small size of GIST, there are other factors contributing to the low preoperative diagnosis rate: (1) EUS demonstrates superior diagnostic capability for mesenchymal tissue GIST compared to conventional gastroscopy; however, most patients still opt for conventional gastroscopy; (2) Patients with concurrent GC and GIST primarily seek medical attention due to symptoms related to GC, resulting in a rarity of clinical recognition. Consequently, some clinicians may prioritize the diagnosis of GC while overlooking the presence of GIST; and (3) Some GISTs are extraluminal. Studies have shown that epigastric discomfort, dull pain, upper gastrointestinal bleeding, or melena may occur when the diameter of GIST is > 5 cm, and bleeding is the first symptom in most patients[55]. The clinical signs of synchronous GC and GIST lack specificity, and the symptoms of GIST are often masked by GC[45], probably because most GISTs are small in diameter (68% ≤ 2 cm).

In this study, the median age of concurrent GC and GIST was 62 years and combined with the literature review[7-41], the median age was 70 years (range: 45-93 years, 47 reports, 157 patients) (Table 3), which is similar to the median age at diagnosis for GIST (range: 66-69 years)[55]. Older people may have specific changes in gene expression profiles, lower immunity, and greater susceptibility to synchronous tumors[45]. The male to female ratio in this study was 8.5:1.0, and combined with other studies[7-41], the ratio was 3.4:1.0 (Table 3). The latest statistics report that GC incidence is two times higher in males than in females[56], while GIST has almost equal gender distribution[55].

The preoperative diagnosis rate of synchronous GIST and GC is low, and diagnosis is usually made during intraoperative exploration or postoperative pathological examination[6,30,45]. GIST is often misdiagnosed as metastatic lymph nodes from epithelial-mesenchymal transition or GC recurrence and metastasis. In our study, the preoperative diagnostic rate of suspicious GIST was 15% with CT, 21% with gastroscopy, and 63% with intraoperative exploration. Lin *et al*[45] found that among 42 patients with synchronous GC and GIST, only one (2.4%) was diagnosed preoperatively. Therefore, it is necessary for clinicians to carefully improve imaging examinations such as endoscopy and CT before surgery, and conduct comprehensive and meticulous exploration during surgery. If suspicious lesions are found, a routine biopsy or intraoperative frozen examination is performed to confirm the diagnosis, and a detailed analysis of specimens after surgery is required.

Table 2 The clinical, histological and immunohistochemical characteristics of gastrointestinal stromal tumor in 19 patients

No.	CT	EGD	Location	Origin	Size (cm)	Type	Growth pattern	Mitotic index (HPF)	Risk category	CD117	CD34	Dog-1	S-100	SMA	VIM	IM
1	GIST	GIST	Antrum	Submucosal	9.0	Spindle, epithelioid	Intraluminal	< 5/50	High	+	+	+	-	-	NA	Yes
2	(-)	(-)	Body	Muscularis	0.4	NA	Intramural	< 5/50	Very low	++	+++	+++	-	-	NA	No
3	(-)	(-)	Body	Subserous	1.0	Spindle	Extraluminal	< 5/50	Low	+	+	+	-	-	+	No
4	Mass	(-)	Duodenum	NA	2.0	Spindle	Extraluminal	< 5/50	Low	+	+	+	-	-	+	No
5	(-)	(-)	Jejunum	NA	1.5	Spindle	Extraluminal	< 5/50	Low	++	+	+++	-		NA	No
6	(-)	GIST	Fundus	Muscularis	1.5	Spindle	Extraluminal	< 5/50	Low	+	+	+	-	-	+	No
7	GIST	GIST	Body	NA	5.0	Spindle	Extraluminal	< 5/50	Low	+	+	+	-	-	+	No
8	Mass	Mass	Fundus	Subserous	1.0	Spindle	Intraluminal	< 5/50	Low	+	+	+	-	NA	NA	No
9	(-)	Mass	Duodenum	NA	4.0	Spindle	Extraluminal	< 5/50	Low	+	+	+	-	-	+	No
10	(-)	(-)	Cardia	Subserous	0.2	Spindle	Extraluminal	< 5/50	Very low	+	+	+	-	-	NA	No
11	GIST	GIST	Body	Muscularis	12.0	Spindle	Extraluminal, intraluminal	6-10/50	High	+	+	+	-	-	+	Yes
12	(-)	(-)	Jejunum	NA	4.0	Spindle	Extraluminal	< 5/50	Low	+	-	+	-	-	+	No
13	(-)	(-)	Body	Muscularis	0.4	Spindle	Intramural	< 5/50	Very low	+	+	+	-	-	NA	No
14	(-)	(-)	Fundus	Subserous	0.4	Spindle	Extraluminal	< 5/50	Very low	++	+++	+++	-	NA	NA	No
15	(-)	(-)	Body	Submucosal	0.6	Spindle	Intramural	< 5/50	Very low	+	+	+	-	-	NA	No
16	(-)	(-)	Body	Subserous	3.0.	Spindle	Extraluminal	< 5/50	Low	+	+	+	-	-	+	No
17	(-)	(-)	Antrum	Muscularis	< 1.0	NA	Intramural	< 5/50	Very low	+	+	NA	NA	NA	NA	No
18	(-)	(-)	Cardia, fundus	Subserous	0.4	Spindle	Extraluminal	< 5/50	Low	+	+	+	NA	-	NA	No
19	(-)	(-)	Body	Subserous	1.3	Spindle	Extraluminal	< 5/50	Very low	+	+	-	-	NA	+	No

NA: Not assessed; CT: Computed tomography; EGD: Esophagogastroduodenoscopy; V-L: Very low; L: Low; IN: Intermediate; H: High; IM: Imatinib mesylate; GC: Gastric cancer; GIST: Gastrointestinal stromal tumor.

In the present study, the median maximum diameter of the GC was 3.5 cm (range: 1.5-10.0 cm), and the most common appearance of GC was ulcerative (53%), which was similar to that reported by Maiorana *et al*[6] (50%) and Cai *et al*[25] (50%). Summarizing this study and literature review[7-41], we found that the median maximum diameter of the GC was 4 cm (range: 1.0-10.2 cm). GC is usually located in the lower third of the stomach (42%), stage I (42%), poorly differentiated (42%), and intestinal adenocarcinoma (51%) (Table 3). Therefore, we hypothesized that the occurrence of GIST might have an inhibitory effect on the progression of GC. This was a finding not encountered before in the literature. However, this conjecture is solely based on the findings of pertinent global research due to limited case numbers and a dearth of molecular biological mechanism investigations, thereby insufficiently substantiating this conclusion.

Table 3 Details of the clinical, histological, immunohistochemical, and outcomes of concurrent gastric cancer and gastrointestinal stromal tumor summarized in this study and literature review

Ref.	Sex	Age in yr	GC					GIST					Outcome
			Location	Size (cm)	TNM status	Lauren	Differentiation	Location	Size (cm)	Risk	CD117	CD34	
Maiorana *et al*[6], 2000	F	81	Cardias	4.0	T2bN0M0, IB	Intestinal	NA	Fundus	5.0	L	NA		21 m, DOD
	F	79	Antrum	2.0	T1bN0M0, IA	Diffuse		Pylorus	6.0	H		+	54 m, PFS
	M	75	Antrum	4.0	T2bN1M0, IIA	Intestinal		Antrum	5.0	L			12 m, PFS
	F	79	Pylorus	1.2	T2aN1M0, IIA	Intestinal		Cardias	5.0	L		+	28 m, PFS
	M	79	Antrum	2.0	T2aN0M0, IB	Intestinal		Cardias	0.6	V-L		+	75 m, PFS
Bircan *et al*[7], 2004	71	Antrum	5.7	T3NxM0	Intestinal	P	Cardias	0.5	V-L	+	+	NA	71
	77	Cardias	7.5	T2N1M0, IIA	NA	M	Cardias	0.6	V-L	+	+	NA	77
Villias *et al*[8], 2008	M	78	Antrum	NA	T1N0M0, IA	Intestinal	M	Antrum	0.9	V-L	+	+	NA
Lin *et al*[9], 2006	F	70	Cardias	1.7	T1N0M0, IA	NA	P, SRCC	Fundus	1.1	V-L	+	+	14 m, PFS
Liu *et al*[10], 2018	M	72	Antrum	4.0	T2N1M0, IIA	NA	M	Fundus	2.0	V-L	+	+	18 m, PFS
Wronski *et al*[11], 2006	F	64	Antrum	5.0	T4N0M0, IIB	Diffuse	NA	Cardias	2.0	L	+	+	NA
	M	66	Cardias	1.0	T1N0M0, IA	Intestinal	NA	Cardias	1.0	V-L	+	+	NA
Theodosopoulos *et al*[63], 2011	M	80	Antrum	6.5	T1N0M0, IA	Intestinal	W	Body	3.0	IN	+	NA	12 m, PFS
Rauf *et al*[46], 2006	F	70	Antrum, body	10.0.	T4N1M0, IIIA	Diffuse	P, SRCC	Body	2.0	L	+	+	18 m, DOD
Namikawa *et al*[14], 2021	M	74	Body	2.0	T2N0M0, IB	NA	M	Body	2.2	L	NA	NA	1 m, PFS
Shimodate *et al*[15], 2014	M	79	Body	3.0	T1bN0M0, IA	NA	NA	Body	1.3	V-L	+	+	NA
Khoshnevis *et al*[16], 2013	F	64	Pylorus	6.0	T4N0M0, IIIA	Diffuse	P, SRCC	Fundus, body	1.0	H	+	NA	4 m, PFS
Namikawa *et al*[17], 2016	M	58	Body	9.0	T2N1M0, IIA	Diffuse	SRCC	Body	21.0	H	NA	NA	4 m, PFS
Kaffes *et al*[18], 2002	M	78	Antrum	NA	T1N0M0, IA	Diffuse	P	Body	1.5	ND	NA	+	20 m, PFS
Uchiyama *et al*[19], 2007	M	74	Antrum	1.5	T1aN0M0, IA	Intestinal	M-P	Body	0.8	L	+	+	NA

Salemis *et al*[20], 2008	F	78	Antrum	6.5	T4N2M0, IIIA	Diffuse	P	Body	1.0	L	+	+	14 m, DOD
Narasimhamurthy *et al*[21], 2010	M	65	Cardias	4.0	T4NxM0	Diffuse	P	Antrum	2.5	L	+	NA	NA
Ferreira *et al*[22], 2010	M	52	NA	10.2	T3N1M0, IIB	NA	NA	NA	1.1	V-L	+	+	NA
	F	65	NA	4.8	T3N1M0, IIB	NA	NA	NA	0.7	V-L	+	+	
Gonçalves *et al*[23], 2010	M	74	NA	NA	NA	NA	NA	NA	1.2	V-L	NA	NA	5 m, DOD
	M	67	NA	NA	NA	NA	NA	NA	0.3	V-L	NA	NA	2 m, DOD
Jeong *et al*[24], 2011	M	74	Antrum	3.3	T1aN0M0, IA	Intestinal	M	Body	2.0	V-L	+	+	NA
Cai *et al*[25], 2013	M	47	Cardias	8.0	T3N1M0, IIB	NA	P	Cardias	2.0	V-L	+	+	NA
	M	80	Antrum	2.0	T1N0M0, IA		P	Cardias	1.5	V-L	+	+	
	M	60	Antrum	8.0	T3N0M0, IIA			Antrum	0.6	V-L	+	+	
	F	67	Antrum	4.0	T3N1M0, IIB			Body	0.8	V-L	+	+	
	M	78	Pylorus	6.0	T4N2M0, IIIA			Body	2.5	L	+	+	
	M	78	Body	10.0	T3N1M0, IIB			Body	1.4	L	+	+	
	F	59	Body	4.0	T2N1M0, IIA		P	Body	0.8	L	+	+	
	M	80	Antrum	6.0	T2N0M0, IB		P	Body	5.0	L	+	+	
Liszka *et al*[26], 2007	M	53	NA	NA	NA	NA	NA	NA	NA	V-L	+	NA	NA
	M	63	NA	NA	NA	NA	NA	NA	NA	L	+	NA	
Yamamoto *et al*[27], 2012	M	67	Body	3.0	T4N0M0, IIB	Diffuse	P	Body	3.0	L	+	+	NA
Gülpınar *et al*[28], 2014	M	75	Antrum	NA	T1N1M0, IB	NA	M	Antrum	1.0		NA	NA	NA
Trihia *et al*[29], 2019	M	79	Cardias	8.5	NA	Intestinal	M-P	Body	0.9	L	+	+	Days, DOD
Yan *et al*[30], 2013	M	53	U	NA	T4N0M0, IIIA	NA	P	NA	0.4	V-L	NA		NA
	M	51	U	NA	T4N3M0, IIIB		M-P		0.8	V-L	+		
	M	62	U	NA	T4N2M0, IIIA		P		0.8	V-L	NA		
	F	73	L	NA	T4N3M0, IIIB		P, SRCC		0.2	V-L	NA		
	M	68	M	NA	T1N0M0, IA		M		0.8	V-L	NA		
	F	46	L	NA	T1bN0M0, IA		P, SRCCM		2.5	L	+		
	M	78	U	NA	T4N1M0, IIIA		M		1.5	V-L	+		

	M	66	U	NA	T4N3M0, IIIB		M-P		1.5	V-L	+		
	M	85	U, M	NA	T4N2M0, IIIA		P		1.0	V-L	+		
	M	68	L	NA	T4N0M0, IIB		M		0.8	V-L	+		
	M	69	U	NA	T4N0M0, IIB		P, SRCC		2.0	V-L	+		
	M	77	U	NA	T2N1M0, IIA		M		0.2	V-L	+		
	M	71	L	NA	T4N3M0, IIIB		M-P		0.6	V-L	+		
	F	77	L	NA	T4N3M0, IIIB		M-P		0.5	V-L	+		
	F	70	L	NA	T1bN0M0, IA				0.6	V-L	+		
Vogel *et al*[31], 2011	M	79	Body	6.0	T1N0M0, IA	Diffuse	P, SRCC	Body	0.8	V-L	+	NA	12 m, PFS
[1]Ozgun *et al*[32], 2009	M	78	Body	NA	NA	NA	NA	Antrum	10.0	H	+	+	
Hsiao *et al*[33], 2009	M	75	Cardias	1.0	T1N0M0, IA	NA	W	Cardias	3.3	L	+	+	6 m, DOD
Kountourakis *et al*[34], 2008	F	72	NA	NA	NA	Diffuse	NA	NA	1.8	V-L	+	+	6 m, PFS
Lee *et al*[35], 2007	M	82	Body	9.5	T4NxM1, IV	NA	NA	Body	1.5	L	+	+	NA
Chen *et al*[36], 2001	M	72	Pylorus	1.5	NA	NA	NA	Body	2.5	V-L	+	+	NA
[1]Katsoulis *et al*[37], 2007	F	78	Cardias	NA	T4N3aM0, IIIB	Diffuse	P	Antrum	0.9	V-L	+	NA	NA
[1]Liu *et al*[38], 2002	M	70	Cardia, fundus	8.5	T4N0M1, IV	Intestinal	NA	Cardia	NA	V-L	+	+	3 m, DOD
[1]Toyoda *et al*[39], 2009	F	83	Body	9.0	T4NxM0	Intestinal	P	Body	4.5	H	+	+	6 m, DOD
[1]Matsuno *et al*[40], 2021	M	68	Body	5.0	T3N0M0, IIA	NA	M	Body	0.5	V-L	+	NA	2.5 yr, PFS
[1]Kleist *et al*[41], 2010	F	86	Body	6.0	NA	Intestinal	SRCC	Body	6.0	IN	+	+	11 m, PFS
	M	78	Body	6.0	NA	NA	SRCC	Body	5.5	IN	+	+	4 m, DOD
[1]Trabelsi *et al*[42], 2008	M	54	NA	NA	NA	Diffuse	NA	NA	1.0	V-L	NA	NA	NA
[1]Zámecník *et al*[64], 2005	F	93	Fundus	NA	LGIN, 0	NA	NA	Fundus	4.5	L	+	+	NA
[1]Idema *et al*[43], 2008	M	71	Body	5.0	T4N2M0, III A	Intestinal	SRCC	Body	0.6	V-L	+	+	30 m, DOD
Alkaaki *et al*[65], 2018	M	55	Cardia	1.7	T1aNxM0	NA	NA	Antrum	10	H	-	+	NA
[1]Bi *et al*[66], 2009	F	73	Fundus, body	4.0	T4N2M0, III A	Intestinal	W	Fundus	4	L	+	+	NA
[1]Firat *et al*[44], 2010	M	63	Cardia	9.0	T4N3bM0, IIIB	Intestinal	NA	Cardia	0.4	V-L	+	+	13 m, DOD

	M	60	Body	4.0	T1N0M0, IA	Intestinal		Body	0.5	V-L	+	+	12 m, PFS
Telugu *et al*[67], 2016	M	63	Cardia	4.0	T3N1M0, IIB	NA	M	Fundus	1.0	V-L	-	+	7 m, PFS
Lin *et al*[45], 2014	M (32), F (10)	> 60 (30), ≤ 60 (12)	NA	NA	IA (14), IB (8), IIA (5), IIB (1), IIIA (7), IIIB (4), III C (3)	NA	W (6), M (21), P (10), SRCC (5)	U (14), M (20), L (8)	≤ 2 (35), 2-5 (7)	V-L (35), L (4), IN (2), H (1)	+ (28)	+ (25)	3-yr (62.6), 5-yr (57.8%)
Liu *et al*[52], 2009	M (19), F (3)	64.5, (Med)	NA	NA	NA	NA	NA	Cardias (1), fundus (7), body (13), antrum (1)	0.8 (Med)	< L			5-yr (31.8%)
Present study	M (17), F (2)	62 (Med)	U (5), M (6), L (7), W (1)	3.5 (Med)	0 (1), IA (3), IB (3), IIA (3), IIB (3), III A (4), IIIC (2)	Diffuse (6), intestinal (5), mixed (3)	M-P (7), M (5), P (5), W (1)	Body (8), fundus (3), antrum (2), Cardia (2)	1.4 (Med)	L (10), V-L (7), H (2)	+ (19)	+ (18), - (1)	3-yr (73.9%), 5-yr (59.2%)
All	M (122), F (35)	70 (Med)	U (26), M (23), L (35)	4 (Med)	0 (2), IA (33), IB (16), IIA (17), IIB (13), IIIA (21), IIIB (11), IIIC (5), IV (2)	Diffuse (19), intestinal (23), mixed (3)	M-P (13), M (38), P (45), W (10)	U (43), M (66), L (20)	1.2 (Med)	V-L (84), L (35), IN (5), H (9)	- (2)	- (1)	3-yr (54.5%), 5-yr (46.7%)

[1]Collision tumor.

GC: Gastric cancer; GIST: Gastrointestinal stromal tumor; M: Male; F: Female; Med: Median; DOD: Dead of disease; U: Upper one-third of the stomach; M: Middle one-third of the stomach; L: Lower one-third of the stomach; LGIN: Low-grade intraepithelial neoplasia; M-P: Moderately to poorly differentiated; M: Moderately differentiated; P: Poorly differentiated; W: Well differentiated; SRCC: Signet-ring cell carcinoma; V-L: Very low; L: Low; IN: Intermediate; H: High; SRCC: Signet-ring cell carcinoma; NA: Not assessed; PFS: Progression-free survival; pTNM: Pathological tumor-node-metastasis.

In the case of GC occurring concomitantly with GIST, we found that GISTs were most frequently located in the gastric body (42%), with a maximum diameter of 1.4 cm (68% ≤ 2 cm), most often occurred in the subserosal layer, and the most common growth pattern was extraluminal (Table 2). These results were similar to our summary[7-41], with 51% of GISTs located in the middle third of the stomach, and the median largest diameter of GISTs was 1.2 cm (78% ≤ 2 cm) (Table 3). Yan *et al*[30] reported that 93% of GISTs simultaneously occurring with GC were < 2 cm in diameter, and Agaimy *et al*[57] found that 73% of GISTs were < 5 cm in diameter. Liu *et al*[52] found that GISTs that occurred simultaneously with GC were small, with a median diameter of 0.8 cm (range: 0.2-2.5 cm), while the median value of pure GIST was 7.5 cm (range: 1.5-30.0 cm). At present, the most practical value for the diagnosis of GIST is the proto-oncogene c-kit gene expression product CD-117 (80%-100%) and CD-34 (56%-83%)[55-57]. In our study, the positive rates of CD117 and CD34 in GIST co-occurring with GC were 100% and 95%, respectively; similar to the results reported by Liu *et al*[52] (CD117 92.6%, CD34 96.3%). Lin *et al*[45] found that compared with pure GIST, the positive rate of CD117 (66.7%) and CD34 (59.5%) in synchronous GC combined with GIST was lower. On the contrary, Liszka *et al*[26] found that the positive expression rate of CD117 in GIST combined with other tumors and GIST alone was 100%, and the positive rate of CD34 was 54.5% and 56.7%, respectively, with no significant difference. Combined with the literature review[7-41], we found that only two cases were negative for CD117 expression and one was negative for CD34 expression (Table 3). Liu *et al*[52] found that most incidental GISTs (90.7%) had low mitotic activity and low risk, while only 1.9% of clinical GIST cases had low risk. Cai *et al*[25] and Liszka *et al*[26] found that patients with synchronously occurring GIST and other tumors had a lower risk of invasion and a smaller tumor diameter than patients with GIST alone. Yan *et al*[30] reported that almost all GISTs occurring concomitantly with GC were stratified as very low or low risk. We found that 89% of GISTs were low or very low risk. When combined with other studies[7-41], we found that 89% of GISTs co-occurring with GC were classified as low or very low risk (Table 3). Liu *et al*[58] conducted a retrospective analysis on 24 patients diagnosed with GC

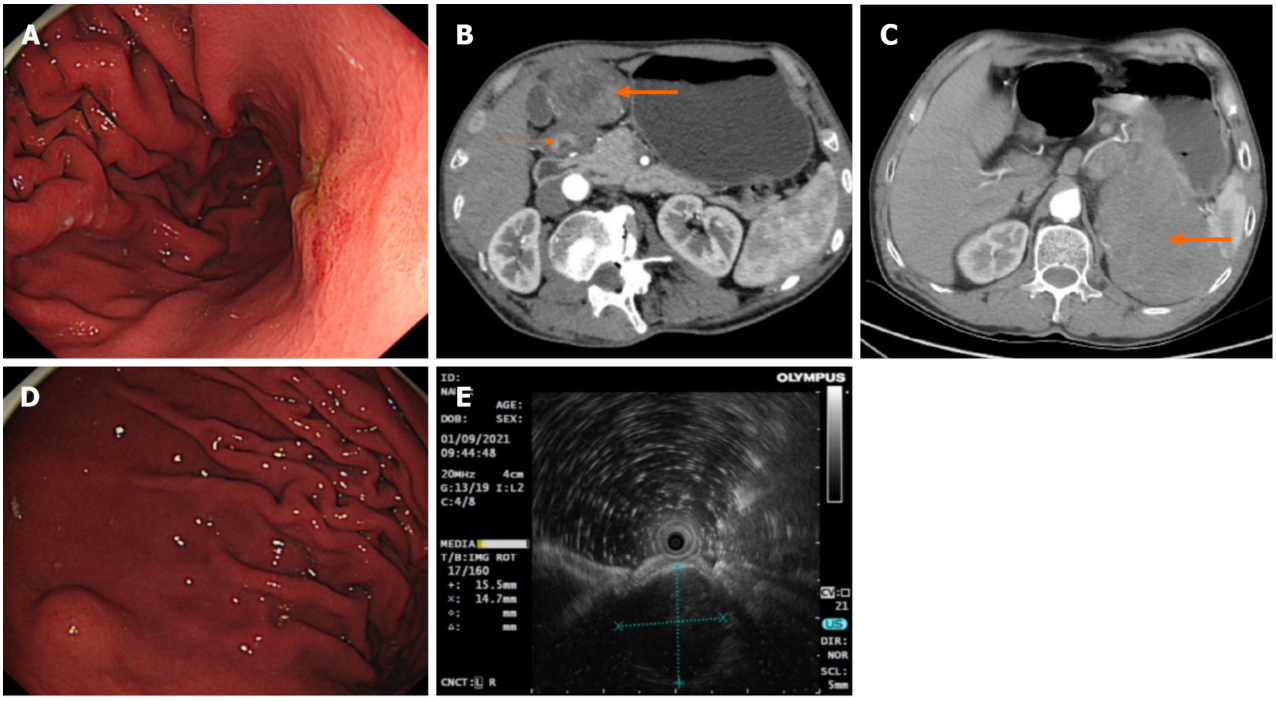

DOI: 10.4251/wjgo.v15.i10.1807 **Copyright** ©The Author(s) 2023.

Figure 1 Gastroscopic and imaging features of gastric cancer concomitant with gastrointestinal stromal tumor. A: Ulcerative gastric adenocarcinoma (patient 6); B: Pyloric adenocarcinoma (thin arrow) and intraluminal gastrointestinal stromal tumor (GIST; thick arrow) leading to pyloric obstruction (patient 1); C: Giant GIST (9.5 cm × 10.9 cm × 11.7 cm, arrow) showing intraluminal and extraluminal growth, compressing the spleen and left kidney (patient 11); D: Suspicious GIST under gastroscopy (patient 6); E: Suspicious GIST on ultrasound Endoscopy (patient 6).

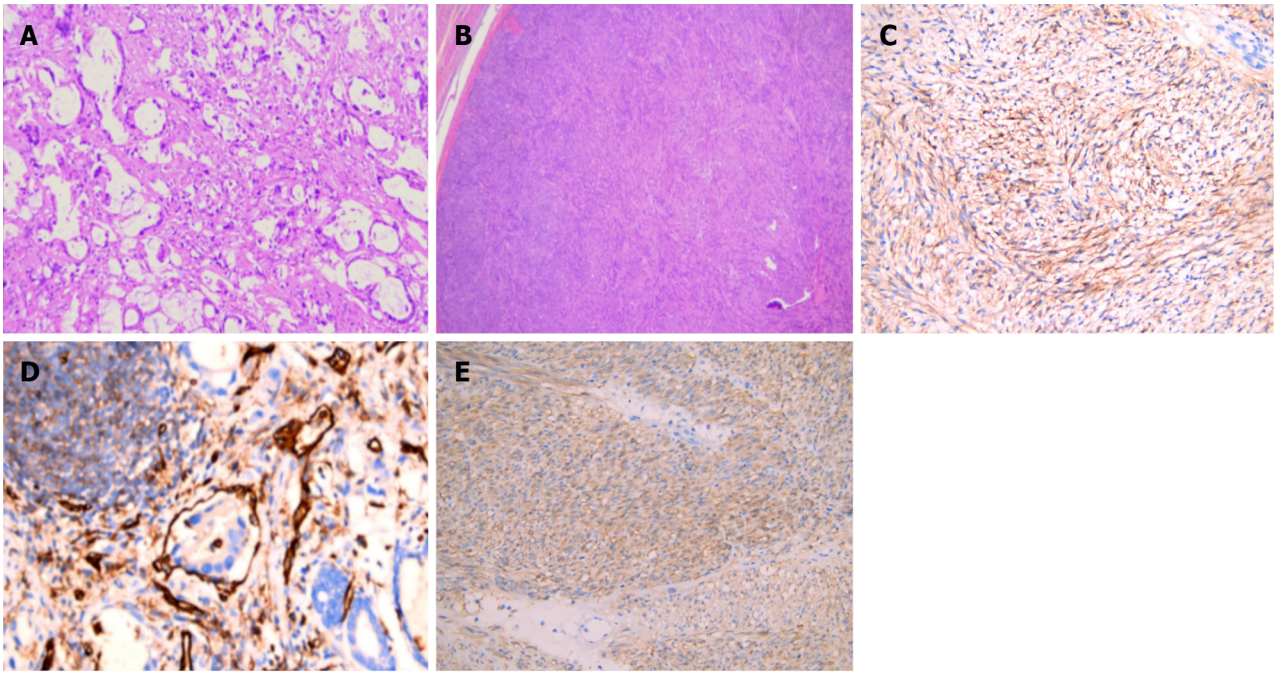

DOI: 10.4251/wjgo.v15.i10.1807 **Copyright** ©The Author(s) 2023.

Figure 2 Pathological and immunohistochemical features of gastric cancer concomitant with gastrointestinal stromal tumor. A: Microscopically showing gastric adenocarcinoma (patient 6; HE, 100 ×); B: Microscopically showing gastric stromal tumor (patient 6; HE, 100 ×); C: CD117 positive under microscope (patient 6; immunohistochemical staining, 200 ×); D: CD34 positive under microscope (patient 6; immunohistochemical staining, 200 ×); E: Dog-1 positive under microscope (patient 6; immunohistochemical staining, 200 ×).

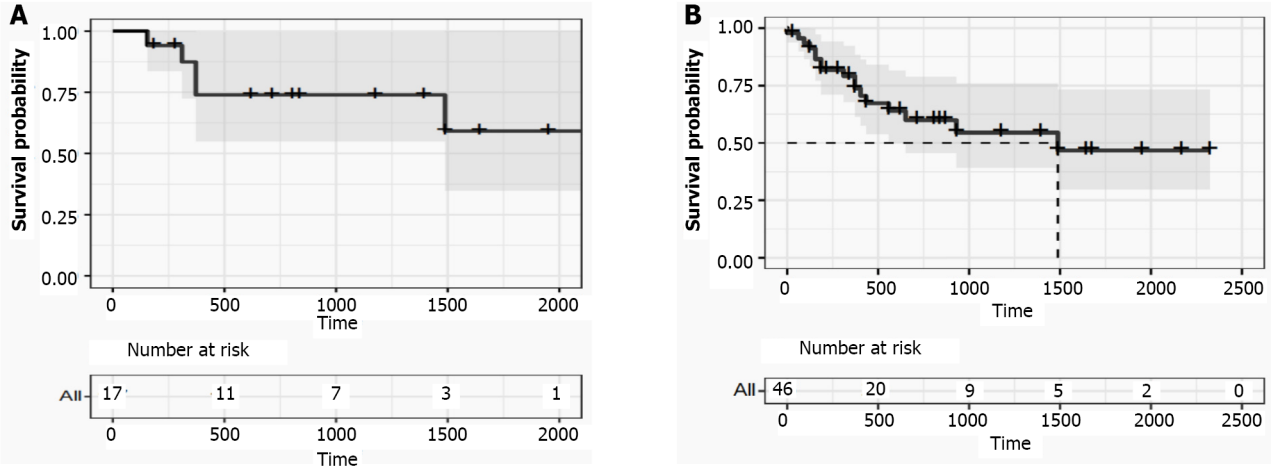

DOI: 10.4251/wjgo.v15.i10.1807 **Copyright** ©The Author(s) 2023.

Figure 3 Kaplan-Meier survival curves. A: 19 patients with gastric cancer (GC) accompanying gastrointestinal stromal tumor (GIST) in this study; B: 46 patients with GC accompanying GIST in this study and the literature reviewed.

combined with GISTs. The findings revealed that the occurrence of GIST combined with GC was more prevalent among elderly male patients, while GIST predominantly exhibited low-risk characteristics. Similarly, Liu *et al*[59] conducted an analysis on 26 patients diagnosed with GC and GISTs, revealing that the Fletcher classification typically indicates a very low or low risk of invasion in patients with GIST and GC. These findings may be related to the following factors: Widespread KIT/PDGFRA mutations in early tumorigenesis. Since additional mutations are required for GIST progression, synchronized tumors may influence the environment, release factors that inhibit the acquisition of further genetic changes, or inhibit GIST growth[30]. It may also be incidental that GIST develops later than GC.

At present, the etiology of GC co-occurrence with GIST is unclear. Some researchers believe that it is an accidental phenomenon[6,11], and others believe that several unknown carcinogens induce simultaneous proliferation and tumorigenesis of epithelial and stromal cells, such as gene mutation, nitrite, and *Helicobacter pylori*[6,7,9,11,18,30,34,37,38,46-49]. Gene mutations may lead to the interaction of two adjacent tissues, interfering with mesothelial and epithelial cell growth regulation, thereby inducing different tumors in two tissues of the same organ. Through next-generation sequencing, Liu *et al*[10] detected that GC and GIST had significantly different gene mutations at the molecular level (TP53 and KIT gene mutations, respectively). Some researchers have hypothesized that there might be a field effect, with etiological cofactors leading to these two lesions[60]. Based on the high correlation between clinical and microscopic GIST and GC, we believe that GC and GIST may be affected by the same unknown carcinogen, resulting in the simultaneous proliferation of epithelial and stromal cells.

Synchronous GC and GIST treatment is comprehensive and based on surgery. The surgical method is mainly based on GC, and adjuvant IM therapy should be given to patients with intermediate- and high-risk GIST after surgery[55]. In our study, all patients were given chemotherapy based on GC after surgery, and imatinib (IM) therapy was also given to patients with high-risk GIST. Xu *et al*[61] demonstrated that apatinib exhibits promising therapeutic potential and tolerability in patients with GC complicated by GISTs who have shown resistance to IM in combination with chemotherapy. However, there is still no conclusion on whether there is any interaction between chemotherapy for GC and IM treatment for GIST and the time sequence of medication.

For patients with synchronously occurring GC and GIST, studies have shown that regardless of the Fletcher grade of GIST, GC is the main factor affecting the prognosis[35,45,51]. Liu *et al*[52] conducted a follow-up study on 22 patients with synchronously occurring GC and GIST who underwent surgery and found that the 5-year survival rate after surgery was 31.8%, and the average survival time was 3 years. Lin *et al*[45] found that GIST risk stratification, postoperative oral IM, and synchronous GC were independent predictors of survival; the 3-year survival rate was 62.6%, the 5-year survival rate was 57.8%, and the 5-year overall survival rate of patients with synchronous GC was lower than that of patients with nonsynchronous GC (very low/low: 60.2% *vs* 98.6%; moderate/high risk: 33.3% *vs* 98.1%). In our study, the 3-year cumulative survival rate of 19 patients with concurrent GC and GIST was 73.9%, and the 5-year cumulative survival rate was 59.2%. We analyzed the survival of 46 patients with synchronous GC and GIST by combining the patients in this study (n = 17) and those reviewed in the literature (n = 29) (Figure 3B)[6-67]. The 3-year cumulative survival rate was 54.5%, the 5-year cumulative survival rate was 46.7%, the median survival time was 4 years, and none of the GISTs recurred during follow-up. In addition to the report by Liu *et al*[52], the 5-year survival rate of patients with GC combined with GIST in our study and in most studies was higher than that of patients with simple curable GC treated with surgery (5-year survival rate: 45%)[62], and similar to that of patients with simple GIST treated with complete resection (5-year survival rate: 50%-65%)[55]. To our knowledge, this is a finding that has not been encountered before in the literature. The reasons may be as follows: In patients with GC combined with GIST, most GC is early stage (42%), and most GIST is very low or low risk (89%). We hypothesize that there may be mutual inhibition between GC and GIST in the pathogenesis and progression. It is crucial to emphasize that our conjecture is solely based on a comprehensive analysis of current research findings both domestically and internationally. However, in order to validate this hypothesis,

extensive medical records and molecular biological investigations are imperative due to the absence of studies elucidating the underlying molecular mechanisms. In contrast, distinct findings emerge when comparing and analyzing GC patients with GIST and those diagnosed solely with GIST. Liu *et al*[58] conducted a comparative analysis between GC patients with GIST (n = 24) and gastric GIST patients (n = 217), revealing significantly lower 5-year disease-free survival rate and disease-specific survival rate in the former group compared to the non-synchronous group (54.9% *vs* 93.5%, $P < 0.001$; 37.9% *vs* 89.9%, $P < 0.001$). Similarly, Liu *et al*[59] conducted an analysis on a cohort of 26 patients with synchronous GC (group A) and 96 patients with gastric GIST (group B). The findings revealed that the Fletcher classification ($P < 0.05$) and synchronous GC ($P < 0.01$) were identified as independent prognostic factors.

LIMITATION

Our study had some limitations. Firstly, the research data quality could be better, with a limited number of cases (19 cases) and insufficient pathological research data. Additionally, more comprehensive test results and genetic and molecular data must be needed to support statistically significant conclusions based on limited information. Methodologically, this study is a retrospective single-centre investigation lacking prospective and case-control studies (including patients with superficial GC and Simple GIST patients) and molecular biological mechanism exploration. Regarding the study's content, an in-depth investigation of H. pylori was not conducted. Consequently, this study remains at a preliminary stage of exploration. This study concludes that further investigations are required to validate and supplement the conjecture. The future research will require enhancements in data quality, research methods, and a deeper exploration of the content.

CONCLUSION

Synchronous of GIST and GC are more common than previously considered. There are specific clinicopathological features between GC and GIST, such as those commonly seen in older men, GC is usually poorly differentiated intestinal-type early adenocarcinoma located in the lower third of the stomach, and GIST is usually small-diameter, low risk or very low risk located in the gastric body. We hypothesize that GC and GIST may be affected by the same unknown carcinogen, resulting in the simultaneous proliferation of epithelial and stromal cells. GC and GIST may have mutual inhibitory effects on the pathogenesis and disease progression. Importantly, a substantial amount of case data and studies on molecular biological mechanisms are imperative to validate this hypothesis.

ACKNOWLEDGEMENTS

The authors thanks professor Yu-Min Li for his comments on this manuscript and professor Ai-Lin Song, Xiao Chen, Ying-Xin Kang for their expert consultation on this article. All the authors thank the enrolled patients for their support of the data.

FOOTNOTES

Author contributions: Liu J performed data collection, statistical analysis, literature collection, and manuscript writing; Huang BJ, Tang FT, and Ding FF participated in the investigation and revision; Li YM designed, supervised, and guided this study; and all authors contributed to the article and approved the submitted version.

Supported by the Fundamental Research Funds for the Central Universities, No. lzujbky-2022-sp08.

Informed consent statement: Informed written or verbal consent were obtained from the patient for publication of this report and any accompanying images.

Conflict-of-interest statement: The authors declare that they have no conflict of interest to disclose.

CARE Checklist (2016) statement: The authors have read the CARE Checklist (2016), and the manuscript was prepared and revised according to the CARE Checklist (2016).

Country/Territory of origin: China

ORCID number: Yu-Min Li 0000-0002-9267-1412.

S-Editor: Chen YL
L-Editor: A
P-Editor: Chen YL

REFERENCES

1 **Menge F**, Jakob J, Kasper B, Smakic A, Gaiser T, Hohenberger P. Clinical Presentation of Gastrointestinal Stromal Tumors. *Visc Med* 2018; **34**: 335-340 [PMID: 30498699 DOI: 10.1159/000494303]
2 **Rabin I**, Chikman B, Lavy R, Sandbank J, Maklakovsky M, Gold-Deutch R, Halpren Z, Wassermann I, Halevy A. Gastrointestinal stromal tumors: a 19 year experience. *Isr Med Assoc J* 2009; **11**: 98-102 [PMID: 19432038]
3 **Nilsson B**, Bümming P, Meis-Kindblom JM, Odén A, Dortok A, Gustavsson B, Sablinska K, Kindblom LG. Gastrointestinal stromal tumors: the incidence, prevalence, clinical course, and prognostication in the preimatinib mesylate era--a population-based study in western Sweden. *Cancer* 2005; **103**: 821-829 [PMID: 15648083 DOI: 10.1002/cncr.20862]
4 **Goettsch WG**, Bos SD, Breekveldt-Postma N, Casparie M, Herings RM, Hogendoorn PC. Incidence of gastrointestinal stromal tumours is underestimated: results of a nation-wide study. *Eur J Cancer* 2005; **41**: 2868-2872 [PMID: 16293410 DOI: 10.1016/j.ejca.2005.09.009]
5 **Nishida T**, Hirota S. Biological and clinical review of stromal tumors in the gastrointestinal tract. *Histol Histopathol* 2000; **15**: 1293-1301 [PMID: 11005253 DOI: 10.14670/HH-15.1293]
6 **Maiorana A**, Fante R, Maria Cesinaro A, Adriana Fano R. Synchronous occurrence of epithelial and stromal tumors in the stomach: a report of 6 cases. *Arch Pathol Lab Med* 2000; **124**: 682-686 [PMID: 10782147 DOI: 10.5858/2000-124-0682-SOOEAS]
7 **Bircan S**, Candir O, Aydin S, Başpinar S, Bülbül M, Kapucuoğlu N, Karahan N, Ciriş M. Synchronous primary adenocarcinoma and gastrointestinal stromal tumor in the stomach: a report of two cases. *Turk J Gastroenterol* 2004; **15**: 187-191 [PMID: 15492920]
8 **Villias C**, Gourgiotis S, Veloudis G, Sampaziotis D, Moreas H. Synchronous early gastric cancer and gastrointestinal stromal tumor in the stomach of a patient with idiopathic thrombocytopenic purpura. *J Dig Dis* 2008; **9**: 104-107 [PMID: 18419644 DOI: 10.1111/j.1751-2980.2008.00330.x]
9 **Lin YL**, Tzeng JE, Wei CK, Lin CW. Small gastrointestinal stromal tumor concomitant with early gastric cancer: a case report. *World J Gastroenterol* 2006; **12**: 815-817 [PMID: 16521203 DOI: 10.3748/wjg.v12.i5.815]
10 **Liu S**, Liu H, Dong Y, Wang F, Wang H, Chen J. Gastric carcinoma with a gastrointestinal stromal tumor - A case report and literature review. *Med Sci (Paris)* 2018; **34** Focus issue F1: 15-19 [PMID: 30403169 DOI: 10.1051/medsci/201834f103]
11 **Wronski M**, Ziarkiewicz-Wroblewska B, Gornicka B, Cebulski W, Slodkowski M, Wasiutynski A, Krasnodebski IW. Synchronous occurrence of gastrointestinal stromal tumors and other primary gastrointestinal neoplasms. *World J Gastroenterol* 2006; **12**: 5360-5362 [PMID: 16981268 DOI: 10.3748/wjg.v12.i33.5360]
12 **A/L Chandrasekaran T**, Sahid NA, Maiyauen TK. Synchronous Gastrointestinal Stromal Tumor (GIST) with pancreatic adenocarcinoma: A case report. *Ann Med Surg (Lond)* 2022; **77**: 103588 [PMID: 35638052 DOI: 10.1016/j.amsu.2022.103588]
13 **Vasilakaki T**, Koulia K, Tsavari A, Arkoumani E, Kouroumpas E, Pavlis A, Christopoulos G, Stamatiou K, Manoloudaki K, Zisis D. Synchronous gastric gastrointestinal stromal tumor and colon adenocarcinoma: a case report. *Case Rep Oncol Med* 2014; **2014**: 305848 [PMID: 25197591 DOI: 10.1155/2014/305848]
14 **Namikawa T**, Maeda M, Yokota K, Tanioka N, Iwabu J, Munekage M, Uemura S, Maeda H, Kitagawa H, Nagata Y, Kobayashi M, Hanazaki K. Laparoscopic Distal Gastrectomy for Synchronous Gastric Cancer and Gastrointestinal Stromal Tumor With Situs Inversus Totalis. *In Vivo* 2021; **35**: 913-918 [PMID: 33622883 DOI: 10.21873/invivo.12331]
15 **Shimodate Y**, Sugiura K, Mitani Y, Hamaguchi K, Doi A, Nishimura N, Fujita H, Mouri H, Matsueda K, Yamamoto H. [A case report of endosonography used for the diagnosis of early gastric cancer and gastrointestinal stromal tumor]. *Nihon Shokakibyo Gakkai Zasshi* 2014; **111**: 1976-1982 [PMID: 25283226]
16 **Khoshnevis J**, Rakhshan A, Sobhiyeh MR, Gholizadeh B, Rahbari A, Adhami F, Lotfollahzadeh S. Simultaneous gastric adenocarcinoma and gastrointestinal stromal tumor of the stomach: a case report. *Iran J Cancer Prev* 2013; **6**: 55-58 [PMID: 25250111]
17 **Namikawa T**, Munekage E, Munekage M, Maeda M, Yatabe T, Kitagawa H, Sakamoto K, Obatake M, Kobayashi M, Hanazaki K. Synchronous Large Gastrointestinal Stromal Tumor and Adenocarcinoma in the Stomach Treated with Imatinib Mesylate Followed by Total Gastrectomy. *Anticancer Res* 2016; **36**: 1855-1859 [PMID: 27069170]
18 **Kaffes A**, Hughes L, Hollinshead J, Katelaris P. Synchronous primary adenocarcinoma, mucosa-associated lymphoid tissue lymphoma and a stromal tumor in a Helicobacter pylori-infected stomach. *J Gastroenterol Hepatol* 2002; **17**: 1033-1036 [PMID: 12167128 DOI: 10.1046/j.1440-1746.2002.02649.x]
19 **Uchiyama S**, Nagano M, Takahashi N, Hidaka H, Matsuda H, Nagaike K, Maehara N, Hotokezaka M, Chijiiwa K. Synchronous adenocarcinoma and gastrointestinal stromal tumors of the stomach treated laparoscopically. *Int J Clin Oncol* 2007; **12**: 478-481 [PMID: 18071869 DOI: 10.1007/s10147-007-0684-8]
20 **Salemis NS**, Gourgiotis S, Tsiambas E, Karameris A, Tsohataridis E. Synchronous occurrence of advanced adenocarcinoma with a stromal tumor in the stomach: a case report. *J Gastrointestin Liver Dis* 2008; **17**: 213-215 [PMID: 18568146]
21 **Narasimhamurthy MS**, Vallachira GP, Mahadev PS. Synchronous adenocarcinoma and gastrointestinal stromal tumor in the stomach. *Saudi J Gastroenterol* 2010; **16**: 218-220 [PMID: 20616420 DOI: 10.4103/1319-3767.65196]
22 **Ferreira SS**, Werutsky G, Toneto MG, Alves JM, Piantá CD, Breunig RC, Brondani da Rocha A, Grivicich I, Garicochea B. Synchronous gastrointestinal stromal tumors (GIST) and other primary cancers: case series of a single institution experience. *Int J Surg* 2010; **8**: 314-317 [PMID: 20380900 DOI: 10.1016/j.ijsu.2010.03.008]
23 **Gonçalves R**, Linhares E, Albagli R, Valadão M, Vilhena B, Romano S, Ferreira CG. Occurrence of other tumors in patients with GIST. *Surg Oncol* 2010; **19**: e140-e143 [PMID: 20675121 DOI: 10.1016/j.suronc.2010.06.004]
24 **Jeong SH**, Lee YJ, Park ST, Choi SK, Hong SC, Jung EJ, Ju YT, Jeong CY, Ha WS. Synchronous Adenocarcinoma and Gastrointestinal Stromal Tumor of the Stomach Treated by a Combination of Laparoscopy-assisted Distal Gastrectomy and Wedge Resection. *J Gastric Cancer* 2011; **11**: 55-58 [PMID: 22076202 DOI: 10.5230/jgc.2011.11.1.55]

25 **Cai R**, Ren G, Wang DB. Synchronous adenocarcinoma and gastrointestinal stromal tumors in the stomach. *World J Gastroenterol* 2013; **19**: 3117-3123 [PMID: 23716992 DOI: 10.3748/wjg.v19.i20.3117]

26 **Liszka Ł**, Zielińska-Pajak E, Pajak J, Gołka D, Huszno J. Coexistence of gastrointestinal stromal tumors with other neoplasms. *J Gastroenterol* 2007; **42**: 641-649 [PMID: 17701127 DOI: 10.1007/s00535-007-2082-4]

27 **Yamamoto D**, Hamada Y, Tsubota Y, Kawakami K, Yamamoto C, Yamamoto M. Simultaneous development of adenocarcinoma and gastrointestinal stromal tumor (GIST) in the stomach: case report. *World J Surg Oncol* 2012; **10**: 6 [PMID: 22230934 DOI: 10.1186/1477-7819-10-6]

28 **Gülpınar K**, Öziş E, Özdemir S, Korkmaz A. Synchronous occurance of adenocarcinoma and gastrointestinal stromal tumor of the stomach. *Turk J Gastroenterol* 2014; **25** Suppl 1: 256-257 [PMID: 25910328 DOI: 10.5152/tjg.2014.3873]

29 **Trihia HJ**. Coexistence of Gastric Cancer and Multiple Small Gastrointestinal Stromal Tumors: Report of a Unique Case and Review of the Literature. *Gastrointest Tumors* 2019; **5**: 63-67 [PMID: 30976576 DOI: 10.1159/000495178]

30 **Yan Y**, Li Z, Liu Y, Zhang L, Li J, Ji J. Coexistence of gastrointestinal stromal tumors and gastric adenocarcinomas. *Tumour Biol* 2013; **34**: 919-927 [PMID: 23283817 DOI: 10.1007/s13277-012-0627-5]

31 **Vogel Y**, Müller C, Uhl W, Tannapfel A. [Coexistence of multifocal gastric adenocarcinoma with signet-ring cell morphology and a gastrointestinal stromal tumour in a stomach with hp-associated gastritis]. *Z Gastroenterol* 2011; **49**: 201-206 [PMID: 21298606 DOI: 10.1055/s-0029-1245593]

32 **Ozgun YM**, Ergul E, Sisman IC, Kusdemir A. Gastric adenocarcinoma and GIST (collision tumors) of the stomach presenting with perforation; first report. *Bratisl Lek Listy* 2009; **110**: 504-505 [PMID: 19750991]

33 **Hsiao HH**, Yang SF, Liu YC, Yang MJ, Lin SF. Synchronous gastrointestinal stromal tumor and adenocarcinoma at the gastroesophageal junction. *Kaohsiung J Med Sci* 2009; **25**: 338-341 [PMID: 19560999 DOI: 10.1016/S1607-551X(09)70525-X]

34 **Kountourakis P**, Arnogiannaki N, Stavrinides I, Apostolikas N, Rigatos G. Concomitant gastric adenocarcinoma and stromal tumor in a woman with polymyalgia rheumatica. *World J Gastroenterol* 2008; **14**: 6750-6752 [PMID: 19034984 DOI: 10.3748/wjg.14.6750]

35 **Lee FY**, Jan YJ, Wang J, Yu CC, Wu CC. Synchronous gastric gastrointestinal stromal tumor and signet-ring cell adenocarcinoma: a case report. *Int J Surg Pathol* 2007; **15**: 397-400 [PMID: 17913950 DOI: 10.1177/1066896907302369]

36 **Chen JH**, Chen CC, Tzeng LM, Tsay SH, Chiang JH, Lu CC, Chang FY, Lee SD. Resection of triple synchronous tumors--gastric adenocarcinoma, gallbladder adenocarcinoma and stromal tumor of the stomach. *Zhonghua Yi Xue Za Zhi (Taipei)* 2001; **64**: 655-660 [PMID: 11853221]

37 **Katsoulis IE**, Bossi M, Richman PI, Livingstone JI. Collision of adenocarcinoma and gastrointestinal stromal tumour (GIST) in the stomach: report of a case. *Int Semin Surg Oncol* 2007; **4**: 2 [PMID: 17222335 DOI: 10.1186/1477-7800-4-2]

38 **Liu SW**, Chen GH, Hsieh PP. Collision tumor of the stomach: a case report of mixed gastrointestinal stromal tumor and adenocarcinoma. *J Clin Gastroenterol* 2002; **35**: 332-334 [PMID: 12352297 DOI: 10.1097/00004836-200210000-00010]

39 **Toyoda A**, Komaba A, Yoshizumi H, Hanaoka R, Sakuma S, Ichinohe A, Kawana H, Harigaya K. Collision of advanced gastric adenocarcinoma and gastrointestinal stromal tumour: a case report. *BMJ Case Rep* 2009; **2009** [PMID: 22110555 DOI: 10.1136/bcr.07.2009.2075]

40 **Matsuno K**, Kanazawa Y, Kakinuma D, Hagiwara N, Ando F, Masuda Y, Fujita I, Arai H, Nomura T, Kato S, Yoshiyuki T, Peng WX, Yoshida H. Preoperatively diagnosed gastric collision tumor with mixed adenocarcinoma and gastrointestinal stromal tumor: a case report and literature review. *Clin J Gastroenterol* 2021; **14**: 494-499 [PMID: 33512639 DOI: 10.1007/s12328-021-01343-4]

41 **Kleist B**, Lasota J, Miettinen M. Gastrointestinal stromal tumor and gastric adenocarcinoma collision tumors. *Hum Pathol* 2010; **41**: 1034-1039 [PMID: 20381123 DOI: 10.1016/j.humpath.2009.11.017]

42 **Trabelsi A**, Stita W, Mokni M, Yacoubi T, Mestiri S, Korbi SY. Collision epithelial and stromal tumours of the stomach: a case report. *Pathologica* 2008; **100**: 18-20 [PMID: 18686521]

43 **Idema DL**, Daryanani D, Sterk LM, Klaase JM. Collision tumor of the stomach: a case of an adenocarcinoma and a gastrointestinal stromal tumor. *Case Rep Gastroenterol* 2008; **2**: 456-460 [PMID: 21897799 DOI: 10.1159/000129707]

44 **Firat Ö**, Çalişkan C, Karaca C, Sezak M, Özütemız Ö, Ersın S, Güler A. Coexistence of gastric cancer and gastrointestinal stromal tumor: report of two cases. *Turk J Gastroenterol* 2010; **21**: 302-304 [PMID: 20931437 DOI: 10.4318/tjg.2010.0105]

45 **Lin M**, Lin JX, Huang CM, Zheng CH, Li P, Xie JW, Wang JB, Lu J. Prognostic analysis of gastric gastrointestinal stromal tumor with synchronous gastric cancer. *World J Surg Oncol* 2014; **12**: 25 [PMID: 24479763 DOI: 10.1186/1477-7819-12-25]

46 **Rauf F**, Ahmad Z, Muzzafar S, Hussaini AS. Synchronous occurrence of gastrointestinal stromal tumor and gastric adenocarcinoma: a case report. *J Pak Med Assoc* 2006; **56**: 184-186 [PMID: 16711342]

47 **Sugimura T**, Fujimura S, Baba T. Tumor production in the glandular stomach and alimentary tract of the rat by N-methyl-N'-nitro-N-nitrosoguanidine. *Cancer Res* 1970; **30**: 455-465 [PMID: 5458974]

48 **Cohen A**, Geller SA, Horowitz I, Toth LS, Werther JL. Experimental models for gastric leiomyosarcoma. The effects of N-methyl-N'-nitro-N-nitrosoguanidine in combination with stress, aspirin, or sodium taurocholate. *Cancer* 1984; **53**: 1088-1092 [PMID: 6692300 DOI: 10.1002/1097-0142(19840301)53:5<1088::AID-CNCR2820530512>3.0.CO;2-Y]

49 **Andea AA**, Lucas C, Cheng JD, Adsay NV. Synchronous occurrence of epithelial and stromal tumors in the stomach. *Arch Pathol Lab Med* 2001; **125**: 318-319 [PMID: 11231473 DOI: 10.5858/2001-125-0318-SOOEAS]

50 **Amin MB**, Edge SB, Greene FL, Brierley JD. AJCC cancer staging manual. 8th ed. New York: Springer, 2017 [DOI: 10.1007/978-3-319-40618-3]

51 **Fletcher CD**, Berman JJ, Corless C, Gorstein F, Lasota J, Longley BJ, Miettinen M, O'Leary TJ, Remotti H, Rubin BP, Shmookler B, Sobin LH, Weiss SW. Diagnosis of gastrointestinal stromal tumors: A consensus approach. *Hum Pathol* 2002; **33**: 459-465 [PMID: 12094370 DOI: 10.1053/hupa.2002.123545]

52 **Liu YJ**, Yang Z, Hao LS, Xia L, Jia QB, Wu XT. Synchronous incidental gastrointestinal stromal and epithelial malignant tumors. *World J Gastroenterol* 2009; **15**: 2027-2031 [PMID: 19399938 DOI: 10.3748/wjg.15.2027]

53 **Perez EA**, Livingstone AS, Franceschi D, Rocha-Lima C, Lee DJ, Hodgson N, Jorda M, Koniaris LG. Current incidence and outcomes of gastrointestinal mesenchymal tumors including gastrointestinal stromal tumors. *J Am Coll Surg* 2006; **202**: 623-629 [PMID: 16571433 DOI: 10.1016/j.jamcollsurg.2006.01.002]

54 **Kawanowa K**, Sakuma Y, Sakurai S, Hishima T, Iwasaki Y, Saito K, Hosoya Y, Nakajima T, Funata N. High incidence of microscopic gastrointestinal stromal tumors in the stomach. *Hum Pathol* 2006; **37**: 1527-1535 [PMID: 16996566 DOI: 10.1016/j.humpath.2006.07.002]

55 **Joensuu H**. Gastrointestinal stromal tumor (GIST). *Ann Oncol* 2006; **17** Suppl 10: x280-x286 [PMID: 17018739 DOI:

10.1093/annonc/mdl274]
56 **Sung H**, Ferlay J, Siegel RL, Laversanne M, Soerjomataram I, Jemal A, Bray F. Global Cancer Statistics 2020: GLOBOCAN Estimates of Incidence and Mortality Worldwide for 36 Cancers in 185 Countries. *CA Cancer J Clin* 2021; **71**: 209-249 [PMID: 33538338 DOI: 10.3322/caac.21660]
57 **Agaimy A**, Wünsch PH, Sobin LH, Lasota J, Miettinen M. Occurrence of other malignancies in patients with gastrointestinal stromal tumors. *Semin Diagn Pathol* 2006; **23**: 120-129 [PMID: 17193825 DOI: 10.1053/j.semdp.2006.09.004]
58 **Liu Z**, Liu S, Zheng G, Yang J, Hong L, Sun L, Fan D, Zhang H, Feng F. Clinicopathological features and prognosis of coexistence of gastric gastrointestinal stromal tumor and gastric cancer. *Medicine (Baltimore)* 2016; **95**: e5373 [PMID: 27828865 DOI: 10.1097/MD.0000000000005373]
59 **Liu XL**, Wang JB, Huang CM, Zheng CH, Li P, Xie JW, Lin JX. [Clinicopathologic features and prognostic factors of gastric gastrointestinal stromal tumor with synchronous gastric cancer]. *Zhonghua Wei Chang Wai Ke Za Zhi* 2012; **15**: 247-250 [PMID: 22454170]
60 **Almaça J**, Tian Y, Aldehni F, Ousingsawat J, Kongsuphol P, Rock JR, Harfe BD, Schreiber R, Kunzelmann K. TMEM16 proteins produce volume-regulated chloride currents that are reduced in mice lacking TMEM16A. *J Biol Chem* 2009; **284**: 28571-28578 [PMID: 19654323 DOI: 10.1074/jbc.M109.010074]
61 **Xu H**, Zhou S, Hu Q, Cao D. Apatinib treatment for unresectable gastrointestinal stromal tumor with synchronous gastric cancer. *Precis Clin Med* 2020; **3**: 67-70 [PMID: 35693429 DOI: 10.1093/pcmedi/pbaa005]
62 **Thrumurthy SG**, Chaudry MA, Chau I, Allum W. Does surgery have a role in managing incurable gastric cancer? *Nat Rev Clin Oncol* 2015; **12**: 676-682 [PMID: 26260039 DOI: 10.1038/nrclinonc.2015.132]
63 **Theodosopoulos T**, Dellaportas D, Psychogiou V, Gennatas K, Kondi-Pafiti A, Gkiokas G, Papaconstantinou I, Polymeneas G. Synchronous gastric adenocarcinoma and gastrointestinal stromal tumor (GIST) of the stomach: a case report. *World J Surg Oncol* 2011; **9**: 60 [PMID: 21615935 DOI: 10.1186/1477-7819-9-60]
64 **Zámecník M**, Sosna B, Chlumská A. Gastrointestinal stromal tumor (GIST) with glandular component. A report of an unusual tumor resembling adenosarcoma. *Cesk Patol* 2005; **41**: 150-156 [PMID: 16382991]
65 **Alkaaki A**, Abdulhadi B, Aljiffry M, Nassif M, Al-Maghrabi H, Maghrabi AA. Coexistence of Primary GEJ Adenocarcinoma and Pedunculated Gastric Gastrointestinal Stromal Tumor. *Case Rep Surg* 2018; **2018**: 4378368 [PMID: 29992077 DOI: 10.1155/2018/4378368]
66 **Bi R**, Sheng W, Wang J. Collision tumor of the stomach: gastric adenocarcinoma intermixed with gastrointestinal stromal tumor. *Pathol Int* 2009; **59**: 880-883 [PMID: 20021614 DOI: 10.1111/j.1440-1827.2009.02460.x]
67 **Telugu RB**, Pushparaj M, Masih D, Pulimood A. Synchronous Appearance of Adenocarcinoma and Gastrointestinal Stromal Tumour (GIST) of the Stomach: A Case Report. *J Clin Diagn Res* 2016; **10**: ED16-ED18 [PMID: 27042477 DOI: 10.7860/JCDR/2016/17636.7289]

World Journal of Gastrointestinal Oncology

Submit a Manuscript: https://www.f6publishing.com

World J Gastrointest Oncol 2023 October 15; 15(10): 1823-1828

DOI: 10.4251/wjgo.v15.i10.1823

ISSN 1948-5204 (online)

CASE REPORT

Comprehensive next-generation sequencing reveals double primary colorectal carcinoma missed by diagnostic imaging: A case report

Yan-Jun Qu, Qian-Shi Zhang, Bo Wang, Feng Zhang, Evenki Pan, Chun-Yan Zhao, Si-Ye Liu, Li-Ping Fang

Specialty type: Oncology

Provenance and peer review: Unsolicited article; Externally peer reviewed.

Peer-review model: Single blind

Peer-review report's scientific quality classification

Grade A (Excellent): 0
Grade B (Very good): B
Grade C (Good): C
Grade D (Fair): 0
Grade E (Poor): 0

P-Reviewer: Sridharan G, India; Tanabe H, Japan

Received: June 5, 2023
Peer-review started: June 5, 2023
First decision: July 8, 2023
Revised: July 14, 2023
Accepted: August 28, 2023
Article in press: August 28, 2023
Published online: October 15, 2023

Yan-Jun Qu, Li-Ping Fang, Department of Medical Oncology, The Second Hospital of Dalian Medical University, Dalian 116023, Liaoning Province, China

Qian-Shi Zhang, Bo Wang, Feng Zhang, Department of Gastrointestinal Surgery, The Second Hospital of Dalian Medical University, Dalian 116023, Liaoning Province, China

Evenki Pan, Chun-Yan Zhao, Si-Ye Liu, Department of Medical, Nanjing Geneseeq Technology Inc., Nanjing 211500, Jiangsu Province, China

Corresponding author: Li-Ping Fang, MD, Professor, Department of Medical Oncology, The Second Hospital of Dalian Medical University, No. 467 Zhongshan Road, Shahekou District, Dalian 116023, Liaoning Province, China. fangliping10000@dmu.edu.cn

Abstract

BACKGROUND

Multiple primary colorectal carcinoma (MPCC) is a rare clinical disease, which is challenging to differentiate from metastatic disease using histopathological methods. Next-generation sequencing (NGS) has been employed to identify multiple primary cancers.

CASE SUMMARY

This study a rare case of a 63-year-old male patient diagnosed with MPCC by targeted NGS, which was initially missed by radiological evaluation. The patient was found to have two tumors located on the surface of the colorectum which had distinct genomic alterations. Based on wild-type *KRAS* detected in the unresected tumor, the patient benefited from the epidermal growth factor receptor (EGFR) inhibitor cetuximab treatment, but developed novel mutations including *KIF5B-RET* fusion, which provides a possible resistance mechanism to anti-EGFR therapy.

CONCLUSION

Our case highlights the necessity of using genetic testing for primary tumor diagnosis and the application of serial plasma circulating tumor DNA profiling for dynamic disease monitoring.

Key Words: Multiple primary colorectal carcinoma; Next-generation sequencing; Cetuximab; RET fusion; Case report

Core Tip: We report a rare case of a 63-year-old male patient diagnosed with multiple primary colorectal carcinomas through targeted next-generation sequencing, which was initially missed by diagnostic imaging. The patient was found to have two tumors located on the colorectal surface which had different genomic alterations, as evidenced by immunohistochemistry staining. The patient benefited from treatment with the epidermal growth factor receptor inhibitor cetuximab due to the wild-type *KRAS* detected in the unresected tumor. This case emphasizes the importance of genetic testing for primary tumor diagnosis and the need for longitudinal circulating tumor DNA profiling to develop effective therapeutic strategies.

Citation: Qu YJ, Zhang QS, Wang B, Zhang F, Pan E, Zhao CY, Liu SY, Fang LP. Comprehensive next-generation sequencing reveals double primary colorectal carcinoma missed by diagnostic imaging: A case report. *World J Gastrointest Oncol* 2023; 15(10): 1823-1828
URL: https://www.wjgnet.com/1948-5204/full/v15/i10/1823.htm
DOI: https://dx.doi.org/10.4251/wjgo.v15.i10.1823

INTRODUCTION

Colorectal cancer (CRC) is one of the most lethal and prevalent malignancies worldwide, with approximately half of CRC patients eventually developing metastatic CRC[1]. However, the occurrence of multiple primary colorectal carcinoma (MPCC) is rare (between 1.1% and 8.1%)[2]. MPCC is defined as the discovery of two or more primary colorectal carcinomas in an individual occurring either synchronously or metachronously[3]. Preoperative detection of multiple primary cancers is important when planning treatment. Nevertheless, current diagnostic criteria may not identify all MPCC patients, leading to inappropriate treatment and follow-up plans[4]. To reduce the rate of misdiagnosis or missed diagnosis, recent studies have proposed the use of molecular testing and genomic profiling[5]. Herein, we report a case of MPCC that was initially missed *via* imaging but was diagnosed using next-generation sequencing (NGS). The patient was found to have two tumors on the surface of the colorectum which had completely different mutation patterns. Furthermore, a *KIF5B-RET* fusion was identified following cetuximab resistance, which has not been previously reported in CRC.

CASE PRESENTATION

Chief complaints

A 63-year-old man presented with hematochezia and abdominal pain in June 2020.

History of present illness

He was diagnosed with colorectal carcinoma initially.

History of past illness

He had no major illnesses in the past.

Personal and family history

He and his family both had no history of cancer.

Physical examination

The patient's vital signs were normal.

Laboratory examinations

To search for an efficient therapeutic strategy, genomic DNA from the formalin-fixed paraffin-embedded sample of lesion A and circulating tumor DNA (ctDNA) from plasma were subjected to targeted NGS of 425 cancer-related genes (Nanjing Geneseeq Technology Inc.) (Figure 1A). A comparison of the genetic alterations in lesion A and B can be found in Supplementary Table 1.

Imaging examinations

The computed tomography (CT) scan showed two lesions (defined as A and B) on the liver. Endoscopic resection revealed that the two lesions were located on the surface of the colon, and only lesion A was removed (Figure 2).

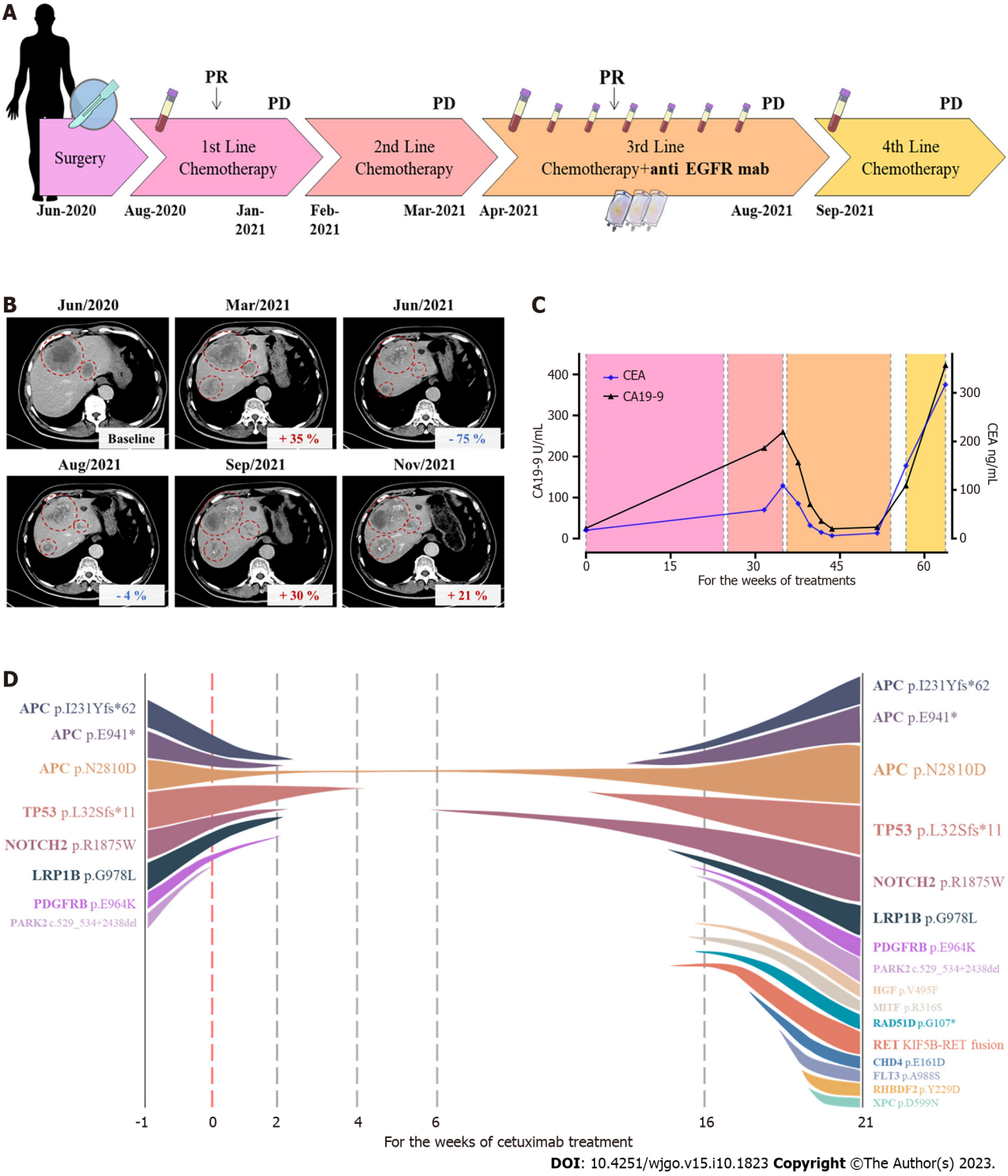

DOI: 10.4251/wjgo.v15.i10.1823 **Copyright** ©The Author(s) 2023.

Figure 1 Sequence of the patient's multiline treatments and computed tomography images, the levels of colorectal cancer biomarkers, and allele frequencies of circulating tumor DNA alterations during treatments. A: Timeline of multiline therapies received by the patient; B: Computed tomography images of liver metastases during treatment. Lesions are indicated by the red circles. The number represents the change in the size of liver metastases compared with the previous image; C: The levels of the colorectal cancer biomarkers carcinoembryonic antigen and carbohydrate antigen 19-9 are shown by the blue and black lines, respectively. The four background colors represent each treatment line; D: The allele frequencies of circulating tumor DNA alterations are shown during cetuximab treatment. CEA: Carcinoembryonic antigen; CA19-9: Carbohydrate antigen 19-9; PR: Partial response; PD: Progressive disease.

FINAL DIAGNOSIS

He was diagnosed with stage IV (pT3N1M1) colorectal carcinoma with liver metastases in June 2020.

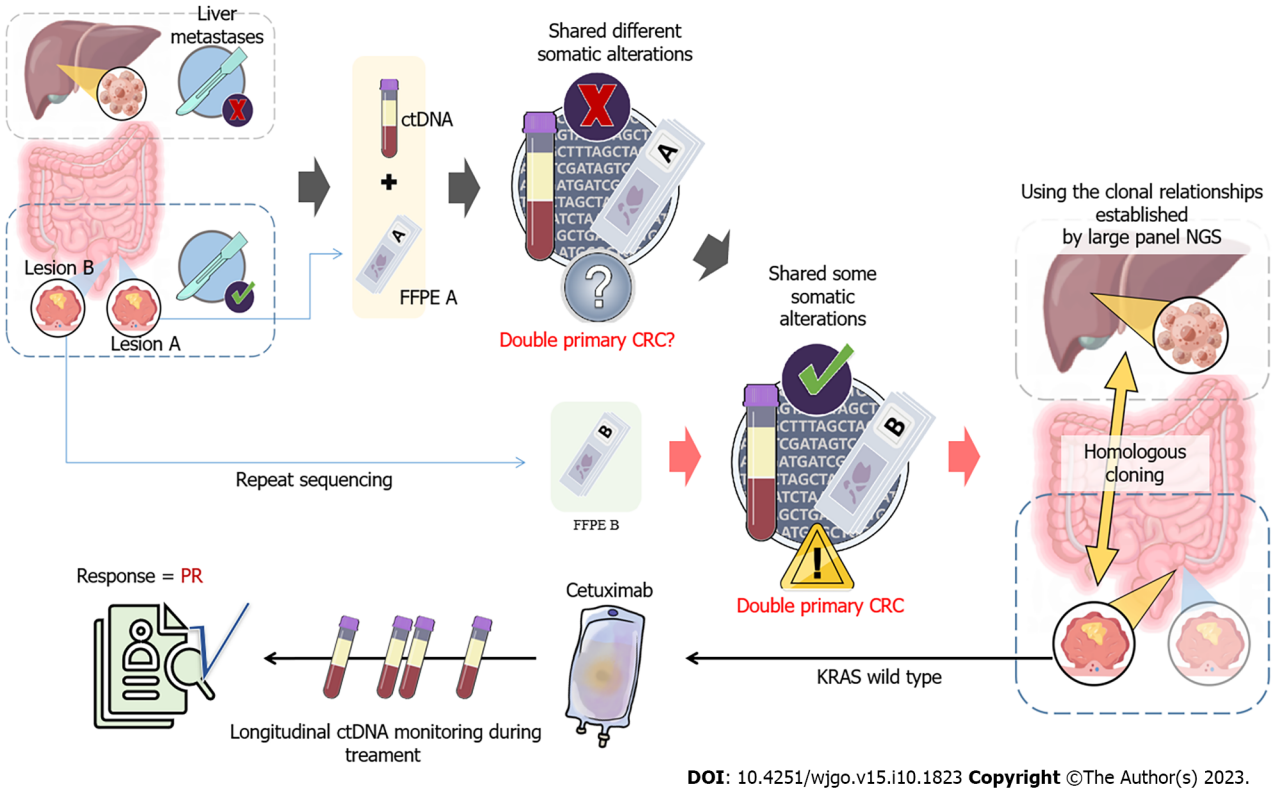

DOI: 10.4251/wjgo.v15.i10.1823 **Copyright** ©The Author(s) 2023.

Figure 2 Schematic diagram of the use of targeted next-generation sequencing for the diagnosis of two primary colorectal tumors, and the corresponding treatment and efficacy. NGS: Next-generation sequencing; FFPE: Formalin-fixed paraffin-embedded; CRC: Colorectal cancer.

TREATMENT

As the patient presented with intestinal bleeding, endoscopic resection was performed to alleviate his symptoms. Based on the identification of *KRAS* G12D with a mutation allelic frequency (MAF) of 41.9% identified in lesion A, the patient was administered XELOX plus bevacizumab (oxaliplatin 130 mg/m^2 on day 1, capecitabine 1500 mg/m^2 twice daily for 14 d, bevacizumab 7.5 mg/kg day 1) every 3 wk as first-line treatment. The patient achieved an initial partial response (PR) with sustained response ongoing for 11 mo. In January 2021, the tumor was evaluated as progressive disease (PD), and second-line chemotherapy was initiated with irinotecan (180 mg/m^2 day 1), raltitrexed (3 mg/m^2 day 1) and bevacizumab (5 mg/kg day 1) every 2 wk. Unfortunately, the liver lesion size increased by 35% compared to baseline, indicating a PD (Figure 1B). In April 2021, both plasma and lesion B were subjected to NGS and four identical mutation types were identified, with no *KRAS* mutations (Supplementary Table 1). A comparison of genomic alterations between lesion A and B revealed completely different mutation landscapes. Furthermore, immunohistochemistry illustrated significant differences between the two lesions (Supplementary Figure 1), which confirmed the diagnosis of MPCC. As the patient had wild-type *KRAS*, he was treated with irinotecan (180 mg/m^2 day 1), raltitrexed (3 mg/m^2 day 1), plus cetuximab (500 mg/m^2 day 1), a monoclonal antibody that blocks the epidermal growth factor receptor (EGFR), every 2 wk in April 2021. Plasma ctDNA sequencing and CT scans were conducted every 2 wk and 2 mo, respectively (Figure 1B and C). Two months later, it was observed that the size of liver metastases had decreased by 75% compared to the previous examination and ctDNA had rapidly decreased to less than 1% (Figure 1B and D). Moreover, the tumor markers for CRC, carcinoembryonic antigen (CEA) and carbohydrate antigen 19-9 (CA19-9) also significantly decreased to normal levels (Figure 1C), indicating a PR.

OUTCOME AND FOLLOW-UP

In August 2021, stable disease was observed with a 4% decrease in liver metastasis size compared to the previous examination, and no significant increase in CEA and CA19-9 Levels was observed (Figure1B and C). However, the allele frequencies (AFs) of ctDNA alterations in plasma samples were considerably elevated (Figure 1D and Supplementary Table 1). One month later, the tumor size had increased by 30% compared to the previous month, with a significant increase in CEA and CA19-9 levels (Figure 1B and C), indicating a PD. Due to the occurrence of *KIF5B-RET* fusion (MAF = 18.5%), we recommended the use of pralsetinib, a selective RET inhibitor, but the patient refused. Consequently, the fourth-line chemotherapy with XELOX and bevacizumab was administered. Two months later, the tumor size had increased by 21% (Figure 1B). Unfortunately, the patient later passed away due to hepatic failure in November 2021.

DISCUSSION

MPCC was initially discovered by Warren and Gates in 1941[6]. Despite its rarity, the occurrence of MPCC is showing an upward trend[2]. Due to a lack of understanding regarding MPCC and limited diagnostic techniques, it is always challenging to distinguish between multiple primary cancers and tumor metastasis. The emergence of NGS has already changed the landscape of cancer studies and is now widely used in the diagnosis of multiple primary cancers[7,8]. In our case, lesions A and B, were initially misdiagnosed as a primary lesion with metastasis due to their similar features. Thus, only tumor A and plasma samples were subjected to targeted NGS, revealing a completely different mutation pattern. Further targeted NGS on lesion B showed that these two tumor lesions, A and B, did not share any mutations. Through genetic profiling, it was confirmed that lesions A and B were independent primary lesions. Of note, the molecular variations identified by NGS aided in the diagnosis of both primary tumors. It was also hypothesized that tumor B may have played a role in the development of liver metastases, but the patient declined a liver biopsy. Subsequent NGS supported this hypothesis, as there was a strong correlation between tumor B and plasma ctDNA.

Surgical intervention has long been the ideal choice for cancer patients[9], but not for patients with metastatic lesions. Our patient presented with intestinal bleeding, and we opted for surgery to ease his symptoms. For those patients who cannot undergo surgery, radiotherapy and chemotherapy are the primary methods for disease control[10]. In addition, targeted therapy is an alternative approach that has proven to be effective in prolonging the overall survival rate of CRC patients[1]. The first targeted agent for CRC approved by the Food and Drug Administration was cetuximab, a monoclonal antibody that blocks EGFR, in 2004[11]. The efficacy of anti-EGFR therapy is dependent on the mutational status of downstream signaling molecules of the EGFR pathway, such as *KRAS*, *NRAS*, *PIK3CA*, and *BRAF*. Patients with a *KRAS* wild-type tumor are more likely to respond to this therapy[12]. In our patient, lesion B and ctDNA showed wild-type *KRAS*, while lesion A, which was removed, had a *KRAS* G12D mutation. Therefore, cetuximab was administered and the patient benefited from this treatment, with a decrease in liver tumor size, a reduction in AF of ctDNA, and lower serum tumor markers (CEA and CA19-9). Initially, the patient was found to have drug resistance by NGS, followed by serum tumor markers and a CT scan. Previous reports indicate that serial ctDNA profiling can detect disease progression earlier than CT scans[13]. Additionally, continuous monitoring of ctDNA can provide a more accurate understanding of the tumor, which can improve personalized treatment decisions[14]. To the best of our knowledge, this is the first time *KIF5B-RET* fusion has been discovered in a CRC patient with resistance to cetuximab. The emerging RET fusion variant is a significant driver gene for drug resistance in multiple progressive cancers, such as non-small cell lung cancer. Zhu *et al* [15] reported that the emergence of the *KIF5B-RET* fusion gene may cause acquired resistance to EGFR-tyrosine kinase inhibitors in EGFR-mutant lung adenocarcinomas[15]. Hence, we propose that this *KIF5B-RET* fusion gene may be a novel factor contributing to acquired resistance to cetuximab in *KRAS* wild-type CRCs. Nevertheless, the patient declined treatment with pralsetinib, a targeted RET inhibitor.

The limitations of the single case presentation in this study should be noted. While the *KIF5B-RET* fusion is a possible resistance mechanism to cetuximab, more pre-clinical research and clinical data are required to confirm its potential. NGS is a powerful tool that can provide valuable insights into an individual's genetic composition[16]. It can help identify genomic variations potentially linked to certain diseases or conditions, allowing for earlier diagnosis and selection of more effective treatment[17]. In this particular case, NGS played a pivotal role in diagnosing MPCC and offered direction for its treatment.

CONCLUSION

In summary, we report the rare case of a 63-year-old male patient with MPCC diagnosed through genetic profiling. The patient was treated with cetuximab based on wild-type *KRAS* identified on the lesion and later developed novel mutations including *KIF5B-RET* fusion, which provides a possible resistance mechanism to anti-EGFR therapy. This case highlights the necessity of using genetic testing for identifying primary tumors and the importance of longitudinal ctDNA profiling, which may trigger the development of effective therapeutic strategies.

FOOTNOTES

Author contributions: Qu YJ, Zhang QS, Wang B and Zhang F contributed equally to this work; All authors contributed to data analysis and drafting or revising the manuscript; All authors agreed on the journal to which the article is submitted, provided final approval of the version to be published, and agreed to be accountable for all aspects of the study.

Informed consent statement: This research was approved by the Ethics Committee of The Second Hospital of Dalian Medical University. Written informed consent to publish the clinical details and images were obtained from the patient.

Conflict-of-interest statement: Authors Evenki Pan and Chunyan Zhao are employed by Nanjing Geneseeq Technology Inc. The remaining authors declare that the research was conducted in the absence of any commercial or financial relationships that could be construed as a potential conflict of interest.

CARE Checklist (2016) statement: The authors have read the CARE Checklist (2016), and the manuscript was prepared and revised according to the CARE Checklist (2016).

Country/Territory of origin: China

ORCID number: Yan-Jun Qu 0000-0001-7336-1778; Qian-Shi Zhang 0000-0003-3336-9934; Bo Wang 0000-0003-4172-9271; Evenki Pan 0000-0001-9214-5108; Li-Ping Fang 0000-0001-5848-5627.

S-Editor: Fan JR
L-Editor: A
P-Editor: Yu HG

REFERENCES

1 **Xie YH**, Chen YX, Fang JY. Comprehensive review of targeted therapy for colorectal cancer. *Signal Transduct Target Ther* 2020; **5**: 22 [PMID: 32296018 DOI: 10.1038/s41392-020-0116-z]
2 **Lam AK**, Chan SS, Leung M. Synchronous colorectal cancer: clinical, pathological and molecular implications. *World J Gastroenterol* 2014; **20**: 6815-6820 [PMID: 24944471 DOI: 10.3748/wjg.v20.i22.6815]
3 **Wang HZ**, Huang XF, Wang Y, Ji JF, Gu J. Clinical features, diagnosis, treatment and prognosis of multiple primary colorectal carcinoma. *World J Gastroenterol* 2004; **10**: 2136-2139 [PMID: 15237453 DOI: 10.3748/wjg.v10.i14.2136]
4 **Lee SH**, Ahn BK, Baek SU. Multiple primary cancers in extracolonic sites with colorectal cancer. *Int J Colorectal Dis* 2009; **24**: 301-304 [PMID: 18797886 DOI: 10.1007/s00384-008-0583-0]
5 **Lin MW**, Wu CT, Kuo SW, Chang YL, Yang PC. Clinicopathology and genetic profile of synchronous multiple small adenocarcinomas: implication for surgical treatment of an uncommon lung malignancy. *Ann Surg Oncol* 2014; **21**: 2555-2562 [PMID: 24643899 DOI: 10.1245/s10434-014-3642-5]
6 **Warren S**, Gates O. Carcinoma of ceruminous gland. *Am J Pathol* 1941; **17**: 821-826.3 [PMID: 19970598]
7 **Ravella L**, Barritault M, Bringuier PP, Chalabreysse L, Thivolet-Bejui F, Maury JM, Duruisseaux M, Brevet M. [Multiple lung carcinoma: Primary or intrapulmonary metastasis?]. *Ann Pathol* 2018; **38**: 202-205 [PMID: 29555057 DOI: 10.1016/j.annpat.2018.02.001]
8 **Chang JC**, Alex D, Bott M, Tan KS, Seshan V, Golden A, Sauter JL, Buonocore DJ, Vanderbilt CM, Gupta S, Desmeules P, Bodd FM, Riely GJ, Rusch VW, Jones DR, Arcila ME, Travis WD, Ladanyi M, Rekhtman N. Comprehensive Next-Generation Sequencing Unambiguously Distinguishes Separate Primary Lung Carcinomas From Intrapulmonary Metastases: Comparison with Standard Histopathologic Approach. *Clin Cancer Res* 2019; **25**: 7113-7125 [PMID: 31471310 DOI: 10.1158/1078-0432.CCR-19-1700]
9 **Schreuders EH**, Ruco A, Rabeneck L, Schoen RE, Sung JJ, Young GP, Kuipers EJ. Colorectal cancer screening: a global overview of existing programmes. *Gut* 2015; **64**: 1637-1649 [PMID: 26041752 DOI: 10.1136/gutjnl-2014-309086]
10 **Brown KGM**, Solomon MJ, Mahon K, O'Shannassy S. Management of colorectal cancer. *BMJ* 2019; **366**: l4561 [PMID: 31439545 DOI: 10.1136/bmj.l4561]
11 **Chu E**. An update on the current and emerging targeted agents in metastatic colorectal cancer. *Clin Colorectal Cancer* 2012; **11**: 1-13 [PMID: 21752724 DOI: 10.1016/j.clcc.2011.05.005]
12 **Saridaki Z**, Georgoulias V, Souglakos J. Mechanisms of resistance to anti-EGFR monoclonal antibody treatment in metastatic colorectal cancer. *World J Gastroenterol* 2010; **16**: 1177-1187 [PMID: 20222160 DOI: 10.3748/wjg.v16.i10.1177]
13 **Zhang C**, Chen Z, Chong X, Chen Y, Wang Z, Yu R, Sun T, Chen X, Shao Y, Zhang X, Gao J, Shen L. Clinical implications of plasma ctDNA features and dynamics in gastric cancer treated with HER2-targeted therapies. *Clin Transl Med* 2020; **10**: e254 [PMID: 33377634 DOI: 10.1002/ctm2.254]
14 **Kim S**, Lim Y, Kang JK, Kim HP, Roh H, Kim SY, Lee D, Bang D, Jeong SY, Park KJ, Han SW, Kim TY. Dynamic changes in longitudinal circulating tumour DNA profile during metastatic colorectal cancer treatment. *Br J Cancer* 2022; **127**: 898-907 [PMID: 35643791 DOI: 10.1038/s41416-022-01837-z]
15 **Zhu YC**, Wang WX, Zhang QX, Xu CW, Zhuang W, Du KQ, Chen G, Lv TF, Song Y. The KIF5B-RET Fusion Gene Mutation as a Novel Mechanism of Acquired EGFR Tyrosine Kinase Inhibitor Resistance in Lung Adenocarcinoma. *Clin Lung Cancer* 2019; **20**: e73-e76 [PMID: 30366769 DOI: 10.1016/j.cllc.2018.09.011]
16 **Hussen BM**, Abdullah ST, Salihi A, Sabir DK, Sidiq KR, Rasul MF, Hidayat HJ, Ghafouri-Fard S, Taheri M, Jamali E. The emerging roles of NGS in clinical oncology and personalized medicine. *Pathol Res Pract* 2022; **230**: 153760 [PMID: 35033746 DOI: 10.1016/j.prp.2022.153760]
17 **Mosele F**, Remon J, Mateo J, Westphalen CB, Barlesi F, Lolkema MP, Normanno N, Scarpa A, Robson M, Meric-Bernstam F, Wagle N, Stenzinger A, Bonastre J, Bayle A, Michiels S, Bièche I, Rouleau E, Jezdic S, Douillard JY, Reis-Filho JS, Dienstmann R, André F. Recommendations for the use of next-generation sequencing (NGS) for patients with metastatic cancers: a report from the ESMO Precision Medicine Working Group. *Ann Oncol* 2020; **31**: 1491-1505 [PMID: 32853681 DOI: 10.1016/j.annonc.2020.07.014]

World Journal of Gastrointestinal Oncology

Submit a Manuscript: https://www.f6publishing.com

World J Gastrointest Oncol 2023 October 15; 15(10): 1829-1834

DOI: 10.4251/wjgo.v15.i10.1829

ISSN 1948-5204 (online)

CASE REPORT

Response to osimertinib in a colorectal cancer patient with an *EGFR* T790M mutation: A case report

Blake Buzard, Lindsey Douglass, Beth Gustafson, Jennifer Buckley, Marc Roth, Lara Kujtan, Dhruv Bansal

Specialty type: Oncology

Provenance and peer review: Unsolicited article; Externally peer reviewed.

Peer-review model: Single blind

Peer-review report's scientific quality classification

Grade A (Excellent): A
Grade B (Very good): 0
Grade C (Good): C
Grade D (Fair): 0
Grade E (Poor): 0

P-Reviewer: Ji DYX, China; Lin Q, China

Received: July 21, 2023
Peer-review started: July 21, 2023
First decision: August 23, 2023
Revised: September 6, 2023
Accepted: September 18, 2023
Article in press: September 18, 2023
Published online: October 15, 2023

Blake Buzard, Lindsey Douglass, Beth Gustafson, Jennifer Buckley, Marc Roth, Cancer Institute, St. Luke's Hospital, Kansas, MO 64111, United States

Lara Kujtan, Department of Medical Oncology, University of Missouri - Kansas City, Kansas, MO 64108, United States

Dhruv Bansal, Department of Hematology/Oncology, St. Luke's Cancer Institute, Kansas, MO 64111, United States

Corresponding author: Lara Kujtan, MD, Associate Professor, Department of Medical Oncology, University of Missouri - Kansas City, No. 2310 Holmes St, Kansas, MO 64108, United States. kujtanl@umsystem.edu

Abstract

BACKGROUND

Although common in lung cancer, somatic epidermal growth factor receptor (*EGFR*) mutations are rarely found in colorectal cancer, occurring in approximately 3% of cases. Treatment with anti-EGFR antibodies is commonplace, but *EGFR* tyrosine kinase inhibitors are not standard treatments in colorectal cancer. Here we report a case of sustained response to osimertinib in a colorectal cancer patient with an *EGFR* T790M mutation on cell-free DNA analysis.

CASE SUMMARY

A 72-year old woman with a past medical history of post-polio syndrome confined to a wheelchair, scoliosis and hypothyroidism presented with metastatic sigmoid colon adenocarcinoma with hepatic metastases. Next generation sequencing revealed a *RAS/RAF* wild-type, microsatellite stable, PD-L1 negative malignancy. Mutations in *TP3* and *APC* were also identified, as well as *EGFR* amplification. Cell-free DNA analysis revealed an *EGFR* T790M mutation. She was unable to tolerate first-line treatment with panitumumab, 5-fluorouracil and leucovorin, progressed on second-line treatment with trifluridine/tipiracil plus bevacizumab, and was unable to tolerate third-line treatment with regorafenib. She was started on fourth-line treatment with off-label osimertinib, with clinical response – decrease in size of hepatic metastases and a pericardial effusion. She remained on treatment with osimertinib for seven months.

CONCLUSION

This case shows the benefit of multi-gene sequencing assays to identify potential therapeutic options in patients with refractory disease.

Key Words: Colorectal cancer; Osimertinib; Epidermal growth factor receptor T790M; Precision oncology; Tyrosine kinase inhibitor; Case report

Core Tip: Somatic epidermal growth factor receptor (*EGFR*) mutations are rarely found in colorectal cancer. Treatment with anti-EGFR antibodies is commonplace, but *EGFR* tyrosine kinase inhibitors are not standard in colorectal cancer. Here we report a case of sustained response to osimertinib in a metastatic colorectal cancer patient with an *EGFR* T790M mutation detected with cell-free DNA. She progressed on three lines of treatment, and received fourth-line treatment with off-label osimertinib, with clinical response. She received treatment with osimertinib for seven months. This case shows the benefit of multi-gene sequencing assays to identify potential therapeutic options in patients with refractory disease.

Citation: Buzard B, Douglass L, Gustafson B, Buckley J, Roth M, Kujtan L, Bansal D. Response to osimertinib in a colorectal cancer patient with an *EGFR* T790M mutation: A case report. *World J Gastrointest Oncol* 2023; 15(10): 1829-1834
URL: https://www.wjgnet.com/1948-5204/full/v15/i10/1829.htm
DOI: https://dx.doi.org/10.4251/wjgo.v15.i10.1829

INTRODUCTION

Although common in lung cancer, somatic epidermal growth factor receptor (*EGFR*) mutations are rarely found in colorectal cancer, occurring in approximately 3% of cases[1]. Treatment with anti-EGFR antibodies is commonplace, but *EGFR* tyrosine kinase (TK) inhibitors (TKIs) are not standard treatments in colorectal cancer. Here we report a case of sustained response to osimertinib in a colorectal cancer patient with an *EGFR* T790M mutation on cell-free DNA analysis.

CASE PRESENTATION

Chief complaints

Our patient is a 72-year-old white female who presented with a chief complaint of right upper quadrant pain.

History of present illness

She was diagnosed with metastatic sigmoid colon adenocarcinoma with liver involvement in November 2020 (Table 1).

History of past illness

She was a former light smoker who quit 10 years before the diagnosis of colon cancer.

Personal and family history

The patient had a past medical history of post-polio syndrome confined to a wheelchair, scoliosis, and hypothyroidism.

Physical examination

Physical examination findings were significant for mild tenderness to palpation in the right upper quadrant without abdominal distention as well as chronic muscle wasting and decreased muscle tone secondary to post-polio syndrome. Her Eastern Cooperative Oncology Group (ECOG) performance status was 3.

Laboratory examinations

Next-generation sequencing (NGS) covering over 600 genes was performed on the liver biopsy and revealed a *RAS/RAF* wild-type, microsatellite stable, PD-L1 negative malignancy. In addition, *TP53* and *APC* mutations and *EGFR* amplification with C-terminal deletion in exons 27-28 were discovered. Cell-free DNA analysis revealed an *EGFR* p.T790M exon 20 somatic mutation with a variant allele frequency (VAF) of 12.3%.

Imaging examinations

Computed tomography (CT) imaging revealed hepatic metastases at diagnosis.

FINAL DIAGNOSIS

She was diagnosed with metastatic sigmoid colon adenocarcinoma with liver involvement in November 2020 (Table 1).

Table 1 Timeline of events

Date	Event
November 2020	Diagnosed with metastatic colon adenocarcinoma and started on panitumumab, 5-fluorouracil and leucovorin
January 2021	Switched to trifluridine/tipiracil
November 2021	Disease progression on CT imaging
December 2021	Switched to regorafenib
February 2022	Switched to osimertinib
November 2023	Died

TREATMENT

She desired to preserve her quality of life and minimize side effects and trips to the cancer center. With these goals in mind, she declined standard frontline treatment options, including FOLFOX and FOLFIRI. This patient was discussed at our molecular tumor board in December 2020. At that time, anti-EGFR antibody therapy was recommended as *EGFR* amplification was thought to be secondary to the *EGFR* exon 27-28 deletion and truncation of the C-terminal domain leading to a paradoxical, ligand-independent downstream activation of the MAPK pathway[2]. She initially received panitumumab, 5-fluorouracil, and leucovorin. However, shortly after receiving panitumumab, the patient complained of post-nasal drainage and difficulty swallowing. She declined further treatment with this regimen. Pursuant to her goals of minimizing time spent at the cancer center and using the least toxic regimen, she was transitioned to treatment with trifluridine/tipiracil plus bevacizumab in January 2021[3]. Imaging revealed treatment response with subsequent progression in November 2021, eleven months after initiation of treatment.

Subsequently, she was initiated on third-line treatment with regorafenib in December 2021. The patient experienced multiple treatment interruptions due to poor tolerability (primarily grade 3 hypertension), and the decision was made to stop regorafenib. Her case was re-presented at the molecular tumor board in January 2022. Recommendations at that time were to pursue clinical trial options for anti-EGFR therapy or off-label *EGFR* TKI therapy. An ECOG performance status of 3 precluded enrollment in local therapeutic clinical trials, and the patient expressed that she did not wish to travel. The decision was made to initiate off-label osimertinib.

She started osimertinib 80 mg daily in February 2022. The VAF of the *EGFR* T790M mutation was 13.3%. Two weeks after initiating osimertinib, the patient developed an acneiform rash on both cheeks. Oral minocycline was prescribed, and the rash improved within two weeks. Worsening fatigue and an elevated total bilirubin of 2.1 mg/dL were noted within the first month of therapy. Her fatigue improved, and bilirubin normalized by the start of cycle two without dose modifications. Between March and April of 2022, the patient developed grade 2 anemia and grade 2 thrombocytopenia, both of which were monitored. A CT chest, abdomen, and pelvis with contrast was obtained five weeks after initiating osimertinib and revealed a decrease in the size of liver metastases and an unchanged appearance of the primary sigmoid colon malignancy. The VAF of the *EGFR* T790M mutation was then 2.1%, which correlated with the response seen on imaging (Figure 1).

OUTCOME AND FOLLOW-UP

In June 2022, a CT scan revealed portal vein thrombosis, and apixaban was initiated. In addition, the osimertinib dose was reduced from 80 mg to 40 mg daily due to the aforementioned hematologic toxicities.

This same CT scan obtained five months after the initiation of osimertinib revealed further improvement in hepatic metastases with a decrease in the size of the dominant hepatic mass from 11.9 cm at the time of initiation of therapy to 8.4 cm (Figure 2). An echocardiogram revealed a decrease in the size of a pericardial effusion, which was present at the time of initiation of osimertinib. Subsequent imaging seven months after initiation of treatment revealed progression of hepatic metastases and new onset large volume ascites and peritoneal carcinomatosis. She decided to pursue hospice at this juncture and passed away two weeks later.

DISCUSSION

Our patient presented with metastatic colorectal cancer, which became refractory to treatment with trifluridine/tipiracil and bevacizumab. In addition, as described above, she had an intolerance to panitumumab and regorafenib. Cell-free DNA analysis revealed an *EGFR* T790M mutation. The patient's case was referred to our molecular tumor board, and the recommendation was to consider a trial of osimertinib. The patient had a response for over six months. While there is preclinical evidence for utilizing osimertinib in colon cancer, we could find only one clinical case report of using osimertinib in colon cancer[4,5].

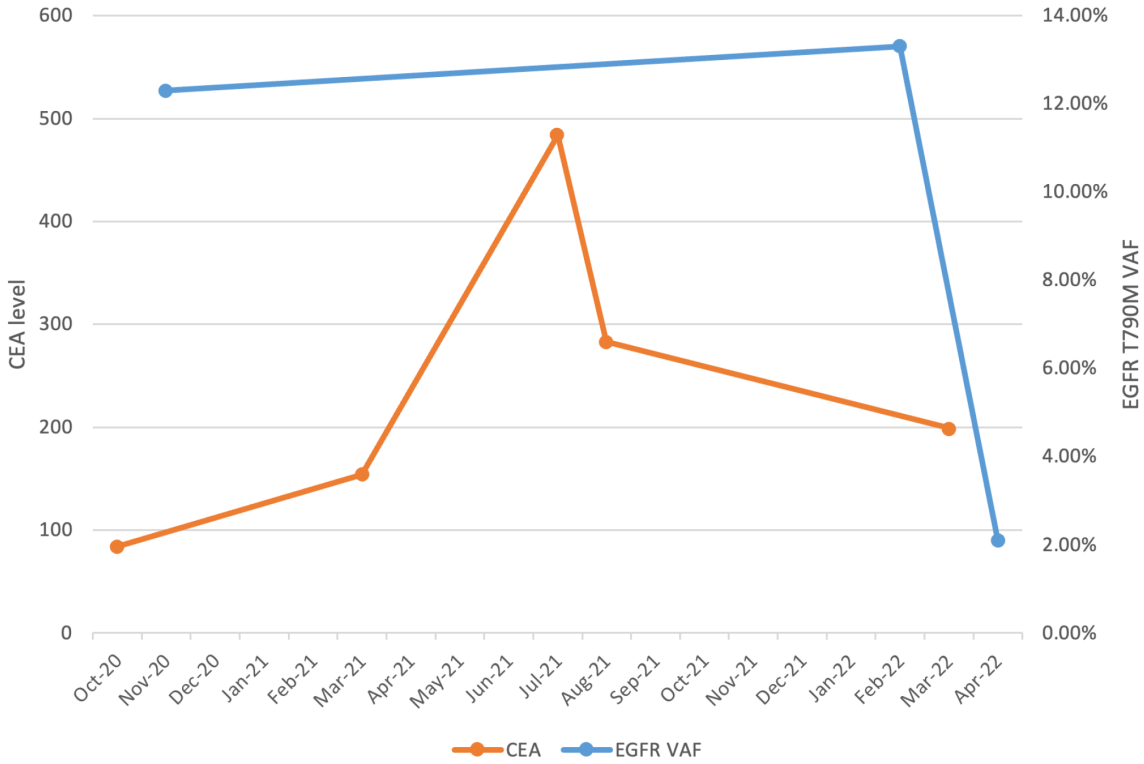

DOI: 10.4251/wjgo.v15.i10.1829

Figure 1 Serial cell-free DNA analyses and carcinoembryonic antigen levels over time. Osimertinib was initiated in February 2022, and imaging in April 2022 confirmed treatment response with a decrease in size of the hepatic metastases. CEA: Carcinoembryonic antigen; CEGFR: Epidermal growth factor receptor; VAF: Variant allele frequency.

The *EGFR* gene is located on chromosome 7p12-13 and encodes a transmembrane receptor composed of extracellular ligand binding and intracellular TK domains[6]. *EGFR* regulation is tightly controlled, and variations within the *EGFR* signaling pathway play a key role in solid tumor oncogenesis. Commercially available *EGFR* antagonists include the monoclonal antibodies (mAbs) panitumumab and cetuximab and act by preventing epidermal growth factor ligand binding to the external *EGFR* domain. *EGFR* mAbs are considered a standard of care in treating patients with metastatic colorectal cancer lacking activating mutations in *KRAS/NRAS* downstream of *EGFR*[7].

In contrast to these mAbs, *EGFR* TKIs block intracellular signaling cascades through competition with adenine triphosphate. While both approaches lead to the inhibition of *EGFR* autophosphorylation, TKI efficacy is restricted to cancers that carry *EGFR* mutations in the TK domain (exons 18-21). Still, these mutations are rarely seen in colorectal cancer[8]. Available TKIs against *EGFR* TK mutations are approved for non-small cell lung cancer and include first-generation agents gefitinib and erlotinib and second-generation agents afatinib and dacomitinib[9]. Osimertinib is the only approved third-generation *EGFR* TKI and has efficacy against *EGFR* T790M, a mutation resistant to first- and second-generation *EGFR* TKIs[10].

There are currently no guidelines to direct therapy selection in *EGFR*-mutated colorectal cancer. However, case reports exist describing the efficacy of erlotinib in *EGFR* mutant colorectal cancer[11,12]. More recently, a 50-year-old Japanese woman with an *EGFR* T790M lung lesion from a colorectal primary responded to osimertinib for 95 days[5]. The patient was noted positive for *RAS* mutant G13D at diagnosis, which is downstream of *EGFR*. Mutations of this pathway are established as strong negative predictive markers, and may preclude efficacy of these therapies. This patient also had an uncommon *EGFR* L861Q mutation compounded with the *EGFR* T790M at the time of osimertinib initiation. It is speculated by the authors the patient originally only had the *EGFR* L861Q mutation and the T790M was acquired during the clinical course prior to starting osimertinib. With one mutation acquired during the clinical course, it is possible another resistance mechanism was acquired after starting osimertinib. This hypothesis along with the *RAS* mutation are potential explanations for the short response time noted compared to our patient. However, such cases highlight the additional options afforded to these patients by utilizing multi-gene sequencing panels.

The use of NGS in metastatic colorectal cancers is becoming standard in an effort to identify additional therapeutic options in the refractory setting. However, guidelines currently recommend testing for only a limited set of genes, including *NRAS, KRAS, BRAF* V600E, and mismatch repair/ microsatellite instability, with consideration to test for *HER2* amplifications and *NTRK* fusions in the refractory disease setting[9]. A retrospective review of 23 US-based oncology practices demonstrates that even these limited gene panels are underutilized; only 40% of patients underwent guideline-recommended genomic testing for any of these genomic markers, a rate that has not increased since 2013[13,14].

Cell-free DNA plays an increasingly pivotal role in minimal residual disease monitoring for individuals with colon cancer[15]. Both tumor-informed and tumor-agnostic approaches are being investigated[16]. The clinical case described in this paper demonstrates the prospect of using cell-free DNA for response assessment, in addition to standard tumor

markers such as carcinoembryonic antigen, as illustrated in Figure 1.

Our patient had a response to osimertinib for over six months of therapy. The previously under-recognized factor of the time-related burden that patients undergoing oncologic treatments experience is coming to the forefront with recent research[17]. We customized her treatment to meet her goals of minimizing toxicity and time spent traveling to the cancer center. In alignment with these goals, most of her visits were performed virtually.

This case shows the benefit of large panel multi-gene sequencing assays to identify potential therapeutic options in patients with refractory disease. Molecular tumor boards are integral in identifying patients appropriate for a targeted therapy approach and procuring these much-needed therapies. As demonstrated in this case, precision medicine holds promise to tailor patient treatments to align with their goals and expectations.

CONCLUSION

This case shows the benefit of large panel multi-gene sequencing assays to identify potential therapeutic options in patients with refractory disease. Molecular tumor boards are integral in identifying patients appropriate for a targeted therapy approach and procuring these much-needed therapies. As demonstrated in this case, precision medicine holds promise to tailor patient treatments to align with their goals and expectations.

FOOTNOTES

Author contributions: All authors contributed to manuscript writing; all authors have read and approved the final manuscript.

Informed consent statement: Consent for this publication was received from the patient's legal guardian.

Conflict-of-interest statement: The authors declare no conflicts of interest.

CARE Checklist (2016) statement: The authors have read the CARE Checklist (2016), and the manuscript was prepared and revised according to the CARE Checklist (2016).

Country/Territory of origin: United States

ORCID number: Lara Kujtan 0000-0001-9758-1777; Dhruv Bansal 0000-0002-6357-6897.

S-Editor: Lin C
L-Editor: A
P-Editor: Zhang XD

REFERENCES

1 **Kim N**, Cho D, Kim H, Kim S, Cha YJ, Greulich H, Bass A, Cho HS, Cho J. Colorectal adenocarcinoma-derived EGFR mutants are oncogenic and sensitive to EGFR-targeted monoclonal antibodies, cetuximab and panitumumab. *Int J Cancer* 2020; **146**: 2194-2200 [PMID: 31290142 DOI: 10.1002/ijc.32499]

2 **Park AK**, Francis JM, Park WY, Park JO, Cho J. Constitutive asymmetric dimerization drives oncogenic activation of epidermal growth factor receptor carboxyl-terminal deletion mutants. *Oncotarget* 2015; **6**: 8839-8850 [PMID: 25826094 DOI: 10.18632/oncotarget.3559]

3 **Van Cutsem E**, Danielewicz I, Saunders MP, Pfeiffer P, Argilés G, Borg C, Glynne-Jones R, Punt CJA, Van de Wouw AJ, Fedyanin M, Stroyakovskiy D, Kroening H, Garcia-Alfonso P, Wasan H, Falcone A, Fougeray R, Egorov A, Amellal N, Moiseyenko V. First-line trifluridine/tipiracil + bevacizumab in patients with unresectable metastatic colorectal cancer: final survival analysis in the TASCO1 study. *Br J Cancer* 2022; **126**: 1548-1554 [PMID: 35440667 DOI: 10.1038/s41416-022-01737-2]

4 **Guo L**, Huang S, Wang X. PUMA mediates the anti-cancer effect of osimertinib in colon cancer cells. *Onco Targets Ther* 2017; **10**: 5281-5288 [PMID: 29138581 DOI: 10.2147/OTT.S139382]

5 **Yanagisawa A**, Kinehara Y, Kijima R, Tanaka M, Ninomiya R, Jokoji R, Tachibana I. Metastatic Lung Tumors from Colorectal Cancer with EGFR Mutations That Responded to Osimertinib. *Intern Med* 2023; **62**: 769-773 [PMID: 35871578 DOI: 10.2169/internalmedicine.0002-22]

6 **Mitsudomi T**, Yatabe Y. Epidermal growth factor receptor in relation to tumor development: EGFR gene and cancer. *FEBS J* 2010; **277**: 301-308 [PMID: 19922469 DOI: 10.1111/j.1742-4658.2009.07448.x]

7 **Cai WQ**, Zeng LS, Wang LF, Wang YY, Cheng JT, Zhang Y, Han ZW, Zhou Y, Huang SL, Wang XW, Peng XC, Xiang Y, Ma Z, Cui SZ, Xin HW. The Latest Battles Between EGFR Monoclonal Antibodies and Resistant Tumor Cells. *Front Oncol* 2020; **10**: 1249 [PMID: 32793499 DOI: 10.3389/fonc.2020.01249]

8 **Altunel E**, Aljamal AA, Mantyh J, Deak K, Glover W, McCall SJ, Datto M, Strickler J, Hsu DS. Characterization of the Epidermal Growth

Factor Receptor T790M Mutation in Colorectal Cancer. *JCO Precis Oncol* 2018; **2**: 1-7 [PMID: 35135168 DOI: 10.1200/PO.18.00194]

9 **Marin-Acevedo JA**, Pellini B, Kimbrough EO, Hicks JK, Chiappori A. Treatment Strategies for Non-Small Cell Lung Cancer with Common EGFR Mutations: A Review of the History of EGFR TKIs Approval and Emerging Data. *Cancers (Basel)* 2023; **15** [PMID: 36765587 DOI: 10.3390/cancers15030629]

10 **Remon J**, Steuer CE, Ramalingam SS, Felip E. Osimertinib and other third-generation EGFR TKI in EGFR-mutant NSCLC patients. *Ann Oncol* 2018; **29**: i20-i27 [PMID: 29462255 DOI: 10.1093/annonc/mdx704]

11 **Yarom N**, Jonker DJ. The role of the epidermal growth factor receptor in the mechanism and treatment of colorectal cancer. *Discov Med* 2011; **11**: 95-105 [PMID: 21356164]

12 **Li Y**, Zhang HB, Chen X, Yang X, Ye Y, Bekaii-Saab T, Zheng Y, Zhang Y. A Rare EGFR-SEPT14 Fusion in a Patient with Colorectal Adenocarcinoma Responding to Erlotinib. *Oncologist* 2020; **25**: 203-207 [PMID: 32162810 DOI: 10.1634/theoncologist.2019-0405]

13 **Gutierrez ME**, Price KS, Lanman RB, Nagy RJ, Shah I, Mathura S, Mulcahy M, Norden AD, Goldberg SL. Genomic Profiling for KRAS, NRAS, BRAF, Microsatellite Instability, and Mismatch Repair Deficiency Among Patients With Metastatic Colon Cancer. *JCO Precis Oncol* 2019; **3** [PMID: 32923867 DOI: 10.1200/PO.19.00274]

14 **Iyer P**, Deng M, Handorf EA, Nakhoda S, Dotan E. Assessing Oncologists' Adoption of Biomarker Testing in Metastatic Colorectal Cancer Using Real-World Data. *JNCI Cancer Spectr* 2022; **6** [PMID: 36149298 DOI: 10.1093/jncics/pkac065]

15 **Venook AP**. Colorectal Cancer Surveillance With Circulating Tumor DNA Assay. *JAMA Netw Open* 2022; **5**: e221100 [PMID: 35258585 DOI: 10.1001/jamanetworkopen.2022.1100]

16 **Gong J**, Hendifar A, Gangi A, Zaghiyan K, Atkins K, Nasseri Y, Murrell Z, Figueiredo JC, Salvy S, Haile R, Hitchins M. Clinical Applications of Minimal Residual Disease Assessments by Tumor-Informed and Tumor-Uninformed Circulating Tumor DNA in Colorectal Cancer. *Cancers (Basel)* 2021; **13** [PMID: 34572774 DOI: 10.3390/cancers13184547]

17 **Gupta A**, Jensen EH, Virnig BA, Beg MS. Time-Related Burdens of Cancer Care. *JCO Oncol Pract* 2022; **18**: 245-246 [PMID: 34709950 DOI: 10.1200/OP.21.00662]

Published by **Baishideng Publishing Group Inc**
7041 Koll Center Parkway, Suite 160, Pleasanton, CA 94566, USA
Telephone: +1-925-3991568
E-mail: bpgoffice@wjgnet.com
Help Desk: https://www.f6publishing.com/helpdesk
https://www.wjgnet.com